HYDROTHERMAL RECONSTRUCTION AND LITHOGEOCHEMISTRY OF THE ARGYLE OROGENIC GOLD DEPOSIT, BAIE VERTE, NEWFOUNDLAND

by Maciej Pawlukiewicz

A Thesis submitted
to the School of Graduate Studies in partial fulfillment of the
requirements for the degree of

Master of Science

Department of Earth Sciences

Memorial University of Newfoundland

St. John’s, Newfoundland and Labrador, Canada

December 2019

Abstract

The Argyle orogenic gold deposit (543,000 t @2.19 g/t Au indicated, and 517,000 t @1.82 g/t Au inferred resources) is located within Lower Ordovician Snooks Arm Group, Baie Verte Peninsula, Newfoundland. Gold mineralization is hosted as inclusions in secondary pyrite and at pyrite crystal boundaries in a ~50 m thick E-W striking, gently N-dipping tholeiitic gabbro sill. The short distance (200-300 m) from the Scrape thrust, rheological contrast within the heterogenous gabbro and a high content of coarse, reactive ilmenomagnetite were critical to the localization of gold mineralization. Two hydrothermal alteration events affected the gabbro: 1) early, pre-mineralization epidote-albite alteration; and 2) later, mineralization-related sericite-quartz-ankerite-(albite-chlorite-rutile-pyrite-gold) alteration. Within the mineralization-related alteration there are three assemblages: 1) distal chlorite-calcite-rutile ± epidote-albite (30-70 m); 2) intermediate chlorite-epidote-albite-calcite ± ankerite-rutile-hematite-sericite-pyrite (5-30 m); and 3) proximal sericite-quartz-ankerite ± albite-chlorite-rutile-sooty pyrite-gold (2-25 m). Lithogeochemistry, mineral chemistry and short-wave infrared (SWIR) spectroscopy were used to identify mineralogical, geochemical and spectral vectors to alteration and mineralization, which may aid in future mineral exploration.

Acknowledgements

I would like to thank my supervisor, Dr. Stephen Piercey for his guidance, humour and conversations during my time at the Memorial University of Newfoundland. Steve’s supervision style has allowed for a large degree of independence and flexibility regarding the direction of this research project. During a time of hardship when my summer fieldwork data was stolen, Steve was most supportive and empathetic, which has encouraged me to return to the field. I would like to thank Dr. Graham Layne for being on my supervisory committee and reviewing this manuscript. I am particularly grateful to Matthew Manor for the early feedback, manuscript review and advice. I would like to acknowledge the remaining members of the Piercey research group, namely Robert King, Carly Mueller and Nikola Denisova for their camaraderie, jokes, daily discussions and Saturday night dinners. Additionally, I would like to express my gratitude to Dr. Philip Lypaczewski for the discussions regarding SWIR data and Dr. Wanda Aylward for access to and assistance with SEM-EDS and EMPA.

The support of the exploration team at Anaconda Mining Inc., namely David Copeland, Steve Barrett, Paul McNeill, Dean Courage, Linsey Gale and Mike Kelly, is greatly appreciated. The folks from the Anaconda exploration team have made me feel most welcome in Baie Verte. I am especially thankful to David Copeland, who has co-designed this Master’s project and has been involved in the development of the ideas regarding the geology of the Argyle gold deposit.

I would like to thank my parents – Maria and Janusz, and my brother Michal for their constant support and their understanding that infrequent visits home are an unfortunate reality in the life of a geologist.

Financial support for this Master's thesis has been provided by Anaconda Mining Ltd., the GeoExplore program from InnovateNL (a part of the Newfoundland and Labrador Department of Trade, Culture, Industry and Innovation), an NSERC Collaborative Research and Development Grant and an NSERC Discovery Grant to Dr. Stephen J. Piercey, and Society of Economic Geologists' Graduate Student Fellowship to Maciej Pawlukiewicz.

Table of Contents

List of Tables

Chapter 2

List of Figures

Chapter 1

Chapter 2

List of Abbreviations

2D, 3D	two-, three-dimensional
Ab	albite
Alt	alteration
Ank	ankerite
aq	aqueous
Au	gold
Avg	average
BBL	Baie Verte Brompton Line
BVOT	Baie Verte Oceanic Tract
BX	breccia
Calc	calcite
Carb	carbonate
Ccp	chalcopyrite
Chl	chlorite
cm	centimeter
D	depth
EDS	energy dispersive x-ray
Ep	epidote
EPMA	electron probe microanalysis
Eq	equation
Fig(s)	figure
FW	footwall
g/t	grams per ton
HFSE	high field strength elements
HREE	heavy rare earth elements
HW	hanging wall
ICP-ES	inductively coupled emission mass spectroscopy
ICP-MS	inductively coupled plasma mass spectrometry
Ilm	ilmenite
Int	intrusion
km	kilometer
LFSE	light field strength elements
LOI	loss-on-ignition
LREE	light rare earth elements
Mag	magnetite
m	meters

MBX	mafic breccia
MCT	mafic crystal tuff
MD	mafic dyke
MF	mafic flow
MLT	mafic lapilli tuff
mm	millimeter
Ms	muscovite
MT	mafic tuff
Mt	million tonnes
nm	nanometers
PCA	principal component analysis
Ph	phengite
ppb	parts per billion
ppm	parts per million
Py	pyrite
Qtz	quartz
REE	rare earth elements
Rut	rutile
SEM	scanning electron microscope
Ser	sericite
SWIR	short-wave infrared
vol.	volume
WL	wavelength
wt %	weight percent

List of Appendices

Chapter 1: Introduction to the Argyle Orogenic Gold Deposit, Baie Verte, north-central Newfoundland

The Argyle orogenic gold deposit (543,000 t @ 2.19 g/t Au indicated, and 517,000 t @ 1.82 g/t Au inferred) is located within the Baie Verte Mining District, 1 km west of the community of Ming's Bight in north-central Newfoundland (Copeland et al., 2015; Sparrow et al., 2017; Cullen et al., 2018). The deposit was discovered in 2012 and is situated near the Stog'er Tight (204,100 t @ 3.59 g/t Au indicated and 252,100 t @ 3.27 g/t Au inferred) and Pine Cove (1,560,000 t @ 1.67g/t Au indicated and 208,700 t grading 1.57 g/t Au inferred) gold mines within Anaconda Mining's Point Rousse Project; the Pine Cove mill is located only 3-4.5 km from the Argyle and Stog'er Tight deposits (Copeland et al., 2015). The Baie Verte Peninsula (Figs. 1.1-1.2) hosts numerous gold occurrences, discovered predominantly in the 1980s (Evans, 2004). The gold occurrences are primarily hosted by Lower Ordovician volcanic cover sequences (Snooks Arm Group) and ophiolitic rocks of the Baie Verte oceanic tract (BVOT) (Williams et al., 1988; Bédard et al., 1998; van Staal, 2007).

There have been no previous academic studies undertaken on the Argyle deposit; hence, its structure, geology, lithology, mineralogy and chemistry are yet to be fully determined. Piercey and Copeland (2017) suggested that the Argyle deposit is hosted by a similar gabbroic intrusion to the Stog'er Tight deposit located 2 km to the west from Argyle. The structural control on mineralization at Stog'er Tight has been described by Kirkwood and Dubé (1992) and a M.Sc. project focusing on Stog'er Tight by Ramezani

(1992) has defined the geology, geochemistry and U-Pb geochronology of the deposit. The study by Ramezani (1992) has been superseded by Ramezani et al. (2000) and additional Re-Os dating was undertaken by Kerr and Selby (2012). However, there have been no modern geological studies on the hydrothermal footprint of either of these deposits.

The objectives of this Master's project are: 1) document the geology, lithostratigraphy, structure, and primary and secondary alteration mineralogy of the Argyle gold deposit; 2) evaluate the role that primary mineralogy and host rock chemical reactivity played in the localization of mineralization and test this using primary textural and lithogeochemical variations in the gabbroic and volcanic host rocks of the Argyle deposit; 3) outline the alteration mineralogy, mineral assemblages, and paragenesis of alteration assemblages to understand their spatial distributions in the Argyle deposit; 4) utilize alteration lithogeochemistry and associated mass balance calculations to document the mass and elemental changes associated with alteration in the Argyle deposit; 5) create spatial and chemical vectors to gold mineralization and elucidate the chemical processes associated with gold formation and fluid-rock interaction in the Argyle deposit; 6) document the mineralogy and mineral chemistry by utilizing scanning electron microscopy (SEM) and electron probe microanalysis (EPMA) to evaluate the variations in mineral chemistry as a function of paragenesis and proximity to mineralization in the Argyle deposit; and 7) integrate results to characterize the hydrothermal footprint of the Argyle deposit, and provide vectors to the gold mineralization.

1.1 Exploration History

The Baie Verte Peninsula has a long history of mineral exploration and mining, dating back to the opening of the Terra Nova and Tilt Cove copper mines in 1860 and 1864, respectively (Evans, 2004). Until the 1980s, gold in the Baie Verte Peninsula was produced primarily as a by-product from VMS deposits (Evans, 2004; Skulski et al., 2009). Gold exploration between 1984 and 1989 led to the numerous orogenic gold (i.e., gold-only) discoveries, including the Nugget Pond, Deer Cove, Pine Cove and Stog'er Tight deposits.

Stog'er Tight was discovered by Noranda Exploration Company Ltd. in 1987 through a soil geochemistry survey and trenching (Ramezani, 1992). In the following years, seven similar gabbro-hosted zones (Gabbro Zone, Gabbro West, Gabbro East, Cliff Zone, West Zone, South Zone and East Zone) (Figs. 1.3 and 1.4) were identified through geochemical, geological and geophysical surveys and an 8,000 m drilling campaign (Evans, 2004). Ming Minerals Inc. acquired the property from Noranda in 1995 and processed a 30,735 t bulk sample @ 3.25 g/t; the project was discontinued after the head grade for gold was lower than projected (Copeland et al., 2015). Supplementary trenching and drilling were carried out by Tenacity Gold Mining Company Ltd. in 2006, which estimated an indicated resource of 96,000 t @ 7.04 g/t Au and an inferred resource of 53,000 t @ 5.75 g/t Au (Copeland et al., 2015). The head grade of 1.92 g/t Au in a 28,695 t bulk sample was significantly lower than the estimated grade in core of 4.8 g/t Au, due to mining dilution (Copeland et al., 2015). The Stog'er Tight Mining Lease was acquired by 1512513 10Alberta Ltd. and optioned to Anaconda Mining in 2012 (Copeland et al., 2015). Since the discovery of the Stog'er Tight deposit, a total of 18,073.73 m of diamond drilling in 282 holes has been completed on the Stog’er Tight property, including 97 holes totaling 5,738.73 m and extensive mining by Anaconda (Cullen et al., 2018). Regional exploration undertaken by Anaconda targeted gold mineralization hosted in gabbros similar to the intrusions at the Stog’er Tight deposit.

The gold mineralization at Argyle was discovered by Anaconda Mining Inc. in 2012 through prospecting, B-horizon soil sampling, soil geochemistry and trenching in a previously unexplored area (Copeland et al., 2015; Sparrow et al., 2017). Trenching in 2014 and 2015 exposed gold mineralization associated with quartz-veined, pyrite-chlorite-carbonate-quartz altered gabbro; the subsequent channel sampling revealed gold mineralization associated with the altered gabbro, including 3.75 g/t Au over 16 m in trench AEtr14-8, 1.31 g/t Au over 11 m in trench AEtr14-12 and 1.89 g/t Au over 10 m in AEtr15-18 (Evans, 2014; Sparrow et al., 2017). Follow-up drilling in 2016 and 2017 outlined a mineralized zone (Fig. 1.5) with associated hydrothermal alteration across a strike length of 685 m and 225 m down-dip with encouraging assay results, such as: 6.09 g/t over 8.9 m (AE-16-11), 9.31 g/t over 6.0 m (AE-16-39), 5.52 g/t over 15.0 m (AE-16-40) and 12.47 g/t over 5.0 m (AE-17-58) (Fig. 1.6) (Cullen et al., 2018). An initial National Instrument (NI) 43-101 mineral resource estimate for Argyle in 2018 defined an indicated mineral resource of 543,000 t @ 2.19 g/t Au and an inferred mineral resource of 517,000 t @ 1.82 g/t Au (Cullen et al., 2018).

1.2 Tectonic Evolution and Regional Geology

Newfoundland is subdivided into four tectonostratigraphic zones: Humber, Dunnage, Gander and Avalon (Fig. 1.1A), which were sutured together during the Paleozoic Appalachian orogenesis (500-250 Ma), as a result of the closure of Iapetus and Rheic oceans and the subsequent amalgamation of Pangea (Williams, 1979, 1995; Williams et al., 1988; van Staal, 2007).

The Dunnage Zone is comprised of variably preserved continental- and oceanic arc, back-arc, and ophiolitic rocks and is subdivided into the peri-Laurentian Notre Dame subzone, which was accreted onto the Laurentian margin with its Dashwood infrastructure during the second phase of the Taconic orogeny in the Lower to Middle Ordovician, and the peri-Gondwanan Exploits subzone, which was accreted onto the Gander Margin during the Early Ordovician Penobscot orogeny (van Staal, 2007; van Staal et al., 2012). The Silurian Salinic orogeny led to the accretion of the leading edge of Ganderia to Laurentia and the Devonian Acadian orogeny resulted from the convergence of Avalonia and Ganderia that led to the subsequent closure of the Acadian Seaway (van Staal, 2007; van Staal et al., 2012). These events led to the amalgamation of the main tectonostratigraphic zones in Newfoundland and were important for the orogenic gold mineralization in the region.

The Baie Verte Peninsula (Fig. 1.1B) is underlain by two discrete tectonostratigraphic belts, the Humber Zone and the Notre Dame subzone of the Dunnage Zone, which are separated by the Baie Verte line (BVL), a complex brittle-ductile shear zone that contains ophiolite slivers along its length (Williams, 1979; Williams and St-Julien, 1982; Castonguay et al., 2014). The Humber Zone to the west of the BVL is a remnant of a passive continental margin of Laurentia and consists of Neoproterozoic to Early Paleozoic metasedimentary rocks of the Fleur de Lys Supergroup that were deposited on Precambrian (Grenvillian) basement, whereas the peri-Laurentian Notre Dame subzone in the Baie Verte Peninsula consist of: 1) Cambrian-Ordovician ophiolitic sequences that are remnants of the Iapetus Ocean; 2) an Early Ordovician volcanic- to volcanosedimentary cover sequence; 3) Silurian terrestrial volcanic and sedimentary rocks; and 4) Silurian intrusive rocks (Evans, 2004; van Staal, 2007; Skulski et al., 2009; van Staal et al., 2012).

1.3 Local Geology

The Baie Verte oceanic tract (BVOT) consists of four Cambro-Ordovician ophiolite suites: 1) the Advocate Complex; 2) the Betts Cove Complex; 3) the Pacquet Complex; and 4) the Point Rousse Complex (Fig. 1.1B; Hibbard, 1983; Skulski et al., 2010). The Point Rousse Complex (PRC) is centered in the Baie Verte flexure, in the northern coastal area of the Baie Verte Peninsula where the northeast-southwest trend of the BVL sharply changes to an east-west orientation (Fig. 1.2; Skulski et al., 2009; Sparrow et al., 2017). The Advocate, Betts Cove, and Pacquet complexes represent Cambrian-Ordovician (488-485 Ma) partial to full ophiolite sequences that contain varying amounts of ultramafic, gabbroic and mafic volcanic rocks (Hibbard, 1983; Bédard, 1999; Bédard et al., 2000; Skulski et al., 2010). The Point Rousse Complex represents an Ordovician ophiolite sequence (Fig. 1.3), which is correlative to the Snooks Arm Group stratigraphy and to a lesser degree with the Pacquet Complex (Tuach and Kennedy, 1978; Hibbard, 1983;

Bédard, 1999; Bédard et al., 2000; Skulski et al., 2010). The Point Rousse Complex comprises mafic volcanic rocks, including high-Ti tholeiitic basalts, calc-alkaline basalt, clinopyroxene-phyric tuff and tuff breccia, banded magnetite and jasper iron-formation, and mafic epiclastic wackes and conglomerates (Bédard, 1999; Bédard et al., 2000; Evans, 2004; Skulski et al., 2010; Sparrow et al., 2017). The volcanic cover sequence is underlain by ophiolitic plutonic rocks located in an east-trending synclinorium (Fig. 1.2; Norman and Strong, 1975; Ramezani et al., 2000), and is exposed in the core of the syncline, with ophiolitic rocks constrained to and exposed on fault-bounded structural blocks on its northern and southern rims. The high-angle faults and thrust faults dip moderately to the northwest (Castonguay et al., 2009; Sparrow et al., 2017).

The rocks in the Point Rousse Complex record at least four deformation events (D_1-D_4) (Castonguay et al., 2009). The fabrics related to the D_1 deformation were formed as a result of the obduction of ophiolites during the Taconian Orogeny but are mostly poorly preserved due to the overprinting by later deformation events (Castonguay et al., 2009). D_2 represents the main tectonometamorphic phase on the peninsula and is responsible for the general northerly dip of the units, the north-dipping S_2 foliation and the down-dip, northerly stretching lineations (Castonguay et al., 2009; Sparrow et al., 2017). The deformation associated with the D_2 event, interpreted to be related to the crustal thickening and transpression during the Silurian Salinic orogeny, resulted in south-directed thrusting, folding and shearing, and the formation of meter-scale south-directed shear zones parallel to S_2, such as the Scrape thrust, which juxtaposed the Point Rousse Complex over the Pacquet Harbour Group (Hibbard, 1983; Dunning et al., 1990; Skulski et al., 2009;

Castonguay et al., 2009; Skulski et al., 2010). Post-D_2 (i.e., D_3) extensional shear bands in the Scrape thrust footwall show normal sense reactivation (Jamieson et al., 1993; Castonguay et al., 2009). Fabrics associated with the D_3 extensional event are expressed as shallowly inclined to recumbent folds, which affect earlier fabrics and are likely related to Devonian extension and core complex formation (Anderson et al., 2001; Castonguay et al., 2009). The D_4 deformation is marked by north-northeast trending anticlines and synclines (F_4), affecting structures related to D_1-D_3 and generally bestowing a double-plunging nature to the earlier folds (Castonguay et al., 2009; Sparrow et al., 2017).

The orogenic gold occurrences in the Baie Verte Peninsula are either hosted in wallrock or in quartz veins (Evans, 2004). Mineralization is spatially associated with, and typically on the hanging wall sides of, D_2-related thrust sheets, such as the Scrape thrust and Deer Cove sole thrust (Kirkwood and Dubé, 1992; Dubé et al., 1993; Evans, 2004; Castonguay et al., 2009, 2014; Skulski et al., 2009, 2010). Thrusting and orogenic gold mineralization are interpreted to be Silurian to Devonian in age, based on a 420 ± 5 Ma U-Pb age for hydrothermal zircon at Stog'er Tight and a 420 ± 7 Ma Re-Os age for pyrite from Pine Cove (Ramezani et al., 2000; Kerr and Selby, 2012).

1.4 Stratigraphy

The Pine Cove, Argyle, and Stog'er Tight gold deposits are hosted by Cambro-Ordovician rocks of the Snooks Arm Group in the Point Rousse Complex (Fig. 1.3) (Bédard, 1999; Bédard et al., 2000; Skulski et al., 2010). The underlying Pacquet Complex, and its correlative rocks in the Betts Cove Complex, represent partially preserved ophiolite stratigraphy, and hosts Au-rich and base metal-bearing volcanogenic massive sulfide (VMS) deposits, including the Betts Cove, Tilt Cove and Rambler-Ming deposits (Tuach et al., 1988; Dimmell et al., 1999; Bédard et al., 2000; Evans, 2004).

These rocks are overlain and in thrust contact with the Snooks Arm Group volcaniclastic cover sequence that overlies the ophiolitic rocks on the Baie Verte Peninsula. The Scrape Point Formation is stratigraphically lowest part of the cover sequence and is truncated by the north-dipping Scrape thrust, which separates the Snooks Arm Group from the serpentinised ultramafic rocks of the Point Rousse Complex (Bédard, 1999; Skulski et al., 2010). The bottom part of the Scrape Point Formation contains the Nugget Pond horizon (~Goldenville horizon), which is composed of a basal conglomerate cemented by jasper that is overlain by red siltstones and a jasper-magnetite iron formation; these rocks host both the Nugget Pond and Goldenville gold deposits (Skulski et al., 2009). The top of the Scrape Point Formation is composed of a coarser green siltstone and tuffaceous wackes, locally overlain and interbedded with mafic tuffs and high-Ti tholeiitic basalts (Skulski et al., 2009, 2010). Gabbros coeval with the Scrape Point Formation host the Stog'er Tight and Argyle gold deposits and the Animal Pond prospect (Ramezani et al., 2000; Skulski et al., 2010). The Bobby Cove Formation consists of calc-alkaline volcaniclastic rocks, calc-alkaline basalts and turbiditic rocks, and the overlying Venam's Bight Formation comprises high-Ti tholeiitic basalts interbedded with volcanic breccias and red mudstones; the latter formation hosts the Pine Cove gold deposit (Skulski et al., 2009, 2010). The Balsam Bud Cove Formation consists predominantly of felsic tuffs, siltstones and shales overlain by the tholeiitic high-Ti basalts of the Round Harbor Formation that comprises the uppermost part of the Snooks Arm Group (Skulski et al., 2009, 2010).

1.5 Deposit Geology

Argyle and Stog’er Tight deposits (Figs. 1.4 and 1.6) are underlain by mafic volcanic and sedimentary rocks of the Scrape Point and Bobby Cove formations, including massive basalt flows interbedded with green mudstone, tuffs, clinopyroxene-phyric lapilli and crystal tuffs (Bédard et al., 2000; Skulski et al., 2009, 2010). These are cut by gabbroic sills and mafic dykes that are variably deformed, with foliation intensity ranging from weak to proto-mylonitic (Bédard, 1999; Bédard et al., 2000; Skulski et al., 2009, 2010; Sparrow et al., 2017).

The volcaniclastic cover sequence at Stog’er Tight is intruded by three 11 to 70 m thick gabbroic sills that trend northwest-southeast and dip to the north (Fig. 1.4 and 1.5) (Kirkwood and Dubé, 1992; Ramezani et al., 2000). The sills display weakly to moderately sheared southern contacts and, intact chilled northern contacts (Kirkwood and Dubé, 1992). The Fe-Ti-rich gabbro body that hosts mineralization at Stog’er Tight differs from the barren Fe-Ti-poor gabbro sill to the north by its increased concentration of ilmenomagnetite (Ramezani et al., 2000).

Ramezani (1992) recognized 4 alteration zones at Stog’er Tight, progressing inward towards gold mineralization: 1) chlorite-calcite; 2) ankerite-sericite; 3) chlorite-magnetite; and 4) red albite-pyrite (± gold). Gold at Stog’er Tight occurs as fine-grained (<0.5 mm) micro-veinlets and disseminated blebs within coarse pyrite crystals and less frequently as visible gold flakes where pyrite has been weathered (Ramezani et al., 2000). Gold-bearing pyrite mineralization is spatially restricted to highly altered gabbro, which is often adjacent to shear-parallel veins (Ramezani et al., 2000). The highest gold grades at Stog'er Tight are associated with coarse, mottled pyrite (Copeland et al., 2015).

The rock units at Argyle deposit are roughly east-west striking, dip gently towards the north-northwest and are in the hanging wall of the Scrape thrust, which outcrops 200-300 m to the south (Figs. 1.6 and 1.7) (Sparrow et al., 2017). Gold mineralization at Argyle is hosted in a ~50 m thick Fe-Ti-rich gabbroic sill, which is similar to the Ordovician (483 Ma +3/-2 U-Pb zircon age) suite of gabbroic rocks dated by Ramezani (1992) at the Stog'er Tight (Piercey and Copeland, 2017). The mineralization has a strike length of 685 m and is defined down-dip for 225 m (Sparrow et al., 2017). Gabbroic host rocks exhibit a roughly symmetrical alteration zone (30 to 70 m) with a distinctive mineralization zonation, from distal to proximal: 1) patchy epidote-albite-magnetite; 2) epidote-albite-chlorite; 3) epidote-albite-chlorite-rutile; and 4) pervasive albite-muscovite-iron carbonate-black chlorite ± pyrite-gold and quartz veins (Piercey and Copeland, 2017; Sparrow et al., 2017). Gold is associated with sooty black tarnished, inclusion-rich subhedral to anhedral pyrite crystals (1-5 wt. %) in the most intensely altered zones and typically resides on pyrite grain margins, in fractures, or as fine inclusions within pyrite crystals (Piercey and Copeland, 2017; Sparrow et al., 2017). Trace amounts of disseminated euhedral pyrite crystals can be found in all units and alteration assemblages in the Argyle deposit. Quartz veins tend to be abundant within mineralized zones proximal to faults and shear zones; there is minimal gold hosted exclusively within quartz veins at Argyle.

1.6 Orogenic Gold Deposits

Orogenic gold deposits are epigenetic, structurally controlled deposits that form in accreted terranes along convergent margins (Fig. 1.8), typically during late orogenic shifts from compressional to transpressional or transtensional regimes (Groves, 1993; Kerrich and Cassidy, 1994; McCuaig and Kerrich, 1998; Poulsen, 2000). Orogenic gold can be hosted in diverse lithologies, including felsic plutonic rocks, banded iron-formations, mafic volcanic rocks, and metasedimentary rocks (Groves et al., 2003; Goldfarb and Groves, 2015). The deposits form along second- and third-order structures that are splays from regional-scale fault zones (e.g. Baie Verte line; Destor-Porcupine deformation zone; Lefroy shear zone), are associated with highly-strained brittle, brittle-ductile or ductile zones at depths of 3-20 km (Fig. 1.9), and are typically at greenschist facies or near the greenschist-amphibolite facies boundary (Dubé and Gosselin, 2007). Orogenic gold mineralization is temporally related to either the metamorphic peak or post-peak metamorphism (Poulsen, 2000; Goldfarb and Groves, 2015).

The source of the ore-forming fluids has been a subject of debate. Most research favors the metamorphic dehydration model (Phillips and Groves, 1983; Robert and Kelly, 1987; Kerrich, 1989; Goldfarb et al., 1991; Groves et al., 1993; Phillips and Powell, 2010; Groves et al., 2019) over the magmatic-hydrothermal model (Giggenbach, 1986; Sillitoe, 1989; Sillitoe and Bonham Jr, 1990; Spooner, 1993) as the fluid source for orogenic gold deposits as reviewed by Pitcairn et al. (2015). In the metamorphic dehydration model ore-forming fluids are generated during accretion when progressive crustal subduction leads to prograde metamorphism from greenschist to amphibolite facies, which results in the devolatilization of the down-going slab and/or rocks in the accretionary complex (Fig. 1.10) (Pitcairn et al., 2014; Groves et al., 2019). The expelled fluids are then focused along crustal-scale shear zones within accreted rocks in the accretionary complex (Pitcairn et al., 2014; Goldfarb and Groves, 2015).

Orogenic gold mineralization can be spatially associated with quartz-carbonate veins and/or strongly altered wallrock. The gold mineralization in the Argyle and Stog'er deposits is associated with wallrock sulfidation. The reaction of fluids with wall rock around the veins and deformation zones results in distinct alteration halos due to fluid-rock interaction, and fluid dispersion and diffusion into the adjacent wallrock (Mikucki, 1998; Ridley and Diamond, 2000). Minerals common in alteration zones in orogenic gold deposits include: carbonates, sericite, biotite, albite, chlorite, pyrite, pyrrhotite, arsenopyrite and quartz (Colvine et al., 1988). Locally abundant minerals can include: hematite, anhydrite, Ti-bearing minerals, tourmaline and scheelite (Kerrich, 1983). In some deposits rare diopside, chloritoid, staurolite, cordierite, and garnet may also be found (Colvine et al., 1988).

Ore fluids in orogenic gold systems globally have a consistent chemistry, which typically includes: 5-20 mol % CO_2, 0.01-0.36 mol% H_2S, a pH of 5.5, salinity of 3-7 wt. % NaCl equivalent with Na>K>Ca,Mg, in addition significant concentrations of CH_4 and N_2 have been recorded in some deposits (Ridley and Diamond, 2000; Goldfarb and Groves, 2015). The interaction of host rocks with ore fluids typically results in significant introduction or remobilization of SiO_2, CO_2, K_2O, H_2O, S, and Au with irregular distributions of Na_2O, Sb, Ag, As, Te, B, Bi and W (Kerrich, 1983; Burrows and Spooner, 1986; Bierlein et al., 1999; Eilu et al., 2001; Bierlein, 2000; Dinel et al., 2008). Al_2O_3, Sc, Ti, V, Y, Zr, Nb, Th and REE are usually immobile during metasomatism (Kerrich, 1983; Bierlein, 2000; Eilu et al., 2001; Dinel et al., 2008). Elemental enrichments and depletions in orogenic gold deposits, expressed by wallrock alteration, are highly variable and dependent on fluid and host rock compositions (Kerrich, 1983; Mikucki, 1998; Bierlein et al., 1999; Eilu et al., 2001; Bierlein, 2000; Dinel et al., 2008). Despite the introduction of the above elements to altered host rock in many orogenic gold deposits there is no universal compositional halo around orogenic Au deposits, which is likely due to the fact that the deposits are rock buffered and this strongly influences the chemical and mineralogical makeup of the alteration assemblages in these deposits (Colvine et al., 1988).

Thermodynamic data and estimated ore-fluid conditions suggest that $Au(HS)_2^-$ is the principal gold transporting complex at temperatures <350°C (Mikucki, 1998; Ridley and Diamond, 2000; Williams-Jones et al., 2009). Calculations indicate thermodynamic stability of $AuCl_2^-$ complexes at temperatures >350°C, low pH and high fO_2, however the pH of orogenic gold fluids is generally near-neutral and $Au(HS)_2^-$ remains the dominant species of transport (Mikucki, 1998; Ridley and Diamond, 2000; Williams-Jones et al., 2009). Gold precipitation in orogenic systems takes place as a result of: 1) mixing of different fluids; 2) phase separation in response to pressure changes; 3) temperature changes related to adiabatic or conductive cooling of ore fluids; or 4) fluid-wallrock interaction (Wilkinson and Johnston, 1996; Mikucki, 1998; Weatherley and Henley, 2013). Fluid cooling is only important under high temperatures at deeper crustal levels (Mikucki, 1998). McCuaig and Kerrich (1998) determined that orogenic gold deposits are characterized by consistent $\delta^{13}C_{fluid}$ values, which suggests that fluid mixing is an insignificant gold precipitation mechanism. Phase separation is an important process near the brittle-ductile boundary, at fault jogs, where there are transitions between different order structures, and during seismic events where flash vaporization takes place and there are significant fluid pressure gradient changes (Wilkinson and Johnston, 1996; Weatherley and Henley, 2013). The relative importance of phase separation decreases from greenschist to amphibolite facies due to decreased brittle deformation with depth in the crust (Mikucki, 1998). Wallrock sulfidation is one of the most important gold precipitation mechanisms over a large range of P-T conditions and at all crustal levels in orogenic gold deposits (Mikucki, 1998; Ridley and Diamond, 2000; Robb, 2004). Sulfidation involves the destabilization of $Au(HS)_2^-$ complexes through a reaction between the ore fluids and Fe, or some other reductant, in the host rocks (Seward, 1973; Mikucki, 1998). Wallrock-hosted deposits typically contain gold in the form of microscopic particles that are spatially associated with, and hosted by, sulfide minerals (Mikucki, 1998; Williams-Jones et al., 2009). The interaction of the $Au(HS)_{2-}$ in the fluid with Fe in the wallrock promotes metal precipitation by changing both pH and redox state of the fluid (Robb, 2004), resulting in Au precipitation as follows (Mikucki, 1998; Williams-Jones et al., 2009):

$$FeO_{(rock)} + 2H_2S^o = FeS_{2(py)} + H_2O + H_{2(g)}$$

and

$$Au(HS)_{2-} + H^+ + \frac{1}{2}H_{2(g)} = Au + 2H_2S^o.$$

1.7 Thesis objectives

This study focuses on examining the hydrothermal footprint of the strongly metasomatized gabbro-hosted mineralization in the Argyle deposit by documenting the hydrothermal alteration footprint of the deposit, the host stratigraphy and structure, and the relationship of these characteristics to gold distribution in the deposit in order to understand the setting, style, exploration footprint, and genesis of the Argyle deposit. The detailed thesis objectives include:

- document the alteration facies, zonation, and distribution using field methods (mapping, graphic core logging), lithogeochemistry, petrography and short-wave infrared spectroscopy;
- define the structural, stratigraphic, mineralogical, and chemical controls on the localization of mineralization and document the alteration footprint and its genesis within the Argyle deposit using field methods, petrography and scanning electron microscopy, lithogeochemistry and mineral chemistry;
- characterize the least altered samples using petrography and lithogeochemistry to understand primary chemical and mineralogical attributes of the Argyle gabbro, its genesis, and to establish a baseline for quantitative calculations of the chemical and mineralogical changes associated with alteration in the deposit;
- document the secondary, hydrothermal alteration facies, paragenesis, distribution, and the chemical and mineralogical changes associated with the alteration footprint within the Argyle deposit;

- evaluate the variations in mineral chemistry as a function of paragenesis and proximity to mineralization and link this with the spatial distribution of white mica and chlorite SWIR reflectance and its relationship to alteration zones and mineral chemistry; and
- develop field, mineralogical, mineral chemical, and lithogeochemical vectors towards mineralization in the Argyle deposit and to illustrate their potential for utility in understanding gabbro-hosted orogenic gold deposits on the Baie Verte Peninsula and deposits in similar environments globally.

1.8 Co-authorship Statement

This research project was designed by Dr. Stephen J. Piercey and David A. Copeland. Primary research including sample collection, core logging, hyperspectral analysis and optical microscopy has been conducted by the author. Scanning electron microscopy and electron microprobe analyses were undertaken by the author under the supervision of Dr. Wanda Aylward at the Memorial University. The primary editor of this thesis was Dr. Stephen J. Piercey with secondary editing by Dr. Graham Layne.

1.9 Presentation

This thesis is composed of three chapters with accompanying appendices. Chapter 1 provides background information, and the layout and objectives of this thesis. Chapter 2 is the main body of the thesis and contains the detailed methodology, descriptions of the lithology, alteration assemblages, mineralization and an alteration model for the Argyle deposit based on data from graphic drill core logging, optical microscopy, whole-rock analyses (ICP-MS), scanning electron microscope-energy dispersive X-ray spectroscopy (SEM-EDS), electron microprobe analysis (EMPA) and short-wave infrared (SWIR) spectroscopy. This chapter provides evidence for the evolution of the Argyle deposit and discusses controls on mineralization and alteration. It is anticipated that this chapter will be published as a peer reviewed journal article in the future. Chapter 3 summarizes the conclusions of the research and establishes direction for potential future research. The appendices contain supplementary material for Chapter 2 and include digitized drill hole logs, cross-sections, geochemical data and hyperspectral datasets, electron microprobe data and scanning electron microscope results.

1.10 References

Anderson, S., Jamieson, R. A., Reynolds, P., and Dunning, G., 2001, Devonian extension in northwestern Newfoundland: $^{40}Ar/^{39}Ar$ and U-Pb data from the Ming's Bight area, Baie Verte Peninsula: Journal of Geology, v. 109, p. 191–211.

Bédard, J. H., 1999, Petrogenesis of boninites from the Betts Cove ophiolite, Newfoundland, Canada: identification of subducted source components: Journal of Petrology, v. 40, p. 1853–1889.

Bédard, J. H., Lauziere, K., Tremblay, A., and Sangster, A., 1998, Evidence for forearc seafloor spreading from the Betts Cove ophiolite, Newfoundland: oceanic crust of boninitic affinity: Tectonophysics, v. 284, p. 233–245.

Bédard, J. H., Lauziere, K., Tremblay, A., Sangster, A. L., Douma, S., and Dec, T., 2000, Betts Cove ophiolite and its cover rocks: Geological Survey of Canada Bulletin, v. 550, 76 p.

Bierlein, F. P., 2000, Wall-rock petrology and geochemistry in alteration halos associated with mesothermal gold mineralization, central Victoria, Australia: Economic Geology, v. 95, p. 283–311.

Bierlein, F. P., Foster, D. A., McKnight, S., and Arne, D. C., 1999, Timing of gold mineralisation in the Ballarat goldfields, central Victoria: Constraints from ^{40}Ar/^{39}Ar results: Australian Journal of Earth Sciences, v. 46, p. 301–309.

Burrows, D. R. and Spooner, E. T. C., 1986, The Mcintyre Cu-Au Deposit, Timmins, Ontario, Canada: in MacDonald, A. J., ed., Gold ‘86 An International Symposium on the Geology of Gold Deposits, Konsult International, Willowdale, Ontario, Canada, p. 23–39.

Castonguay, S., Skulski, T., van Staal, C., and Currie, M., 2009, New insights on the structural geology of the Pacquet Harbour Group and Point Rousse Complex, Baie Verte Peninsula, Newfoundland: Newfoundland and Labrador Department of Natural Resources, Geological Survey, Report 09-1, p. 147–158.

Castonguay, S., van Staal, C. R., Joyce, N., Skulski, T., and Hibbard, J. P., 2014, Taconic metamorphism preserved in the Baie Verte Peninsula, Newfoundland Appalachians: Geochronological evidence for ophiolite obduction and subduction and exhumation of the leading edge of the Laurentian (Humber) margin during closure of the Taconic Seaway: Geoscience Canada, v. 41, p. 459–482.

Colvine, A. C., Fyon, J. A., Heather, K. B., Marmont, S., Smith, P. M., and Troop, D. G., 1988, Archean lode gold deposits in Ontario: Ontario Geological Survey, Miscellaneous Paper 139, 136 p.

Copeland, D. A., Pitman, C., Evans, D. T. W., McNeill, P., and Slepcev, G., 2015, Mineral resource and mineral reserve update on the Pine Cove Mine and mineral resource estimate on the Stog'er Tight deposit, Point Rousse Project Baie Verte. NI-43-101 Technical Report: Anaconda Mining Inc., Newfoundland and Labrador, Canada, 249 p.

Cullen, M., Pitman, C., Copeland, D. A., McNeill, P., and Slepcev, G., 2018, Mineral resource and mineral reserve update on the Point Rousse Project, Baie Verte, Newfoundland and Labrador, Canada, NI-43-101 Technical Report: Anaconda Mining Inc., Newfoundland and Labrador, Canada, 285 p.

Dimmell, P., Bradley, P., and MacGillivray, G., 1999, The base metal/gold deposit in the Rambler area Baie Verte Peninsula, Newfoundland: in Evans, D. T. W. and Kerr, A., eds., Geology and mineral deposits of the Northern Dunnage Zone, Newfoundland Appalachians: Geological Association of Canada, Mineralogical Association of Canada Joint Annual Meeting, Memorial University, St. John's, Newfoundland, May 2001, Program with Abstracts, p. 57–70.

Dinel, E., Fowler, A. D., Ayer, J., Still, A., Tylee, K., and Barr, E., 2008, Lithogeochemical and stratigraphic controls on gold mineralization within the metavolcanic rocks of the Hoyle Pond mine, Timmins, Ontario: Economic Geology, v. 103, p. 1341–1363.

Dubé, B. and Gosselin, P., 2007, Greenstone-hosted quartz-carbonate vein deposits: in Goodfellow, W. D., ed., Mineral deposits of Canada: A Synthesis of Major Deposit-Types, District Metallogeny, the Evolution of Geological Provinces And Exploration Methods: Geological Association of Canada, Mineral Deposits Division, Special Publication No. 5, p. 49–73.

Dubé, B., Lauzière, K., and Poulsen, H. K., 1993, The Deer Cove deposit: an example of "thrust"- related breccia-vein type gold mineralization in the Baie Verte Peninsula, Newfoundland: Geological Survey of Canada, Current Research, Paper 93-1D, p. 1–10.

Dunning, G. R., O’Brien, S. J., Colman-Sadd, S. P., Blackwood, R. F., Dickson, W. L., O’Neill, P. P., and Krogh, T. E., 1990, Silurian orogeny in the Newfoundland Appalachians: Journal of Geology, v. 98, p. 895–913.

Eilu, P., Mikucki, E. J., and Dugdale, A. L., 2001, Alteration zoning and primary geochemical dispersion at the Bronzewing lode-gold deposit, Western Australia: Mineralium Deposita, v. 36, p. 13–31.

Evans, D. T. W., 2004, Epigenetic gold occurrences, Baie Verte Peninsula, (NTS 12H/09, 16 and 12I/01) Newfoundland: Government of Newfoundland and Labrador, Department of Natural Resources, Geological Survey, Mineral Resource Report No. 11, 157 p.

Evans, D. T. W., 2014, Mineral Licence 012433M Baie Verte Peninsula, Newfoundland NTS 12H/16. Assessment Report, Silvertip Exploration Consultants Incorporated, 33 p.

Giggenbach, W. F., 1986, The use of gas chemistry in delineating the origin of fluids discharged over the Taupo volcanic zone: a review: in International Volcanological Congress, Proceedings Symposium, Hamilton, New Zealand, v. 5, p. 47-50.

Goldfarb, R. J. and Groves, D. I., 2015, Orogenic gold: Common or evolving fluid and metal sources through time: Lithos, v. 233, p. 2–26.

Goldfarb, R. J., Snee, L. W., Miller, L. D., and Newberry, R. J., 1991, Rapid dewatering of the crust deduced from ages of mesothermal gold deposits: Nature, v. 354, p. 296–298.

Groves, D. I., 1993, The crustal continuum model for late-Archaean lode-gold deposits of the Yilgarn block, Western Australia: Mineralium Deposita, v. 28, p. 366–374.

Groves, D. I., and Santosh, M., 2016, The giant Jiaodong gold province: the key to a unified model for orogenic gold deposits?: Geoscience Frontiers, v. 7, p. 409-418.

Groves, D. I., Barley, M. E., Barnicoat, A. C., Cassidy, K. F., Fare, R. J., Hagemann, S. G., Ho, S. E., Hronsky, J. M. A., Mikucki, E. J., Mueller, A. G., McNaughton, N. J., Perring, C. S., Ridley, J. R., and Vearncombe, J. R., 1992, Sub-greenschist to granulite-hosted Archaean lode-gold deposits of the Yilgarn craton: a depositional continuum from deep-sourced hydrothermal fluids in crustal-scale plumbing systems: The University of Western Australia Publication, v. 22, p. 325–327.

Groves, D. I., Goldfarb, R. J., Robert, F., and Hart, C. J. R., 2003, Gold deposits in metamorphic belts: overview of current understanding, outstanding problems, future research, and exploration significance: Economic Geology, v. 98, p. 1–29.

Groves, D. I., Santosh, M., Deng, J., Wang, Q., Yang, L., and Zhang, L., 2019, A holistic model for the origin of orogenic gold deposits and its implications for exploration: Mineralium Deposita, v. 54, p. 1-18.

Herrmann, W., Blake, M., Doyle, M., Huston, D., Kamprad, J., Merry, N., and Pontual, S., 2001, Short wavelength infrared (SWIR) spectral analysis of hydrothermal alteration zones associated with base metal sulfide deposits at Rosebery and Western Tharsis, Tasmania, and Highway-Reward, Queensland: Economic Geology, v. 96, p. 939–955.

Hibbard, J., 1983, Geology of the Baie Verte Peninsula, Newfoundland: Government of Newfoundland and Labrador, Department of Mines and Energy, Mineral Development Division, Memoir 2, 280 p.

Jamieson, R. A., Anderson, S., and McDonald, L., 1993, Slip on the Scrape; an extensional allochthon east of the Baie Verte Line, Newfoundland: Geological Society of America: Program with Abstracts, v. 25, p. 26

Kerr, A. and Selby, D., 2012, The timing of epigenetic gold mineralization on the Baie Verte Peninsula, Newfoundland, Canada: new evidence from Re-Os pyrite geochronology: Mineralium Deposita, v. 47, p. 325–337.

Kerrich, R., 1983, Geochemistry of Gold Deposits of the Abitibi Greenstone Belt: Canadian Institute of Mining and Metallurgy, Special Paper, v. 27, p. 1-75.

Kerrich, R., 1989, Geodynamic setting and hydraulic regimes: shear zone hosted mesothermal gold deposits: in Bursnall, J. T., ed., Mineralization and Shear Zones: Geological Association of Canada, Short Course No. 6, p. 89-128.

Kerrich, R. and Cassidy, K. F., 1994, Temporal relationships of lode gold mineralization to accretion, magmatism, metamorphism and deformation—Archean to present: A review: Ore Geology Reviews, v. 9, p. 263–310.

Kerrich, R., Goldfarb, R. J., and Richards, J. P., 2005, Metallogenic provinces in an evolving geodynamic framework. Economic Geology, v. 100, p. 1097–1136.

Kirkwood, D. and Dubé, B., 1992, Structural control of sill-hosted gold mineralization: the Stog’er Tight gold deposit, Baie Verte Peninsula, northwestern Newfoundland: Geological Survey of Canada, Current Research, Paper 92-1D, p. 211–221.

McCuaig, T. C. and Kerrich, R., 1998, P-T-T deformation-fluid characteristics of lode gold deposits: evidence from alteration systematics: Ore Geology Reviews, v. 12, p. 381–453.

Mikucki, E. J., 1998, Hydrothermal transport and depositional processes in Archaean lode-gold systems: A review: Ore Geology Reviews, v. 13, p. 307–321.

Norman, R. E. and Strong, D. F., 1975, The geology and geochemistry of ophiolitic rocks exposed at Ming’s Bight, Newfoundland: Canadian Journal of Earth Sciences, v. 12, p. 777-797.

Phillips, G. N. and Groves D. I., 1983, The nature of Archaean gold-bearing fluids as deduced from gold deposits of western Australia: Journal of the Geological Society of Australia, v. 30, p. 25–39.

Phillips, G. N., Powell, R., 2010, Formation of gold deposits: a metamorphic devolatilization model: Journal of Metamorphic Geology, v. 28, p. 689-718.

Piercey, S. J. and Copeland, D. A., 2017, Host-rock reactivity in the generation of gabbro-hosted orogenic Au in the Baie Verte Peninsula, Newfoundland, Canada: GAC-Newfoundland and Labrador Section, 2017 Spring Technical Meeting, Program with Abstracts, St. John’s, Newfoundland, v. 53, p. 250.

Pitcairn, I. K., Craw, D., and Teagle, D. A. H., 2014, The gold conveyor belt: Large-scale gold mobility in an active orogen: Ore Geology Reviews, v. 62, p. 129–142.

Pitcairn, I. K., Craw, D., and Teagle, D. A. H., 2015, Metabasalts as sources of metals in orogenic gold deposits: Mineralium Deposita, v. 50, p. 373–390.

Poulsen, K. H., 2000, Geological classification of Canadian gold deposits: Geological Survey of Canada, Bulletin, v. 540, 106 p.

Ramezani, J., 1992, The geology, geochemistry and U-Pb geochronology of the Stog’er Tight Gold Prospect, Baie Verte Peninsula, Newfoundland. M.Sc. thesis, Memorial University of Newfoundland, St. John’s, Newfoundland, 312 p.

Ramezani, J., Dunning, G. R., and Wilson, M. R., 2000, Geologic setting, geochemistry of alteration, and U-Pb age of hydrothermal zircon from the Silurian Stog'er Tight Gold Prospect, Newfoundland Appalachians, Canada: Exploration and Mining Geology, v. 9, p. 171-188.

Ridley, J. R. and Diamond, L. W., 2000, Fluid chemistry of orogenic lode deposits and implications for genetic models: Economic Geology, Reviews, v. 13, p. 141–162.

Robb, L., 2004, Introduction to ore-forming processes. Wiley-Blackwell, Oxford, UK, 386 p.

Robert, F. and Kelly, W. C., 1987, Ore-forming fluids in Archean gold-bearing quartz veins at the Sigma mine, Abitibi greenstone belt, Quebec, Canada. Economic Geology, v. 82, p. 1464–1482.

Seward, T. M., 1973, Thio complexes of gold and the transport of gold in hydrothermal ore solutions: Geochimica et Cosmochimica Acta, v. 37, p. 379–399.

Sillitoe, R. H., 1989, Gold deposits in western pacific island arcs: the magmatic connection: Economic Geology Monograph, v. 6, p. 274–291.

Sillitoe, R. H. and Bonham Jr., H. F., 1990, Sediment-hosted gold deposits: Distal products of magmatic-hydrothermal systems: Geology, v. 18, p. 157–161.

Skulski, T., Castonguay, S., van Staal, C. R., Rogers, N., McNicoll, V., Kerr, A., and Escayola, M., 2009, Baie Verte Peninsula: an evolving geological story: Geological Association of Canada, Newfoundland and Labrador Section, Annual Field Trip Guide, St. John's, Newfoundland, v. 60, p. 1–60.

Skulski, T., Castonguay, S., McNicoll, V., van Staal, C., Kidd, W., Rogers, N., Morris, W., Ugalde, H., Slavinski, H., and Spicer, W., 2010, Tectonostratigraphy of the Baie Verte oceanic tract and its ophiolite cover sequence on the Baie Verte Peninsula: Geological Survey, Newfoundland and Labrador Department of Natural Resources, Current Research, Report 10-1, p. 315–337.

Sparrow, B., Barrett, S., Copeland, D. A., and Walsh, M., 2017, Argyle Prospect Mineral Licences 012433M (11th year) and 020060M (5th year) Point Rousse Project, Baie Verte Peninsula, NL NTS sheet 12H/16, Assessment Report: Anaconda Mining Inc., Newfoundland and Labrador, Canada, 481 p.

Spooner, E. T. C., 1993, Magmatic sulphide/volatile interaction as a mechanism for producing chalcophile element enriched, Archean Au-quartz, epithermal Au-Ag and Au skarn hydrothermal ore fluids: Ore Geology Reviews, v. 7, p. 359–379.

Tuach, J., 1976, Structural and stratigraphic setting of the Ming and other sulfide deposits in the Rambler area, Newfoundland: Unpub. M.Sc. thesis, Memorial University of Newfoundland, St. John's, Newfoundland, Canada, 128 p.

Tuach, J. and Kennedy, M. J., 1978, The geologic setting of the Ming and other sulfide deposits, Consolidated Rambler Mines, Northeast Newfoundland: Economic Geology, v. 73, p. 192-206.

Tuach, J., Dean, P. L., Swinden, H. S., O'Driscoll, C. F., Kean, B. F., and Evans, D. T. W., 1988, Gold mineralization in Newfoundland: A 1988 review: Newfoundland Department of Mines and Energy, Mineral Development Division, Report 88-1, p. 279-306.

van Staal, C. R., 2007, Pre-Carboniferous tectonic evolution and metallogeny of the Canadian Appalachians: in Goodfellow, W. D., ed. Mineral Deposits of Canada: A Synthesis of Major Deposit Types, District Metallogeny, the Evolution of Geological Provinces and Exploration Methods: Geological Association of Canada, Mineral Deposits Division, Special Publications no. 5, p. 793–818.

van Staal, C. R., Barr, S. M., and Percival, J., 2012, Lithospheric architecture and tectonic evolution of the Canadian Appalachians and associated Atlantic Margin: in Percival, J. A., Cook, F. A. and Clowes, R. M., eds., Tectonic styles in Canada: the LITHOPROBE perspective: Geological Association of Canada, Special Paper 49, p. 41-95.

Weatherley, D. K. and Henley, R. W., 2013, Flash vaporization during earthquakes evidenced by gold deposits: Nature Geoscience, v. 6, p. 294-298.

Wilkinson, J. J. and Johnston, J. D., 1996, Pressure fluctuations, phase separation, and gold precipitation during seismic fracture propagation: Geology, v. 24, p. 395–398.

Williams, H., 1979, Appalachian orogen in Canada: Canadian Journal of Earth Sciences, v. 16, p. 792–807.

Williams, H., 1995, Geology of the Appalachian-Caledonian Orogen in Canada and Greenland: Geological Survey of Canada, Ottawa, Ontario, Canada, 944 p.

Williams, H. and St. Julien, P., 1982, The Baie Verte Brompton Line: Early Paleozoic continent ocean interface in the Canadian Appalachians; in St. Julien, P., and Beland, J., eds., Major Structural zones and faults of the northern Appalachians: Geological Association of Canada, Special Paper No. 24, p. 177-208.

Williams, H., Colman-Sadd, S. P., and Swinden, H. S., 1988, Tectonic-stratigraphic subdivisions of central Newfoundland: Geological Survey of Canada, Current Research, Paper 88-1B, p. 91–98.

Williams-Jones, A. E., Bowell, R. J., and Migdisov, A. A., 2009, Gold in solution: Elements, v. 5, p. 281–287.

Ybarra S.J., 2019 (in revision). Hydrothermal Alteration and Lithogeochemistry of the Pine Cove Orogenic Gold Deposit, Baie Verte Peninsula, Newfoundland, Canada. Unpublished MSc thesis, Memorial University of Newfoundland, St. John’s, NL, Canada, 160 p.

Ybarra, S., Piercey, S., Layne, G. D., Copeland, D. A., and McNeil, P., 2017, Alteration halo and lithogeochemistry of the Pine Cove orogenic gold deposit, Baie Verte Peninsula, Newfoundland, Canada: GAC-Newfoundland and Labrador Section, 2017 Spring Technical Meeting, Program with Abstracts, St. John’s, Newfoundland: Atlantic Geology, p. 250.

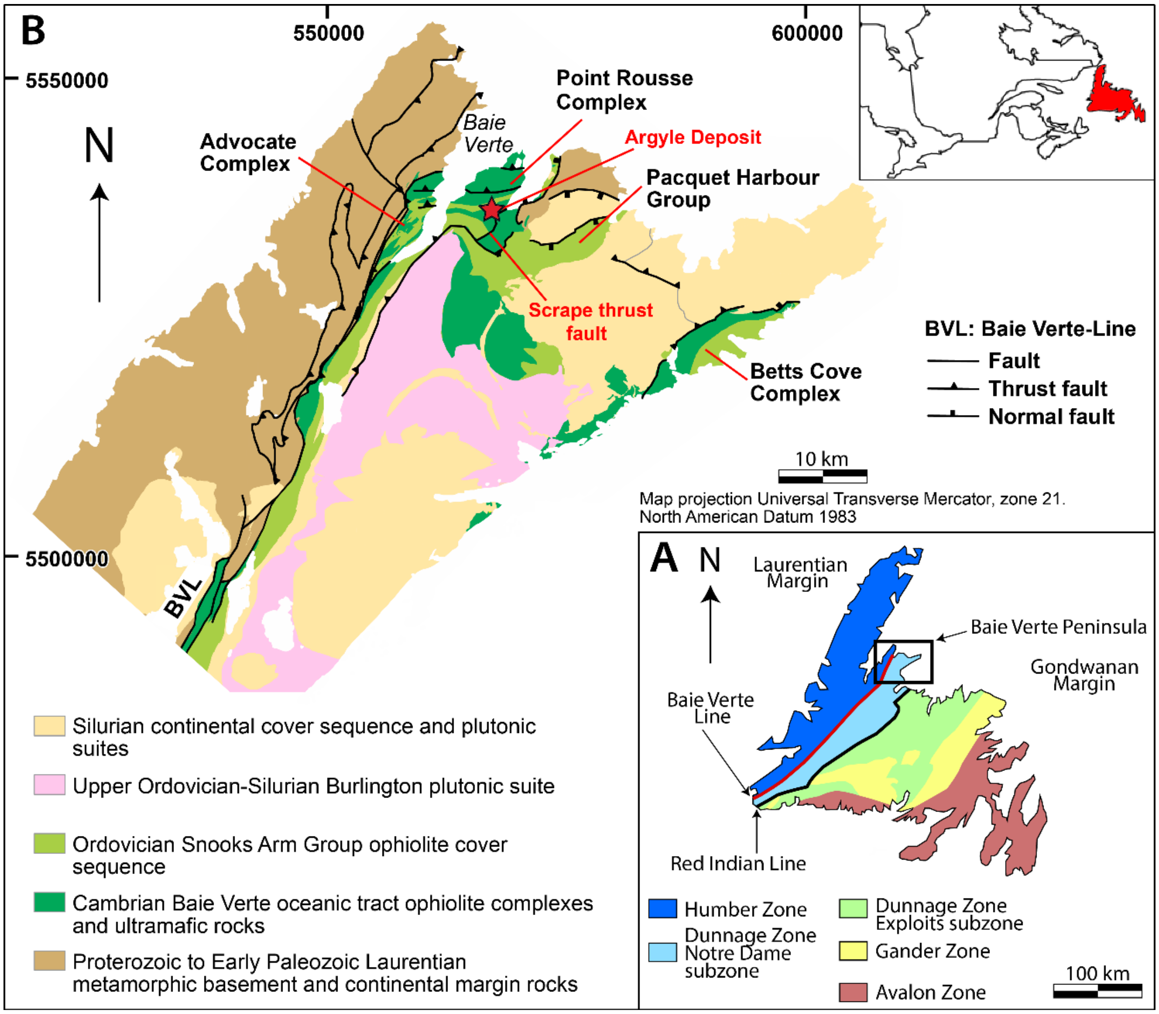

Figure 1.1. A) Simplified map of tectonostratigraphic terranes of Newfoundland (modified after Williams, 1979 and Skulski et al., 2010). B) Geology map of the Baie Verte Peninsula (modified after Skulski et al., 2010 and Ybarra, 2019). Inset shows the location of the Baie Verte Peninsula in Newfoundland.

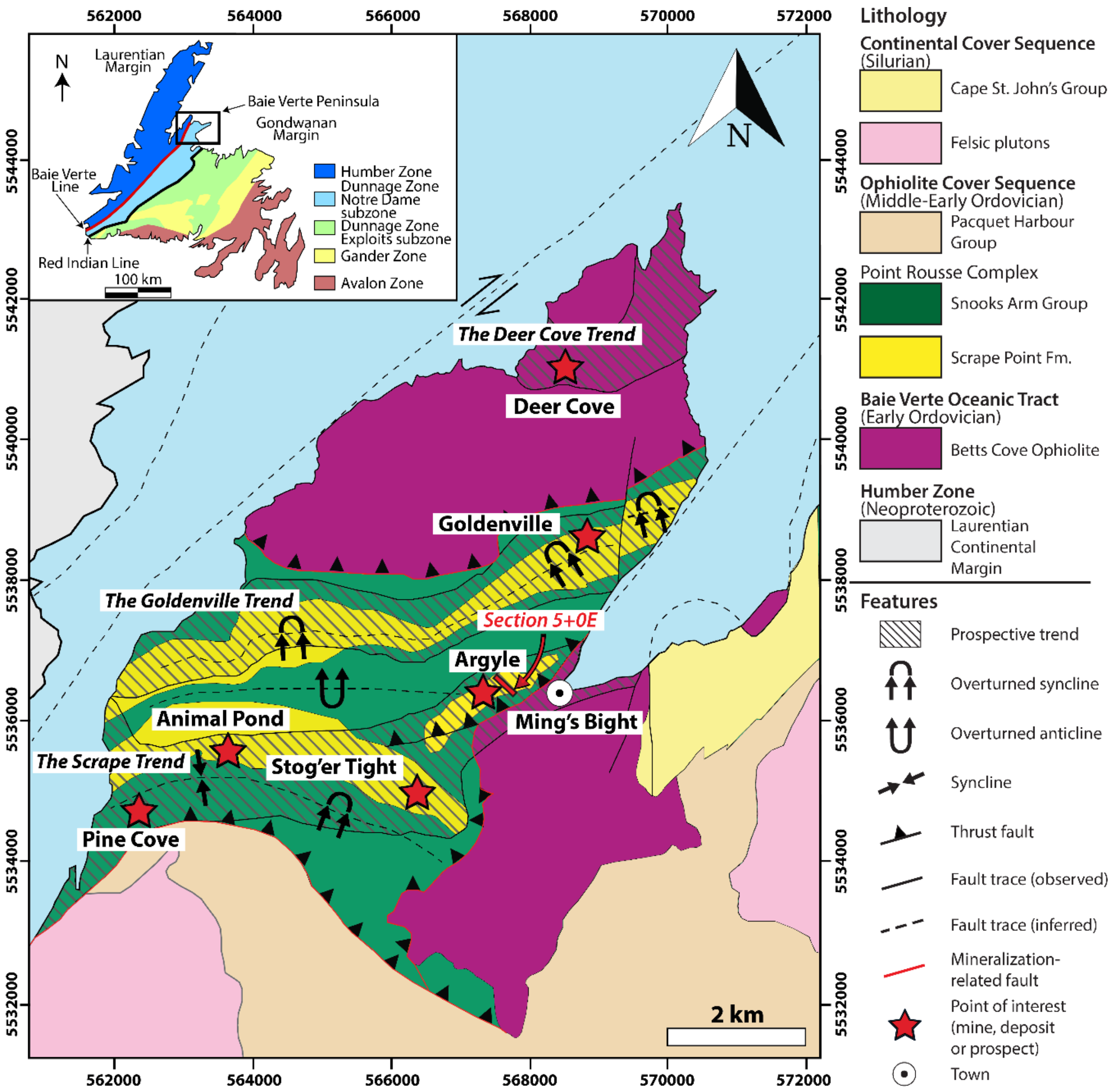

Figure 1.2. Simplified geological map of the Point Rousse project on the Baie Verte Peninsula. Relative position of Argyle, Stog'er Tight and Animal Pond deposits are symbolized by red stars. Modified from Skulski et al. (2010) and Anaconda Mining's NI 43-101 for the Point Rousse Project by Cullen et al. (2018). Inset shows the location of the Baie Verte Peninsula in Newfoundland.

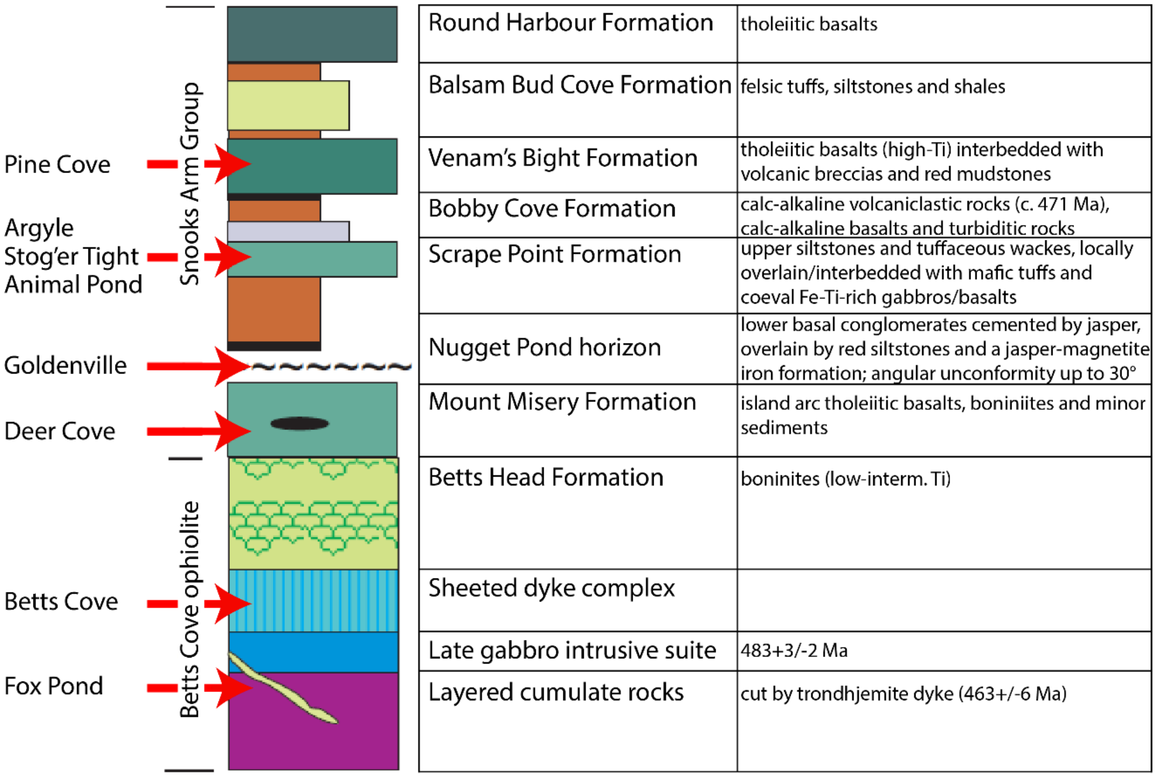

Round Harbour Formation	tholeiitic basalts
Balsam Bud Cove Formation	felsic tuffs, siltstones and shales
Venam’s Bight Formation	tholeiitic basalts (high-Ti) interbedded with volcanic breccias and red mudstones
Bobby Cove Formation	calc-alkaline volcaniclastic rocks (c. 471 Ma), calc-alkaline basalts and turbiditic rocks
Scrape Point Formation	upper siltstones and tuffaceous wackes, locally overlain/interbedded with mafic tuffs and coeval Fe-Ti-rich gabbros/basalts
Nugget Pond horizon	lower basal conglomerates cemented by jasper, overlain by red siltstones and a jasper-magnetite iron formation; angular unconformity up to 30°
Mount Misery Formation	island arc tholeiitic basalts, boniniites and minor sediments
Betts Head Formation	boninites (low-interm. Ti)
Sheeted dyke complex	
Late gabbro intrusive suite	483+3/-2 Ma
Layered cumulate rocks	cut by trondhjemite dyke (463+/-6 Ma)

Figure 1.3. Stratigraphy of the Point Rousse Complex (modified after Skulski et al., 2009).

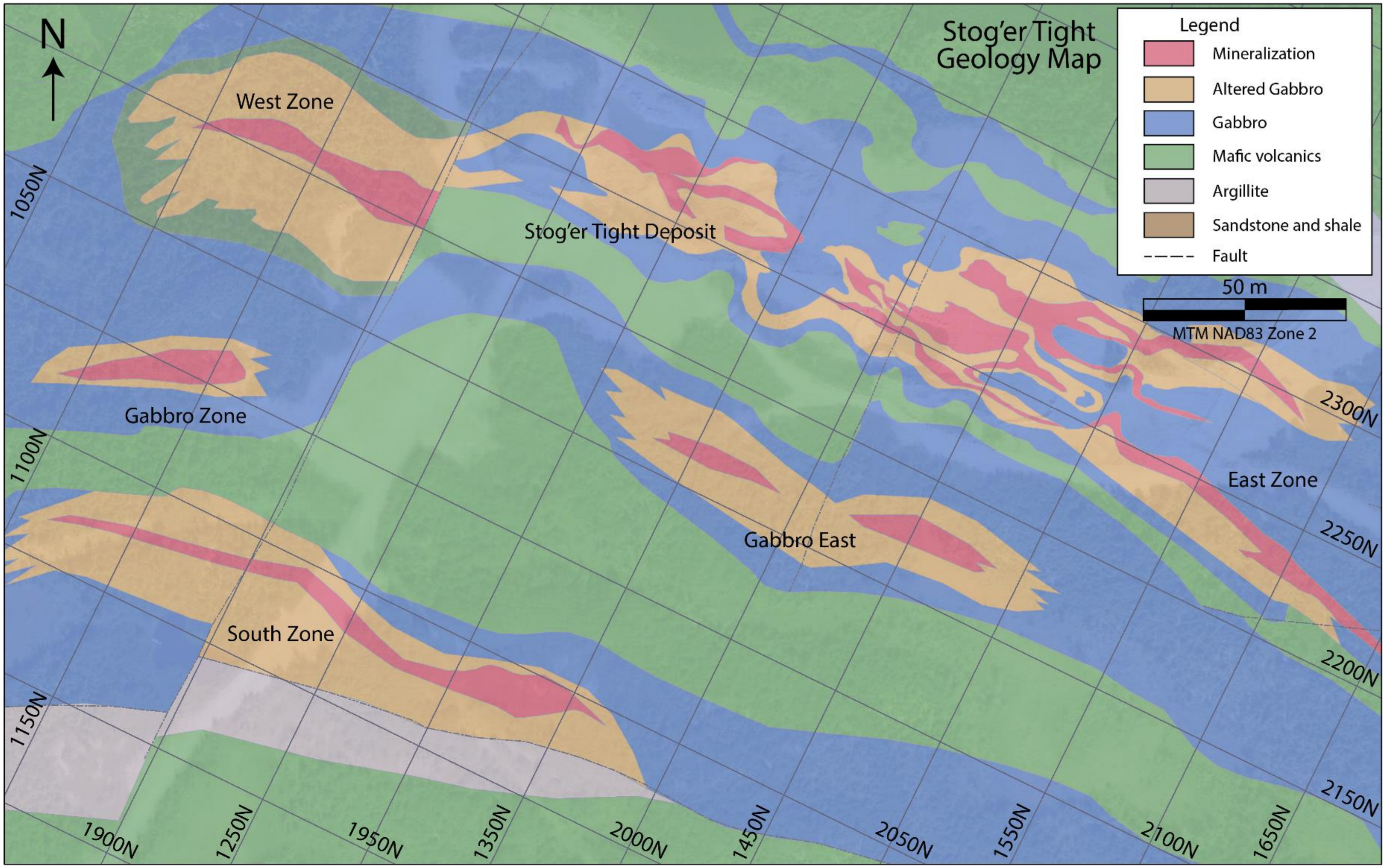

Figure 1.4. Geology map of Stog'er Tight deposit (Cliff Zone and Gabbro West out of view; modified after Copeland et al., 2015).

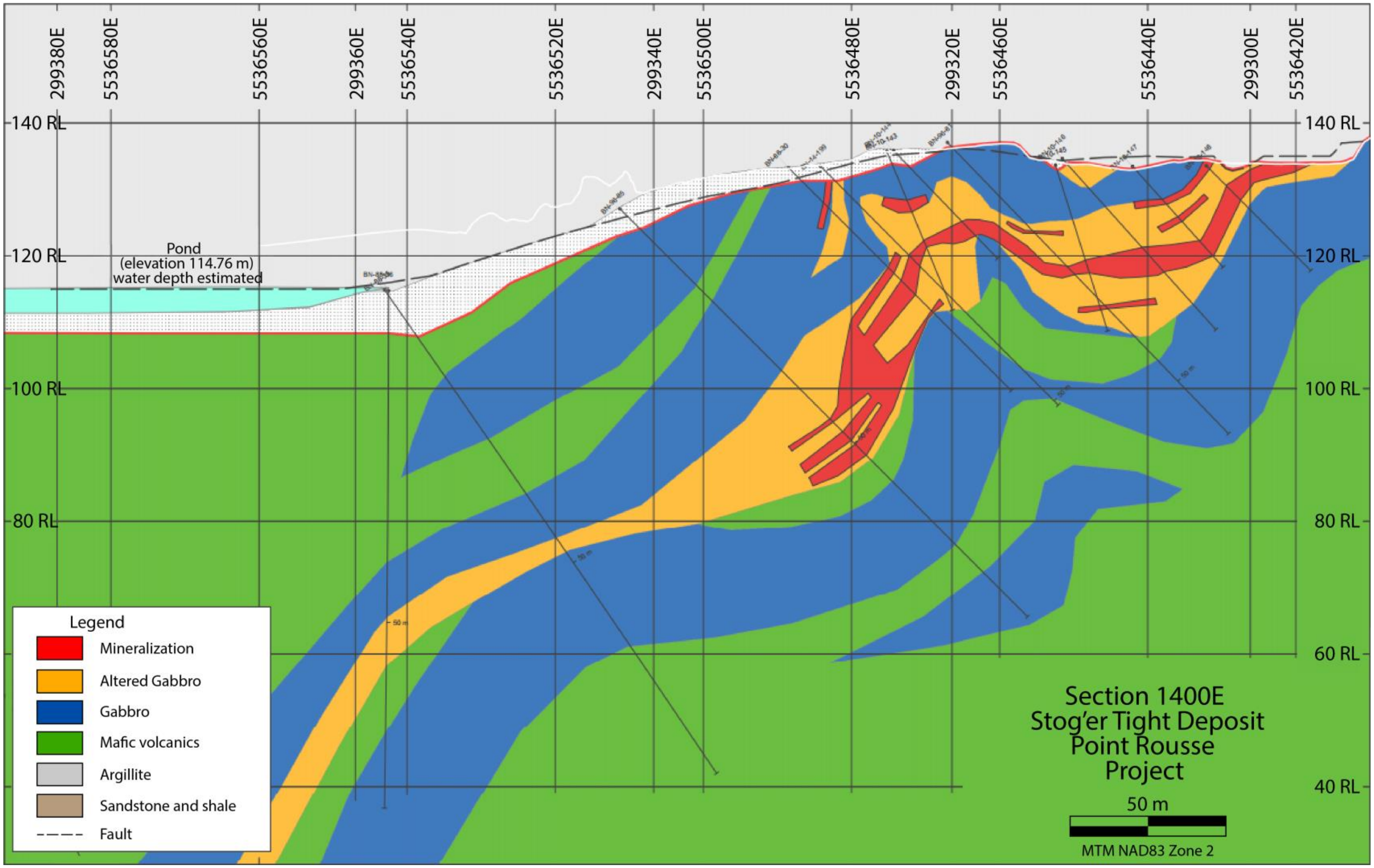

Figure 1.5. Section 1400E Stog'er Tight deposit (modified after Copeland et al., 2015).

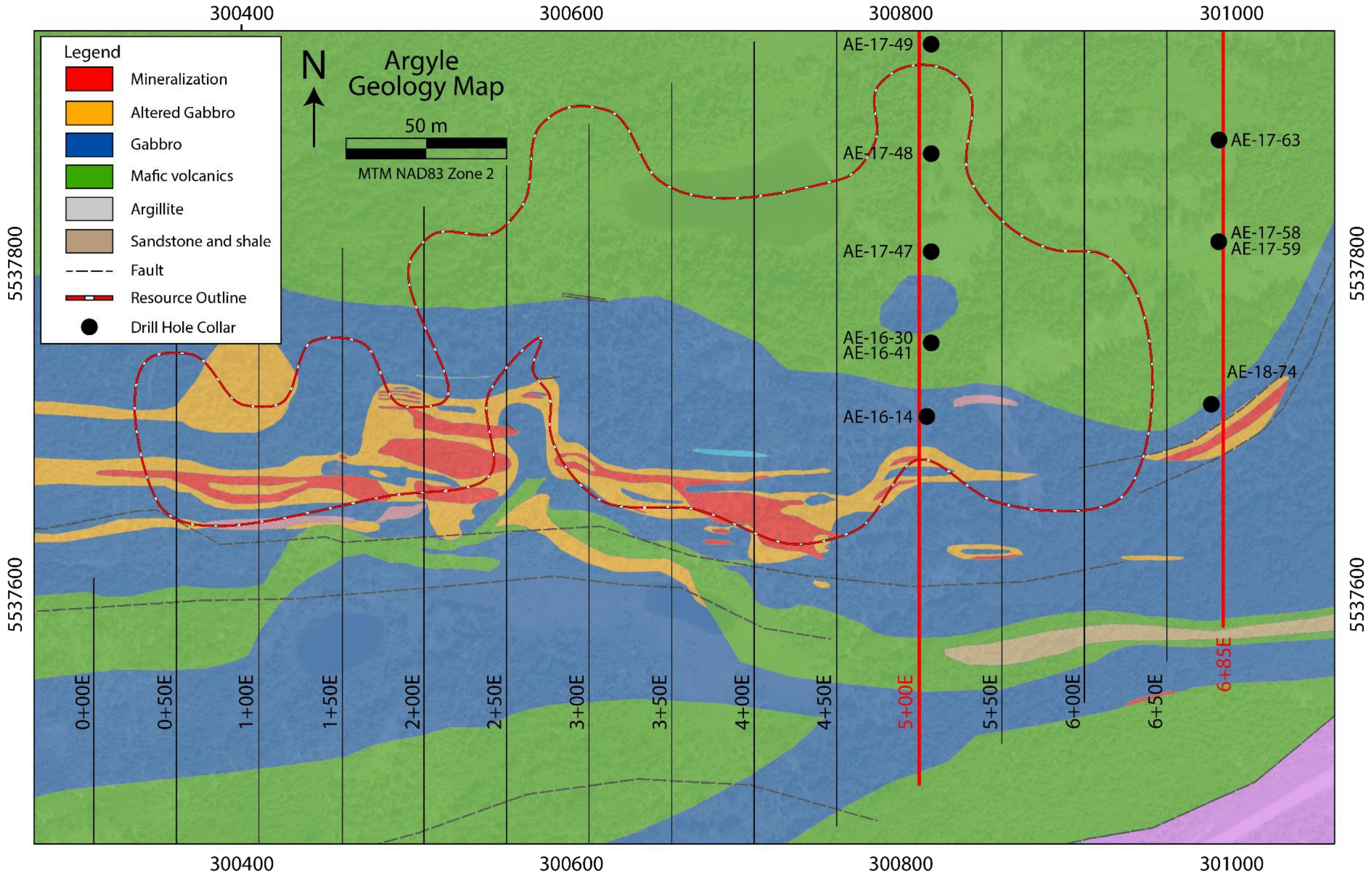

Figure 1.6. Geological map of the Argyle deposit (modified after Anaconda Mining Inc. Press Release, January 8th, 2018).

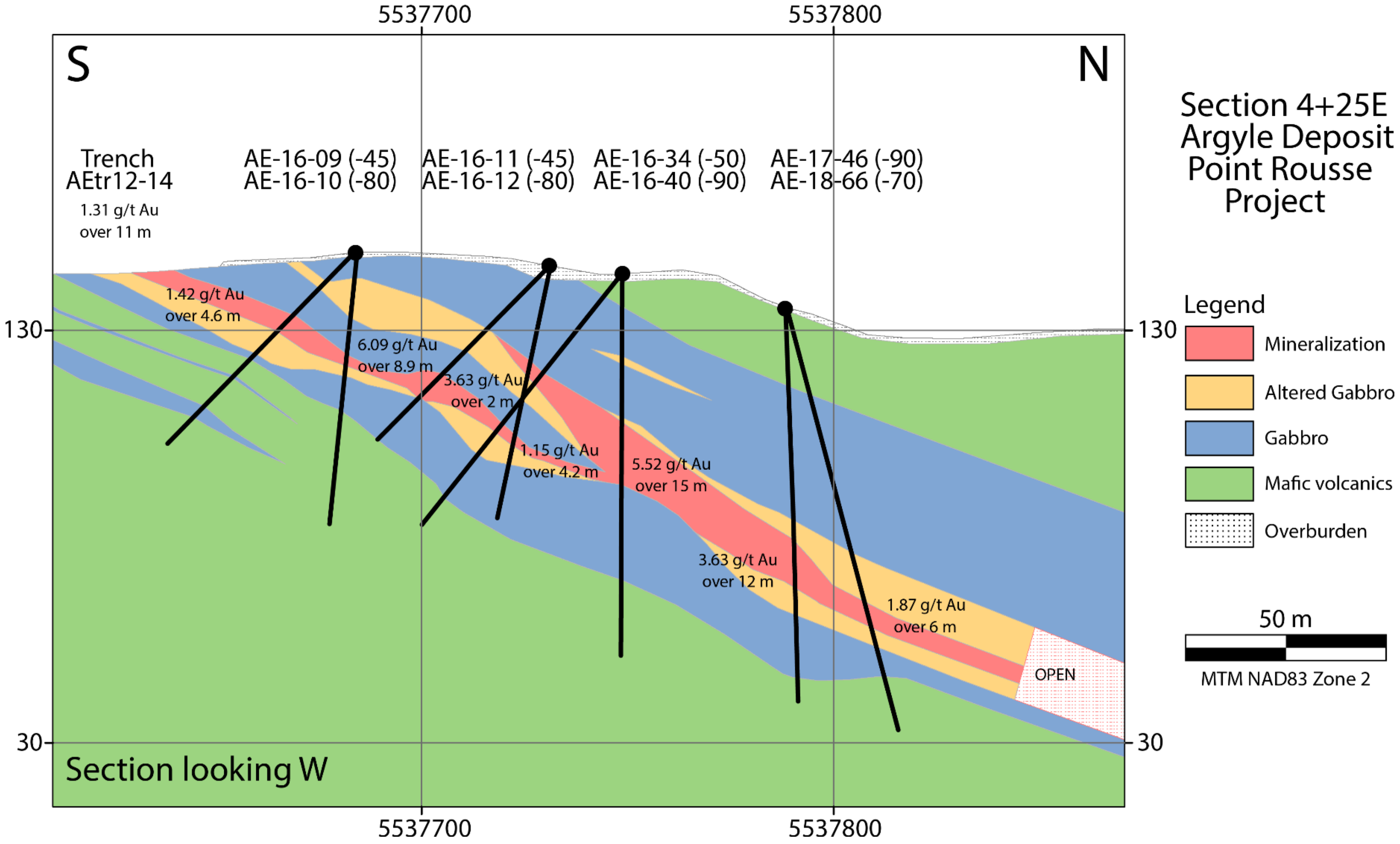

Figure 1.7. Section 4+25E Argyle deposit (modified after Sparrow et al., 2017).

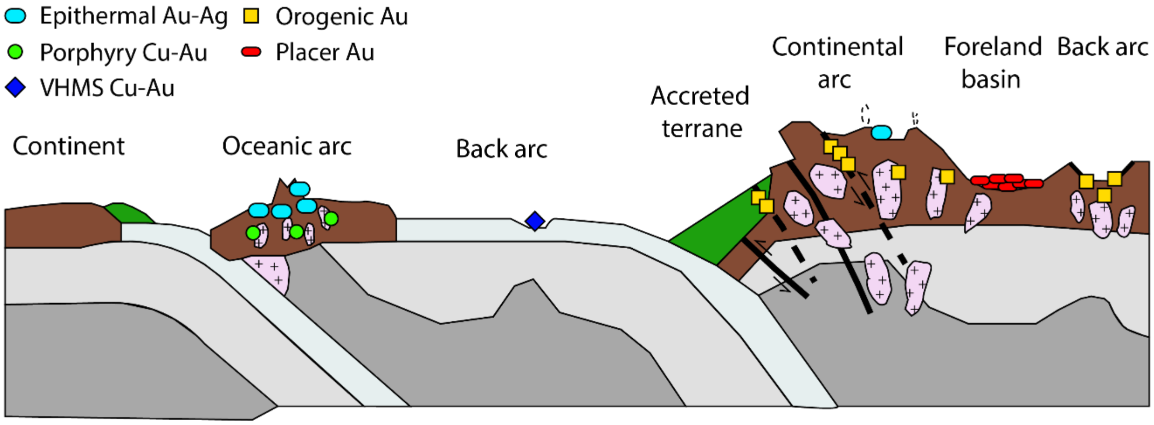

Figure 1.8. Tectonic settings in which gold deposits form. Orogenic gold deposits are found in deformed forearcs and backarcs, in addition to sheared margins of continental arc batholiths (modified after Goldfarb and Groves, 2015).

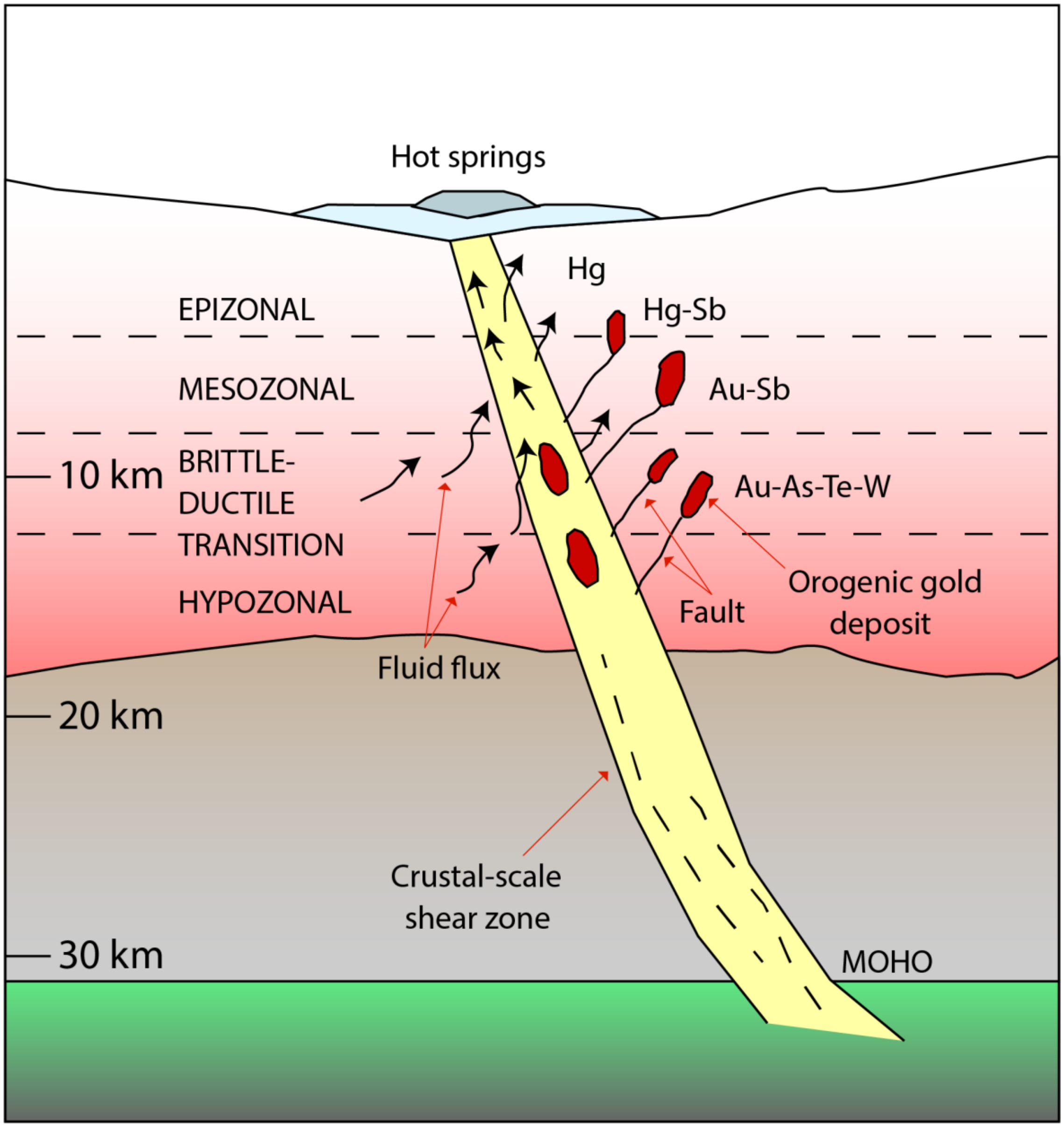

Figure 1.9. Depth of formation of orogenic gold deposits (modified after Groves and Santosh, 2016 and Groves et al., 2019).

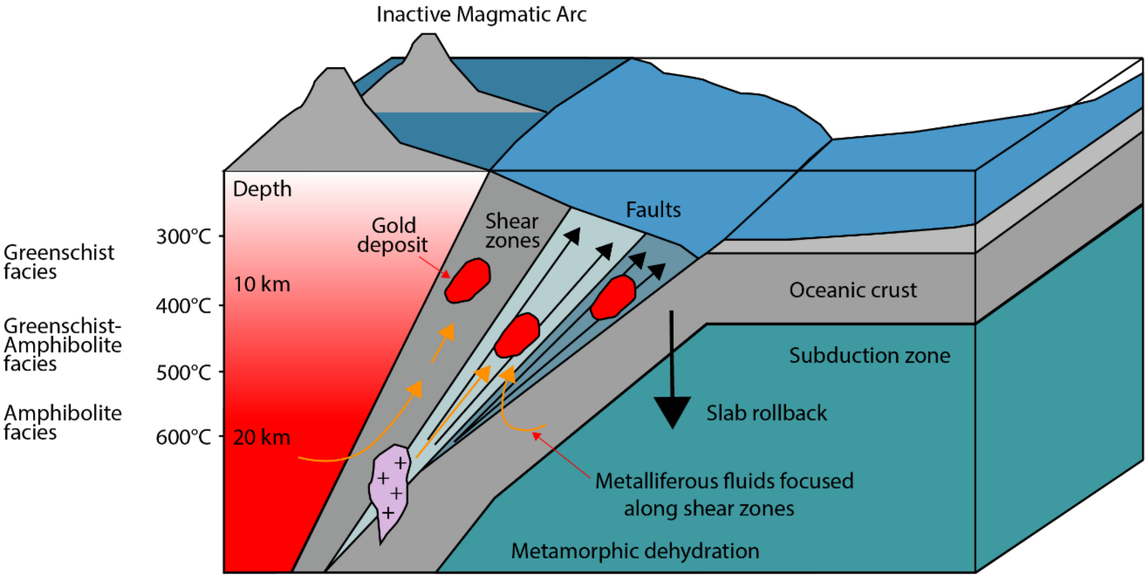

Figure 1.10. Flow of fluid into accreted oceanic arc derived from prograde metamorphism of a subducting slab and overlying material (modified after Kerrich et al., 2005).

Chapter 2: Hydrothermal Reconstruction and Lithogeochemistry of the Argyle Orogenic Gold Deposit, Baie Verte, Newfoundland, Canada

2.1 Abstract

The Argyle gold deposit (543,000 t @2.19 g/t Au indicated, and 517,000 t @1.82 g/t Au inferred resources), Baie Verte Peninsula, Newfoundland, Canada is hosted within the Scrape Point Formation of the Lower Ordovician Snooks Arm Group. Orogenic, structurally controlled stratabound gold mineralization is hosted within a 50-70 m thick, E-W striking, gently (22°-27°) north-dipping tholeiitic gabbro sill, which intruded the Scrape Point Formation volcaniclastic cover sequence rocks.

Both structure and gabbro grain size influenced the localization of mineralization. Mineralization at Argyle is associated with gabbroic rocks located in the hanging wall above the Scrape thrust fault. Gabbro grain size affected the localization of mineralization such that mineralization is associated with coarse-grained and pegmatitic gabbros. It is interpreted that these coarser-grained zones located in the centre of the gabbro sills acted as rigid blocks and were preferentially faulted relative to the aphanitic and fine-grained chilled margins of the sill, creating structural damage zones that were preferentially metasomatized due to increased permeability. Gold predominantly occurs as inclusions in pyrite or along boundaries between pyrite grains hosted in the gabbroic wallrock, typically <1 m from quartz-ankerite altered vein margins. The highest gold grades are associated with locally remobilized gold in sooty black tarnished, anhedral inclusion-bearing pyrite associated with black chlorite veinlets. Partial to complete replacement of Fe-Ti oxides

proximal to gold-bearing pyrite suggests that wallrock sulfidation was the main gold precipitation mechanism, and occurred due to the interaction of an $Au(HS)_2^-$-bearing hydrothermal fluid with coarse ilmenomagnetite in the Fe-Ti-rich host gabbro. The coincidence of structure-related fluid flow associated with regional tectonism, coupled with the textural and compositional character of host gabbros was critical for the localization of mineralization in the Argyle deposit.

Two separate hydrothermal events are recorded in the Argyle gabbro: early epidote-albite alteration that was pre-mineralization, followed by partial destruction of this assemblage by younger, mineralization-related sericite-quartz-ankerite-(albite-chlorite-rutile-pyrite-gold) alteration. Within the mineralization-related alteration there are three distinct zones: 1) distal chlorite-calcite-rutile ± epidote-albite (30-70 m); 2) intermediate chlorite-epidote-albite-calcite ± ankerite-rutile-hematite-sericite-pyrite (5-30 m); and 3) proximal sericite-quartz-ankerite ± albite-chlorite-rutile-sooty pyrite-gold (2-25 m). Distal alteration zones in the gabbro typically occur at chilled contacts with hanging-wall and footwall volcaniclastic rocks and within the finer-grained gabbro away from the centre of the sill. Intermediate alteration generally forms a diffuse semi-concentric compositional halo around the periphery of the proximal alteration in medium to coarse-grained gabbro and is interpreted to represent lower intensity diffuse metasomatism further from the centre of hydrothermal fluid flow. The proximal alteration zone is the most intensely hydrothermally altered zone, occurs in the coarse-grained to pegmatitic centre of the sill, and is associated with increases in pyrite-gold mineralization and quartz-ankerite veins. The observed alteration zonation suggests that the deformed, coarse-grained pegmatitic gabbro acted as the main fluid conduit for gold mineralization. Further, the deposit is interpreted to have formed at a shallow crustal level (estimate of depth; ~3-6 km), as evidenced by mineral assemblages concurrent with shallow-level greenschist-facies "sericite-ankerite" deposit class. Wide alteration zones in the gabbro (from proximal up to 25 m) indicate less-focused fluid flow at shallow crustal depths.

The Argyle gabbros have E-MORB affinities with Fe-Ti-enrichment, whereas footwall volcaniclastic rocks have calc-alkaline affinities consistent with derivation from a volcanic arc and/or contamination by continental crust. Fluid-rock interaction associated with gold mineralization caused significant elemental changes in the host gabbroic rocks at Argyle. In general, there are Na_2O depletions associated with feldspar destruction and sericite-quartz-ankerite alteration, and this is coupled with LOI, CO_2, S, Au and As enrichments that increase with alteration intensity, reflecting ankerite, pyrite, gold and arsenopyrite involvement during mineralization. Pathfinder elements (Bi, W, As, Te and S) also show strong mass gains with increasing alteration, and correlate with Au. Mass change calculations, principal component analysis and mobile element indicators, such as $CO_2/CaO+MgO+FeO$ and 3K/Al, indicate that carbonate and sericite-quartz alteration were the most significant hydrothermal alteration processes that affected the Argyle gabbro and are of greater intensity proximal to mineralization.

Short wave infrared spectroscopic (SWIR) data for AlOH and FeOH absorption features illustrate zonation in both white mica and chlorite. The proximal alteration zone contains 'short wavelength' white mica (AlOH; <2,198 nm) and Fe-rich chlorite (FeOH >2,255 nm), and there are progressive increases in AlOH and a decrease in FeOH wavelengths distal to mineralization. EPMA data supports the SWIR spectroscopy results and indicates that Fe-rich chlorite, Al-rich muscovite and ankerite are closely associated with gold mineralization.

A combination of the aforementioned techniques, core-logging and cross-sections has been used to define the hydrothermal footprint of gold mineralization in tholeiitic gabbros on the Baie Verte Peninsula. The vectors developed can be applied to similar mafic-rich orogenic Au environments globally for both greenfields exploration and also in evaluating existing datasets in prospective brownfields areas.

2.2 Introduction

Orogenic gold deposits are significant contributors to global gold production and their geological characteristics are well-understood (Groves et al., 1998; Goldfarb et al., 2001; Goldfarb et al., 2005; Phillips and Powell, 2010; Pitcairn et al., 2014, 2015; Goldfarb and Groves, 2015; Groves et al., 2019). Orogenic gold deposits form in accretionary orogens during shifts from compressional to transtensional or transpressional regimes and are spatially associated with regional-scale crustal structures in metamorphic belts (Groves, 1993, Kerrich and Cassidy, 1994, Robert et al., 1997; McCuaig and Kerrich, 1998; Kerrich et al., 2000; Upton and Craw, 2013). The formation of orogenic gold deposits is linked to large-scale hydrothermal fluid flow along these regional scale structures driven by metamorphic dehydration at depth and subsequent transport and deposition within crustal-scale fault zones at higher crustal levels (3-20 km) (Phillips and Groves, 1983; Kerrich, 1983; Groves et al., 1992; Kerrich and Cassidy, 1994; Kerrich et al., 2000; Groves et al., 2003; Kerrich et al., 2005; Pitcairn et al., 2014, 2015; Goldfarb and Groves, 2015; Groves et al., 2019).

Global research into the geochemistry and vectoring in orogenic gold deposits (e.g. Kerrich, 1983; Bierlein, 2000; Eilu et al. 2001; Dinel et al., 2008) highlights a typical suite of elemental enrichments (e.g. SiO_2, CO_2, K_2O, H_2O, S, and Au with irregular influxes of Na, Sb, Ag, As, Te, B, Bi and W) and low base metal contents, which are highly variable and dependent on host rock and fluid compositions. The heterogeneities in these rock buffered systems lead to a lack of consistency in alteration compositional haloes around orogenic gold deposits, thus these deposits lack a simple and robust geochemical exploration criterion. Nevertheless, recent technological advances in analytical lithogeochemistry and field-based infrared spectroscopy have been applied to orogenic gold deposits (e.g. Yang et al. 2011; Wang et al., 2017), allowing one to map subtle changes in both bulk rock geochemistry and white mica and chlorite chemistry, thus enhancing the resolution of the hydrothermal footprint of these deposits and providing vectors for orogenic Au hydrothermal systems. Despite this, very little research has been undertaken in the last decade on bulk rock lithogeochemical footprints in orogenic Au systems globally (e.g., Perrouty et al., 2019), particularly so in the Appalachians. This is also the case for hyperspectral mapping of alteration minerals in Appalachian orogenic gold systems. Thus, the hydrothermal footprints of gold deposits in young accretionary orogens like the Appalachians is still poorly understood. This creates an opportunity to test and compare hydrothermal footprints between belts that are associated with true accretionary tectonics versus Archean environments, where the nature of tectonics is still debated (e.g., Bleeker and Hall, 2007; Stern, 2008).

The tectonic evolution of the Appalachian orogen (500-250 Ma) resulted in the accretion and variable preservation of greenstone terranes (i.e., ophiolites and related rocks) along the length of orogen in eastern North America (Williams, 1979, 1995; Williams et al., 1988; van Staal, 2007). During the Silurian Salinic orogen numerous orogenic gold deposits formed as part of regional-scale hydrothermal fluid system in the Newfoundland Appalachians (Cawood et al., 1994; Wilson et al., 1994; Ramezani et al., 2000; van Staal, 2007).

The Baie Verte gold belt, Newfoundland, is similar to other orogenic gold districts world-wide and is associated with the Baie Verte line and subsidiary faults, a regional-scale complex brittle-ductile shear zone system that separates Proterozoic and Paleozoic continental rocks of the Humber Zone from ophiolitic and cover rocks of the Notre Dame subzone of the Dunnage Zone in Newfoundland (Williams, 1979; Williams and St-Julien, 1982; Castonguay et al., 2014). The Baie Verte line is of the scale and extent typical of orogenic gold-hosting environments (e.g., Dubé and Gosselin, 2007) and has a prolonged tectonothermal history and evidence for orogenic fluid flow (Williams and St-Julien, 1982; Castonguay et al., 2014; Menzel et al., 2018). Majority of the deposits are spatially related to the Scrape thrust, a second-order splay off the Baie Verte Line, and are located in the hanging wall to this fault, and include gabbro hosted deposits (e.g., Stog’er Tight mine and Argyle deposit), basalt-hosted deposits (e.g., Pine Cove mine), and iron formation-hosted deposits (e.g., Goldenville deposit) (Ramezani et al., 2000; Evans, 2004; Castonguay et al., 2009; Skulski et al., 2009, 2010; Ybarra et al., 2017; Cullen et al., 2018). The Argyle deposit, the subject of this manuscript, occurs in the hanging wall of the Scrape thrust, roughly 300m north of where the fault outcrops on surface (e.g., Cullen et al., 2018).

The Argyle deposit in the Baie Verte gold belt (543,000 t @2.19 g/t Au indicated and 517,000 t @1.82 g/t Au inferred resources; Cullen et al., 2018) was discovered in 2014, and is associated with the Scrape thrust and a tholeiitic gabbro sill of the Scrape Point Formation of the Snooks Arm Group. The deposit is exceptionally well preserved and provides an outstanding opportunity to study the processes of wall rock sulfidation and the hydrothermal footprint associated with mafic-hosted orogenic Au deposits. This manuscript integrates fieldwork, lithogeochemistry, mineralogical and mineral chemical work, textural analysis, and short wave infrared spectroscopy (SWIR) to: 1) document the geology and mineralogy of or the Argyle gold deposit, its contained mineralization and hydrothermal footprint; 2) utilize integrated field, geochemical, mineralogical, and spectral information to develop vectors towards mineralization; and 3) utilized the above to understand the main controls and processes that led to gold formation and host rock metasomatism. The results provide both a quantitative and qualitative insight into the processes and controls involved in the formation of the Argyle gold deposit and provide scalable vectors to mineralization. These results have implications not only for the genesis of the Argyle deposit, but also those studying and exploring for orogenic Au in other greenstone terranes in Paleozoic accretionary orogens and Precambrian greenstone belts.

2.3 Geological Setting

Paleozoic Appalachian orogen (500-250 Ma) in Newfoundland consists of four tectonostratigraphic zones: Humber, Dunnage, Gander and Avalon zones (Fig 2.1A), which formed as result of the closure of Iapetus Ocean and the amalgamation of Pangea (Williams, 1979; Williams et al., 1988; Williams, 1995; van Staal, 2007). The Baie Verte Peninsula contains rocks of both the Humber Zone and the Dunnage Zone, which lie in fault contact along the Baie Verte line (BVL), a regional-scale brittle-ductile shear zone (Fig 2.1B; Williams, 1979; Williams and St-Julien, 1982; Castonguay et al., 2014). The Humber Zone, which lies to the west of the BVL, represents early Paleozoic rocks of the Laurentian passive continental margin that were deposited on Precambrian (Grenvillian) basement (e.g., Williams, 1979). The Dunnage Zone within Newfoundland is comprised of Notre Dame and Exploits subzones, which represent Cambrian-Ordovician arc, back-arc, and ophiolitic rocks that formed along the ancient Laurentian and Gondwanan margins, respectively (Fig 2.1B; Williams, 1979; Williams and St-Julien, 1982; Hibbard, 1983; Dunning and Krogh, 1985; Cawood and Dunning, 1993; Evans, 2004; van Staal, 2007; Skulski et al., 2009; van Staal et al., 2012). The Notre Dame subzone, which hosts the Argyle deposit, is represented by rocks of arc, backarc, and ophiolitic origins that were accreted onto the peri-Laurentian margin during the Lower to Middle Ordovician Taconic (Stage 2) orogeny (500-450 Ma) (Evans, 2004; van Staal, 2007; Skulski et al., 2009; van Staal et al., 2012).

On the Baie Verte Peninsula four ophiolitic suites constitute the Baie Verte oceanic tract (BVOT): 1) the Advocate Complex; 2) the Betts Cove Complex; 3) the Pacquet

Complex; and 4) the Point Rousse Complex (Fig. 2.1B; Hibbard, 1983; Skulski et al., 2010). All ophiolite sequences on the Baie Verte Peninsula are correlative and their stratigraphy is typified by the rocks of the Betts Cove ophiolite (489 Ma) and the Snooks Arm Group volcanic cover sequence (<487 Ma to 467 Ma; Skulski et al., 2010). The Cambro-Ordovician Advocate, Betts Cove and Pacquet complexes are partially to fully intact ophiolite sequences, comprised of ultramafic, gabbroic and mafic rocks (Hibbard, 1983; Bédard, 1999; Bédard et al., 2000; Skulski et al., 2010). The Point Rousse Complex, which is centered in the Baie Verte flexure, contains Ordovician volcanic cover sequence underlain by ophiolitic rocks that are correlatable with the Snooks Arm Group of the Betts Cove Complex and to a lesser extent to the upper Pacquet Complex (Fig. 2.2; Tuach, 1976; Tuach and Kennedy, 1978; Hibbard, 1983; Bédard, 1999; Bédard et al., 2000; Skulski et al., 2010). The Point Rousse Complex is situated in an east-trending synclinorium (Fig. 2.2), where the volcanic cover sequence is exposed in the centre of the syncline that that is fault bounded with high-angle fault and thrust faults generally dipping to the northwest resulting in the exposure of ophiolitic rocks on both its northern and southern rims (Fig. 2.2; Norman and Strong, 1975; Ramezani et al., 2000; Castonguay et al., 2009; Skulski et al., 2010).

The Point Rousse Complex records four deformation events (D_1-D_4), with poorly preserved D_1 ophiolite obduction-related fabrics that formed during the Taconian Orogeny (Castonguay et al., 2009). The main tectonostratigraphic phase, $D_{2,}$ caused the predominant northerly dip of the units with a north-dipping S_2 foliation and down-dip northerly stretching lineations (Castonguay et al., 2009; Sparrow et al., 2017). D_2 deformation led to south-directed thrusting, folding and shearing, and the creation of S_2 parallel, meter-scale south-directed shear zones, such as the Scrape thrust, which juxtaposed the Point Rousse Complex over the Pacquet Complex; D_2 is interpreted to be related to the crustal thickening and transpression during the Silurian Salinic orogeny (Hibbard, 1983; Dunning et al., 1990; Skulski et al., 2009; Castonguay et al., 2009; Skulski et al., 2010). D_3-related fabrics are expressed as shallowly inclined to recumbent folds, which deform earlier fabrics related to extension associated with Devonian core complex formation (Anderson et al., 2001; Castonguay et al., 2009). D_3 event fabrics also show normal sense reactivation as extensional shear bands in the footwall of the Scrape thrust fault (Jamieson et al., 1993; Anderson et al., 2001; Castonguay et al., 2009). D_4 deformation affected D_1-D_3 fabrics, north-northeast trending anticlines and synclines, resulting regionally in double-plunging folds (F_4) (Castonguay et al., 2009; Sparrow et al., 2017).

The stratigraphy of the Point Rousse Complex volcanic cover sequence is locally separated from the underlying Mount Misery Formation of the Pacquet Complex by an angular unconformity, which comprises island arc tholeiitic basalts, boninites and minor sedimentary rocks, and is host to the past-producing Deer Cove gold deposit (Fig 2.3; Hibbard, 1983; Bédard, 1999; Bédard et al., 2000; Skulski et al., 2009, 2010). The Mount Misery Formation also hosts the Tilt Cove Cu-VMS deposit (489 Ma; Dunning and Krogh, 1985) in the Betts Cove Complex (Upadhyay and Strong, 1973; Bédard, 1999; Bédard et al., 2000; Skulski et al., 2009, 2010). The Scrape Point Formation is the lowest part of the Snooks Arm Group and is subdivided into: 1) lower basal conglomerates cemented by jasper and overlain by red siltstones and a jasper-magnetite iron formation (the Nugget

Pond horizon), which hosts the Goldenville gold deposit; and 2) upper siltstones and tuffaceous wackes, in places overlain or interbedded with mafic tuffs and coeval tholeiitic Fe-Ti-rich gabbros or basalts, which are host to gold mineralization at the Argyle deposit, the Stog'er Tight mine and the Animal Pond prospect (Ramezani, 1992; Bédard, 1999; Bédard et al., 2000; Ramezani et al., 2000; Sangster et al., 2008; Skulski et al., 2010). The Bobby Cove Formation overlies the Scrape Point Formation and comprises calc-alkaline volcaniclastic rocks (470 Ma; V. McNicoll, unpublished data, 2007; Skulski et al., 2010), calc-alkaline basalts and turbiditic rocks, whereas the overlying Venam's Bight Formation consists of high-Ti tholeiitic basalts interbedded with volcanic breccias and red mudstones; the latter unit hosts the Pine Cove gold deposit (Skulski et al., 2009, 2010; Ybarra et al., 2017). The Balsam Bud Cove Formation overlies the Venam's Bight Formation and consists predominantly of felsic tuffs (467 Ma; V. McNicoll, unpublished data, 2007; Skulski et al., 2010), siltstones and shales overlain by the uppermost part of the Snooks Arm Group, the Round Harbor Formation, which contains tholeiitic high-Ti basalts (Bédard, 1999; Bédard et al., 2000; Skulski et al., 2009, 2010).

The orogenic gold occurrences in the Baie Verte Peninsula are hosted in wallrock or in quartz-carbonate veins where the gold mineralization is spatially related to the hanging wall sides of thrust sheets associated with D_2 deformation, such as the Scrape thrust and the Deer Cove sole thrust (Kirkwood and Dubé, 1992; Dubé et al., 1993; Evans, 2004; Castonguay et al., 2009, 2014; Skulski et al., 2009, 2010). The hydrothermal zircon (420 ± 5 Ma) U-Pb and pyrite (420 ± 7 Ma) Re-Os ages at Stog'er Tight and Pine Cove respectively, indicate Silurian to Devonian timing of thrusting and orogenic gold mineralization within the Point Rousse Complex volcanic cover sequence (Ramezani et al., 2000; Kerr and Selby, 2012).

2.4 Geology of the Argyle Au deposit

The Argyle deposit (Fig. 2.4) is located 1 km west of the community of Ming's Bight on the Baie Verte Peninsula, Newfoundland, Canada (Fig. 2.2). Gold mineralization is stratabound within a 50-70 m thick, E-W striking, gently (22°-27°) north-dipping tholeiitic gabbro sill (Fig. 2.5), which intruded Snooks Arm Group mafic volcaniclastic rocks. The gabbro is part of the Scrape Point Formation and occurs as a tabular heterogeneous body with a variety of textures and grain-sizes, with aphanitic to fine-grained chilled margins at contacts with the volcaniclastic rocks, that grade into coarse-grained to pegmatitic gabbro with large feldspar laths at the centre of the intrusion (Fig. 2.6A). The intrusion is sill-like with weak open folds and thickening of hydrothermal alteration along fold hinges (Figs. 2.4-2.5 and Appendix B). The other units in the Argyle deposit can be grouped into: 1) hanging wall volcaniclastic rocks; 2) footwall volcaniclastic rocks; 3) footwall diabase; and 4) late mafic dykes. The hanging wall to the gabbro sill consists of mafic flows, basaltic pillow lavas, and mafic lapilli tuffs and breccias (Fig. 2.6B-D). At the far eastern extent of the deposit (section 6+85E) a dense purple-black magnetite-hematite-silica-pyrite-bearing hanging wall iron formation has been intersected (Fig. 2.6E), but is interpreted to be distinct from Goldenville horizon and Nugget Pond horizon in both geological features and stratigraphic position. Hanging wall pillow lavas can exhibit mm-cm scale chlorite-epidote-quartz selvages with quartz and carbonate alteration of pillow margins, interpreted to be near syn-depositional seafloor alteration (Fig

2.6D; e.g., Skirrow and Franklin, 1994). The footwall to the gabbro consists of mafic lapilli tuff and crystal tuff, which commonly contain abundant quartz and calcite; green and maroon argillite; and fresh diabase that is conformable to stratigraphy (Fig. 2.6F-G). Aphanitic to fine-grained olive green to dark grey cm-scale mafic dykes crosscut all units in the Argyle deposit.

The Argyle deposit is located in the hanging-wall of a second-order splay fault off the Baie Verte Line, the Scrape thrust, which outcrops 300 m to the south of the deposit (Fig. 2.2). Coarse-grained to pegmatitic gabbro in the centre of the tabular sill is significantly more faulted and deformed compared to the finer grained margins in contact with volcaniclastic rocks; the intensity of brittle deformation increases with gabbro grain-size. The deformed gabbro in the centre of sill consists of meter-scale damage zones that contain broken and fractured gabbro with abundant quartz-carbonate veining, pyrite-gold mineralization and rare fault gouge. (Fig. 2.5).

Fabrics in the gabbro are very weakly developed; however, foliation in the gabbro increases in proximity to shear zones, and in rare cases grades into a strong mylonitic fabric. There is a local alignment of ‘wisp-shaped’ rutile, iron carbonate alteration and chlorite in the gabbro in the alteration zone and along fractures in the gabbro.

Foliated, flattened clasts sub-parallel to bedding are common in the hanging wall and footwall volcaniclastic rocks, reflecting the weak open folding of the geological units at Argyle (Fig. 2.5) and are difficult to distinguish from the original fabric. The damage zones in the deposit are discerned by systematic logging of quartz-carbonate veins in the strongly metasomatized alteration zones (e.g., Appendix A.1.3; AE-16-43, 94.1-108.5m).

2.5 Mineralization and Alteration

2.5.1 Alteration

The hydrothermal alteration at the Argyle deposit is confined to the gabbro sill and there were two separate hydrothermal events that affected the gabbro: an early epidote-albite alteration, which replaced the igneous plagioclase feldspar and is interpreted as pre-mineralization and unrelated to gold mineralization, and the later gold-related hydrothermal alteration, typified by carbonate and sericite alteration that overprints the epidote-albite alteration. Paragenetic relationships of alteration assemblages and ore minerals are summarized in Figure 2.10. Regardless of type, hydrothermal alteration of the host gabbro is most intense in the deformed centre of the sill, decreases in intensity away from the fault zone (Fig. 2.5 and Appendix B) and terminates near the contact with hanging-wall volcaniclastic rocks. Alteration in the footwall is locally truncated by faults at depth, near to the contact with footwall volcaniclastic rocks. In some cases, alteration zones terminate against footwall volcaniclastic rocks when not truncated by structures (e.g. AE-16-03; Appendix A).

Within the gold-related alteration there are three distinct hydrothermal alteration assemblages: 1) distal chlorite-calcite-rutile ± epidote-albite (30-70 m); 2) intermediate chlorite-epidote-albite-calcite ± ankerite-rutile-hematite-sericite-pyrite (5-30 m); and 3) proximal sericite-quartz-ankerite ± albite-chlorite-rutile-inclusion-rich pyrite-gold (2-25

m) (Figs. 2.7-2.9). The hydrothermal alteration assemblages are centred around mineralization with the proximal zone located predominantly in the centre of the gabbro sill where gabbro is most deformed. Intermediate alteration forms a diffuse, semi-concentric compositional halo around the proximal zone and the distal alteration defines the outer envelope of hydrothermal activity.

The distal chlorite-calcite alteration is poorly defined and is generally similar to the regional greenschist metamorphic assemblages consisting of medium to dark green chlorite-rich assemblage, but with distinctive tan-yellow ‘wisp-shaped’ (Fig. 2.7A-B) rutile overprinting primary Fe-Ti oxides (Fig. 2.10). Distal alteration (30-70 m) occurs predominantly in aphanitic to fine-grained gabbro at or near chilled margin contacts with the hanging wall and footwall volcaniclastic rocks.

The intermediate alteration zone consists of chlorite-epidote-albite-calcite ± ankerite-rutile-hematite-muscovite-pyrite (Fig. 2.8). The alteration is typified by the replacement of igneous pyroxene by chlorite and plagioclase feldspar by epidote and albite giving the rock a pale greenish-yellow to light grey colour. The original igneous Fe-Ti minerals are only partially replaced by alteration phases and are often highlighted by tan-yellow “wisp-shaped” rutile alteration (Figs. 2.7B and 2.10).

The proximal alteration (2-25 m) contains gabbro that is pervasively altered to sericite-quartz-ankerite ± albite-chlorite-rutile-pyrite-gold (Fig. 2.9A-C). The proximal alteration is associated with fracturing of the gabbro, intense destruction of primary igneous textures and early albite-epidote alteration. Locally, the proximal zone gabbro contains coarse-grained to locally pegmatoidal feldspar that is altered to grey-pinkish albite. The albite, and associated epidote are interpreted to be pre-mineralization alteration (Fig. 2.10). This assemblage is overprinted by intense sericite-quartz-ankerite ± black chlorite-sooty pyrite-gold, resulting in a pale brown-yellow-grey-green massive appearance. Generally, the feldspars are replaced by sericite, pyroxene is replaced by chlorite, and the entire rock is overprinted by mm- to cm-scale veins of quartz and ankerite. Primary igneous ilmenite/ilmenomagnetite grains are partly to fully replaced by inclusion-rich, black tarnished sooty, subhedral-anhedral pyrite that form clusters in the wall rock and are associated with gold (see Mineralization below). The proximal assemblage also contains tan-brown, locally sheared, wispy rutile (Fig. 2.9B) that overprints Fe-Ti-oxides. All of the above assemblages are crosscut by black chlorite veinlets (Fig. 2.10).

The zonation of alteration assemblages is spatially variable. The distal alteration assemblage transitions to the intermediate assemblage over <1 m and is characterized by an increase in albite (± epidote-ankerite), and is typically accompanied by an increase in grain-size from fine- to medium- and/or coarse-grained gabbro. In some cases, the transition from the intermediate to proximal alteration zone is between 1.5 to 3 m and is accompanied by a change from mottled green-yellow chlorite-epidote dominated gabbro to fractured and locally sheared, coarse grained gabbro dominated by chlorite and other proximal alteration minerals. In other cases, the transition is abrupt, spanning <30 cm and accompanied by extensive fracturing of the gabbro associated with intense sericite-ankerite-quartz-pyrite alteration resulting in massive tan-coloured gabbro. In most sections through the Argyle deposit the alteration zones are well-defined and show a gradual transition from distal, through intermediate to proximal hydrothermal alteration zones; however, in rare cases an abrupt change from distal to proximal zones is observed. Further, in some cases the zonation pattern and symmetry is disrupted by late faults that crosscut the host intrusion.

The volcaniclastic and volcanic country rocks have experienced regional lower greenschist metamorphism and contain weak chlorite-actinolite-calcite-epidote alteration. In some cases, hanging-wall volcaniclastic rocks, especially hyaloclastites and mafic pillow flows, show primary volcanogenic alteration typified by epidote-chlorite-carbonate, quartz alteration and local bleaching; the latter two are particularly pronounced in pillow selvages. Where present, gold-related metasomatism of the volcaniclastic rocks is restricted to small (<75 cm) areas around the faults or fractures zones and consist of moderate-strong sericite alteration. In a number of drill holes, the footwall crystal tuffs are weakly bleached and contain quartz veining.

2.5.2 Mineralization

Gold mineralization at Argyle is stratabound and restricted to highly fractured gabbroic rocks, typically in 0.5 to 4 m wide zones and associated with the proximal alteration assemblage (Fig. 2.10). Gold mineralization is generally hosted in the coarsest, pegmatoidal gabbros, and is spatially associated with the presence of the coarsest-grained Fe-Ti minerals. Gold is hosted in inclusion-rich, black tarnished sooty, anhedral-subhedral pyrite grains that are 1-40 mm in size (Figs. 2.9B and 2.9D-F). The sooty pyrite grains are distinctive from the barren euhedral pyrite crystals that are disseminated in all alteration zones of the gabbro and volcaniclastic rocks. Euhedral pyrite crystals are interpreted to have formed post-mineralization and are likely metamorphic in origin. Despite being proximal to quartz-carbonate veins, gold is not found within veins, but is hosted predominantly by pyrite in wall rock near the margins of narrow (<1 m) irregularly oriented quartz-carbonate veins in the proximal alteration zone.

Gold-bearing pyrite grains at Argyle exhibit varying textures including: inclusion-rich and inclusion-poor grains; cracked grains with irregular edges; and grains that are annealed or recrystallized (Figs. 2.9D-F). The inclusion-rich pyrite grains contain various minerals (<1 vol%) including: gold, tellurides, chalcopyrite, arsenopyrite, sphalerite, rutile, titanite, skeletal magnetite, ilmenite, apatite and xenotime (SEM-EDS, e.g. Appendix G.2.9).

Gold in the Argyle deposit occurs predominantly as native gold, and rare Au-telluride grains (calaverite). Gold is associated with pyrite grains and occurs as: inclusions within the pyrite grains, blebs along fractures and pyrite grain margins, free gold or as intergrowths with ankerite, chlorite, albite, quartz or zircon. The coarsest gold (~1000 µm) grains occurs as blebs and fracture-infill between pyrite grain margins. Fracture-related gold is commonly associated with the paragenetically late black chlorite veinlets (Fig. 2.10).

2.6 Lithogeochemistry

2.6.1 Methods

A total of 225 drill core samples were analyzed for whole-rock geochemistry. Samples were collected to understand both primary petrological processes and chemostratigraphy, as well as superimposed alteration. Samples were taken from representative lithologies and host rocks, including the host gabbro, surrounding volcaniclastic rocks, and cross-cutting mafic dykes. For least altered/primary samples, gabbro with minimal hydrothermal alteration minerals and veins were chosen. These samples were selected to provide a baseline, to which altered samples could be compared. Altered samples were taken to map the hydrothermal footprint of the Argyle deposit and were selected spatially to obtain downhole profiles, according to alteration assemblage, and as a function of alteration intensity.

All samples were half or quartered drill core, roughly 20 cm in length. Samples were crushed in standard jaw crusher and pulverized in mild steel. Samples were analyzed for various elements using the complete characterization package (CCP-PKG01) at ALS Minerals Ltd. in Sudbury, Ontario (Appendix C). Major elements were analyzed using lithium borate fusion pre-preparation with subsequent dissolution of the fused bead in acid and an inductively coupled plasma atomic emission spectroscopy (ICP-AES) finish. Total carbon and sulfur were analyzed using Leco, whereas base metals were determined following a four-acid dissolution and an inductively coupled plasma mass spectrometry (ICP-MS) finish. Trace elements, including high field strength elements (HFSE), low field strength elements (LFSE), and rare earth elements (REE) were determined using lithium borate fusion pre-preparation, dissolution of the fused material in acid and an ICP-MS finish. Volatile elements (e.g., Sb, As, Te) were determined via an aqua regia digestion with an ICP-MS finish. Gold was analyzed separately using fire assay pre-preparation and an ICP-AES (AuICP21) finish, whereas inorganic carbon was analyzed using perchloric acid digestion and analysis by coulometer (C-GAS05). Precision and accuracy were determined by replicate analysis of a matrix matched, internal basalt standard (SLV_MC), in addition to ALS internal standards. The measure of precision (%RSD) for basalt reference materials was <4% for major elements and <10% for detectable trace elements except for Cs, Cd, Ta, Mo, U, Pb and Au (10%, 11%, 17%, 18%, 26%, 63% and 83%, respectively). The measure of accuracy (%RD) was <3% for all detectable elements except for Ta, Pb and Au (9%, 9% and 30%, respectively, due to compositions at or near the lower detection limits; Appendix C).

2.6.2 Results

Representative whole-rock analyses for the Argyle dataset are presented in Table 2.1. All gabbro samples from Argyle were affected by hydrothermal alteration and this limits the elements that can be used for understanding primary petrological processes and determination of primary chemostratigraphy. In general, the major elements (excluding Al_2O_3), base metals, LFSE and volatile elements are mobile in hydrothermal fluids and during alteration/metamorphism, and were also likely mobile during the formation of the Argyle deposit. In contrast, REE (excluding Eu) and HFSE are typically considered immobile under most circumstances, but may become mobilized under certain conditions during intense hydrothermal alteration (e.g., MacLean, 1988; MacLean and Barrett, 1993). In general, the mobile elements are utilized for understanding the hydrothermal footprint of mineralization, whereas the immobile elements and ratios are utilized to understand the primary geochemistry of the gabbro and the volcaniclastic rocks to identify their magmatic affinities, tectonic environments, and regional correlations. The combination of mobile and immobile element geochemistry was also utilized to undertake the mass balance calculations to quantify element mobility in the Argyle deposit (e.g., MacLean and Barrett, 1993).

2.6.2.1 Principal Component Analysis of Lithogeochemical Data

Principal component analysis (PCA) has been undertaken using Reflex ioGAS 7.0 software to determine elemental associations in the Argyle lithogeochemistry dataset. PCA is based on either a co-variance matrix or a correlation matrix (Appendix E), and was used for exploratory data analysis to determine the causes of variability in the dataset, correlation between different variables and grouping of the correlated variables into principal components, to understand the processes that are recorded in the Argyle lithogeochemical dataset. The data was Z-score scaled and log-centered prior to PCA to ease the positive skewing in the dataset, so as to minimize the effects of non-normality, and to minimize the effects of outliers on the PCA (e.g., Davis, 2002).

Elements that had concentration values below the limit of detection in more than 10% of the samples were censored (i.e. removed) from the dataset prior to running the PCA, so as to avoid generating false components based on the censored values. Elements that contained censored values in <10% of samples were retained in the dataset and samples with concentrations below the detection limit were assigned concentrations equal to 0.5x the detection limit of the element. Rare earth elements (REE) and high field strength elements (HFSE) are assumed to be immobile and therefore only one REE (Lu) and one HFSE (Y) were included in the analysis. If all REE and HFSE were included in PCA, these elements would strongly correlate and mask potential effects of other elemental correlations in the PCA. Following the reduction of data, the 26 elements and oxides that remained for PCA were: SiO_2, Al_2O_3, Fe_2O_3, CaO, MgO, Na_2O, K_2O, TiO_2, MnO, P_2O_5, LOI, Ba, Cs, Lu, Rb, Sr, V, W, Y, As, Sb, Co, Cu, Sc, Zn and CO_2. The summary of main principal components is presented in Table 2.2.

The scree plot (Fig. 2.11A), which orders eigenvalue by their relative significance for all components, shows 5 principal components with eigenvalues >1. However, principal components 4 and 5, show no significant additional elemental associations, as the majority of elements in PC4 and PC5 are already associated with PC1-PC3. Additionally, the graphical representation of data using bivariate plots (Fig. 2.11B-C) illustrates the clustering of associated elements, which further suggests that all significant data is well represented by the first 3 principal components, which account for 65.91% of total dataset variance.

The first principal component (PC1; (Fig. 2.11B-C) accounts for 31.88% of variance and shows negative loadings for MgO-CaO-Sc-Co-V, which reflects original mafic mineral phases and plagioclase feldspar (e.g., Sr, CaO) in the least altered gabbros. Positive loadings on PC1 are associated with potassic and carbonate alteration (LOI, K_2O, CO_2, Cs, Rb, Ba), monazite/xenotime (P_2O_5, Y, Lu) and quartz-albite (SiO_2, Na_2O), whereas zero loadings on PC1 are highlighted by Fe_2O_3-TiO_2 (i.e. Fe-Ti-oxide minerals) and Al_2O_3. The second principal component (PC2; Fig. 2.11B) accounts for 19.46% of variance and shows negative loadings on LOI-K_2O-CO_2-Cs-Rb-Ba that correlate with potassic and carbonate alteration. Positive loadings on PC2 are associated with other alteration types and primary igneous mineralogy (Fe_2O_3, TiO_2, MgO, CaO, Sc, Co, V, Sr). The third principal component (PC3; Fig 2.11C) accounts for 14.57% of variance and shows significant negative loadings associated with the destruction of albite alteration (SiO_2, Na_2O and Al_2O_3), and positive loadings associated with other alteration types and mineralization (SiO_2, Fe_2O_3, TiO_2, Mn and Zn).

2.6.2.2 Immobile Element Magmatic Affinity Monitors

The immobile trace elements Zr, Yb, Nb, and Th are used to infer the primary magmatic affinities of the Argyle host rocks (e.g., MacLean and Kranidiotis, 1987; MacLean and Barrett, 1993; Ross and Bédard, 1999). The Argyle gabbros, and footwall and hanging wall volcaniclastic rocks all have subalkaline Nb/Y ratios and have compositions that range from basaltic to andesitic (Fig. 2.12). The volcaniclastic rocks have predominantly basaltic affinities, consistent with their field descriptions. In contrast, the gabbros have compositions that range from basaltic to andesitic, but notably the distal and intermediate samples are predominantly basaltic, whereas the proximal altered samples have a wide range of higher Zr/Ti ratios, potentially reflecting Ti (± Zr) mobility during the intense alteration in the presence of CO_2 (e.g., Murphy and Hynes, 1986), which is recorded in these rocks.

The Th-Yb space (Fig 2.13A) indicates that the majority of gabbroic samples have tholeiitic to transitional affinities with Th/Yb = 0.35, with some strongly altered gabbro samples having higher values. A small, but significant number of gabbro samples from all alteration zones, contain elevated Th/Yb and have calc-alkaline to transitional affinities; this Th-enrichment is also evident on primitive mantle normalized plots (Fig. 2.14). The hanging wall volcaniclastic rocks have similar Th/Yb values indicating that they have tholeiitic affinities, whereas footwall volcaniclastic rocks have higher Th/Yb and calc-alkaline affinities. In contrast to Th-Yb, in La-Yb and Zr-Y space (Figs. 2.13B-C) the gabbroic samples plot towards higher La/Yb and Zr/Y with transitional to calc-alkalic affinities, which may reflect potential mobility of La and Zr and is supported by the presence of hydrothermal zircon, monazite and xenotime in some of the alteration assemblages at Argyle and other gabbro-hosted mineralization regionally (Ramezani et al., 2000; Piercey and Copeland, 2017). Given the potential mobility of La and Zr, it suggests that Th-Yb may be unreliable as well; however, the evidence for Fe-Ti-enrichment, TiO_2 >1.5 wt. % in most samples, and coarse-grained ilmenomagnetite in the gabbros favours a tholeiitic magma series with evidence for Fe-Ti-enrichment (e.g., Irvine and Baragar, 1971; Jensen, 1976). Hanging wall volcaniclastic rocks have La/Yb = 2.6 (Fig. 2.13B), indicating that they have tholeiitic affinities, in contrast to footwall volcaniclastic rocks which have higher La/Yb and calc-alkaline affinities. In Zr-Y space, the hanging wall volcaniclastic rocks indicate transitional affinities, whereas footwall volcaniclastics have higher Zr/Y and calc-alkaline affinities (Fig. 2.13C). In contrast to gabbroic samples, the affinities of hanging wall volcaniclastic rocks consistently classify as tholeiitic-transitional, whereas footwall volchangcaniclastic rocks have calc-alkaline affinities in Th-Yb, La-Yb and Zr-Yb space. That consistency may reflect the lack of hydrothermal zircon, monazite and xenotime in the hanging wall and footwall volcaniclastic rocks. Gabbroic samples from the Argyle deposit plot along a single trend line on an immobile-immobile element pair in Th-Yb space (Fig. 2.13D), which indicates that the gabbros are cogenetic and have a common precursor (e.g., MacLean, 1990).

Primitive mantle normalized multi-element plots for the Argyle gabbros and host volcaniclastic rocks are shown in Figure 2.14. The gabbroic samples all show broadly similar smooth patterns with LREE-enrichment, and predominantly flat to positive Nb relative to Th and La (i.e., Nb/Th$_{\text{pm-normalized}}$ >1)(Figs. 2.14A-C); these signatures are similar to enriched mid-ocean ridge basalt (E-MORB)-type magmas (e.g., McDonough and Sun, 1995). Generally, the REE plots show progressively higher immobile element enrichment with more intense metasomatism of the gabbro, features common to rocks that have experienced mass loss associated with hydrothermal alteration (e.g., MacLean, 1990). Further, the samples from the proximal alteration zone, and to a lesser extent the intermediate zone, have some samples with variable Ti anomalies, ranging from positive to negative, and some have low La and Ce contents, reflecting potential mobility of these elements, as suggested above. Similarly, Zr and Hf are enriched relative to Nd and Sm, which is an attribute of some E-MORB basalts and the presence of this relationship in the least altered samples suggests that it is a primary petrological feature; however, this enrichment is greatest in the proximal altered gabbro samples, indicating minor mobility of Zr and Hf. In contrast, Th is generally smooth and only shows positive Th relative to Nb in some samples (i.e. a negative Nb anomaly relative to Th and La), which is interpreted to reflect either subduction-related metasomatism and/or continental crustal contamination (see below).

Hanging-wall volcaniclastic rocks (Fig. 2.14D) from Argyle have flat E-MORB-like signatures, whereas the footwall volcaniclastic rocks have LREE-enriched patterns with negative Nb anomalies relative to Th and La and slight depletions in Ti (Fig. 2.14E), which are indicative of continental crustal contamination and/or slab metasomatism common to arc magmas (Pearce, 1983; Piercey et al., 2002; Murphy, 2007). Footwall volcaniclastic rocks at Argyle show a slight enrichment in Zr, which is typically depleted in mafic arc rocks; however the smoothness of the multi-element patterns suggest that this feature is common to the source (Murphy, 2007). Samples from both volcaniclastic units at Argyle in Figs. 2.14D-E show smooth elemental patterns indicating their immobility, which contrasts the highly variable sample-to-primitive mantle ratios for the altered gabbro samples (Figs. 2.14B-C).

The Th-Nb-La systematics of the Argyle gabbros and volcaniclastic rocks illustrate two suites of samples: one with negative Nb relative to Th and La and a second suite with flat to positive Nb relative to Th and La (i.e., a non-arc signature) (Figs. 2.13-2.14). In Figure 2.15A the majority of gabbro samples, regardless of alteration type, are within the mantle arrays proximal to E-MORB, with a similar distribution in Nb/Th-La/Sm space (Fig. 2.15B). Similarly, the hanging wall volcaniclastic rocks have similar low Th/Yb and high Nb/Th ratios and are within the non-arc array (Fig. 2.15A-B). In contrast, the gabbro samples and the footwall volcaniclastic rocks with negative Nb anomalies on primitive mantle normalized plots (Fig. 2.15B) plot proximal to the continental arc fields with elevated Th/Yb and low Nb/Yb (Fig. 2.15A). Further, there seems to be a discontinuous array from the E-MORB box to the continental arc fields in both diagrams, suggesting that: 1) the E-MORB rocks were contaminated by rocks with arc-like signatures or continental crust (e.g., gabbros); and/or 2) they represent rocks that have experienced slab metasomatism and are true arc signatures (e.g., footwall volcaniclastic rocks).

2.6.2.3 Mobile Element Geochemistry

All gabbro samples from the Argyle deposit have been metasomatized. Samples from all alteration zones have very high chlorite-carbonate-pyrite index values (55-95) (CCPI; $100*(MgO+Fe_2O_3)/(MgO+Fe_2O_3+CaO+Na_2O)$; Large et al., 2001) and low-medium Hashimoto alteration index values (15-45) (AI; $100*(MgO+K_2O)/(MgO+K_2O+CaO+Na_2O)$; Ishikawa et al., 1976), with many proximal alteration zone samples plotting near the ankerite node and defining a broadly linear trend between the ankerite and albite nodes (Fig. 2.16A). Albite (Na/Al) and sericite (3K/Al) (Fig. 2.16B) saturation indices show that many proximal gabbro samples exhibit a strong albite alteration, whereas other proximal samples are defined by extreme sericite alteration. A similar distribution exists in Al_2O_3/Na_2O-Na_2O space where the albite altered samples have $Na_2O>5\%$, whereas sericite altered samples generally have higher Al_2O_3/Na_2O ratios and $Na_2O<2\%$ (Fig. 2.16C).

Carbonate ($CO_2/CaO+MgO+FeO$) and sericite (3K/Al) saturation indices in Figure 2.16D generally show that high sericite index samples also contain elevated carbonate index values, but the overall correlation is weak. Carbonate saturation indices, however, do exhibit a correlation between the degree of carbonate alteration and proximity to mineralization (Figs. 2.16E-F). In particular, while calcite is found in all alteration zones, the ankerite saturation level is exceeded almost exclusively by the proximal gabbro samples and where present, ankerite tends to overprint the early calcite alteration.

K/Ti, Y/Ti, Rb/Ti indices show an increase in Y, K and Rb against the relatively conserved behavior of Ti in proximal gabbro (Table 2.3), indicating mobility of these elements (e.g., Eilu et al. 2001). A suite of pathfinder elements typical of orogenic gold mineralization (Au, As, Bi, Te and W), in addition to S, Zr, Ba and Rb all exhibit elevated values in the proximal zone to mineralization, whereas base metals (Cu, Ni, Pb) and other elements (Ag, Sb and Sr) show no correlation with Au (Table 2.3).

2.6.2.4 Mass Change Calculations

2.6.2.4.1 Methods

Mass change calculations are utilized to quantify elemental changes during alteration as they take into account the effects of mass and volume changes during alteration and allow determination of absolute elemental gains and losses of mobile elements during alteration processes (Gresens, 1967; MacLean, 1990; MacLean and Barrett, 1993). Samples from Argyle gabbro all plot along a single alteration line in immobile element space (Fig. 2.13D), thus a single precursor method (e.g., MacLean, 1990; MacLean and Barrrett, 1993) has been used for quantifying mass changes during alteration of the host gabbro at Argyle. The linearity of Th-Yb (Fig. 2.13D) and the coherency of most immobile elements on primitive mantle normalized plots suggest that these elements have been predominantly immobile during alteration with minor exceptions (see below).

The least altered gabbro precursor was selected based on the following criteria: 1) the lack of alteration minerals and ‘freshness’ of the gabbro using optical microscopy and in hand specimen; and 2) low LOI (<3%), CO_2 (<0.5%) and base metal values (Pb <1 ppm; Zn <100 ppm; Ni <100 ppm; Cu <100 ppm), low alteration index values (AI <35), and composition similar to E-MORB from the literature (e.g., McDonough and Sun, 1995). Effectively all gabbro at Argyle has experienced pre-gold mineralization epidote-albite alteration. Thus, mass balance calculations herein record only the gold mineralization-related hydrothermal alteration event and the elemental gains and losses reflect gold forming fluid-rock interaction processes.

The single precursor method involves the following steps:

1) Calculation of an enrichment factor (EF) by comparing an immobile element in the altered sample to the precursor: EF = i_p / i_a, where i_p = concentration of immobile element i in the least altered precursor and i_a = immobile element i in the altered sample. Al_2O_3 has been used as a constant as Al_2O_3 is present in both the precursor and alteration minerals and was likely conserved during alteration reactions.
2) The reconstructed elemental compositions (RC) of each sample were calculated by multiplying the elemental abundances in the altered rock by the EF: RC = EF*Z_a , where Z_a = the concentration of some element (a) in the altered rock.
3) Mass changes (MC) are then calculated by comparing the difference in the concentration of elements between the precursor relative to those in the least altered precursor: MC = RC – PC.

2.6.2.4.2 Results

Major element mass changes across the three alteration zones are generally subtle. Correlation coefficients of Argyle gabbro lithogeochemical samples, the entire mass change result dataset and Tukey plots are found in Appendix F.

Major elements SiO_2, Fe_2O_3, CaO, K_2O, P_2O_5 and TiO_2 show minor gains, up to 2.4% in the proximal zone, whereas Na_2O is depleted. LOI, CO_2, S, Au and As progressively increase with alteration intensity, reflecting the abundance of iron carbonate, pyrite, gold and arsenopyrite. SiO_2, Fe_2O_3, K_2O, TiO_2, P_2O_5, Zr and REE show minor losses in the distal and intermediate zones, and minor gains in the proximal zone, highlighting the presence of quartz veins, pyrite, iron carbonate, muscovite, rutile, phosphate minerals and zircon. Major element oxide mass change plots that show the most significant mass changes and their related processes are presented in Figs. 2.17A-C.

A number of metals (Bi, W, Zr), semi-metals (As, Te), and non-metals (S) show a strong associations with gold content, and are enriched exclusively in the proximal alteration zone (Figs. 2.18A-H); S, Se, As, and Bi exhibit Pearson correlation coefficient values of 0.92, 0.88, 0.77 and 0.67 with Au (Appendix F)

2.7 Electron Probe Microanalysis (EPMA)

2.7.1 Methods

Representative polished thin sections from the distal, intermediate and proximal alteration zones at Argyle were analyzed for major element concentrations of white mica, chlorite and carbonate using a JEOL JXA-8230 electron probe microanalyzer (EPMA) with a W filament source and 5 wavelength dispersive spectrometers (WDS) at Memorial University of Newfoundland. Micas and chlorites were analyzed for 16 elements (K, Ca, Na, Al, Si, Mg, Cu, Ni, Fe, Mn, Cr, V, Ti, Ba, F, Cl), whereas carbonates were analyzed for 6 elements (Fe, Mn, Ca, Sr, Mg, Ba). These minerals were analyzed to quantitatively characterize mineral chemical variations of alteration assemblages at Argyle.

White mica (n=24), chlorite (n=44), and carbonate (n=23) from distal, intermediate and proximal gabbro alteration zones from Argyle were collected to identify chemical changes in mineral species in the different alteration zones. The analyses of white mica and chlorite were undertaken using a spot size of 5-15 µm at an intensity of 20 nA and a voltage of 15 kV with an X-ray takeoff angle of 40 degrees for a count time of 10-30 seconds dependent on element analyzed with off-peak count times equal to half the peak count time. LIF, LDE1, PET and TAP crystals were used to determine elemental concentrations. Both synthetic and natural mineral phases were used as calibration standards. The analyses of carbonates were undertaken using a spot size of 5-15 µm at an intensity of 5 nA and a voltage of 15 kV with an X-ray takeoff angle of 40 degrees for a count time of 20-30 seconds, with off-peak count times equal to half the peak count time. LIF, PET and TAP crystals were used to determine elemental concentrations. Both synthetic and natural mineral phases were used as calibration standards. The secondary Astimex biotite, chlorite and dolomite standards were measured at the beginning and end of each analyses and every 25 points to check if their known compositions are consistently reproduced by the instrument. The compiled results for white mica, chlorite and carbonate EMPA analyses are found in Appendix D.

Chlorite geothermometry was undertaken (n = 44) to provide quantitative estimates on the temperatures of fluid-rock interaction at Argyle. Five chlorite geothermometers were tested (Kranidiotis and MacLean, 1987; Cathelineau, 1988; Jowett, 1991; Zang and

Fyfe, 1995; Xie et al., 1997); however, only the calculated temperatures using the Kranidiotis and MacLean (1987) chlorite geothermometer were consistent with the 250-350 °C temperature range for a "sericite-ankerite" mesozonal deposit class defined by Mikucki and Ridley (1993), which agrees with the observations of gangue mineral alteration assemblage and ore zone sulfide species; and has shown general temperature zoning between distal and intermediate alteration zones. Other chlorite geothermometers (e.g. Jowett, 1991) estimated temperatures that coincide with the "biotite-ankerite" mesozonal deposit class (320-420 °C) in Mikucki and Ridley (1993). Biotite and pyrrhotite have not been observed at Argyle, thus the lower T Kranidiotis and MacLean (1987) is best calibrated for the mineral assemblages observed at Argyle. Kranidiotis and MacLean (1987) geothermometry equation is $T\,(^{o}C) = 106 * Al^{iv} + 18$, with Al^{iv} corrected to $Al^{iv} + 0.7\,Fe/(Fe + Mg)$ to account for the changes associated with Fe/Fe + Mg ratio of chlorite; this thermometer determines the temperature of chlorite formation as a function of the Fe/Fe + Mg ratio of the chlorite and the Al in the tetrahedral site in chlorite.

2.7.2 Results

Mineral chemical data for chlorite is shown in Figure 2.19A and there is a clear progression in mineral chemistry from distal to proximal zones from pycnochlorite in the distal zone, pycnochlorite and ripidolite in the intermediate zone, and brunsvigite in the proximal zone. In general, the proximal zone chlorites have greater Fe relative to the distal chlorite, which are Fe-Mg-bearing (Fig. 2.19B). Chlorites from the distal alteration zone (n = 13) yield temperatures ranging from 224-291 °C with a mean of 257 °C (± 6 °C (1σ)). Chlorites from the intermediate alteration zone (n = 19) yield temperatures of 261-294 °C and a mean of 281 °C (± 2 °C). Chlorites from the proximal zone (n = 12) yield temperatures that overlapped with those from the intermediate zone and range from 266-296 °C with a mean of 282 °C (± 3 °C). The results are shown in Fig. 2.19C and the temperature calculations can be found in Appendix D.

White mica mineral chemical data are summarized in Figure 2.19D in Al (apfu) vs Fe+Mg+Si (apfu) space. This plot illustrates that white mica from the proximal alteration zone at Argyle is muscovitic and has experienced a low degree of Tschermak substitution. The other zones had insufficient white mica for analysis due to the extremely small size of mica crystals.

Carbonate data shown on the Ca-Fe-Mg ternary plot in Fig. 2.19E define two carbonate species: calcite and ankerite. Ankerite is only found in the proximal zone at Argyle, whereas calcite is abundant throughout the deposit and distributed across all alteration zones.

2.8 Short-wave Infrared Spectroscopy

2.8.1 Methods

1,524 hyperspectral measurements were recorded of all lithologies present at the Argyle deposit. Measurements were recorded for each geochemical sample and at downhole intervals with <5 m spacing in 47 diamond drill holes. The samples were analyzed on site, at the Anaconda Mining Stog’er Tight core shack in Baie Verte using a Terraspec™ mineral spectrometer with a Hi-Brite Muglight or High Intensity Contact Probe. Drill core samples analyzed were fresh, cleaned prior to measurements, and dried, but this entailed insignificant amounts of preparation. Terraspec™ has been optimized using a white reference disk either every 20 samples or every 20 minutes to minimize instrument drift. Precision and accuracy were monitored using an internal pyrophyllite reference material.

Hyperspectral data acquisition has been undertaken using RS3 software and processed using The Spectral Geologist version number 7.1.0.069 (”TSG”). Hull correction was applied to a fourth order polynomial fitting curve that was used over Al-OH and Al(Mg,Fe)-OH absorption wavelengths (2,185-2,225 nm and 2,245-2,265 nm, respectively) to calculate hyperspectral scalars. Infrared reflectance spectra were additionally analyzed as described in Lypaczewski and Rivard (2018). Spectra were interpolated to 0.1 nm and convolved with a Gaussian function with a full width half maximum (FWHM) of 20 nm to reduce noise. A majority of spectra produced diagnostic features for SWIR-active minerals. The SWIR absorption data is reported in Appendix C.

The SWIR spectroscopy enables the ability to identify specific mineral phases and their compositions as a result of light absorption by molecular bonds in a mineral sample (e.g., King et al., 2004; Pontual et al., 2008), with different absorption features being produced due to vibrations caused by the stretching or the bending motions of molecular bonds in various mineral phases (Bishop et al., 2008). Minerals that tend to reflect short-wave infrared radiation most often contain chemical bonds between CO_3, OH, NH_4, SO_4, Fe, Mg and Al, which create indicative absorption spectra for specific mineral phases, including phyllosilicates, sulfates and carbonates (Thompson et al., 1999; Herrmann et al., 2001; Pontual et al., 2008).

The 2,190-2,225 nm and 2245-2260 nm absorption hulls reflect the presence of Al-OH and Fe-OH bonds in minerals such as chlorite or white mica and are the most commonly used absorption features in orogenic gold systems for mapping of SWIR-active alteration minerals (Roache et al., 2011; Yang et al., 2011; Halley et al., 2015; Laakso et al., 2016). The diagnostic absorption features are related to the octahedrally coordinated atoms, such as Ca^{2+}, Mg^{2+}, Fe^{2+}, Fe^{3+}, Al^{3+}, Cr^{3+} and Ti^{4+} with hydroxyl groups (Clark et al., 1990; Wang et al., 2017). For example, the white mica absorption at 2,200 nm is caused by a combination of stretching and bending vibrations of the octahedral Al^{3+} ($\upsilon + \delta$) with OH (Bishop et al., 2008; Wang et al., 2017). The absorption features are present at exact wavelengths, thus allowing for precise mineral identification based on the absorption wavelengths (Herrmann et al., 2001). Chemical variations in white mica composition result in a shift of the Al-OH absorption hull, dependent on the element that is substituted into the crystal structure of the mineral. The absorption hull for the K-rich white mica ranges between 2,190-2,198 nm. Substitution of Na^{+} for K^{+}, results in a paragonitic white mica composition with shorter wavelength at 2,180-2,190 nm. Progressively more intense degree of Tschermak's substitution of Fe^{2+} and/or Mg^{2+} into the lattice results in longer wavelength phengitic white mica (>2208 nm). Mg- and Fe- rich chlorites also show diagnostic absorption hulls at 2,245-2,265 nm for FeOH and the less diagnostic 2,320-2,360 nm hull for MgOH bonds (Herrmann et al., 2001; Laakso et al., 2016). Laakso et al. (2016) state that mixed absorption profiles could result from the presence of two or more phases with similar compositions. Water, for example has a number of absorption features in the SWIR spectrum (1450 nm, 1920 nm and 2700 nm); hence, its presence results in a ramped-down absorption feature between 1,000-2,700 nm that obscures and interferes with other SWIR-active minerals (King et al., 2004).

2.8.2 Results

Alteration zones at Argyle have white mica AlOH absorption wavelengths that range from 2,182-2,228 nm, with most proximal white mica having 2,190-2,200 nm (muscovitic; AlOH <2198nm), and most distal white mica having 2,210-2,228 nm (phengitic; AlOH >2208 nm; Fig. 2.20A). Locally, in the distal zones the phengite white mica species extend into the volcaniclastic rocks past the mineralization-hosting gabbroic sill and could potentially be used as a vector toward mineralization on the Baie Verte Peninsula.

The hyperspectral data suggests that overall FeOH and MgOH in silicates show less variation within the Argyle deposit. Generally, chlorite proximal to mineralization is dominantly Fe-chlorite (>2,255 nm), whereas distal to mineralization chlorite found in gabbro, mafic dykes, volcaniclastic rocks in the hanging-wall and footwall are Fe-Mg/Mg-chlorite (<2,255 nm) (Fig. 2.20B). The ratio of the AlOH to FeOH absorption depth (Al-OH/Fe-OH) increases from distal alteration gabbro (0.62), through intermediate alteration (1.01) to proximal alteration gabbro (2.50), reflecting the significant decrease in the content of chlorite relative to white mica with increasing distance to gold mineralization (Appendix C).

2.9 Discussion

2.9.1 Structure and Deformation

Orogenic gold deposits world-wide are intimately associated with regional-scale crustal structures in metamorphic belts (Robert et al., 1997; Kerrich et al., 2000). The formation of orogenic gold deposits is attributed to large-scale hydrothermal fluid flow where there is an intimate linkage of fluid generation at depth driven by metamorphic dehydration and subsequent transport and deposition within crustal-scale fault zones at higher crustal levels (Kerrich, 1983; Phillips and Groves, 1983; Robert and Kelly, 1987; Colvine et al., 1988; Robert, 1990; Groves et al., 1992; Groves, 1993; Kerrich and Cassidy, 1994; Kerrich et al., 2000; Groves et al., 2003; Kerrich et al., 2005; Robert et al., 2005; Dubé and Gosselin, 2007; Phillips and Powell, 2010; Pitcairn et al., 2014, 2015; Goldfarb and Groves, 2015; Groves et al., 2019). The deposits typically form in the hanging wall locations of second- and third-order compressional to oblique slip brittle-ductile shear zones, at distances generally <5 km from the first-order regional scale structures (Robert, 1990; Dubé and Gosselin, 2007). For example, the largest orogenic gold district globally, the Timmins-Porcupine gold camp, Ontario, has produced >67 MOz of gold from multiple world-class deposits that occur at distances <5 km away from the Porcupine-Destor deformation zone (e.g., Dubé and Gosselin, 2007; Bateman et al., 2008). In most global orogenic gold camps deposits are associated with faults that contain curvatures, flexures and/or dilatational jogs, which allow both upward migration of hydrothermal fluids and provide suitable structural traps for deposition of gold-bearing fluids (Teagle et al., 1990; Cox et al., 1991; Groves et al., 1995; Colvine et al., 1998; McCuaig and Kerrich, 1998;

Craw, 2002; Bateman and Hagemann, 2004; Pitcairn et al., 2006; Vielreicher et al., 2016; Wilson et al., 2016).

The Baie Verte gold belt is similar to global orogenic gold districts. The deposits are associated with the regional scale Baie Verte line, a complex brittle-ductile shear zone that marks the suture between Proterozoic to Paleozoic continental rocks of Humber Zone and ophiolitic and cover rocks of the Notre Dame subzone of the Dunnage Zone (Williams, 1979; Williams and St-Julien, 1982; Castonguay et al., 2014). This regional scale structure is of the scale and extent of many global gold hosting environments (e.g., Dubé and Gosselin, 2007) and has a protracted tectonothermal history and evidence of orogenic fluid flow (Williams and St-Julien, 1982; Castonguay et al., 2014; Menzel et al., 2018). The deposits themselves are spatially associated with a second-order splay fault off the Baie Verte Line, the Scrape thrust, which outcrops 300 m to the south of the Argyle deposit and is spatially associated with the Argyle, Stog'er Tight and Pine Cove gold deposits, all of which formed in the hanging-wall to the fault (Ramezani et al., 2000; Evans, 2004; Castonguay et al., 2009; Skulski et al., 2009, 2010; Ybarra et al., 2017; Cullen et al., 2018). Given these structural relationships parallels can be drawn between the Baie Verte gold camp and the global tectonothermal settings of orogenic gold deposits.

The regional-scale structural controls of the Scrape thrust translate well to deposit-scale. At the Argyle deposit the stratigraphy and rheology controlled the localization of brittle deformation, subsequent fluid flow and the localization of gold mineralization.

The rigid gabbroic sill (50-70 m) that is host to gold mineralization was preferentially faulted relative to the volcaniclastic rocks that it intruded. Extreme grain-size heterogeneity (in many cases over <5 m) exists within the vari-textured gabbro; the rheological contrast between the coarse-grained to pegmatitic centre of the sill and the aphanitic chilled margins was greater than the contrast between aphanitic gabbro at stratigraphic contacts with the mafic tuffs and other volcaniclastic rocks. The faulted centre of the sill contains fault-fill quartz-carbonate veins and rare fault gouge, in comparison to wide, less focused deformation zones within distal gabbro and volcaniclastic rocks that are not sealed by veins. In some cases, late faults cross-cut the host intrusion. The stratigraphic, mineralogical and rheological contrasts focused the deformation in the coarsest parts of the sill, which governed the location of subsequent fluid flow and gold mineralization in the gabbro.

The coincidence of structure-related fluid flow associated with regional tectonism, coupled with the textural and compositional character of host gabbros was critical for the localization of mineralization in the Argyle deposit.

2.9.2 Reactivity of the Wallrock

Gold mineralization in orogenic gold deposits globally is spatially linked to strongly altered wallrock and/or quartz-carbonate veins, as a result of different gold precipitation mechanisms (Teagle et al., 1990; Colvine et al., 1998; Vielreicher et al., 2016). Gold precipitation in orogenic gold systems results from: 1) phase separation in response to pressure changes; 2) temperature changes related to conductive or adiabatic cooling of ore fluids; 3) mixing of fluids; and 4) fluid-wallrock reactions (Wilkinson and Johnston, 1996; Mikucki, 1998; Weatherley and Henley, 2013).

The interaction between the wallrock and hydrothermal fluids results in characteristic alteration mineral assemblages around zones of deformation and veins, forming alteration haloes by fluid dispersion and diffusion into surrounding wallrock (Neall, 1987; Mikucki, 1998; Ridley and Diamond, 2000). Wallrock reactivity has been documented as an important process in the deposition of gold by desulfidization of bisulfide complexes ($Au(HS)_2^-$) during reaction of hydrothermal fluids with Fe-rich wallrock. This is especially common in deposits hosted in reactive mafic host rocks (e.g. Bourbeau Sill in Chibougamau, Abitibi; Golden Mile Dolerite in Eastern Goldfields, Yilgarn), but also in felsic-hosted gold deposits with abundant Fe-bearing mineral components (e.g. White River area, Yukon) (Phillips, 1986; Neall, 1987; Dubé et al., 1987; Mikucki, 1998; Ridley and Diamond, 2000; Mernagh et al., 2004; O'Connor-Parsons and Stanley, 2007; MacKenzie, 2010).

Gold mineralization at Argyle is predominantly hosted in the gabbro wallrock, typically <1 m from the quartz-carbonate vein margins and commonly associated with sooty, inclusion-bearing pyrite grains hosted within the gabbro. These relationships at the macro-scale, coupled with micro-scale relationships (e.g., Fig. 2.9A-F), suggest that wallrock sulfidation was a critical process in the formation of the Argyle deposit. For example, the coarsest grained gabbros host mineralization (see above) and pegmatoidal zones that contain the coarsest grained Fe-Ti oxides (e.g. ilmenomagnetite) would have had the largest surface area available for reacting with Au-bearing fluids. Furthermore, many gold-bearing pyrite grains have relict rutile inclusions (after ilmenite) that are spatially associated with ilmenomagnetite (Fig. 2.9D), and which are proximal to gold grains, suggesting that the ilmenomagnetite acted as a chemical trap for the precipitation of hydrothermal (“sooty”) pyrite and gold. In orogenic gold systems, Au is generally transported as an $Au(HS)_2^-$ molecule in near neutral fluids (e.g., Mikucki, 1998; Robb, 2004; Williams-Jones et al., 2009). Reaction of such a fluid with the ilmenite-bearing gabbro would result in pH and redox change of the fluid, destabilization the $Au(HS)_2^-$ complexes, and formation of gold, pyrite, and rutile (modified after Ramezani et al., 2000):

$$(1)\quad \underset{\text{ilmenite}}{FeTiO_{3(s)}} + \underset{\text{gold bisulfide}}{Au(HS)_2^-{}_{(aq)}} + \underset{H^+}{4H^+_{(aq)}} = \underset{\text{pyrite}}{FeS_{2(s)}} + \underset{\text{gold}}{Au_{(s)}} + \underset{\text{rutile}}{TiO_{2(s)}} + \underset{\text{water}}{3H_2O_{(l)}}$$

Wallrock properties not only controlled gold deposition, but also the alteration distribution as there is strong correlation between the alteration intensity and grain-size in the gabbro. In particular, coarse-grained to pegmatitic gabbro exhibits most intense hydrothermal alteration and it is interpreted that it had a larger surface area of reactive ilmenomagnetite crystals and a higher permeability for fluid flow at the time of gold formation. In contrast, the finer grained gabbro is weakly epidote-albite altered or has minor bright-tan altered Ti oxides in the distal alteration zones. In many cases, the hydrothermally altered gabbro terminates against footwall volcaniclastic rocks that are unaffected by hydrothermal fluids. Given their calc-alkalic affinities and low Fe-Ti contents, it suggests they were less chemically receptive hosts for mineralization and therefore not subject to the same degree of hydrothermal alteration, in contrast to the Fe-Ti-enriched gabbro sill.

2.9.3 Relationships between Short-wave Infrared Spectroscopy, Mineral Chemistry, Alteration Mineralogy and Lithogeochemistry

Short wave infrared spectroscopy is a powerful tool in real-time alteration footprint mapping. In the Argyle deposit, the SWIR data show definitive variations in spectral signatures and mineral chemistry with proximity to mineralization (Table 2.3). Proximal alteration is defined by AlOH absorption wavelengths ~2199 nm, typical of muscovite, whereas intermediate (~2210 nm, muscovitic phengite) and distal (~2216 nm, phengite) alteration zones exhibit progressively longer-wavelength white mica. Mineral chemical data confirms the SWIR data with white mica in the proximal zone having muscovitic signatures (Fig. 2.19D). The presence of muscovite in the proximal alteration is reflective of the proximal sericite-quartz-ankerite alteration and likely formed via the partial destruction of feldspar and chlorite in the gabbro: (Colvine et al., 1988):

$$(2)\quad \underset{\text{albite}}{\mathrm{NaAlSi_3O_8}} + \underset{\text{chlorite}}{\mathrm{(Mg,Fe)_5Al_2Si_3O_{10}(OH)_8}} + \underset{\text{calcite}}{\mathrm{5CaCO_3}} + \underset{\text{fluid}}{\mathrm{K^+}} = \underset{\text{sericite}}{\mathrm{KAl_3Si_3O_{10}(OH)_2}} +$$

$$\underset{\text{ankerite}}{\mathrm{5Ca(Mg,Fe)(CO_3)_2}} + \underset{\text{quartz}}{\mathrm{3SiO_2}} + \underset{\text{fluid}}{\mathrm{3H_2O}} + \mathrm{Na^+}$$

Outside of the proximal zones the white mica was too fine-grained for EPMA analysis, despite being identified by SWIR, and this is likely due to the weaker sericite alteration of plagioclase. These mineral chemical vectors are also reflected in alteration indices (e.g. 3K/Al, K/Ti and $(K_2O+CO_2)/(K_2O+CO_2+Na_2O+Al_2O_3)$, which also show similar zoning and progressively increase with proximity to mineralization (Table 3).

In contrast to the muscovite, SWIR data for chlorite shows subtler variations. In particular, there are only small differences in the FeOH absorption wavelengths between the various alteration zones in the Argyle gabbro (Table 2.3). The proximal alteration zones have average FeOH absorption wavelengths (~2,256 nm) typical of Fe-rich chlorite, whereas the intermediate (~2,255 nm) and distal (~2,254 nm) alteration zones have shorter wavelengths indicative of Fe-Mg-chlorite. A number of dark fine-grained distal gabbro samples were considered “aspectral”, despite identification of chlorite in the same samples by optical microscopy. However, this is large part due to their lack of reflectance, rather than the presence or absence of chlorite. Mineral chemistry is a much more robust indicator of chemical variation in chlorite than SWIR (Fig. 2.19A-B). In particular, chlorite from the proximal zone chlorites are brunsvigite/Fe-rich chlorite, whereas intermediate and distal zones exhibit pycnochlorite/Fe-Mg chlorite. This change in chemistry is also reflected in chlorite geothermometry, indicating a progressive increase in the temperature of chlorite formation, and fluid-rock interaction, from the distal zone (257 ± 6 ^{o}C) to the proximal zone (282 ^{o}C ± 3 ^{o}C).

Despite subtleties in recognition of chlorite by SWIR spectroscopy, the relative proportions of white mica, chlorite, and Fe-carbonate can be defined by real-time SWIR spectroscopy using the depth of absorption hulls for AlOH and FeOH (e.g. Ybarra et al., 2017; Ybarra, 2019). As the muscovite content increases there is a coincident increase in the AlOH depth. Similarly, the presence of chlorite results in FeOH absorption hulls and the ratio of AlOH/FeOH depth features reflects the increase in relative abundance of muscovite to chlorite in the alteration assemblage (Table 2.3); this ratio shows an increase in the AlOH/FeOH from distal (0.64) to intermediate (0.96) and proximal (2.6) reflecting an increase in abundance of sericite relative to chlorite with proximity to mineralization.

The SWIR data, mineral chemistry and various alteration indices all exhibit similar patterns that outline the gold-related sericite-ankerite-quartz-dominated hydrothermal alteration in the Argyle deposit. These findings demonstrate that SWIR spectroscopy is a powerful tool for real time rapid identification of subtle mineral chemistry variations and a powerful vectoring tool in orogenic gold systems.

2.9.4 Vectors to Mineralization

The Argyle gold deposit reflects the complex interplay between structure, tectonothermally-driven fluid flow, and reaction with host rocks that resulted in gold precipitation. Various tools, ranging from the field to micro-analytical, provide key vectors to mineralization, which are applicable to not only the Baie Verte Peninsula, but also similar greenschist-facies mafic-hosted gold environments worldwide. Key vectors to mineralization within the Argyle deposit include:

1) distance from the Scrape thrust – Argyle, as well as the Stog’er Tight and Pine Cove gold deposits, are located in the hanging-wall of the Scrape thrust <2 km away from the thrust surface. It is interpreted that the thrust was the main fluid conduit for Au-bearing fluids and was responsible for fracturing of the host gabbro to allow Au-bearing fluid infiltration.
2) gabbro grain-size – mineralization in the Argyle deposit is found within the coarser, pegmatoidal parts of gabbros. It is interpreted that these pegmatite

zones nucleated brittle deformation, which enhanced permeability and helped focus fluid flow throughout the gabbro.

3) host rock composition – gabbros with E-MORB signatures and the Fe-Ti-enrichment (Fe_2O_3 >11.5 wt. % and TiO_2 >1.5 wt. %) were critical for host rock reactivity as Fe-Ti promoted destabilization of $Au(HS)_2^-$ complexes in the Au-bearing fluid via sulfidation of wall rock leading to the formation of observed inclusion-rich pyrite and associated gold.
4) chemical vectors – the hydrothermal footprint of alteration proximal to gold mineralization can be recognized using: enrichments in CO_2 (>6.5 wt.%) and K_2O (>1 wt.%); Au (>DL), Bi (>DL), W (>7 ppm), Zr (>500 ppm), As (>60 ppm), Se (>0.5 ppm) and Te (>DL), and S (>500 ppm); depletion in Sb (<0.35 ppm); elevated alteration indices CO_2/CaO (>1), CO_2/LOI (>0.6), CO_2/(Mg+Fe+Ca) (>0.8), CO_2/(Ca+Mg+Fe-0.5*(S+As)) (>0.6), (K_2O+CO_2)/(K_2O+CO_2+Na_2O+ Al_2O_3) (>0.25), 3K/Al (>0.25), K/Ti (>0.25), Y/Ti (>35) and Rb/Ti (>10); and low AI (<30) and CCPI (<59) values.
5) SWIR – AlOH and FeOH absorption features. The distal alteration is defined by the long-wavelength mica (~2,220 nm; phengite) and short wavelength chlorite (~2,250 nm; Fe-Mg-chlorite) with gradual zonation into the proximal zone defined by short-wavelength mica (~2,198 nm; muscovite) and long-wavelength chlorite (~2,260; Fe-chlorite). Mineral chemical data confirms the SWIR results with pycnochlorite being associated with the distal alteration zone and muscovite white mica and brunsvigite chlorite found in the proximal zone.

2.10. Conclusions

The key conclusions of this manuscript include:

1) The localization of gold mineralization in the Argyle orogenic gold deposit reflects the coincidence of structure-related tectono-thermal fluid flow coupled with host-rock sulfidation due to the textural and compositional character of gabbroic host rocks.
2) The Argyle gabbro and volcaniclastic hanging-wall have tholeiitic affinities with E-MORB signatures. In contrast, the volcaniclastic footwall has calc-alkalic signatures that were influenced by subducted slab metasomatism and/or continental crustal contamination.
3) The Argyle gabbro has experienced two episodes of hydrothermal alteration: 1) epidote-albite, which affected gabbroic rocks regionally throughout the Baie Verte area; 2) mineralization-related alteration. Mineralization-related alteration was focused in the central, pegmatoidal portions of gabbroic sills and is spatially associated with fractures associated with the Scrape thrust fault.
4) Mineralization-related hydrothermal alteration at Argyle can be divided into three assemblages: 1) distal chlorite-calcite-rutile ± epidote-albite (30-70 m); 2) intermediate chlorite-epidote-albite-calcite ± ankerite-rutile-hematite-sericite-pyrite (5-30 m); and 3) proximal sericite-quartz-ankerite ± albite-chlorite-rutile-sooty pyrite-gold (2-25 m). The alteration assemblage distribution is controlled by the grain-size of the gabbro, wherein pegmatoidal gabbros preferentially host mineralization and are interpreted to have induced

brittle deformation and enhanced permeability, and the Fe-Ti-rich chemistry of the gabbro, which acted as a chemical trap for $Au(HS)_2^-$ - bearing fluids.

5) The key depositional process for gold at Argyle was wallrock sulfidation. The majority of gold mineralization is hosted within the gabbro, <1 m from quartz-carbonate veins. The highest gold grades coincide with black chlorite veinlets; however, gold is also present in fractures between pyrite grains and as inclusions of native gold, gold-calaverite, gold-arsenopyrite and gold-chalcopyrite.
6) The key alteration type in the Argyle deposit is the proximal sericite-quartz-ankerite-(albite-chlorite-pyrite-gold). The proximal zone is best mapped by: 1) alteration indices that represent carbonate (e.g. $CO_2/(Ca+Mg+Fe-0.5*(S+As))$) and sericite (e.g. 3K/Al) alteration; 2) pathfinder elements for orogenic gold with increase in Au, As, Bi, Te, W, Zr, Ba, Rb and REE, and decrease in Sb and Sr; 3) mass changes with gains in major oxides SiO_2, Fe_2O_3, CaO, K_2O, P_2O_5 and TiO_2, and Na_2O mass loss; and 4) major element gains with elevated CO_2, K_2O, LOI, Fe_2O_3, TiO_2, MnO, P_2O_5 and S, and decrease in CaO, MgO and Cr_2O_3. The outer alteration footprint, i.e. the distal alteration zone is best defined by an elevated LOI and CO_2-related alteration indices (e.g. CO_2/CaO) relative to the least altered background.
7) SWIR and mineral chemical data exhibit zonation in white mica and chlorite species with proximity to mineralization, consisting of muscovite (~2,198 nm), brunsvigite/Fe-chlorite (~2,260 nm) and ankerite proximal to mineralization

and phengite (~2,214 nm), pycnochlorite/Fe-Mg-chlorite (~2,250 nm), and calcite distal from mineralization. Therefore, SWIR offers a quick and reliable way to discern the relative distance from mineralization.

8) The geological, geochemical and spectral vectors defined in this thesis quantify the anomalous values for various elements, alteration indices and spectral signatures associated with proximal alteration that may be used for further targeting of orogenic gold mineralization in mafic rocks in greenstone belts world-wide.

2.11. References

Anderson, S., Jamieson, R. A., Reynolds, P., and Dunning, G., 2001, Devonian extension in northwestern Newfoundland: ^{40}Ar/^{39}Ar and U-Pb data from the Ming’s Bight area, Baie Verte Peninsula: Journal of Geology, v. 109, p. 191–211.

Bateman, R., and Hagemann, S., 2004, Gold mineralisation throughout about 45 Ma of Archaean orogenesis: protracted flux of gold in the Golden Mile, Yilgarn Craton, Western Australia: Mineralium Deposita, v. 39, p. 536-559.

Bateman, R., Ayer, J. A., and Dubé, B., 2008, The Timmins-Porcupine gold camp, Ontario: Anatomy of an Archean greenstone belt and ontogeny of gold mineralization Economic Geology, v. 103, p. 1285-1308.

Bédard, J. H., 1999, Petrogenesis of boninites from the Betts Cove ophiolite, Newfoundland, Canada: identification of subducted source components: Journal of Petrology, v. 40, p. 1853–1889.

Bédard, J. H., Lauziere, K., Tremblay, A., Sangster, A. L., Douma, S., and Dec, T., 2000, Betts Cove ophiolite and its cover rocks: Geological Survey of Canada Bulletin v. 550, 76 p.

Bierlein, F. P., 2000, Wall-rock petrology and geochemistry in alteration halos associated with mesothermal gold mineralization, central Victoria, Australia: Economic Geology, v. 95, p. 283–311.

Bishop, J. L., Dobrea, E. Z. N., McKeown, N. K., Parente, M., Ehlmann, B. L., Michalski, J. R., Milliken, R. E., Poulet, F., Swayze, G. A., and Mustard, J. F., 2008, Phyllosilicate diversity and past aqueous activity revealed at Mawrth Vallis, Mars: Science, v. 321, p. 830–833.

Bleeker, W., and Hall, B., 2007, The Slave craton: geological and metallogenic evolution, in Goodfellow, W. D., ed., Mineral Deposits of Canada: A Synthesis of Major Deposit-types, District Metallogeny, the Evolution of Geological Provinces, and Exploration Methods, Special Publication 5, Mineral Deposits Division, Geological Association of Canada, p. 849-879.

Castonguay, S., Skulski, T., van Staal, C., and Currie, M., 2009, New insights on the structural geology of the Pacquet Harbour Group and Point Rousse Complex, Baie Verte Peninsula, Newfoundland: Newfoundland and Labrador Department of Natural Resources, Geological Survey, Report, p. 147–158.

Castonguay, S., van Staal, C. R., Joyce, N., Skulski, T., and Hibbard, J. P., 2014, Taconic metamorphism preserved in the Baie Verte Peninsula, Newfoundland

Appalachians: Geochronological evidence for ophiolite obduction and subduction and exhumation of the leading edge of the Laurentian (Humber) margin during closure of the Taconic Seaway: Geoscience Canada, v. 41, p. 459–482.

Cathelineau, M., 1988, Site occupancy in chlorites and illites as a function of temperature: Clay Minerals, v. 23, p. 471-485.

Cawood, P. A., and Dunning, G. R., 1993, Silurian age for movement on the Baie Verte Line: Implications for accretionary tectonics in the northern Appalachians: Geological Society of America, Program with Abstracts, v. 25, p. A422.

Cawood, P. A. and Dunning, G. R., Lux, D., and van Gool, J. A. M., 1994, Timing of peak metamorphism and deformation along the Appalachian margin of Laurentia in Newfoundland: Silurian and not Ordovician: Geology, v. 22., p. 399-402.

Christie, A. B., and Brathwaite, R. L., 1986, Epithermal gold-silver and porphyry copper deposits of the Hauraki goldfields—A review. In: Henley, R. W., Hedenquist, J. W., and Roberts, P. J., eds., Guide to the active epithermal (geothermal) systems and precious metal deposits of New Zealand: Monograph series on mineral deposits, Berlin, Gebruder Borntraeger, v. 26, p. 129–145.

Clark, R. N., King, T. V., Klejwa, M., Swayze, G. A., and Vergo, N., 1990, High spectral resolution reflectance spectroscopy of minerals. Journal of Geophysical Research: Solid Earth, v. 95, p. 12653–12680.

Colvine, A. C., Fyon, J. A., Heather, K. B., Marmont, S., Smith, P. M., and Troop, D. G., 1988, Archean lode gold deposits in Ontario: Ontario Geological Survey, Miscellaneous Paper 139, 136 p.

Cox, S. F., Wall, V. J., Etheridge, M. A., and Potter, T. F., 1991, Deformational and metamorphic processes in the formation of mesothermal vein-hosted gold deposits – examples from the Lachlan Fold Belt in central Victoria, Australia: Ore Geology Reviews, v. 6, p. 391-423.

Cullen, M., Pitman, C., Copeland, D. A., McNeill, P., and Slepcev, G., 2018, Mineral resource and mineral reserve update on the Point Rousse Project, Baie Verte, Newfoundland and Labrador, Canada, Technical Report NI43-101: Anaconda Mining Inc., Newfoundland and Labrador, Canada, 285 p.

Craw, D., 2002, Geochemistry of late metamorphic hydrothermal alteration and graphitisation of host rock, Macraes Gold Mine, Otago Schist, New Zealand: Chemical Geology, v. 191, p. 257-275.

Davis, J. C., 2002, Statistics and Data Analysis in Geology, Third Edition: New York, John Wiley and Sons, 638 p.

Dinel, E., Fowler, A. D., Ayer, J., Still, A., Tylee, K., and Barr, E., 2008, Lithogeochemical and stratigraphic controls on gold mineralization within the metavolcanic rocks of the Hoyle Pond mine, Timmins, Ontario: Economic Geology, v. 103, p. 1341–1363.

Dubé, B. and Gosselin, P., 2007, Greenstone-hosted quartz-carbonate vein deposits. In: Goodfellow, W. D., ed., Mineral deposits of Canada: A Synthesis of Major Deposit-Types, District Metallogeny, the Evolution of Geological Provinces And Exploration Methods: Geological Association of Canada, Mineral Deposits Division, Special Publication No. 5, p. 49–73.

Dubé, T. B., Guha, J. and Rocheleau, M., 1987, Alteration patterns related to gold mineralization and their relation to CO_2/H_2O ratios: Mineralogy and Petrology, v. 37, p. 267-291.

Dubé, B., Lauzière, K., and Poulsen, H. K., 1993, The Deer Cove deposit: an example of "thrust"- related breccia-vein type gold mineralization in the Baie Verte Peninsula, Newfoundland: Geological Survey of Canada, Current Research, Paper 93-1D, p. 1–10.

Dunning, G. R., and Krogh, T. E., 1985, Geochronology of ophiolites of the Newfoundland Appalachians: Canadian Journal of Earth Sciences, v. 22, p. 1659-1670.

Dunning, G. R., O'Brien, S. J., Colman-Sadd, S. P., Blackwood, R. F., Dickson, W. L., O'Neill, P. P., and Krogh, T. E., 1990, Silurian orogeny in the Newfoundland Appalachians: Journal of Geology, v. 98, p. 895–913.

Evans, D. T. W., 2004, Epigenetic gold occurrences, Baie Verte Peninsula, (NTS 12H/09, 16 and 12I/01) Newfoundland: Government of Newfoundland and Labrador, Department of Natural Resources, Geological Survey, Mineral Resource Report No. 11, 157 p.

Eilu, P. K., 1999, Atlas of alteration assemblages, styles and zoning in orogenic lode-gold deposits in a variety of host rock and metamorphic settings: University of Western Newfoundland, Geology and Geophysics Department, v. 30, 58 p.

Eilu, P. K., Mikucki, E. J. and Groves, D. I., 1998, Wallrock alteration and primary geochemical dispersion in lode-gold exploration: Society for Geology Applied to Mineral Deposits, Short Course Notes, 65 p.

Eilu, P., and Groves, D. I., 2001, Primary alteration and geochemical dispersion haloes of Archaean orogenic gold deposits in the Yilgarn Craton: the pre-weathering scenario: Geochemistry: Exploration, Environment, Analysis, v. 1, p. 183-200.

Goldfarb, R. J. and Groves, D. I., 2015, Orogenic gold: Common or evolving fluid and metal sources through time: Lithos, v. 233, p. 2–26.

Goldfarb, R. J., Groves, D.I., and Gardoll, S., 2001, Orogenic gold and geologic time; a global synthesis: Ore Geology Reviews, v. 18, p. 1–75.

Goldfarb R.J., Baker, T., Dubé, B., Groves, D. I., Hart, C. J. R., and Gosselin, P., 2005, Distribution, character, and genesis of gold deposits in metamorphic terranes, in Goldfarb, R. J., and Richards, J. P., eds., Economic Geology, 100th Anniversary Volume, v. 100, p. 1001-1033.

Gresens, R. L., 1967, Composition-volume relationships of metasomatism: Chemical Geology, v. 2, p. 47–65.

Groves, D. I., 1993, The crustal continuum model for late-Archaean lode-gold deposits of the Yilgarn block, Western Australia: Mineralium Deposita, v. 28, p. 366–374.

Groves, D. I., Barley, M. E., Barnicoat, A. C., Cassidy, K. F., Fare, R. J., Hagemann, S. G., Ho, S. E., Hronsky, J. M. A., Mikucki, E. J., Mueller, A. G., McNaughton, N. J., Perring, C. S., Ridley, J. R., and Vearncombe, J. R., 1992, Sub-greenschist to granulite-hosted Archaean lode-gold deposits of the Yilgarn craton: a depositional continuum from deep-sourced hydrothermal fluids in crustal-scale plumbing systems: The University of Western Australia Publication, v. 22, p. 325–327.

Groves D. I., Goldfarb, R. J., Gebre-Mariam, M., Hagemann, S. G., Robert, F., 1998, Orogenic gold deposits–a proposed classification in the context of their crustal distribution and relationship to other gold deposit types: Ore Geology Reviews, v. 13, p. 7–27.

Groves, D. I., Goldfarb, R. J., Robert, F., and Hart, C. J. R., 2003, Gold deposits in metamorphic belts: overview of current understanding, outstanding problems, future research, and exploration significance: Economic Geology, v. 98, p. 1–29.

Groves, D. I., Santosh, M., Deng, J., Wang, Q., Yang, L., and Zhang, L., 2019, A holistic model for the origin of orogenic gold deposits and its implications for exploration: Mineralium Deposita, v. 54, p. 1-18.

Halley, S., Dilles, J., and Tosdal, R., 2015, Footprints: Hydrothermal alteration and geochemical dispersion around porphyry copper deposits: Society Of Economic Geology Newsletter v. 100, p. 12-19.

Herrmann, W., Blake, M., Doyle, M., Huston, D., Kamprad, J., Merry, N., and Pontual, S., 2001, Short wavelength infrared (SWIR) spectral analysis of hydrothermal alteration zones associated with base metal sulfide deposits at Rosebery and Western Tharsis, Tasmania, and Highway-Reward, Queensland: Economic Geology, v. 96, p. 939–955.

Hibbard, J., 1983, Geology of the Baie Verte Peninsula, Newfoundland: Government of Newfoundland and Labrador, Department of Mines and Energy, Mineral Development Division, v. 2, 280 p.

Irvine, T. N., and Baragar, W. R. A., 1971, A guide to the chemical classification of the common volcanic rocks: Canadian Journal of Earth Sciences, v. 8, p. 523-548.

Ishikawa, Y., Sawaguchi, T., Iwaya, S., and Horiguchi, M., 1976, Delineation of prospecting targets for Kuroko deposits based on modes of volcanism of underlying dacite and alteration haloes: Mining Geology, v. 26, p. 105-117.

Jamieson, R. A., Anderson, S., and McDonald, L., 1993, Slip on the Scrape; an extensional allochthon east of the Baie Verte Line, Newfoundland: Geological Society of America: Program with Abstracts, v. 25, p. 26

Jensen, L. S., 1976, A new cation plot for classifying subalkalic volcanic rocks: Ontario Geological Survey Special Paper, v. 66, p. 1-22.

Jowett, E. C., 1991, Fitting iron and magnesium into the hydrothermal chlorite geothermometer: GAC/MAC/SEG Joint Annual Meeting, Program with Abstracts, Toronto, May 27-29, 1991, v. 16.

Kerr, A. and Selby, D., 2012, The timing of epigenetic gold mineralization on the Baie Verte Peninsula, Newfoundland, Canada: new evidence from Re-Os pyrite geochronology: Mineralium Deposita, v. 47, p. 325–337.

Kerrich, R., 1983, Geochemistry of Gold Deposits of the Abitibi Greenstone Belt: Canadian Institute of Mining and Metallurgy, Special Paper, v. 27, p. 1-75.

Kerrich, R. and Cassidy, K. F., 1994, Temporal relationships of lode gold mineralization to accretion, magmatism, metamorphism and deformation—Archean to present: A review: Ore Geology Reviews, v. 9, p. 263–310.

Kerrich, R., Goldfarb, R., Groves, D., and Garwin, S., 2000, The geodynamic of world-class gold deposits: characteristics, space-time distribution and origins: Reviews in Economic Geology, v. 13, p. 501-551.

Kerrich, R., Goldfarb, R. J., and Richards, J. P., 2005, Metallogenic provinces in an evolving geodynamic framework. Economic Geology, v. 100, p. 1097–1136.

King, P. L., Ramsey, M. S., and Swayze, G. A., 2004, Infrared spectroscopy in geochemistry, exploration geochemistry and remote sensing: Mineralogical Association of Canada, Short Course Series, v. 33, 284 pp.

Kirkwood, D. and Dubé, B., 1992, Structural control of sill-hosted gold mineralization: the Stog'er Tight gold deposit, Baie Verte Peninsula, northwestern Newfoundland: Geological Survey of Canada, Current Research, Paper 92-1D, p. 211–221.

Kranidiotis, P. and MacLean, W. H., 1987, Systematics of chlorite alteration at the Phelps Dodge massive sulfide deposit, Matagami, Quebec: Economic Geology, v. 82, p. 1898-1911.

Laakso, K., Peter, J., Rivard, B., and White, H., 2016, Short-wave infrared spectral and geochemical characteristics of hydrothermal alteration at the Archean Izok Lake Zn-Cu-Pb-Ag volcanogenic massive sulfide deposit, Nunavut, Canada: Application in exploration target vectoring: Economic Geology, v. 111, p. 1223–1239.

Large, R. R., Gemmell, J. B., Paulick, H., and Huston, D. L., 2001. The alteration box plot: A simple approach to understanding the relationship between alteration mineralogy and lithogeochemistry associated with volcanic-hosted massive sulfide deposits: Economic Geology, v. 96, p. 957-971.

Lypaczewski, P. and Rivard, B., 2018, Estimating the Mg# and Al^{vi} content of biotite and chlorite from shortwave infrared reflectance spectroscopy: Predictive equations and recommendations for their use: International Journal of Applied Earth Observation and Geoinformation, v. 68, p. 116–126.

MacKenzie, D., Craw, D., Cooley, M. and Fleming, A., 2010, Lithogeochemical localisation of disseminated gold in the White River area, Yukon, Canada: Mineralium Deposita, v. 45, p. 683-705.

MacLean, W., 1988, Rare earth element mobility at constant inter-REE ratios in the alteration zone at the Phelps Dodge massive sulphide deposit, Matagami, Quebec. Mineralium Deposita, v. 23, p. 231– 238.

MacLean, W., 1990, Mass change calculations in altered rock series. Mineralium Deposita, v. 25, p. 44–49.

MacLean, W. and Barrett, T., 1993, Lithogeochemical techniques using immobile elements: Journal of Geochemical Exploration, v. 48, v. 109–133.

MacLean, W. and Kranidiotis, P., 1987, Immobile elements as monitors of mass transfer in hydrothermal alteration; Phelps Dodge massive sulfide deposit, Matagami, Quebec. Economic Geology, v. 82, p. 951–962.

McCuaig, T. C. and Kerrich, R., 1998, P-T-T deformation-fluid characteristics of lode gold deposits: evidence from alteration systematics: Ore Geology Reviews, v. 12, p. 381–453.

McDonough, W. F. and Sun, S. S., 1995, The composition of the earth: Chemical Geology, v. 120, p. 223–253.

Menzel, M. D., Garrido, C. J., López Sánchez-Vizcaíno, V., Marchesi, C., Hidas, K., Escayola, M. P., and Delgado Huertas, A., 2018, Carbonation of mantle peridotite by CO_2-rich fluids: the formation of listvenites in the Advocate ophiolite complex (Newfoundland, Canada): Lithos, v. 323, p. 238-261.

Mernagh, T. P., Heinrich, C. A., Mikucki, E.J., 2004, Temperature gradients recorded by fluid inclusions and hydrothermal alteration at the Mount Charlotte gold deposit, Kalgoorlie, Australia: Canadian Mineralogist, v. 42, p. 1383-1403.

Mikucki, E. J., 1998, Hydrothermal transport and depositional processes in Archaean lode-gold systems: A review: Ore Geology Reviews, v. 13, p. 307–321.

Mikucki, E. J., and Ridley, J. R., 1993, The hydrothermal fluid of Archaean lode-gold deposits at different metamorphic grades: compositional constraints from ore and wallrock alteration assemblages: Mineralium Deposita, v. 28, p. 469-481.

Murphy, J. B., 2007, Igneous Rock Associations 8: Arc Magmatism II: geochemical and isotopic characteristics: Geoscience Canada, v. 34, p. 7-36.

Murphy, J. B., and Hynes, A. J., 1986, Contrasting secondary mobility of Ti, P, Zr, Nb, and Y in two metabasaltic suites in the Appalachians: Canadian Journal of Earth Sciences, v. 23, p. 1138-1144.

Neall, F. B., 1987, Sulphidation of iron-rich rocks as a precipitation mechanism for large Archaean gold deposits in Western Australia: thermodynamic confirmation. In: Ho, S. E., Groves, D. I., eds., Recent Advances in Understanding Precambrian Gold Deposits: University of Western Australia, Geology Department, p. 265-269.

Norman, R. E. and Strong, D. F., 1975, The geology and geochemistry of ophiolitic rocks exposed at Ming's Bight, Newfoundland: Canadian Journal of Earth Sciences, v. 12, p. 777-797.

O’Connor-Parsons, T. and Stanley, C. R., 2007, Downhole lithogeochemical patterns relating to chemostratigraphy and igneous fractionation processes in the Golden Mile dolerite, Western Australia: Geochemistry: Exploration, Environment, Analysis, v. 7, p. 109-127.

Pearce, J. A., 1983, Role of sub-continental lithosphere in magma genesis at active continental margins. In: Hawkesworth, C. J. and Norry, M. J. Shiva, eds., Continental Basalts and Mantle Xenoliths, Nantwich, UK., p. 230–249.

Pearce, J. A., 1996, A user’s guide to basalt discrimination diagrams. Trace element geochemistry of volcanic rocks: Applications for massive sulphide exploration: Geological Association of Canada, Short Course Notes, v. 12, p. 79-113.

Pearce, J. A., 2014, Immobile element fingerprinting of ophiolites: Elements, v. 10, p. 101-108.

Perrouty, S., Linnen, R. L., Lesher, C. M., Olivo, G.R., Piercey, S. J., Gaillard, N., Clark, J. R. and Enkin, R.J., 2019, Expanding the size of multi-parameter metasomatic footprints in gold exploration: utilization of mafic dykes in the Canadian Malartic district, Québec, Canada: Mineralium Deposita, v. 54, p.761-786.

Phillips, G. N., 1986, Geology and alteration in the Golden Mile Kalgoorlie: Economic Geology, v. 81, p. 779-808.

Phillips, G. N. and Groves D. I., 1983, The nature of Archaean gold-bearing fluids as deduced from gold deposits of western Australia: Journal of the Geological Society of Australia, v. 30, p. 25–39.

Phillips, G. N., Powell, R., 2010, Formation of gold deposits: a metamorphic devolatilization model: Journal of Metamorphic Geology, v. 28, p. 689-718.

Piercey, S. J. and Copeland, D. A., 2017, Host-rock reactivity in the generation of gabbro-hosted orogenic Au in the Baie Verte Peninsula, Newfoundland, Canada: Atlantic Geology, GAC-Newfoundland and Labrador Section, 2017 Spring Technical Meeting, Program with Abstracts, St. John's, Newfoundland, v. 53, p. 250.

Piercey, S. J., Mortensen, J. K., Murphy, D. C., Paradis, S., and Creaser, R. A., 2002, Geochemistry and tectonic significance of alkalic mafic magmatism in the Yukon-Tanana terrane, Finlayson Lake region, Yukon. Canadian Journal of Earth Sciences, v. 39, p. 1729–1744.

Pitcairn, I. K., Teagle, D. A., Craw, D., Olivo, G. R., Kerrich, R., and Brewer, T. S., 2006, Sources of metals and fluids in orogenic gold deposits: Insights from the Otago and Alpine Schists, New Zealand: Economic Geology, v. 101, p. 1525-1546.

Pitcairn, I. K., Craw, D., and Teagle, D. A. H., 2014, The gold conveyor belt: Large-scale gold mobility in an active orogen: Ore Geology Reviews, v. 62, p. 129–142.

Pitcairn, I. K., Craw, D., and Teagle, D. A. H., 2015, Metabasalts as sources of metals in orogenic gold deposits: Mineralium Deposita, v. 50, p. 373–390.

Pontual, S., Merry, N., and Gamson, P., 2008, Spectral interpretation-field manual. GMEX. Spectral analysis guides for mineral exploration: AusSpec International Pty. Ltd., Victoria, Australia, 189 p.

Ramezani, J., 1992, The geology, geochemistry and U-Pb geochronology of the Stog’er Tight Gold Prospect, Baie Verte Peninsula, Newfoundland. M.Sc. thesis, Memorial University of Newfoundland, St. John’s, Newfoundland, 312 p.

Ramezani, J., Dunning, G. R., and Wilson, M. R., 2000, Geologic setting, geochemistry of alteration, and U-Pb age of hydrothermal zircon from the Silurian Stog'er Tight Gold Prospect, Newfoundland Appalachians, Canada: Exploration and Mining Geology, v. 9, p. 171-188.

Ridley, J. R. and Diamond, L. W., 2000, Fluid chemistry of orogenic lode deposits and implications for genetic models: Economic Geology, Reviews, v. 13, p. 141–162.

Roache, T., Walshe, J., Huntington, J., Quigley, M., Yang, K., Bil, B., Blake, K., and Hyvärinen, T., 2011, Epidote–clinozoisite as a hyperspectral tool in exploration for Archean gold: Australian Journal of Earth Sciences, v. 58, p. 813–822.

Robb, L., 2004, Introduction to ore-forming processes. Wiley-Blackwell, Oxford, UK, 386 p.

Robert, F., 1990, Structural setting and control of gold-quartz veins of the Val d'Or area, southeastern Abitibi subprovince. In: Ho, S.E., Robert, F., and Groves, D.I., eds., Gold and Base-Metal Mineralization in the Abitibi Subprovince, Canada, with

Emphasis on the Quebec Segment: University of Western Australia, Short Course Notes, v. 24, p. 167-210.

Robert, F. and Kelly, W. C., 1987, Ore-forming fluids in Archean gold-bearing quartz veins at the Sigma mine, Abitibi greenstone belt, Quebec, Canada. Economic Geology, v. 82, p. 1464–1482.

Robert, F., Poulsen, K. H., and Dubé, B., 1997, Gold deposits and their geological classification, in Gubins, A. G., ed., Proceedings of Exploration'97: Fourth Decennial International Conference on Mineral Exploration, p. 209-220.

Robert, F., Poulsen, K. H., Cassidy, K. F., and Hodgson, C. J., 2005, Gold metallogeny of the Yilgarn and Superior cratons, in Goldfarb, R. J., and Richards, J. P., eds., Economic Geology, 100th Anniversary Volume, v. 100, p. 1001-1033.

Ross, P. S. and Bédard, J. H., 2009, Magmatic affinity of modern and ancient subalkaline volcanic rocks determined from trace-element discriminant diagrams: Canadian Journal of Earth Sciences, v. 46, p. 823–839.

Sangster, A. L., Douma, S. L., and Lavigne, J., 2008, Base metal and gold deposits of the Betts Cove Complex, Baie Verte Peninsula, Newfoundland. Geological Association of Canada, Mineral Deposits Division, Special Publication No. 5, p. 703–721.

Skirrow, R. G., and Franklin, J. M., 1994, Silicification and metal leaching in semiconformable alteration beneath the Chisel Lake massive sulfide deposit, Snow Lake, Manitoba: Economic Geology, v. 89, p. 31-50.

Skulski, T., Castonguay, S., van Staal, C. R., Rogers, N., McNicoll, V., Kerr, A., and Escayola, M., 2009, Baie Verte Peninsula: an evolving geological story: Geological Association of Canada, Newfoundland and Labrador Section, Annual Field Trip Guide, St. John’s, Newfoundland, v. 60, p. 1–60.

Skulski, T., Castonguay, S., McNicoll, V., van Staal, C., Kidd, W., Rogers, N., Morris, W., Ugalde, H., Slavinski, H., and Spicer, W., 2010, Tectonostratigraphy of the Baie Verte oceanic tract and its ophiolite cover sequence on the Baie Verte Peninsula: Geological Survey, Newfoundland and Labrador Department of Natural Resources, Current Research, Report 10-1, p. 315–337.

Sparrow, B., Barrett, S., Copeland, D. A., and Walsh, M., 2017, Argyle Prospect Mineral Licences 012433M (11th year) and 020060M (5th year) Point Rousse Project, Baie Verte Peninsula, NL NTS sheet 12H/16, Assessment Report: Anaconda Mining Inc., Newfoundland and Labrador, Canada, 481 p.

Spitz, G., and Darling, R., 1978, Major and minor element lithogeochemical anomalies surrounding the Louvem copper deposit, Val d'Or, Quebec: Canadian Journal of Earth Sciences, v. 15, p. 1161-1169.

Stern, R. J., 2008, Modern-style plate tectonics began in Neoproterozoic time: An alternative interpretation of Earth's tectonic history: Geological Society of America Special Papers, v. 440, p. 265-280.

Teagle, D. A., Norris, R. J., and Craw, D., 1990, Structural controls on gold-bearing quartz mineralization in a duplex thrust system, Hyde-Macraes Shear Zone, Otago Schist, New Zealand: Economic Geology, v. 85, p. 1711-1719.

Thompson, A. J. B., Hauff, P. L., and Robitaille, A. J., 1999, Alteration mapping in exploration: Application of short-wave infrared (SWIR) spectroscopy: Society of Economic Geology Newsletter, v. 39, p. 15-27.

Tuach, J., 1976, Structural and stratigraphic setting of the Ming and other sulfide deposits in the Rambler area, Newfoundland: Unpub. M.Sc. thesis, Memorial University of Newfoundland, St. John’s, Newfoundland, Canada, 128 p.

Tuach, J. and Kennedy, M. J., 1978, The geologic setting of the Ming and other sulfide deposits, Consolidated Rambler Mines, Northeast Newfoundland: Economic Geology, v. 73, p. 192-206.

Upadhyay, H. D., and Strong, D. F., 1973, Geological Setting of the Betts Cove Copper Deposits, Newfoundland: An example of ophiolite sulfide mineralization. Economic Geology, v. 68, p. 161-167.

Upton, P., and Craw, D., 2013, Extension and gold mineralization in the hanging walls of active convergent continental shear zones: Journal of Structural Geology, v. 64, p. 135-148.

van Staal, C. R., 2007, Pre-Carboniferous tectonic evolution and metallogeny of the Canadian Appalachians. In: Goodfellow, W. D., ed. Mineral Deposits of Canada: A Synthesis of Major Deposit Types, District Metallogeny, the Evolution of Geological Provinces and Exploration Methods: Geological Association of Canada, Mineral Deposits Division, Special Publications no. 5, p. 793–818.

van Staal, C. R., Barr, S. M., and Percival, J., 2012, Lithospheric architecture and tectonic evolution of the Canadian Appalachians and associated Atlantic Margin. In: Percival, J. A., Cook, F. A. and Clowes, R. M., eds., Tectonic styles in Canada: the LITHOPROBE perspective: Geological Association of Canada, Special Paper 49, p. 41-95.

Vielreicher, N. M., Groves, D. I., and McNaughton, N. J., 2016, The giant Kalgoorlie gold field revisited: Geoscience Frontiers, v. 7, p. 359-374.

Wang, R., Cudahy, T., Laukamp, C., Walshe, J. L., Bath, A., Mei, Y., Young, C., Roache, T. J., Jenkins, A., Roberts, M., et al., 2017, White mica as a hyperspectral tool in exploration for the Sunrise Dam and Kanowna Belle gold deposits, Western Australia: Economic Geology, v. 112, p. 1153–1176.

Weatherley, D. K. and Henley, R. W., 2013, Flash vaporization during earthquakes evidenced by gold deposits: Nature Geoscience, v. 6, p. 294-298.

Wilkinson, J. J. and Johnston, J. D., 1996, Pressure fluctuations, phase separation, and gold precipitation during seismic fracture propagation: Geology, v. 24, p. 395–398.

Williams, H., 1979, Appalachian orogen in Canada: Canadian Journal of Earth Sciences, v. 16, p. 792–807.

Williams, H., 1995, Geology of the Appalachian-Caledonian Orogen in Canada and Greenland: Geological Survey of Canada, Ottawa, Ontario, Canada, 944 p.

Williams, H. and St. Julien, P., 1982, The Baie Verte Brompton Line: Early Paleozoic continent ocean interface in the Canadian Appalachians; in St. Julien, P., and Beland, J., eds., Major Structural zones and faults of the northern Appalachians: Geological Association of Canada, Special Paper No. 24, p. 177-208.

Williams, H., Colman-Sadd, S. P., and Swinden, H. S., 1988, Tectonic-stratigraphic subdivisions of central Newfoundland; Geological Survey of Canada, Current Research, Paper 88-1B, p. 91–98.

Williams-Jones, A. E., Bowell, R. J., and Migdisov, A. A., 2009, Gold in solution: Elements, v. 5, p. 281–287.

Wilson, M. R., Dunning, G. R., and Cawood, P. A., 1994, Fluid compositions in crustal-scale plumbing systems related to contrasting styles of Ordovician and Silurian orogenesis, Northern Appalachians, Newfoundland: Mineralogical Magazine, v. 58, p. 977-987.

Wilson, C. J., Osborne, D. J., Robinson, J. A. and Miller, J. M., 2016, Structural constraints and localization of gold mineralization in Leather Jacket Lodes, Ballarat, Victoria, Australia: Economic Geology, v. 111, p. 1073-1098.

Winchester, J. A., and Floyd, P. A., 1976, Geochemical magma type discrimination: application to altered and metamorphosed basic igneous rocks: Earth and Planetary Science Letters, v. 28, p. 459-469.

Xie, X., Byerly, G. R., and Ferrell Jr., R. E., 1997, IIb trioctahedral chlorite from the Barberton greenstone belt: crystal structure and rock composition constraints with implications to geothermometry: Contributions to Mineralogy and Petrology, v. 126, p. 275-291.

Yang, K., Huntington, J., Gemmell, J., and Scott, K., 2011, Variations in composition and abundance of white mica in the hydrothermal alteration system at Hellyer, Tasmania, as revealed by infrared reflectance spectroscopy: Journal of Geochemical Exploration, v. 108, p. 143–156.

Ybarra S.J., 2019 (in revision). Hydrothermal Alteration and Lithogeochemistry of the Pine Cove Orogenic Gold Deposit, Baie Verte Peninsula, Newfoundland, Canada. Unpublished MSc thesis, Memorial University of Newfoundland, St. John’s, NL, Canada, 160 p.

Ybarra, S., Piercey, S., Layne, G. D., Copeland, D. A., and McNeil, P., 2017, Alteration halo and lithogeochemistry of the Pine Cove orogenic gold deposit, Baie Verte Peninsula, Newfoundland, Canada: Atlantic Geology, GAC-Newfoundland and

Labrador Section, 2017 Spring Technical Meeting, Program with Abstracts, St. John’s, Newfoundland, v. 53, p. 250.

Zang, W., and Fyfe, W. S., 1995, Chloritization of the hydrothermally altered bedrock at the Igarapé Bahia gold deposit, Carajás, Brazil: Mineralium Deposita, v. 30, p. 30-38.

Table 2.1. Representative whole-rock analyses for Argyle

Sample ID	294859	294867	I951379	I951368	I951359	294852
Hole ID	AE-16-27	AE-16-26	AE-16-09	AE-16-34	AE-16-40	AE-16-43
Depth (m)	90.95	89.85	26.35	5	4	125.95
Lithology	Gabbro	Gabbro	Gabbro	HW Breccia	HW lapilli tuff	FW lapilli tuff
Alteration	Distal	Intermediate	Proximal	Unaltered	-	-
Assemblage	Ep-Chl-Calc-Rt	Chl-Ep-Ank-Ab-Rut	Ab-Ank-Chl-Ms-Py	Calc-Chl-Ep	Ep-Chl-Calc	Chl-Calc
SiO_2 (%)	50.8	44.5	51.2	51.5	49	54.2
Al_2O_3	15.45	13.45	16.2	16.15	16.9	15.5
Fe_2O_3	11	10.5	9.64	8.05	12	7.57
CaO	8.73	8.17	4.1	5.68	5.47	4.81
MgO	6.62	5.01	1.52	3.81	4.01	6.08
Na_2O	4.04	3.68	6.76	6.14	6.08	5.51
K_2O	0.32	0.97	0.72	0.26	0.02	0.17
Cr_2O_3	0.02	0.012	<0.01	0.02	0.02	0.025
TiO_2	1.62	1.72	1.35	1.65	1.78	0.87
MnO	0.17	0.16	0.11	0.08	0.06	0.09
P_2O_5	0.18	0.2	0.36	0.28	0.19	0.12
SrO	0.04	0.02	0.01	0.01	<0.01	0.01
BaO	0.01	0.01	0.01	<0.01	<0.01	<0.01
LOI	2.46	12.25	6.84	6.61	5.44	6.23
Total	101.46	100.65	98.82	100.24	100.97	101.19
C	0.03	2.89	1.4	1.17	0.75	0.84
S	0.01	0.05	2.28	0.01	<0.01	<0.01
Ba (ppm)	74.3	89.6	47.4	46	10.6	22.2
Ce	19.6	22.8	113.5	18.1	20.8	26.8
Cr	120	90	<10	120	130	190
Cs	0.09	0.23	0.21	0.06	<0.01	0.04
Dy	3.99	4.32	15.6	6.43	7.83	3.35
Er	2.53	2.45	9.17	4.28	4.75	1.88
Eu	1.32	1.42	4.46	1.9	1.7	0.91
Ga	19.7	16.6	21.6	16.9	21.9	18.2
Gd	3.96	4.15	15.05	6.56	6.97	3.04
Ge	<5	<5	<5	<5	<5	<5
Hf	3.4	3.6	17.6	2.6	3	3
Ho	0.81	0.83	3.28	1.5	1.73	0.7
La	7.6	8.8	44.6	8.2	9.2	11.6
Lu	0.31	0.32	1.27	0.59	0.63	0.32
Nb	7	7.8	38.2	5.8	6.4	7
Nd	13.6	14.7	66.9	15.7	16.9	13.2
Pr	2.85	3.25	15.45	2.78	3.03	3.24
Rb	3.9	16.7	10.2	3.1	0.2	2.1
Sm	4.18	4.15	15.55	4.65	5.71	3.12
Sn	1	1	3	4	1	1
Sr	306	179	134.5	113	86.2	122
Ta	0.4	0.7	2.6	0.3	0.4	0.4
Tb	0.66	0.73	2.52	1.05	1.22	0.55
Th	0.62	0.8	3.63	0.53	0.65	4.19
Tm	0.35	0.35	1.36	0.68	0.65	0.31
U	0.27	0.26	1.54	0.37	0.31	2.87
V	276	277	68	177	177	126
W	1	4	12	2	1	1
Y	20	23.2	81.6	34.5	37.4	17.5
Yb	2.16	2.09	8.67	3.78	3.97	1.62
Zr	130	140	811	122	137	118
As	61.6	1.8	74.1	1.5	3.8	1
Bi	0.01	0.01	0.07	<0.01	<0.01	0.01
Hg	<0.01	<0.01	0.01	<0.01	<0.01	<0.01
In	0.01	0.04	0.09	0.03	0.02	0.02

Table 2.1. Representative whole-rock analyses for Argyle

Sample ID	294859	294867	I951379	I951368	I951359	294852
Hole ID	AE-16-27	AE-16-26	AE-16-09	AE-16-34	AE-16-40	AE-16-43
Depth (m)	90.95	89.85	26.35	5	4	125.95
Lithology	Gabbro	Gabbro	Gabbro	HW breccia	HW lapilli tuff	FW lapilli tuff
Alteration	Distal	Intermediate	Proximal	Unaltered	-	-
Assemblage	Ep-Chl-Calc-Rt	Chl-Ep-Ank-Ab-Rut	Ab-Ank-Chl-Ms-Py	Calc-Chl-Ep	Ep-Chl-Calc	Chl-Calc
Re	0.00	0.00	0.00	0.00	0.00	0.00
Sb	0.41	0.08	0.14	0.07	0.29	0.16
Se	0.20	<0.2	3.40	0.30	<0.2	<0.2
Te	0.01	<0.01	0.40	<0.01	<0.01	<0.01
Tl	<0.02	<0.02	<0.02	<0.02	<0.02	<0.02
Ag	<0.5	<0.5	<0.5	<0.5	<0.5	<0.5
Cd	0.5	<0.5	<0.5	<0.5	<0.5	<0.5
Co	39	34	14	31	34	26
Cu	89	34	46	9	5	2
Li	20	20	<10	20	20	20
Mo	<1	<1	2	<1	<1	1
Ni	61	47	1	54	48	103
Pb	<2	<2	2	4	3	10
Sc	31	29	9	31	32	17
Zn	83	52	47	28	37	47
Au	0.001	0.002	5.05	<0.001	<0.001	<0.001
C (%)	<0.05	2.66	1.32	1.06	0.73	0.82
CO_2	0.20	9.8	8.6	3.9	2.7	3
AlOH WL (nm)	2225.01	2201.61	2196.18	N/A	N/A	N/A
AlOH D (%)	0.12	0.13	0.20	N/A	N/A	N/A
FeOH WL (nm)	2253.91	2258.89	2257.16	2256.27	2259.11	2258.03
FeOH D (%)	0.25	0.16	0.10	0.27	0.24	0.32
AlOH D/FeOH D	0.476	0.813	1.904	N/A	N/A	N/A
AlOH D/FeOH D	0.476	0.813	1.904	N/A	N/A	N/A

Abbreviations:
D = depth
WL = wavelength

Units:
HW = hanging wall
FW = footwall

Table 2.2. Principal components from principal component analysis, variance, and elemental associations with positive and negative principal component scores

Component	Variance (%)	Positive Scores	Negative Scores
1	31.88	Y, Lu, P_2O_5	MgO, CaO, Sc, Co, V
2	19.46	Fe_2O_3, TiO_2	CO_2, Cs, Ba, LOI, K_2O, Rb
3	14.57	Fe_2O_3, TiO_2, MnO, Zn	Al_2O_3, Na_2O, SiO_2
4	7.92	LOI, CO_2	As, Cu, Al_2O_3, Ba, Cs
5	5.12	Cu, Al_2O_3, CO_2, Na_2O, W	SiO_2, MnO, Ba, Cs, Sr, Zn

Table 2.3. Average gabbro alteration characteristics

	Distal			Intermediate			Proximal		
	Avg	Min	Max	Avg	Min	Max	Avg	Min	Max
Index AI	35.61	25.7	50	32.97	21.34	67.86	28.96	14.31	48.94
CCPI	60.32	55.07	70.53	59.03	51.27	74.08	58.92	45.81	76.29
CO_2/CaO	0.42	0.01	1.45	0.49	0.01	1.42	1.01	0.01	2.65
CO_2/(Mg+Fe+Ca)	0.20	0.01	0.75	0.27	0.01	0.81	0.44	0.01	1.1
CO_2/(Ca+Mg+Fe-0.5*(S+As))	0.23	-0.08	0.76	0.32	-1.38	2.30	0.63	-24.10	31.58
CO_2/LOI	0.42	0.01	0.95	0.58	0.02	2.17	0.66	0.01	1.35
(K_2O+CO_2)/(K_2O+CO_2+Na_2O+Al_2O_3)	0.16	0.01	0.47	0.20	0.01	0.44	0.28	0.02	0.63
3K/Al	0.08	0.01	0.48	0.16	0.02	0.93	0.26	0.02	1.18
Na/Al	0.33	0.22	0.45	0.33	0.06	0.52	0.36	0.05	0.6
K/Ti	0.08	0.01	0.48	0.16	0.02	0.93	0.26	0.02	1.18
Y/Ti	19.65	12.25	25.07	21.80	12.92	47.76	36.43	11.65	113.37
Rb/Ti	5.00	0.40	20.27	8.91	0.46	101.70	11.16	0.64	118.52
Element S (%)	0.03	0.01	24.70	0.03	0.01	0.41	0.31	0.01	2.73
Au (ppm)	0.00	0.00	0.02	0.02	0.00	0.51	0.75	0.00	10.65
Ag	0.33	0.25	0.5	0.28	0.25	0.50	0.30	0.25	0.7
As	13.33	1	100.5	7.92	1	55.4	27.32	1	244
Bi	0.01	0.01	0.03	0.01	0.01	0.05	0.05	0.01	1.32
Sb	0.31	0.07	0.86	0.24	0.07	0.88	0.18	0.05	0.82
Te	0.01	0.01	0.01	0.01	0.01	0.04	0.13	0.01	4.62
W	1.37	0.5	5.00	2.53	0.5	38	6.63	0.5	29
Zr	160.65	115	363	159.9	118	516	356.69	73	811
Ba	56.6	24.7	135.5	57.1	20.7	264	78.51	20.9	180
Sr	228.37	110	413	195.39	113.5	609	207.83	98.5	558
Cs	0.16	0.02	0.47	0.17	0.01	1.84	0.18	0.03	0.48
Rb	5.65	0.5	21.3	6.64	0.9	56.70	12.25	1	40.5
Cu	47.88	6	171	29.69	3	88	32.81	1	144
Ni	53.4	0.5	92	32.91	0.5	175	14.8	0.5	144
Pb	1.54	1	5	1.63	1	6	2.06	1	6
Zn	73.85	45	132	59.33	47	134	95.3	42	221
SWIR AlOH wavelength (nm)	2216	2191	2227	2210	2189	2227	2199	2188	2227
AlOH depth	0.14	0.06	0.21	0.16	0.03	0.43	0.21	0.02	0.46
FeOH wavelength (nm)	2254	2250	2260	2255	2241	2263	2256	2241	2264
FeOH depth	0.21	0.11	0.32	0.2	0.08	0.34	0.12	0.01	0.27
AlOH depth/FeOH depth	0.64	0.33	0.88	0.96	0.22	4.01	2.6	0.35	16.8

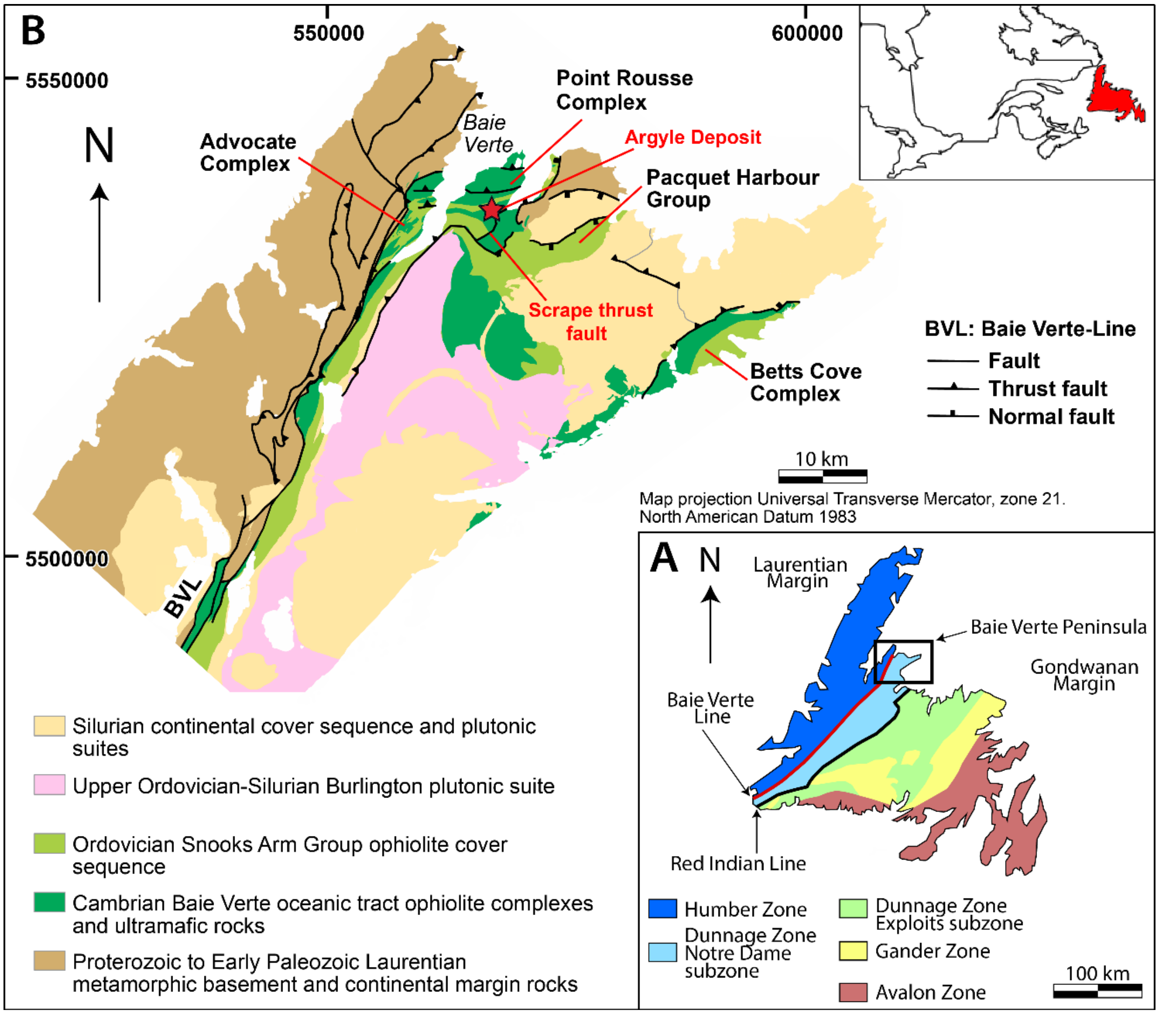

Figure 2.1. A) Simplified map of tectonostratigraphic terranes of Newfoundland (modified after Williams, 1979 and Skulski et al., 2010). B) Geology map of the Baie Verte Peninsula (modified after Skulski et al., 2010 and Ybarra, 2019). Inset shows the location of the Baie Verte Peninsula in Newfoundland.

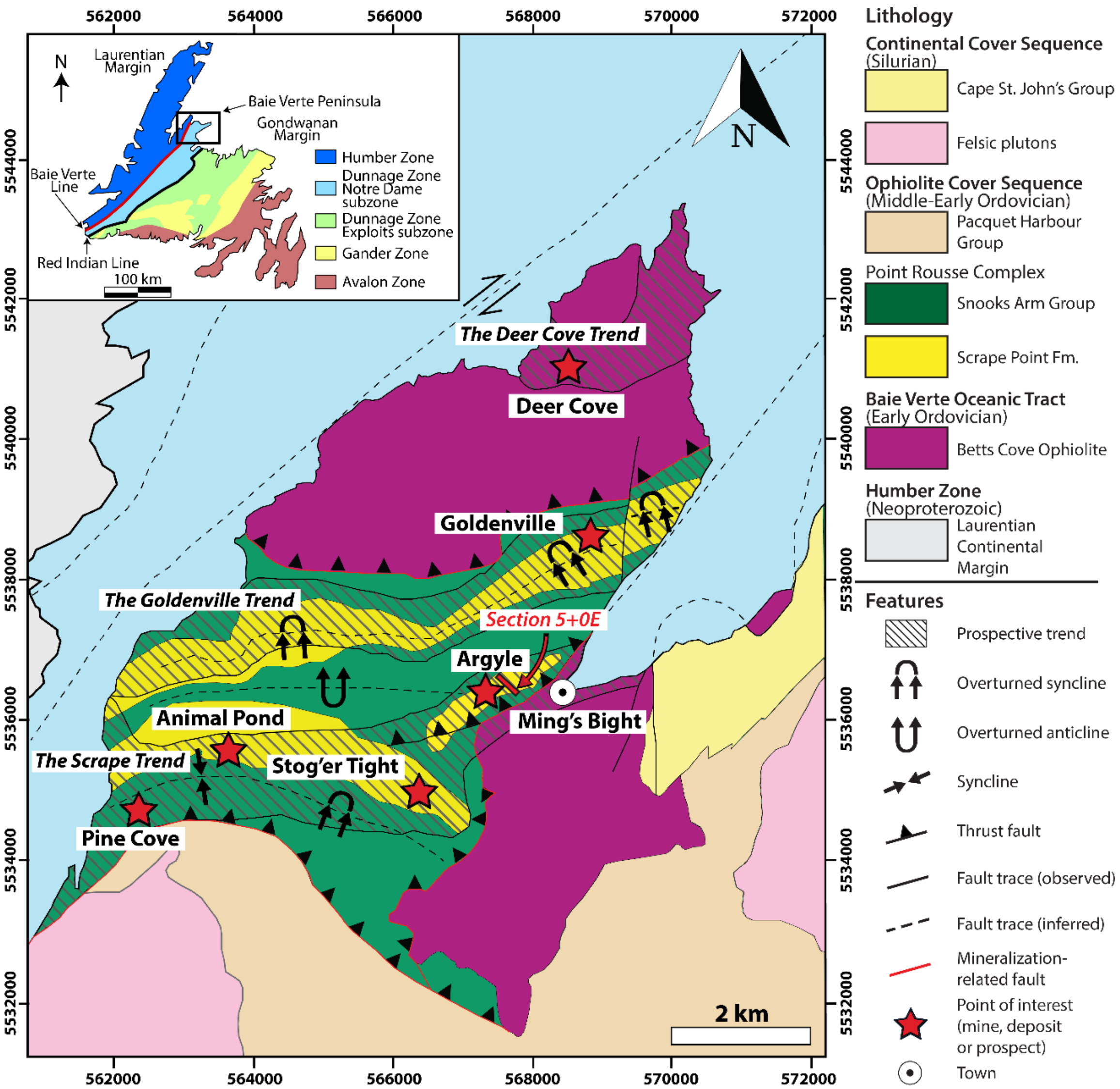

Figure 2.2. Simplified geological map of the Point Rousse project on the Baie Verte Peninsula. Relative position of Argyle, Stog'er Tight and Animal Pond deposits are symbolized by red stars. Modified from Skulski et al. (2010) and Anaconda Mining's NI 43-101 for the Point Rousse Project by Cullen et al. (2018). Inset shows the location of the Baie Verte Peninsula.

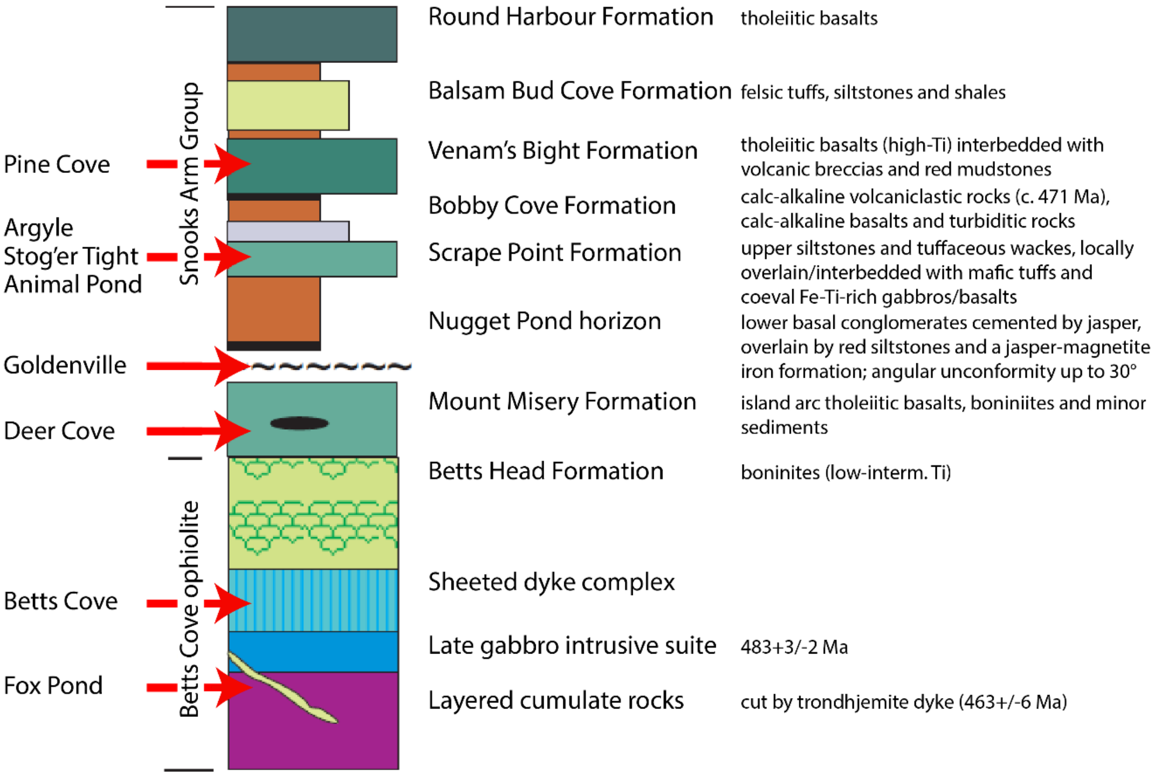

Figure 2.3. Stratigraphy of the Point Rousse Complex (modified after Skulski et al., 2009).

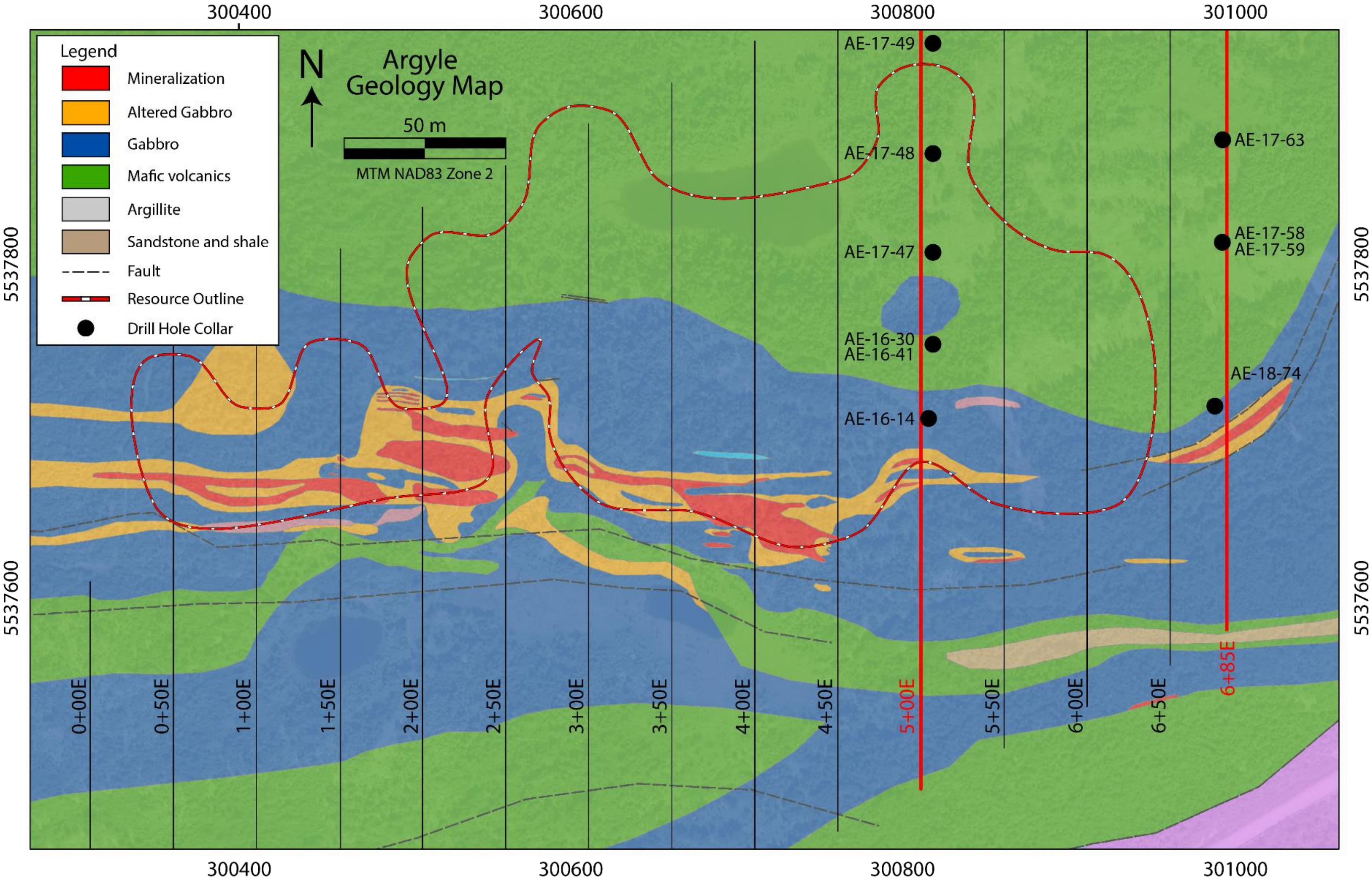

Figure 2.4. Geological map of the Argyle deposit with highlighted sections 5E and 6+85E (modified after Anaconda Mining Inc. Press Release, January 8th, 2018).

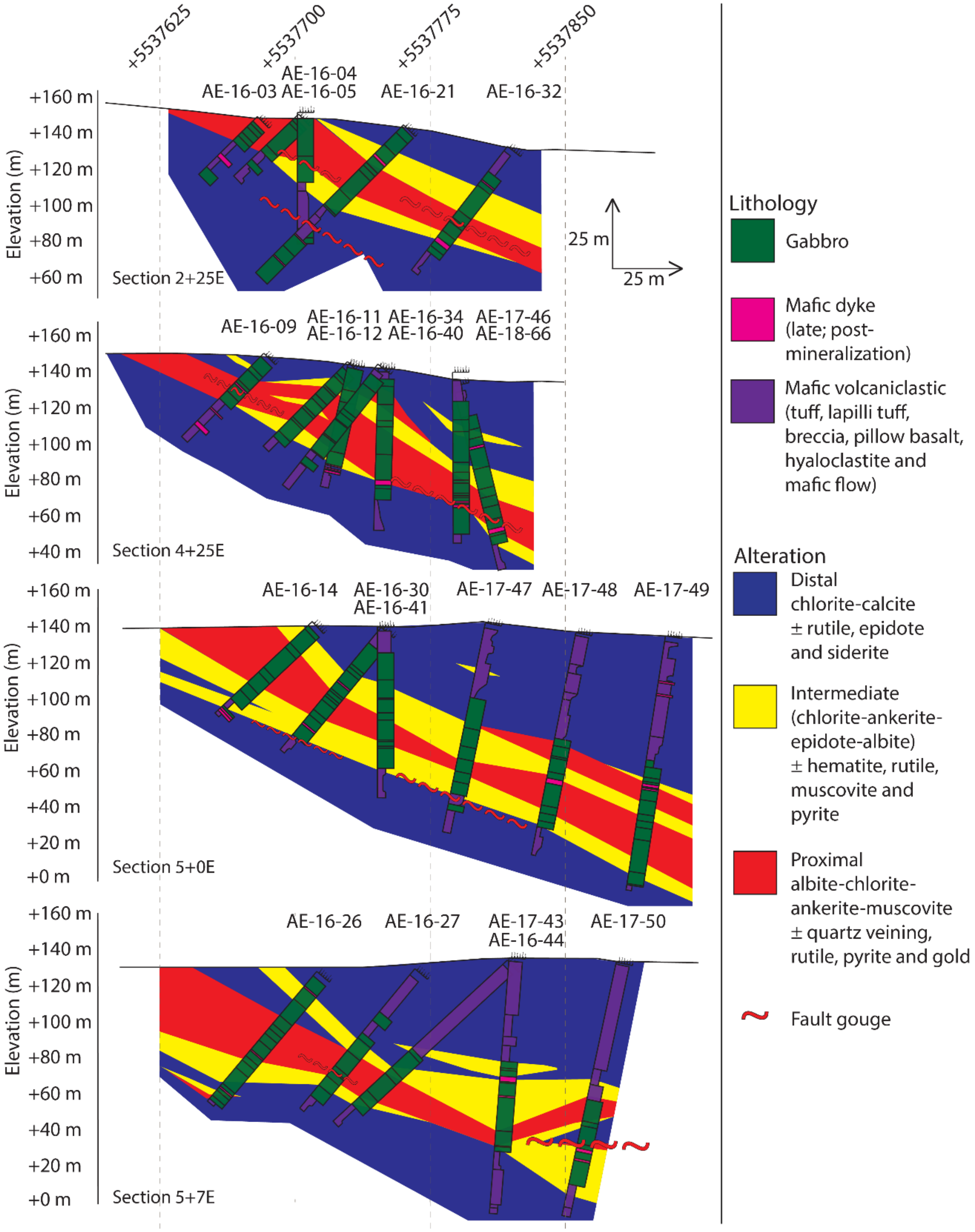

Figure 2.5. Key cross-sections through the Argyle deposit. All sections looking west.

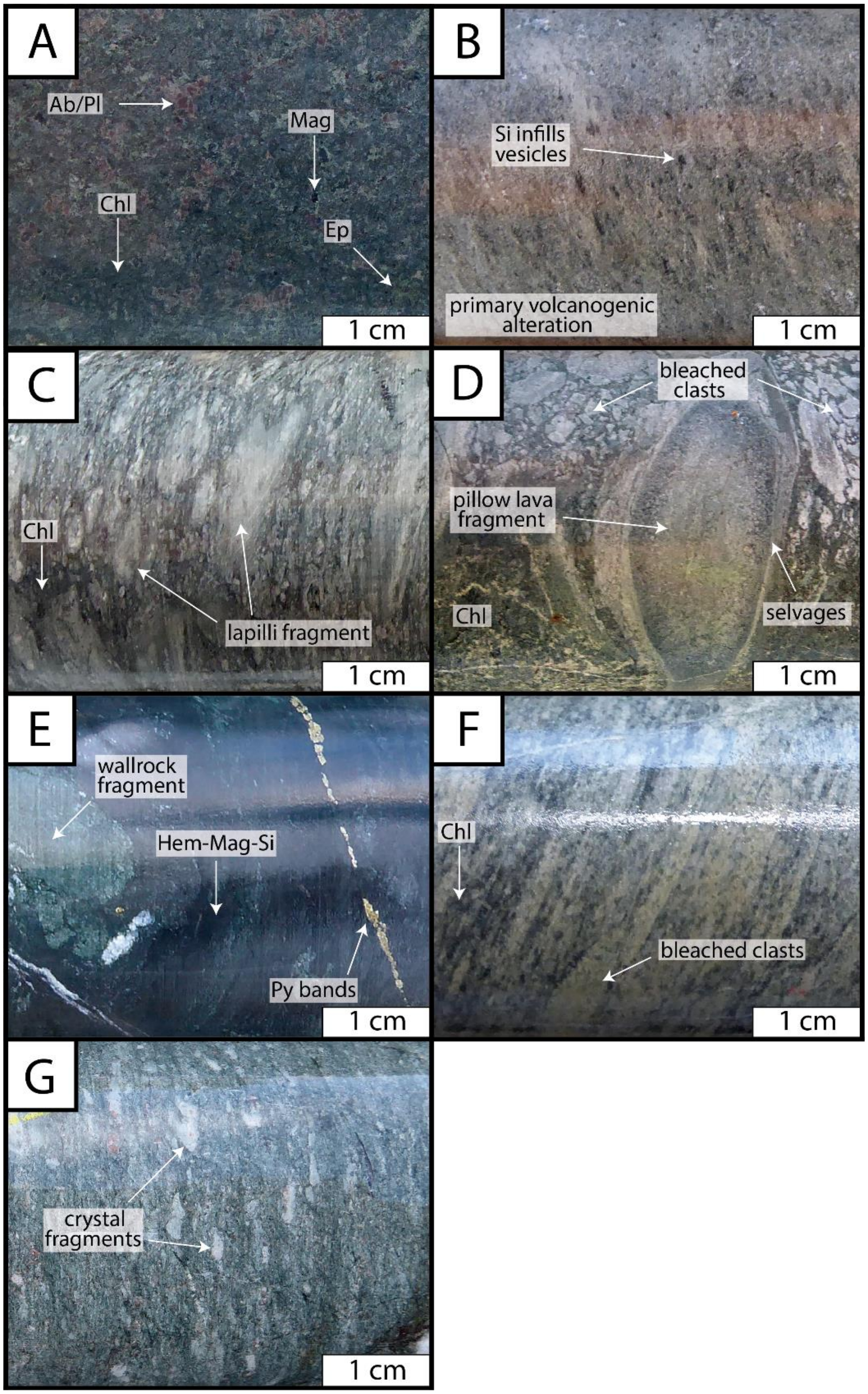

Figure 2.6. Main lithologies of the Argyle deposit. A) Coarse-grained relatively fresh gabbro. B) Hanging wall mafic tuff with primary volcanogenic alteration and black Si infill of vesicles. C) Hanging wall mafic lapilli tuff with bleached clasts. D) Hanging wall mafic breccia with fragments of brecciated clasts and pillow lava fragments, which show chilled margins. E) Hanging wall hematite-magnetite-silica iron formation with chloritized wallrock fragments. F) Footwall mafic lapilli with bleached clasts. J) Footwall crystal tuff with common crystal fragments.

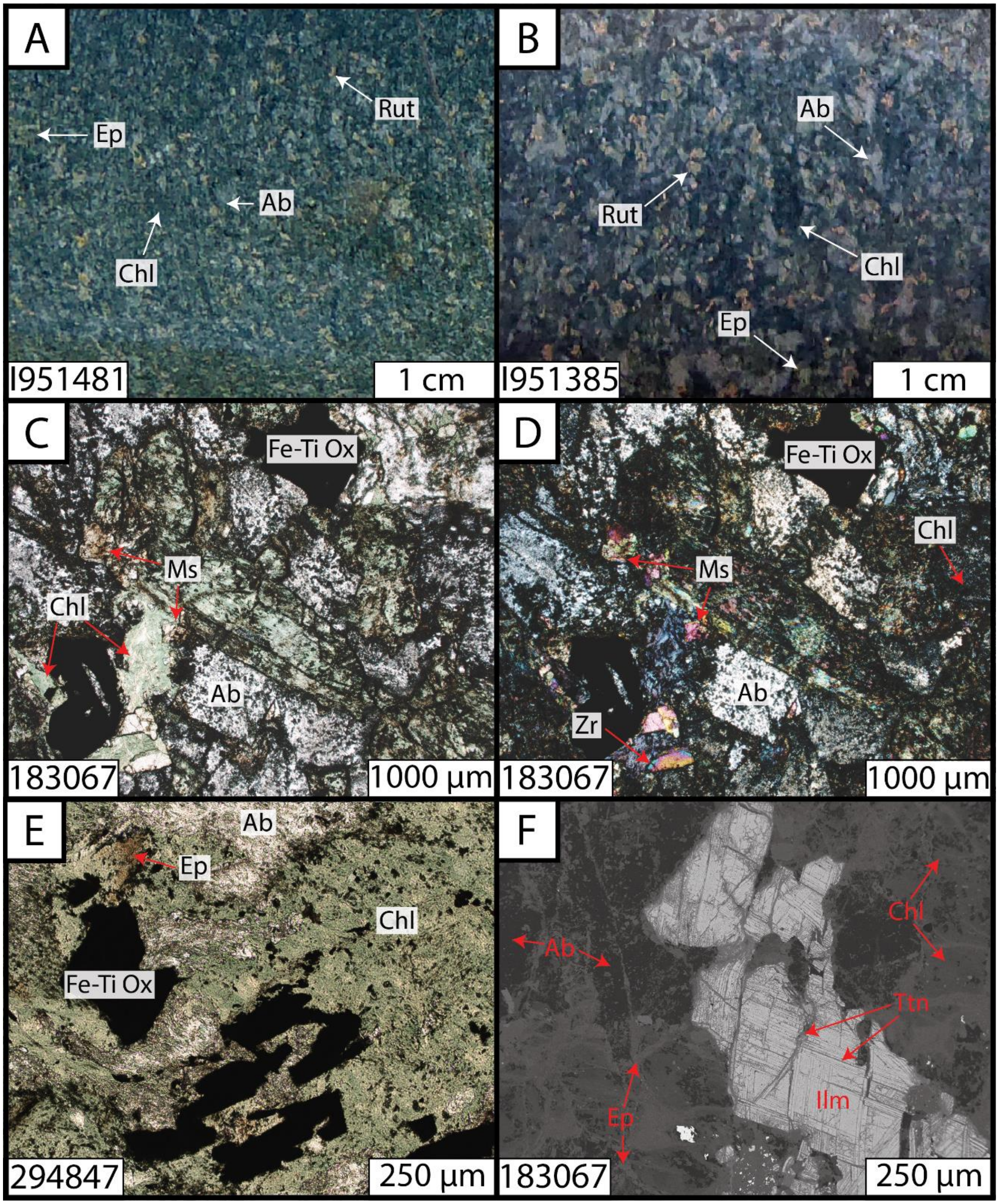

Figure 2.7. Photographs and photomicrographs of distal alteration Argyle gabbro. A) Fine-grained strongly chloritized gabbro with weak albite and rutile alteration. B) Medium-grained chlorite-rutile altered gabbro. C) and D) Weak chlorite epidote alteration of gabbro. E) Chlorite-epidote alteration of gabbro with relatively unaltered Fe-Ti mineral phases. F) Least altered Fe-Ti phase.

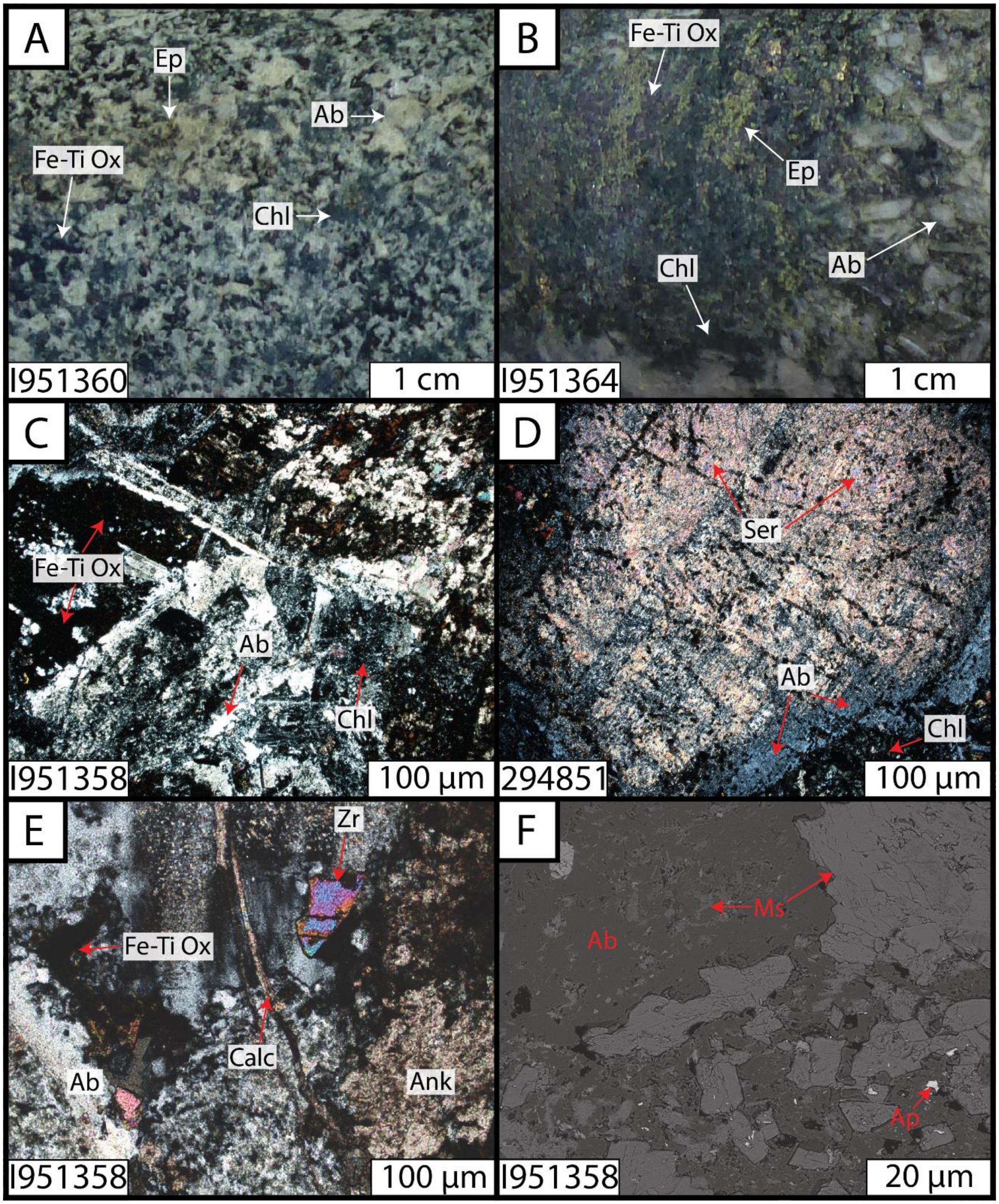

Figure 2.8. Photographs and photomicrographs of intermediate alteration Argyle gabbro. A) Medium-grained chlorite-albite-epidote altered gabbro (intermediate alteration zone). B) Coarse-grained albite-epidote-chlorite altered gabbro (intermediate alteration zone). C) Typical intermediate alteration of gabbro with remnant disintegrating ilmenomagnetite with strong fine-grained dark green-grey chlorite, buff ankerite alteration of pyroxene, and weak-moderate high-birefringence sericite alteration of plagioclase. D) Sericite altered centre of an albite crystal with unaltered albite rim. E) Damaged high-birefringence zircon next to a calcite veinlet within partially moderately ankerite-sericite altered albite crystal. F) SEM backscatter documenting partial sericitization (lighter grey) of albite (darker grey) groundmass.

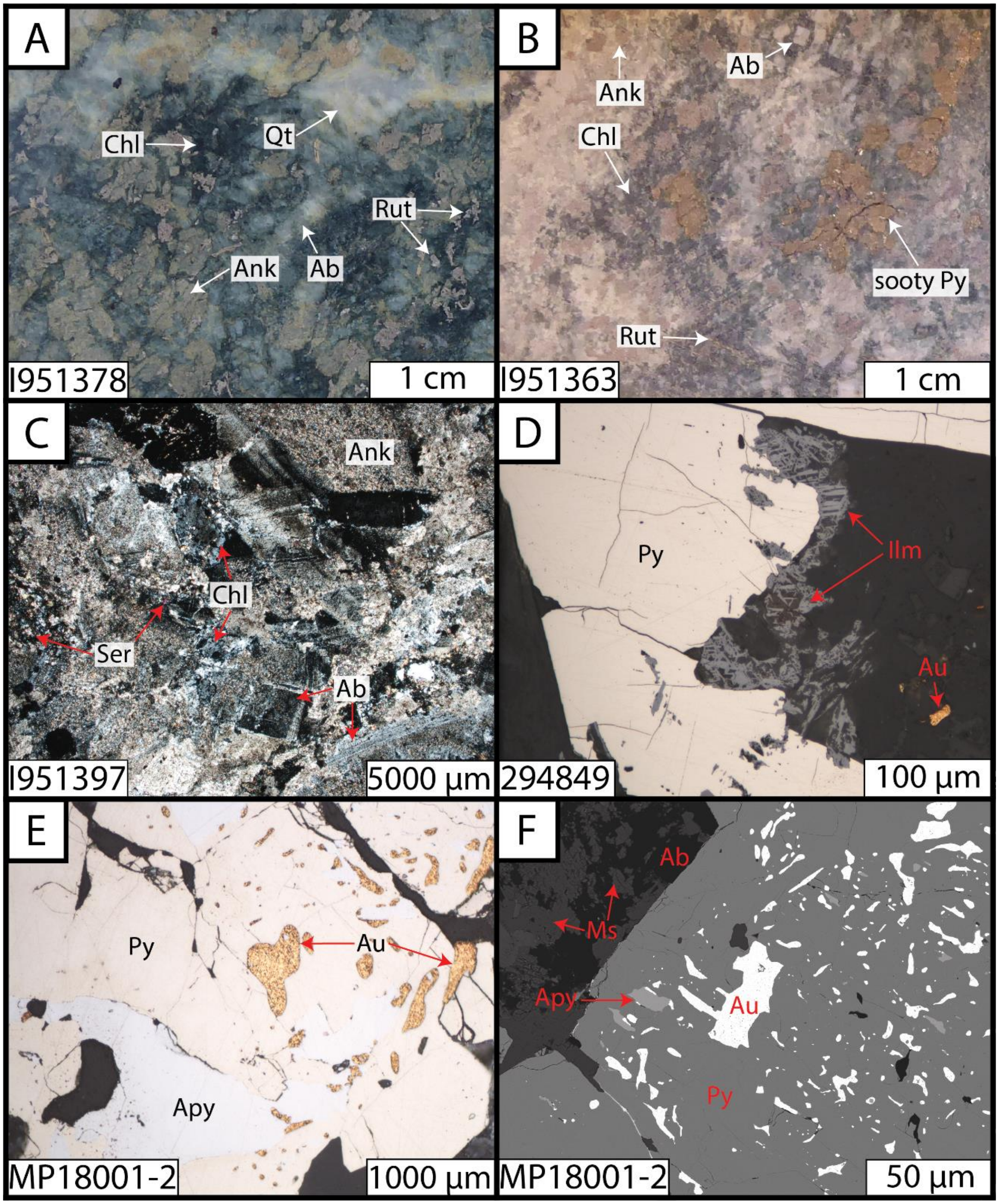

Figure 2.9. Photographs and photomicrographs of proximal alteration Argyle gabbro. A) Tan ankerite overprint of albite-chlorite-rutile altered gabbro, quartz-carbonate veinlet at the top. B) Coarse sooty anhedral pyrite mineralization within albite-quartz-chlorite altered gabbro wallrock. C) Strongly sericite and ankerite altered albite-dominated gabbro. D) Pyrite and gold precipitating at a site previously occupied by ilmenite, note the exsolution lamellae in ilmenite and spatial association of gold with pyrite. E) Gold and arsenopyrite-gold infilling voids and fractures within sooty pyrite. F) Backscatter image of gold infilling voids and fracture within sooty pyrite.

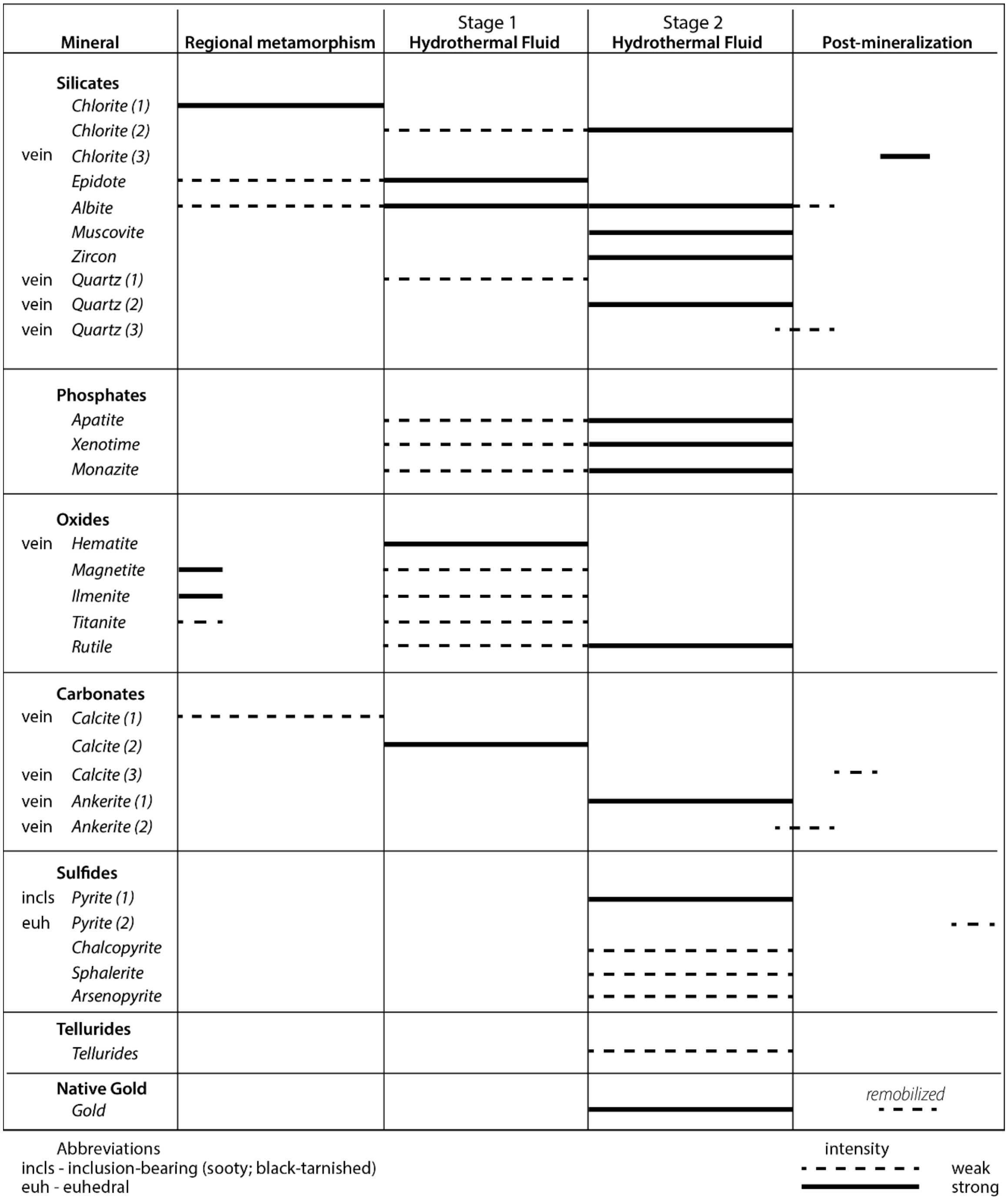

Figure 2.10. Alteration and ore mineral paragenesis at the Argyle deposit.

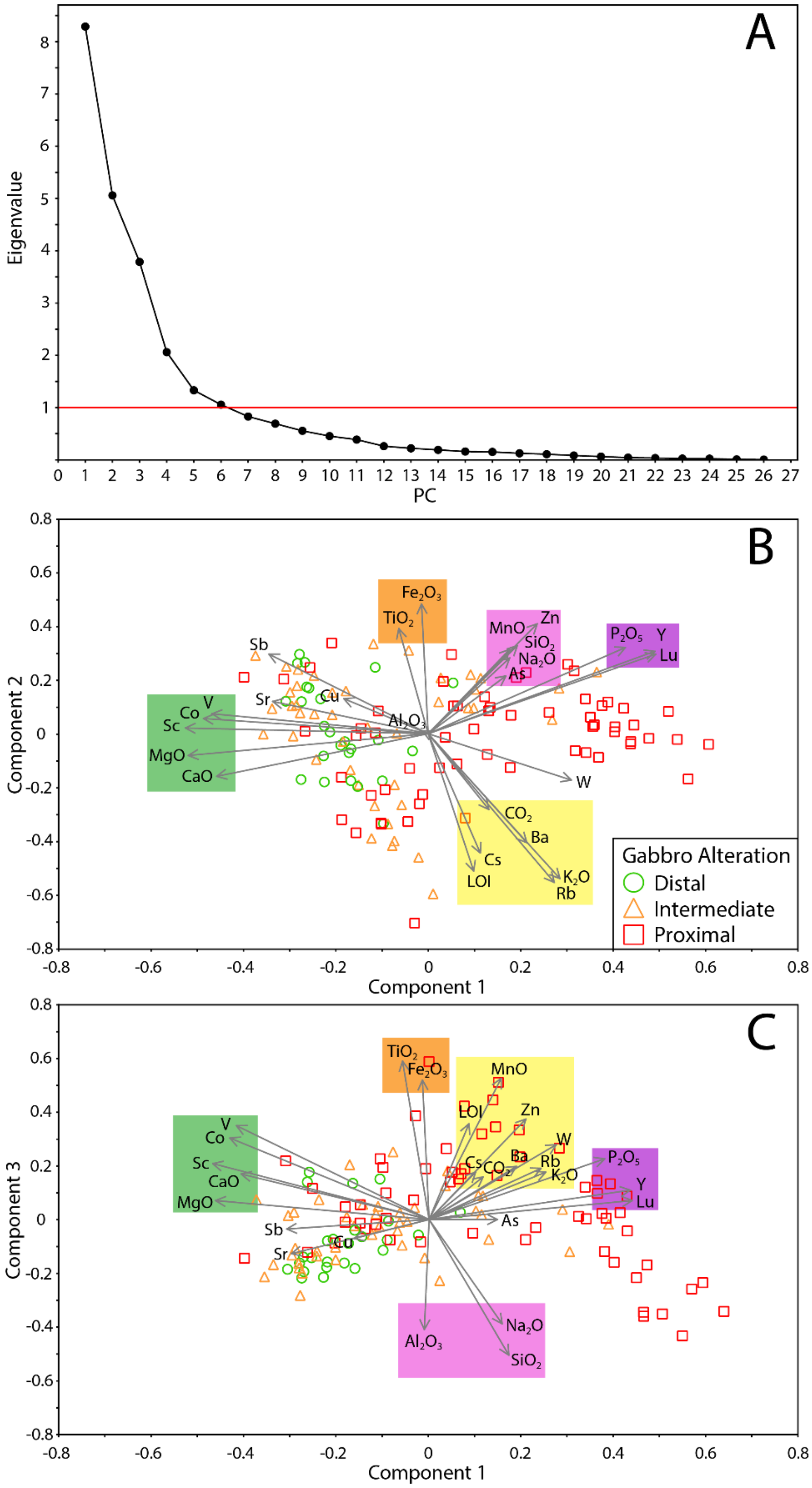

Figure 2.11. Principal component analysis results. A) Scree plot defining the importance of components. B) Plot of component 1 vs component 2, and C) component 1 vs component 3, which highlight elemental associations between elements and inferred processes.

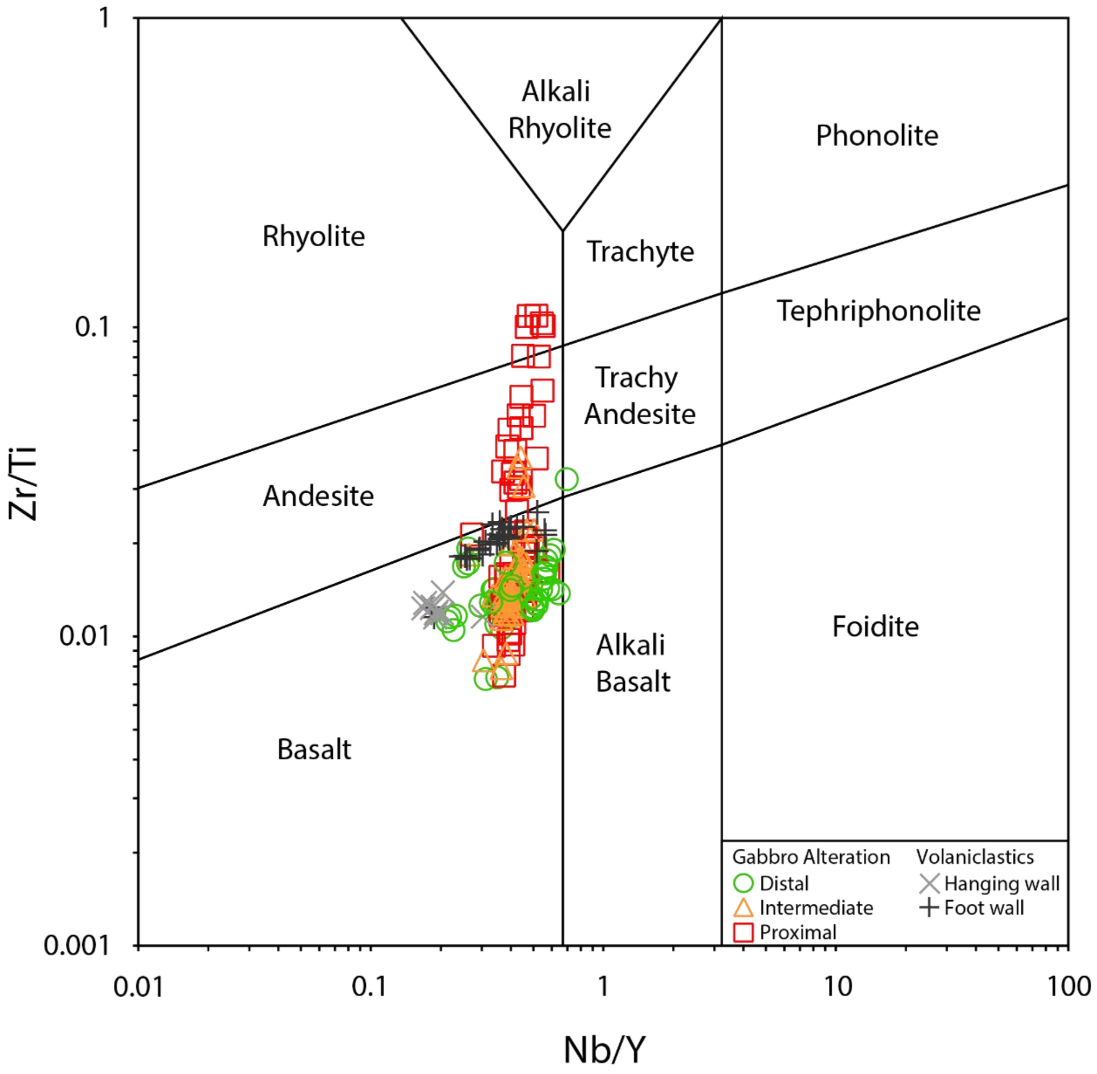

Figure 2.12. Volcanic rock classification from Pearce (1996), modified after Winchester and Floyd (1977). Log Nb/Y vs log Zr/Ti immobile element proxy for the TAS diagram classifies all samples as sub-alkaline.

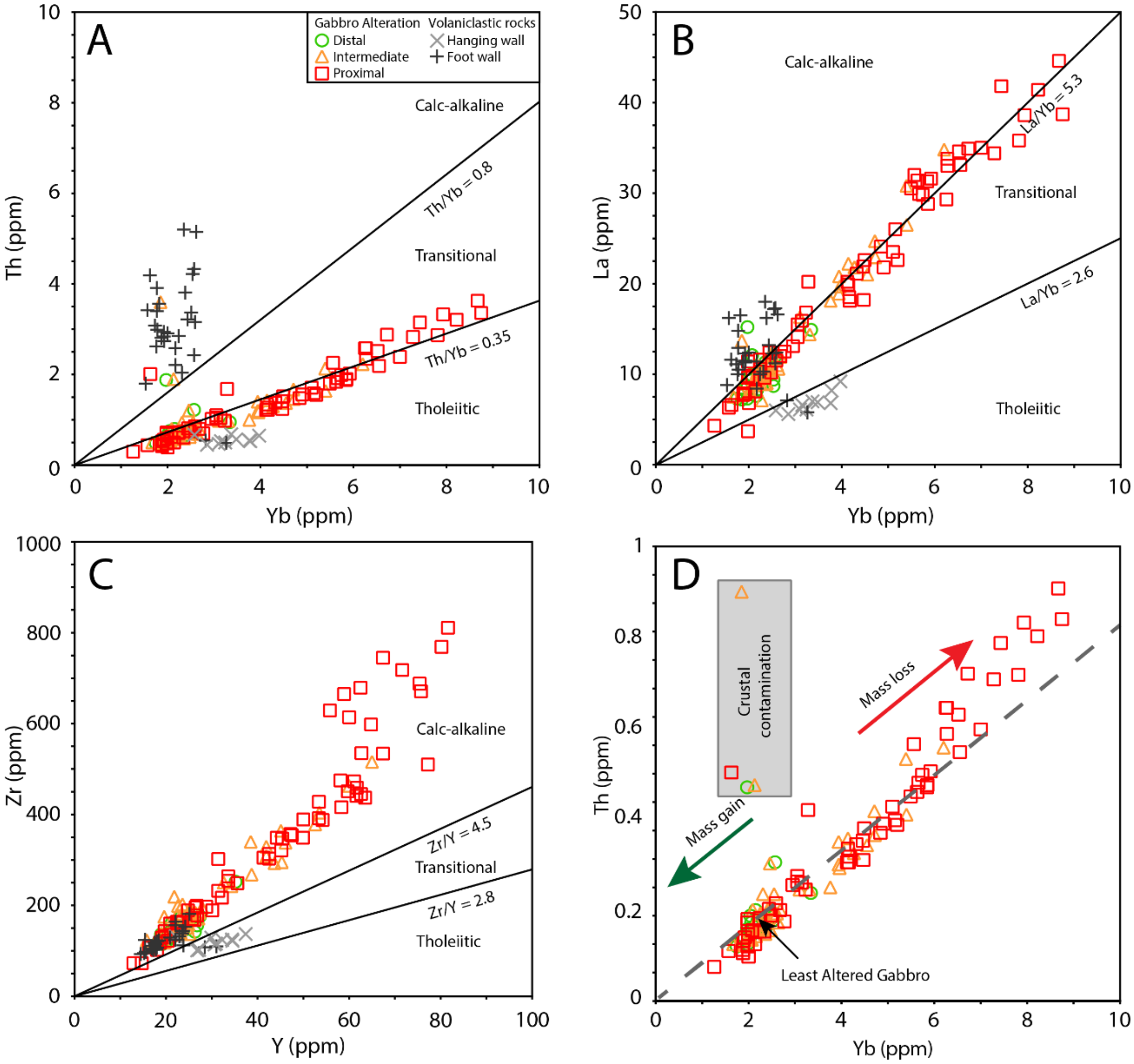

Figure 2.13 Immobile element ratio plots of Argyle samples. A) Ross and Bédard (2009) Yb vs Th magma affinity discrimination diagram, suggests that the gabbro is tholeiitic, which reflects the high TiO_2 content of the gabbro and the presence of Fe-Ti oxides in drill core and thin sections. B and C (Yb vs La and Y vs Zr after Ross and Bédard, 2009) show contrasting associations, which are likely affected by the presence of mobile xenotime and monazite (Piercey and Copeland, 2017). D) Yb vs Th most immobile element plot shows the alteration trend line for the Argyle gabbro. The trend indicates a single gabbro precursor. Mass gain and loss of mobile elements has caused the shift of Nb and Zr relative concentrations in the directions shown by arrows.

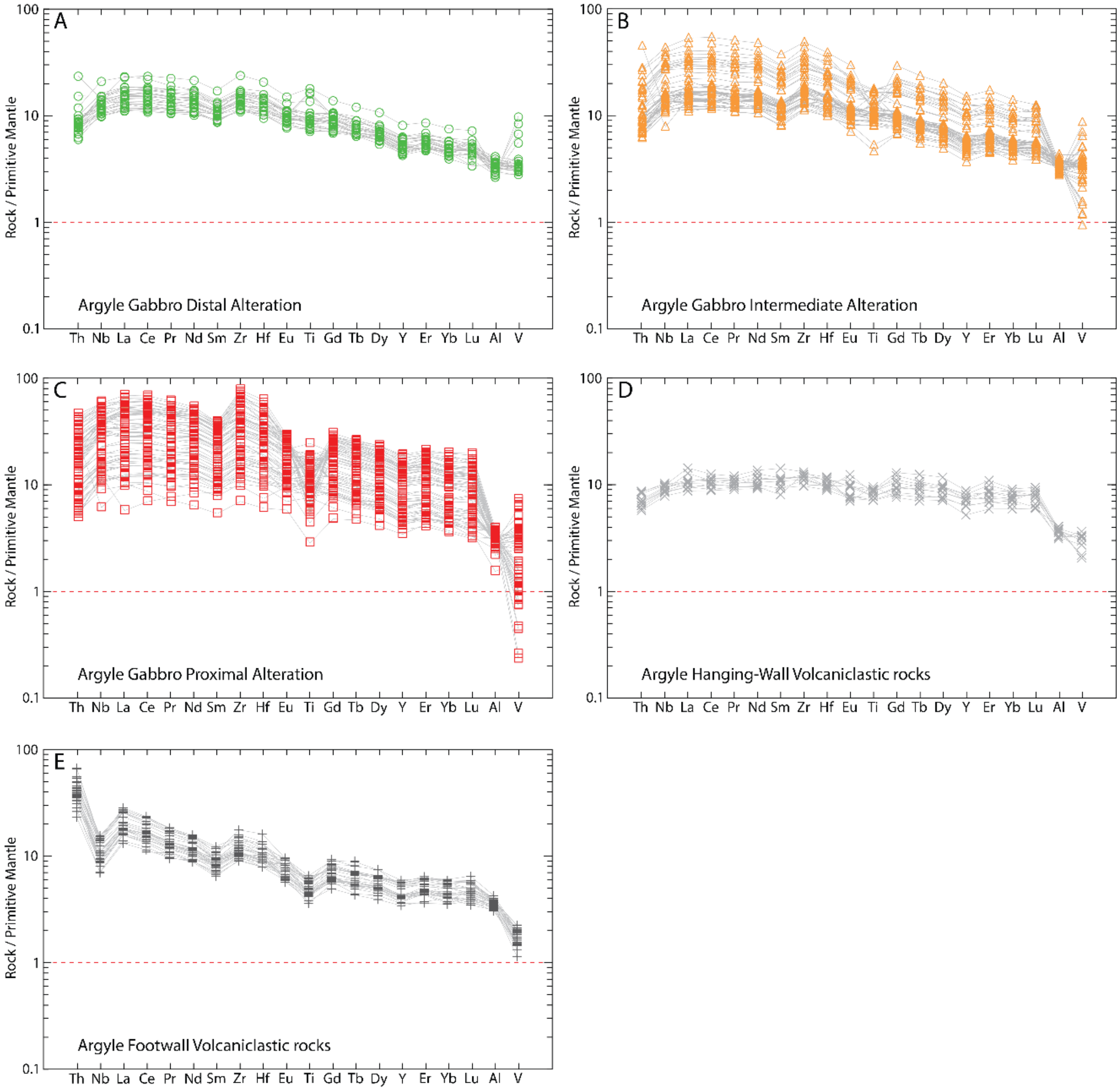

Figure 2.14. PM-normalized plots of samples from the Argyle deposit (normalized to primitive mantle using McDonough and Sun, 1995). A) Argyle distal alteration gabbro. B) Argyle intermediate alteration gabbro. C) Argyle proximal alteration gabbro. D) Argyle hanging wall volcaniclastic rocks. E) Argyle footwall volcaniclastic rocks.

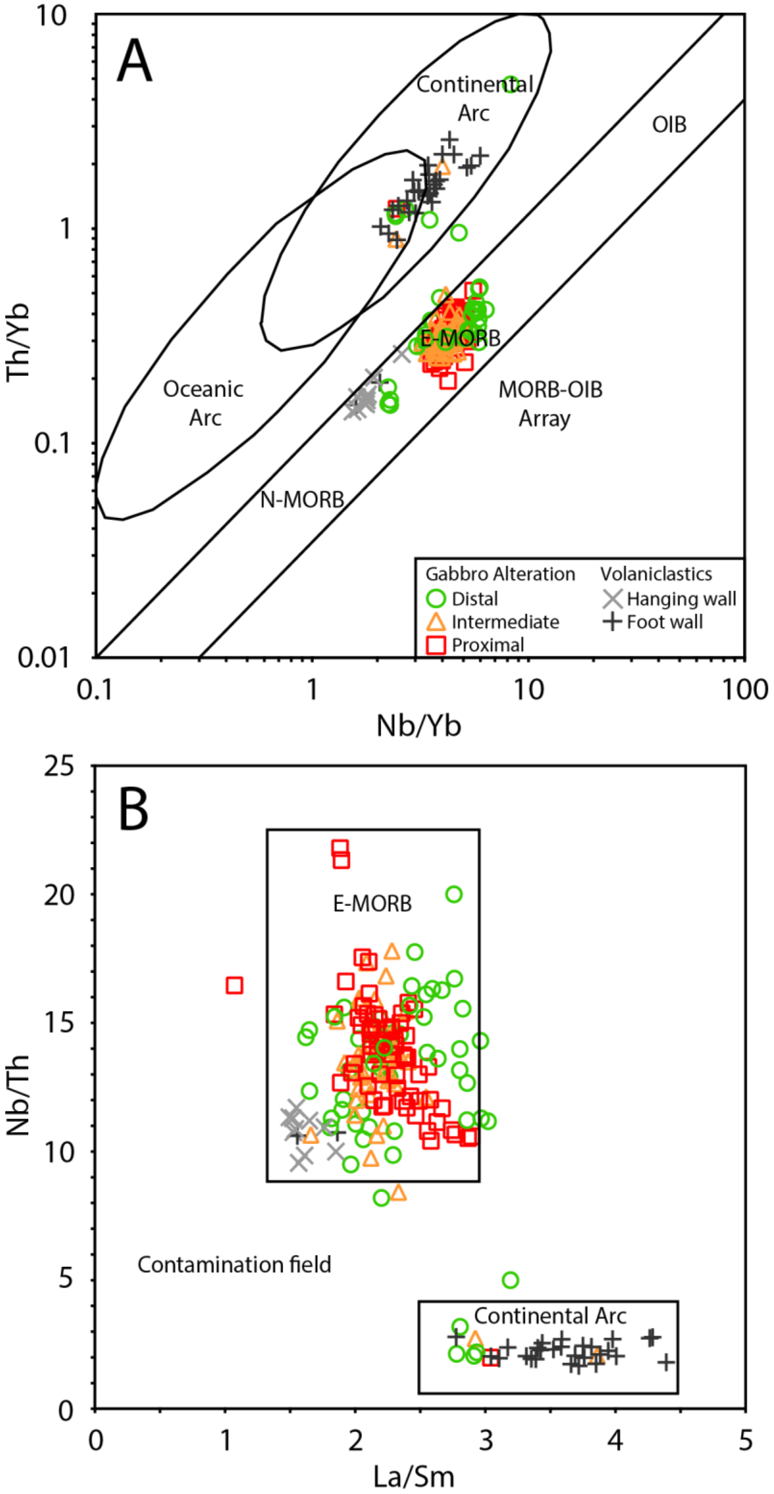

Figure 2.15. Immobile element plots assessing the affinity of magma, source region and contamination of mafic rocks from the Argyle gold deposit A) Pearce (2014) Nb/Th vs Th/Yb tectonic discrimination diagram. B and C) La/Sm vs Nb/Th and Zr vs Th/Nb (Piercey et al., 2002) source region and contamination assessment diagrams.

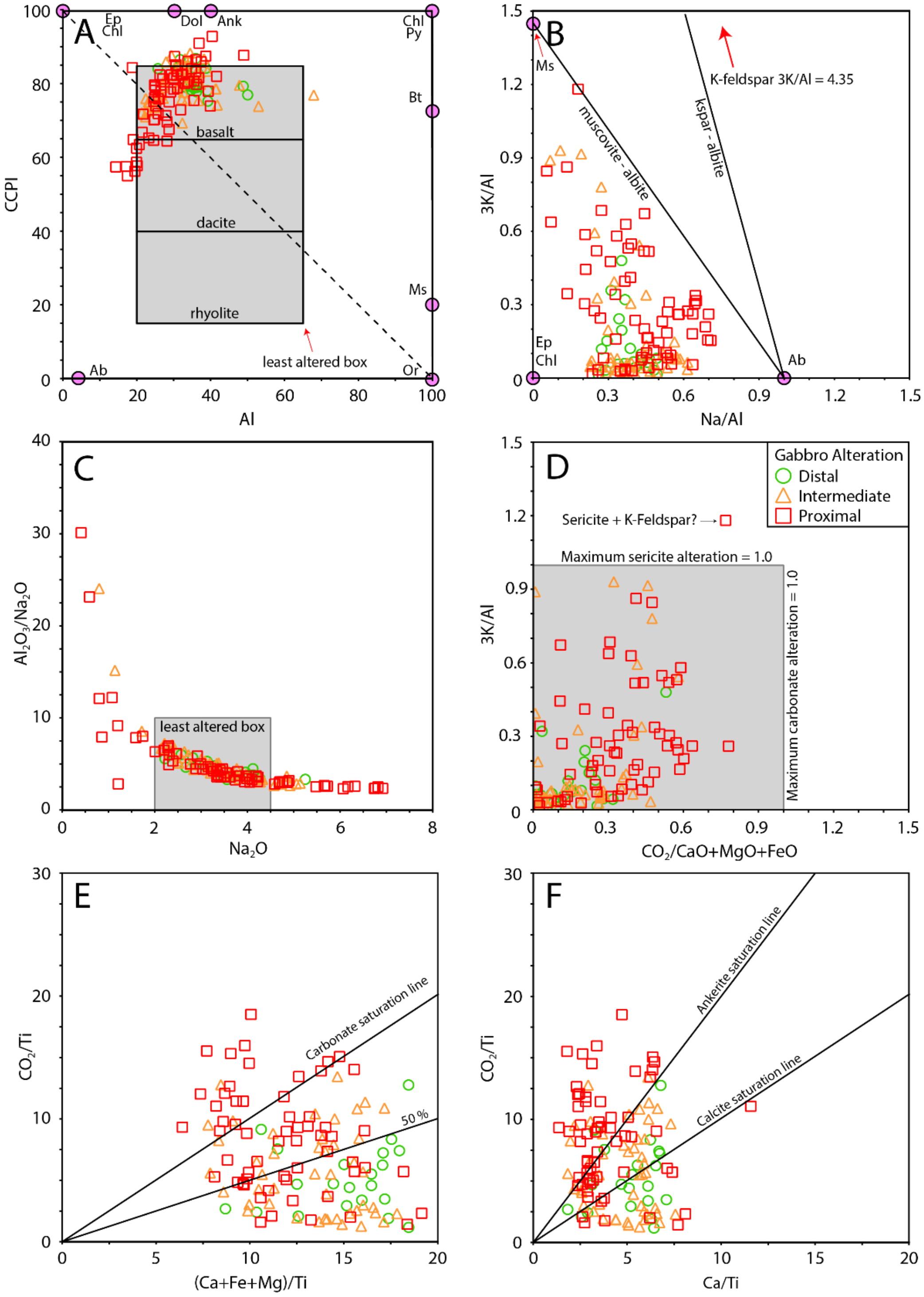

Figure 2.16. Mobile element plots for gabbroic rocks from the Argyle gold deposit. A). Alteration plot - Hashimoto alteration index (AI; Ishikawa et al., 1976) vs. chlorite-carbonate-pyrite index (CCPI; Large et al., 2001) B) Albite saturation index vs. sericite saturation index. C) Sodium alteration plot vs. Spitz-Darling index (Spitz and Darling, 1978). D) Carbonate saturation index vs. Sericite saturation index. E) Ca+Ti+Mg/Ti vs. CO_2/Ti and F) Ca/Ti vs. CO_2/Ti (Christie and Braithwaite, 1988) quantify the carbonate saturation in gabbro samples.

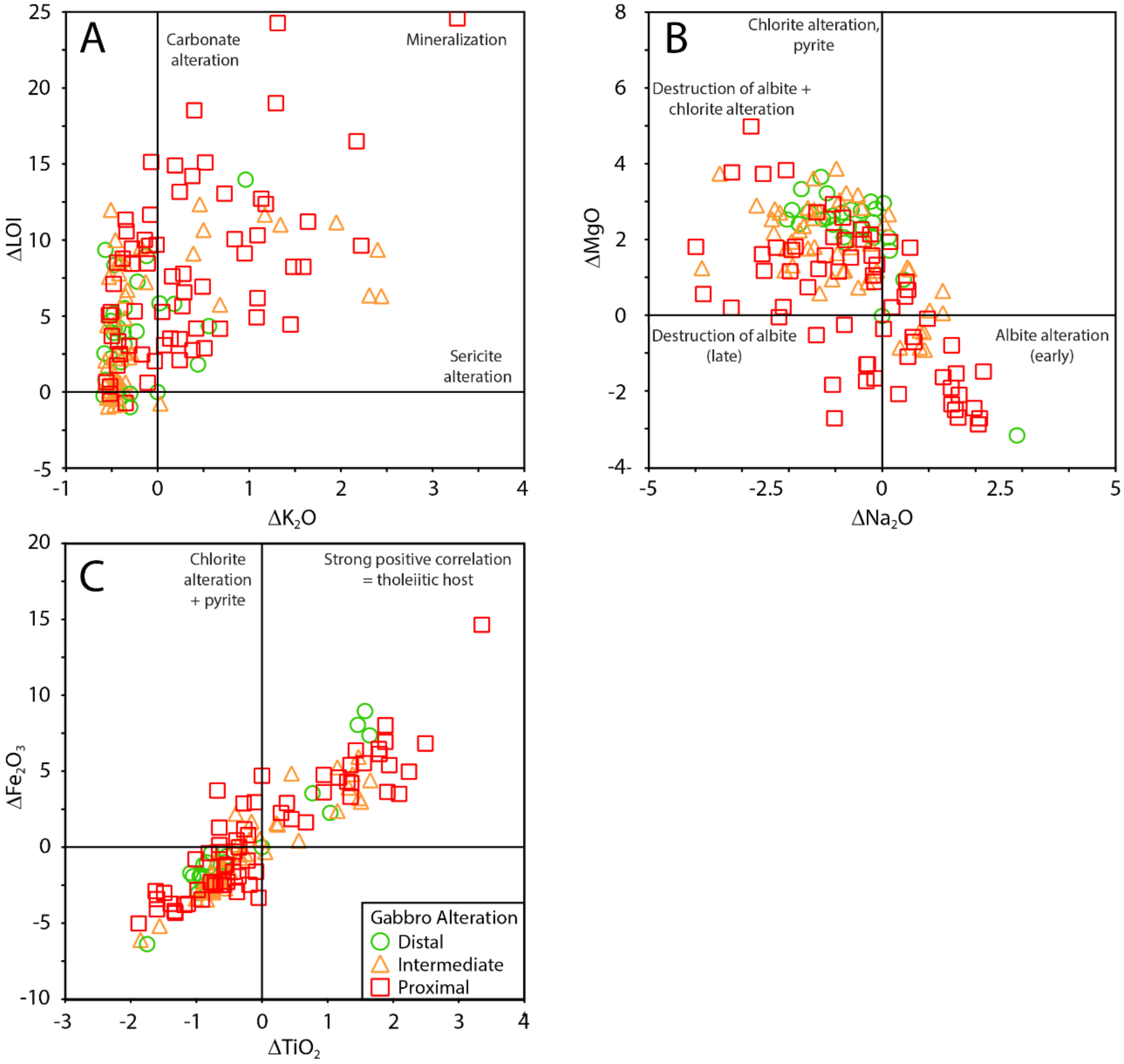

Figure 2.17. Mass change plots that highlight the key processes involved in the hydrothermal alteration of the Argyle gabbro. A) Mass change plot of K_2O vs. LOI, highlighting both sericite and carbonate alteration, highest Au grades are found where correlation between sericite and carbonate is the highest. B) Mass change plot of Na_2O vs MgO, which shows the presence of strong albite alteration (early) in some samples and the destruction (sericite alteration; later) of albite in others. C) Mass change plot of TiO_2 vs Fe_2O_3, which shows a strong positive correlation, highlighting the tholeiitic primary chemistry of the gabbro. Mass losses in proximal zone due to reactive TiO_2 and the strong presence of quartz and ankerite, which could dilute the TiO_2 content.

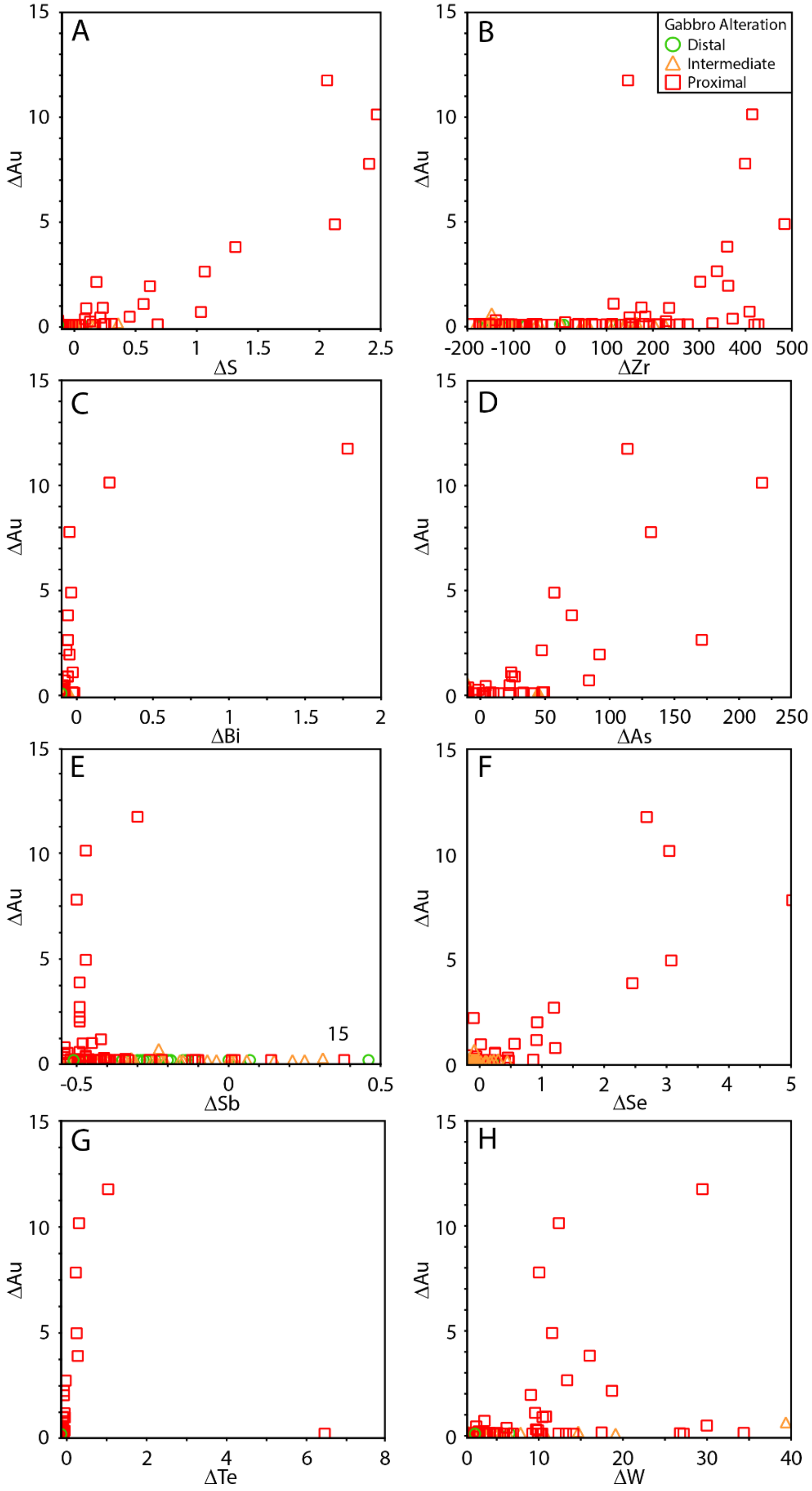

Figure 2.18. Mass change plots of pathfinder minerals related to gold.

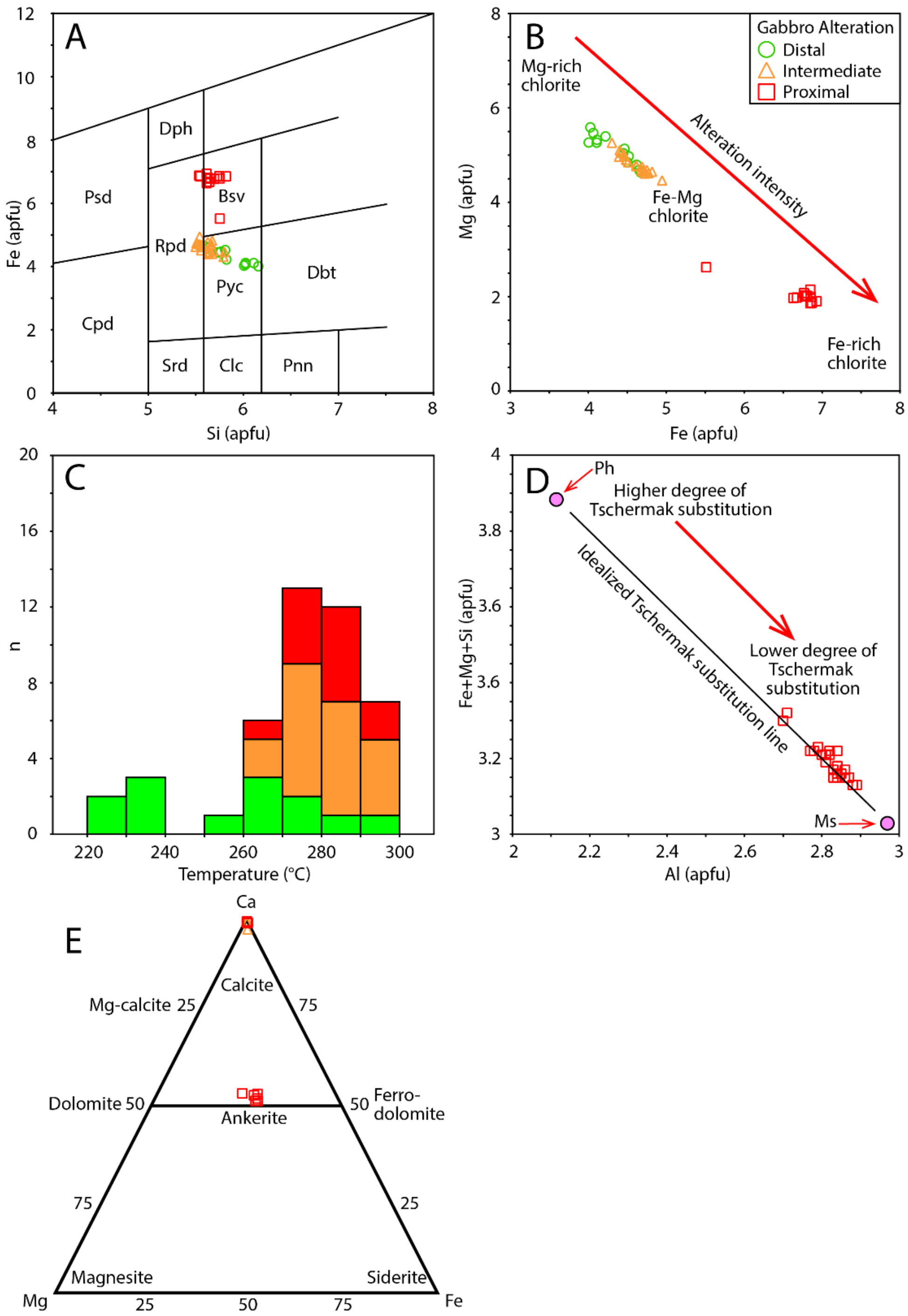

Figure 2.19. Mineral chemistry plots based on EMPA data. A) Si (apfu) vs Fe (apfu) chlorite classification plot. Dph = Daphnite. Psd = Pseudothuringite. Rpd = Ripidolite. Bsv = Brunsvigite. Pyc = Pycnochlorite. Dbt = Diabentite. Corundophilite. Cdp = Corundophilite. Srd = Sheridanite. Clc = Clinochlore. Pnn = Penninite. B) Fe (apfu) vs Mg (apfu) plot shows zoning in chlorite across alteration zones. C) Histogram for temperatures of chlorite defined by the Kranidiotis and MacLean (1987) chlorite geothermometer. Green = distal. Orange = intermediate. Red = proximal. D) Al (apfu) vs Fe+Mg+Si (apfu) shows the muscovitic signature of white mica. E) Ternary Mg-Ca-Fe plot for carbonates indicates the presence of calcite in all alteration zones and ankerite constrained to proximal alteration.

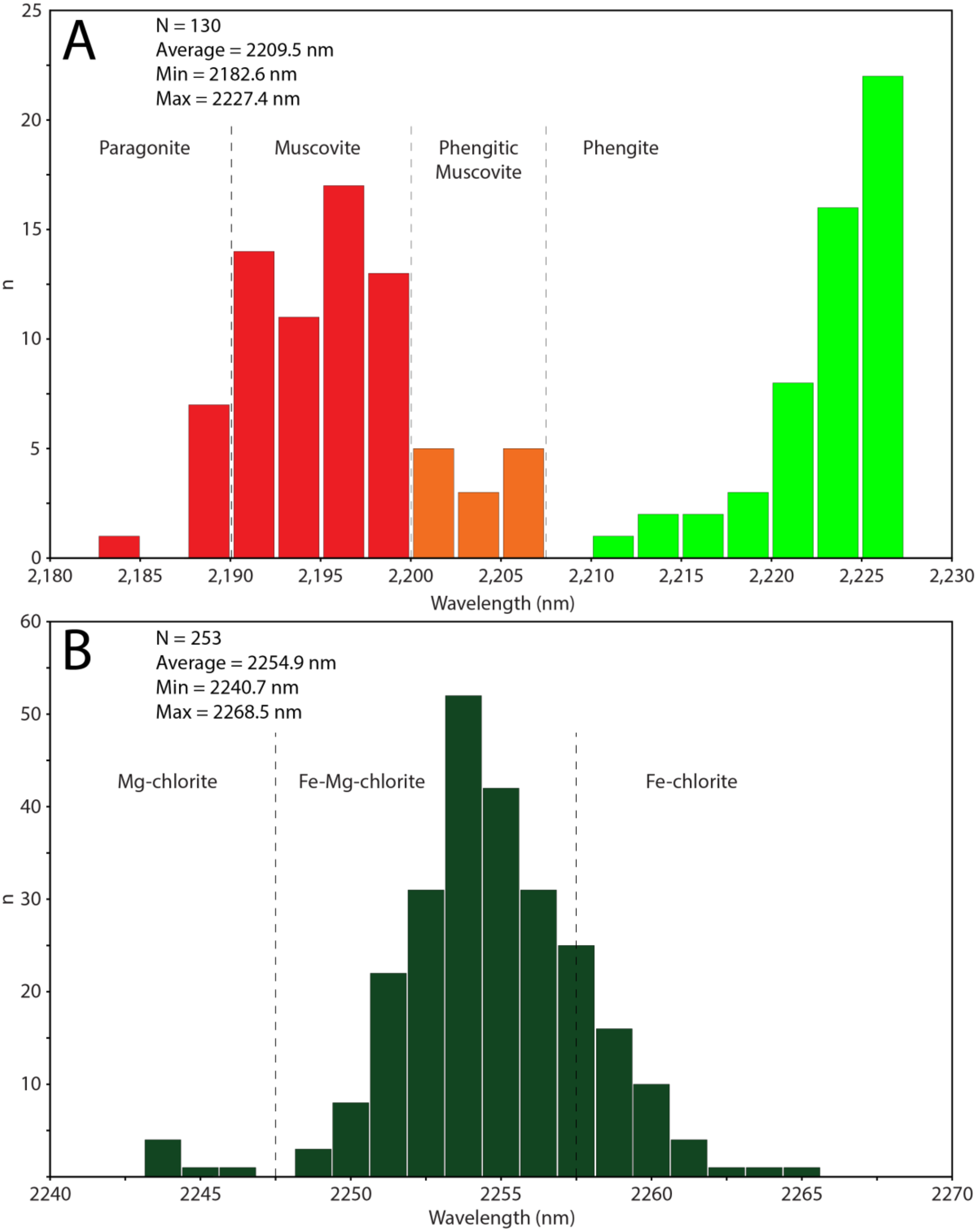

Figure 2.20. Histograms of SWIR data. A) AlOH, and B) FeOH wavelengths of samples from the Argyle deposit. Mineral species thresholds based on pers. comm. F. Lypaczewski.

Chapter 3: Summary and Suggestions for Future Research

3.1 Summary

The Argyle orogenic gold deposit is hosted within a tholeiitic gabbro sill in the Scrape Point Formation of the Snooks Arm Group in Baie Verte, Newfoundland, Canada. It is an ideal location to study the hydrothermal footprint of an orogenic gold deposit due to its location, recent discovery, wealth of abundant drill core, and because of the preservation of hydrothermal alteration and mineralization within the deposit. The combination of drill core logging, lithogeochemistry, SWIR spectroscopy, mineral imaging and mineral chemical techniques provide insight into the key controls on the formation of gold mineralization and hydrothermal alteration in the Argyle deposit and allowed for the development of geological, geochemical, and mineralogical vectors that can be used for further targeting of orogenic gold mineralization in mafic rocks in greenstone belts. The major conclusions from this thesis are as follows:

1) Gold mineralization is coincident with Silurian (to Devonian) tectonically driven (orogenic) fluid flow, and deposition was influenced by the texture and composition of the host gabbros.
2) The Argyle gabbro and volcaniclastic hanging-wall rocks have enriched mid-ocean ridge basalt (E-MORB) signatures and tholeiitic signatures. In contrast, the volcaniclastic footwall to the deposit has calc-alkaline signatures with evidence for slab metasomatism and/or continental crustal contamination.

3) The Argyle gabbro has experienced two episodes of hydrothermal alteration: 1) regional epidote-albite alteration; and 2) mineralization-related, which was associated with faulting and localized to the central parts of the gabbro sills.

4) The Argyle deposit contains three mineralization-related hydrothermal alteration assemblages: 1) distal chlorite-calcite-rutile ± epidote-albite (30-70 m); 2) intermediate chlorite-epidote-albite-calcite ± ankerite-rutile-hematite-sericite-pyrite (5-30 m); and 3) proximal sericite-quartz-ankerite ± albite-chlorite-rutile-sooty pyrite-gold (2-25 m). These alteration assemblages were controlled by host rock composition (Fe-Ti-enrichment), permeability/grain size of the gabbro, and the chemistry of the hydrothermal fluid.

5) Gold mineralization in the Argyle deposit was deposited through wallrock sulfidation and is generally located within 1 m from quartz-carbonate vein margins. Gold occurs as: 1) inclusions in pyrite; and 2) fracture-fill between pyrite grains. The composition of gold-bearing inclusions includes: 1) native gold; 2) gold-calaverite; 3) gold-arsenopyrite; and 4) gold-chalcopyrite. The highest gold grades correlate with late black chlorite veinlets.

6) The key alteration type in the Argyle deposit is the proximal sericite-quartz-ankerite-(albite-chlorite-pyrite-gold). The proximal zone is best mapped by: 1) alteration indices that represent carbonate (e.g. $CO_2/(Ca+Mg+Fe-0.5*(S+As))$) and sericite (e.g. 3K/Al) alteration; 2) pathfinder elements for orogenic gold with elevated Au, As, Bi, Te, W, Zr, Ba, Rb and REE, and low Sb and Sr; 3) mass changes and major elements including gains in SiO_2, Fe_2O_3, CaO, K_2O,

P_2O_5, TiO_2, CO_2, LOI, MnO and S; and loses in Na_2O, MgO and Cr_2O_3. The outer alteration footprint, i.e. the distal alteration zone is best defined by elevated LOI and CO_2 and CO_2/CaO ratios relative to the least altered background.

7) Chlorite and white mica are zoned with distance from the Argyle deposit. SWIR and mineral chemical data illustrate that in proximal to distal there is a shift from muscovite (~2,198 nm), Fe-chlorite/brunsvigite (~2,260 nm) and ankerite proximal to mineralization to Fe-Mg-chlorite/pycnochlorite (~2,250 nm), phengite (~2,214 nm) and calcite distal from mineralization. Short acquisition and processing times and reliability of SWIR data allows for rapid indication of relative distance from gold mineralization.

3.2 Suggestions for future research

The development of the Argyle gold deposit is planned to begin in 2020 and there are interesting opportunities for further academic work to improve the understanding of the deposit, such as:

1) Combination of Argyle lithogeochemistry and drill core logging with datasets from Stog’er Tight and Animal Pond deposits into a regional-scale study on gabbro-hosted gold mineralization. The study could compare and contrast the effects of structure, deformation style and distance from the Scrape thrust fault on the deformation, hydrothermal alteration and gold mineralization in the rigid gabbroic sills. The host rocks in these deposits share a common geochemical

precursor, yet they were affected by different amounts of deformation due to the varying distances from the Scrape thrust, which may have global implications on the understanding of effects of the distance from the controlling structure on gold mineralization in mafic host rocks in greenstone terranes;

2) Age dating of zircon, monazite, xenotime and/or rutile from the Argyle gabbro to constrain the absolute timing of gold mineralization. Gold mineralization age could indicate the relationship to regional tectonic events.
3) Petrography and mineral chemical work showed variations in Fe-Ti oxide phases with distance to gold mineralization at Argyle. A heavy mineral indicator study to document the changes to Fe-Ti oxides resultant from the alteration in orogenic gold deposits in Baie Verte could test the applicability of Fe-Ti minerals as an exploration tool.
4) SWIR spectroscopy of the dark fine-grained Argyle gabbro samples using a “grey reference”, which were deemed as aspectral by the instrument, despite visual and petrographic identification of chlorite in the same samples. A darker, less reflective reference sample could calibrate the instrument to make it possible to detect the absorption hulls for AlOH and FeOH along the SWIR spectrum.

Appendix A: Graphic Logs

Appendix A.1: Graphic Logs Information

Detailed logging and sampling of Argyle, Stog'er Tight and Animal Pond drill core focused on the lithology, alteration assemblages, and mineralization. Fieldwork and data collection took place in October 2017, May-July 2018 and October 2018 at the Stog'er Tight mine core shack. A total of 65 drill holes were logged and 315 samples were collected from 40 different holes, of which 144 were analyzed for whole rock geochemistry. A total of 49 thin sections were made from the collected samples.

The appendix below shows the key and legend for the corresponding 65 drill hole logs. The drill hole naming system follows an XX-YY-ZZZ format, where XX corresponds to deposit name, which is AE for Argyle, AP for Animal Pond and BN for Bradley North (Stog'er Tight). YY corresponds to the year the drilling took place and ZZZ represents the number of the drill hole on a given project. For example, drill hole AE-16-40 was drilled in 2016 and was the 40th drill hole on the Argyle property. The drill holes dip between 45°-90° and rarely exceed 150 m depth.

The graphic logs consist of alteration logged based on visual interpretations recorded in the core shack and reflect the alteration minerals identified in the drill core. In several cases improvements were made to the logs based on petrography or whole-rock geochemical data. Sulfide occurrences are logged in the alteration field based on their relative proportions. Additional notes on mineralization along with alteration and lithology changes are found in the description box.

Table A.1.1. Abbreviation Key for Graphic Logs

Descriptions

alt	Alteration
anh	Anhedral
aph	Aphanitic
calc	Calcite
cg	Coarse-grained
dis	Disseminated
dist	Distal
euh	Euhedral
FLT	Fault
fg	Fine-grained
FOL	Foliation
FW	Footwall
Fm.	Formation
FRC	Fracture
FF	Fracture-filling
grad	Gradual
HW	Hanging wall
str	Intense
int./interm	Intermediate
Fe	Iron
LC	Lower contact
mag / mt	Magnetite
mg	Medium-grained
mod	Moderate
MS	Moderately strong
OVB	Overburden
OVP	Overprint
pegm	Pegmatitic
prox	Proximal
SHR	Shear
SZ	Shear zone
Si	Silica
subh	Subhedral
UC	Upper contact
vn	Vein
vnlt	Veinlet
vcg	Very coarse-grained
vfg	Very fine-grained
wk	Weak

General

E	Easting
EOH	End of hole
m	Meter
N	Northing
UTM	Universal Transverse Mercator

Alteration Minerals

Ab	Albite
Carb	Carbonate
Chl	Chlorite
Ep	Epidote
Hem	Hematite
Py	Pyrite
Qtz	Quartz
Rut	Rutile

Host Rock

BX	Breccia
Flow	Flow
Int	Intrusive unit
Lap	Lapilli tuff
Tuff	Tuff

Table A.1.2. Legend for Graphic Logs

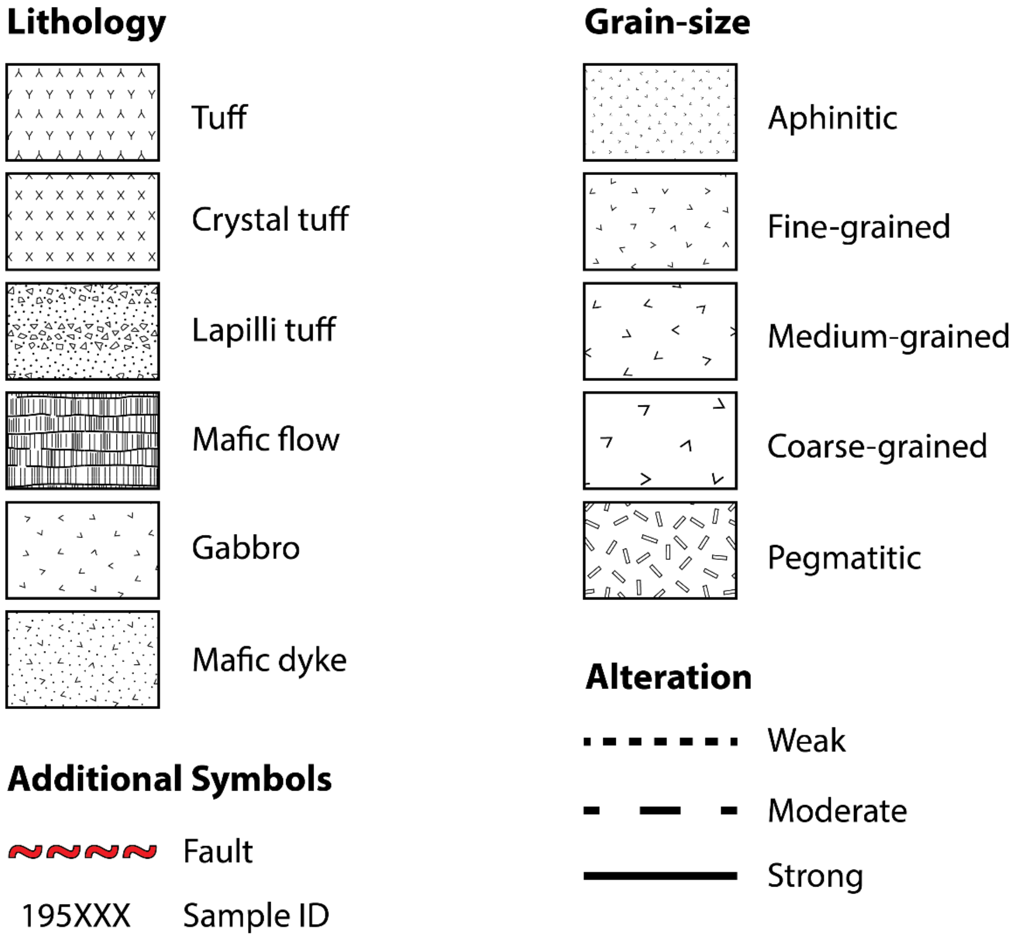

Appendix A.1.3: Graphic Log Compilation

Project: Argyle
Diamond Drill Hole: AE-16-23
Date: 10-13-2018

Section: 0+65E

UTM
300364.1E
5537700N

Azimuth: 180
Dip: -50
Depth: 101 m

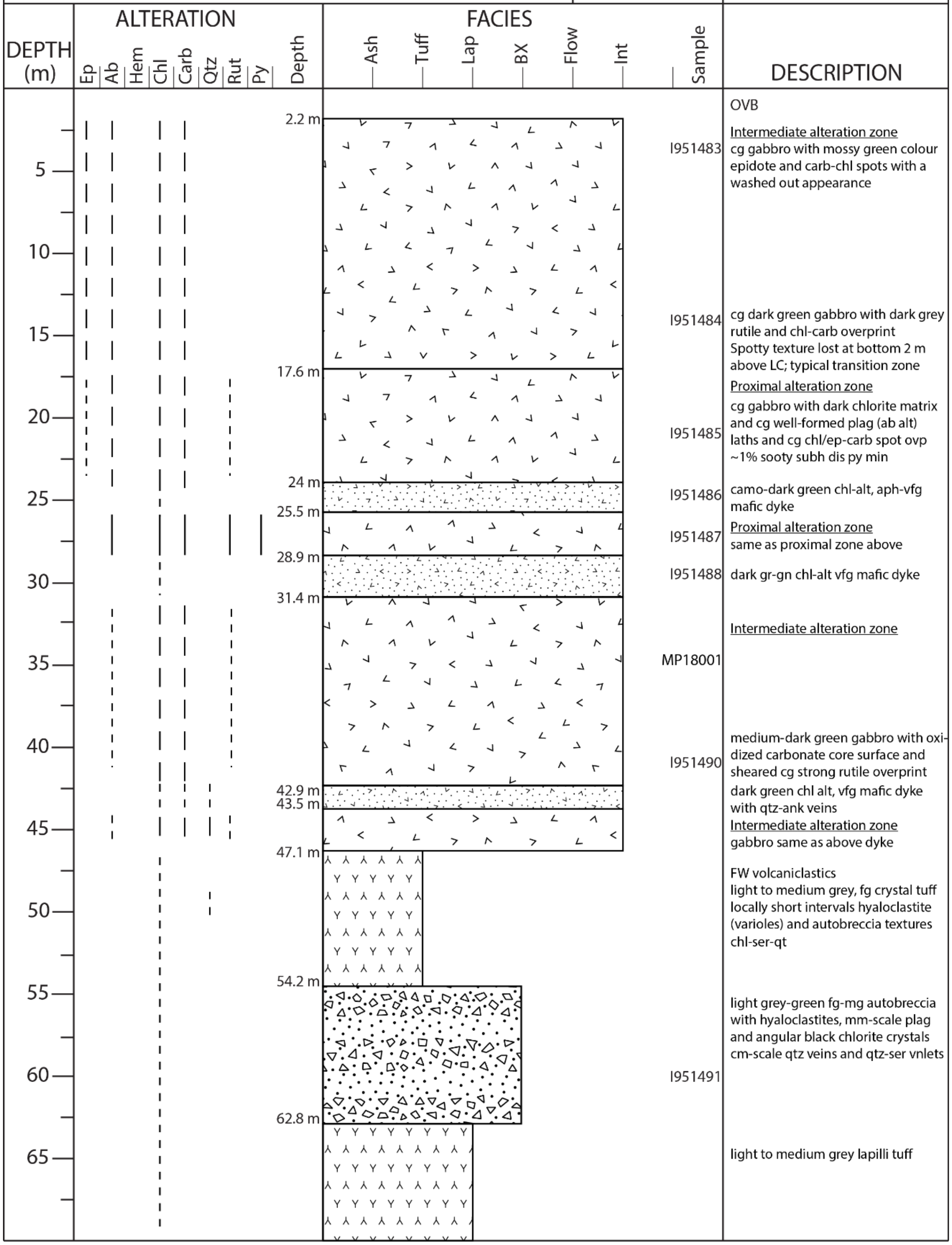

OVB

Intermediate alteration zone
cg gabbro with mossy green colour epidote and carb-chl spots with a washed out appearance

cg dark green gabbro with dark grey rutile and chl-carb overprint
Spotty texture lost at bottom 2 m above LC; typical transition zone

Proximal alteration zone
cg gabbro with dark chlorite matrix and cg well-formed plag (ab alt) laths and cg chl/ep-carb spot ovp
~1% sooty subh dis py min

camo-dark green chl-alt, aph-vfg mafic dyke

Proximal alteration zone
same as proximal zone above

dark gr-gn chl-alt vfg mafic dyke

Intermediate alteration zone

medium-dark green gabbro with oxidized carbonate core surface and sheared cg strong rutile overprint

dark green chl alt, vfg mafic dyke with qtz-ank veins

Intermediate alteration zone
gabbro same as above dyke

FW volcaniclastics
light to medium grey, fg crystal tuff locally short intervals hyaloclastite (varioles) and autobreccia textures
chl-ser-qt

light grey-green fg-mg autobreccia with hyaloclastites, mm-scale plag and angular black chlorite crystals
cm-scale qtz veins and qtz-ser vnlets

light to medium grey lapilli tuff

Project: Argyle
Diamond Drill Hole: AE-16-23
Date: 10-13-2018

Section: 0+65E

UTM
300364.1E
5537700N

Azimuth: 180
Dip: -50
Depth: 101 m

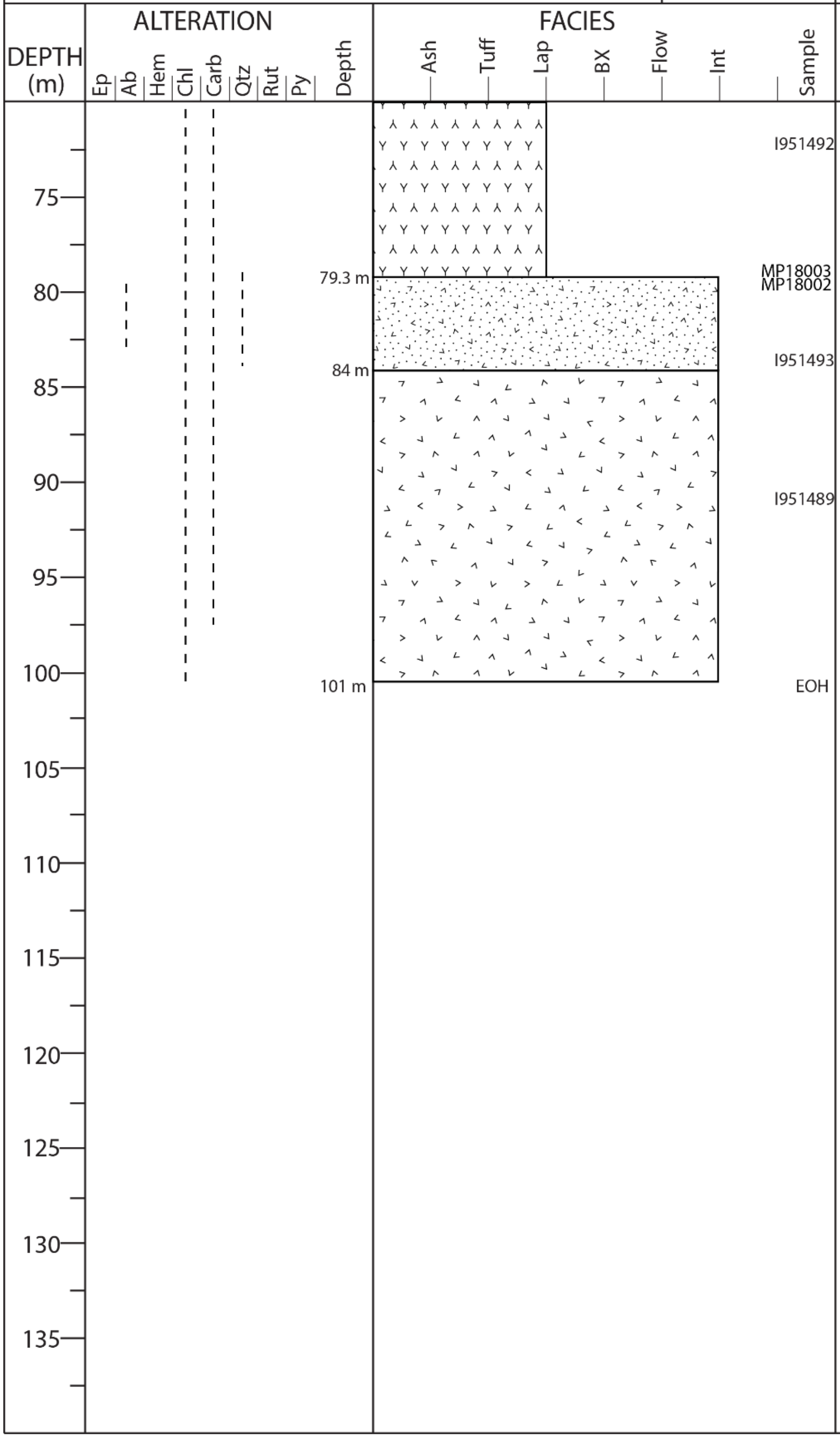

DESCRIPTION

FW volcaniclastics
relatively unaltered lapilli tuff

pyrite min constrained to qt-ab and qt-ank veins in a diabase/mafic dyke
medium grey mg chl-alt mafic dyke with cg plag crystals. 1-2% blebby euhedral py throughout the unit
bleached LC with gabbro

Distal alteration zone
fg dark green gabbro with weak chl-carb alteration

Project: Argyle
Diamond Drill Hole: AE-16-24
Date: 10-13-2018

Section: 0+65E

UTM
300364.1E
5537738.1N

Azimuth: 180
Dip: -50
Depth: 76 m

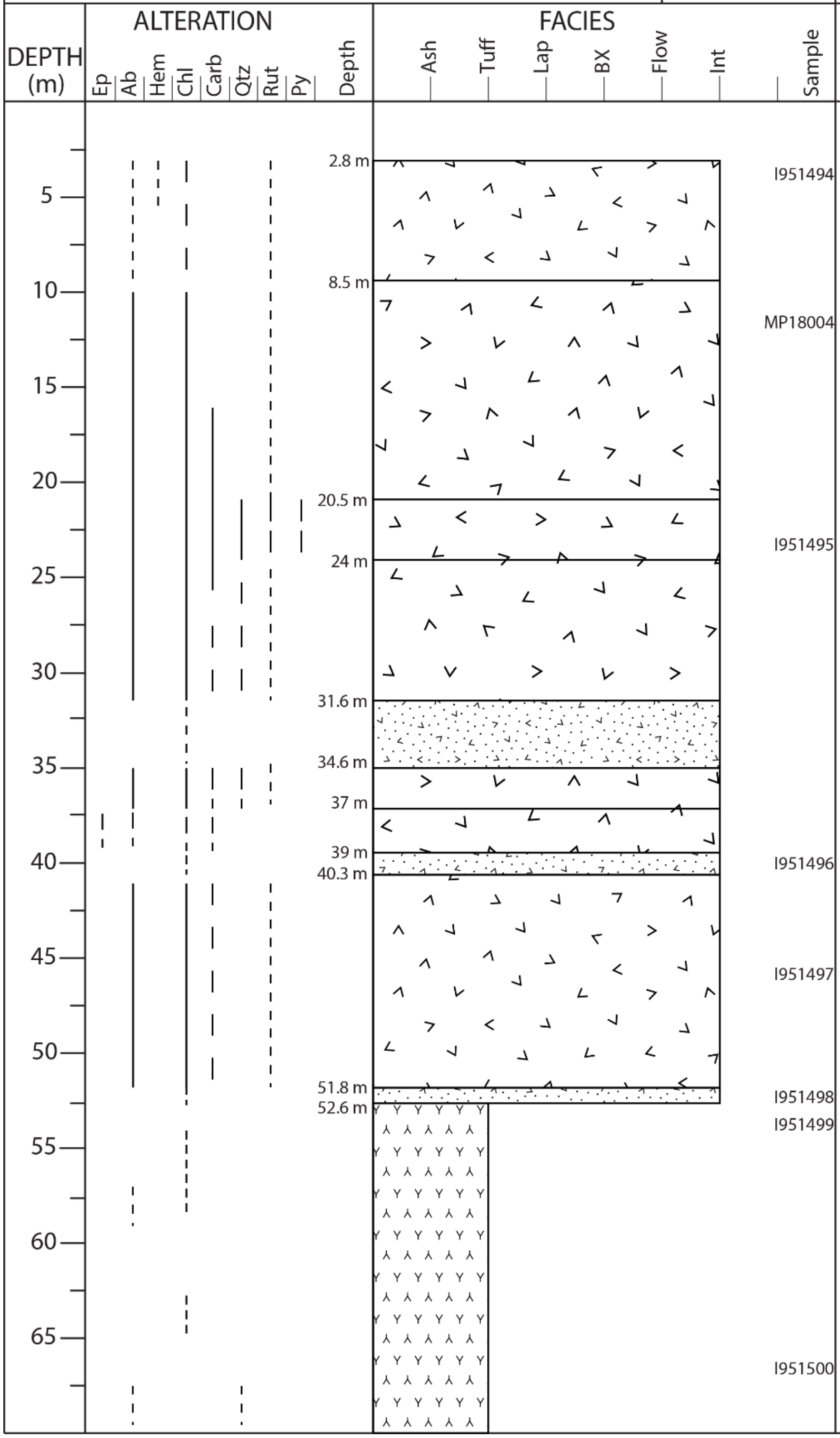

Depth	Sample	DESCRIPTION
		OVB
2.8 m	I951494	Intermediate alteration zone mg-cg spotty gabbro
8.5 m	MP18004	Proximal alteration zone chl-carb-ab-rut alteration to ~17m, downhole increase in strong ank ovp and ab content cg to 11m mg to 17m
20.5 m	I951495	"ore-zone" strongly metasomatized and Si-flooded/bleached cg gabbro
24 m		chl-ab cg proximal alteration of the gabbro
31.6 m		medium grey mg mafic dyke with mm-cm scale qtz-ank veins
34.6 m		Proximal alteration zone gabbro alteration like above
37 m		Intermediate alteration zone mg-cg spotty gabbro
39 m	I951496	fg dark grey-green mafic plag-phyric dyke
40.3 m	I951497	Intermediate alteration zone mg-cg spotty gabbro
51.8 m	I951498	Medium grey fg mafic dyke
52.6 m	I951499	FW ash, pale tan-green moderately altered to ab-chl FW volcaniclastics medium-light grey fg tuff with interbedded ash intervals with less common bleached ash zones and crystal tuff intervals
	I951500	Light grey, silicified mafic tuff Silica infilled voids

Project: Argyle
Diamond Drill Hole: AE-16-24
Date: 10-13-2018

Section: 0+65E

UTM
300364.1E
5537738.1N

Azimuth: 180
Dip: -50
Depth: 76 m

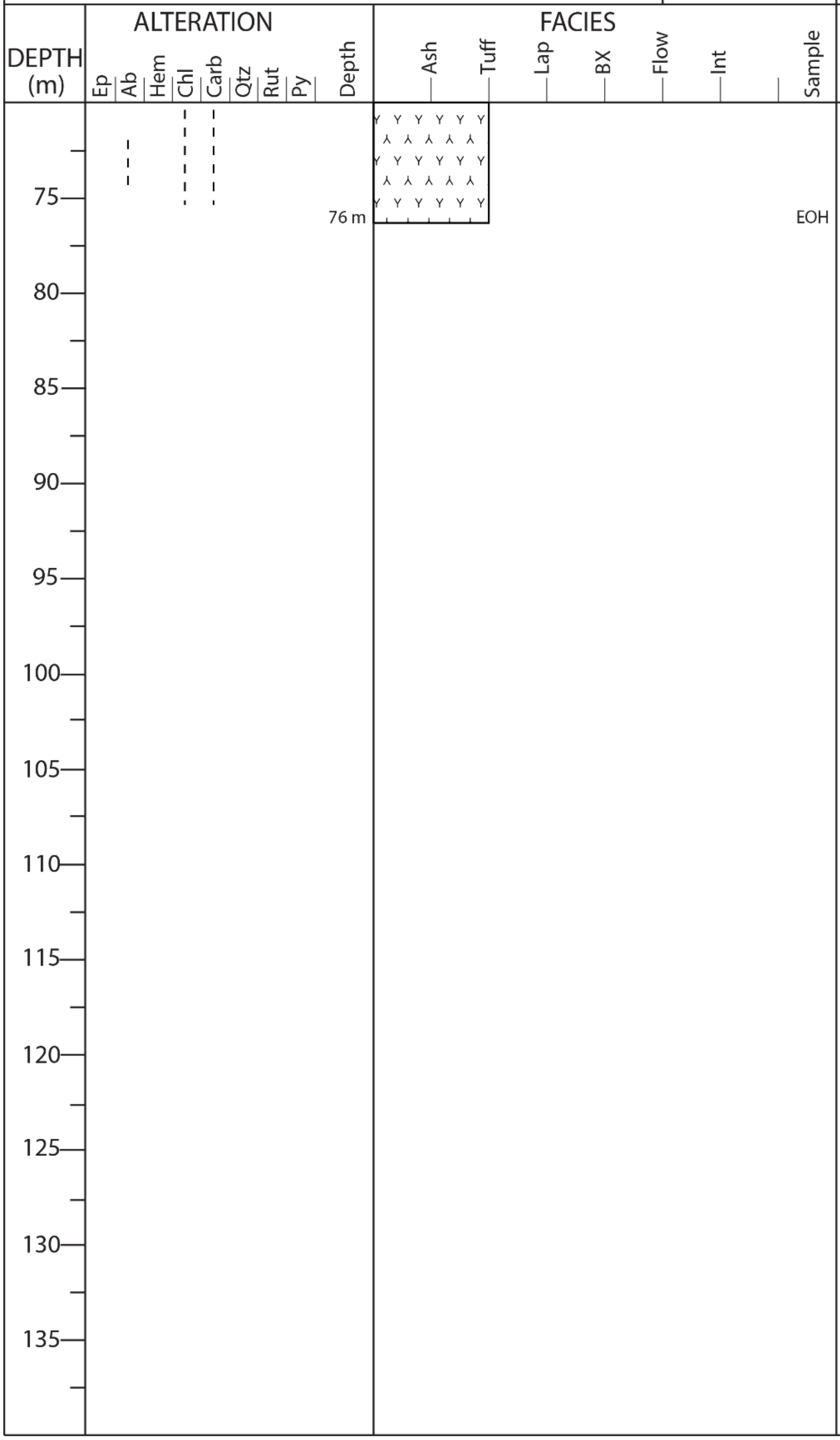

DESCRIPTION

FW volcaniclastics
medium-light grey fg tuff with interbedded ash intervals with less common bleached ash zones and crystal tuff intervals

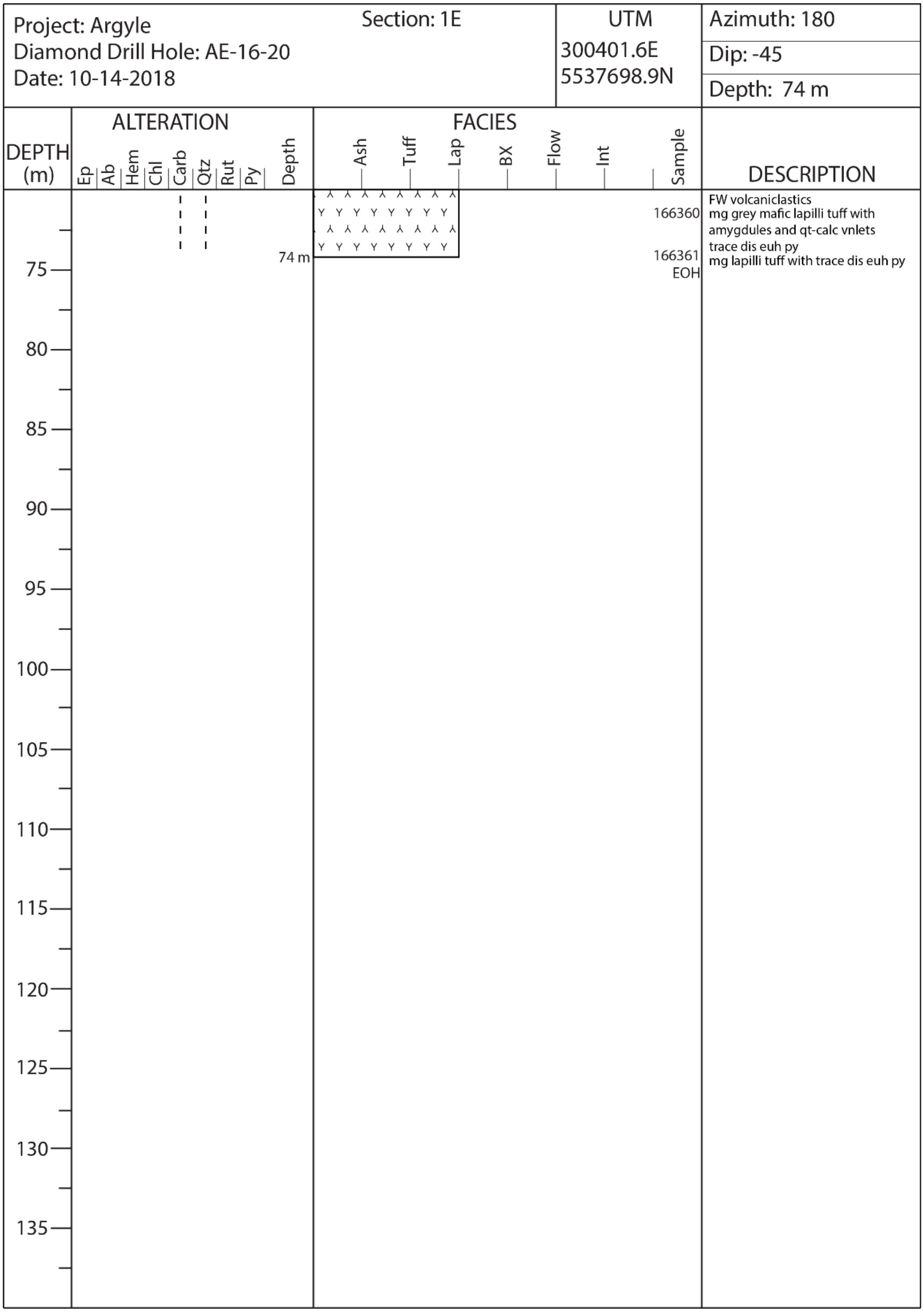

Project: Argyle
Diamond Drill Hole: AE-16-20
Date: 10-14-2018
Section: 1E
UTM
300401.6E
5537698.9N
Azimuth: 180
Dip: -45
Depth: 74 m

DESCRIPTION

FW volcaniclastics
mg grey mafic lapilli tuff with amygdules and qt-calc vnlets trace dis euh py
mg lapilli tuff with trace dis euh py

Project: Argyle
Diamond Drill Hole: AE-16-20
Date: 10-14-2018

Section: 1E

UTM
300401.6E
5537698.9N

Azimuth: 180
Dip: -45
Depth: 74 m

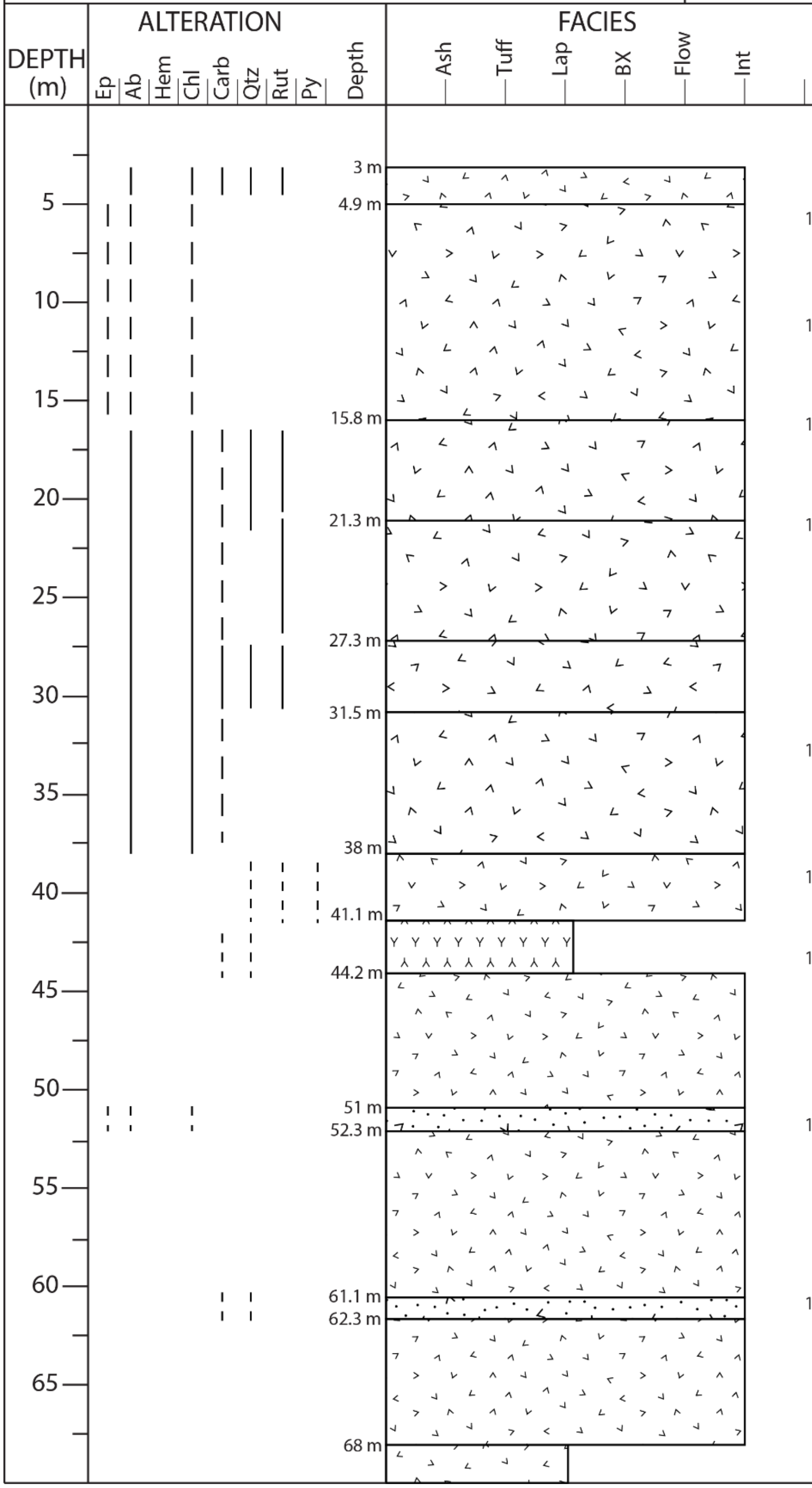

Sample	DESCRIPTION
	OVB
183093	Intermediate alteration zone dark grn-apple green spotty cg gabbro
183094	equigranular mg-cg ep-ab-chl altered gabbro with fibrous chl
183095	Proximal alteration zone "zone" - strongly-mod silica flooded cg gabbro with strong ab-chl wit rut and ank veinlets and spots
183096	cg gabbro with ab-rut-chl-ank alteration with py
	"zone" - like above
183097	strongly ab-rut-chl-ank altered cg-pegm dark green gabbro with mod spotty Fe-carb and rut ovp Sheared 70 cm to LC
183098	fg foliated and sheared mafic dyke with rut-py-qtz and mm-scale py-qtz veinlets
	FW volcaniclastics
183099	medium grey mafic locally weakly sheared crystal tuff qt-cal veins locally Si-flooded
	Distal alteration zone fg gabbro relatively fresh
183100	fg-mg mafic dyke with amygdules with minor ep-ab-chl clots
166359	fg gabbro/diabase with minor qtz-cal veinlets

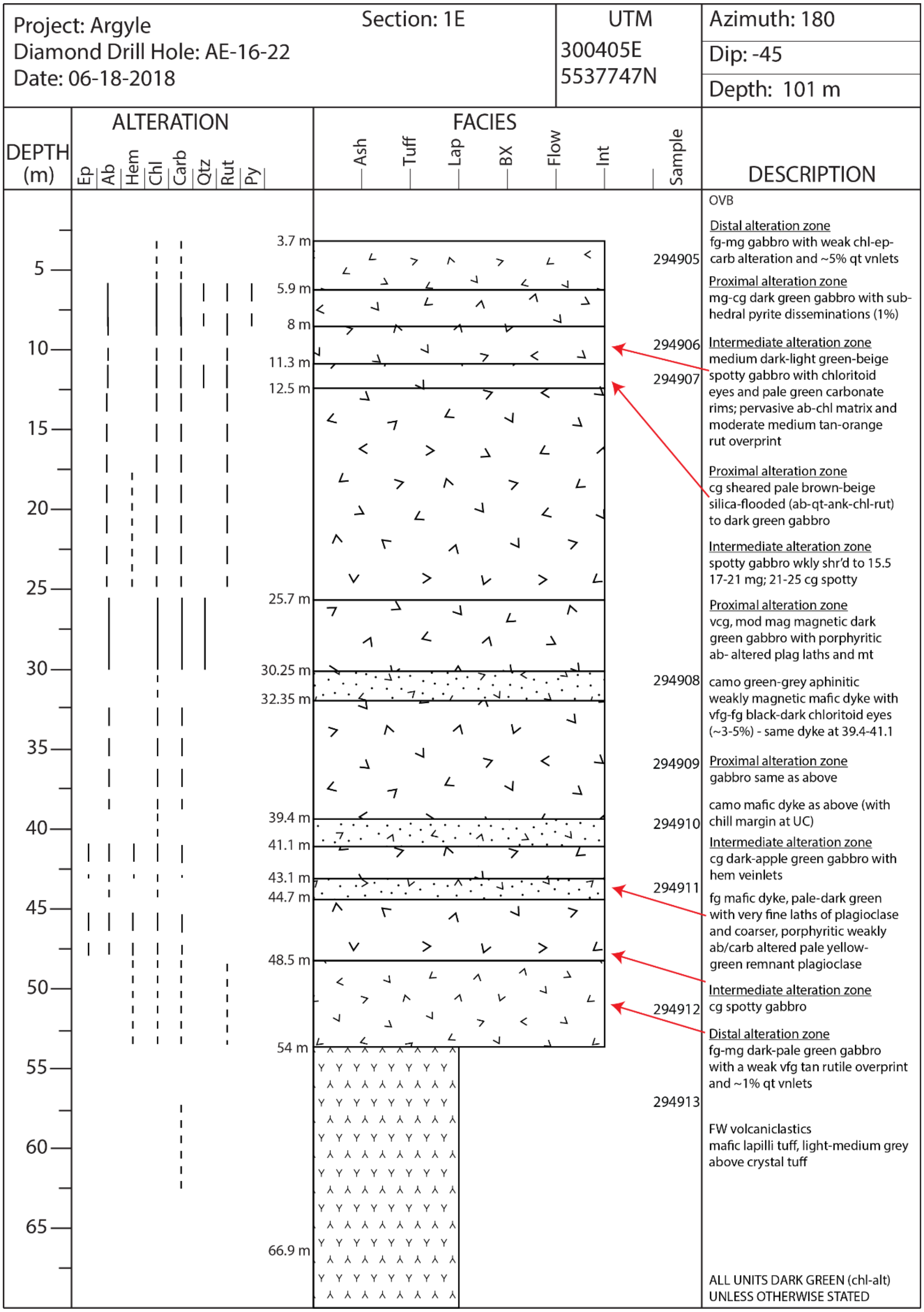

Project: Argyle
Diamond Drill Hole: AE-16-22
Date: 06-18-2018

Section: 1E

UTM
300405E
5537747N

Azimuth: 180
Dip: -45
Depth: 101 m

DESCRIPTION

OVB

Distal alteration zone
fg-mg gabbro with weak chl-ep-carb alteration and ~5% qt vnlets

Proximal alteration zone
mg-cg dark green gabbro with sub-hedral pyrite disseminations (1%)

Intermediate alteration zone
medium dark-light green-beige spotty gabbro with chloritoid eyes and pale green carbonate rims; pervasive ab-chl matrix and moderate medium tan-orange rut overprint

Proximal alteration zone
cg sheared pale brown-beige silica-flooded (ab-qt-ank-chl-rut) to dark green gabbro

Intermediate alteration zone
spotty gabbro wkly shr'd to 15.5 17-21 mg; 21-25 cg spotty

Proximal alteration zone
vcg, mod mag magnetic dark green gabbro with porphyritic ab- altered plag laths and mt

camo green-grey aphinitic weakly magnetic mafic dyke with vfg-fg black-dark chloritoid eyes (~3-5%) - same dyke at 39.4-41.1

Proximal alteration zone
gabbro same as above

camo mafic dyke as above (with chill margin at UC)

Intermediate alteration zone
cg dark-apple green gabbro with hem veinlets

fg mafic dyke, pale-dark green with very fine laths of plagioclase and coarser, porphyritic weakly ab/carb altered pale yellow-green remnant plagioclase

Intermediate alteration zone
cg spotty gabbro

Distal alteration zone
fg-mg dark-pale green gabbro with a weak vfg tan rutile overprint and ~1% qt vnlets

FW volcaniclastics
mafic lapilli tuff, light-medium grey above crystal tuff

ALL UNITS DARK GREEN (chl-alt) UNLESS OTHERWISE STATED

Project: Argyle
Diamond Drill Hole: AE-16-22
Date: 06-18-2018

Section: 1E

UTM
300404.5E
5537746.9N

Azimuth: 180
Dip: -45
Depth: 101 m

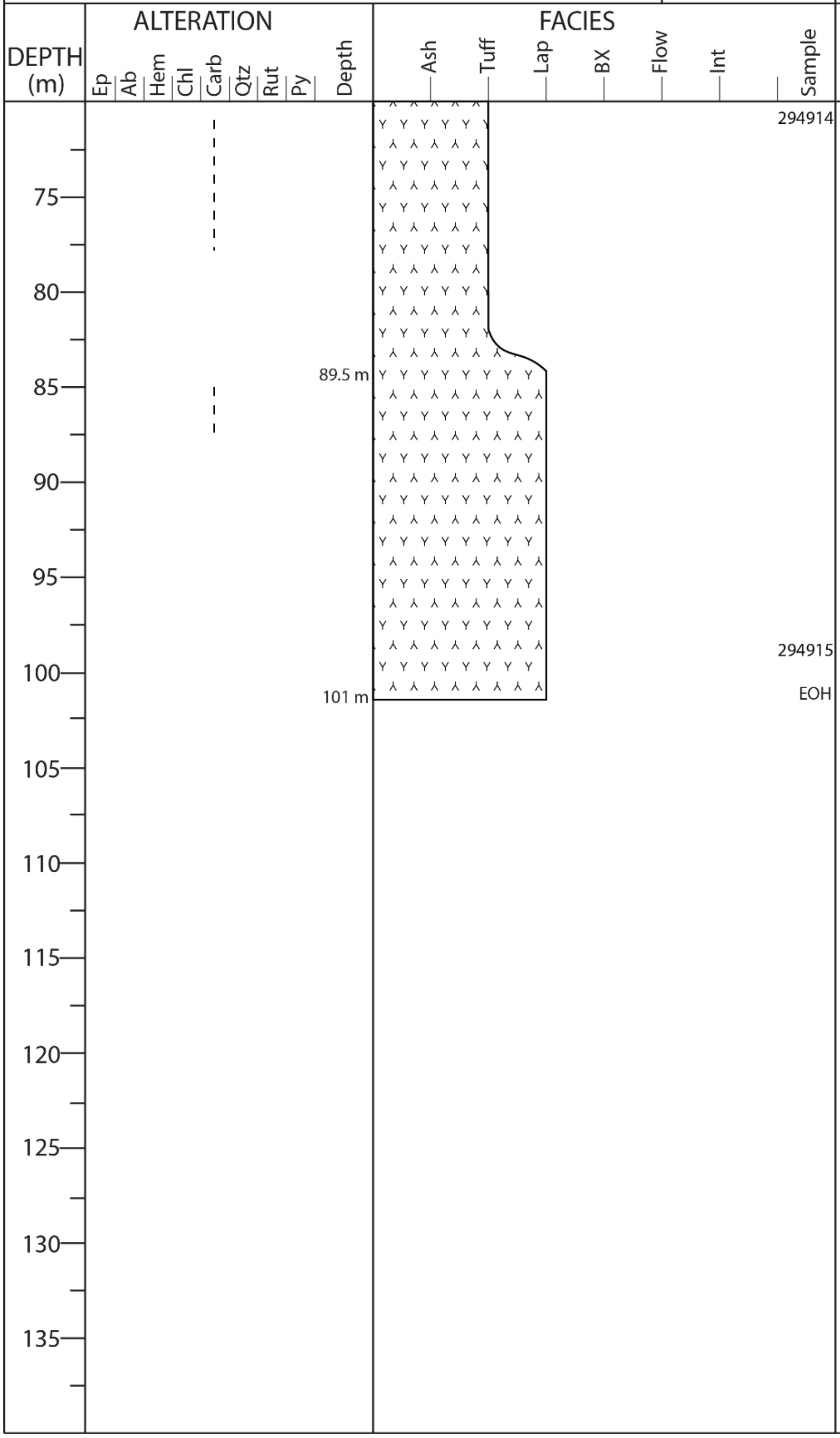

DESCRIPTION

medium grey silica-flooded, weakly bleached crystal tuff (logged as gabbro by Anaconda, perhaps this is an amygdoidal gabbro? although appearance suggests crystal tuff)

mafic crystal tuff or amygdoidal gabbro? grades into lapilli, therefore it is more likely to be a tuff

light-medium grey, mafic lapilli tuff
FOL 55 @90.5
FOL 62 @95.5
FOL 62 @100.5

the fault found typically in the lower portion of the gabbro near LC w/volcs is not present in this hole, hence there is a distal/weakly altered gabbro near LC

Project: Argyle
Diamond Drill Hole: AE-16-06
Date: 10-14-2018

Section: 1+8E

UTM
300481E
5537704N

Azimuth: 180
Dip: -50
Depth: 50 m

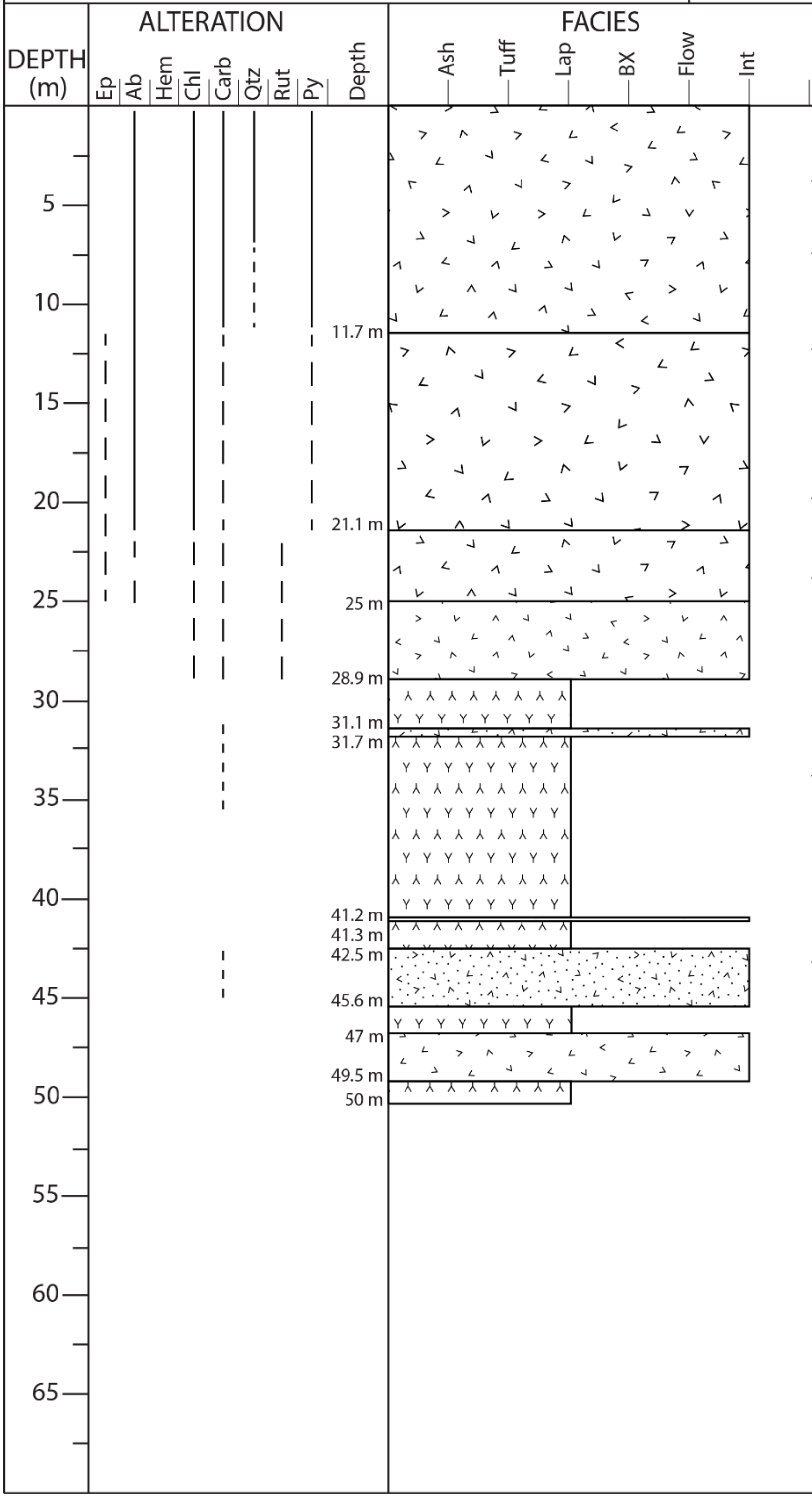

Sample	DESCRIPTION
	<u>Proximal alteration zone</u> "ore-zone" Si-flooded
183077	strong Si-flooded fe carb-chl-abt alt of gabbro with py-bearing qtz vn
183078	strong chl-ab-ank alteration of gabbro with pyrite clots
183079	cg-pegm gabbro with black chl, rut, spotty ank and py
183080	pegmatoidal gabbro with strong ep-chl-black chl alteration with py cubes and ab altered plag laths
	<u>Intermediate alteration zone</u>
183081	ep-ab-chl spotty altered cg gabbro on edge of alt zone
	<u>Distal alteration zone</u> fg gabbro with wk vfg rut ovp
	FW volcaniclastics fg medium-dark grey mafic dyke with bleached contacts and qt-ab vein on LC
183082	mafic tuff with minor calc vnlts well foliated ~80 tca, LC with distal gabbro is sub-parallel (< 10 deg.)
	mafic dyke the same as above
183083	relatively unaltered fg mafic dyke with rare dark green chloritoids and minor cal veinlets. qt-ab on LC
	distal fg-mg unaltered gabbro with chilled LC and UC
EOH	sheared mafic lapilli tuff

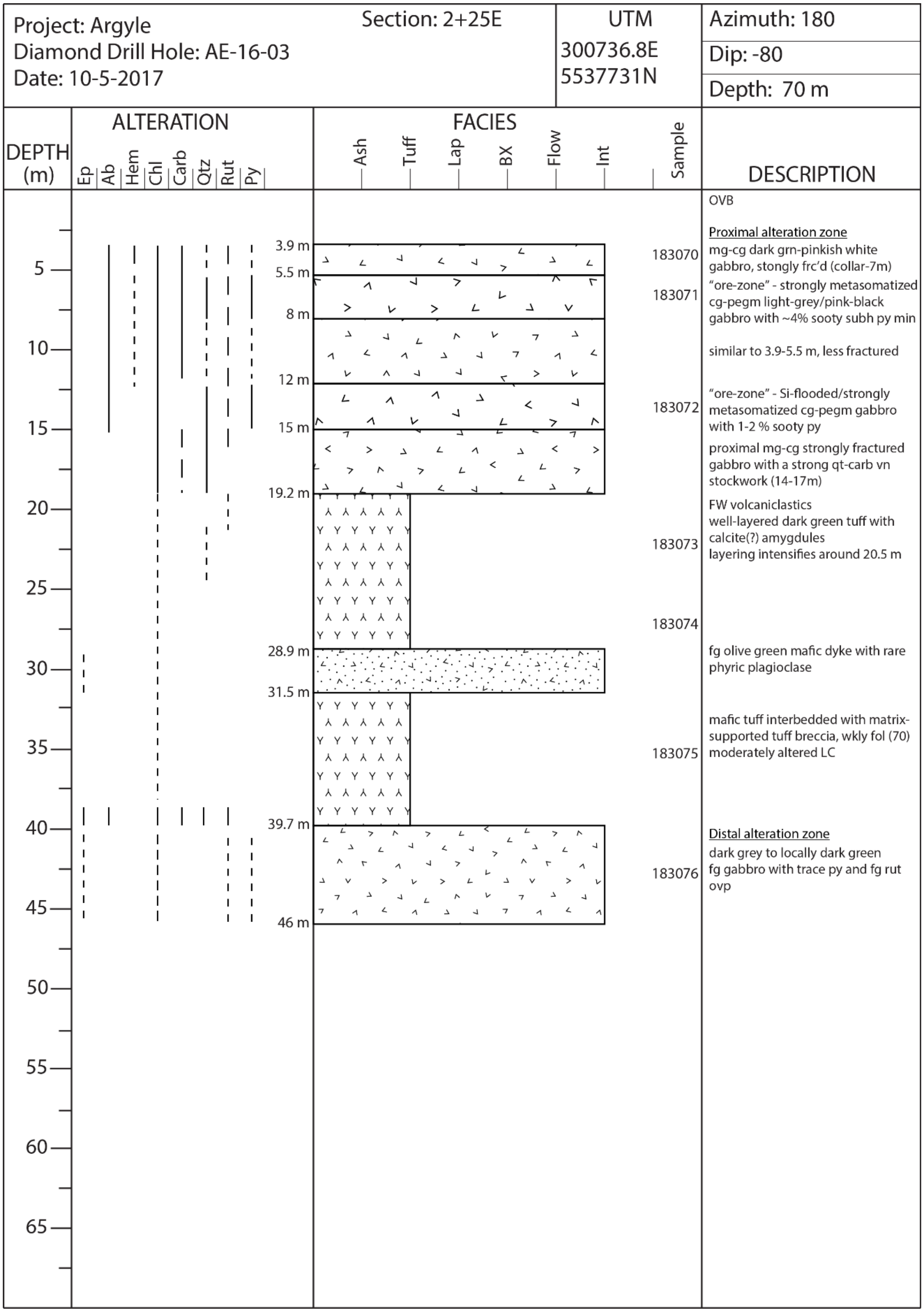

Project: Argyle
Diamond Drill Hole: AE-16-03
Date: 10-5-2017

Section: 2+25E

UTM
300736.8E
5537731N

Azimuth: 180
Dip: -80
Depth: 70 m

Sample	DESCRIPTION
	OVB
	Proximal alteration zone
183070	mg-cg dark grn-pinkish white gabbro, stongly frc'd (collar-7m)
183071	"ore-zone" - strongly metasomatized cg-pegm light-grey/pink-black gabbro with ~4% sooty subh py min
	similar to 3.9-5.5 m, less fractured
183072	"ore-zone" - Si-flooded/strongly metasomatized cg-pegm gabbro with 1-2 % sooty py
	proximal mg-cg strongly fractured gabbro with a strong qt-carb vn stockwork (14-17m)
183073	FW volcaniclastics well-layered dark green tuff with calcite(?) amygdules layering intensifies around 20.5 m
183074	
	fg olive green mafic dyke with rare phyric plagioclase
183075	mafic tuff interbedded with matrix-supported tuff breccia, wkly fol (70) moderately altered LC
	Distal alteration zone
183076	dark grey to locally dark green fg gabbro with trace py and fg rut ovp

Project: Argyle Diamond Drill Hole: AE-16-04 Date: 10-6-2017	Section: 2+25E	UTM 300530.3E 5537703 N	Azimuth: 180 Dip: -45 Depth: 50 m

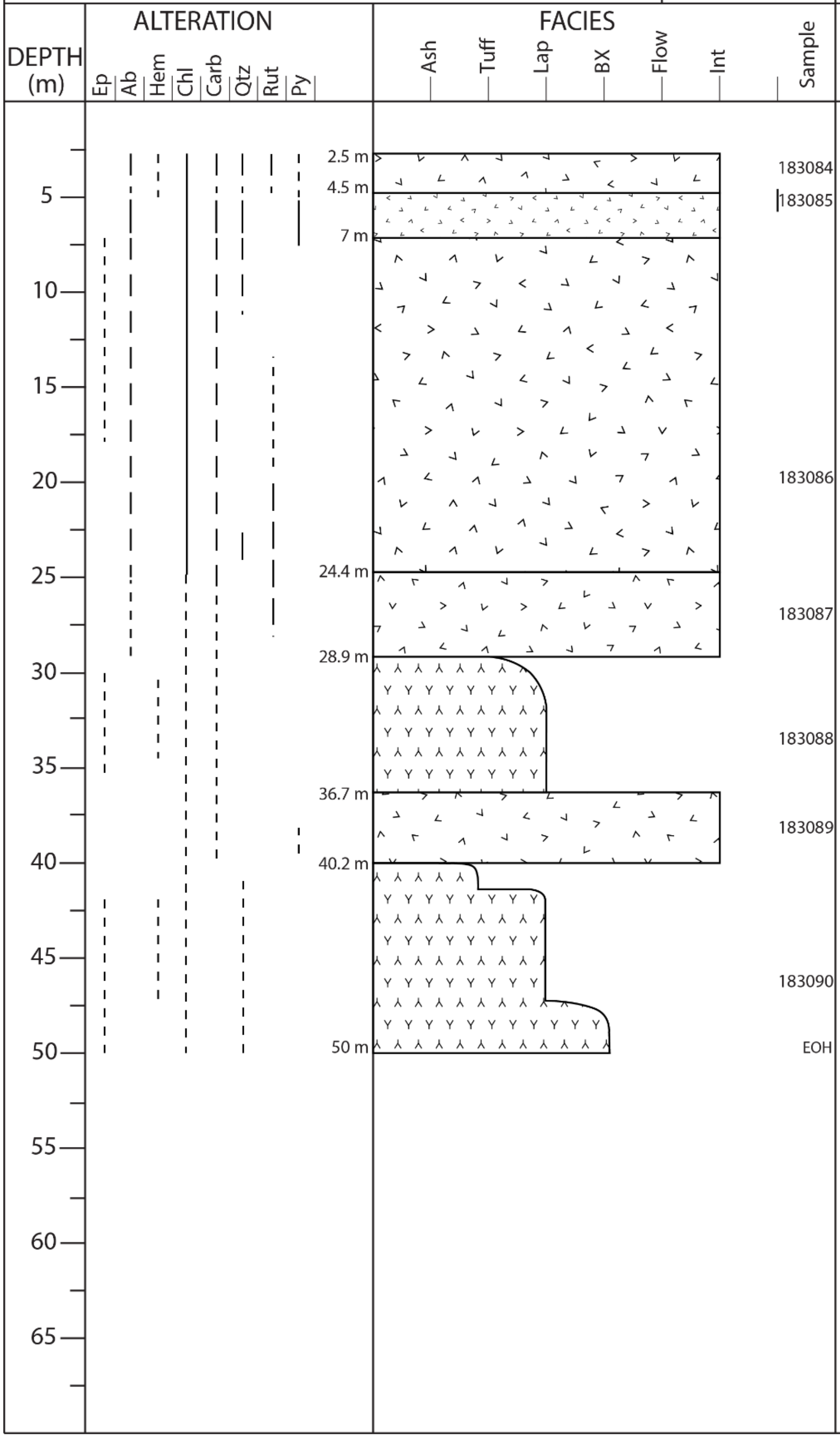

DESCRIPTION

OVB

Proximal alteration zone
light green-light cg greyish pink alt'd gabbro with ank mottled overprint
"ore-zone" - Si-flooded/strongly metasomatized cg-pegm gabbro up to 2 % sooty py
highly fractured/veined to 7m.

mg-cg foliated (65) rut ovp of altered gabbro (very similar to 2.5-4.5m)

disintegrating magnetite (21-23.5 m) this likely shows ilmenomagnetite reacting with hydrothermal fluids (in uphole direction) progressively altering into rutile, as evident by the foliated overprint

Intermediate alteration zone
mg gabbro with a weakly bleached appearence and a weak rut ovp

FW volcaniclastics
mafic tuff coarsens down to lapilli tuff

small fracture zone (35-37 m)

Distal alteration zone
weakly chl-carb altered mg gabbro weakly foliated (75)

matrix-supported mafic ash, coarsens down to tuff bx

Z-fold

Project: Argyle
Diamond Drill Hole: AE-16-05
Date: 5-18-2018

Section: 2+25E

UTM
300736.8E
5537731N

Azimuth: 000
Dip: -90
Depth: 73 m

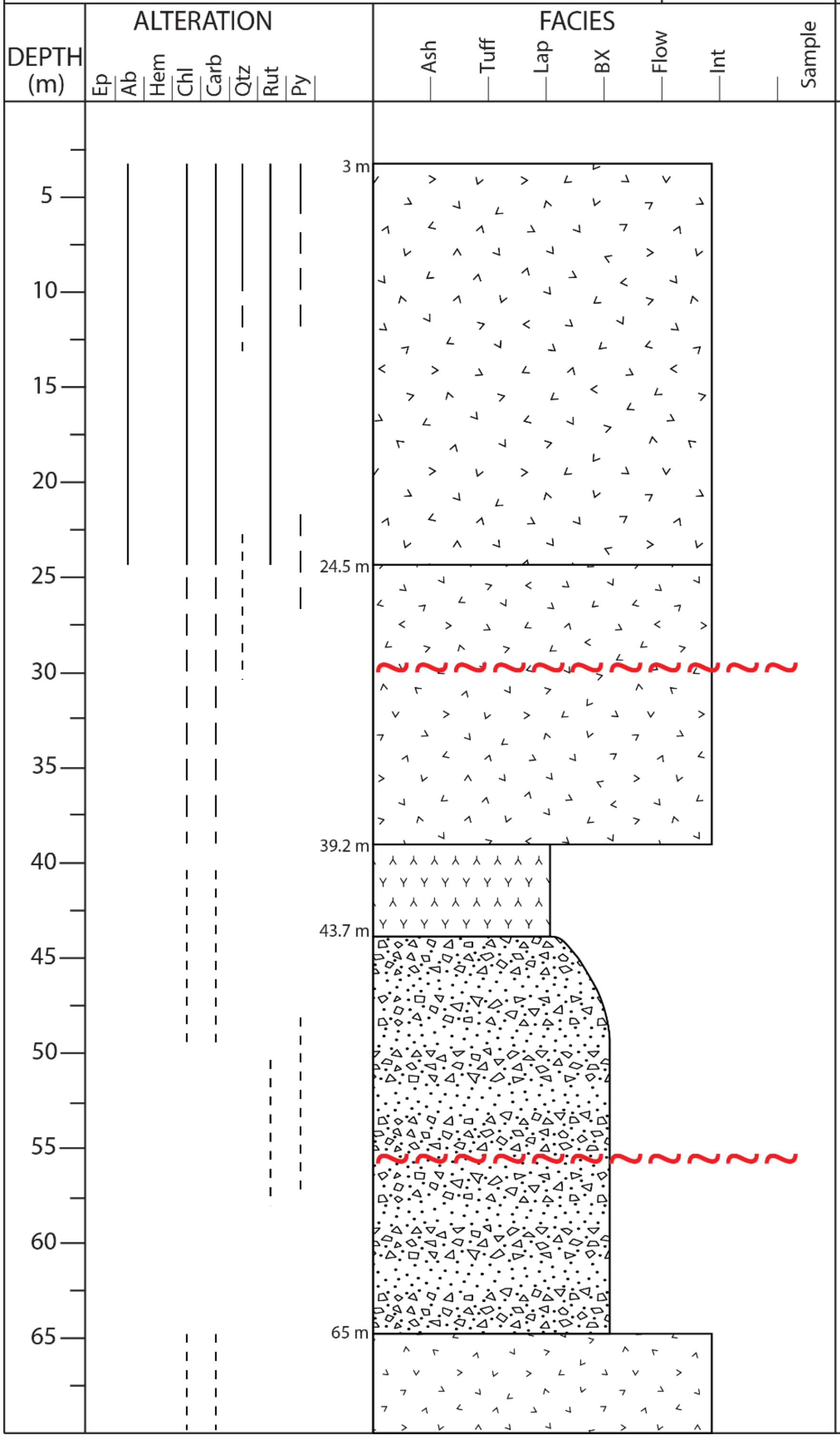

DESCRIPTION

OVB

Proximal alteration zone
dark grn-pinkish light grey cg altered gabbro with well-defined plag laths (ab alt'd) ankerite widely abundant, visible on oxidized core, rutile not foliated

mineralized section ~1% py 4-5
LCT 67@24.5.

gradational change over m-scale to intermediate at LC

Intermediate alteration zone
mg mottled chl-carb-ab altered gabbro; decreasing downhole ank overprint content
from 24.5m

LC cuts across foliation in lapilli tuff

QT VN 27.5-27.9 m , 29-29.3 m
FLT 29-29.5 m
SHR 29.5-30 (53@29.6 m, 40@29.9 m)

FW volcaniclastics
fg mafic lapilli tuff

coarsens from lapilli tuff at UC to tuff breccia by 50m

Fractured (folding?) at LC, increase in qt vn from 63 m

SHR 47.5-54.6.
euh tr dis py 54.8-55.1
FF eu py 50-52.2
fractured LC with qt vn (+chl-ab)
FOL 43@55.8
FOL 52@61
FLT gouge 55.8-56.2

Distal alteration zone
dark green fg gabbro - Bobby Cove Fm? very consistent until EOH, no chilled margin, fg rut overprint

Project: Argyle
Diamond Drill Hole: AE-16-05
Date: 5-18-2018

Section: 2+25E

UTM
300719E
5537790N

Azimuth: 000
Dip: -90
Depth: 73 m

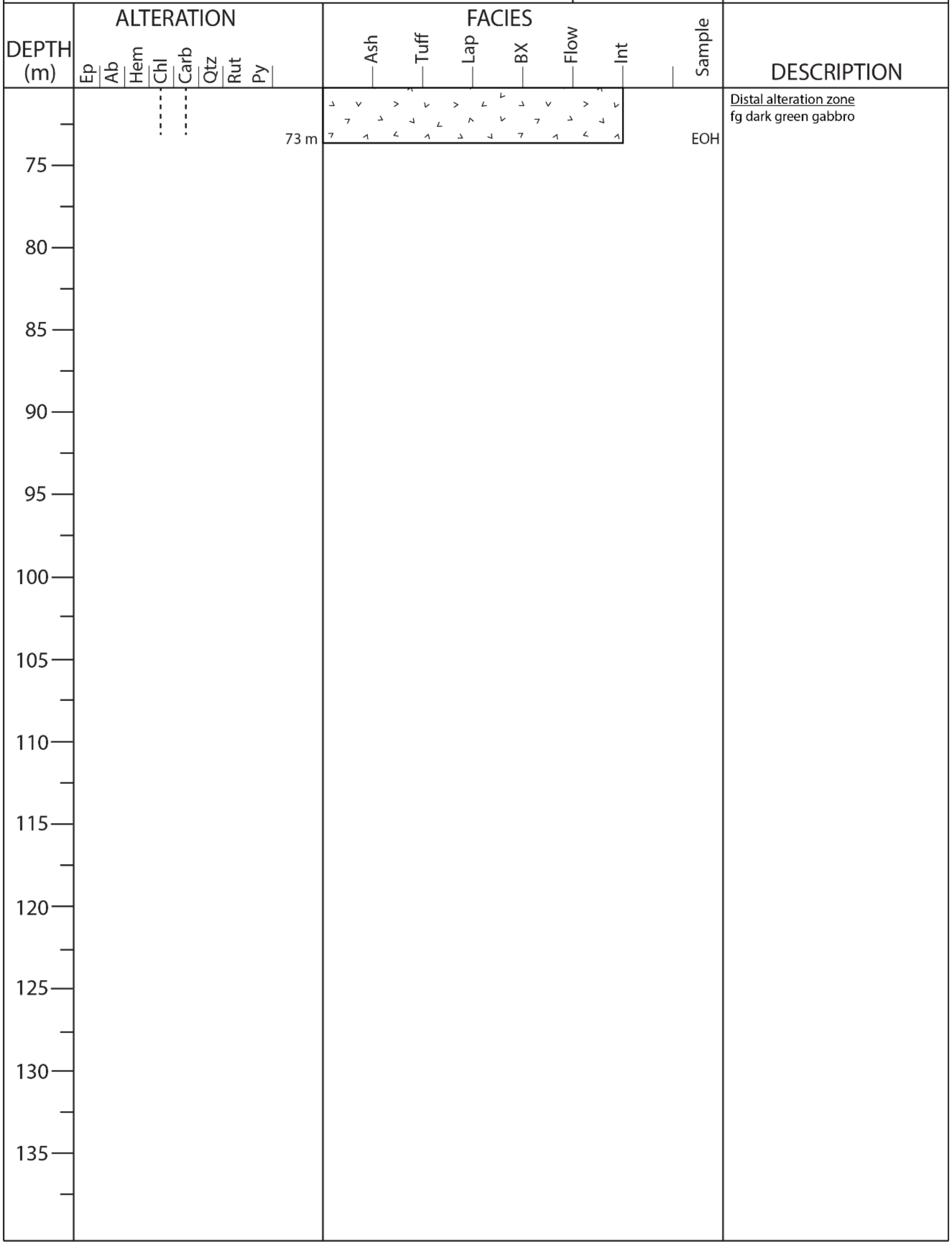

Distal alteration zone
fg dark green gabbro

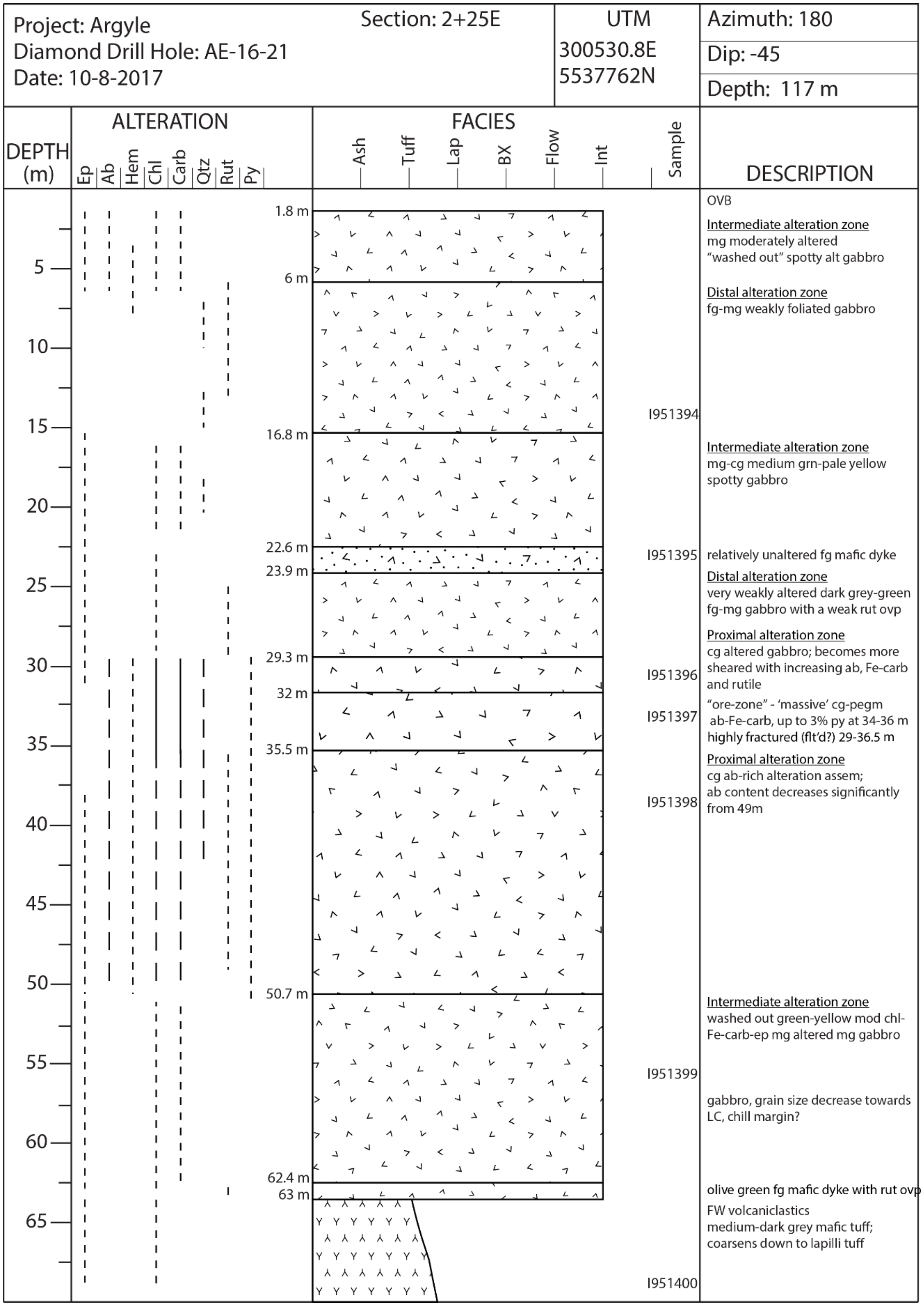

Project: Argyle
Diamond Drill Hole: AE-16-21
Date: 10-8-2017

Section: 2+25E

UTM
300530.8E
5537762N

Azimuth: 180
Dip: -45
Depth: 117 m

OVB

Intermediate alteration zone
mg moderately altered
"washed out" spotty alt gabbro

Distal alteration zone
fg-mg weakly foliated gabbro

Intermediate alteration zone
mg-cg medium grn-pale yellow spotty gabbro

relatively unaltered fg mafic dyke

Distal alteration zone
very weakly altered dark grey-green fg-mg gabbro with a weak rut ovp

Proximal alteration zone
cg altered gabbro; becomes more sheared with increasing ab, Fe-carb and rutile

"ore-zone" - 'massive' cg-pegm ab-Fe-carb, up to 3% py at 34-36 m
highly fractured (flt'd?) 29-36.5 m

Proximal alteration zone
cg ab-rich alteration assem;
ab content decreases significantly from 49m

Intermediate alteration zone
washed out green-yellow mod chl-Fe-carb-ep mg altered mg gabbro

gabbro, grain size decrease towards LC, chill margin?

olive green fg mafic dyke with rut ovp

FW volcaniclastics
medium-dark grey mafic tuff;
coarsens down to lapilli tuff

Project: Argyle
Diamond Drill Hole: AE-16-21
Date: 10-8-2017

Section: 2+25E

UTM
300530.8E
5537762N

Azimuth: 180
Dip: -45
Depth: 117 m

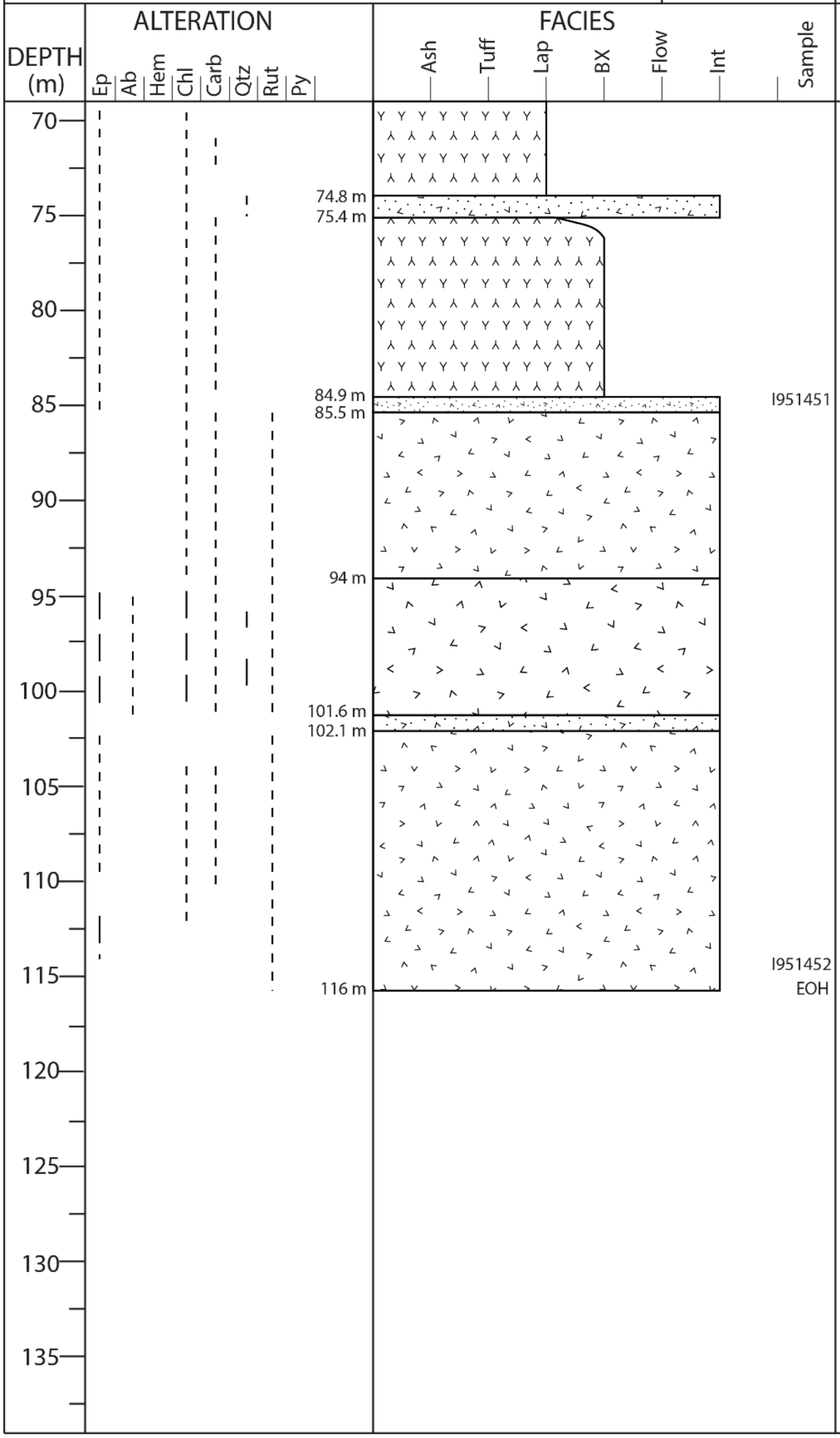

DESCRIPTION

dark grey fg mafic dyke, minor chl alt

dark grey mafic lapilli tuff, coarsens down to a moderately foliated (~30) tuff breccia

aph-fg dark camo green dyke at ct between volcaniclastic tuff breccia and underlying gabbro sill

Distal alteration zone
dark grey fg gabbro, relatively unaltered with rutile overprint gabbro coarsens down to mg, hence UC likely a chill margin

Intermediate alteration zone
moderately to strongly altered mg-cg gabbro with quartz veins (~10 %)

fg olive green mafic dyke with a weak rutile overprint

Distal alteration zone
fg gabbro with locally more intense ep alteration (111.1-116m) including ep veins

Project: Argyle
Diamond Drill Hole: AE-16-32
Date: 10-7-2017

Section: 2+25E

UTM
300527.5E
5537821N

Azimuth: 180
Dip: -50
Depth: 86 m

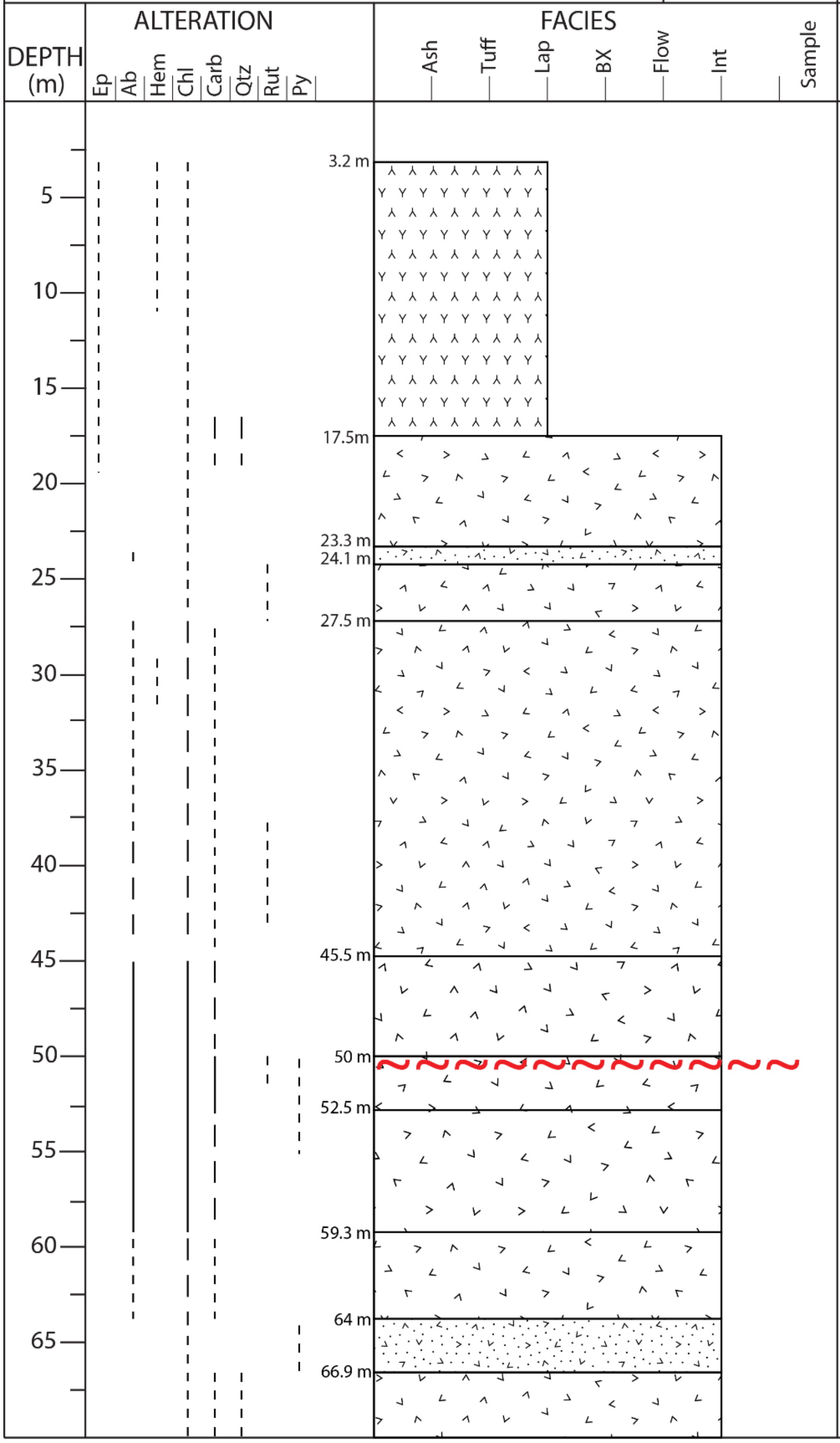

DESCRIPTION

OVB

HW volcaniclastics
dark green-frey mafic lapilli tuff
moderately hematized to 11 m;
well-foliated and disking 15-17.4m
MS qtz-carb veining 17.4-18.5

very broken up around the qt veins at LC, likely a minor FLT zone

Distal alteration zone
weakly chl-ep altered mg gabbro

olive green fg mafic dyke with phyric plag and orange isolated ab crystals

Distal alteration zone
weakly altered mg gabbro with a weak tan rutile overprint

Intermediate alteration zone
moderately bleached mg gabbro with a spotty appearance; ep veins present up to 43m

Proximal alteration zone
cg ab dominates min alt assm

"ore-zone" - Si-flooded/strongly metasomatized cg-pegm gabbro up to 2 % subh py; coincides with FLT/FRC zone (49-51.5m)

similar to 45.5-50 m

Intermediate alteration zone
UC marks transition from ab- to chl-carb- dominated alt assemblage; mottled mg-cg gabbro

dark grey fg mafic dyke with tr dis py

Intermediate alteration zone
mottled mg gabbro with Fe-carb-qt veins (~3-4 %)

Project: Argyle
Diamond Drill Hole: AE-16-32
Date: 10-7-2017

Section: 2+25E

UTM
300527.5E
5537821N

Azimuth: 180
Dip: -50
Depth: 86 m

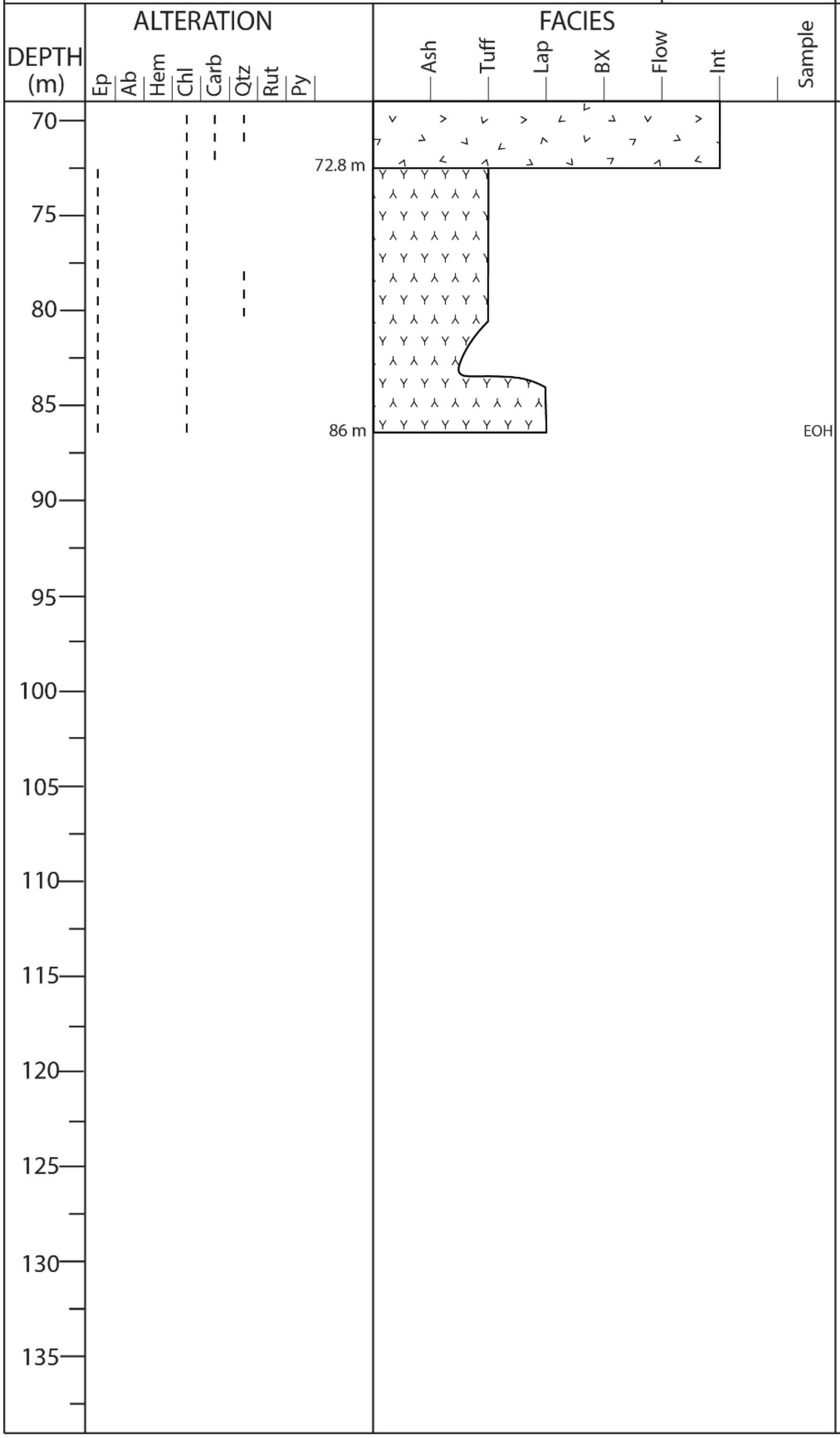

DESCRIPTION

FW volcaniclastics
well-layered (80 tca)
strongly foliated (77.5-78.3 m)
clastic content decrease (80-83 m);
coarsens to EOH

Project: Argyle
Diamond Drill Hole: AE-16-35
Date: 10-9-2017

Section: 3E

UTM
300609.2E
5537711N

Azimuth: 180
Dip: -50
Depth: 74 m

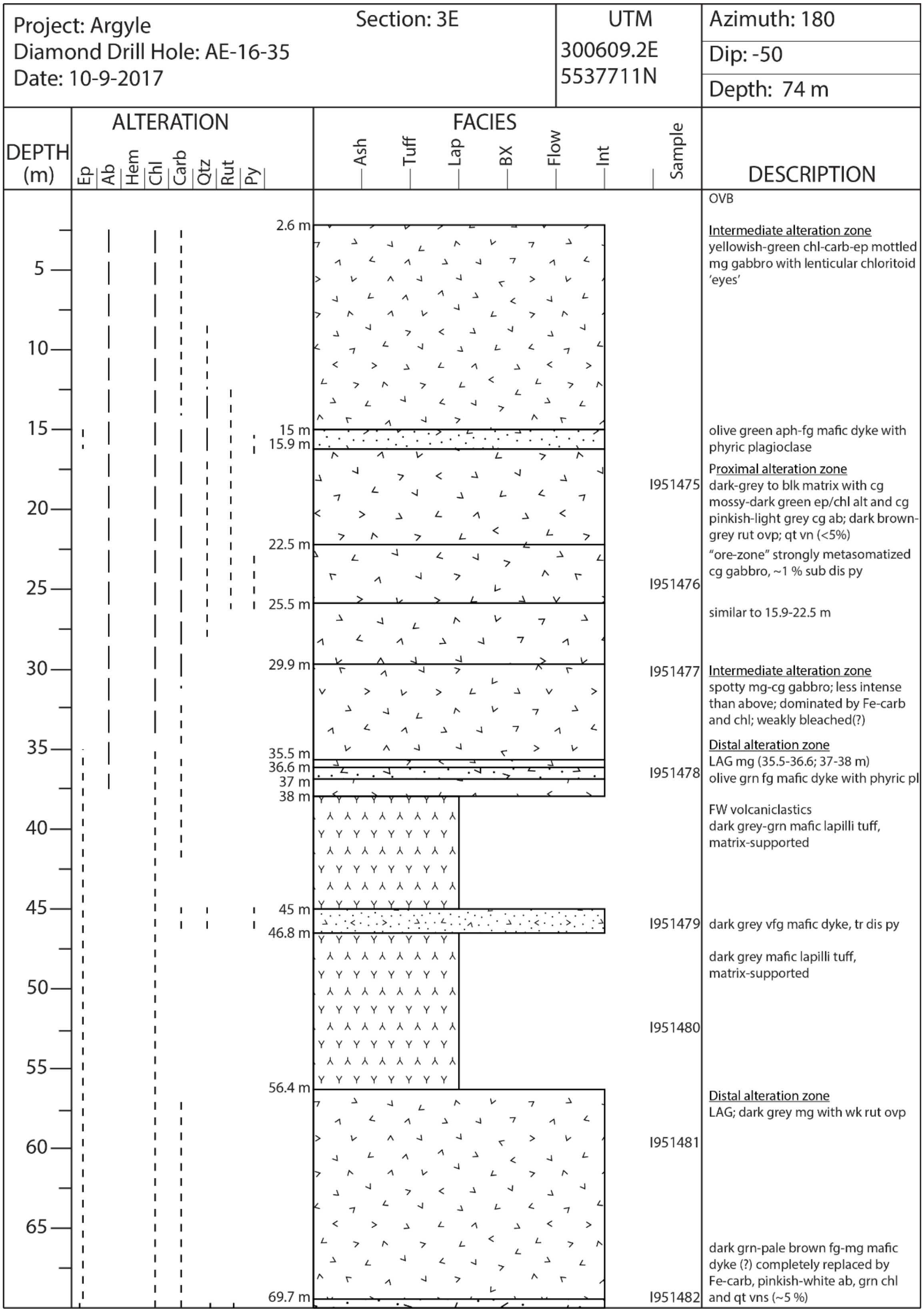

DESCRIPTION

OVB

Intermediate alteration zone
yellowish-green chl-carb-ep mottled mg gabbro with lenticular chloritoid 'eyes'

olive green aph-fg mafic dyke with phyric plagioclase

Proximal alteration zone
dark-grey to blk matrix with cg mossy-dark green ep/chl alt and cg pinkish-light grey cg ab; dark brown-grey rut ovp; qt vn (<5%)

"ore-zone" strongly metasomatized cg gabbro, ~1 % sub dis py

similar to 15.9-22.5 m

Intermediate alteration zone
spotty mg-cg gabbro; less intense than above; dominated by Fe-carb and chl; weakly bleached(?)

Distal alteration zone
LAG mg (35.5-36.6; 37-38 m)
olive grn fg mafic dyke with phyric pl

FW volcaniclastics
dark grey-grn mafic lapilli tuff, matrix-supported

dark grey vfg mafic dyke, tr dis py

dark grey mafic lapilli tuff, matrix-supported

Distal alteration zone
LAG; dark grey mg with wk rut ovp

dark grn-pale brown fg-mg mafic dyke (?) completely replaced by Fe-carb, pinkish-white ab, grn chl and qt vns (~5 %)

Project: Argyle
Diamond Drill Hole: AE-17-35
Date: 10-9-2017

Section: 3E

UTM
300609.2E
553771N

Azimuth: 180
Dip: -50
Depth: 74 m

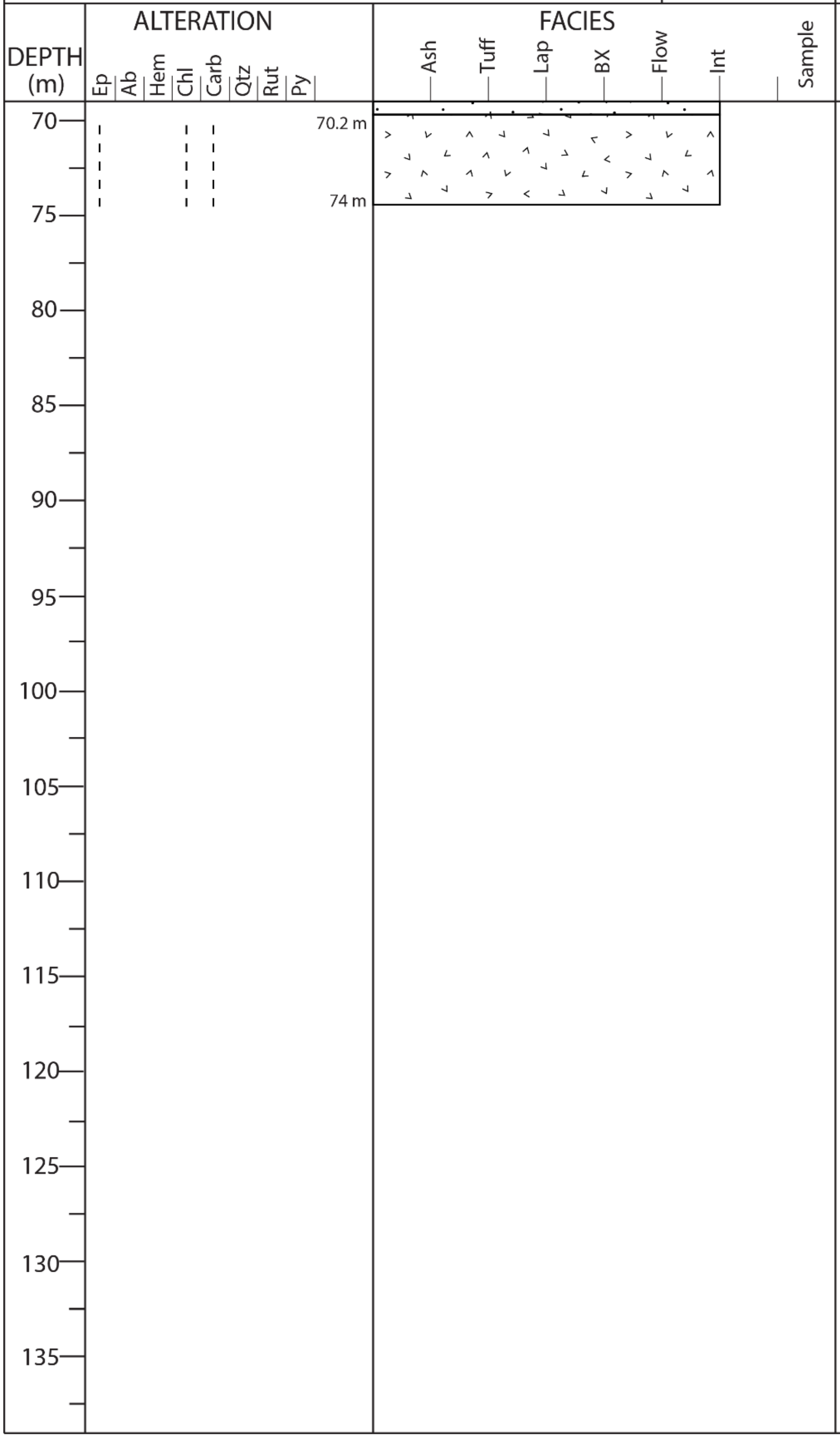

DESCRIPTION

Distal alteration zone
LAG fg-mg with carb veins (71.3-71.5)

Project: Argyle
Diamond Drill Hole: AE-16-36
Date: 10-9-2017

Section: 3E

UTM
300608.2E
5537774N

Azimuth: 180
Dip: - 50
Depth: 68.3 m

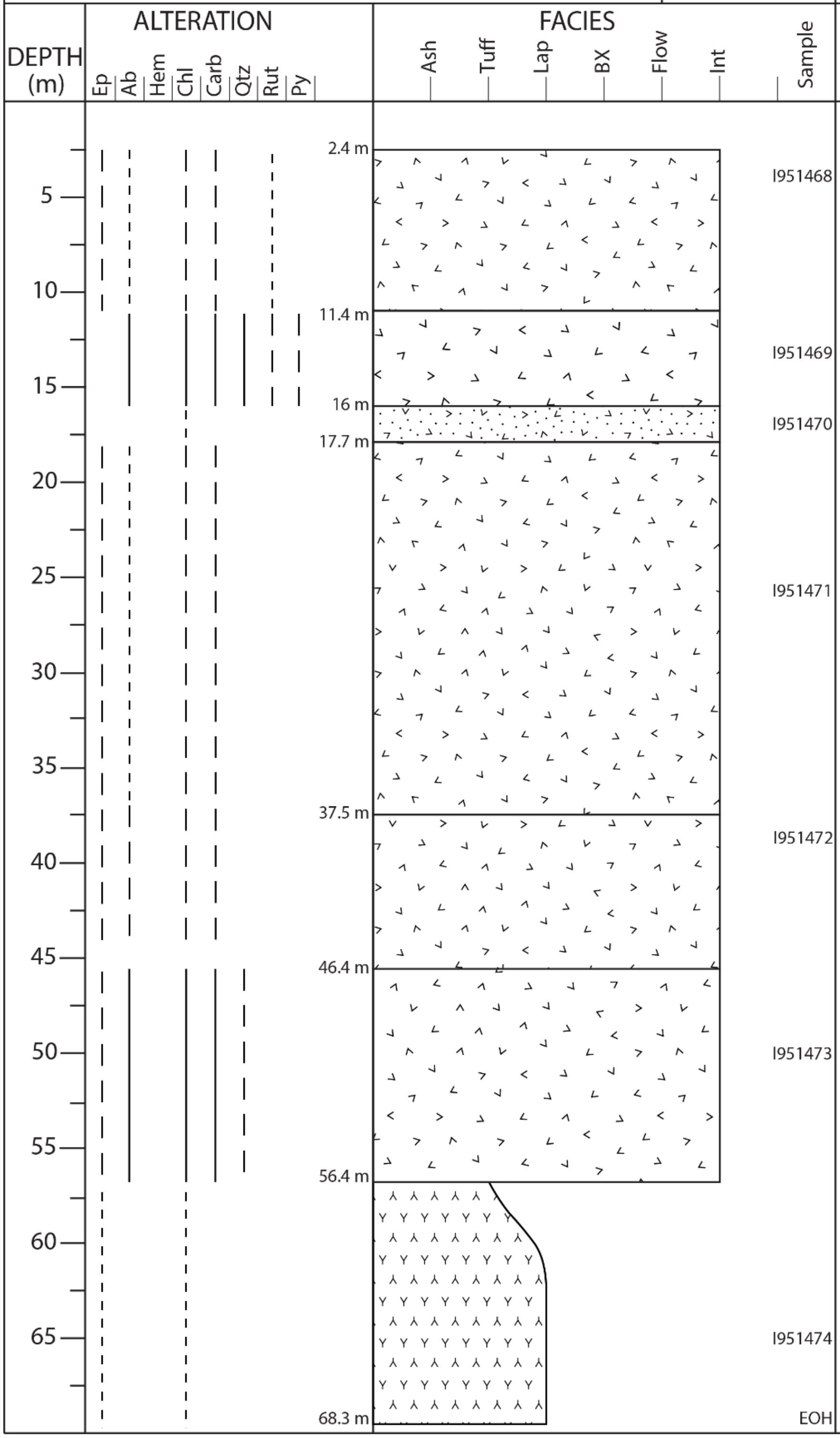

DESCRIPTION

OVB

Intermediate alteration zone
weakly bleached, mottled (chloritoid eyes) appearence; light green-pale yellow with a locally moderate ank spotty ovp; mg
Fe-carb-chl dominated

Proximal alteration zone
stongly metasomatized appearence, ab-qtz-Fe-carb-chl dominated; tr py dis and some min constrained to a mm-scale py veinlet; cg
dark grey fg-mg mafic dyke, aphinitic olive green at contact evidence for fg grey mafic dykes = aph olive dykes?

Intermediate alteration zone
mossy yellow-green to dark green bleached mg gabbro

transition from Fe-carb-chl dominated alteration asm to ab-dominated downhole

mixed zone, mg; transition from ep-dominated to ab-dominated alt assm downhole

Proximal alteration zone
dark grn, mg-cg altered gabbro with tr dis euh py; cg greyish ab with dark chl matrix, rare ep and brownish rut ovp; compared to other Argyle holes with the same alteration assemblage, the intensity of alteration here is moderate relative to stronger alt elsewhere
quartz stockwork, fractured zone 47.6-50.6 m; small shear zone ~55m.

FW volcaniclastics
mafic tuff grading down to well-foliated lapilli tuff

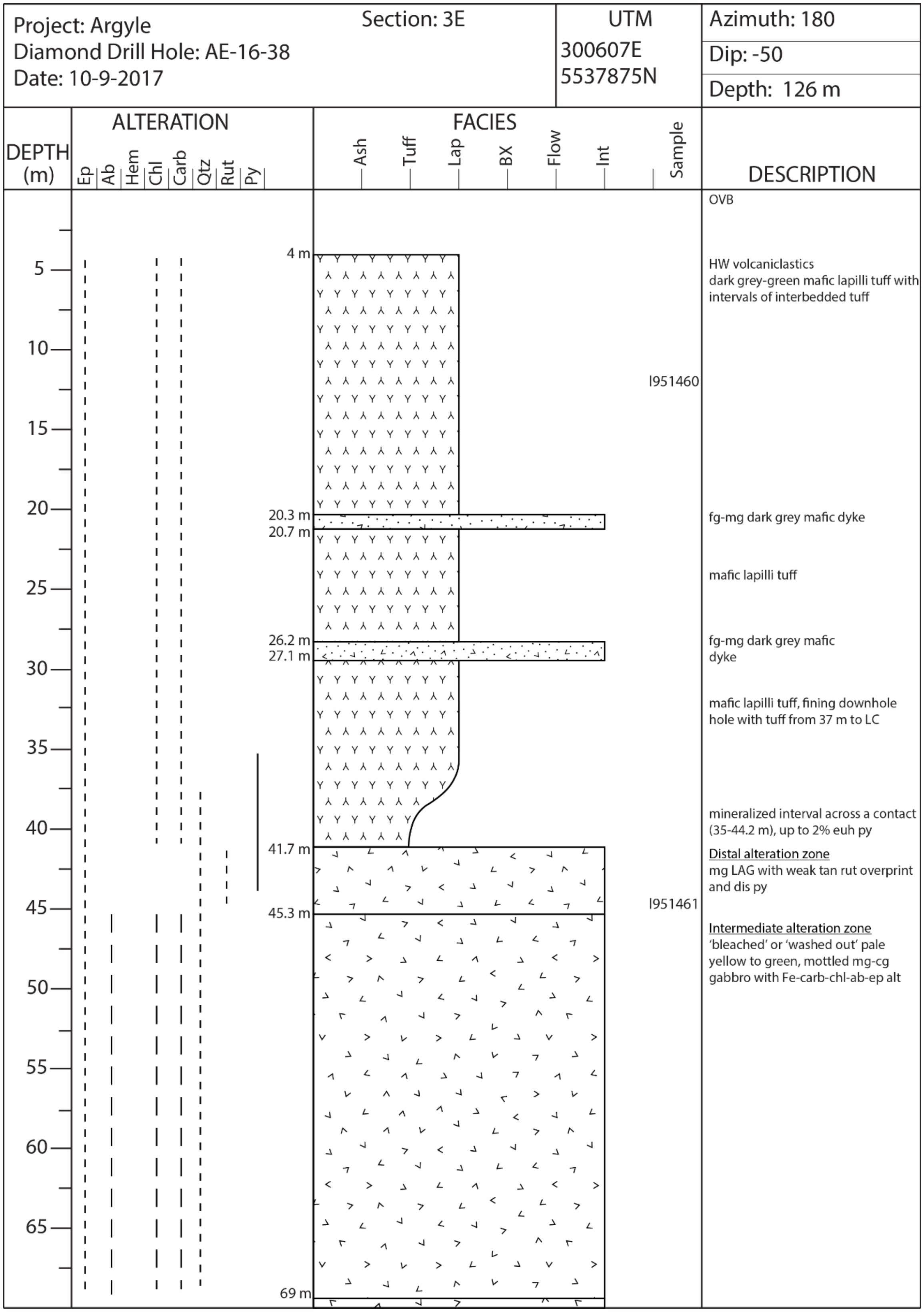

Project: Argyle
Diamond Drill Hole: AE-16-38
Date: 10-9-2017

Section: 3E

UTM
300607E
5537875N

Azimuth: 180
Dip: -50
Depth: 126 m

OVB

HW volcaniclastics
dark grey-green mafic lapilli tuff with intervals of interbedded tuff

fg-mg dark grey mafic dyke

mafic lapilli tuff

fg-mg dark grey mafic dyke

mafic lapilli tuff, fining downhole hole with tuff from 37 m to LC

mineralized interval across a contact (35-44.2 m), up to 2% euh py

Distal alteration zone
mg LAG with weak tan rut overprint and dis py

Intermediate alteration zone
'bleached' or 'washed out' pale yellow to green, mottled mg-cg gabbro with Fe-carb-chl-ab-ep alt

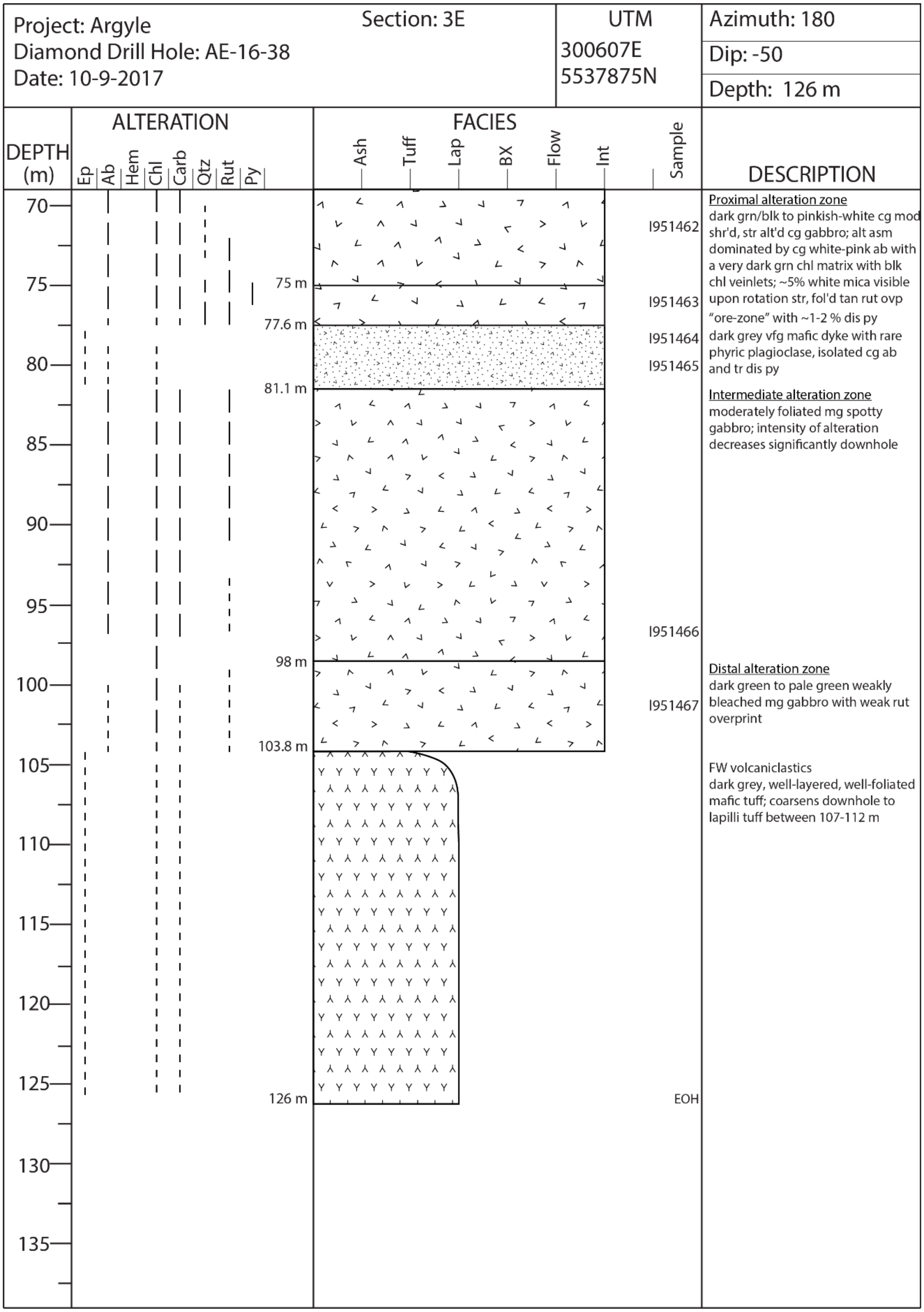

Project: Argyle
Diamond Drill Hole: AE-16-38
Date: 10-9-2017

Section: 3E

UTM
300607E
5537875N

Azimuth: 180
Dip: -50
Depth: 126 m

DESCRIPTION

Proximal alteration zone
dark grn/blk to pinkish-white cg mod shr'd, str alt'd cg gabbro; alt asm dominated by cg white-pink ab with a very dark grn chl matrix with blk chl veinlets; ~5% white mica visible upon rotation str, fol'd tan rut ovp

"ore-zone" with ~1-2 % dis py

dark grey vfg mafic dyke with rare phyric plagioclase, isolated cg ab and tr dis py

Intermediate alteration zone
moderately foliated mg spotty gabbro; intensity of alteration decreases significantly downhole

Distal alteration zone
dark green to pale green weakly bleached mg gabbro with weak rut overprint

FW volcaniclastics
dark grey, well-layered, well-foliated mafic tuff; coarsens downhole to lapilli tuff between 107-112 m

Project: Argyle
Diamond Drill Hole: AE-16-39
Date: 10-9-2017

Section: 3E

UTM
300607E
5537875N

Azimuth: 0
Dip: -90
Depth: 115 m

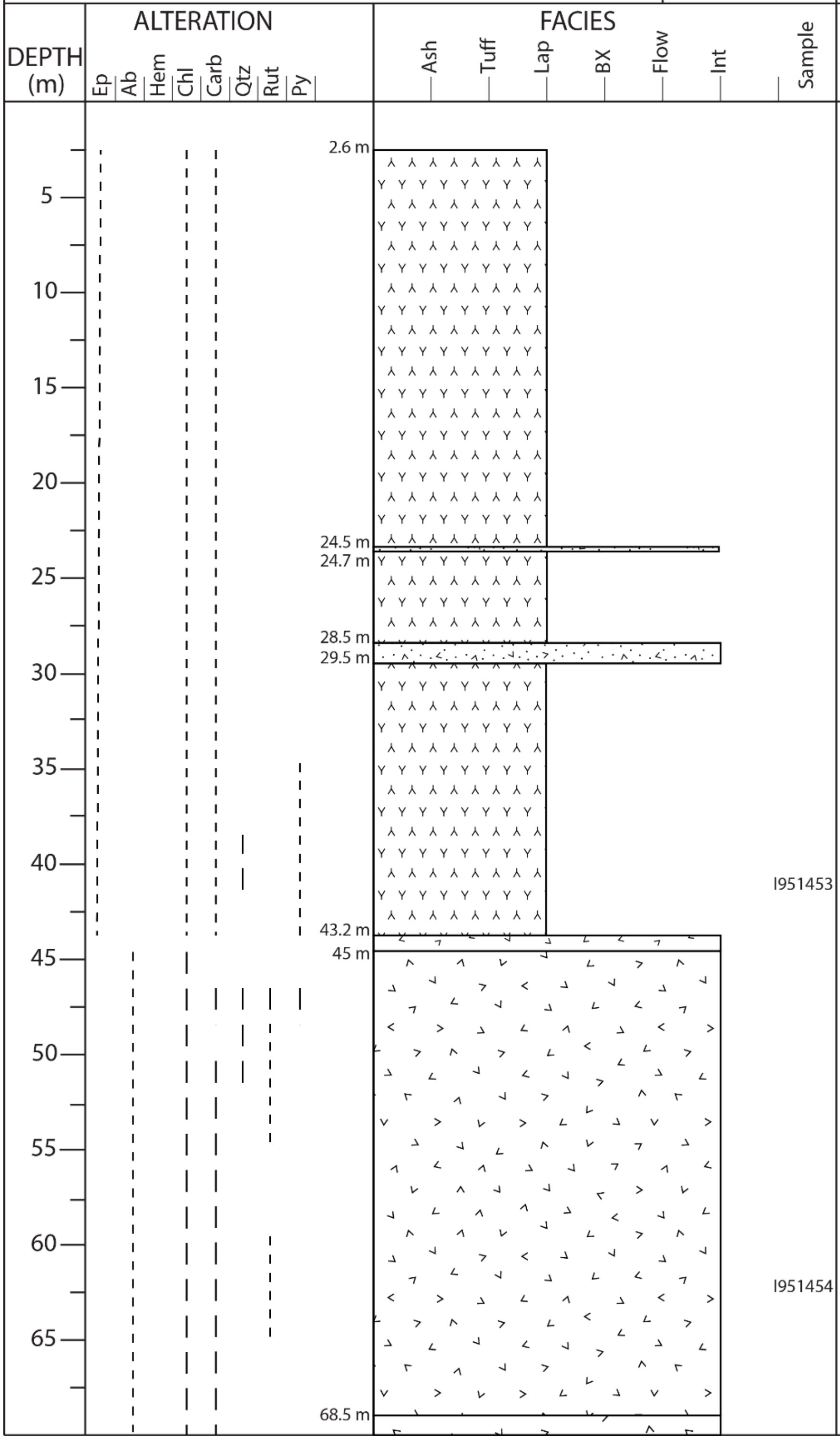

DESCRIPTION

OVB

HW volcaniclastics
mafic lapilli tuff locally interbedded with tuffaceous ash

foliation intensity increases 10.2 - 14.6 m

dark grey fg mafic dyke with rare isolated cg albite crystals (<2 %)

mafic lapilli tuff

dark grey fg mafic dyke with rare isolated cg albite crystals

mafic lapilli tuff with qt vns (10 %)

foliation intensity increases 30 - 36 m

tr dis euh py 34 - 45 m

Distal alteration zone
foliated fg gabbro from UC to 44 m.

Intermediate alteration zone
spotty dark green to brownish-yellow mg (45-52 m) to cg from 52m moderately altered gabbro

core surface is oxidized with a yellow-brown to rusty mottled appearence

chl-Fe-carb-ab dominated assm.

Proximal alteration zone
ab-Fe-carb dominated assemblage

Project: Argyle
Diamond Drill Hole: AE-16-39
Date: 10-9-2017

Section: 3E

UTM
300607E
5537875N

Azimuth: 000
Dip: -90
Depth: 115 m

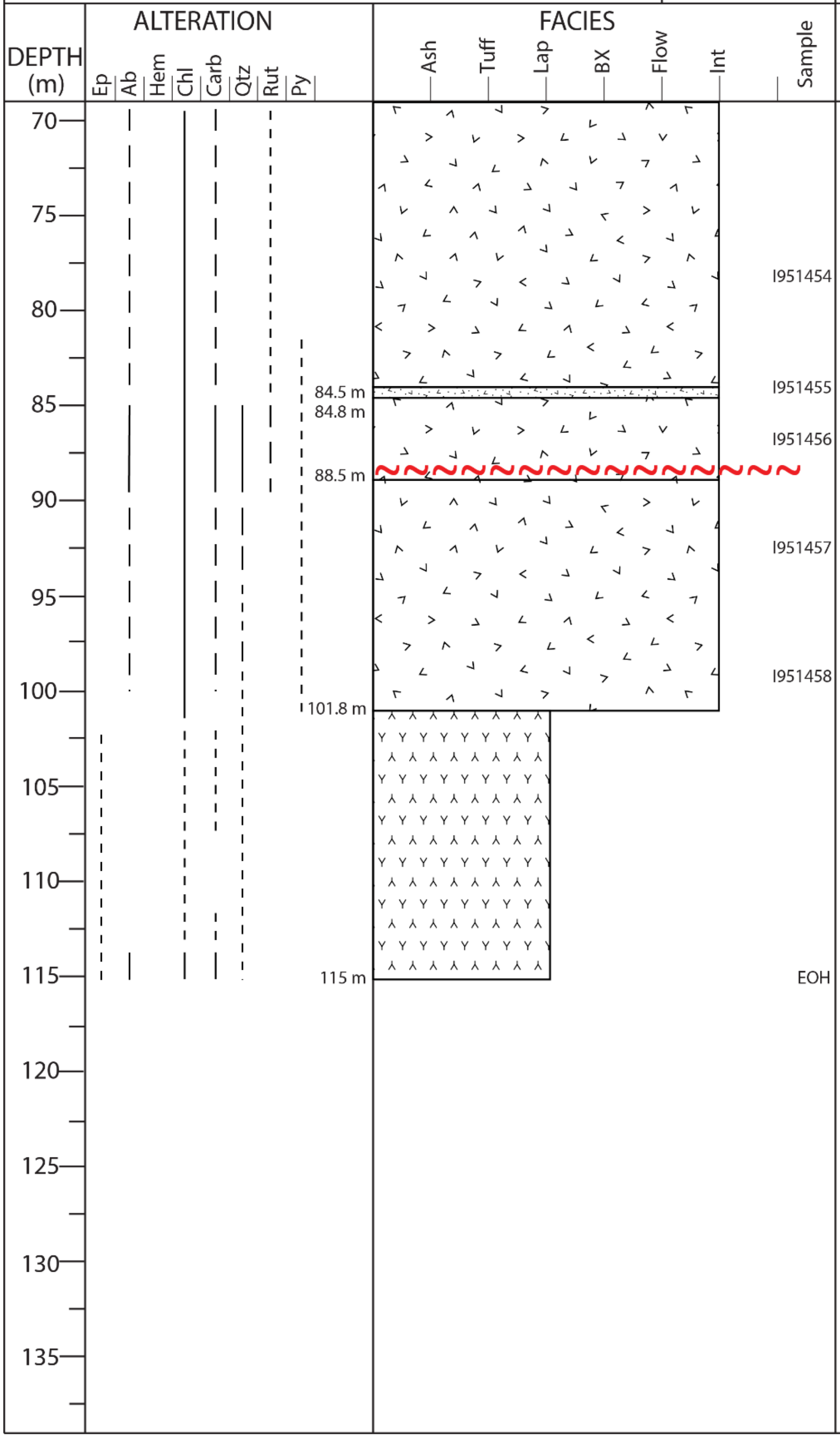

DESCRIPTION

Proximal alteration zone
from 68.5 m alteration assm. is dominated by ab-Fe-carb; cg gabbro

moderately-strongly altered with a spotty appearence

from 75.8 m gabbro develops a stronger foliation/becomes sheared

olive grn-brown vfg sheared mafic dyke

"ore-zone" - strongly metasomatized with intense qt-carb alteration and dis sooty py (5-8 %)

FLT unconsolidated gouge 87.5-88.5
FRC zone 85.5-93 m

Proximal alteration zone
alteration intensity decreases downhole, but dominated by cg pale pink ab

foliation intensity gradually decreases from 88-99.5 m

FW volcaniclastics
mafic lapilli tuff with interbedded tuff

Fe-carb-ser-ab alteration of volcaniclastic material 113.5-114.3 m

Project: Argyle
Diamond Drill Hole: AE-16-09
Date: 10-5-2017

Section: 4+25E

UTM
300733.6E
5537684N

Azimuth: 180
Dip: -45
Depth: 65.35 m

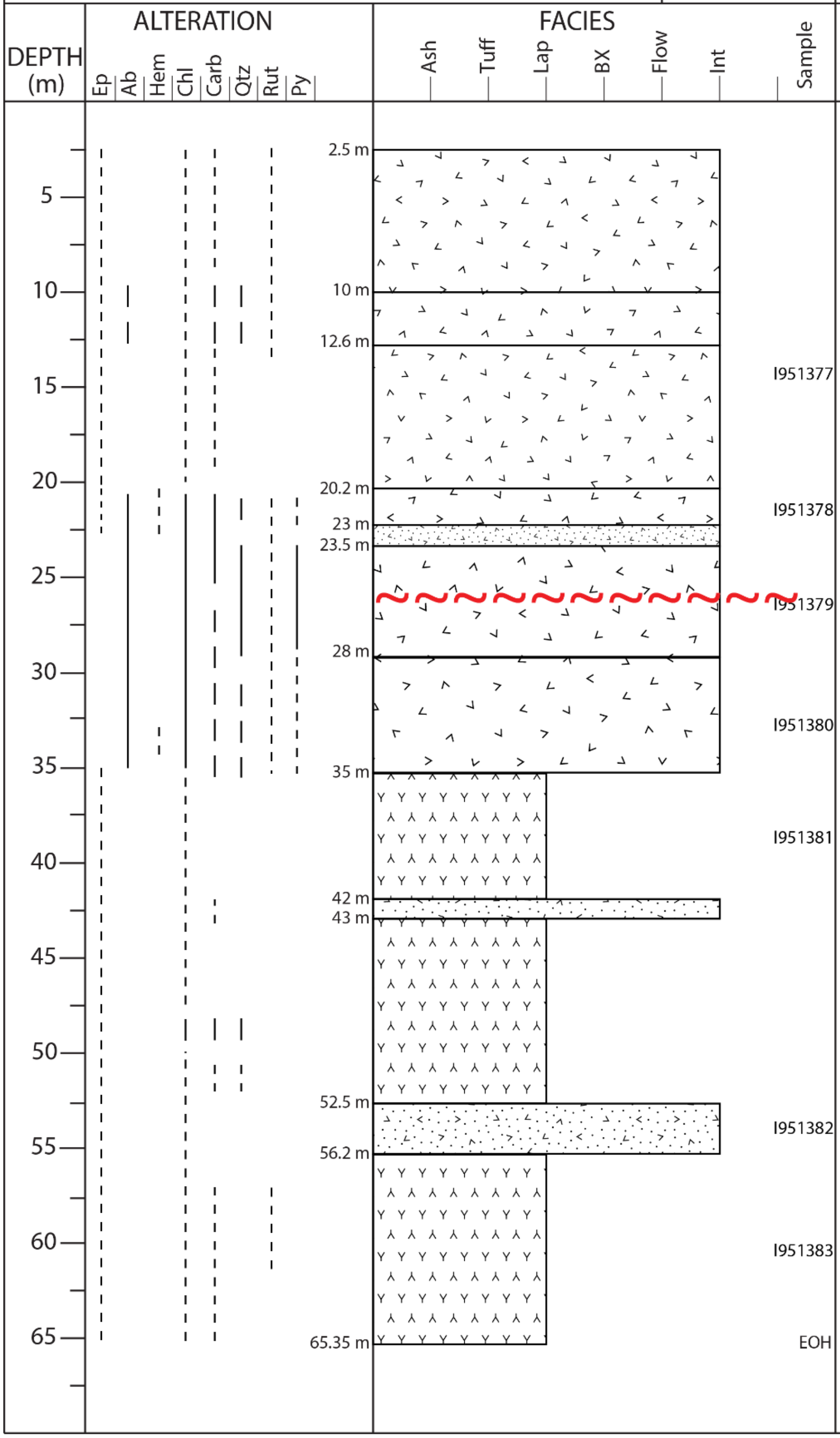

DESCRIPTION

OVB

Distal alteration zone
weakly bleached mg gabbro with a rutile overprint

Intermediate alteration zone
mg mottled gabbro

Distal alteration zone
dark grey to dark green fg-mg gabbro; mt clots (up to 5 %) with rare reaction rims and trace py on fracture planes

Proximal alteration zone
dark green to pale yellow mg-cg gabbro

olive aph-fg mafic dyke

"ore-zone" - Si-flooded/strongly metasomatized cg-pegm gabbro up to 4 % sooty py
severely fractured zone 22-31 m (intense @26 m - FLT?)

cg altered gabbro with brown-pink coarse albite, dark green chlorite matrix and black chlorite veinlets. 5% white mica, quartz carbonate veins (5%) and tan rutile overprint

mafic lapilli tuff, matrix-supported

dark grey fg mafic dyke with tr dis py and mg phyric plagioclase

mafic lapilli tuff, matrix-supported

dark grey fine mafic dyke with euhedral (<1 mm) dis. py and medium phyric plagioclase

dark grey-green mafic lapilli tuff, matrix-supported

Project: Argyle
Diamond Drill Hole: AE-16-12
Date: 10-5-2017

Section: 4+25E

UTM
300736.8E
5537731N

Azimuth: 180
Dip: -80
Depth: 70 m

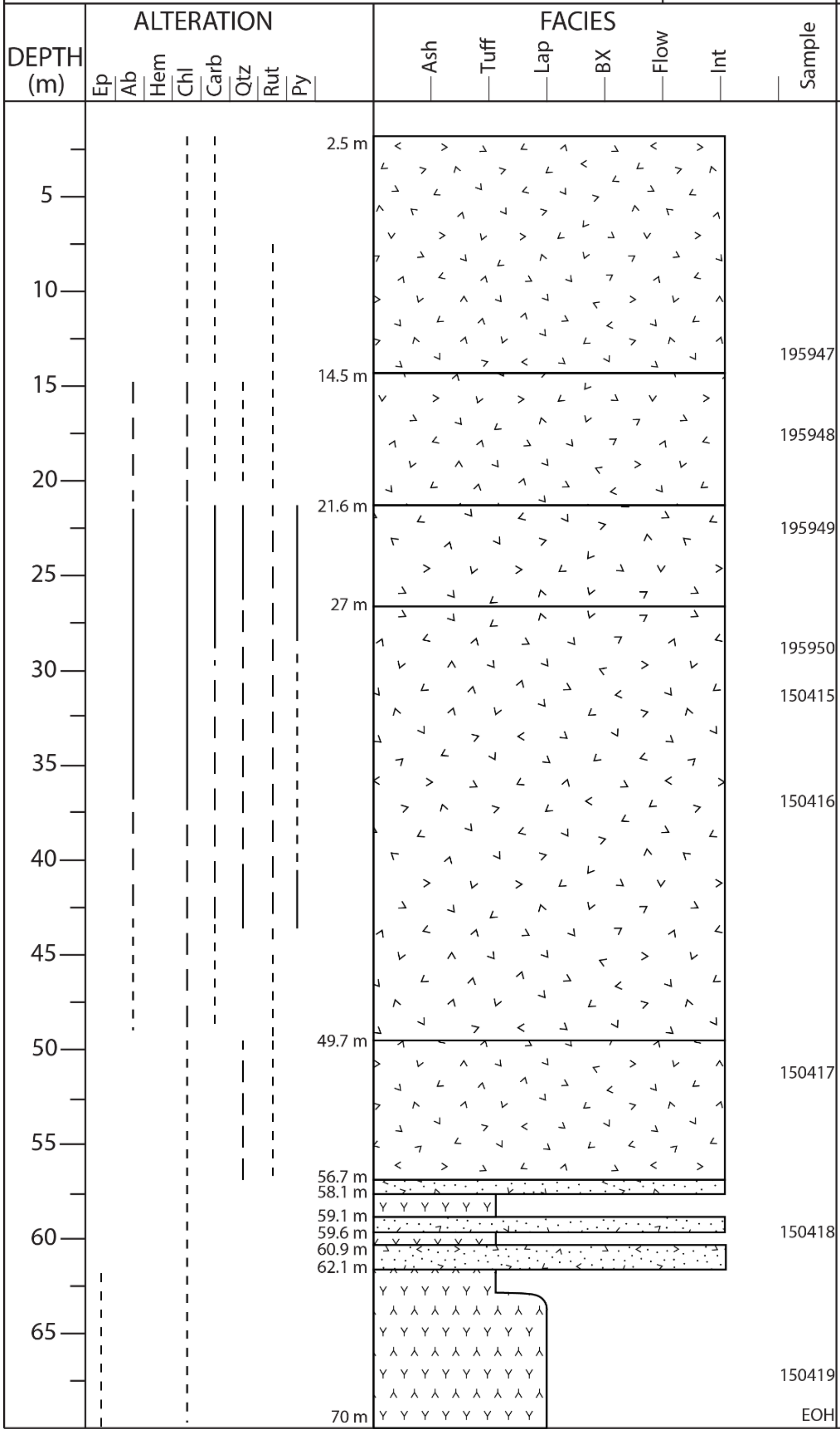

DESCRIPTION

OVB

Distal alteration zone
dark grey mg gabbro with rutile overprint and calcite veinlets

Intermediate alteration zone
mg-cg spotty gabbro with qt-carb veinlets

Proximal alteration zone
“ore-zone” - Si-flooded/strongly metasomatized cg-pegm gabbro
up to 3 % sooty py
qt-healed 24-29m

brownish-pink-grey to dark green to pale cg altered gabbro; dis euh-anh py cubes (3-5 mm, ~4% in the zone) assemblage dominated by brown-pink cg ab crystals with dark green chl infilling spaces around the albite crystals and some blk chl veinlets
5-10% white mica visible upon rotation of the core; ank visible around qt veins and likely present in large amounts, but not well defined without core surface oxidation
fg tan to dark brown rutile overprint

increasingly sheared pegmatoidal gabbro with ab-chl

tr dis py between 22-47m; up to 3% @24-29m and 40.5-44m

Intermediate alteration zone
mg gabbro with a mottled Fe-carb overprint, chilled margin at LC

multiple qt vns at LC

dark grey fg mafic dyke

dark green fg mafic dyke with phyric plag laths

olive fg mafic dyke

dark grey fg mafic tuff, coarsens downhole to lapilli tuff

Project: Argyle
Diamond Drill Hole: AE-16-11
Date: 10-14-2018

Section: 4+25E

UTM
300736.7E
5537730.6N

Azimuth: 180
Dip: -45
Depth: 67 m

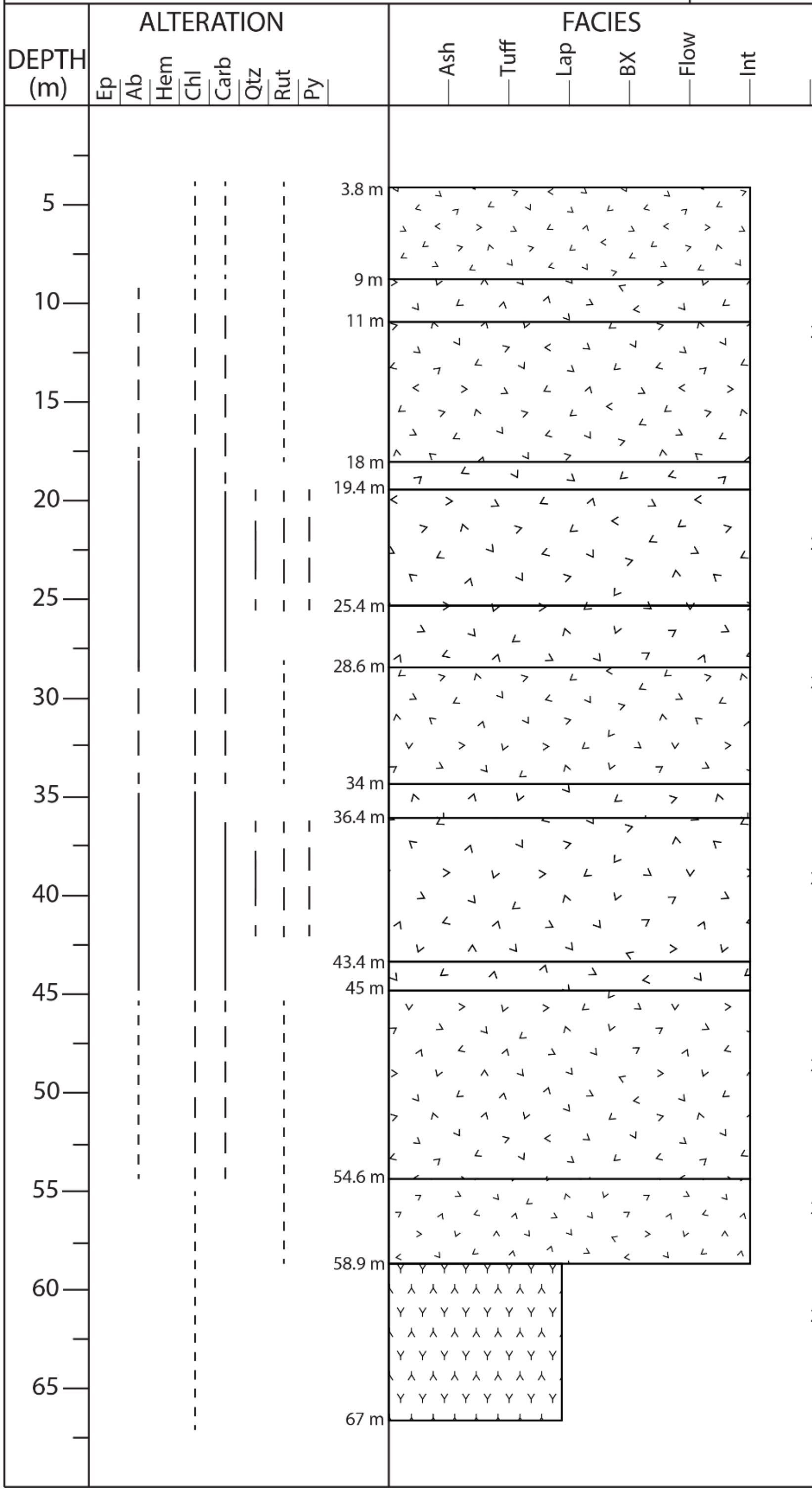

Sample	DESCRIPTION
	OVB
	Distal alteration zone fg dark grn-pale grn/ylw gabbro
	Intermediate alteration zone mg mottled gabbro
294761	spotty mg gabbro, ank ovp dominant with fg-mg chloritoid eyes core is heavily oxidized; approx ct
	Proximal alteration zone regular proximal black/dark grn chl with cg well-formed ab-altd laths
294762	“ore zone” Si-flooded, massive ab with black chl veins and sooty py mineralization
	proximal blk/drk grn gabbro with cg ab laths
294763	Intermediate alteration zone mg spotty gabbro
	Proximal alteration zone blk/drk grn gabbro with cg ab laths
294764	“ore zone” Si-flooded, massive ab with black chl veins and sooty py mineralization
	proximal blk/drk grn gabbro with cg ab laths with heavy (oxidized) Fe-carb spotting
294765	Intermediate alteration zone mg spotty gabbro with strong Fe-carb spotty overprint to 51m, downhole decrease in intensity
294766	Distal alteration zone fg dark grey-green gabbro
294767	FW volcaniclastics medium grey matrix-supported lapilli tuff with small ash and crystal tuff intervals
EOH	This hole shows Fe-carb ovp a more intense Fe-carb overprint in all alteration zones than most Argyle holes. Some similarities in prox zones with some ST section

Project: Argyle
Diamond Drill Hole: AE-16-34
Date: 10-2-2017

Section: 4+25E

UTM
300720.44E
5537748.5N

Azimuth: 180
Dip: -50
Depth: 86 m

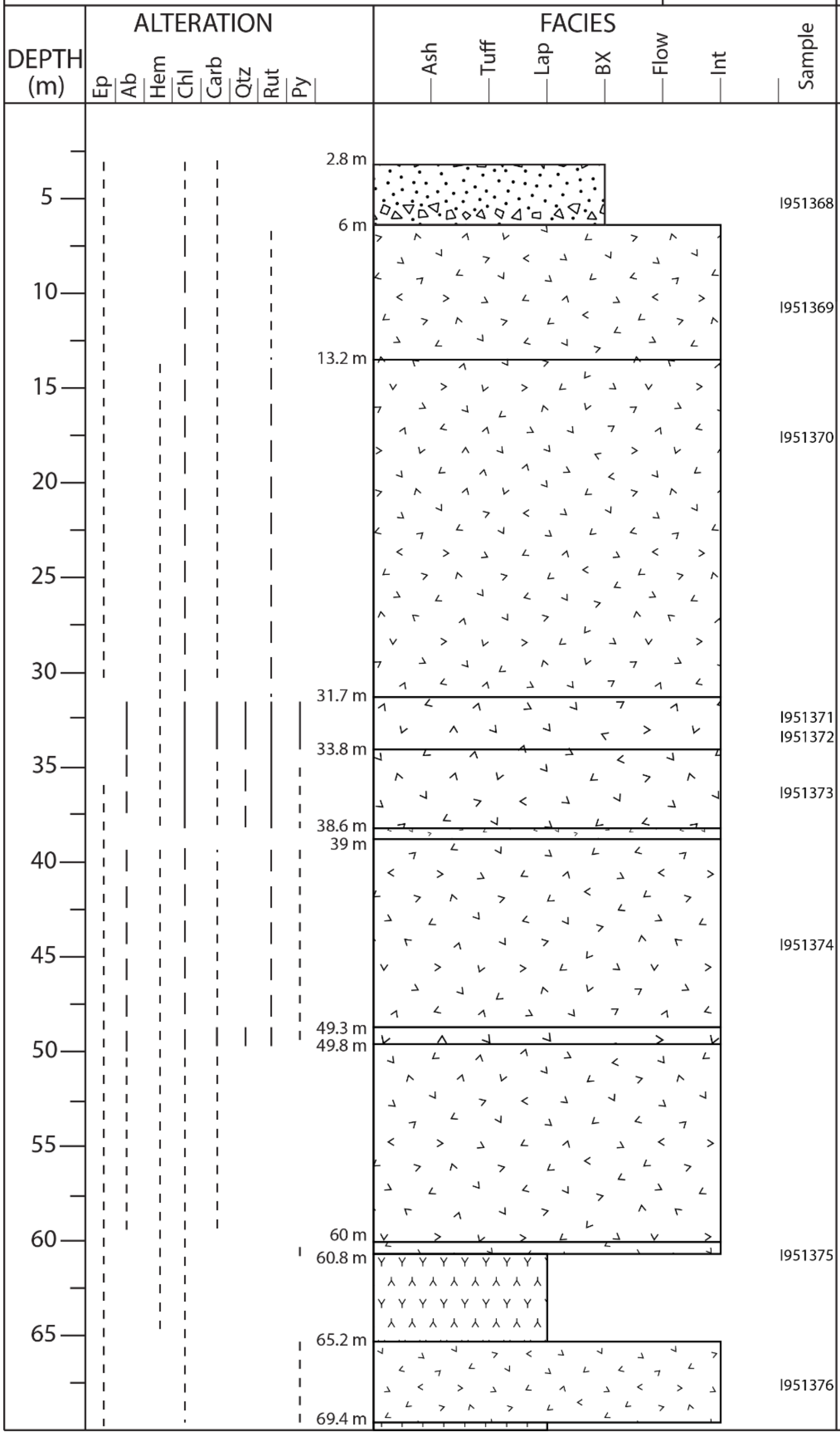

DESCRIPTION

OVB

HW volcaniclastics
dark green to pale-yellow matrix-supported mafic tuff breccia; carb-ep alteration of clasts and chl alteration of matrix; 2-3% mm-scale qt veins

Distal alteration zone
LAG; dark green mg gabbro with mg magnetite (10%), qt-blk chl vns (3%) and v. weak, vfg tan rut ovp

Intermediate alteration zone
pale-dark green chl-ep-ab altered mg gabbro with weak spotty carb and tan rut ovp

"ore-zone" - light-grey to pale-yellow and dark green strongly altered min cg gabbro, sub-anh 3 % sooty py (3-8 mm, avg 4); mineralization in WR in spatial proximity to qt-carb veins (40%); Damage/FRC zone 29-33 m

Proximal alteration zone
dark grn/blk-pinkish white cg gabbro

olive-green aph mafic dyke

Intermediate alteration zone
typical spotty mg-cg altered gabbro

Proximal alteration zone
Intense massive ab alteration with minor green chl and qtz veins (5%)

Intermediate alteration zone
mg-cg gabbro

olive-green fg mafic dyke with tr euh py dis hosted in blk chl crystal

dark grey-grn lapilli tuff;
contains a 20 cm section with ab-Fe-carb-qt material

dark grey-dark green fg mafic dyke. tr dis euh(<5 mm) py; weak chl alt of groundmass and plag
Contains numerous qt, qt-ep and ep veins x-cutting the unit

Project: Argyle
Diamond Drill Hole: AE-16-34
Date: 10-2-2017

Section: 4+25E

UTM
300720.44E
5537748.5N

Azimuth: 180
Dip: -50
Depth: 86 m

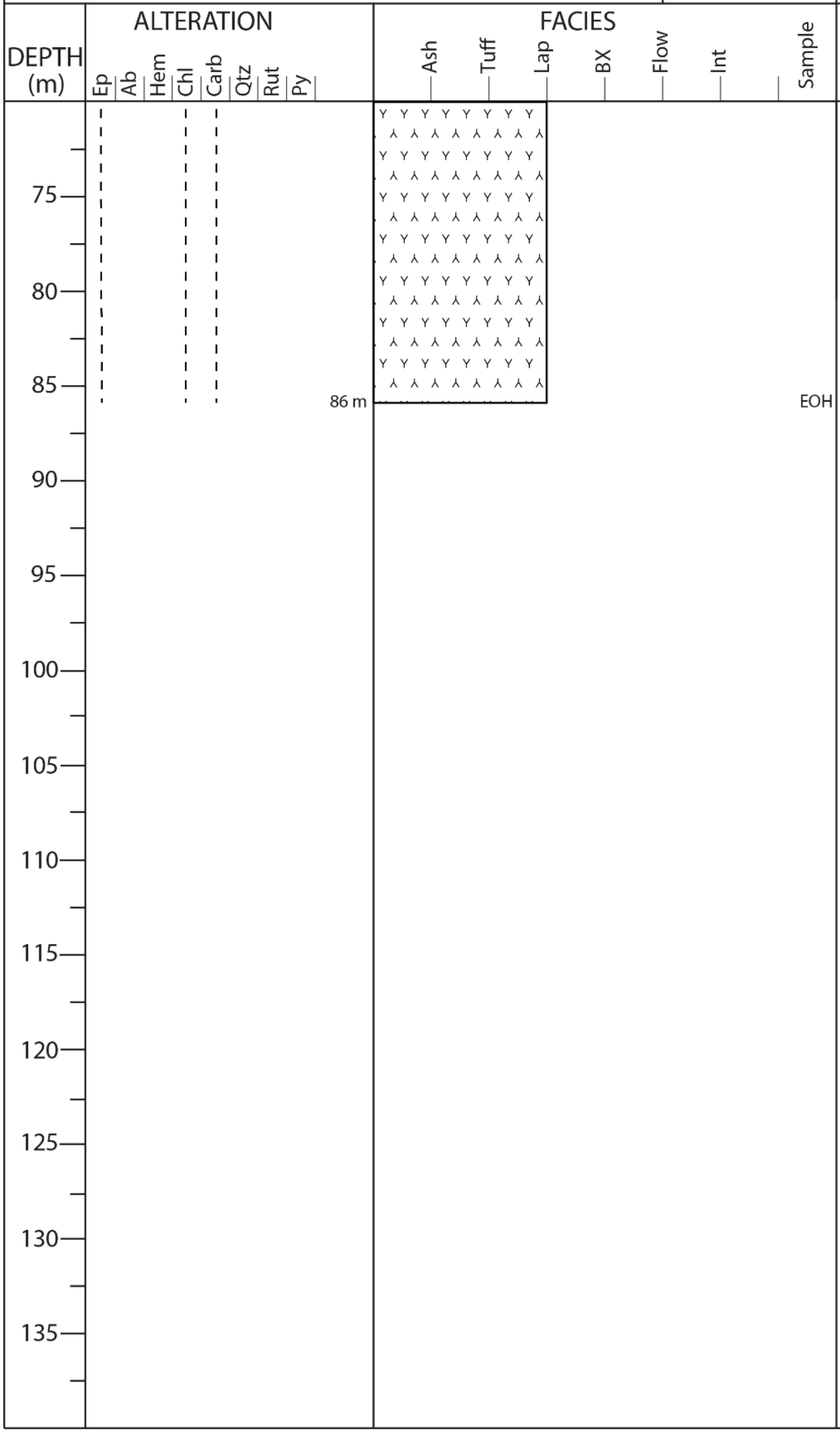

DESCRIPTION

FW volcaniclastics
pistachio light-dark grn lapilli tuff with rare blocky fragments; contains some pink-white amygdules and mm-scale ep vns

Project: Argyle
Diamond Drill Hole: AE-16-40
Date: 10-4-2017

Section: 4+25E

UTM
300720.4E
5537748N

Azimuth: 000
Dip: -90
Depth: 92 m

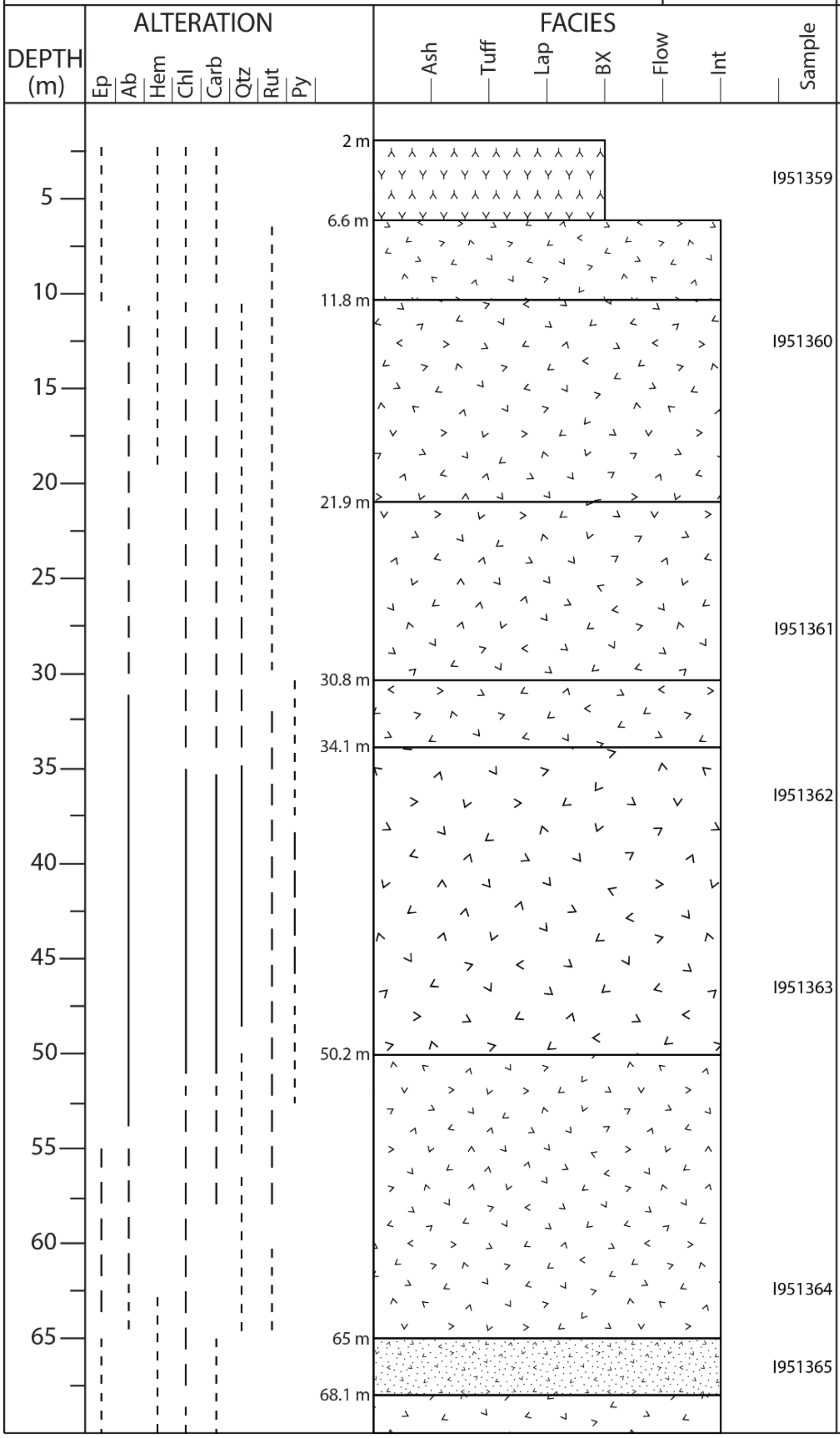

DESCRIPTION

OVB

pale green mafic tuff breccia

Distal alteration zone
fg gabbro with rare qtz veinlets and hem on fracture planes

Intermediate alteration zone
dark green to pale green 'bleached' mg gabbro, which increases downhole from 17.8 m; spotty appearence with lenticular chloritoid 'eyes'; 2% blk chl vns; 2% qt vns

Intermediate alteration zone
mg-cg mod altered gabbro with cg ab-chl dominated alteration assemblage; intensity increases significantly downhole

significant inc in qt and ab

Proximal alteration zone
"ore-zone" - Si-flooded/strongly metasomatized cg-pegm gabbro mineralized across the entire interval
pale yellow to pinkish-light grey and dark green strongly altered gabbro
2-5% dis euh-anh py (up to 4 mm), some dism concentrated together, but not constrained to a specific mineral (i.e. not spatially constrained to qt)
zone dominated by quartz vein stockwork 32-41 m
rapidly diminishing alteration intensity

Distal alteration zone
fg-mg gabbro; some Fe-carb-ab-rut present near UC; most of the unit dominated by chl-Fe-carb-ep and minor qt vnlts

dark grey-green vfg mafic dyke; rare porphyritic ab crystals; chill margin at LC

fresh/least altered fg-mg gabbro

Project: Argyle
Diamond Drill Hole: AE-16-40
Date: 10-4-2017

Section: 4+25E

UTM
300720.4E
5537748N

Azimuth: 000
Dip: -90
Depth: 92 m

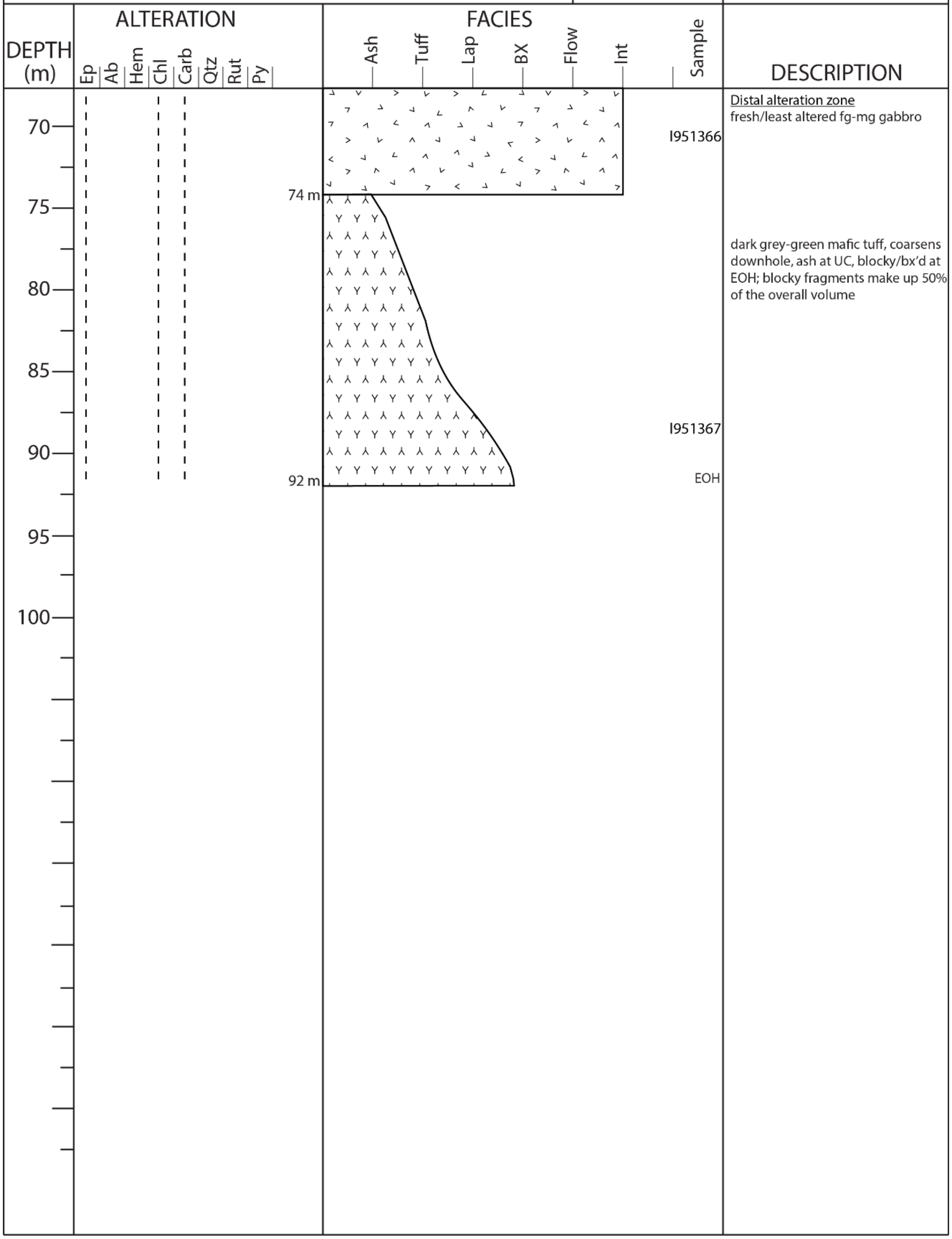

Distal alteration zone
fresh/least altered fg-mg gabbro

dark grey-green mafic tuff, coarsens downhole, ash at UC, blocky/bx'd at EOH; blocky fragments make up 50% of the overall volume

Project: Argyle
Diamond Drill Hole: AE-17-46
Date: 10-4-2017

Section: 4+25E

UTM
300719E
5537790N

Azimuth: 000
Dip: - 90
Depth: 94 m

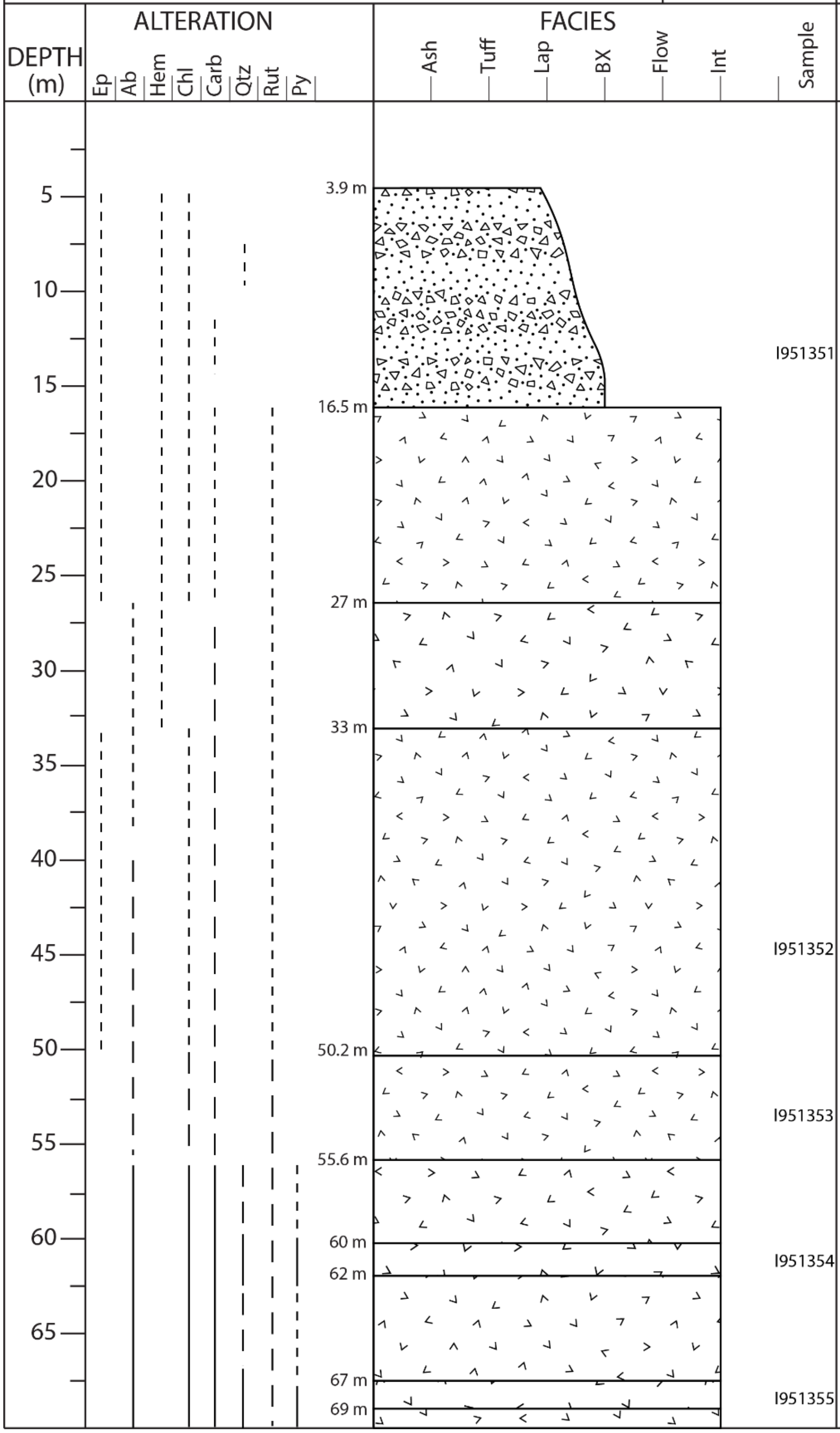

DESCRIPTION

OVB

HW volcaniclastics;
medium grey mafic tuff, coarsens downhole to tuff breccia

pillow lavas from 10 m; volcanic pillows in the mafic tuff breccia unit moss-olive green; weakly ep-chl alt'd black silica makes up 2-3% of vol

Distal alteration zone
mg LAG to 21 m, cg downhole

Intermediate alteration zone
moderately to strongly mottled cg altered gabbro, bleached; chloritoid eyes with carbonate rims

Distal alteration zone
wk-mod altered mg gabbro, locally bleached appearence evident by pale yellow-green patches of Fe-carb-chl/ep and weak rut ovp

moderately well-developed foliation near LC

Intermediate alteration zone
mg altered gabbro with pale yellow Fe-carb patches and rut overprint

Proximal alteration zone
dominated by cg ab, Fe-carb and chl

"ore-zone" - Si-flooded/strongly metasomatized cg-pegm gabbro with a dis py rich zone up to 5%; highly fractured (59-70 m)

same as above zone

"ore zone" dis py-rich zone, up to 8% py; one of the highest observed at Argyle

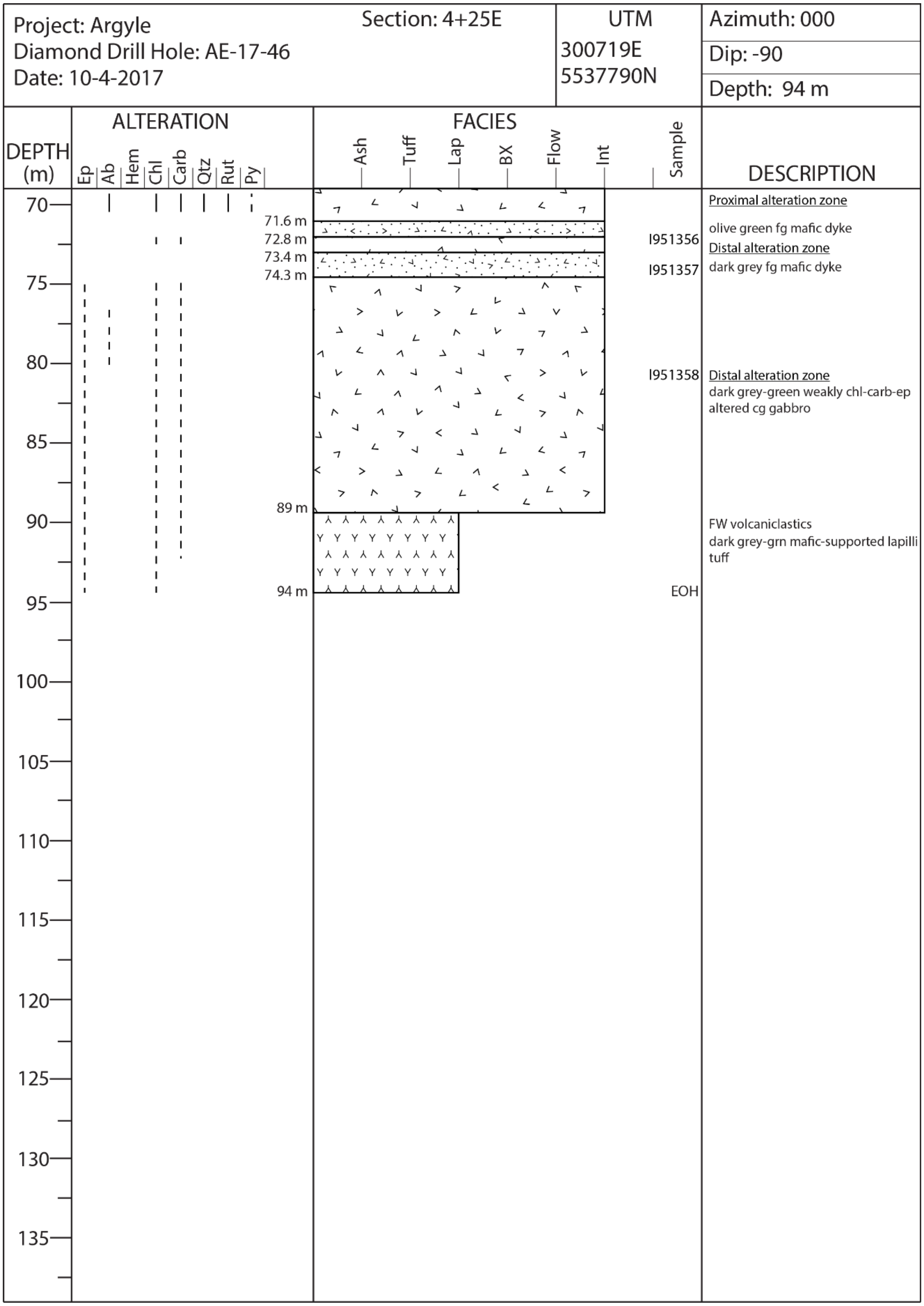

Project: Argyle
Diamond Drill Hole: AE-17-46
Date: 10-4-2017

Section: 4+25E

UTM
300719E
5537790N

Azimuth: 000
Dip: -90
Depth: 94 m

Proximal alteration zone

olive green fg mafic dyke

Distal alteration zone

dark grey fg mafic dyke

Distal alteration zone

dark grey-green weakly chl-carb-ep altered cg gabbro

FW volcaniclastics

dark grey-grn mafic-supported lapilli tuff

Project: Argyle
Diamond Drill Hole: AE-18-66
Date: 10-13-2018

Section: 4+25E

UTM
300718.9E
5537789.8N

Azimuth: 360
Dip: -75
Depth: 106 m

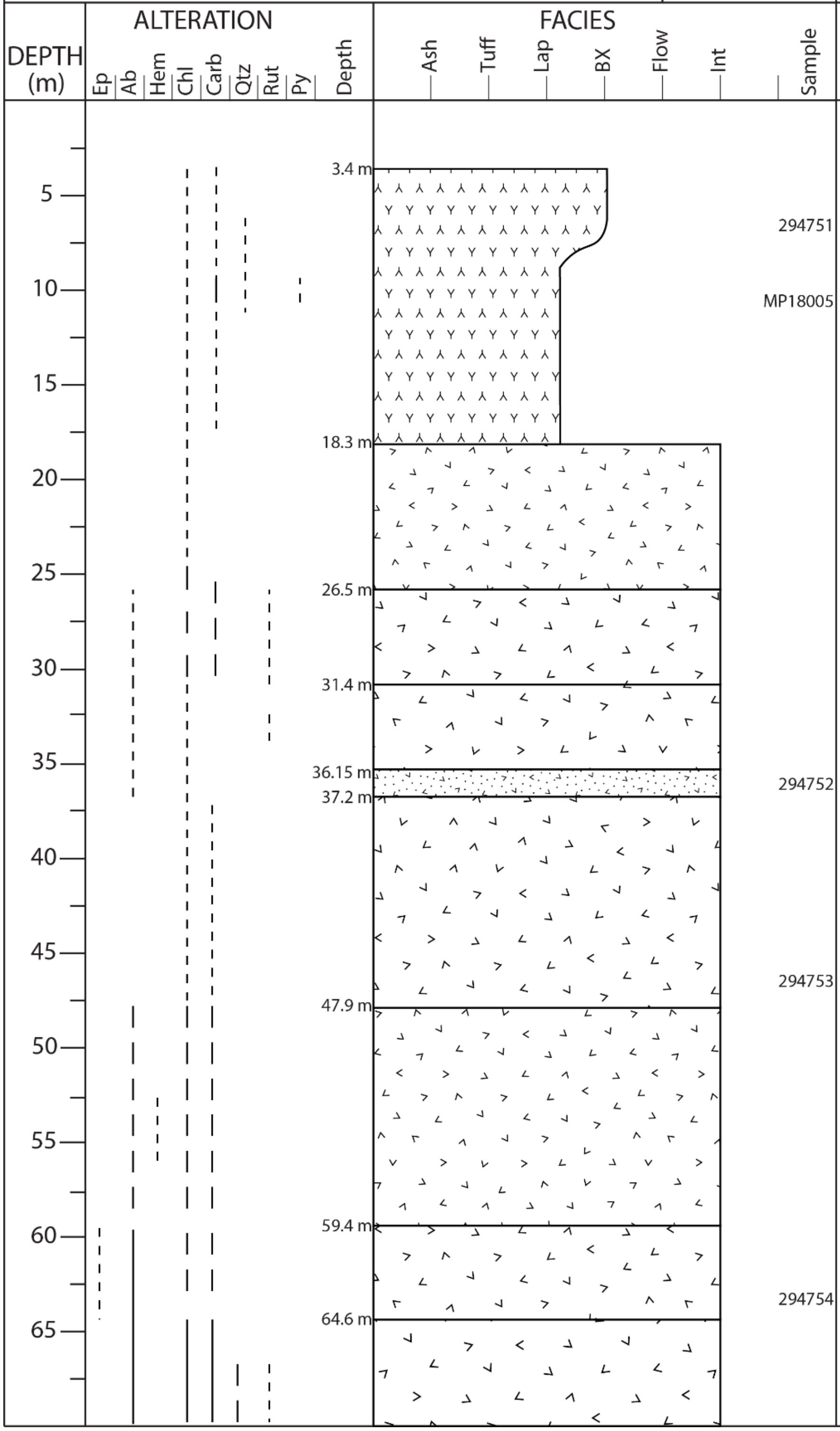

DESCRIPTION

OVB

HW volcaniclastics
medium-dark green-grey mafic lapilli tuff with trace dis euh py in WR and close to vein margins
cm-dm scale qtz-ank veins common

py in qt-carb-ab massive veins ff in tuff bx

Distal alteration zone
dark pale grn fg-mg gabbro with locally wk-mod rut and chloritoids (~5-10%)

Intermediate alteration zone
pale yellow-beige-brown to dark grn cg spotty gabbro with cm-scale qt-carb veins, locally weakly foliated

Distal alteration zone
dark grey cg gabbro with a weak rut ovp

dark green aph-fg mafic dyke weakly-moderately carb altered with isolated ab crystals

Distal alteration zone
as gabbro above

mg gabbro with weak chl-carb spots and magnetite crystals

Intermediate alteration zone
spotty mg gabbro with ab
37.2-59 mg; 59-65 cg

cg gabbro, equivalent to that found in proximal zone at AP (pre-D2)

spotty mg gabbro with ab

Proximal alteration zone
becomes increasingly altered (syn-D2) downhole with increase in spotty carb overprint, qt and sericite

Project: Argyle
Diamond Drill Hole: AE-18-66
Date: 10-13-2018

Section: 4+25E

UTM
300718.9E
5537789.8N

Azimuth: 360
Dip: -75
Depth: 106 m

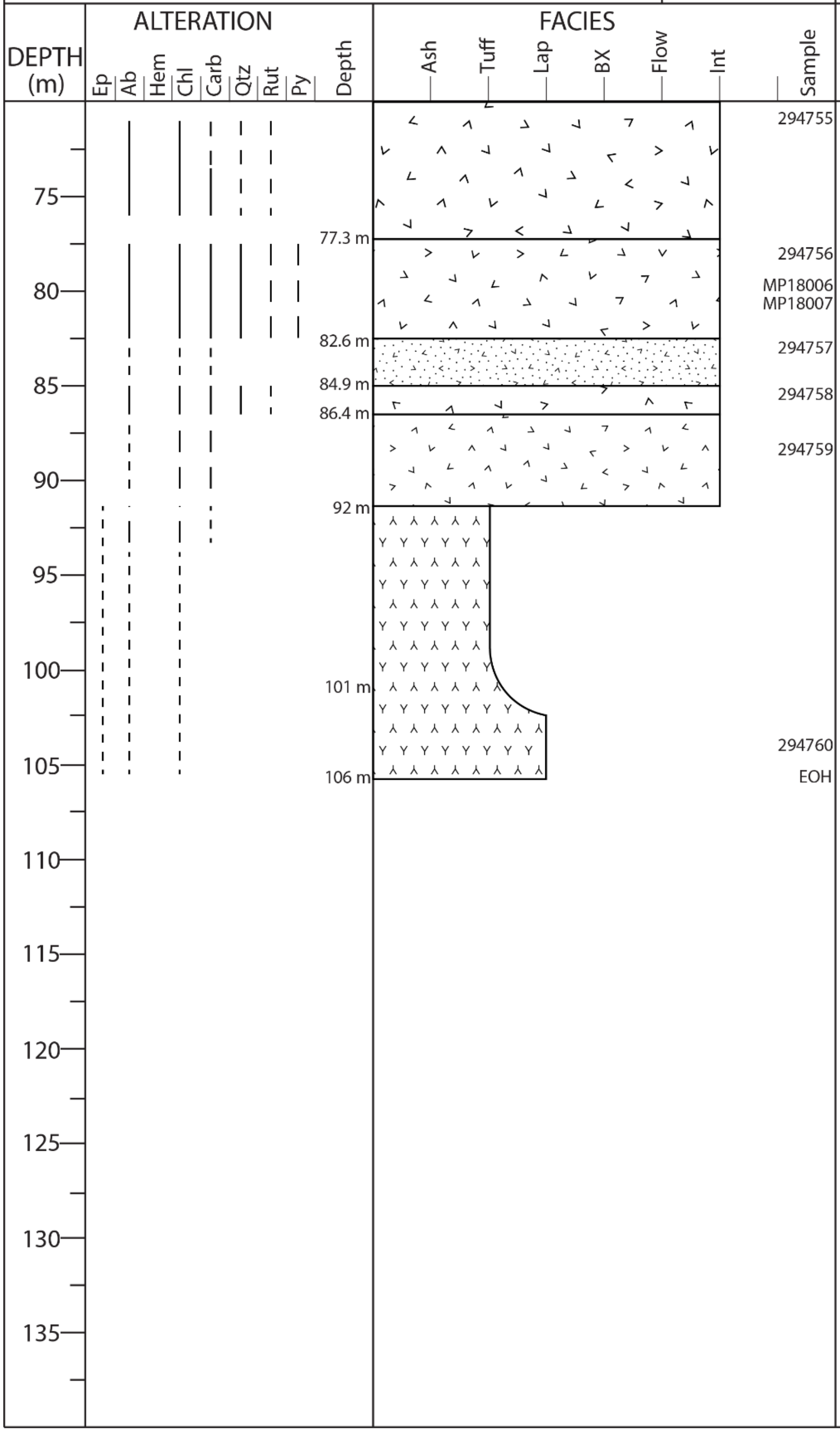

DESCRIPTION

Proximal alteration zone
spotty vcg gabbro, increase in carb-qt-ser alteration

mineralized zone within strongly metasomatized gabbro with massive ab-Fe carb-chl appearance highly Si-flooded with ~5% blebby sooty py and abundant qt veins

aph-fg dark green mafic dyke with isolated ab crystals, post-dates syn-D2 mineralization event, crosscuts the gabbro. Dyke unaffected by hydrothermal alteration

Proximal alteration zone
non-mineralized zone despite the same alteration assemblage as in the mineralized zone above

Intermediate alteration zone
mg-cg gabbro

FW volcaniclastics
mafic crystal tuff interbedded with ash sections and lapilli fragments

lapilli tuff/breccia with chl and apple green ep and pink-orange ab void infill
mm-scale qt veins less abundant compared to HW

Project: Argyle Diamond Drill Hole: AE-16-14 Date: 10-14-2018	Section: 5E	UTM 300805.8E 5537710.2N	Azimuth: 180 Dip: -45 Depth: 75 m

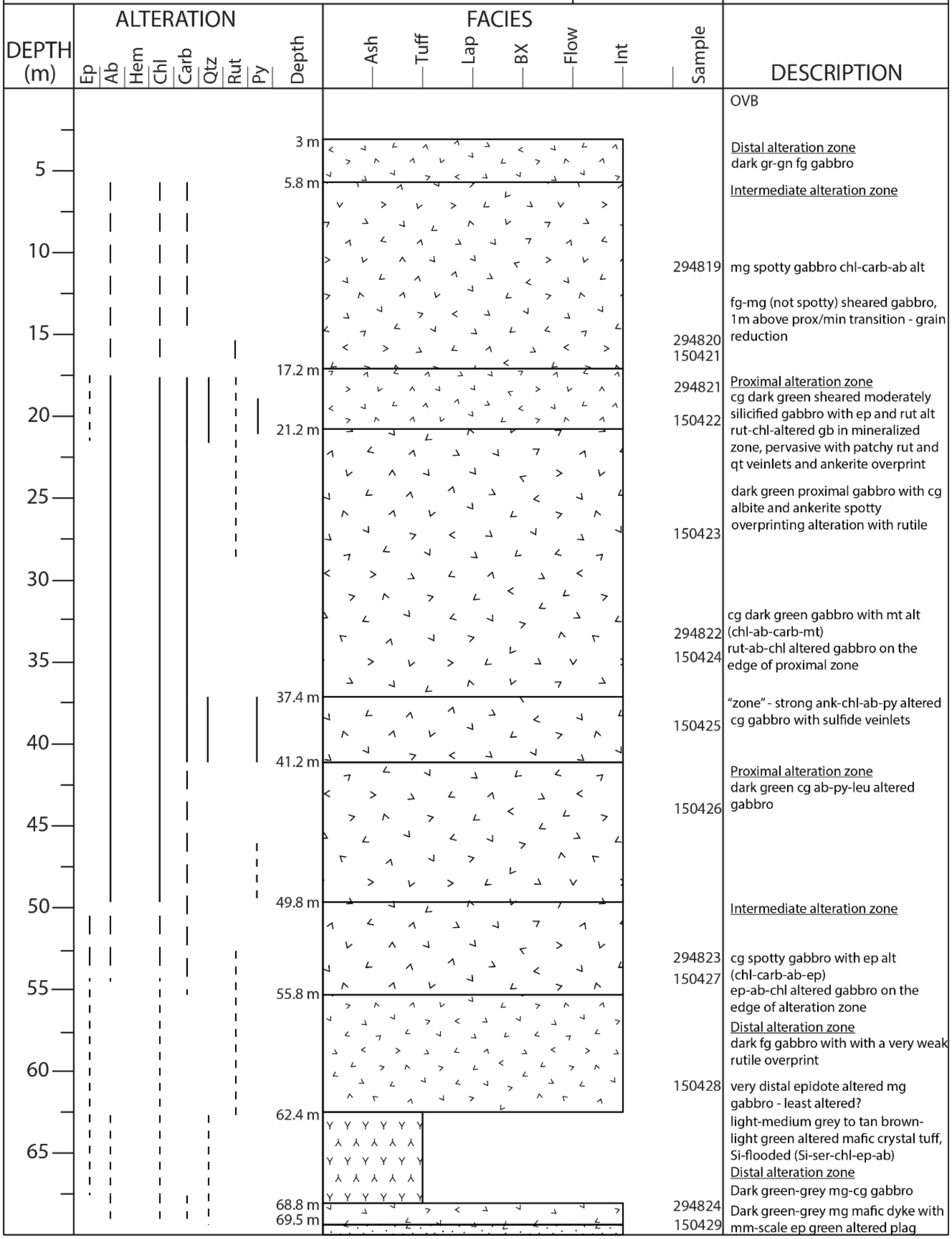

Project: Argyle
Diamond Drill Hole: AE-16-14
Date: 10-14-2018

Section: 5E

UTM
300805.8E
5537710.2N

Azimuth: 180
Dip: -45
Depth: 75 m

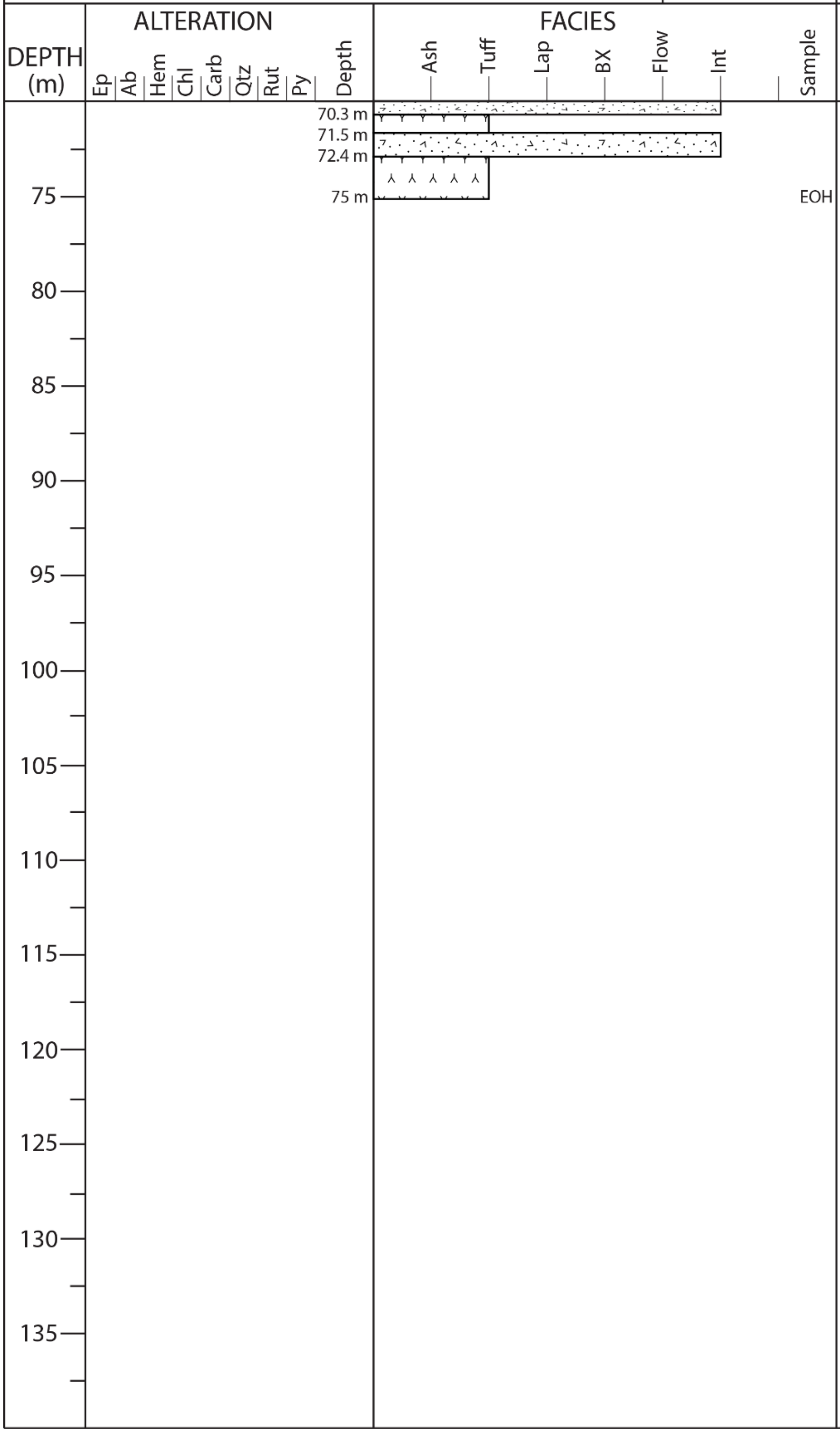

DESCRIPTION

FW volcaniclastics

medium grey alt crystal tuff, as at 65.4-68.8; grades in and out of the regular style of unaltered lapilli tuff

dark grey-green mafic dyke with rare ab crystals

same as volcaniclastics above

Project: Argyle Diamond Drill Hole: AE-16-30 Date: 10-5-2017	UTM 300811.2E 5537747.5N	Azimuth: 180 Dip: -50 Depth: 88 m

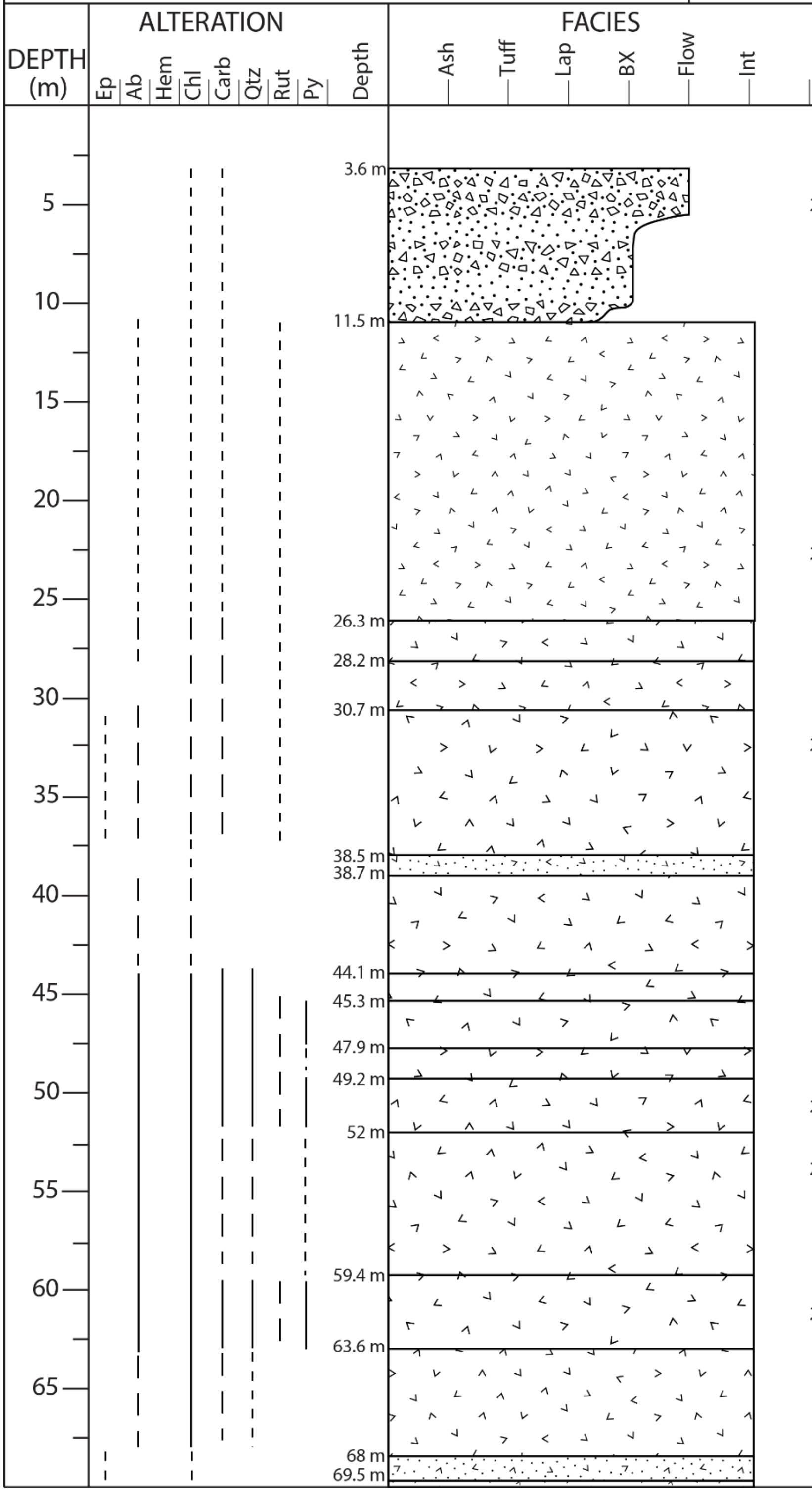

Sample	DESCRIPTION
	OVB
	HW volcaniclastics
294810	pale grey-green patchy alteration of matrix-supported pillow lavas, locally brecciated
	chl-ser-ep-Si-ab
	Distal alteration zone
	medium green-grey fg gabbro with pervasive overprinting chl alteration
294811	mg distal gabbro with wm rut ovp
	Intermediate alteration zone
	mg spotty gabbro
	Distal alteration zone
	mg-cg green-grey distal with rut ovp
	Intermediate alteration zone
294812	cg spotty gabbro
	aph camo grn dyke with 5-10% blk chloritoid eyes
	Intermediate alteration zone
	same as above interm. gabbro bottom ~1.5 m no spotty texture "transition zone" - dark green chl-ab
	Proximal alteration zone
	44.1-45.3, 47.9-49.2, 52-50.4 - cg prox 45.3-47.9, 49.1-52, 59.4-63.6 - "ore-zones"
294813	typical cg black/dark green gabbro with cg ab crystals immediately below a qt-healed fault
294814	cg dark green gabbro with mt and py min
294815	mineralized coarse Si-flooded gabbro with vcg (up to 25 mm brown Fe carb spots)
	Intermediate alteration zone
	spotty mg dark grn-pale/tan brown with rare fuchsite replacing chloritoid eyes
	camo grn aph mafic dyke

Project: Argyle
Diamond Drill Hole: AE-16-30
Date: 10-5-2017

Section: 5E

UTM
300811.2E
5537747.5N

Azimuth: 180
Dip: -50
Depth: 88 m

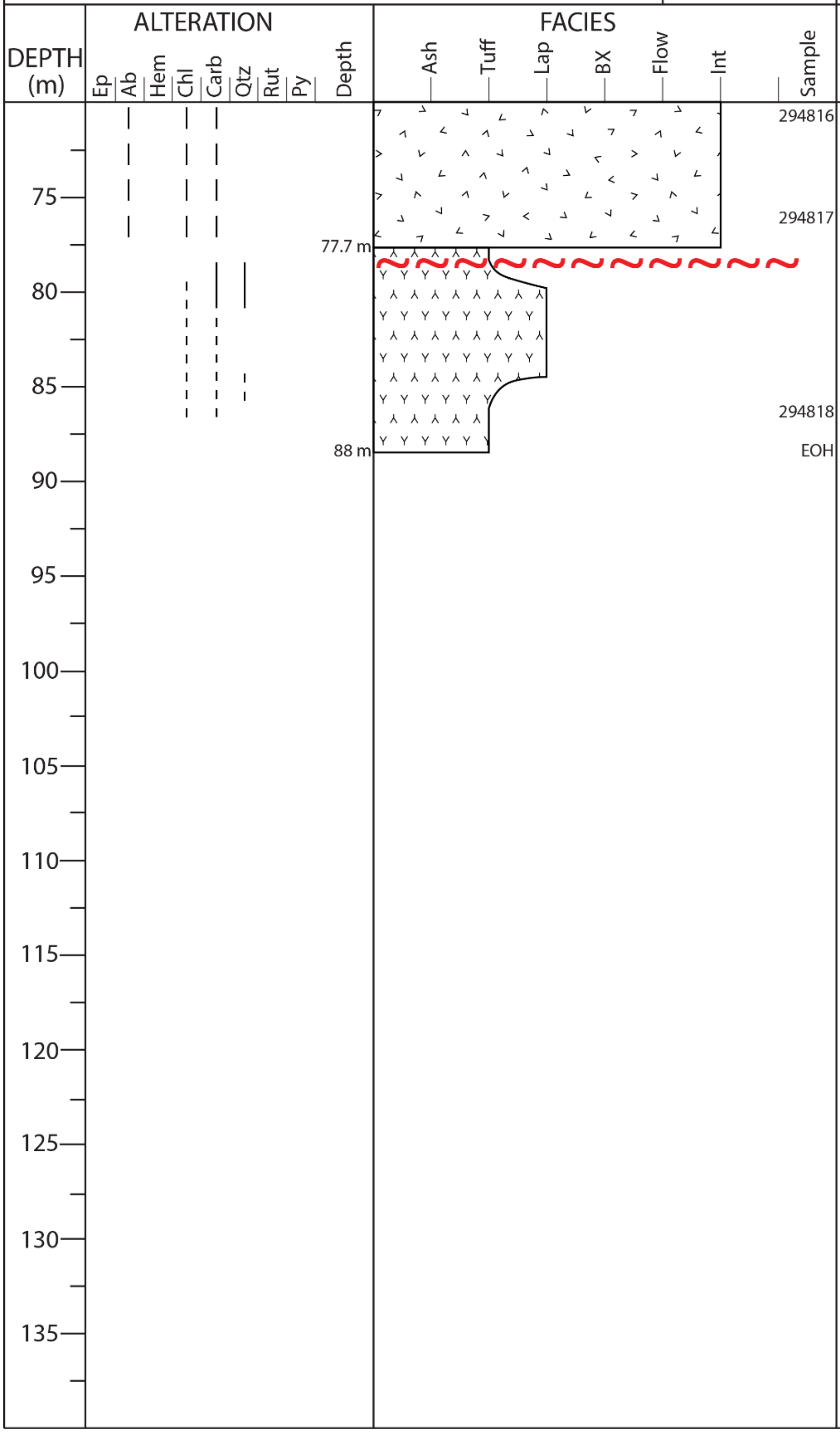

DESCRIPTION

Intermediate alteration zone
mg-cg spotty gabbro

78.7-80.4m - strongly deformed qtz-carb veining and ~2cm wide fault gouges

FW volcaniclastics
well-foliated and folded medium grey-pale medium green mafic lapilli tuff with short intervals of crystal tuff and qt-ank-ab cm-scale veinlets

crystal tuff with remnant foliation

Project: Argyle
Diamond Drill Hole: AE-16-41
Date: 10-14-2018

Section: 5E

UTM
300811.2E
5537747.5N

Azimuth: 000
Dip: -90
Depth: 95 m

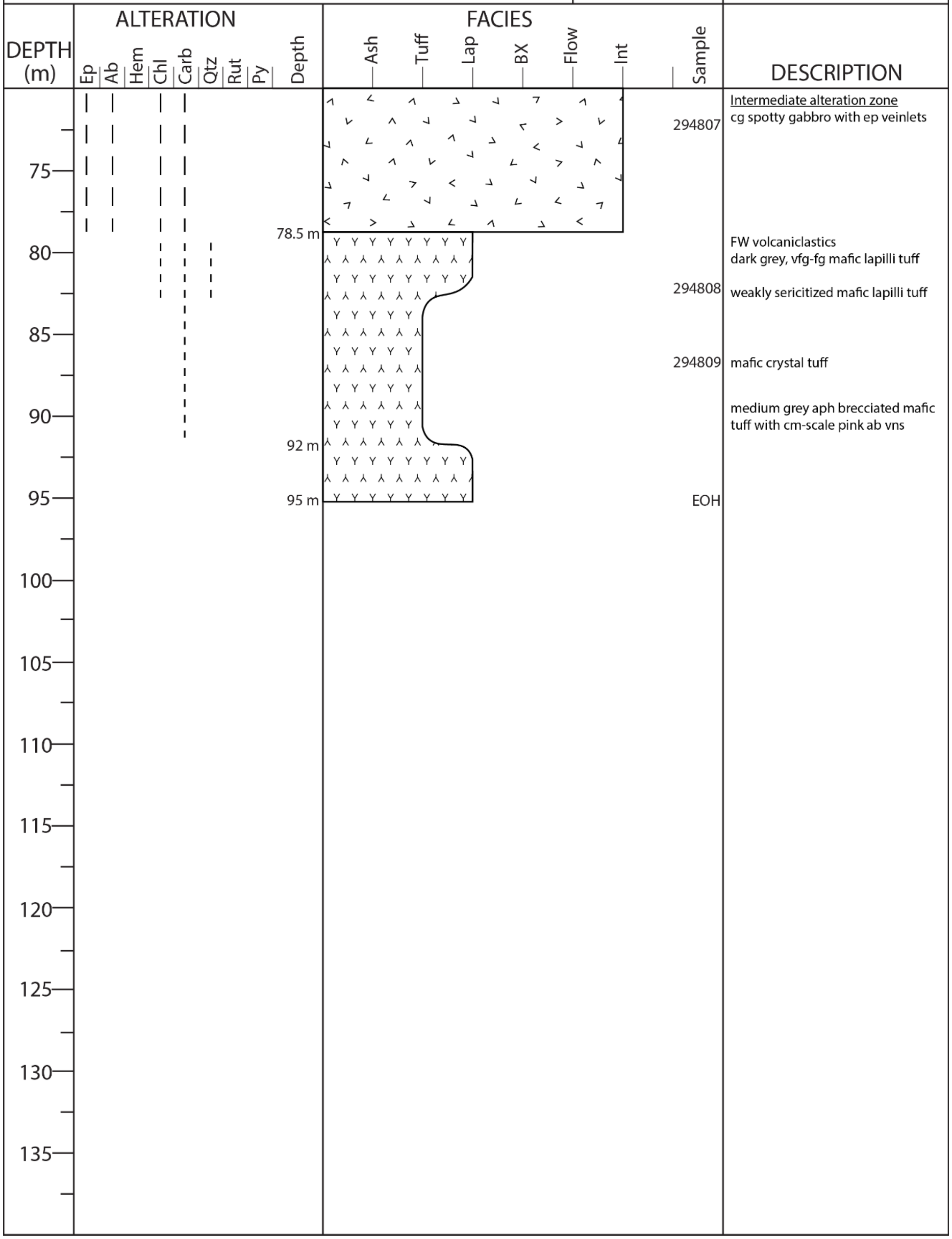

Intermediate alteration zone
cg spotty gabbro with ep veinlets

FW volcaniclastics
dark grey, vfg-fg mafic lapilli tuff

weakly sericitized mafic lapilli tuff

mafic crystal tuff

medium grey aph brecciated mafic tuff with cm-scale pink ab vns

Project: Argyle
Diamond Drill Hole: AE-16-41
Date: 10-14-2018

Section: 5E

UTM
300811.2E
5537747.5N

Azimuth: 000
Dip: -90
Depth: 95 m

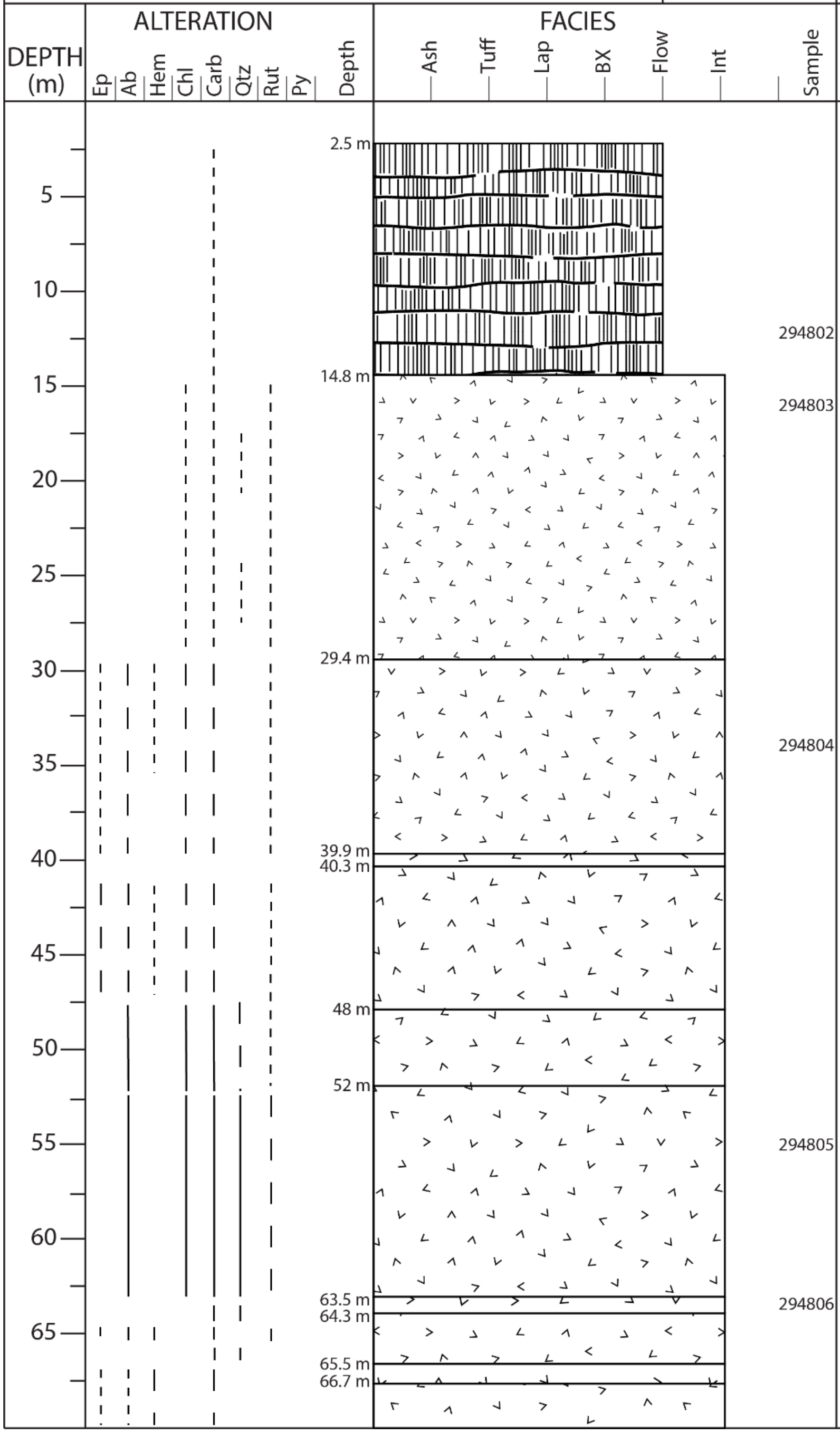

DESCRIPTION

OVB

HW volcaniclastics
dark grey-green aphinitic mafic flow.
weak patchy chl-ep primary volcanogenic alteration
mm-cm ab(pink)-qt veins

HW mafic tuff breccia

fg-mg gabbro with chilled margin

Distal alteration zone
fg gabbro with rut with chilled margin and cm-scale qt veins

Intermediate alteration zone
cg spotty gabbro

cg spotty gabbro, carb-rich with moderate rut ovp

aph medium grn dyke with isolated porphyritic crystals (ab?)

Intermediate alteration zone
dark grn-apple grn mg-cg spotty gabbro

Proximal alteration zone

dark grn/blk cg gabbro with cg ab crystals

"ore-zone" - moderately Si-flooded interval with a proximal alteration assemblage - chl-ab-ank-qt-py mineralized gabbro

silica flooding is not as intense as in e.g. narrow ore-zones in AE-16-30
cg silica-flooded mineralized gabbro related to qt-ank veins

dark grey-grn fg mafic dyke, weakly magnetic

Intermediate alteration zone
cg spotty gabbro

fg mafic dyke; same as above

Intermediate alteration zone
cg spotty gabbro

Project: Argyle
Diamond Drill Hole: AE-17-47
Date: 10-12-2018

Section: 5E

UTM
300814.8E
5537807.2N

Azimuth: 180
Dip: -80
Depth: 119 m

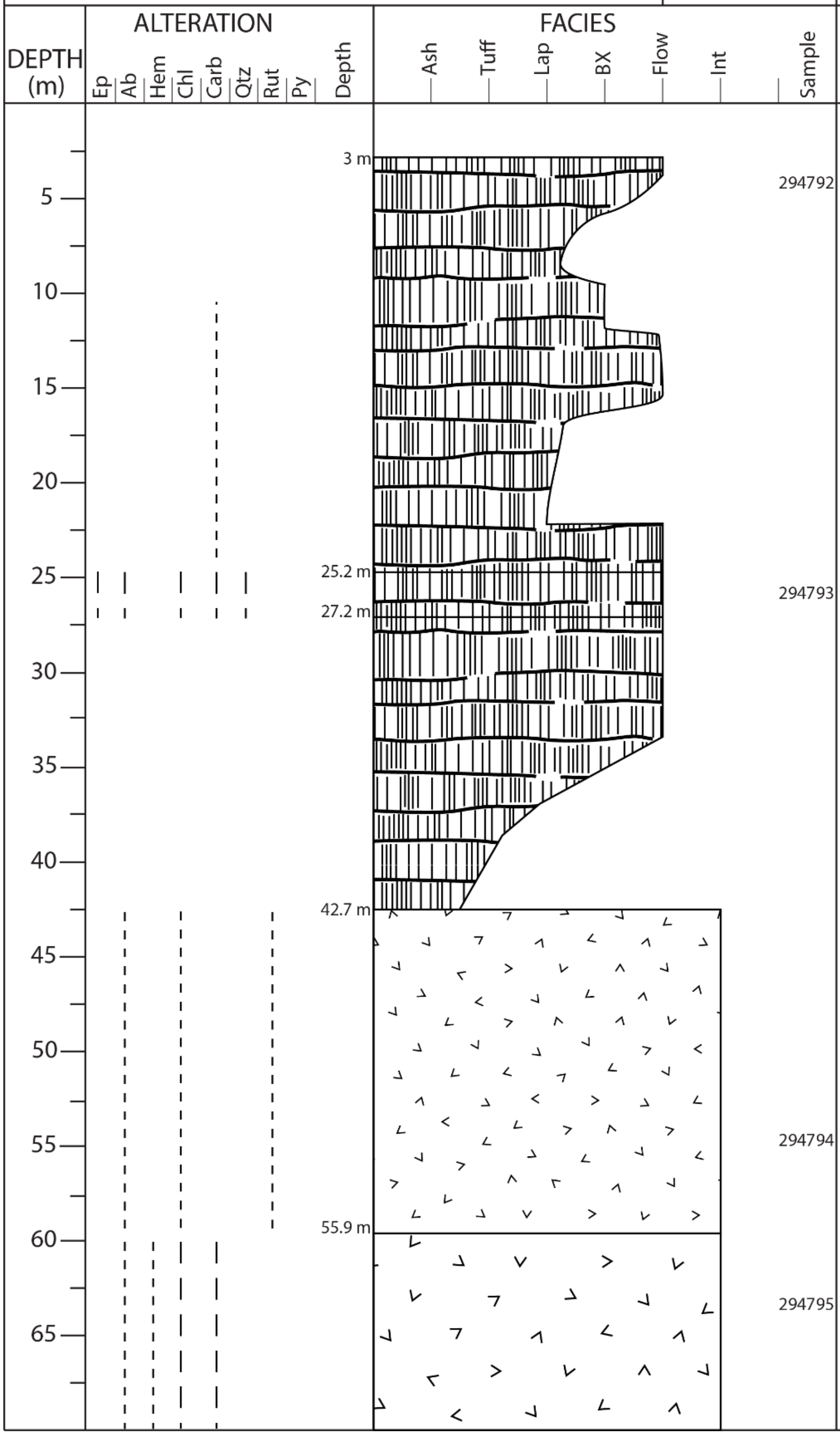

DESCRIPTION

OVB

HW volcaniclastics
mafic flow/hyaloclastite chl-carb alt of clasts with some glassy fragments present between clasts

dark grey mafic lapilli tuff, vfg-mg matrix with weak ep alteration and fracture-filling hematite veinlets rare euhedral dis py

mafic flow ~65%
lapilli tuff ~35%

weakly-moderately Si-flooded altered tan-light grey-pale green carb-qt-chl-ab mafic lapilli tuff, qt veinlets and blebby py min

same as 3-25.2 m

Distal alteration zone
mg gabbro with yellow rutile overprint

Intermediate alteration zone
medium green-pale yellow cg magnetic mottled (chloritoid eyes with carb rims) gabbro

Project: Argyle
Diamond Drill Hole: AE-17-47
Date: 10-12-2018

Section: 5E

UTM
300814.8E
5537807.2N

Azimuth: 180
Dip: -80
Depth: 119 m

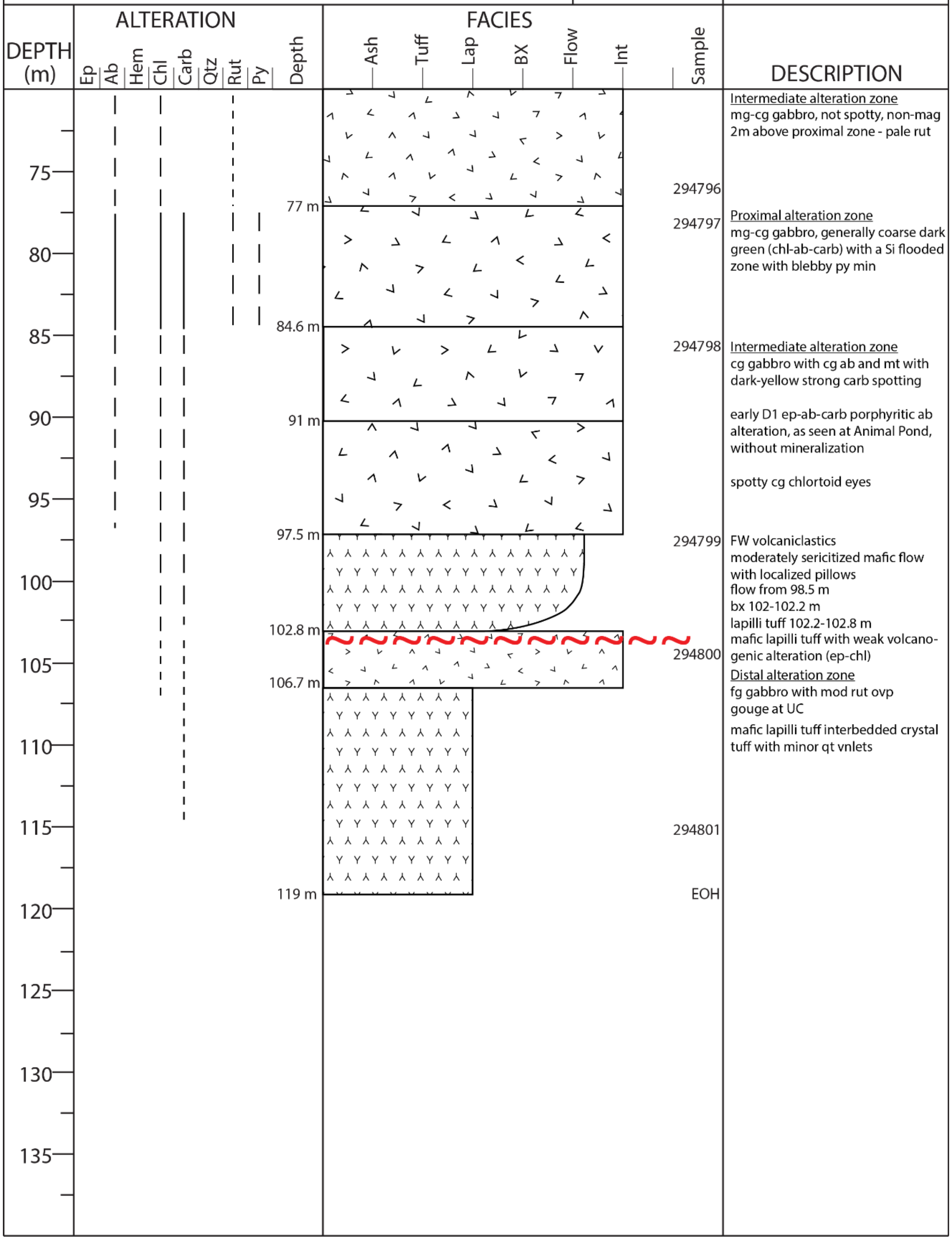

Intermediate alteration zone
mg-cg gabbro, not spotty, non-mag
2m above proximal zone - pale rut

Proximal alteration zone
mg-cg gabbro, generally coarse dark green (chl-ab-carb) with a Si flooded zone with blebby py min

Intermediate alteration zone
cg gabbro with cg ab and mt with dark-yellow strong carb spotting

early D1 ep-ab-carb porphyritic ab alteration, as seen at Animal Pond, without mineralization

spotty cg chlortoid eyes

FW volcaniclastics
moderately sericitized mafic flow with localized pillows
flow from 98.5 m
bx 102-102.2 m
lapilli tuff 102.2-102.8 m
mafic lapilli tuff with weak volcanogenic alteration (ep-chl)

Distal alteration zone
fg gabbro with mod rut ovp
gouge at UC

mafic lapilli tuff interbedded crystal tuff with minor qt vnlets

Project: Argyle
Diamond Drill Hole: AE-17-48
Date: 10-12-2018

Section: 5E

UTM
300812.9E
5537855.9N

Azimuth: 180
Dip: -80
Depth: 126 m

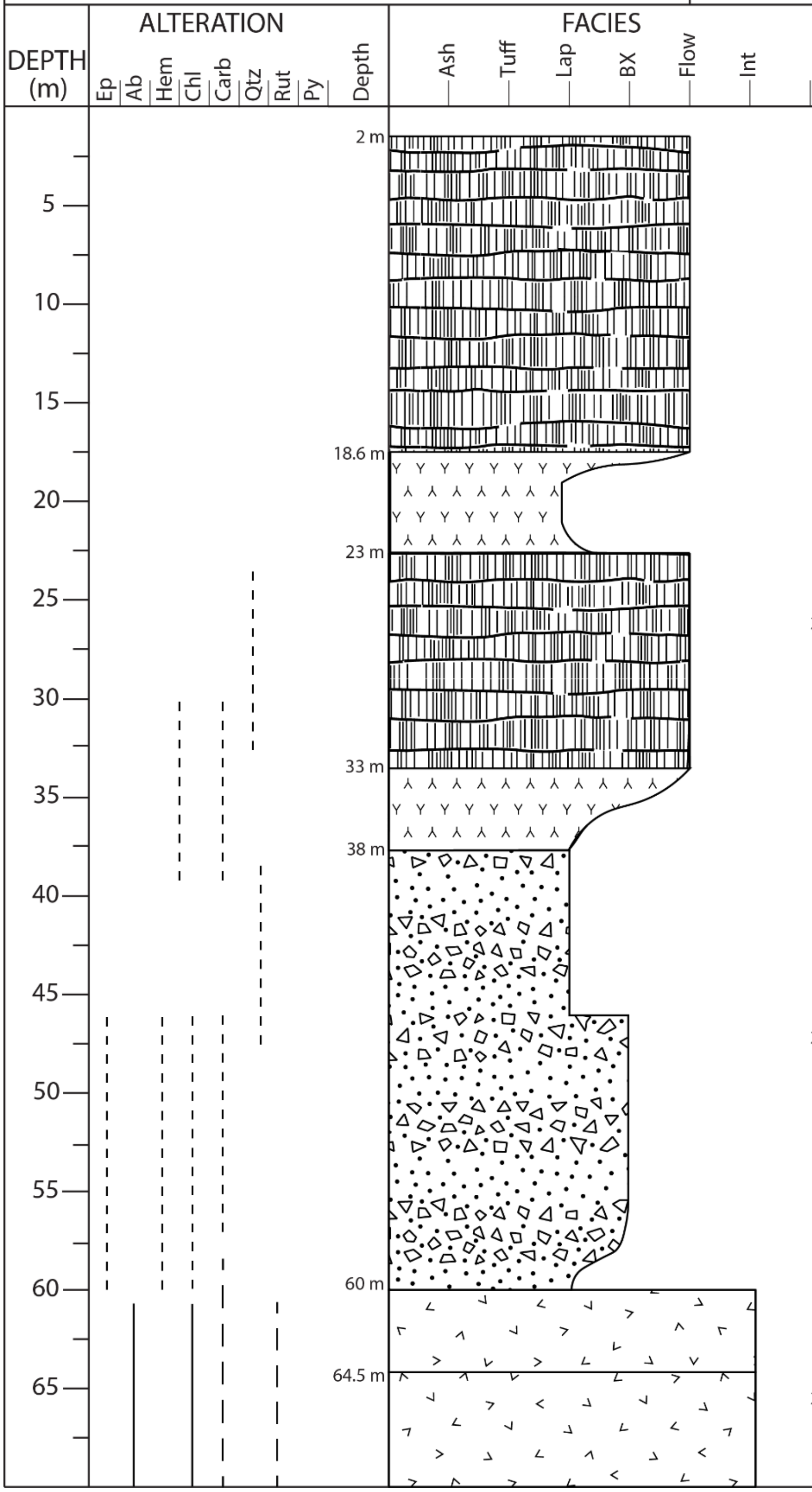

Sample	DESCRIPTION
	OVB
	HW volcaniclastics hyaloclastite with pillow selvages dark green mafic flow with brecciated pillow lavas and lapilli tuff intervals
	dark green lapilli tuff matrix-supported
294782	fg green-grey mafic flow
	dark green mafic flow with brecciated pillow lavas and lapilli tuff intervals
	clast-supported 33-38 m, matrix-supported below
	dark green lapilli tuff, matrix-supported, in which the size of lapilli increases from ~52 m and becomes more massive downhole minor qt and qt-ab veins
294783	moderately altered breccia with dark grey-green-purple matrix and large (>1 cm) yellow-green fractured clasts
	bottom 1m wk-mod ser-ank altered
	<u>Proximal alteration zone</u> aph-vfg chilled margin contains both faulted and qt-healed gabbro and heavily faulted and qt-healed volcaniclastics
294784	fg non-mineralized gabbro mineral lineation defined by chl eyes

Project: Argyle
Diamond Drill Hole: AE-17-48
Date: 10-12-2018

Section: 5E

UTM
300812.9E
5537855.9N

Azimuth: 180
Dip: -80
Depth: 126 m

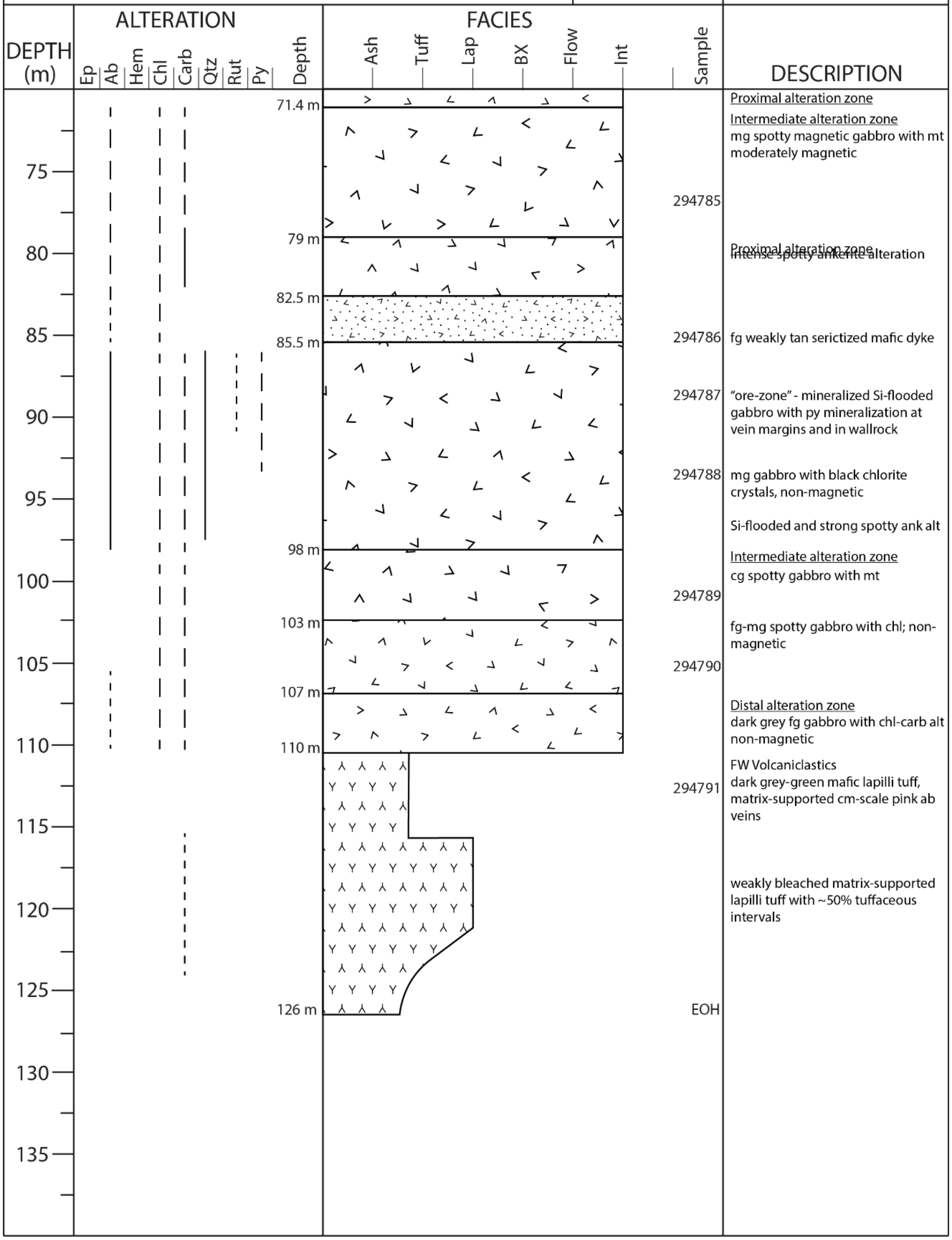

Proximal alteration zone

Intermediate alteration zone
mg spotty magnetic gabbro with mt
moderately magnetic

Proximal alteration zone
intense spotty ankerite alteration

fg weakly tan sericitized mafic dyke

“ore-zone” - mineralized Si-flooded gabbro with py mineralization at vein margins and in wallrock

mg gabbro with black chlorite crystals, non-magnetic

Si-flooded and strong spotty ank alt

Intermediate alteration zone
cg spotty gabbro with mt

fg-mg spotty gabbro with chl; non-magnetic

Distal alteration zone
dark grey fg gabbro with chl-carb alt
non-magnetic

FW Volcaniclastics
dark grey-green mafic lapilli tuff, matrix-supported cm-scale pink ab veins

weakly bleached matrix-supported lapilli tuff with ~50% tuffaceous intervals

Project: Argyle
Diamond Drill Hole: AE-17-49
Date: 10-12-2018

Section: 5E

UTM
300813.1E
5537908.2N

Azimuth: 180
Dip: -80
Depth: 143 m

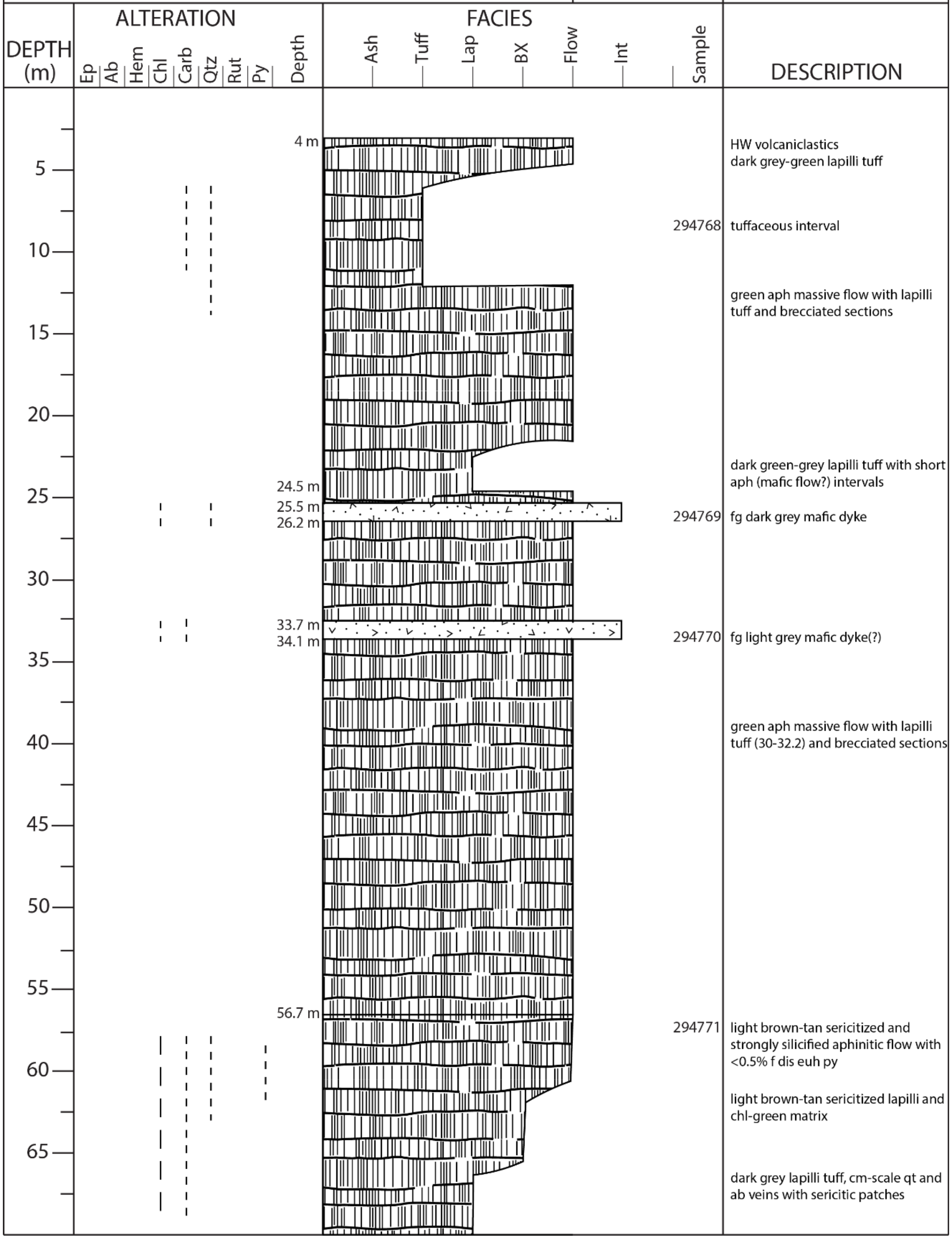

HW volcaniclastics
dark grey-green lapilli tuff

294768 tuffaceous interval

green aph massive flow with lapilli tuff and brecciated sections

dark green-grey lapilli tuff with short aph (mafic flow?) intervals

294769 fg dark grey mafic dyke

294770 fg light grey mafic dyke(?)

green aph massive flow with lapilli tuff (30-32.2) and brecciated sections

294771 light brown-tan sericitized and strongly silicified aphinitic flow with <0.5% f dis euh py

light brown-tan sericitized lapilli and chl-green matrix

dark grey lapilli tuff, cm-scale qt and ab veins with sericitic patches

Project: Argyle
Diamond Drill Hole: AE-17-49
Date: 10-12-2018

Section: 5E

UTM
300813.1E
5537908.2N

Azimuth: 180
Dip: -80
Depth: 143 m

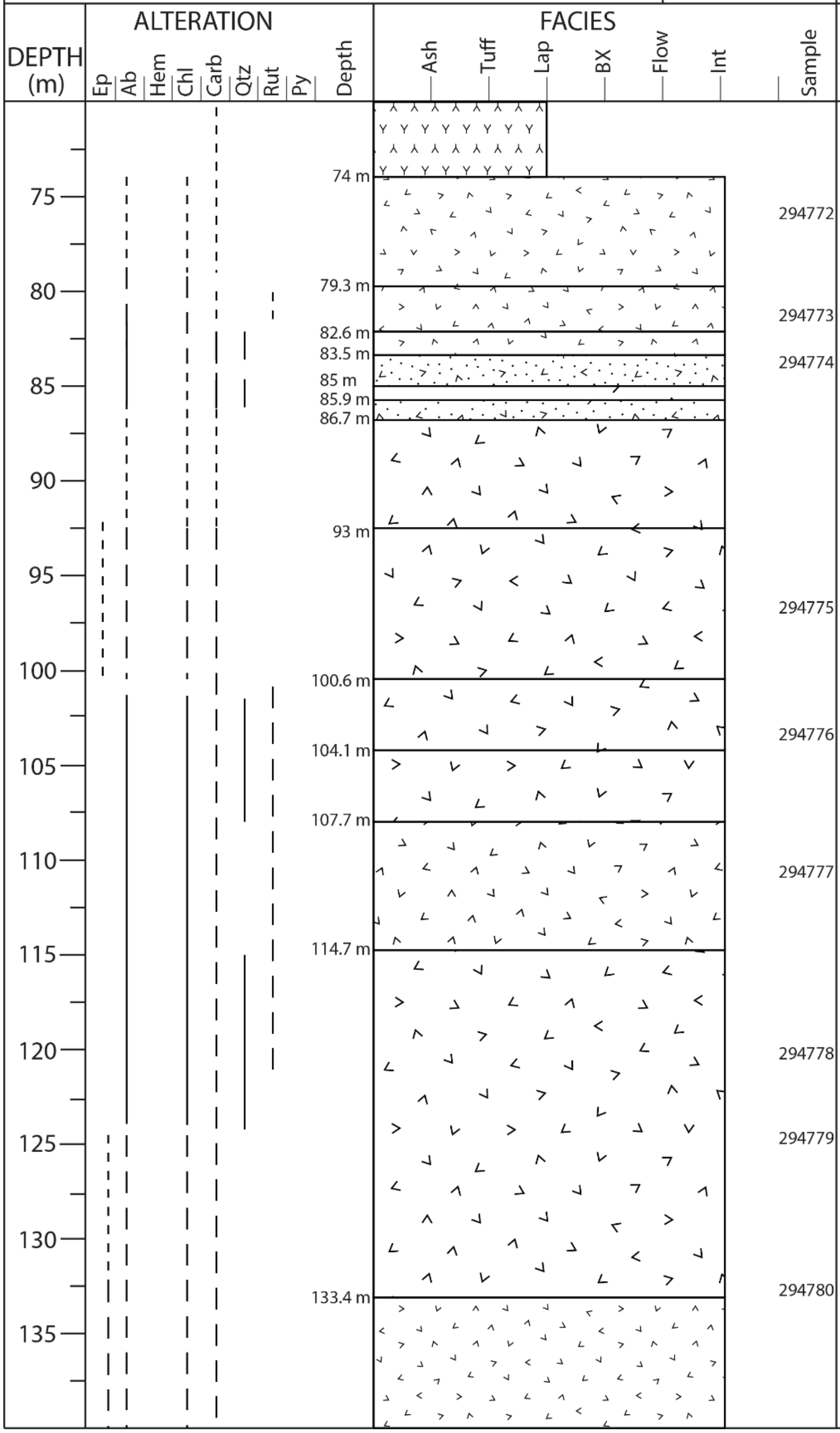

DESCRIPTION

light brown-tan sericitized lapilli and chl-green matrix, cm-scale qt-ab vns

Distal alteration zone
fg dark grey-grn gabbro

Intermediate alteration zone
fg-mg altered gabbro with aligned chloritoid eyes, ab and rut

Proximal alteration zone
fg gabbro (82.6-83.5) mg (85-85.95) aph camo-tan mafic dyke with aligned chloritoid eyes, ser and ab

aph camo dyke

Distal alteration zone
fg dark grey-grn gabbro

Intermediate alteration zone
cg-porphyritic (ab) gabbro with ep, mod-str magnetic

Proximal alteration zone
cg gabbro with a silicified tan-pale grey appearance due to Si flooding with blebby py min

mg-cg dark green gabbro with blebby py min

Intermediate alteration zone
cg gabbro with a silicified tan-pale grey appearance due to Si-flooding with blebby py min
116-121 m mod-str ser ank spotting

cg spotty gabbro with ep, mt (mod-str) and dull lilac-purple transition stage between rut and mt

Distal alteration zone
fg dark grey-grn gabbro

Project: Argyle
Diamond Drill Hole: AE-17-49
Date: 10-12-2018

Section: 5E

UTM
300813.1E
5537908.2N

Azimuth: 180
Dip: -80
Depth: 143 m

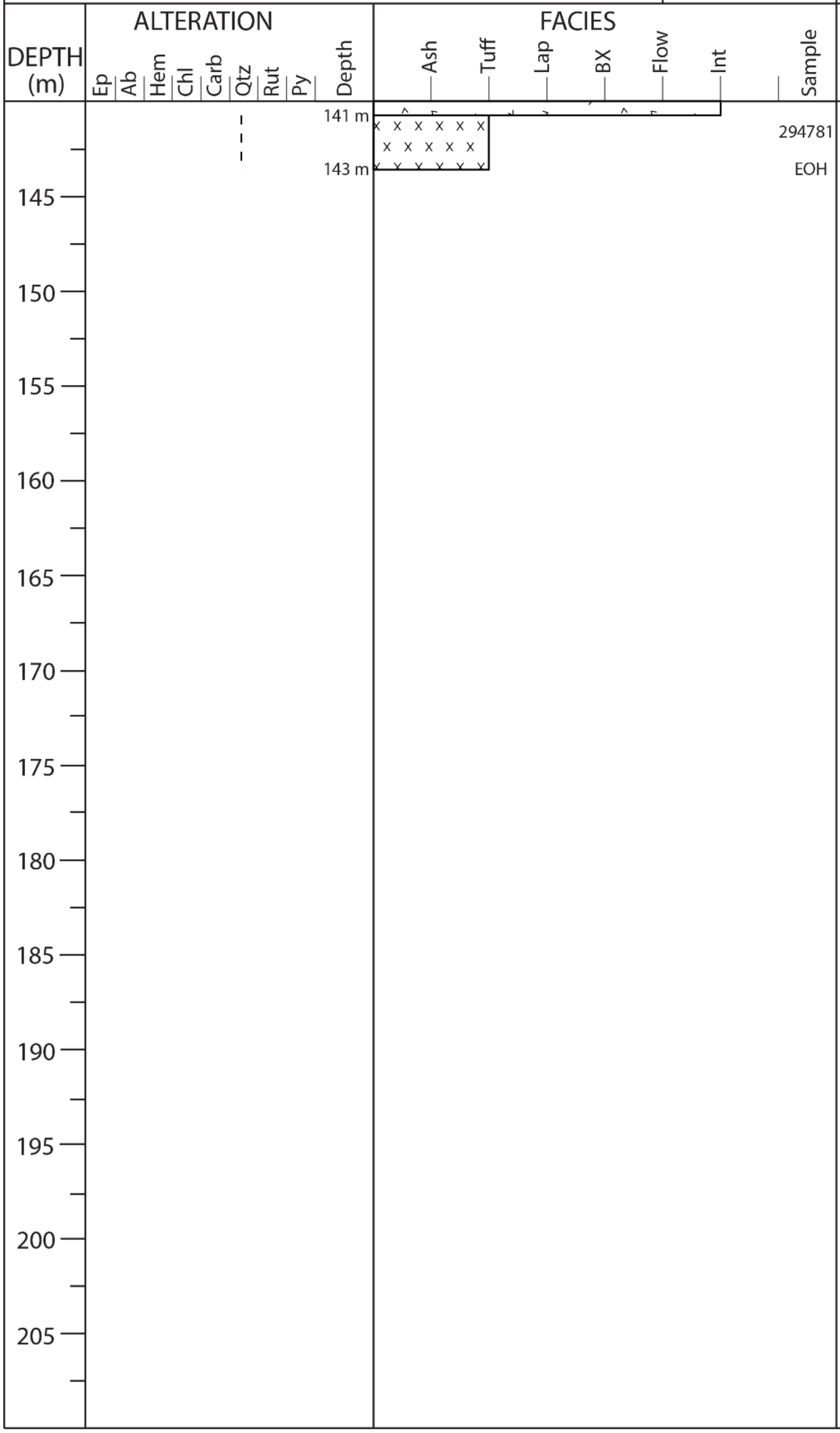

DESCRIPTION

FW volcaniclastics
medium grey crystal tuff with minor interbedded lapilli tuff, mm-cm scale qt-carb veins

Project: Argyle
Diamond Drill Hole: AE-16-26
Date: 6-7-2018

Section: 5+7E

UTM
300859.5E
5537711N

Azimuth: 180
Dip: -50
Depth: 95 m

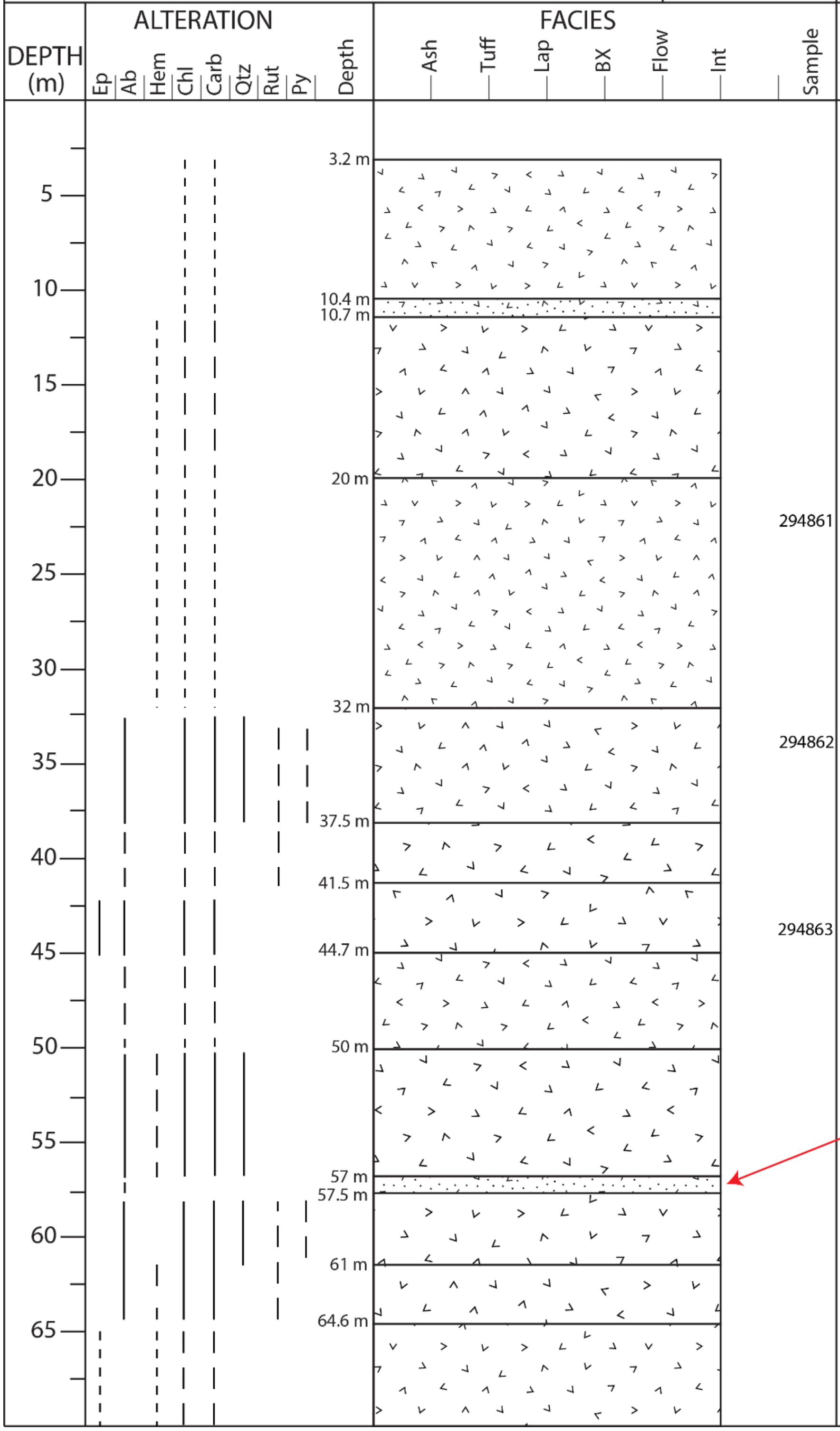

DESCRIPTION

OVB

<u>Distal alteration zone</u>
dark green fg gabbro

fg mafic dyke altered pale-green carbonate with blk chl crystals

<u>Intermediate alteration zone</u>
spotty mg gabbro chl-carb alt with hem on fracture planes

<u>Distal alteration zone</u>
dark green fg gabbro with wk chl-carb spots and hem veinlets

<u>Proximal alteration zone</u>
tan-brown mg heavily metasomatized gabbro (Si-flooded? hard)

<u>Intermediate alteration zone</u>
cg gabbro with rutile overprint, not spotty texture, less ab

<u>Proximal alteration zone</u>
dark green, cg spotty gabbro, highly magnetic with hem veinlets

<u>Intermediate alteration zone</u>
mg gabbro, not spotty

<u>Proximal alteration zone</u>
dark green gabbro with cg ab and hem on frc planes and rut ovp

weakly sericitized aph-fg mafic dyke with ab isolated ab crystals

"ore-zone" tan-brown to pinkish orange Si-flooded zone with pervasive ab, which dominated the alteration assemblage; dis sub-an py

<u>Proximal alteration zone</u>
cg dark green with coarse ab and Fe-carb (chl-ab-ank); magn from 63m

<u>Intermediate alteration zone</u>
spotty gabbro ep-mt alt, highly magnetic mg to 67.4 m, fg from 67.4 m

Project: Argyle
Diamond Drill Hole: AE-16-26
Date: 6-7-2018

Section: 5+7E

UTM
300859.5E
5537711N

Azimuth: 180
Dip: -50
Depth: 95 m

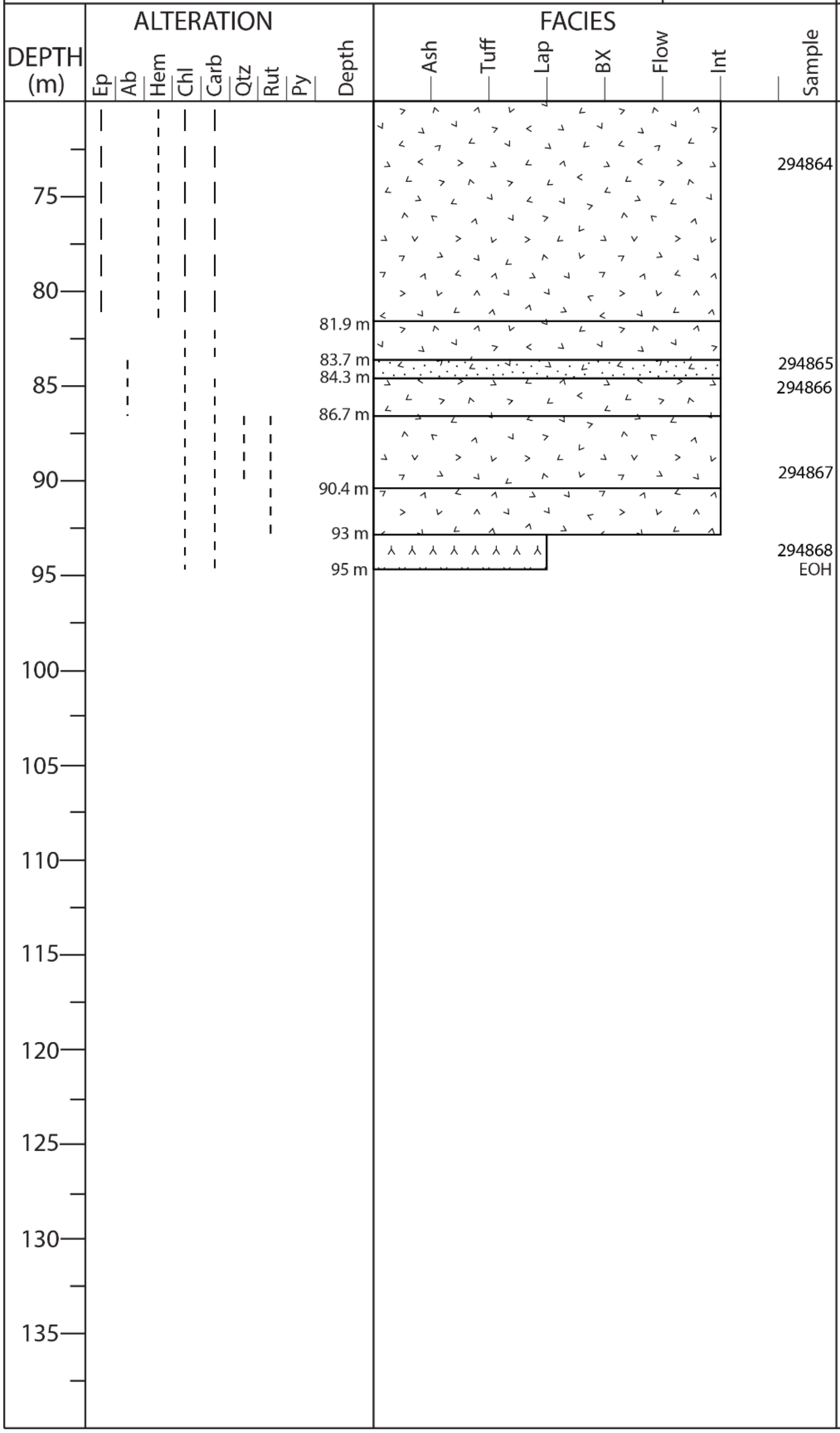

DESCRIPTION

Intermediate alteration zone
dark green to pale green fg-mg spotty gabbro with hem veinlets

Distal alteration zone
fg dark green gabbro with mt

aph mafic dyke, camo-green with weak sericite alteration and relict black chl crystals

Distal alteration zone
fg dark green gabbro

Intermediate alteration zone
fg gabbro with mod ser-chl-carb-rut-py(euh) alt associated with and restricted to the damage zone and 1m shoulders

Distal alteration zone
fg dark green gabbro with rut

FW volcaniclastic
dark grey lapilli tuff with pink ab and yellow-green carb altered clasts

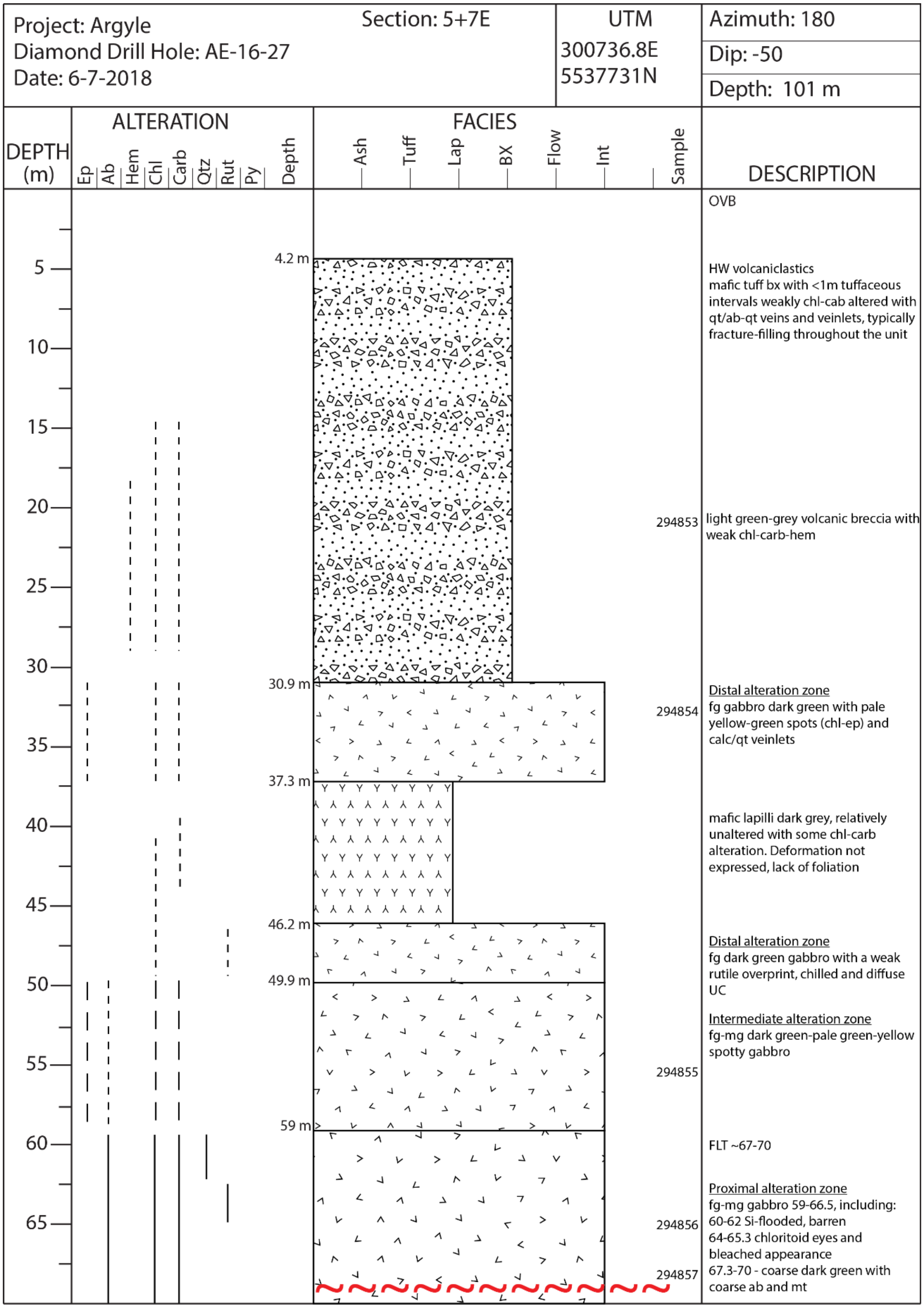

Project: Argyle
Diamond Drill Hole: AE-16-27
Date: 6-7-2018

Section: 5+7E

UTM
300736.8E
5537731N

Azimuth: 180
Dip: -50
Depth: 101 m

OVB

HW volcaniclastics
mafic tuff bx with <1m tuffaceous intervals weakly chl-cab altered with qt/ab-qt veins and veinlets, typically fracture-filling throughout the unit

294853 light green-grey volcanic breccia with weak chl-carb-hem

294854 Distal alteration zone
fg gabbro dark green with pale yellow-green spots (chl-ep) and calc/qt veinlets

mafic lapilli dark grey, relatively unaltered with some chl-carb alteration. Deformation not expressed, lack of foliation

Distal alteration zone
fg dark green gabbro with a weak rutile overprint, chilled and diffuse UC

Intermediate alteration zone
fg-mg dark green-pale green-yellow spotty gabbro

294855

FLT ~67-70

Proximal alteration zone
fg-mg gabbro 59-66.5, including:
294856 60-62 Si-flooded, barren
64-65.3 chloritoid eyes and bleached appearance
294857 67.3-70 - coarse dark green with coarse ab and mt

Project: Argyle
Diamond Drill Hole: AE-16-27
Date: 6-7-2018

Section: 5+7E

UTM
300736.8E
5537731N

Azimuth: 180
Dip: -50
Depth: 101 m

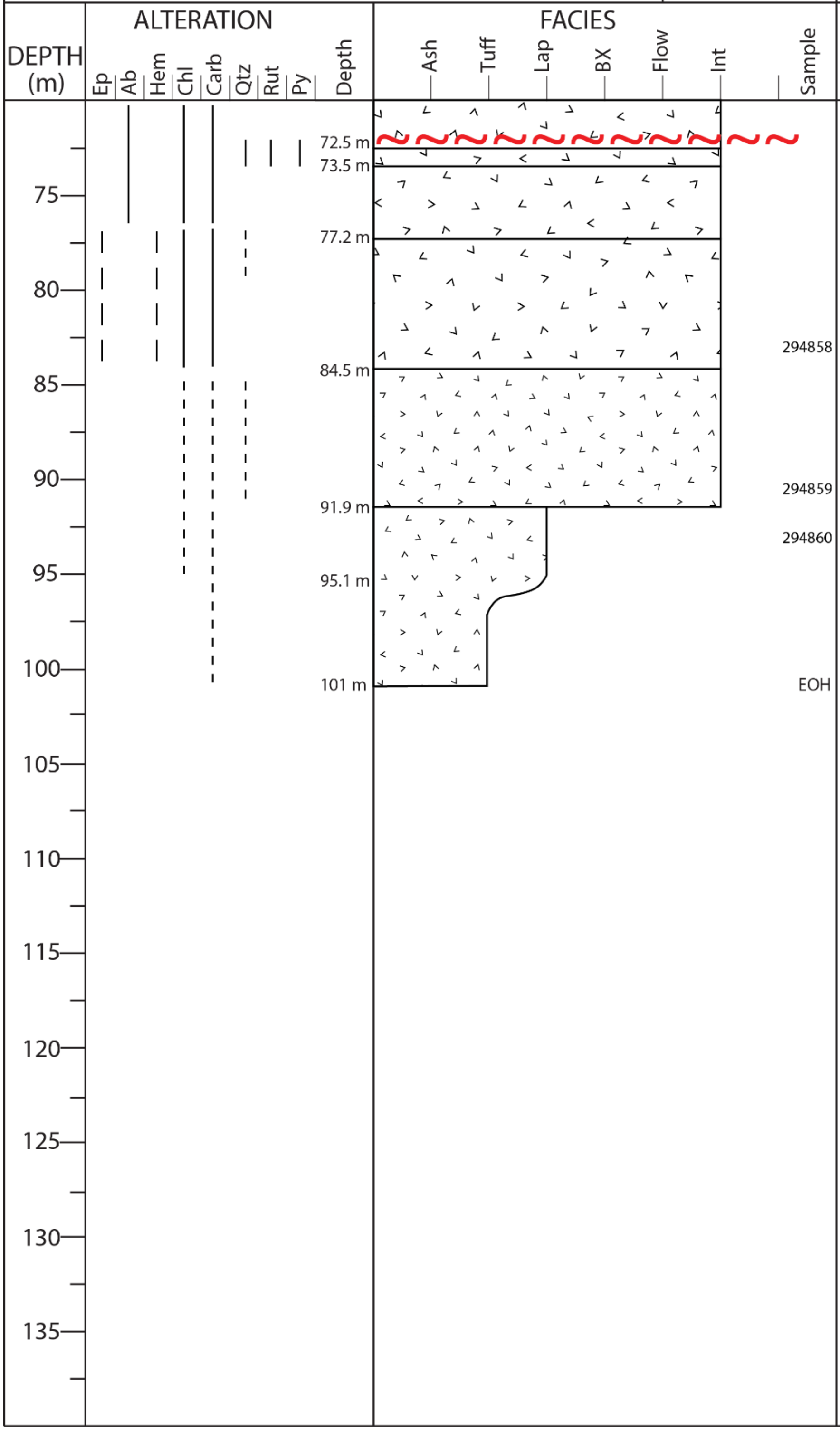

DESCRIPTION

FLT 71-73
SHR 72@72

Proximal alteration zone
72.5-73.5 "zone" - cg metasomatized (>0.5 g/t Au)
changes between rut (66.5-67.3, 70-73.5) and mt (67.3-70, 73.5-77.2)

Intermediate alteration zone
spotty gabbro dark-pale green
77.2-81.3 - cg chl-ep-carb-mt spotty (decrease in ab)
81.3-84.5 - mg spotty gabbro with qt veins and hem veinlets

Distal alteration zone
dark green fg gabbro with vfg rutile overprint

FW volcaniclastic
light grey-pale green crystal tuff (bleaching +silicification) + qt veins

dark grey mafic tuff with wk green chl and qt veins
FOL 70 @ 97.8

Project: Argyle
Diamond Drill Hole: AE-16-43
Date: 6-6-2018

Section: 5+7E

UTM
300859E
5537819N

Azimuth: 180
Dip: -45
Depth: 134 m

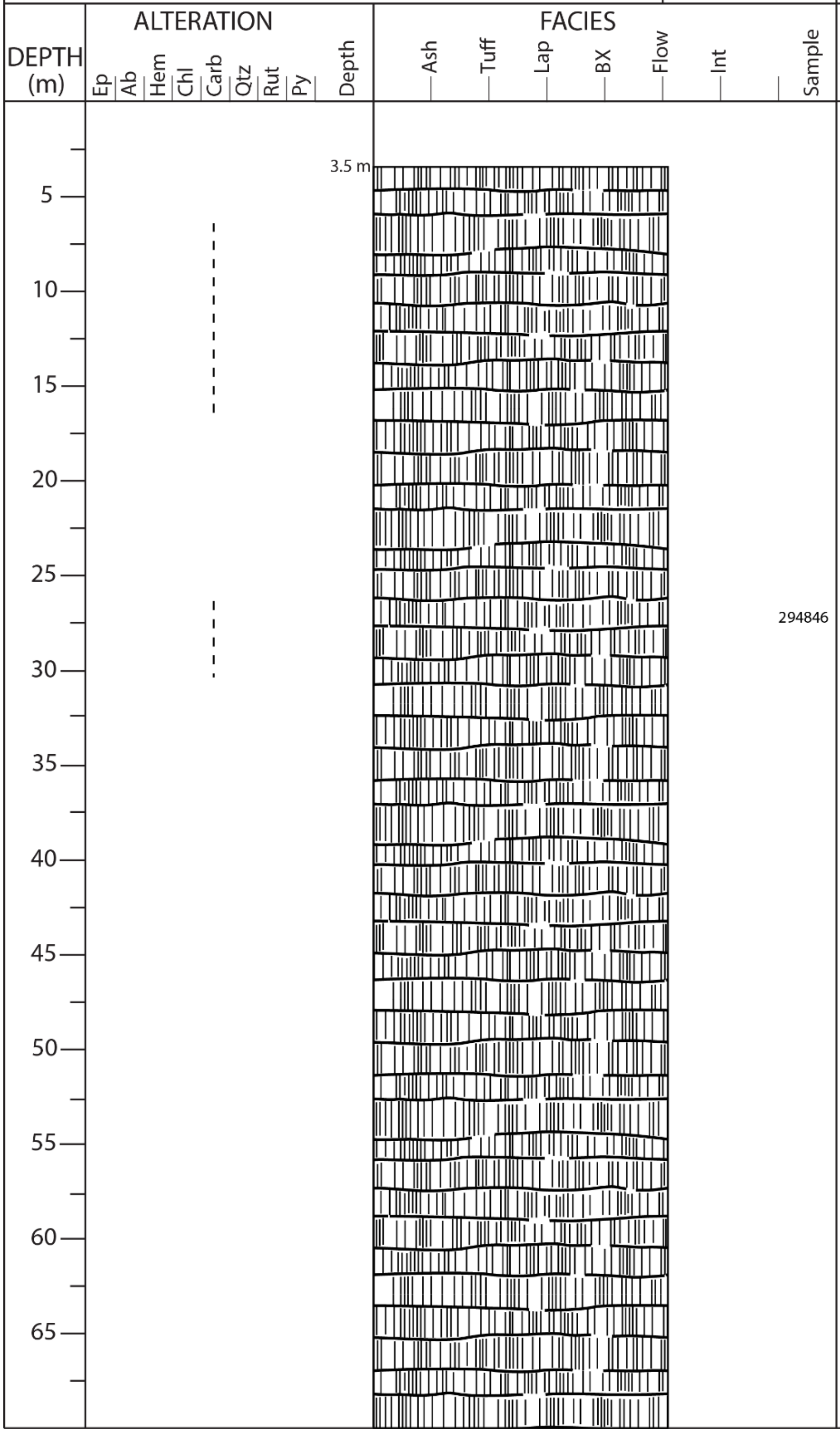

DESCRIPTION

OVB

HW volcaniclastics
medium grey-green mafic flow interbedded with tuff bx (35%) and lapilli tuff (10%)

Typically weakly chl-carb altered (primary volcanogenic alteration) with qt veinlets throughout

weakly-moderately altered (chl-carb) lower contact between HW volcaniclastics and underlying gabbro; this is evident in other holes in this section (5+7 E)

unaltered medium-dark grey from 57-60 m

only a single 'proximal' alteration zone in this hole. Qt vn at LC.

HW light-grey green mafic lapilli tuff with calc veinlets

FRC zones 5-7.5, 9-10, 18-19, 20.5-21

Project: Argyle
Diamond Drill Hole: AE-16-43
Date: 6-6-2018

Section: 5+7E

UTM
300859E
5537819N

Azimuth: 180
Dip: -45
Depth: 134 m

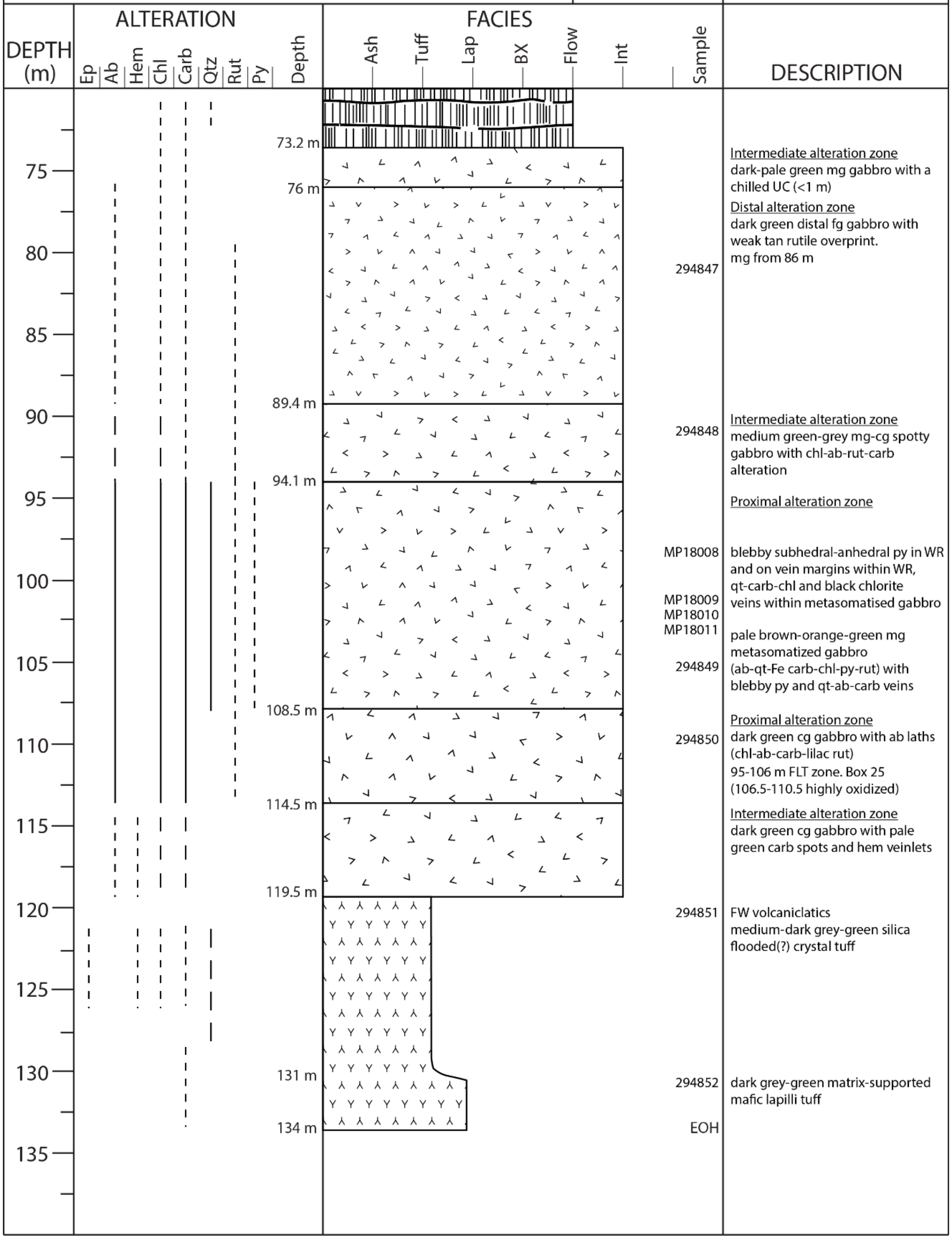

Intermediate alteration zone
dark-pale green mg gabbro with a chilled UC (<1 m)

Distal alteration zone
dark green distal fg gabbro with weak tan rutile overprint.
mg from 86 m

Intermediate alteration zone
medium green-grey mg-cg spotty gabbro with chl-ab-rut-carb alteration

Proximal alteration zone

blebby subhedral-anhedral py in WR and on vein margins within WR, qt-carb-chl and black chlorite veins within metasomatised gabbro

pale brown-orange-green mg metasomatized gabbro (ab-qt-Fe carb-chl-py-rut) with blebby py and qt-ab-carb veins

Proximal alteration zone
dark green cg gabbro with ab laths (chl-ab-carb-lilac rut)
95-106 m FLT zone. Box 25
(106.5-110.5 highly oxidized)

Intermediate alteration zone
dark green cg gabbro with pale green carb spots and hem veinlets

FW volcaniclactics
medium-dark grey-green silica flooded(?) crystal tuff

dark grey-green matrix-supported mafic lapilli tuff

Project: Argyle
Diamond Drill Hole: AE-16-44
Date: 6-6-2018

Section: 5+7E

UTM
300859E
5537819N

Azimuth: 000
Dip: -90
Depth: 143 m

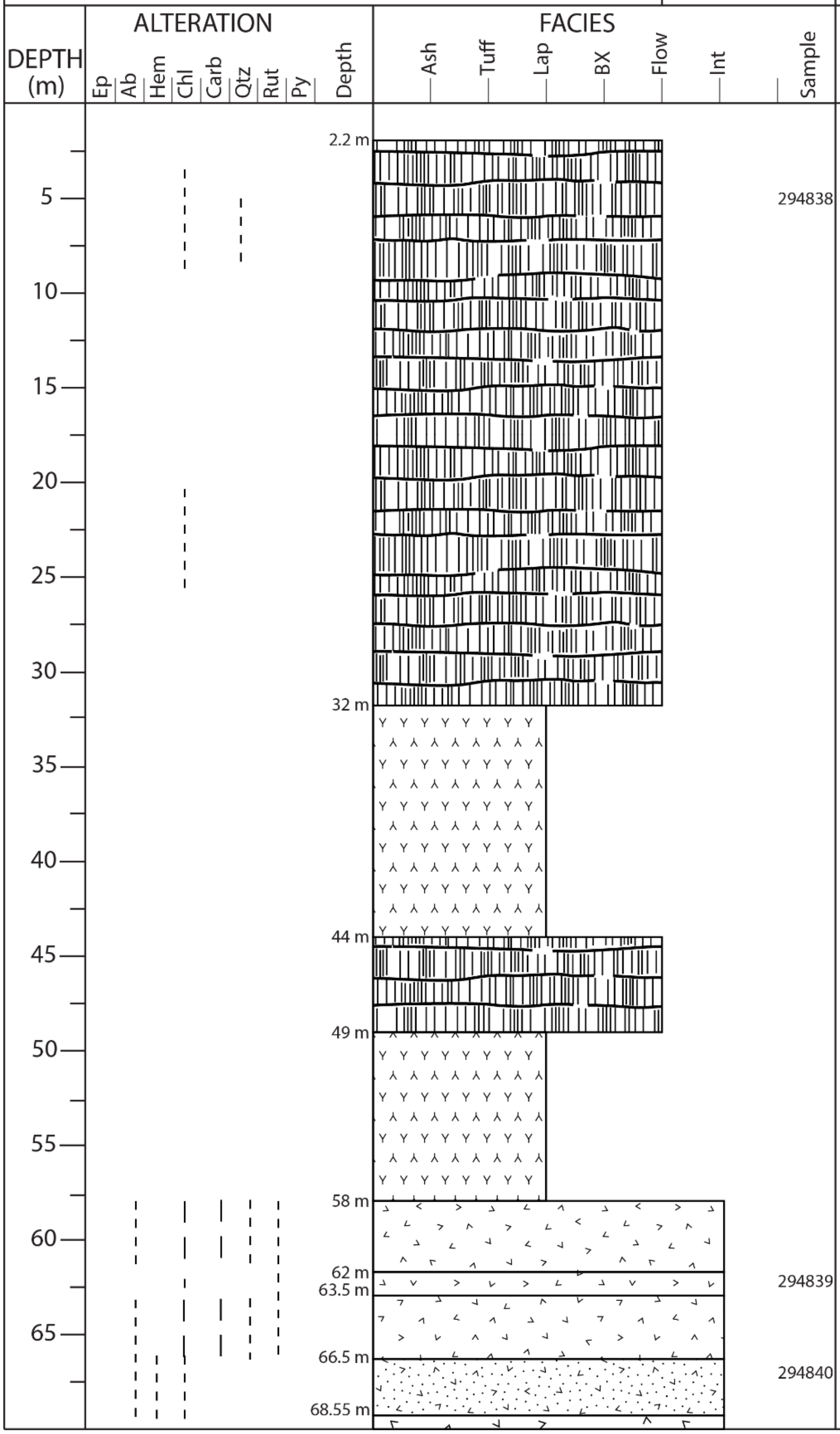

DESCRIPTION

OVB

HW volcaniclastics

pale green mafic flow with chl alt

mafic flow interbedded with intervals of lapilli tuff and tuff bx, well layered/ foliated in lapilli intervals

the unit is consistently chl-carb-ep altered with calc/qt veinlets infilling fractures

generally undeformed to weakly deformed

small FRC zones @ 23-24, 28-29, 46.5-48

FOL 60 @ 12.5
FOL 60 @ 32.5
FOL 60 @ 44
FOL 76 @ 57.9
FOL 72 @ 60.5

<u>Intermediate alteration zone</u>
fg gabbro chl-carb altered at contact
weak-mod alteration (carb-chl) tan-green with stronger fabric in gabbro; chilled LC

Distal alteration zone
medium-dark green fg gabbro with chlorite eyes and weak vfg rutile ovp

Intermediate alteration zone
fg spotty gabbro

dark grey mafic dyke with porphyritic ab crystal and hem veinlets
mt-ab-chl-hem

Project: Argyle
Diamond Drill Hole: AE-16-44
Date: 6-6-2018

Section: 5+7E

UTM
300859E
5537819N

Azimuth: 000
Dip: -90
Depth: 143 m

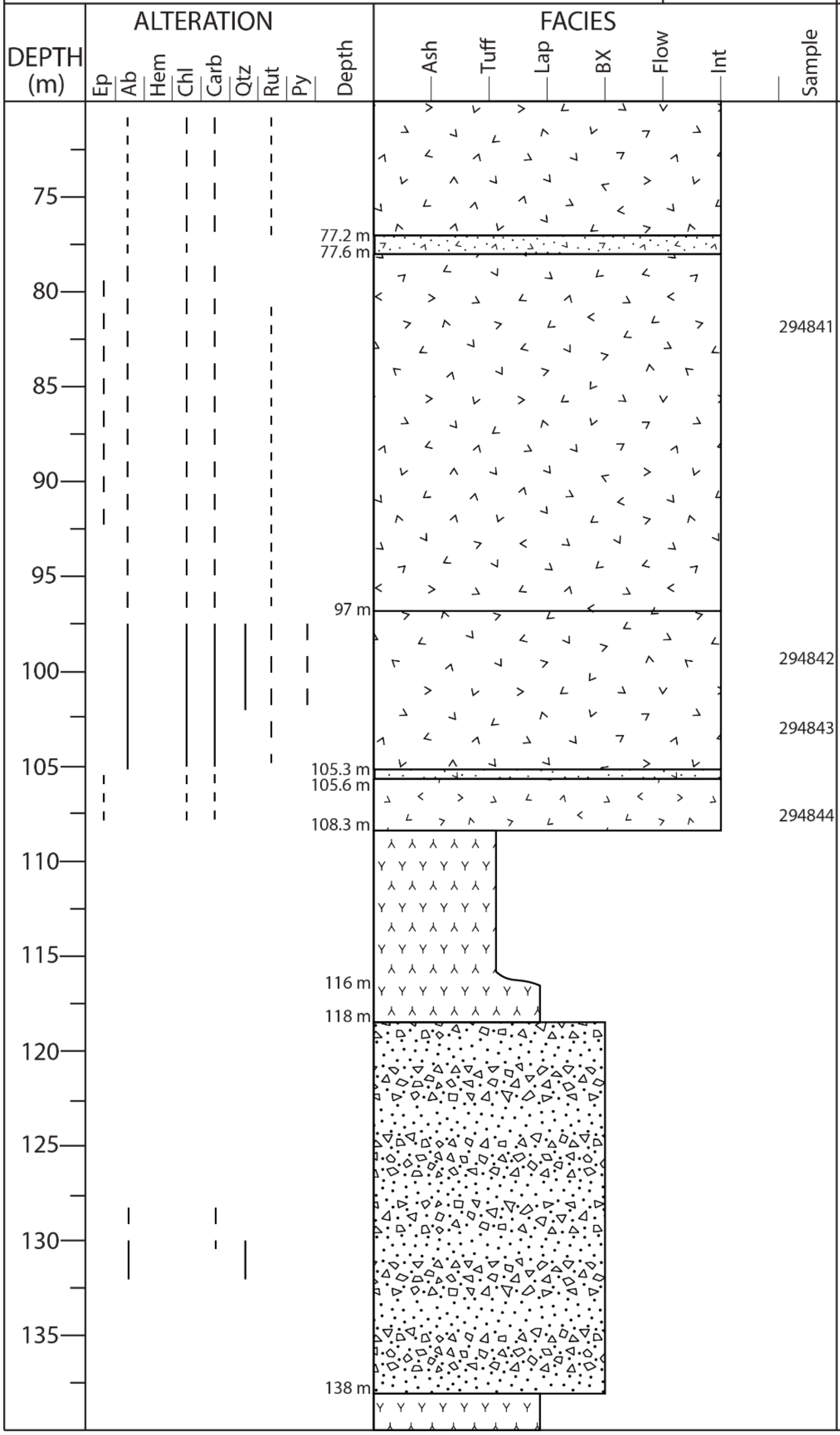

DESCRIPTION

Intermediate alteration zone
dark green-pale green cg spotty gabbro with ep to 73. From 73 dark green m-c gabbro, not spotty with rutile

Distal alteration zone
fg dark grey mafic dyke + rare ab crystals
FRC'd dyke and ~1 m either side

Intermediate alteration zone
dark to apple green cg spotty gabbro with chl-ep-ab-carb-mt alt
dark-pale green to apple-green spotty gabbro
77.6-81.5 fg-mg + mt
81.5-93 cg spotty + ep
93-97 cg spotty + ep
magnetic @ 77-87.5, 92-95.5
SHR 72 @ 78.5
damage zone 76.5-78.5, 86-89, 97.5-100 (qt-healed)

Proximal alteration zone
cg tan-brown-green strongly Si-flooded gabbro with qt-carb(+ab) vn
From 102.5 coarse dark green gabbro with dark chl matrix, c ab laths, heavy carb spots + lilac rut
pale tan brown to dark green heavily metasomatized cg gabbro with ab-Fe carb-qt-chl-rut-py alteration
dark green-pale muave cg gabbro carb-chl-ab-(muave)rut alteration
aph mafic dark dark green with weak sericite alteration with qt and qt-ab veins; sub-vert CTs in broken core

Distal alteration zone
dark green fg gabbro with rutile ovp with chilled gradational margin into FW volcaniclastics
mafic crystal tuff

dark grey-green mafic lapilli tuff much less qt vn and weaker fabric in FW compared to HW

dark grey-green mafic tuff breccia
129-132 ab-carb alt (dist-interm), 130.6-131 ab-qt (prox)

Project: Argyle
Diamond Drill Hole: AE-16-44
Date: 6-6-2018

Section: 5+7E

UTM
300859E
5537819N

Azimuth: 000
Dip: -90
Depth: 143 m

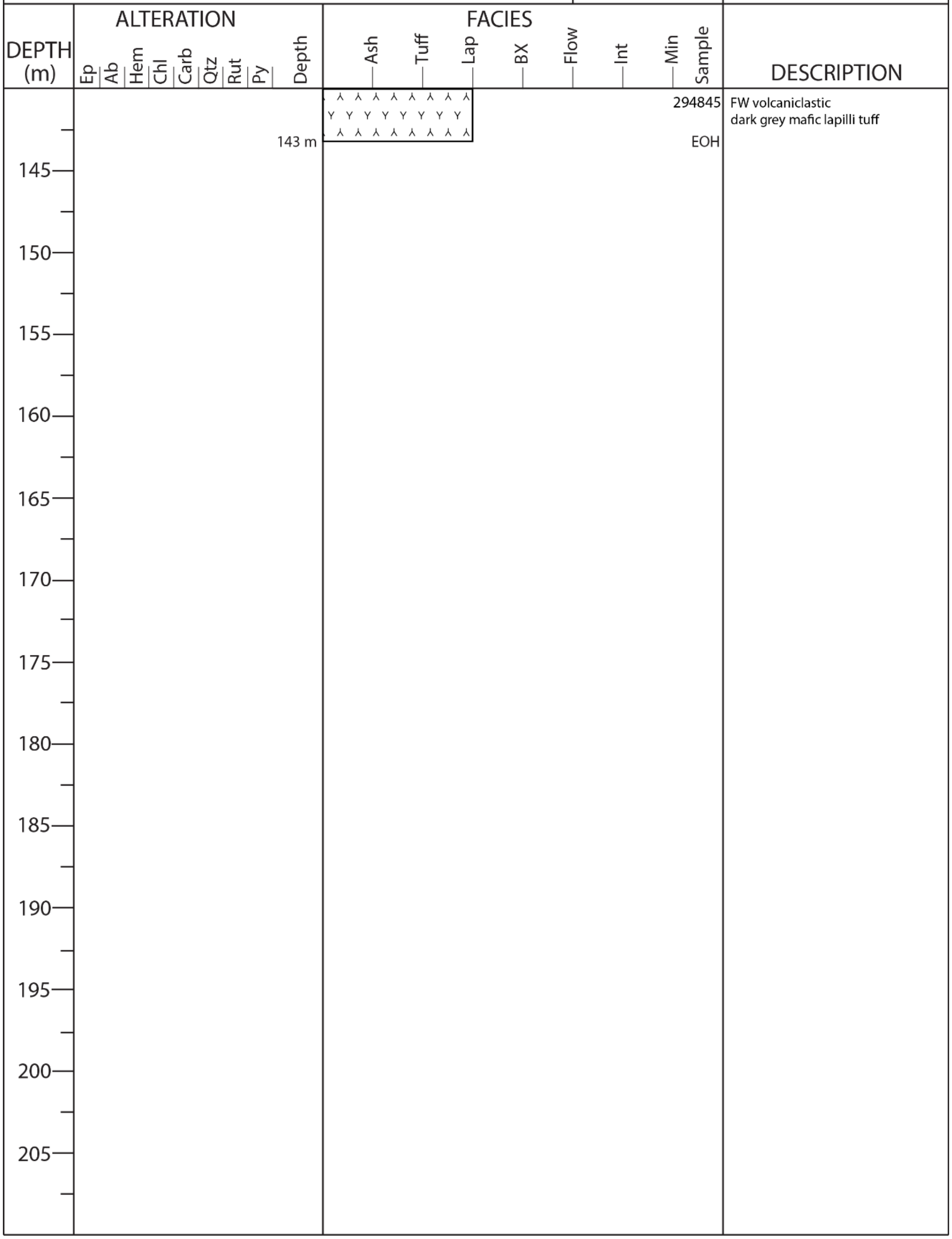

294845 FW volcaniclastic
dark grey mafic lapilli tuff

EOH

Project: Argyle
Diamond Drill Hole: AE-17-50
Date: 10-8-2017

Section: 5+7E

UTM
300860.7E
5537878.5N

Azimuth: 180
Dip: -80
Depth: 145 m

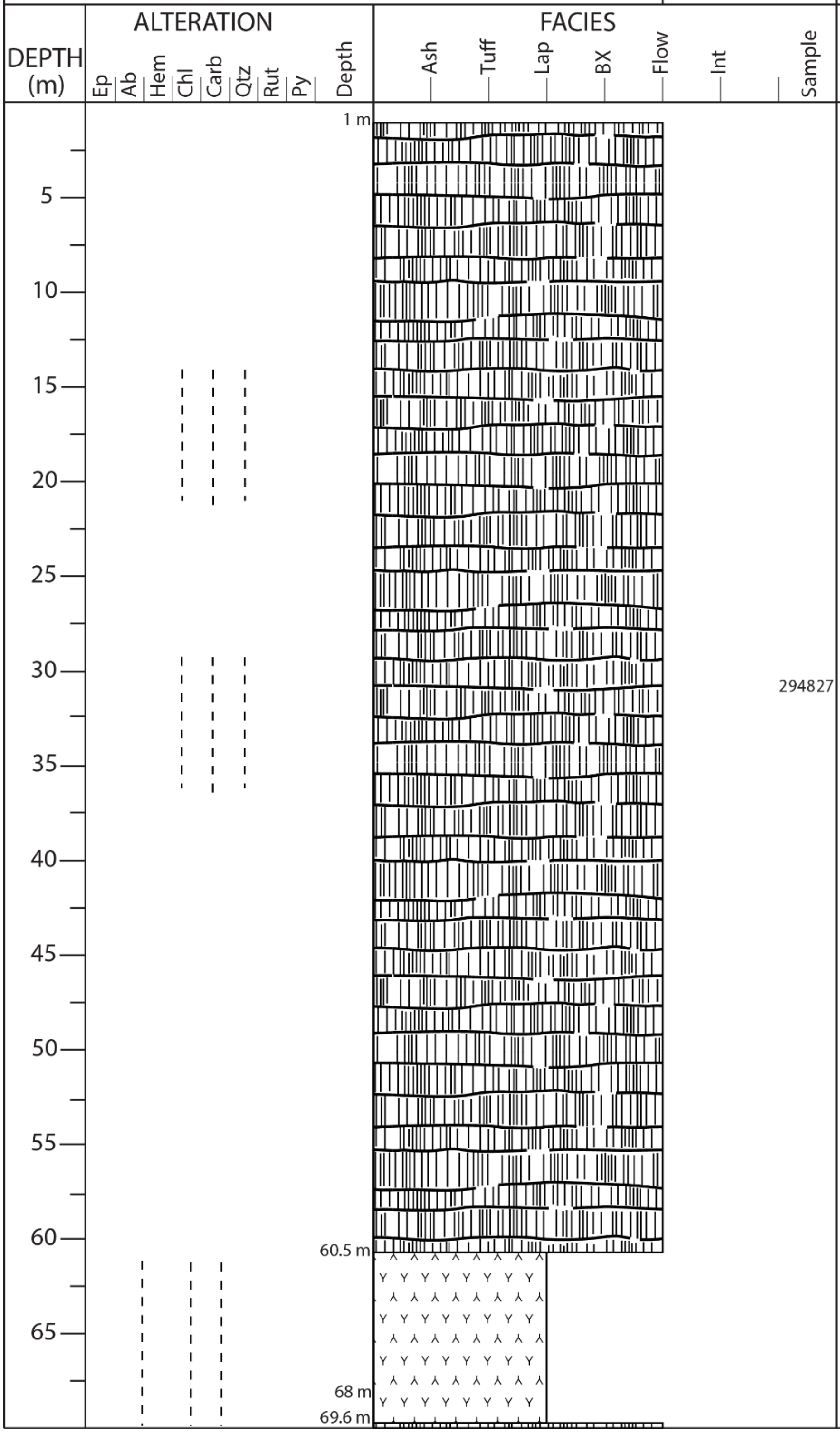

DESCRIPTION

OVB

HW volcaniclastics

continuous unit of predominantly mafic flow with dm-scale tuff breccia intervals consistent distal volcanogenic seafloor alteration (chl-carb+/-ep) and fracture-filling qt veinlets

damage zones with less intensely fractured intervals (15-22.2, 31.1-38.6)

heavily fractured @42.5-46.5m

50-60.50 m gradual change to tuff breccia and mafic lapilli tuff

FOL 64@53
FOL 68@57.8

medium-dark grey mafic lapilli tuff from 60.5m weakly sericitized, increasing downhole to mod @68 from 66.5m orange ab (< 3 mm)

FOL 84@62.1
FOL 86@67.9

dark grey-brown mafic lapilli tuff moderately sericitized
ser-chl-carb-ab

Project: Argyle
Diamond Drill Hole: AE-17-50
Date: 10-8-2017

Section: 5+7E

UTM
300860.7E
5537878.5N

Azimuth: 180
Dip: -80
Depth: 145 m

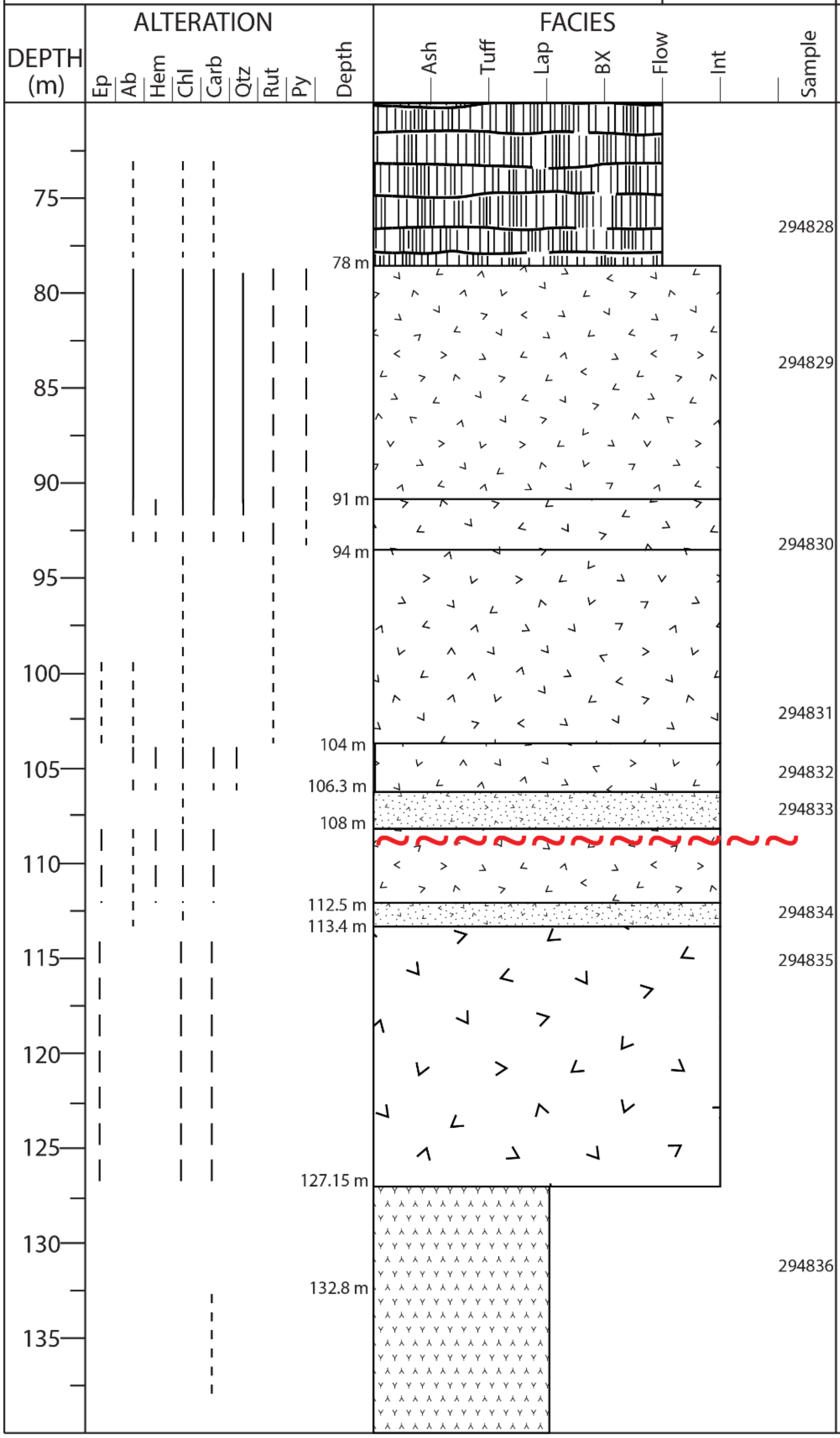

DESCRIPTION

HW volcaniclastics
beige-brown-dark grey-green mafic flow moderately-strongly sericitized
LC concealed by severe sericitization and qt-carb-ab vn

ser-chl-carb-ab

Proximal alteration zone
to 89m fg-mg gabbro ser-ab-ank-qt-chl-rut-py alteration

change in alteration across dm-scale qt-carb vein

from 89m dark green proximal cg ab-Fe-carb-chl-ser-rut-py-qt alt

FRC zones @ ~80-82, ~84-86, ~88-90

Intermediate alteration zone
dark green, not spotty chl-ab-ank cg gabbro

Distal alteration zone
dark green cg gabbro with tan rutile overprint
from 100.5 fg-mg

Proximal alteration zone
fg-mg Si-flooded strongly metasomatized gabbro

Intermediate alteration zone
aphinitic moderately sercitized mafic dyke with elongated black chlorite crystals (<5%)

mg dark green-pale green spotty gabbro; magnetic; weakly sheared near UC

SHR 85 @108.1 sheared rut
minor FLT zone @ 108-110

dark grey fg mafic dyke with porphyritic ab crystals, magnetic

Intermediate alteration zone
cg spotty gabbro with minor ab-ep-mt, magnetic to 117
from 120.5 mg, spotty ab-qt vn at LC

FW volcaniclastics
dark grey with pale tan-green intervals and pink ab veins

mafic lapilli tuff, similar to above with a finer weakly-moderately metasomatized and sericitized (+ab+chl) interval (134.8-136.8)

FOL 72 @134.5
FOL 78 @136.8
FOL 68 @138.6
fold hinge @139.8

Project: Argyle
Diamond Drill Hole: AE-17-50
Date: 10-8-2017

Section: 5+7E

UTM
300860.7E
5537878.5N

Azimuth: 180
Dip: -80
Depth: 145 m

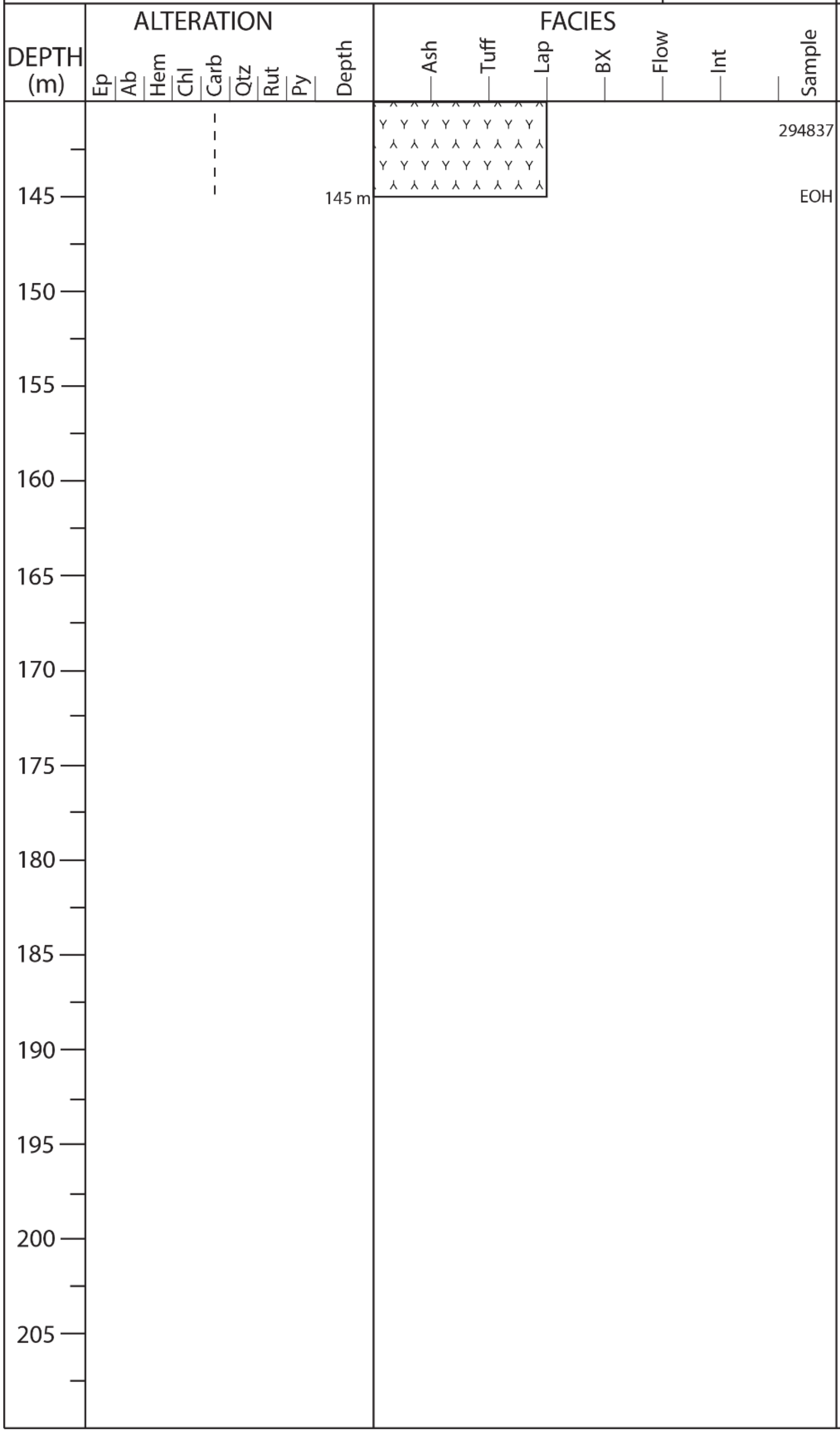

DESCRIPTION

FW volcaniclastics
dark grey; mafic lapilli tuff

FOL 38 @141.5
FOL 68 @142.5
FOL 43 @145

NO ZONE IN THIS HOLE DESPITE
WIDE DISTRIBUTION OF PY (EUH)
(NO ASSAYS ABOVE 0.18 G/T)

Project: Argyle
Diamond Drill Hole: AE-16-29
Date: 10-6-2017

Section: 6+5E

UTM
300952E
5537672N

Azimuth: 180
Dip: -52
Depth: 112 m

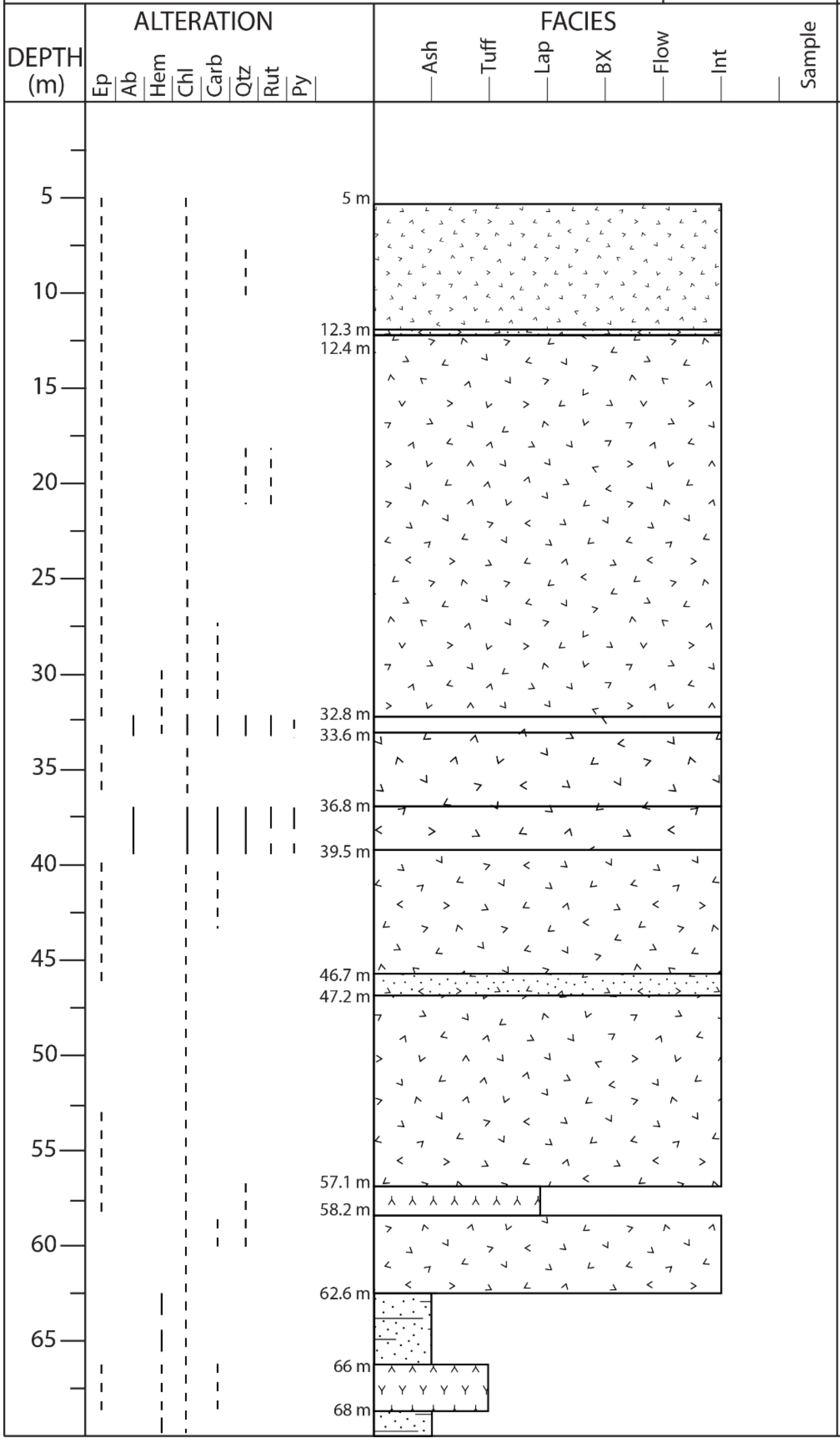

DESCRIPTION

OVB

Distal alteration zone
dark grey fg least altered gabbro

olive green fg mafic dyke (12.3-12.4)

Distal alteration zone
medium grey fg-mg least altered gabbro with fg-mg weak rut ovp and irregular mt-rich intervals

Proximal alteration zone
strong qt veining; proximal alt minerals likely only present due to a large concentration of qt veins; narrow interval, non-mineralized highly fractured (32-39 m)

Distal alteration zone
LAG - a weakly altered gabbro in a damage zone between two highly altered proximal intervals - perhaps shows fault splays above and below this interval - irregular faulting through the sill? i.e. in certain parts only one "proximal" zone, in others two

Proximal alteration zone
cg; qt-ab-Fe-carb-chl dominated

Distal alteration zone
mg LAG with cg magnetite

dark green fg mafic dyke with green phyric chl-altered plagioclase

Distal alteration zone
mg gabbro with locally weakly bleached spotty appearence

dark grey fg mafic lapilli tuff

Distal alteration zone
fg-mg gabbro with numerous mm-cm scale ep and qt-carb veins

maroon argillite; marker horizon at Pine Cove FW

FW volcaniclastics; mafic tuff with well-defined foliation (65 tca)

maroon argillite

Project: Argyle
Diamond Drill Hole: AE-16-29
Date: 10-6-2017

Section: 6+5E

UTM
300952E
5537672N

Azimuth: 180

Dip: -52

Depth: 112 m

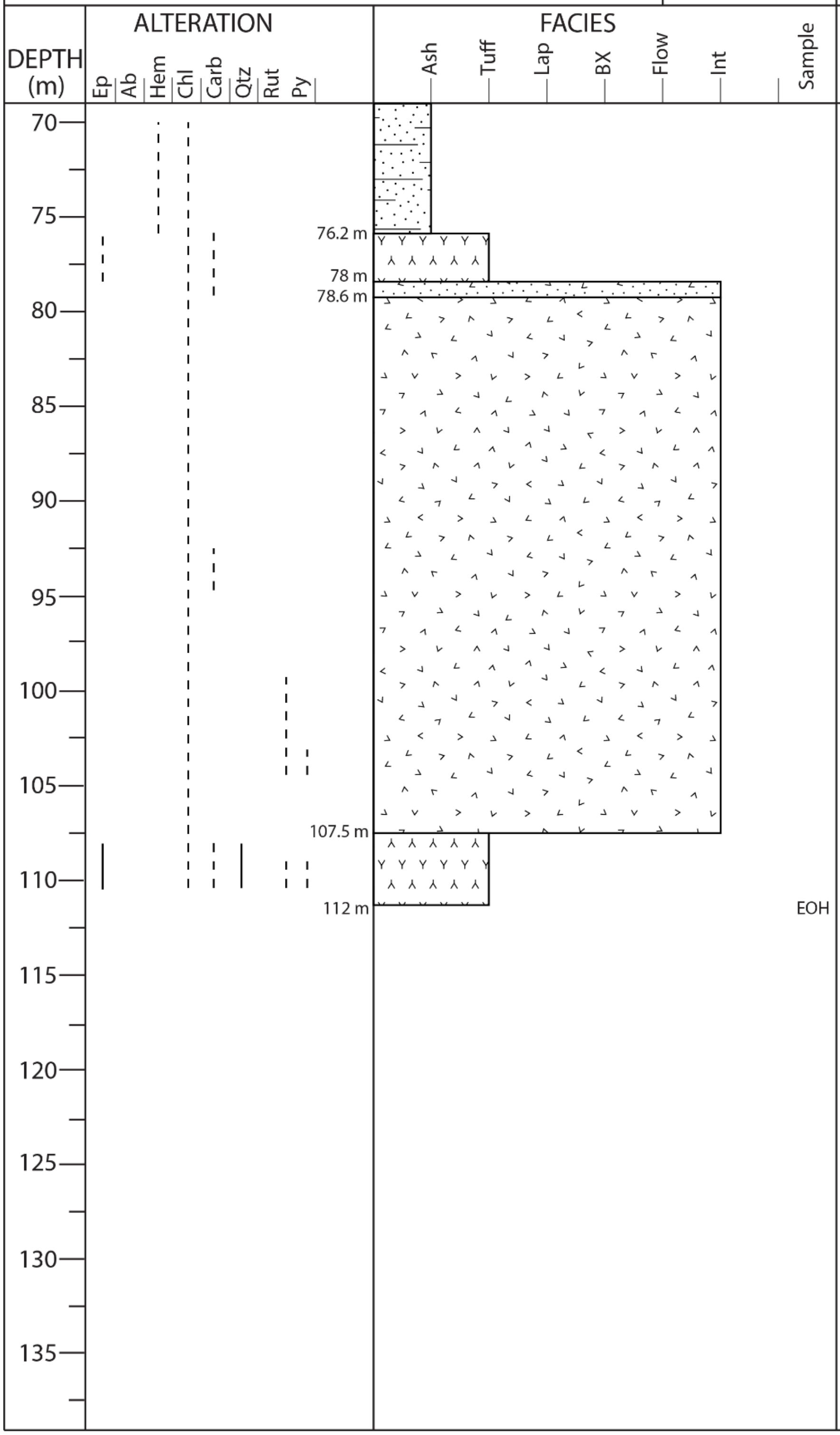

DESCRIPTION

maroon and green finely layered argillite; mt-rich beds

dark grey lapilli tuff

dark grey fg mafic dyke with phyric plagioclase

<u>Distal alteration zone</u>
relatively unaltered fg weak chl; likely a different gabbroic body; much less altered - may belong to Bobby Cove Fm. based on presence of maroon argillite marker horizon

lapilli tuff interbedded with well-bedded ash tuffs and blocky fragments; weakly sericitzied; py present at 109 m, associated with qt veins

Project: Argyle
Diamond Drill Hole: AE-17-58
Date: 10-13-2018

Section: 6+85E

UTM
300987E
5537763N

Azimuth: 180
Dip: -55
Depth: 107 m

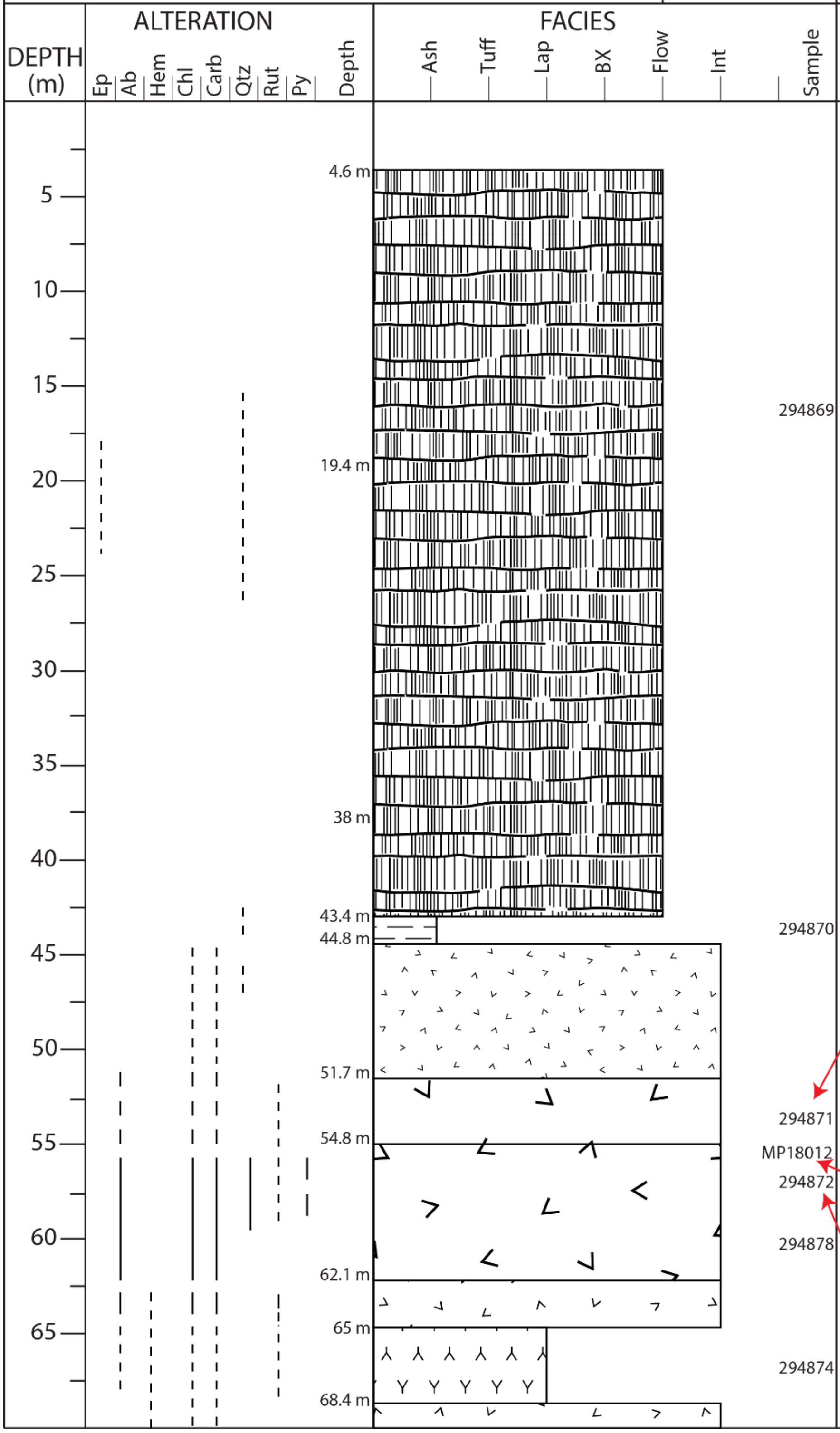

DESCRIPTION

OVB

HW volcaniclastics
mafic pillow lava with hyaloclastites (fragmentation of pillow lavas) with moderate ep-carb-Si alteration in selvages and pillow margins

pillow marigns exhibit cm-thick primary volcanogenic alteration mm-cm scale qt and calc veins

pale green-light grey massive flow with intervals of pillows and breccias minor veins, as above

medium grey-green fg volcanics

maroon-black, vfg-fg magnetite, hematite silica oxide iron formation interbedded with chl-qt altered volcaniclastic material 4-5% euh-subh py intensely magnetic

Distal alteration zone
fg gabbro

Intermediate alteration zone
dark green (not spotty) gabbro with pervasive ab and rutile overprint contains less carbonate than usual spotty intermediate gabbro, wk shr'd

Proximal alteration zone
mineralization in pink-green cg metasomatized gabbro
euh-sub dis pyrite in pink cg ab WR with coarser blebby min constrained to interface between WR and mm-scale black chl veins as well as dis anh py stringer parallel to qt vein zone - proximal pale brown-orange-green cg Si-flooded gabbro (ab-qt-Fe carb-chl-py-rut) with coarse ab

Intermediate alteration zone
spotty fg gabbro with rutile

mafic lapilli tuff between gabbro bodies - chl-carb-ab-qt

Distal alteration zone
fg gabbro

Project: Argyle
Diamond Drill Hole: AE-17-58
Date: 10-13-2018

Section: 6+85E

UTM
300987E
5537763N

Azimuth: 180
Dip: -55
Depth: 107 m

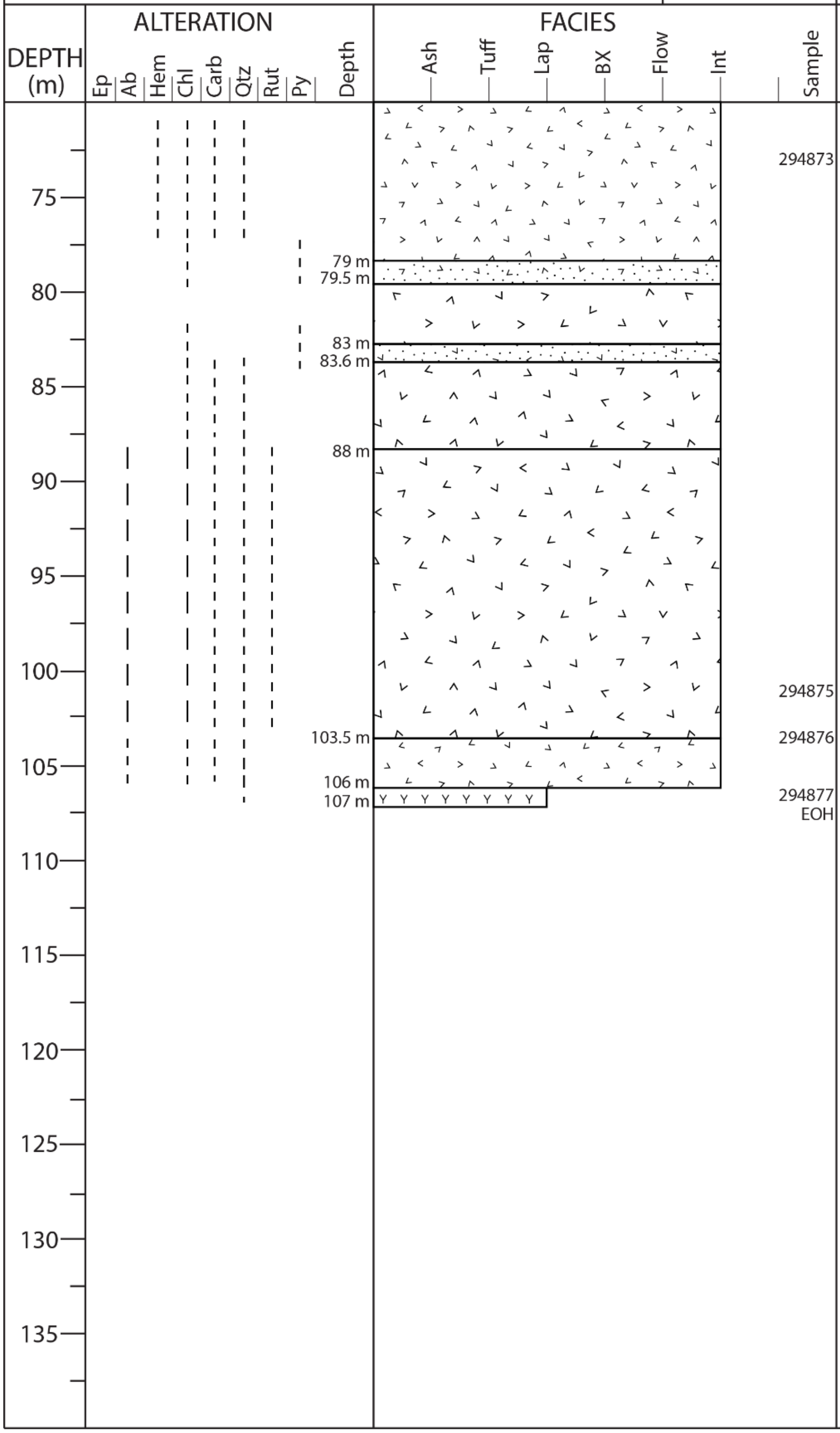

DESCRIPTION

<u>Distal alteration zone</u>
dark green-pale green fg gabbro with weak carb, chl and hem veinlets

medium grey-green fg mafic dyke with ep-chl veinlets and ~1% euh dis py

<u>Distal alteration zone</u>
mg-cg gabbro

same as dyke above

<u>Distal alteration zone</u>
mg-cg gabbro

<u>Intermediate alteration zone</u>
mg gabbro, patchy altered albite ab-chl-qt-rut related to qt-chl-carb veins

<u>Distal alteration zone</u>
dark green fg gabbro with fg rut ovp and qt vns - LAG?

FW volcaniclastics
pale green mafic lapilli tuff/ medium-light green bx
carb-chl-ab-qt

Project: Argyle
Diamond Drill Hole: AE-17-59
Date: 10-13-2018

Section: 6+85E

UTM
300987E
5537763N

Azimuth: 180
Dip: -90
Depth: 146 m

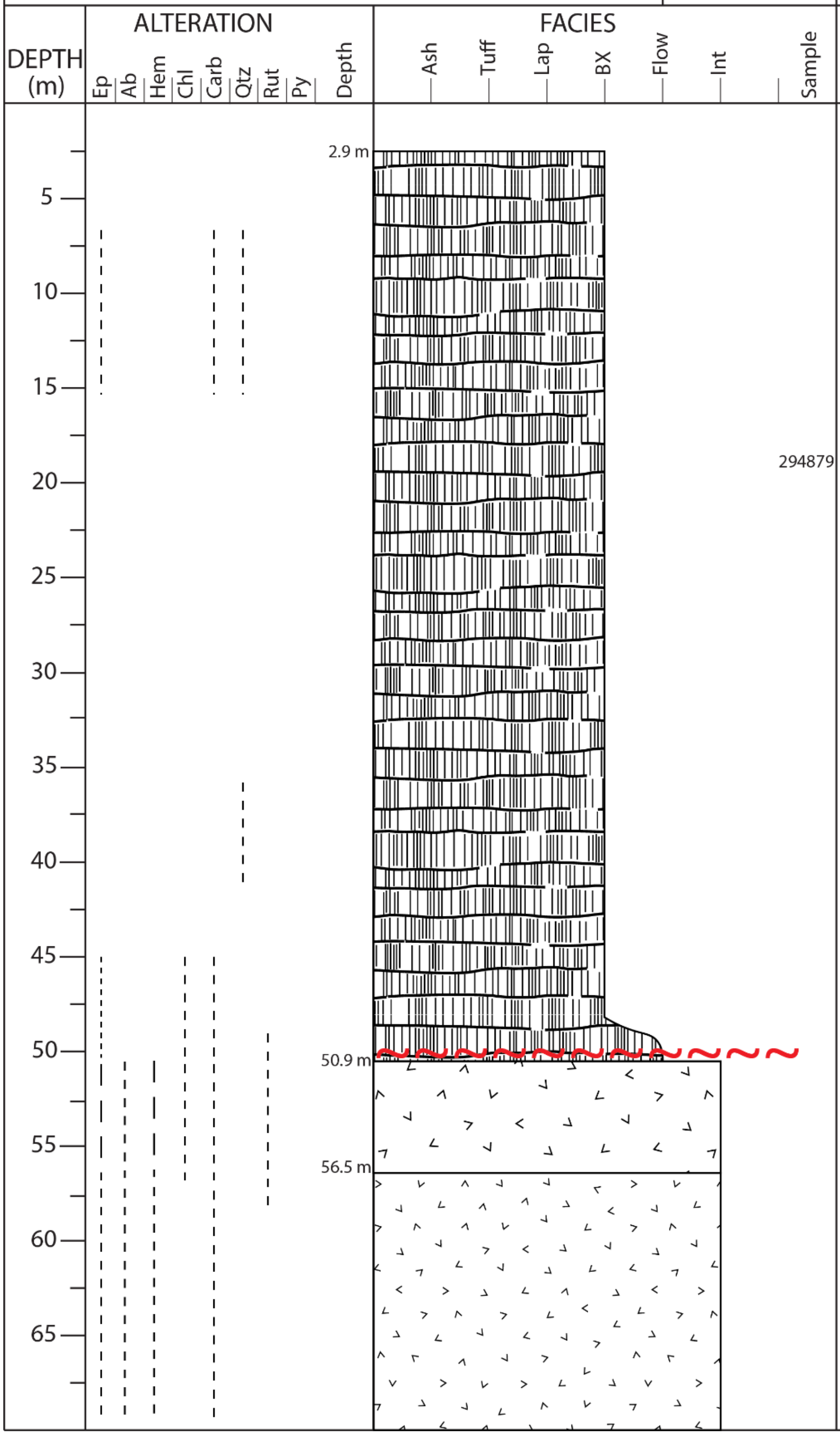

DESCRIPTION

OVB

HW volcaniclastics
medium-green basaltic pillows with mm-cm pillow selvages and weak ep-Si-carb alteration (primary volcanogenic) with hem veinlets

HW pale green mafic flow

weakly ser-carb-chl altered brecciated mafic flow

Intermediate alteration zone

FLT 50-50.5 intense chl alteration

spotty mg-cg chl-carb-rut mod altered, locally foliated gabbro

Distal alteration zone

fg-mg dark-medium green, locally ep-altered distal gabbro

Project: Argyle
Diamond Drill Hole: AE-17-59
Date: 10-13-2018

Section: 6+85E

UTM	
300987E	Azimuth: 180
5537763N	Dip: -90
	Depth: 146 m

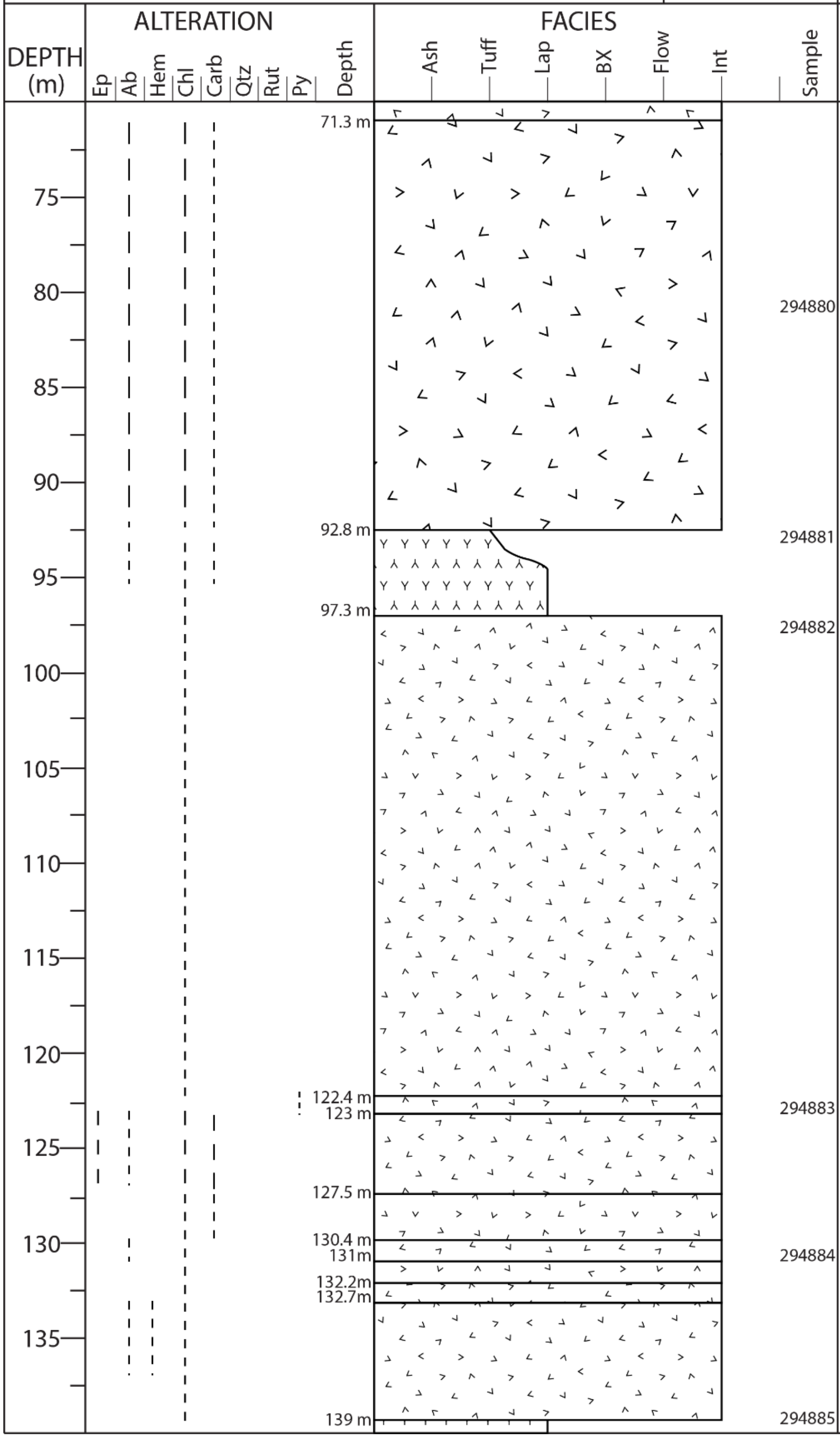

DESCRIPTION

Intermediate alteration zone
dark green to apple green (ep) cg gabbro with cg ab, locally pale green-yellow altered plag/ab laths

dark green coarse spotty magnetic gabbro with chl-ab-carb-ep-mt alt

mafic lapilli tuff between two(?) gabbro dark-grey-green, weakly carb-ab-chl altered
crystal tuff at UC (?)

Distal alteration zone
pale-dark green fg gabbro
LAG with no rutile

fg dark grey mafic dyke with weak chl and euhedral py alteration

Intermediate alteration zone
fg dark-medium green gabbro with weak carb-ep spotting, likely due to proximity to dyke, which acted as a fluid conduit

Distal alteration zone
fg mafic dyke dark green-grey with mm-scale ab(carb?) altered laths

medium grn-gr fg mafic dyke mm-scale plagioclase laths, weakly sheared with hem veinlets

Distal alteration zone
dark green fg-mg gabbro with chl-ep carb-qt alteration

Project: Argyle
Diamond Drill Hole: AE-17-59
Date: 10-13-2018

Section: 6+85E

UTM
300987E
5537763N

Azimuth: 180
Dip: -90
Depth: 146 m

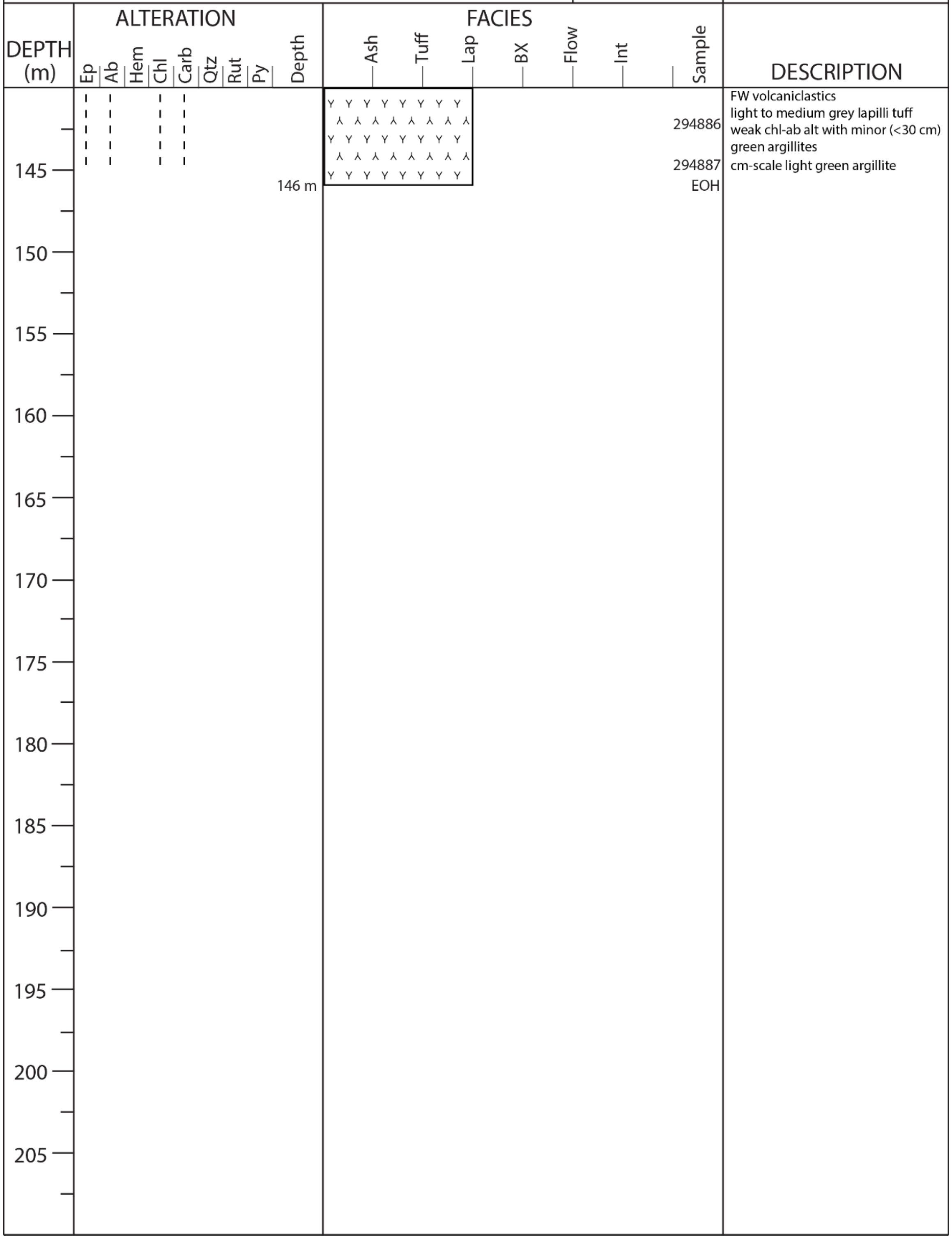

FW volcaniclastics
light to medium grey lapilli tuff
weak chl-ab alt with minor (<30 cm)
green argillites
cm-scale light green argillite

Project: Argyle
Diamond Drill Hole: AE-17-63
Date: 10-13-2018

Section: 6+85E

UTM
300998.9E
5537850.5N

Azimuth: 180
Dip: -80
Depth: 161 m

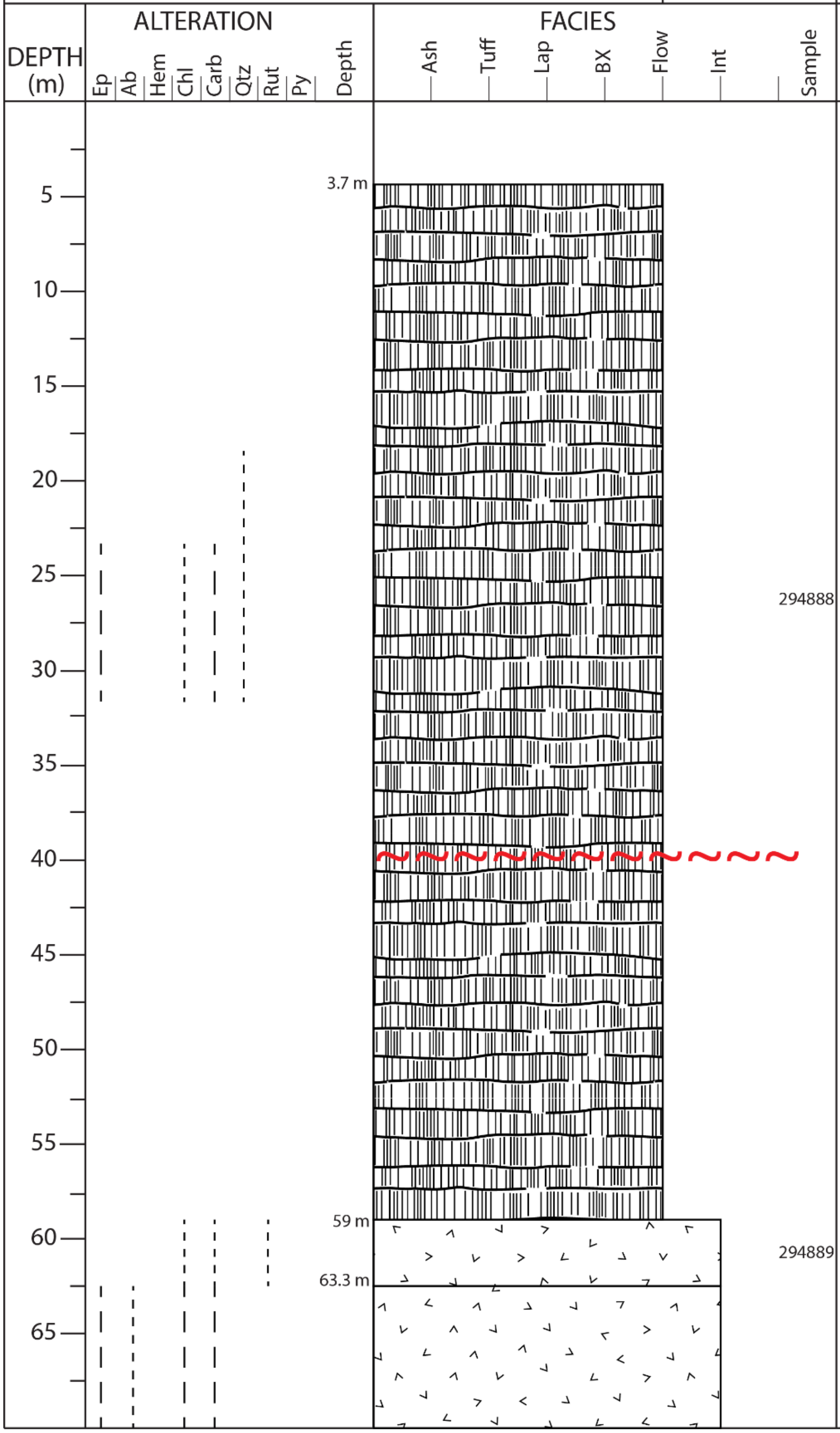

DESCRIPTION

OVB

HW volcaniclastics
medium green-grey basaltic pillow low with minor intervals of brecciated volcanics m-scale pillow lavas (<1.5m) mm-cm scale calc and qt veins primary carb-ep-chl-Si alt

HW mafic pillow lava with hyaloclastites (fragmentation of pillow lavas) with moderate ep-carb-Si alteration in selvages and pillow margins

FLT 39.8-39.9 m

<u>Distal alteration zone</u>
dark green mg gabbro with a weak rutile overprint

<u>Intermediate alteration zone</u>
dark green-apple green mg spotty gabbro

Project: Argyle
Diamond Drill Hole: AE-17-63
Date: 10-13-2018

Section: 6+85E

UTM
300998.9E
5537850.5N

Azimuth: 180
Dip: -80
Depth: 161 m

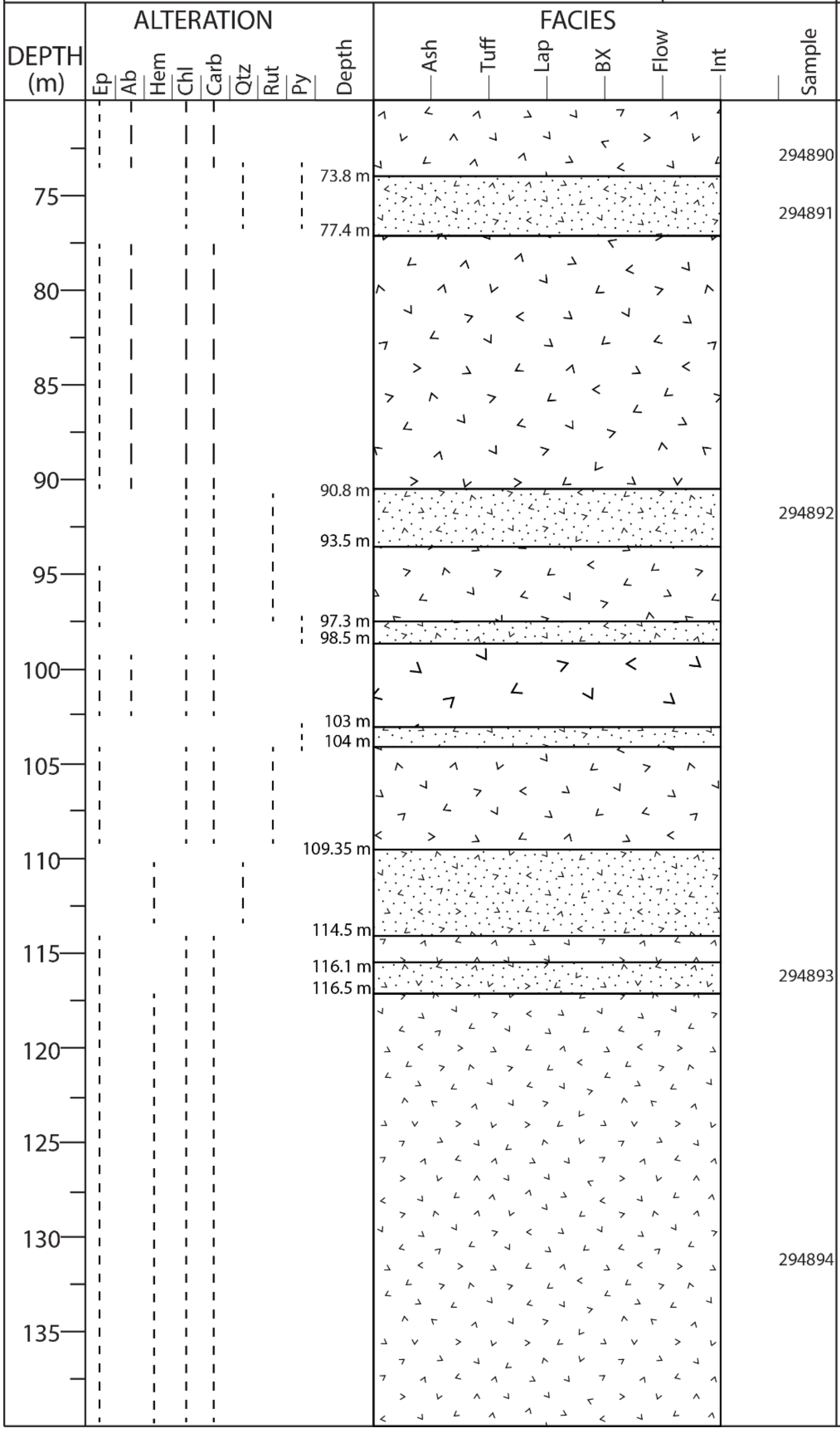

DESCRIPTION

<u>Intermediate alteration zone</u>
dark green to pale green medium spotty gabbro (chl-carb-ab-ep) with hematite veinlets

dark green relatively unaltered mafic dyke with euhedral dis pyrite (~3-4%)

intermediate alt gabbro, same as above, mg-cg

mafic dyke light green grey, where aphintic, medium-dark grey where fg weak chl-carb-rut alt

<u>Distal alteration zone</u>
dark green mg gabbro with a rut overprint near LC with dyke

dark grey aph-fg mafic dyke with 1% dis euh py

dark green-brown to apple grn (ep) cg gabbro with locally porphyritic pl (ab-alt'd)

dark grey aph-fg mafic dyke with 0.5-1% dis euh py

dark green mg gabbro with locally pale grn-yelw/gold cg rut ovp

dark grey fg mafic dyke with rare mm-scale plag laths
common qt, qt-ab, hem vns and vnlts

mafic dyke aph medium green chl alteration and qt vn

distal fg dark-pale green gabbro with chl-ep alteration and ep and qt-hem veinlets

Project: Argyle Diamond Drill Hole: AE-17-63 Date: 10-13-2018	Section: 6+85E	UTM 300998.9E 5537850.5N	Azimuth: 180 Dip: -80 Depth: 161 m

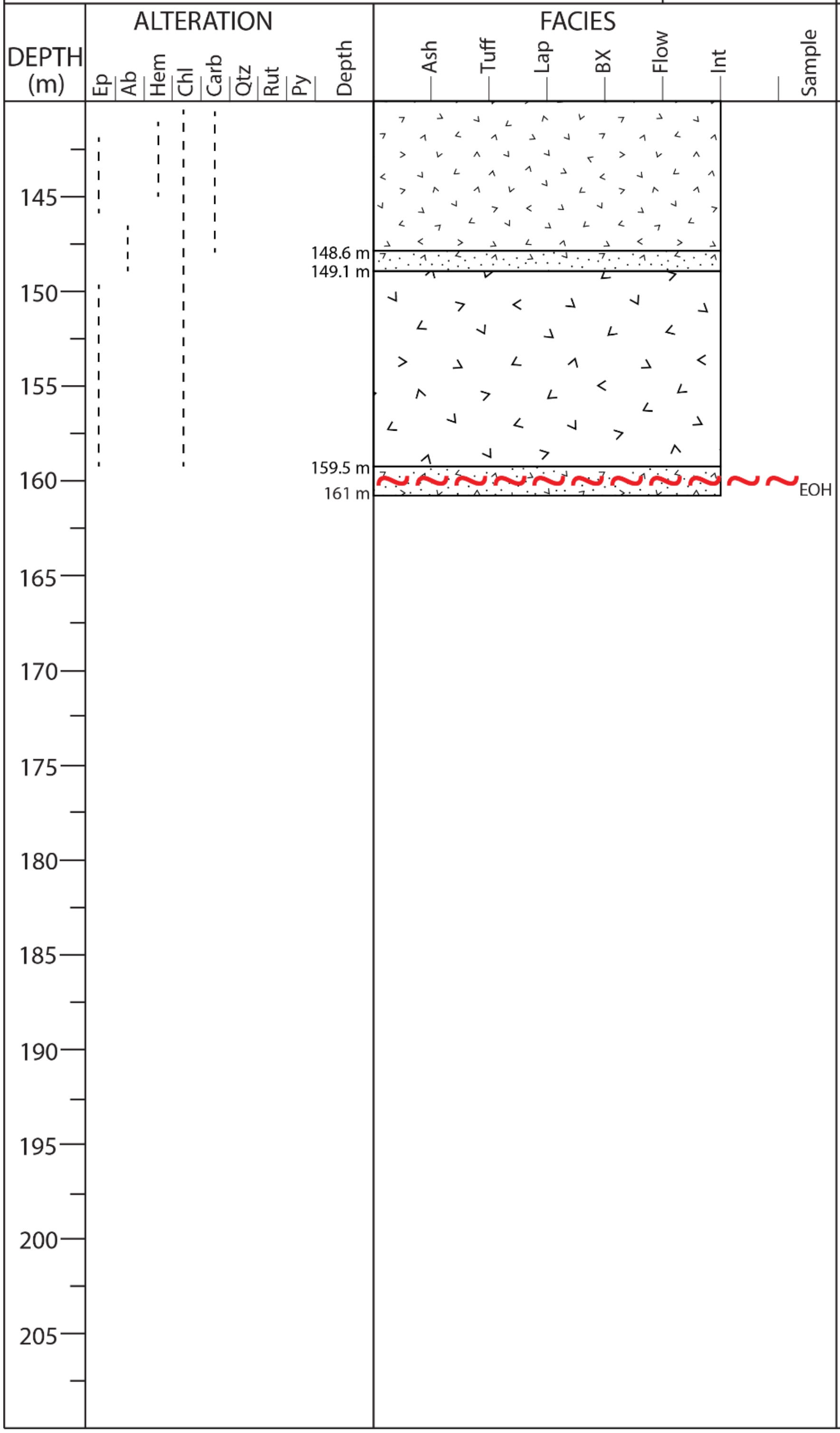

DESCRIPTION

dark grn fg gabbro with locally apple green ep patches

medium grey, fg mafic dyke with black chloritoids (~5%) and isolated ab crystals

medium washed-out green cg gabbro with patchy ep (apple grn)

dark grey mafic dyke with a small FLT zone (160.5-160.85) with gouge; mm-cm qt veins

Project: Argyle
Diamond Drill Hole: AE-18-74
Date: 10-11-2018

Section: 6+85E

UTM
300984.3E
5537717.1N

Azimuth: 180
Dip: -55
Depth: 65.2 m

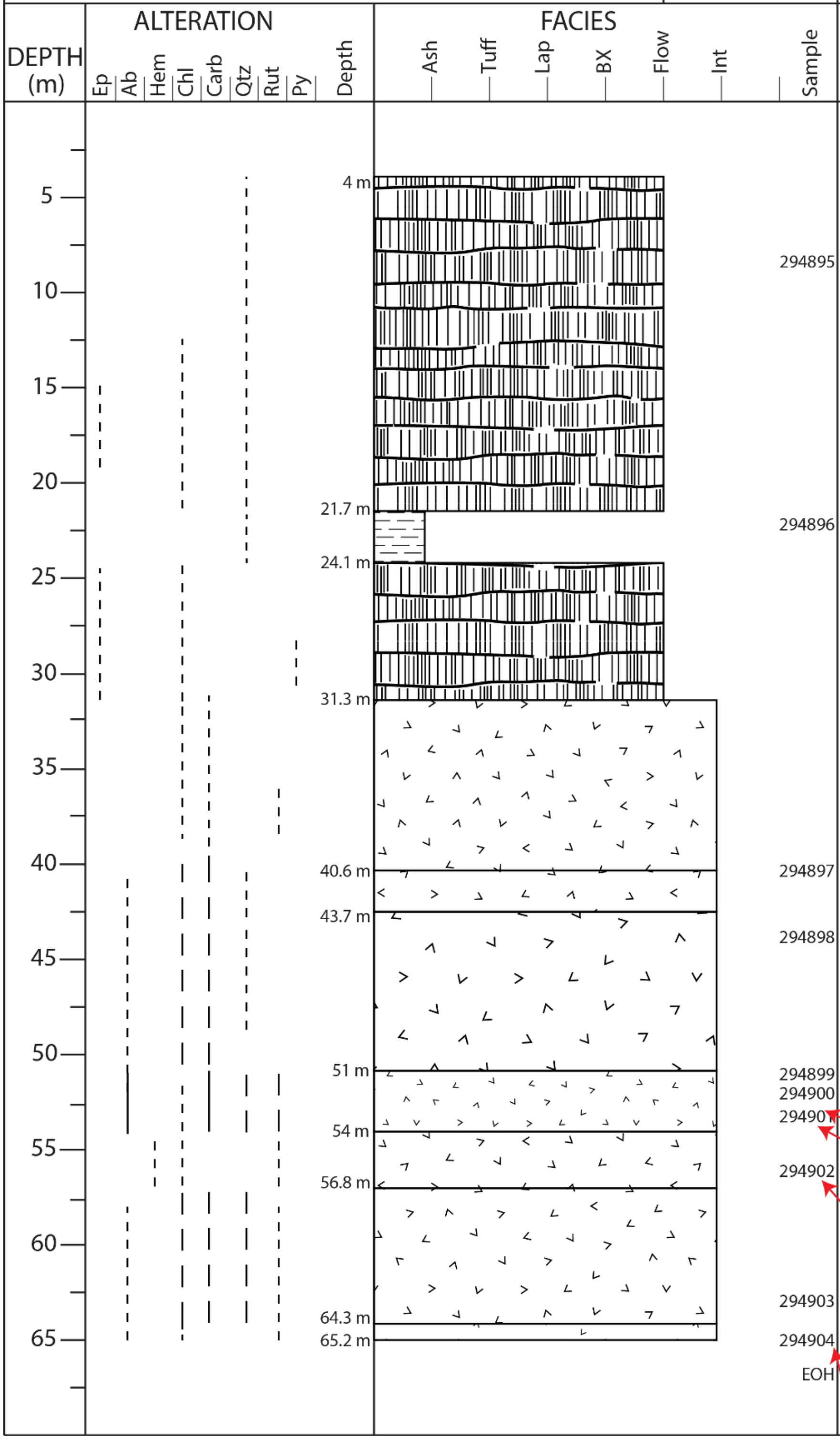

DESCRIPTION

OVB

HW volcaniclastics
light grey-green aph-fg massive mafic flow with tr dis euh py;
locally brecciated with rare pillow selvages and mm-scale qt-carb veins
primary volcanogenic ep-chl-qt

294895

maroon-black fg extremely magetic iron formation (hem-mt-Si) with fragments of mafic flow
3-5% euh-anh pyrite disseminated blebs and stringer sulphide

294896

mg

dark grey-green fg mafic flow with tr dis py throughout the unit and mafic lapilli tuff section towards LC
mm-scale calcite veinlets

Distal alteration zone
mg gabbro

Intermediate alteration zone
mg gabbro with round chloritoid eyes and carbonate rims, chl-ab and bleached matrix
mm-cm scale qt veins

294897

cg dark green gabbro with cg brown-tan rutile overprint and qt veinlets
chl-carb-ab-rut

294898

Proximal alteration zone
Zone (30 g/t), pale tan-green heavily Si-flooded gabbro, with 10-15% blebby and stringer sub-anhedral py
ab-Fe-carb-chl-py-qt-rut

294899
294900

pale-bright-dark green c-m gabbro
heavy Fe-carb overprint
Fe carb-ab-rut-qt-fuch-chl alteration

29490

Intermediate alteration zone
fg gabbro with pale brown-green carb-ser-ab-chl-qt alteration

294902

Distal alteration zone
dark-bright green gabbro with chl-hem-rut alteration; stronger and wider (< 1 cm) hematite veinlets

Intermediate alteration zone
pale tan-medium green Si-flooded mg spotty gabbro
Si-chl-carb-ab-rut alteration

294903
294904

Distal alteration zone
dark green fg gabbro, chl-ab altered with rut overprint

EOH

Project: Animal Pond
Diamond Drill Hole: AE-05-03
Date: 10-16-2018

UTM
296618E
5536859N

Azimuth: 140
Dip: -65
Depth: 67.1 m

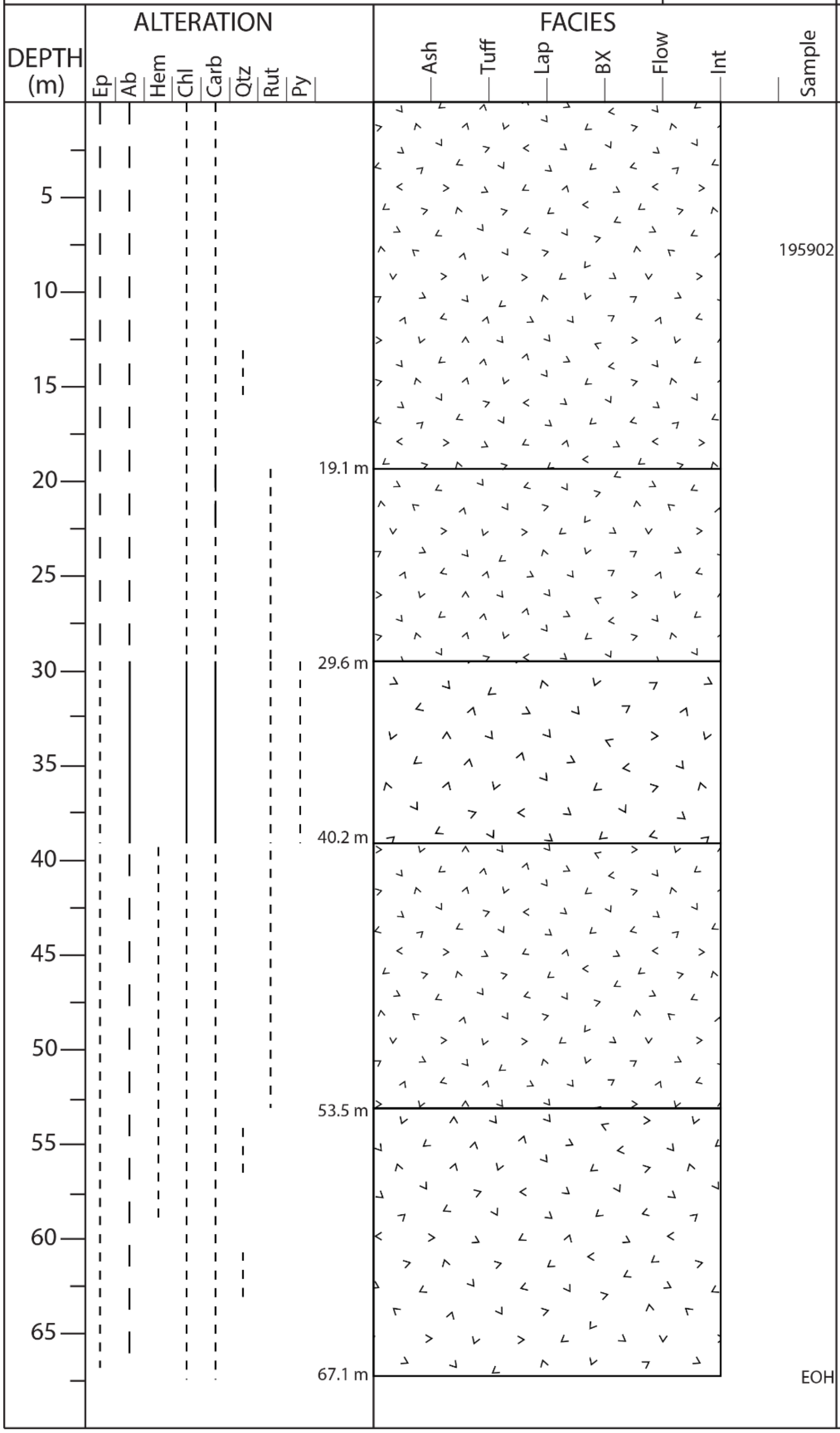

DESCRIPTION

Intermediate alteration zone
mossy green-pale yellow-pink mottled/"spotty" intermediately altered gabbro

some oxidized Fe-carb spots in mg gabbro; less spotty like than intermediate alteration zone above

darker, more green with lesser ep and less spotting, with mg tan-gold yellow rutile overprint

Proximal alteration zone
cg-pegmatitic ab(plag) laths very well formed, clearly unaffected by the later hydrothermal events only affected by the early alteration this alteration zone is not deformed the gabbro at AP hasn't experienced the brittle deformation that the gabbro at Argyle has experienced which possibly explains there is relative lack of gold mineralization (D2) at Animal Pond - a strong contrast with Argyle

Intermediate alteration zone
similar to top of the hole, moderate epidote alteration
more epidote veining

less spotty texture, mg-cg.
very weak hematite veinlets

from 62.5 cg skeletal magnetite instead of rutile overprint - less affected by hydrothermal alteration (D1)

Representative hole of Animal Pond gabbro alteration
- shows D1-related (ep-ab+) hydrothermal alteration
- typical “mottled” / “spotty” texture of gabbro

D1 - ep-ab;
qt, qt-ab veins post-D1, pre-D2

Project: Argyle
Diamond Drill Hole: AE-18-74
Date: 10-11-2018

Section: 6+85E

UTM
300984.3E
5537717.1N

Azimuth: 180
Dip: -55
Depth: 65.2 m

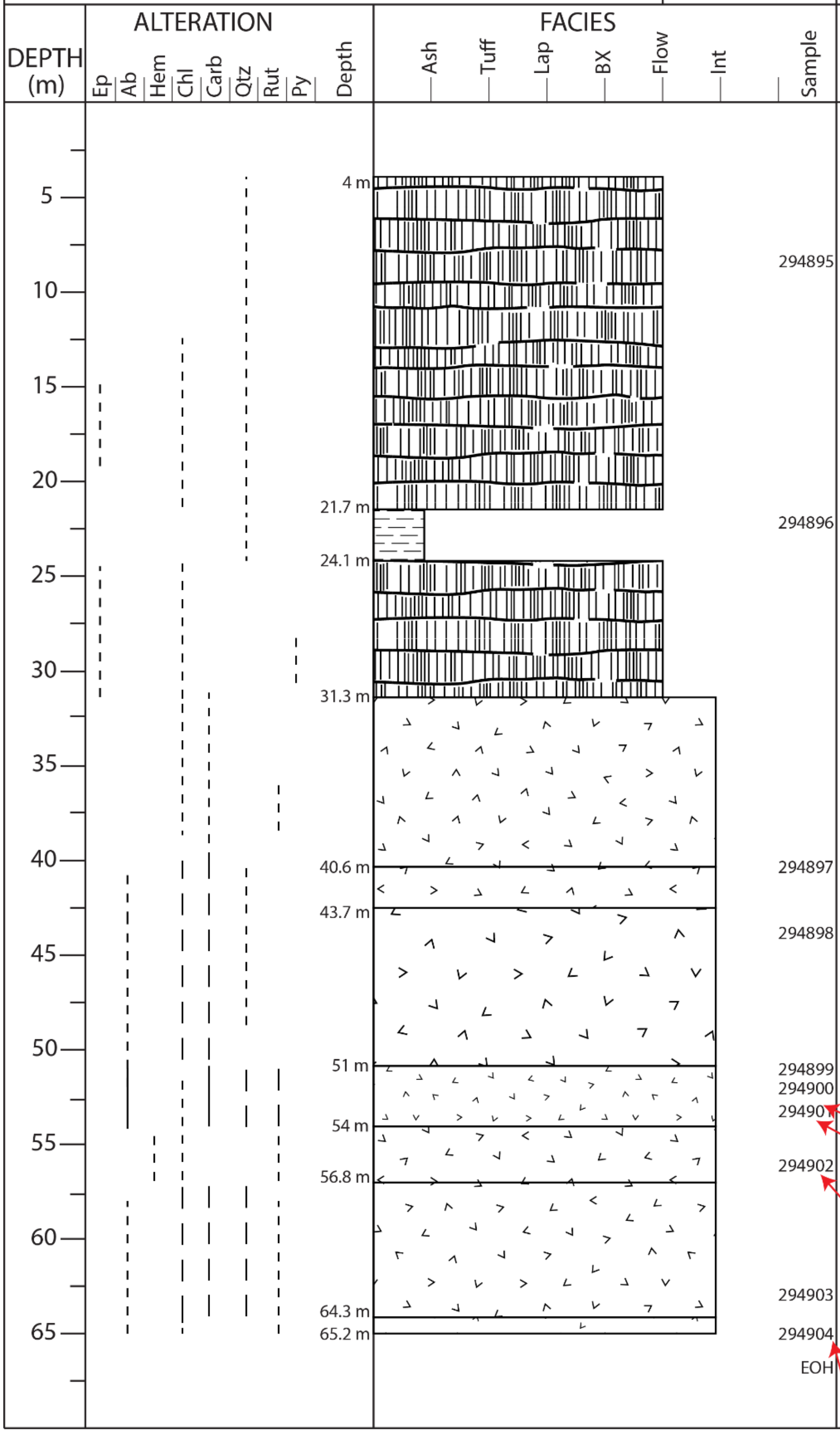

DESCRIPTION

OVB

HW volcaniclastics
light grey-green aph-fg massive
mafic flow with tr dis euh py;
locally brecciated with rare pillow
294895 selvages and mm-scale qt-carb veins
primary volcanogenic ep-chl-qt

maroon-black fg extremely magetic
iron formation (hem-mt-Si) with
fragments of mafic flow
294896 3-5% euh-anh pyrite disseminated
blebs and stringer sulphide

mg

dark grey-green fg mafic flow with
tr dis py throughout the unit and
mafic lapilli tuff section towards LC
mm-scale calcite veinlets

Distal alteration zone
mg gabbro

Intermediate alteration zone
294897 mg gabbro with round chloritoid
eyes and carbonate rims, chl-ab and
bleached matrix
mm-cm scale qt veins
294898 cg dark green gabbro with cg brown-tan rutile overprint and qt veinlets
chl-carb-ab-rut

Proximal alteration zone
Zone (30 g/t), pale tan-green heavily
Si-flooded gabbro, with 10-15%
blebby and stringer sub-anhedral py
294899 ab-Fe-carb-chl-py-qt-rut
294900 pale-bright-dark green c-m gabbro
294901 heavy Fe-carb overprint
Fe carb-ab-rut-qt-fuch-chl alteration

Intermediate alteration zone
294902 fg gabbro with pale brown-green
carb-ser-ab-chl-qt alteration

Distal alteration zone
dark-bright green gabbro with chl-hem-rut alteration; stronger and
wider (< 1 cm) hematite veinlets

Intermediate alteration zone
294903 pale tan-medium green Si-flooded
mg spotty gabbro
294904 Si-chl-carb-ab-rut alteration

EOH
Distal alteration zone
dark green fg gabbro, chl-ab altered
with rut overprint

Project: Stog'er Tight
Diamond Drill Hole: BN-14-186
Date: 10-17-2018
Section: 1262.5E
UTM
299202E
5536529N
Azimuth: 206
Dip: -50
Depth: 76 m

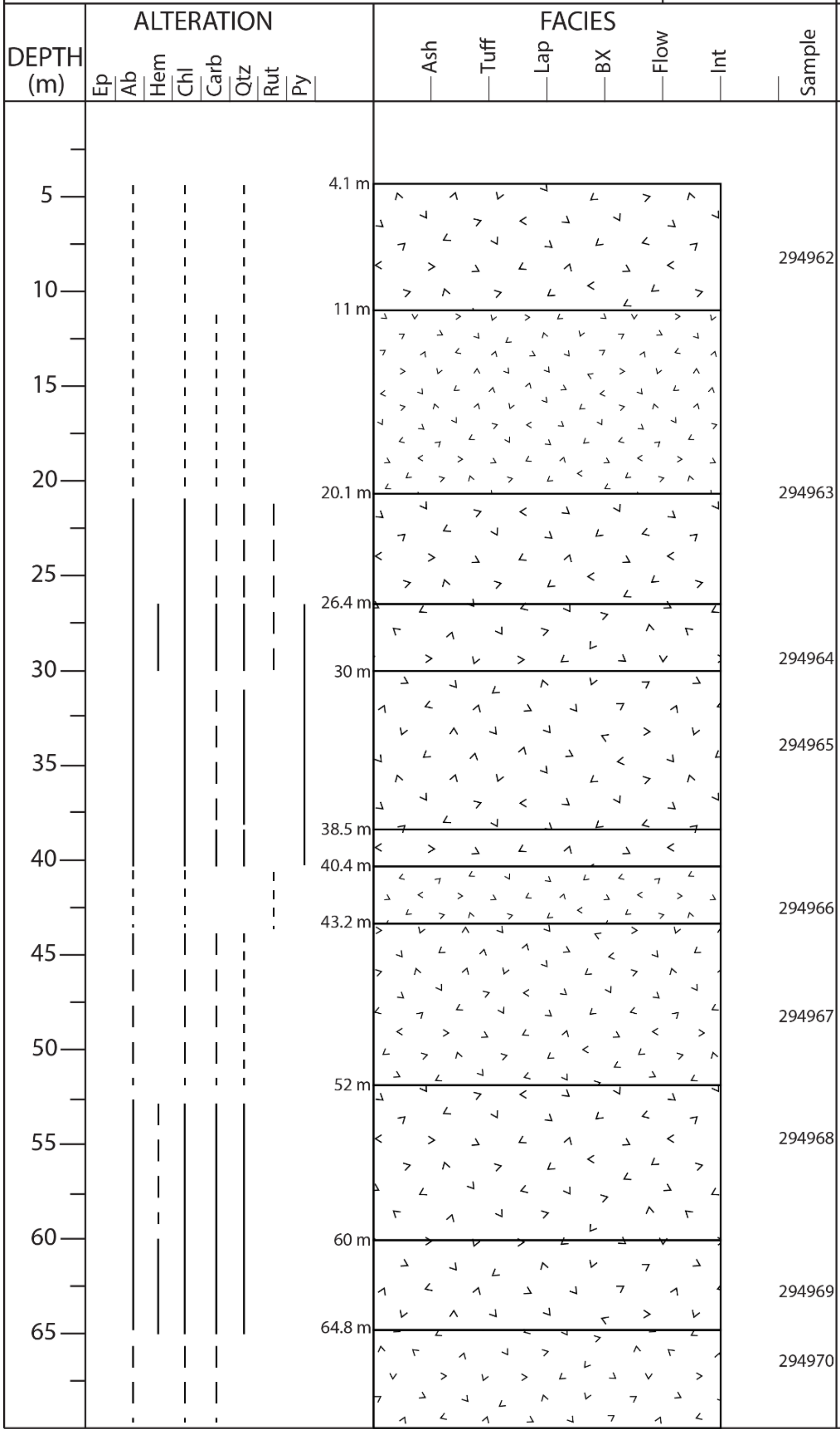

DESCRIPTION

OVB

Distal alteration zone

dark green-grey mg gabbro with cg plagioclase (ab-altered?) laths minor qtz and qtz-carb veinlets dark green mg gabbro with pinkish-white incipient albite

Intermediate alteration zone

strongly sheared and locally folded fg-mg gabbro with chloritoid eyes and strong ab alteration (20.5-25.1), rut ovp and 2-3% dis euh py v strong qtz-carb-chl-abstockwork dark green-pinkish orange (heavily oxidized on fresh surfaces) cg banded (sheared ab-chl) gabbro transitioning to proximal

Proximal alteration zone

banded ab-chl gabbro

"ore-zone" dominated by brick red pegm ab, hem and qt with a strong chl matrix and ~10% milled qtz and subh-anh grungy py

dark grn/blk-orange-pink moderately sheared with late blk chl veinlets associated with mineralization and cg py in vein margins and WR

cg-pegm gabbro with cg py, with heavy mottled ankerite overprint

Distal alteration zone

dark green-grey fg gabbro, weakly sheared with fg ab and rut ovp mm-scale qtz-carb vnlts and ff-hem

Intermediate alteration zone

medium dark green to tan-pale orng strongly foliated chl-ab-ank-qt

Proximal alteration zone (lower)

heavily sheared and folded gabbro with dominant ab-ank-qt-chl alt assemblage and minor dark gr chl matrix (<15%)

"ore-zone" with lower grade and less hem than in the upper ore zone orange-yllw vcg-pegm ab-hem-ank vcg-pegm, milled appearance 60-61.1m qt-chl vn; 25% quartz veins

Intermediate alteration zone

sheared and banded mg ab-chl with w-m ank overprint and

Project: Stog'er Tight
Diamond Drill Hole: BN-14-186
Date: 10-17-2018

Section: 1262.5E

UTM
299202E
5536529N

Azimuth: 206
Dip: -50
Depth: 76 m

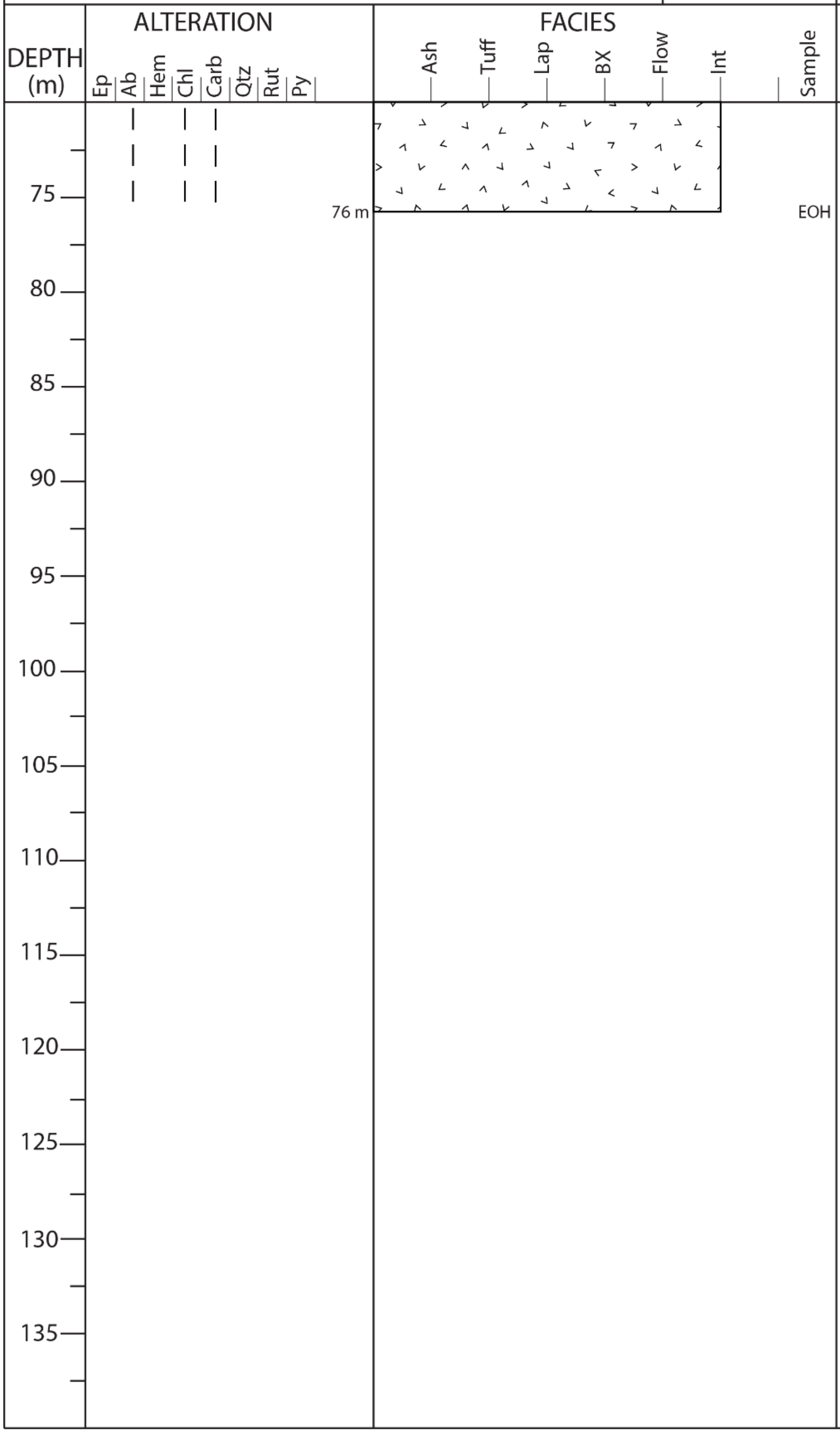

DESCRIPTION

Intermediate alteration zone
sheared to 70.3 m
70.3 - EOH - mod-wkly foliated

Upper proximal zone - sheared outside of ore-zone, typically blk chl-ab orange sheared bands; higher Au grades, common

Lower proximal zone - regularly strongly sheared and tan-pale orange/weakly-moderately sericitized; lower Au grades, Au assays tend to be below LOD

Project: Stog’er Tight
Diamond Drill Hole: BN-14-191
Date: 10-17-2018

Section: 1262.5E

UTM
299200E
5536521N

Azimuth: 206
Dip: -50
Depth: 52 m

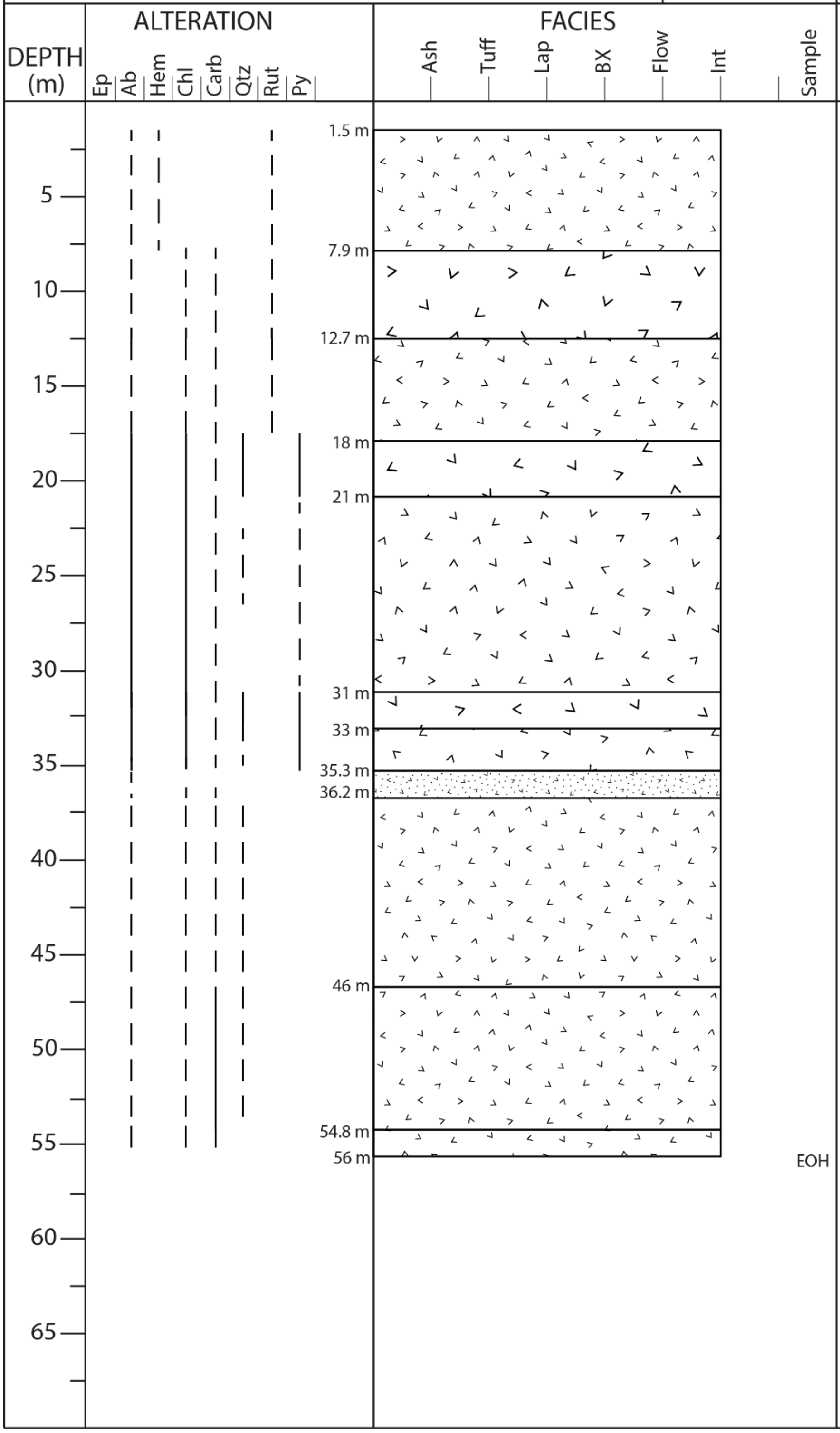

DESCRIPTION

OVB

Distal alteration zone
dark green-grey, fg-mg gabbro with incipient albite; shearing intensity increases from 8 m to LC
tr-0.5% dis euh py

weak orange-tan rut ovp
from 7.9 m signifnant increase in carbonate mottled overprint (oxidized core)

Intermediate alteration zone
mg mod-str sheared and banded gabbro

Proximal alteration zone
“ore zone” - typical ST ab-hem pegm altered gabbro with cg py
3-4% dis euh py (18-24 m)

cg orange-pink to blk/dark grn gabbro with mineralization constrained to qt vn margins and ab in WR, late blk chl veinlets and some fg-mg pyrite in qt veins
strongly magnetic (24-28 m)

“ore zone” i.e. ab-hem pegm gabbro w/ cg py like 18-21 m

cg blk/dark grn to orange-pink prox. gabbro with~ 5% euh-anh py

camo green aph mafic dyke with isolated cg ab crystals

Intermediate alteration zone
fg-mg dark grey gabbro with incip. ab and a mottled oxidized core surface (ank); weakly-moderately sheared from 38m.

increase in ank and ser due to presence of dm-scale qt-ank-chl vns

Distal alteration zone
fg dark grn gabbro with incipient ab

Project: Stog'er Tight
Diamond Drill Hole: BN-14-192
Date: 10-17-2018

Section: 1262.5E

UTM
299192E
5536536N

Azimuth: 206
Dip: -70
Depth: 55 m

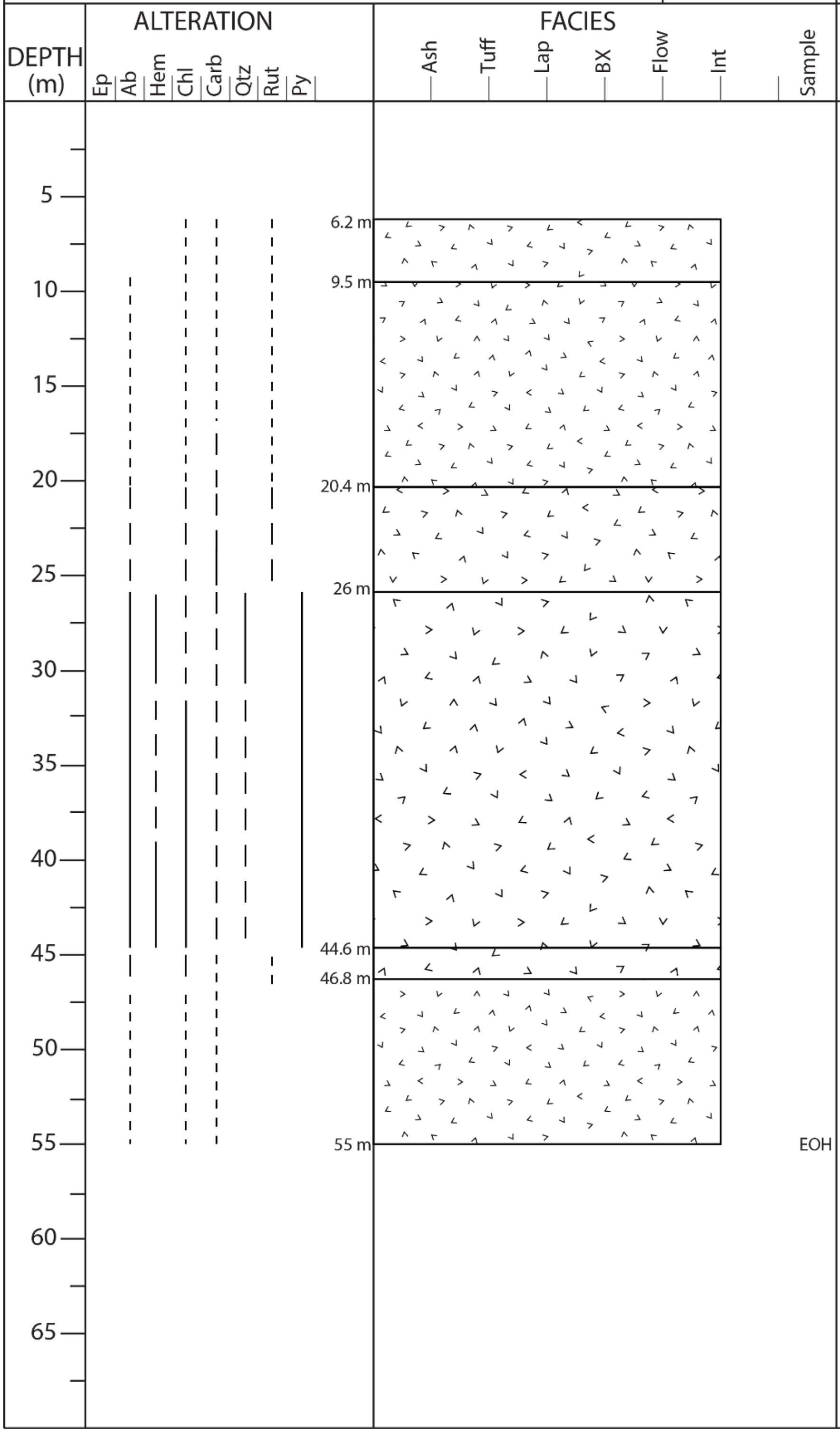

DESCRIPTION

OVB

Distal alteration zone
dark grey fg gabbro with incipient ab
locally weakly sheared
minor qt-carb-chl veins
tr dis py at vein margins

ab-ank alt intensity increases downhole

gradual change to to intermediate alteration mineral assemblage

Intermediate alteration zone
mg sheared gabbro, well expressed by sheared tan rut ovp
mg-cg altered gabbro, increasingly sheared downhole with overall 1-2% tr dis py, euh-subh; ~5% dis euh py (23.8-29.5) and ~3% euh-subh py (33.6-45.8)

Proximal alteration zone
cg orange-pink to black gabbro
26-27.5 - qt-chl vein with strong cg py mineralization on vein margin

consistent proximal zone appearence with other ST sections with presence of AP proximal plag lath precursor (D1-related)

cg strong pyrite mineralization within the unit at vein margins and WR
In WR, where ab is pegmatitic with ank and hem py is both coarser and more abundant

Intermediate alteration zone
cg sheared chl-ab gabbro

Distal alteration zone
dark grey fg gabbro
minor qt-ank and qt-chl veinlets

Project: Stog'er Tight
Diamond Drill Hole: BN-14-190
Date: 10-17-2018

Section: 1287.5E

UTM
299223E
5536521N

Azimuth: 206
Dip: -50
Depth: 82 m

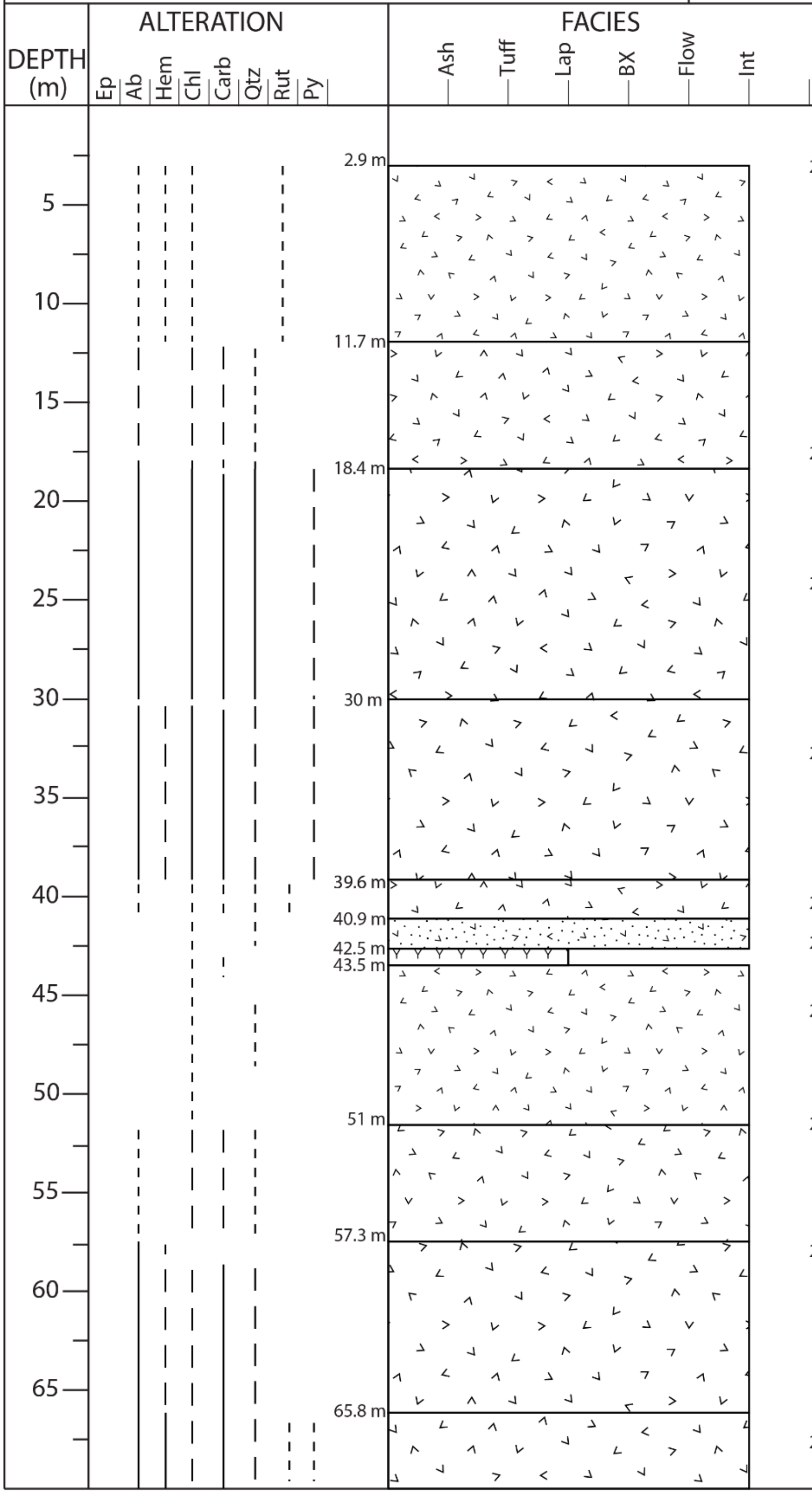

Sample	DESCRIPTION
	OVB
294951	<u>Distal alteration zone</u> dark green gabbro with incipient ab and weak orange-tan rut ovp dark grey-green mg-cg gabbro, with local wk-mod shearing and rut ovp increase towards LC shear-parallel mm-cm scale qt-ank veins
294952	<u>Intermediate alteration zone</u> dark green-pinkish-white (orange on oxidized surfaces) mg-cg shr'd gb locally strongly sheared (well expressed by rut ovp) and strongly magnetic (35.5-40) mg-cg gabbro with ab-chl alteration and ~1-2% dis euh py in WR and vein material common qt-ank-chl-ab cm-scale vns
294953	<u>Proximal alteration zone</u> cg dark green-orange grey gabbro with orange albite <6 mm euhedral-subhedral pyrite cubes (~2%) moderate hematite alteration; porphyritic ab (the same porph, D1-related ab/plag laths seen at AP, e.g. in AP-05-03).
294954	Ore zone dominated by pegmatitic orange-red ab-hem <2% subhedral-anhedral py cubes <20 mm in size
294955	dark green-orange-tan mg-cg sheared banded (chl-ab) gabbro
294956	dark grey-green fine mafic tuff dark grey mafic lapilli tuff
294957	<u>Distal alteration zone</u> dark green-grey fg gabbro with very fine plagioclase laths, wk vfg rut ovp, tr-0.5% dis euh py and wkly sheared and folded intervals minor shear-parallel qt-carb veins
294958	<u>Intermediate alteration zone</u> mod-str strongly sheared dark green-grey gabbro with pale pink ab-ank bands increasing in ab content and intensity downhole
294959	<u>Proximal alteration zone</u> cg tan-coloured sheared ab-ank-hem-qt-ser-chl gabbro shear parallel m-s ser alt
294960	ore zone - pegm ab-hem-qt-fuch-chl-ser, 5% quartz vn

Project: Stog'er Tight
Diamond Drill Hole: BN-14-190
Date: 10-17-2018

Section: 1287.5E

UTM
299223E
5536521N

Azimuth: 206
Dip: -50
Depth: 82 m

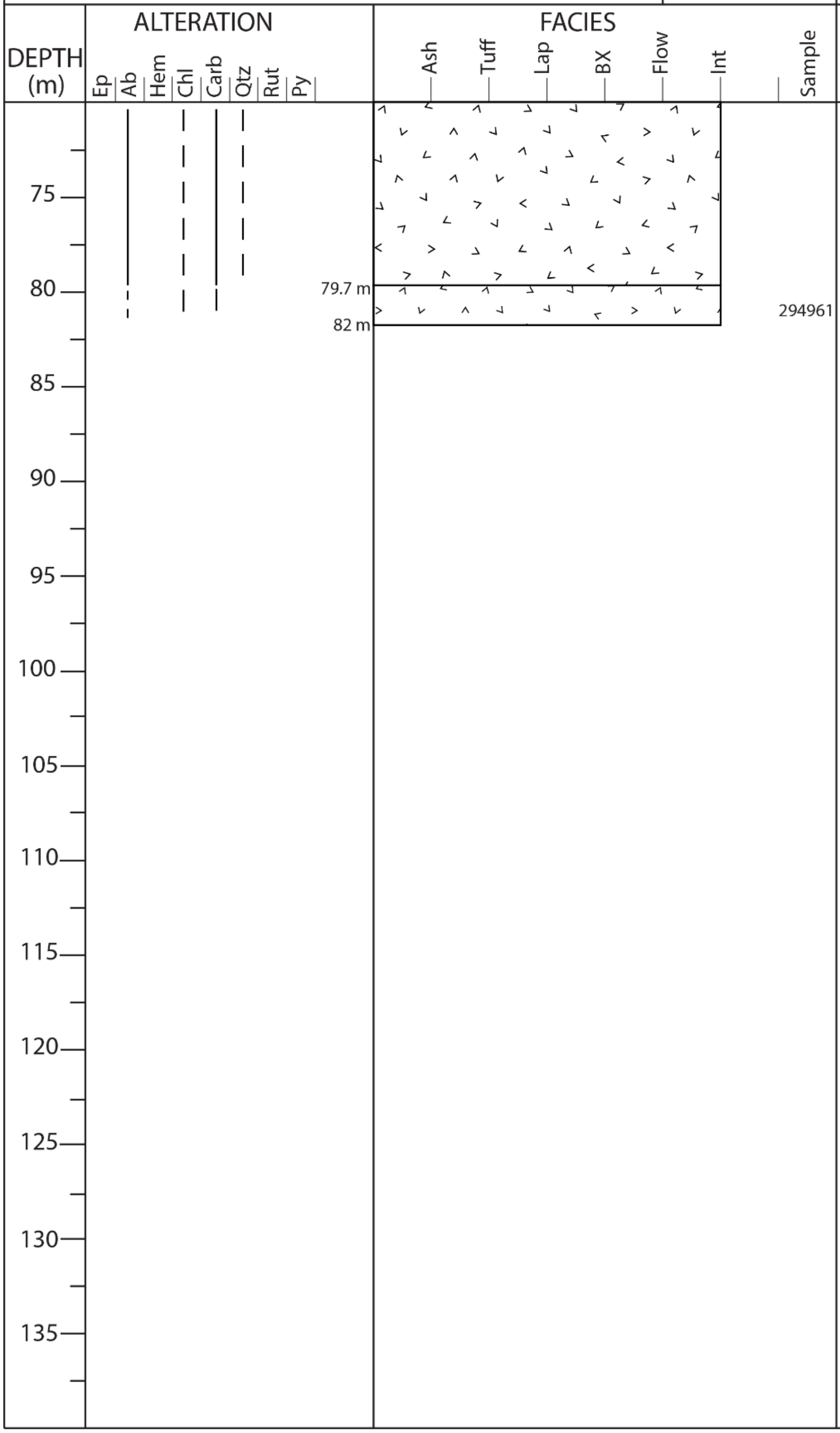

DESCRIPTION

Proximal alteration zone
(cont.)

Intermediate alteration zone
dark-green to pinkish grey (orange oxidised surfaces) gabbro transition to distal; incipient albite and weak ankerite decreasing shearing intensity

Project: Stog'er Tight
Diamond Drill Hole: BN-14-194
Date: 10-17-2018

Section: 1287.5E

UTM
299213E
5536525N

Azimuth: 203
Dip: -60
Depth: 54 m

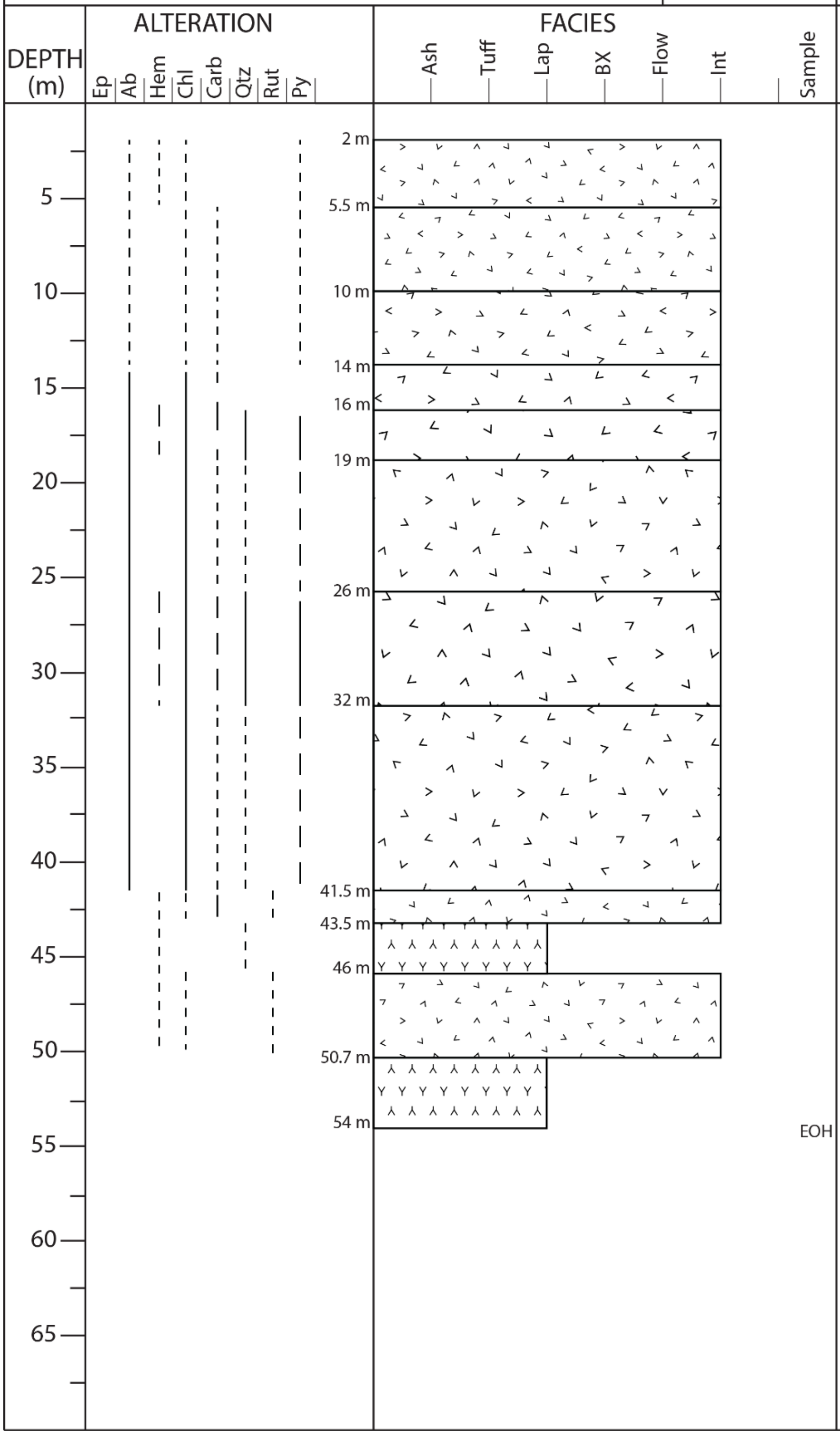

DESCRIPTION

OVB

Distal alteration zone

dark green grey fg gabbro with chl-ab alteration and incipient ab, with increase in mottled ank ovp from 5.5 m minor mm- cm scale qt-ank veins and ff hem

Intermediate alteration zone

fg-mg spotty weakly sheared chloritoids/fuchsite eyes

Proximal alteration zone

black-orange chl-ab sheared gabbro

"zone" -black-pinkish orange cg gabbro with ab-hem rich intervals that are pegm pink/orange-black (more ab-hem-rich)

moderately sheared outside of zones ~2% overall tr dis py anh-euh and py stringers with intervals of ~7% dis py (16-19) and ~10% blebby py (26-29); higher grades correlate with an increase in metasomatism intensity with strong ab-chl and ser alteration faulted LC (~50 cm)

"zone" with a large degree (up to 20%) qt-ank-ab veins

black-orange chl-ab sheared gabbro; locally weakly-moderately sheared; localized folding ~37 m

Intermediate alteration zone

dark grey-green fg-mg similar to 10-14.1 m, shear parallel mm-cm scale qt-ank-chl veinlets

volcaniclastics - ash tuff/mafic dyke

Distal alteration zone

fg gabbro with incipient ab

fresh mafic tuff/lapilli

Project: Stog’er Tight
Diamond Drill Hole: BN-14-195
Date: 10-17-2018

Section: 1300E

UTM
299237E
5536520N

Azimuth: 203
Dip: -55
Depth: 51 m

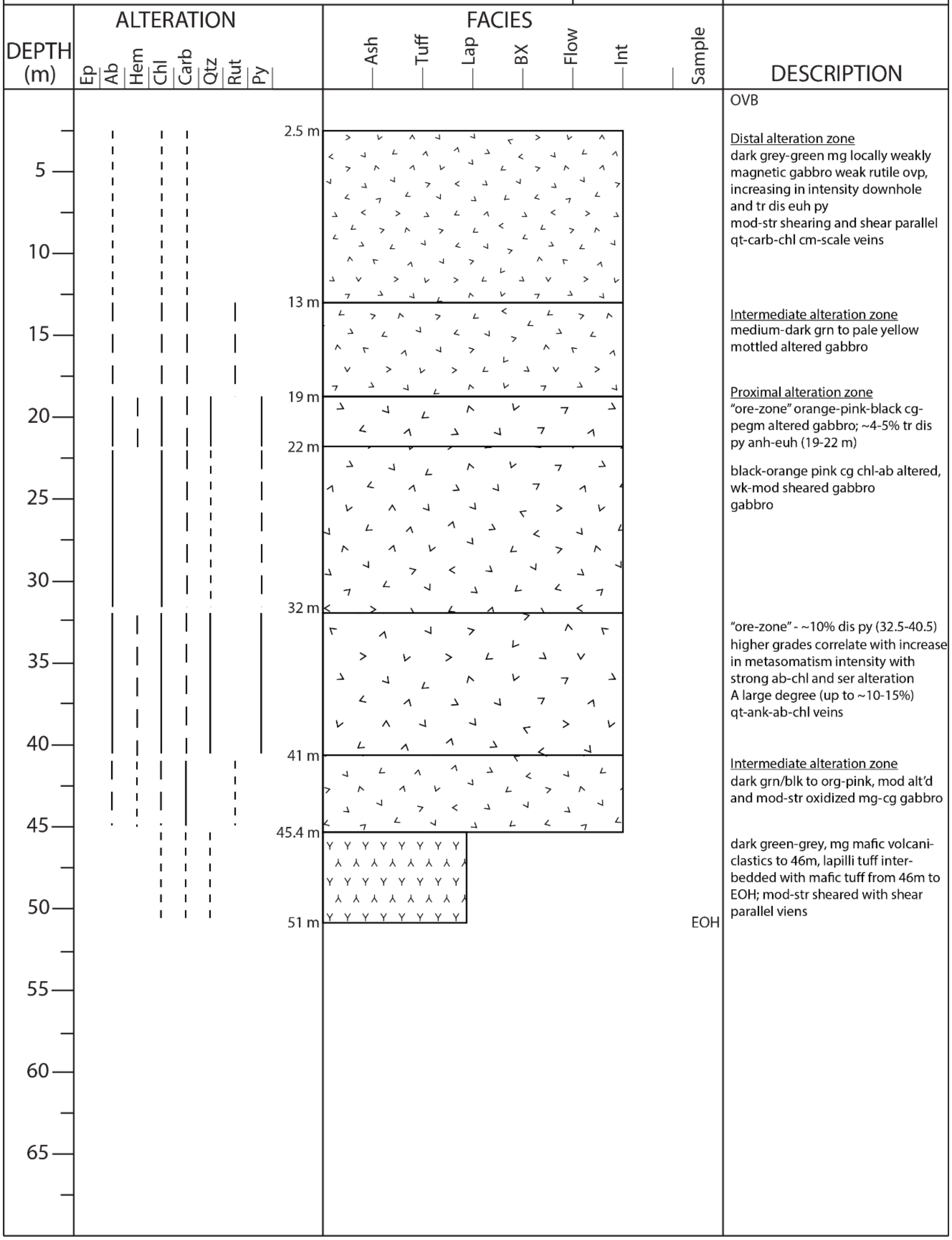

OVB

Distal alteration zone
dark grey-green mg locally weakly magnetic gabbro weak rutile ovp, increasing in intensity downhole and tr dis euh py
mod-str shearing and shear parallel qt-carb-chl cm-scale veins

Intermediate alteration zone
medium-dark grn to pale yellow mottled altered gabbro

Proximal alteration zone
“ore-zone” orange-pink-black cg-pegm altered gabbro; ~4-5% tr dis py anh-euh (19-22 m)

black-orange pink cg chl-ab altered, wk-mod sheared gabbro
gabbro

“ore-zone” - ~10% dis py (32.5-40.5)
higher grades correlate with increase in metasomatism intensity with strong ab-chl and ser alteration
A large degree (up to ~10-15%) qt-ank-ab-chl veins

Intermediate alteration zone
dark grn/blk to org-pink, mod alt’d and mod-str oxidized mg-cg gabbro

dark green-grey, mg mafic volcaniclastics to 46m, lapilli tuff interbedded with mafic tuff from 46m to EOH; mod-str sheared with shear parallel viens

Project: Stog'er Tight
Diamond Drill Hole: BN-14-187
Date: 10-17-2018

Section: 1312.5E

UTM
299250E
5536519N

Azimuth: 206
Dip: -50
Depth: 54.6 m

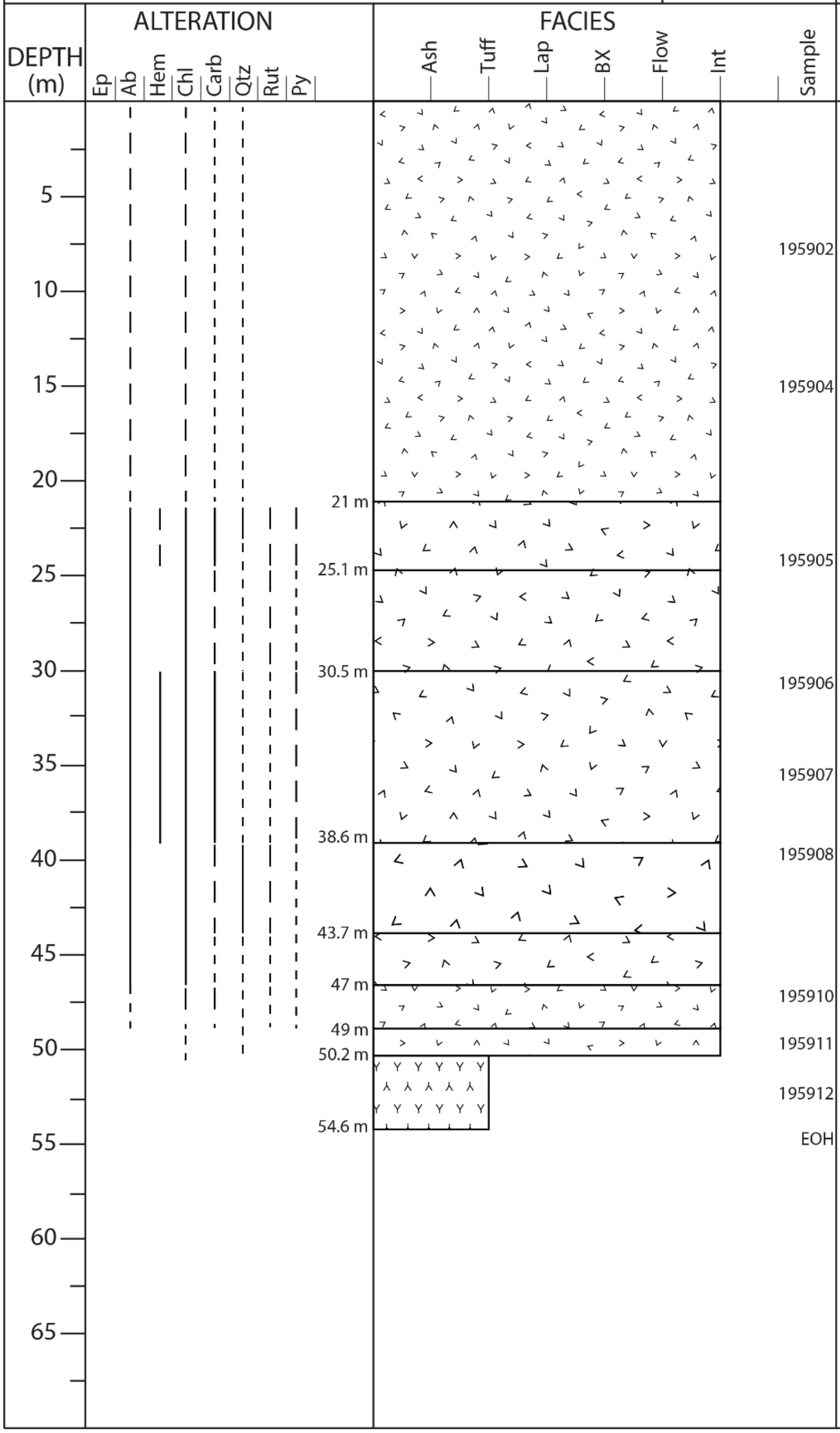

DESCRIPTION

Intermediate alteration zone
mg-fg gabbro, locally where more ank alteration is present and near qt-ank veins, the appearance in spotty (chloritoid eyes)

generally weakly foliated, locally weakly sheared. Shearing intensity increases from 17.5m

Proximal alteration zone
brick red-pegmatitic ab with strong black chl matrix and cg anhedral py "ore-zone"
top 1.5m = 50% qt-ank-late-blk chl veins-qt healed

black-orange (chl-ab) weakly sheared proximal gabbro, non-ore zone

cg with hem-rich zone strong hem veining overprinting black chl-orange ab (cg-pegm) matrix that resembles proximal AP alteration zone with porphyritic laths

resembles proximal alteration zone at AP, overprinted by hem veins

brick red-orange-black pegmatitic ab zone with vcg anhedral py in WR and edges of late black chl veinlets locally moderately sheared and banded where crystal size is smaller

Intermediate alteration zone
dark green/black-orange cg-fg gabbro; ab rapidly decreases in abundance with grain size decrease

Distal alteration zone
dark grey-green fg distal gabbro
unaltered mafic tuff

BN-14-187 - single proximal zone, the lower pale ab-ank-ser proximal alteration zone found in 186 does not exist here - possibly due to lesser degree of brittle deformation in the lower part of the gabbro?

Project: Stog'er Tight
Diamond Drill Hole: BN-14-188
Date: 10-17-2018

Section: 1312.5E

UTM
299245E
5536508N

Azimuth: 206
Dip: -50
Depth: 57.3 m

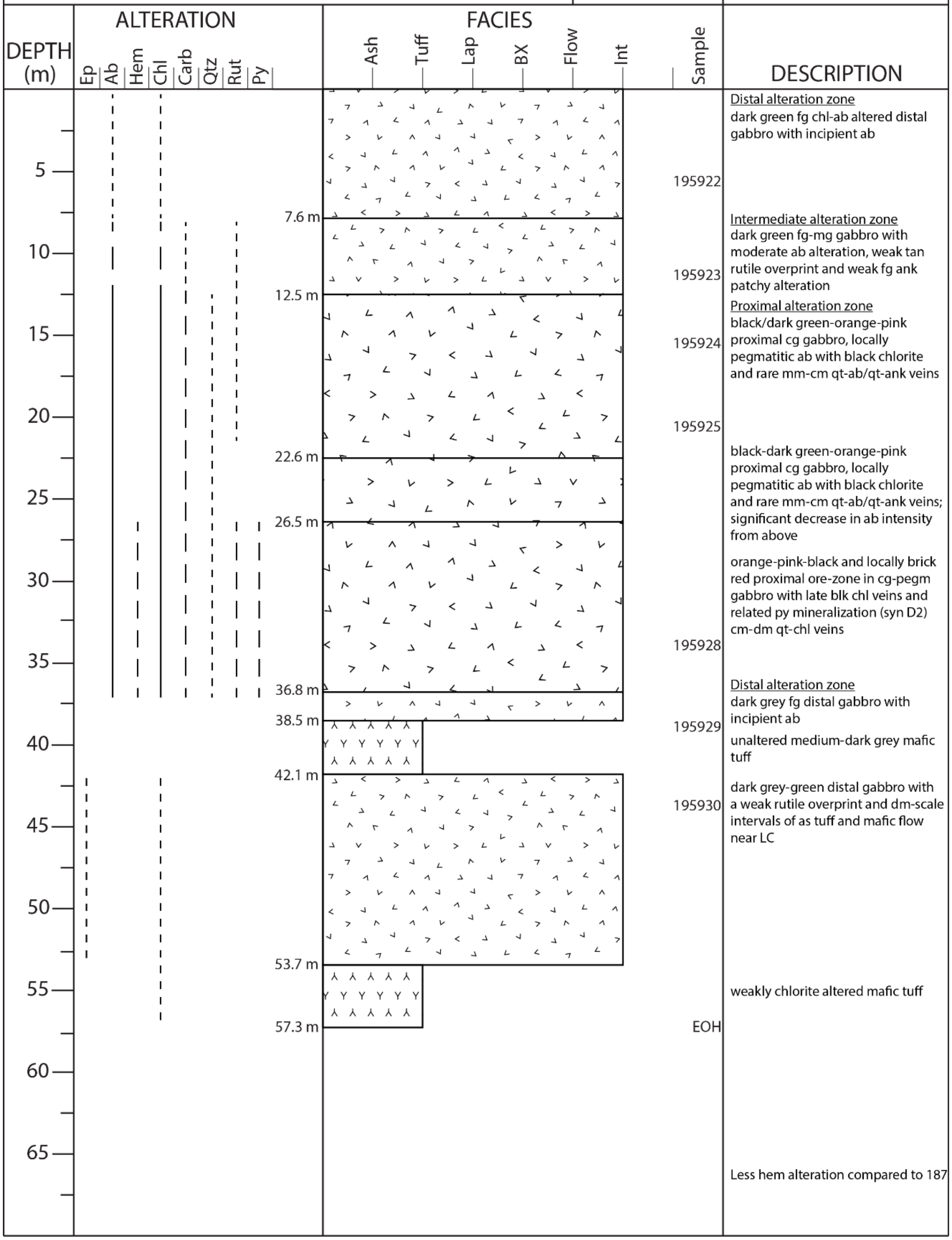

Distal alteration zone
dark green fg chl-ab altered distal gabbro with incipient ab

Intermediate alteration zone
dark green fg-mg gabbro with moderate ab alteration, weak tan rutile overprint and weak fg ank patchy alteration

Proximal alteration zone
black/dark green-orange-pink proximal cg gabbro, locally pegmatitic ab with black chlorite and rare mm-cm qt-ab/qt-ank veins

black-dark green-orange-pink proximal cg gabbro, locally pegmatitic ab with black chlorite and rare mm-cm qt-ab/qt-ank veins; significant decrease in ab intensity from above

orange-pink-black and locally brick red proximal ore-zone in cg-pegm gabbro with late blk chl veins and related py mineralization (syn D2) cm-dm qt-chl veins

Distal alteration zone
dark grey fg distal gabbro with incipient ab

unaltered medium-dark grey mafic tuff

dark grey-green distal gabbro with a weak rutile overprint and dm-scale intervals of as tuff and mafic flow near LC

weakly chlorite altered mafic tuff

Less hem alteration compared to 187

Project: Stog’er Tight
Diamond Drill Hole: BN-14-189
Date: 10-17-2018

Section: 1312.5E

UTM
299239E
5536497N

Azimuth: 206

Dip: -50

Depth: 44.5 m

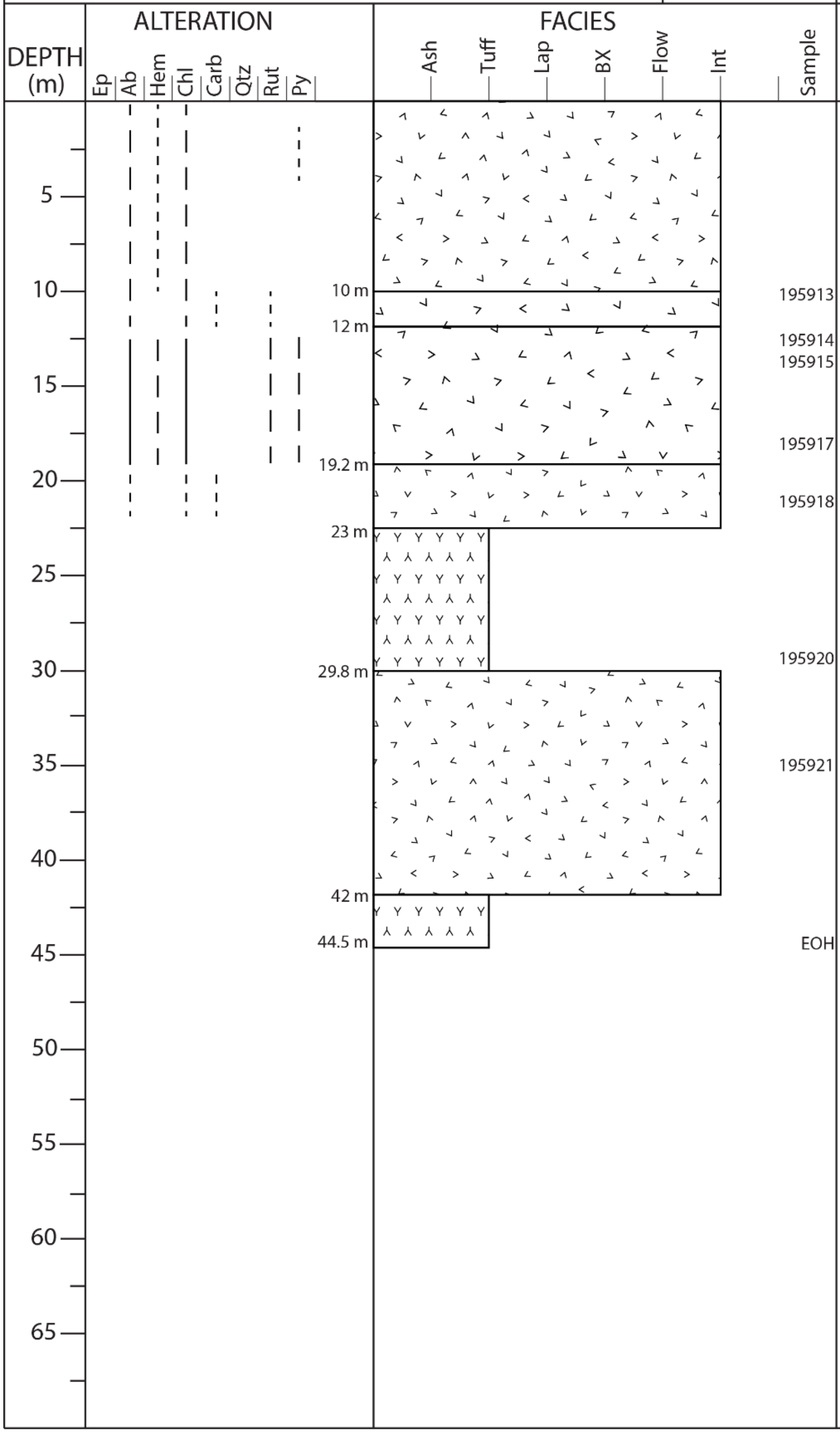

DESCRIPTION

Intermediate alteration zone
sheared mg with some porphyritic (pegm) orange pink ab

Proximal alteration zone
orange-pink-black/dark green cg to locally pegmatitic gabbro (with a red-brick ab-hem interval at 19-19.3) top 2m show well-formed porphyritic laths***

Distal alteration zone
fg-mg gabbro with locally cg ab, weak foliated rutile overprint

matrix-supported matrix lapilli tuff

unaltered dark grey fg-mg diabase

dark grey fg tuff, similar to above diabase

No zone, only small ~30cm section of ab-hem (19-19.3)

***exactly like those found in the proximal zone of Animal Pond; proximal zone = D1 alteration precursor

Later hydrothermal event (syn D2) used these, likely due to their mineralogic properites (mt-bearing, cg)

Some moderate shearing in the form of chl-ab banding in less coarse sections; cm-scale qt-carb veins and possibly healed faults

BN-14-187 - single proximal zone, the lower pale ab-ank-ser proximal alteration zone found in 186 does not exist here - possibly due to lesser degree of brittle deformation in the lower part of the gabbro?

Project: Stog'er Tight
Diamond Drill Hole: BN-14-202
Date: 10-15-2018

Section: 1487.5E

UTM
299405E
5536460N

Azimuth: 000
Dip: -90
Depth: 76 m

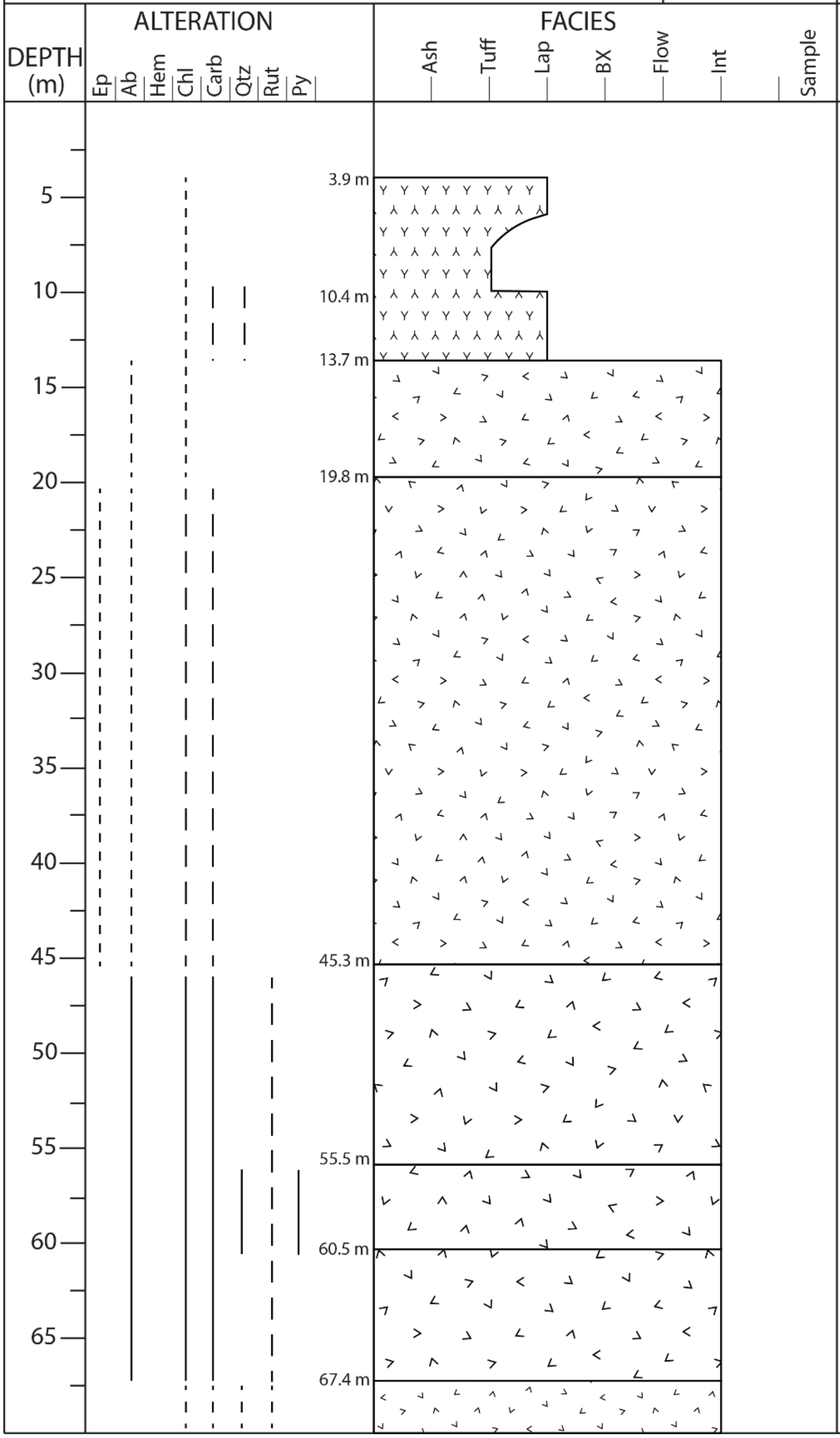

DESCRIPTION

OVB

sheared and locally strongly folded dark grey fg mafic volcanics with some porphyritic plag laths
weak-mod shr TOH-9m; str shr 9-13.7
More intensely sheared section is mod-str oxidized with minor qt-carb vnlets, mostly shear-parallel

Distal alteration zone
dark green-grey mg-cg, locally sheared gabbro with incipient ab cm-scale qt-carb and qt-carb-chl vns

Intermediate alteration zone
mg-cg spotty pale-dark grn gabbro with chlorotoid eyes

vcg from 40 m

Proximal alteration zone
altered gabbro with mod chl-ab intensity increases downhole expressed by increase in ab and qt-ank-chl-ab veining generally ~0.5-1% euh py throughout the unit, with ~15% dis and blebby py (55-55.8) constrained to a highly metasomatized ab-ser alteration

"ore-zone" - ab is cg to locally pegm with blk chl vnlets and cg py grains 55.5-60.5 - ~50% veins, although the ore-zone does not look strongly silicified, although the alteration minerals associated with strong qt-chl-ab veining

dm-m scale qt-carb(+/-chl-ab) veins make up ~10% of total volume locally moderately sheared

Distal alteration zone
distal dark grn-grey fg w/ vfg rut ovp and calc + qt-carb veins/veinlets

Project: Stog'er Tight
Diamond Drill Hole: BN-14-202
Date: 10-15-2018

Section: 1487.5E

UTM
299405E
5536460N

Azimuth: 000

Dip: -90

Depth: 76 m

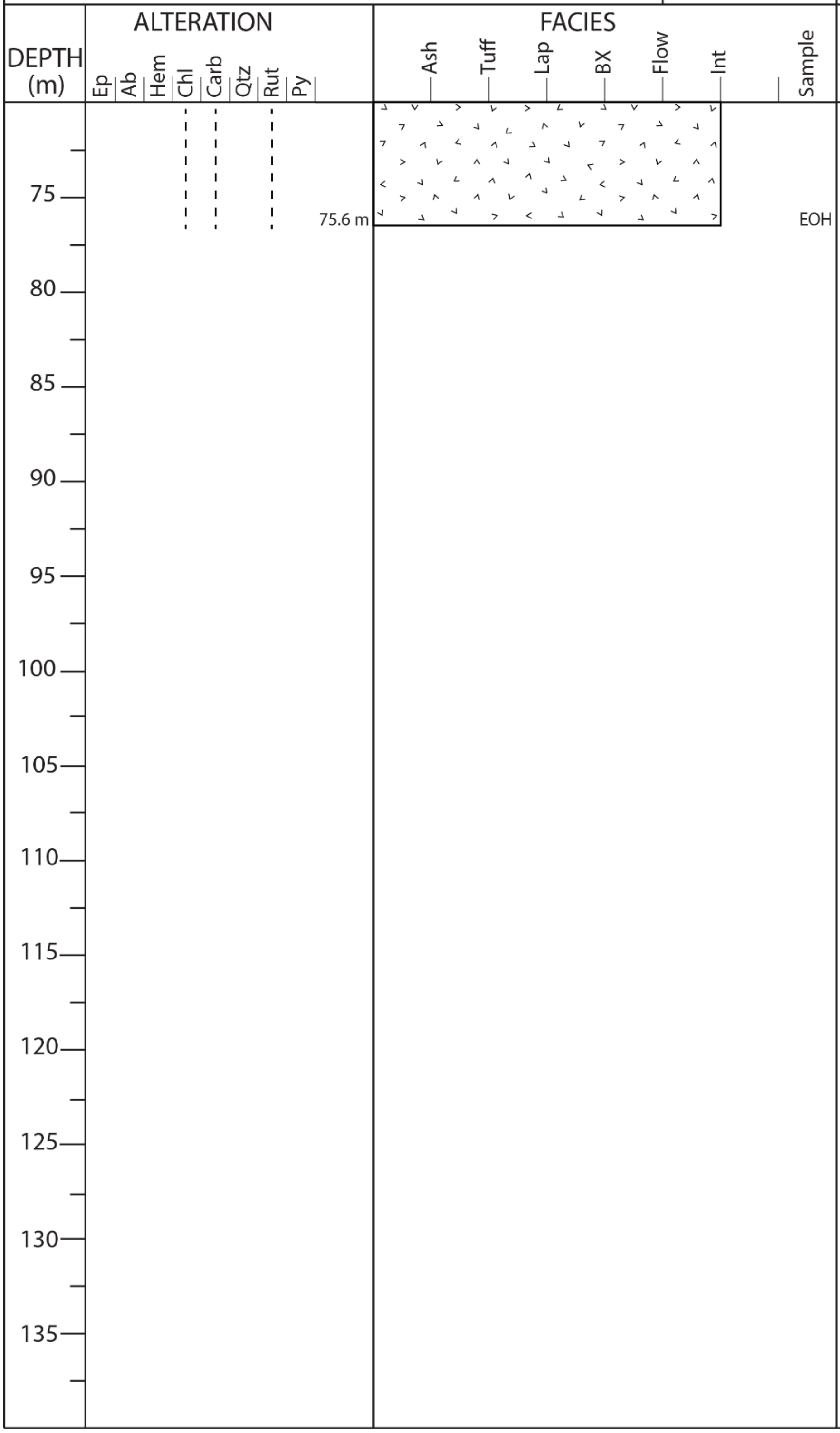

DESCRIPTION

<u>Distal alteration zone</u>
same as in the previous diagram

Proximal zone (45.5-67.4 m) shows very little shearing and is more akin to Argyle than typical Stog'er Tight core (e.g. no regular chl-ab bands)

Project: Stog’er Tight
Diamond Drill Hole: BN-14-203
Date: 10-15-2018

Section: 1487.5E

UTM
299404E
5536460N

Azimuth: 203
Dip: -60
Depth: 58 m

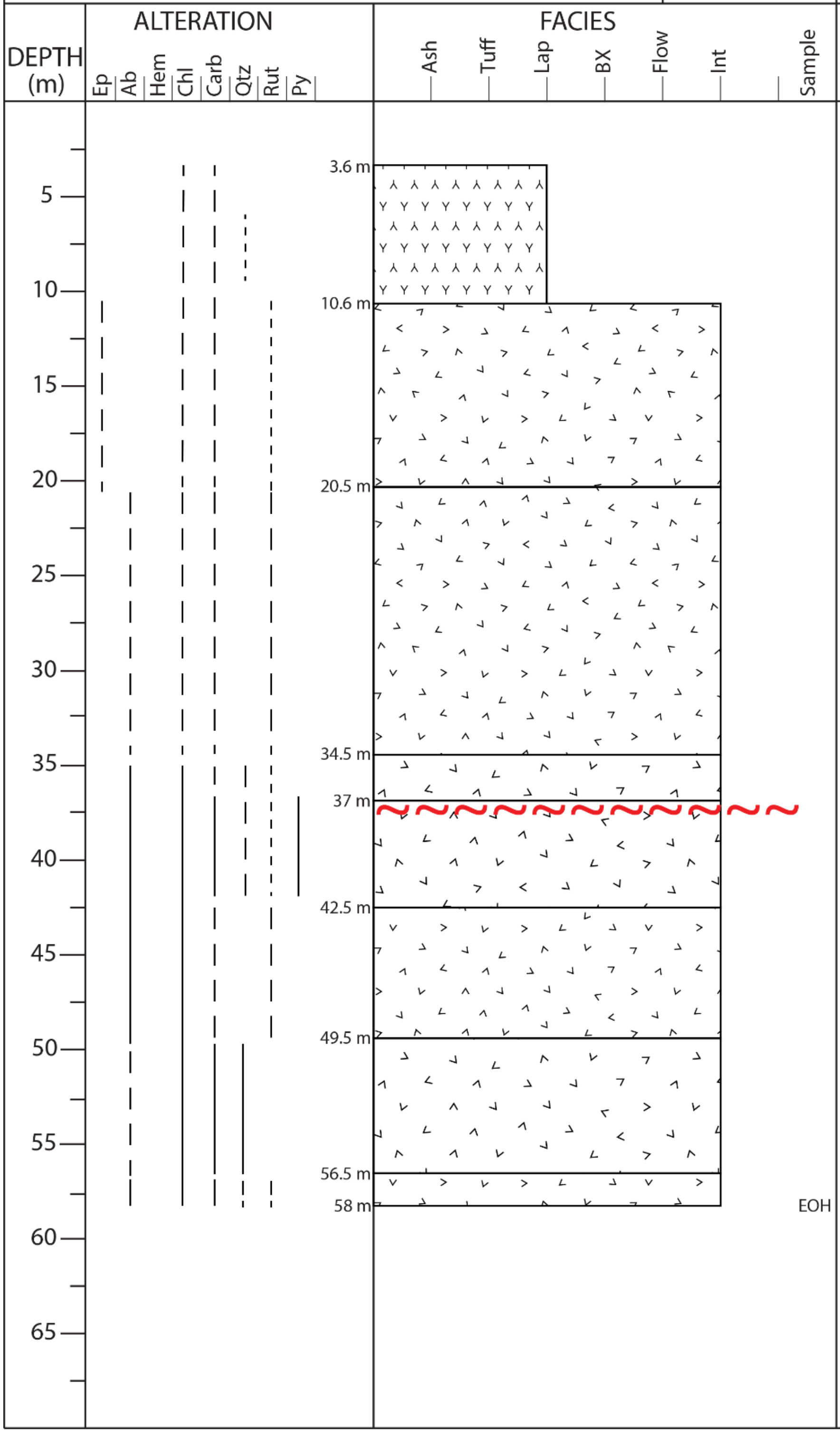

DESCRIPTION

OVB

dark grey, fg strongly sheared and folded mod oxidized mafic tuff with mm-cm qt-carb vn-vnlts

Intermediate alteration zone
dark green, mg-cg gabbro with weak ep-chl-rut-ab alt and tr dis euh py, locally strongly magnetic (23-29.5)

dark green-pale pink mg-cg spotty gabbro with a mg-cg rut ovp

mg from 29.5 m

Proximal alteration zone
cg dark green chl-ab altered gabbro with porphyritic ab; ~6-8% dis and blebby py between 37.5-41, avg ~1% dis py throughout
cm-scale qt-carb-ab-chl cm-scale veins make up 15% of total volume.
minor FLT between 37.45-37.6, very little gouge and locally brecciated

37-42.5 m “ore zone”; ab-dominated pegmatitic gabbro with cg sooty py

mg-fg mod-str sheared banded (chl-ab) gabbro with 0.5-1% tr euh py with apparent FLD (44, 53.2-53.8) cm-scale qt-carb-chl shear-parallel veins

heavily oxidized and locally strongly sericitized proximal altered gabbro with ~30% qt-ank veins and blk chl veinlets; healed qt

decrease in fabric intensity, similar to 42.5-49.5m interval

Project: Stog’er Tight
Diamond Drill Hole: BN-14-204
Date: 10-15-2018

Section: 1487.5E

UTM
299403E
5536424N

Azimuth: 208
Dip: -60
Depth: 75 m

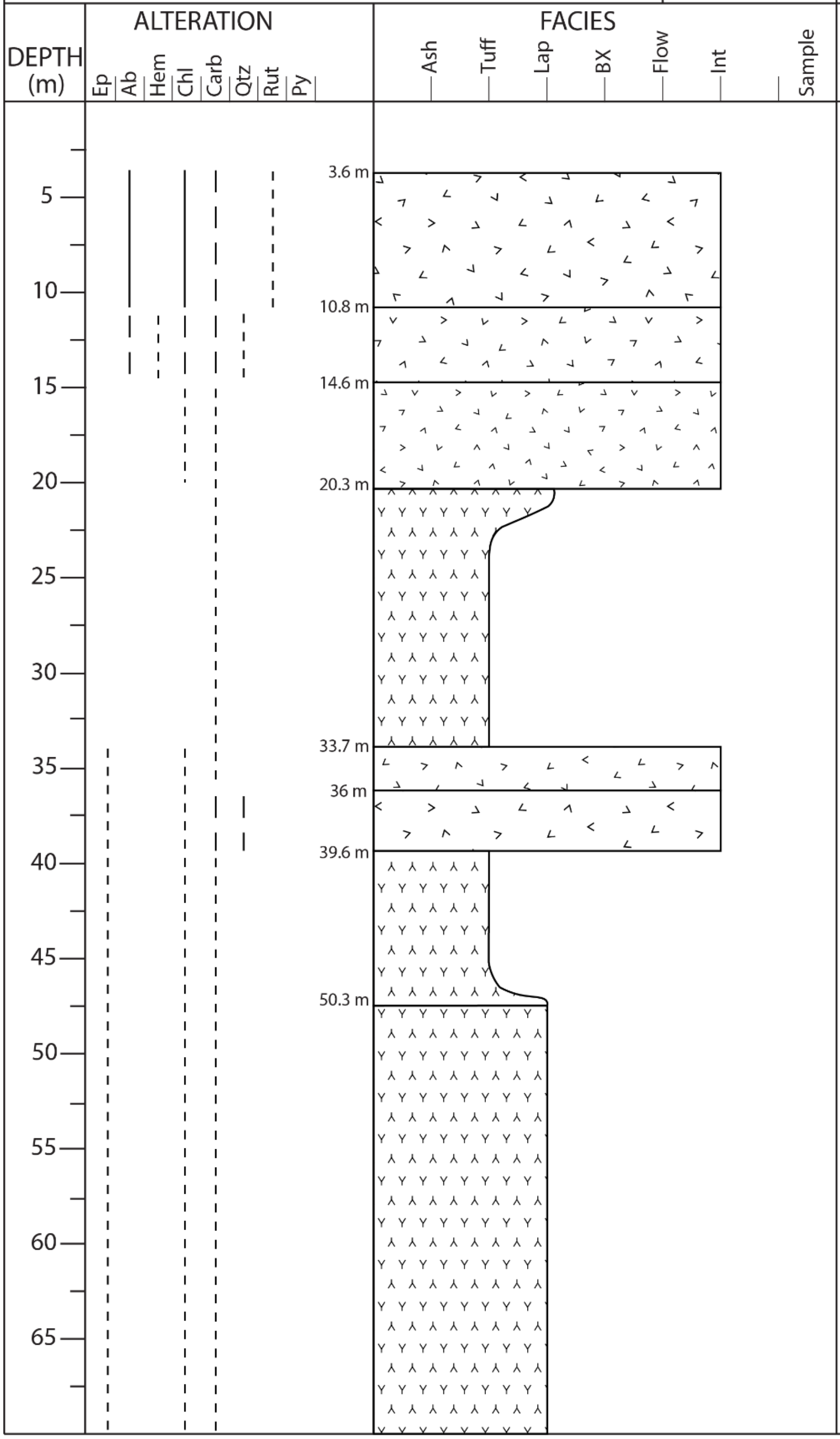

DESCRIPTION

OVB

Proximal alteration zone
mg-cg altered gabbro with strong chl-ab-rut alteration and ~1% euh dis py, locally moderately sheared with mm-scale qt-carb(+/-chl-ab) veinlets

Intermediate alteration zone
dark grey-green to pale grn/yellow moderately sheared and folded gabbro
locally strongly magnetic (9.5-14)
minor FRC/FLT zone (~26)

Distal alteration zone
fg dark grn-grey gabbro

shear parallel qt-carb and ep veinlets

mafic tuff with lapilli at UC; well-foliated

Distal alteration zone
dark green, mg, massive gabbro with a sheared UC (cm-scale); strongly magnetic; qt-carb-chl and hem vnlets common

Intermediate alteration zone
dark grn-pale grn/yellow cg spotty gabbro

dark grey-green mafic tuff with locally mod-str sheared and folded with ep-chl alt
qt-carb shear parallel veins-veinlets, hem ff vnlets and ep vnlets near UC

dark grey-green strongly sheared and folded lapilli tuff with multiple folds in the unit and a short faulted interval (62.5), grades into mafic tuff below; primary volcanogenic alt short qt-carb-chl shear parallel vnlts

Project: Stog’er Tight
Diamond Drill Hole: BN-14-204
Date: 10-15-2018

Section: 1487.5E

UTM
299403E
5536424N

Azimuth: 208
Dip: -60
Depth: 75 m

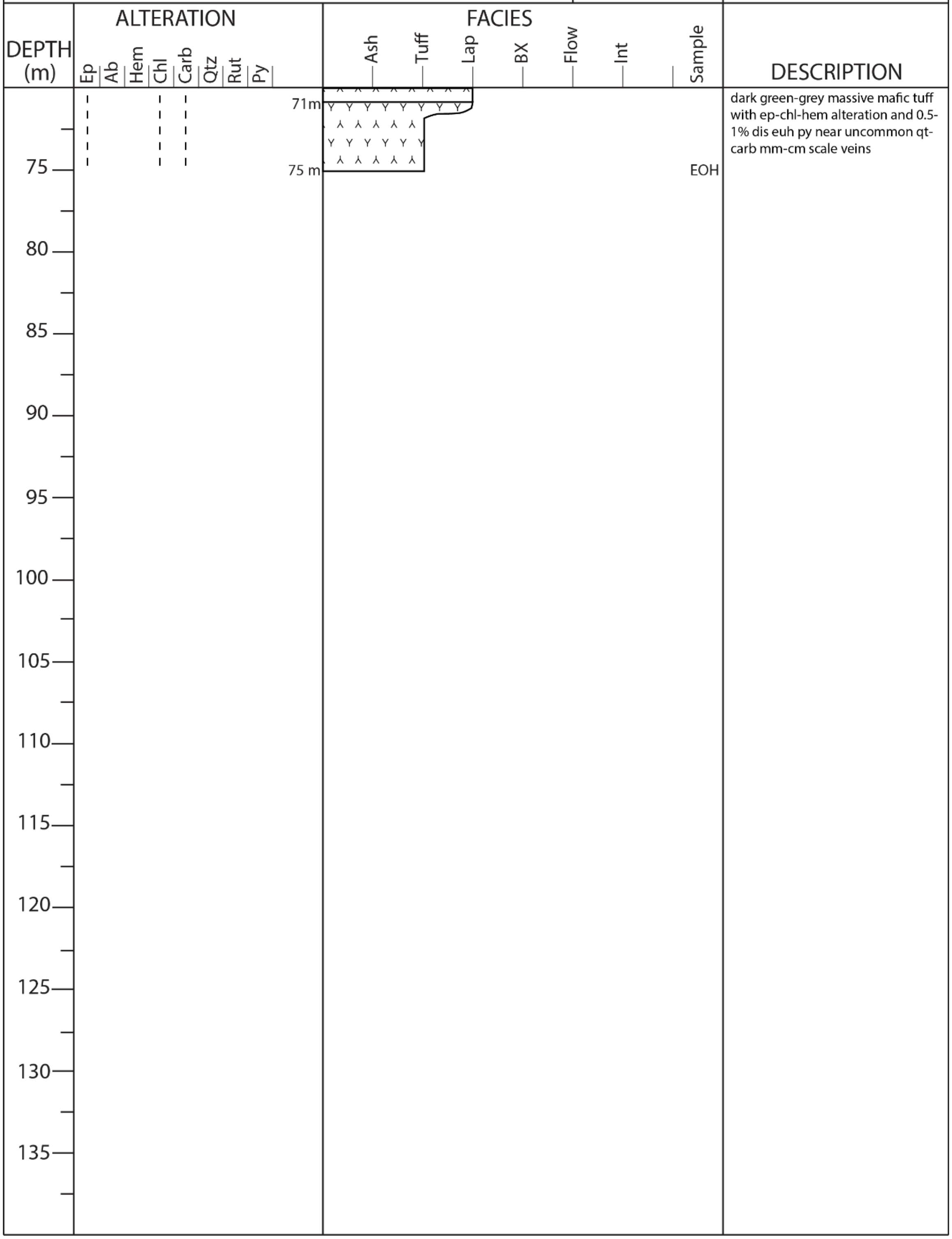

dark green-grey massive mafic tuff with ep-chl-hem alteration and 0.5-1% dis euh py near uncommon qt-carb mm-cm scale veins

Project: Stog’er Tight
Diamond Drill Hole: BN-14-205
Date: 10-15-2018

Section: 1487.5E

UTM
299415E
5536478N

Azimuth: 208
Dip: -75
Depth: 89 m

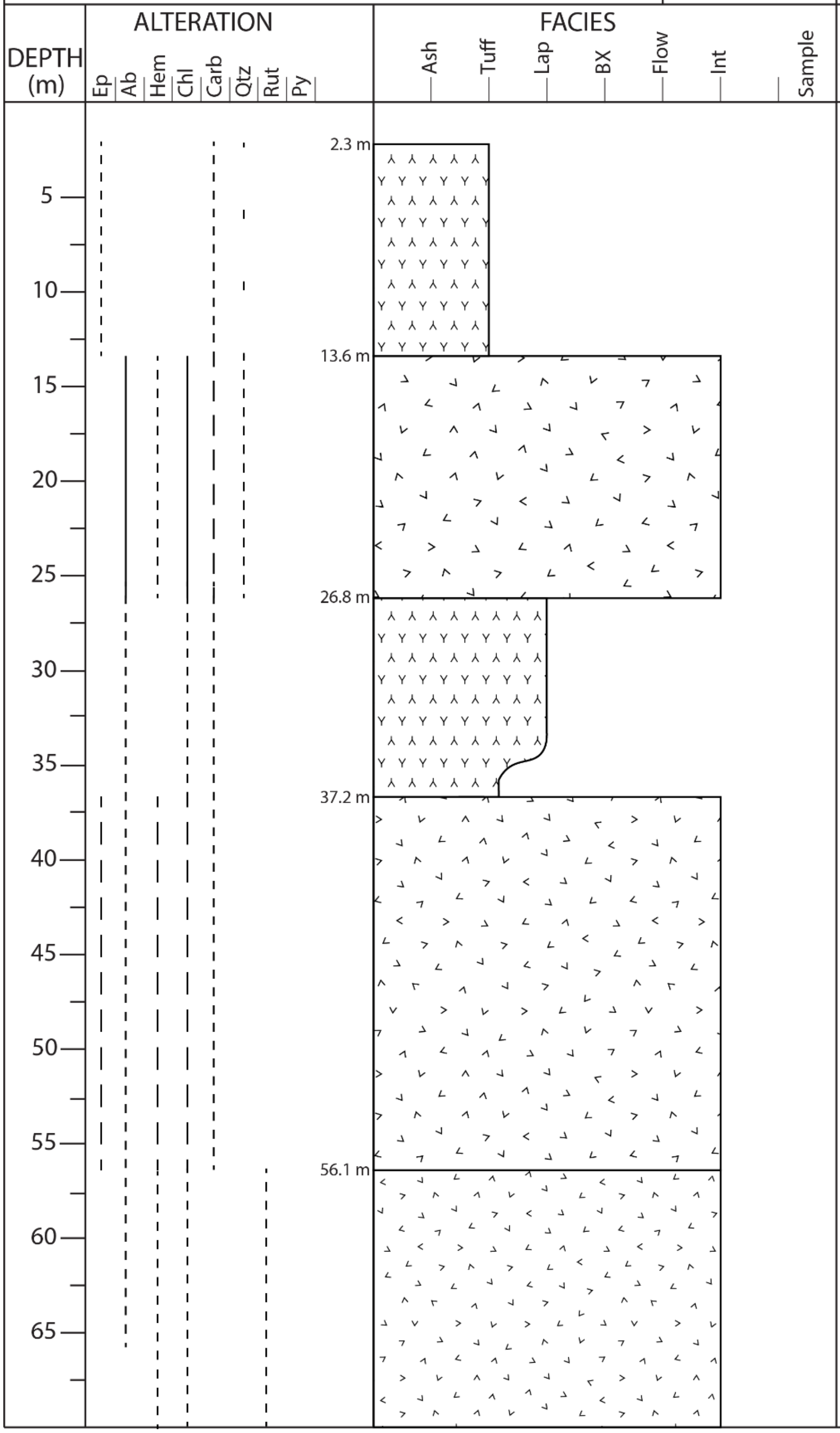

DESCRIPTION

OVB

dark greenish-grey mod-str sheared and folded mafic tuff with lapilli tuff intervals with primary volcanogenic alteration
mm-cm qt-carb veins

Proximal alteration zone
cg strongly banded chl-ab proximal gabbro

medium grey-green, fg-mg str sheared and locally folded mod chl-ab-ser altered gabbro with tr-0.5% dis euh py

cm-scale qt-carb and qt-carb-chl-ab veins

dark greenish-grey mod-str sheared and folded mafic lapilli tuff with phyric plag laths and tuffaceous intervals, tr dis euh py
weakly oxidized to 30.5 m
mm-cm qt-carb veins, increase near LC

Intermediate alteration zone
spotty medium grey-green mg chl-ep-hem intermediately altered gabbro with short sheared intervals and tr-0.5% dis and blebby dis py; locally weakly foliated
minor qt-carb and ff hem vnlts

Distal alteration zone
fg gabbro with incipient fg ab and vfg rut ovp, inor calc and qt-carb veinlets

57.8-59 m - 60% qt-ank-chl-ab veins, no significant change in alt assm

Project: Stog’er Tight
Diamond Drill Hole: BN-14-205
Date: 10-15-2018

Section: 1487.5E

UTM
299415E
5536478N

Azimuth: 208
Dip: -75
Depth: 89 m

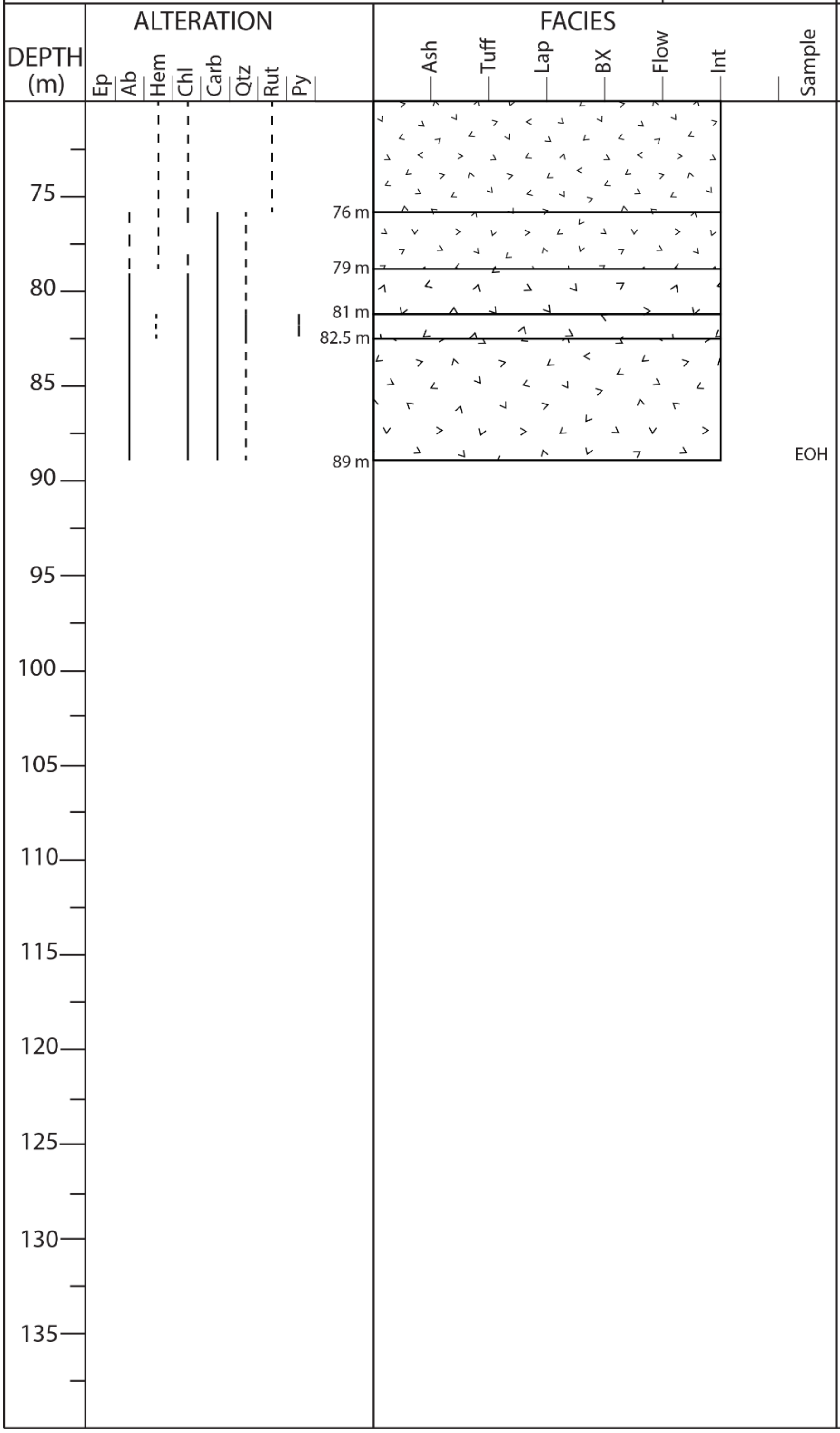

DESCRIPTION

dark green-grey, fg massive weakly chl-ep altered gabbro with rut and porphyritic plag (ab-alt) crystals to ~66m with ff hem veinlets and qt-ank-chl-ab veins (~5%)

Intermediate alteration zone
spotty (lesser degree than Argyle) fg-mg drk-med grn gabbro with pale grn/ylw porph ab

Proximal alteration zone
strongly sheared similar to upper prox zone
81-82.5 m - “ore” zone - intensely sheared

the lower proximal zone is generally a mg-cg strongly ab-chl altered and moderately sheared gabbro with porphyritic plag (ab-alt) crystals (from 84m).

~1-2% dis py throughout the unit and moderately sheared

qt-carb-chl-ab veins common

Both proximal zones show similar alteration mineral assemblages.

The upper zone is less intensely sheared.

An ore-zone with pegmatitic ab and cg py grains only exists in the lower proximal zone.

The lower zone with cg py is cross-cut by more qt veins with ank at WR margins.

The py is hosted mostly either within vein material or at the vein-WR front.

ST gabbro is much more strongly and consistently sheared than Argyle gabbro

The ab-chl mm-cm scale bands are consistently present for ~20 m in this hole.

At Argyle the zones where ab is sheared are significantly less extensive (<1 m) and where present are typically well outlined by mg-cg rutile overprint in the sheared zones, which are not present in this hole.

Appendix B: Cross-sections

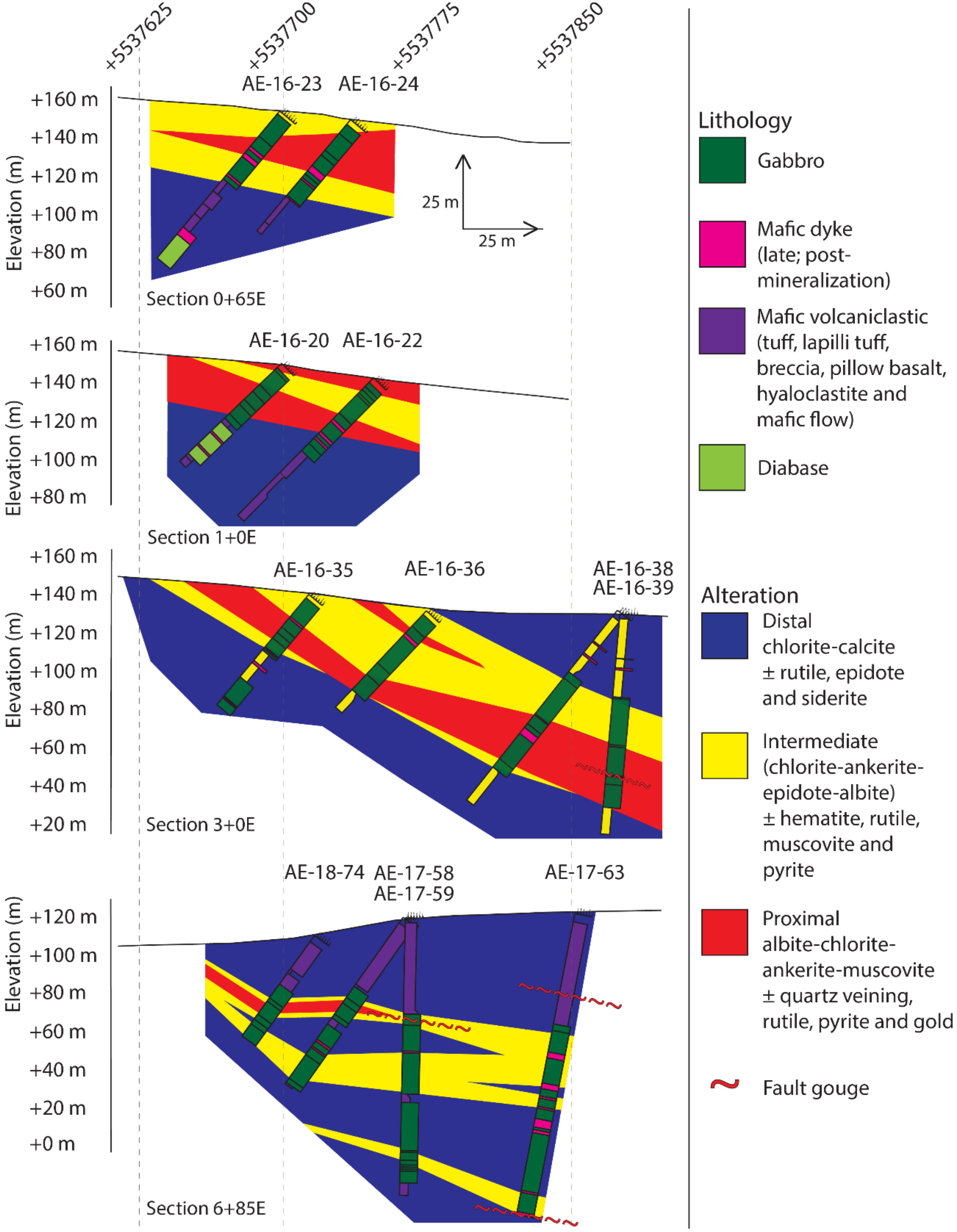

Appendix B.1.1. Cross-sections through the Argyle deposit not used in Chapter 2. All sections facing west.

Appendix C: Whole Rock Geochemistry and Terraspec Data

Table C.1.1. Whole Rock Geochemistry and Terraspec™ Data for Argyle Samples

Sample ID		150420	150421	150422	150423	150424
Hole ID		AE-16-14	AE-16-14	AE-16-14	AE-16-14	AE-16-14
Depth (m)		6.9	16.36	20.44	26.76	34.62
Lithology		Gabbro	Gabbro	Gabbro	Gabbro	Gabbro
Alteration Assemblage		Ep-Ab	Rut-Chl-Py-Ab	Rut-Chl-Qt	Rut-Chl	Rut-Chl-Ab
Alteration		Intermediate	Intermediate	Proximal	Intermediate	Intermediate
SiO_2	*%*	46.90	41.40	42.60	46.60	48.50
Al_2O_3		17.30	14.80	14.50	13.15	13.70
Fe_2O_3		11.50	10.40	9.79	11.35	11.90
CaO		7.92	8.69	8.31	7.04	6.81
MgO		7.20	4.83	4.46	3.35	2.69
Na_2O		3.38	3.50	4.70	4.92	4.69
K_2O		0.06	0.96	0.57	0.18	0.43
Cr_2O_3		0.03	0.01	0.01	<0.01	<0.01
TiO_2		2.15	2.03	1.96	2.75	2.20
MnO		0.15	0.14	0.15	0.22	0.26
P_2O_5		0.24	0.24	0.24	0.66	0.74
SrO		0.03	0.02	0.03	0.02	0.02
BaO		<0.01	0.01	0.01	<0.01	<0.01
LOI		4.34	12.00	12.30	10.15	9.45
Total		101.20	99.03	99.63	100.39	101.39
C		0.18	2.63	2.90	2.40	2.23
S		0.01	0.01	0.01	0.01	0.01
Ba	*ppm*	29.20	69.40	79.90	39.00	43.00
Ce		27.20	23.00	25.50	54.40	67.80
Cr		230.00	80.00	40.00	10.00	10.00
Cs		0.08	0.28	0.15	0.07	0.17
Dy		4.99	4.19	4.50	9.18	10.10
Er		2.74	2.26	2.55	5.11	5.66
Eu		1.78	1.61	1.76	3.07	3.66
Ga		19.10	18.30	18.10	21.60	27.50
Gd		5.18	4.79	5.10	10.85	12.15
Ge		<5	<5	<5	<5	<5
Hf		3.70	3.20	3.50	7.30	8.50
Ho		1.02	0.90	0.93	1.92	2.17
La		10.40	8.80	9.60	21.00	26.50
Lu		0.32	0.29	0.33	0.59	0.71
Nb		9.70	8.60	9.40	20.30	24.30
Nd		18.40	16.20	17.50	37.60	45.60
Pr		4.03	3.32	3.66	7.74	9.78
Rb		1.00	15.10	9.00	2.70	6.90
Sm		5.16	4.09	4.40	9.91	11.95
Sn		2.00	1.00	1.00	4.00	2.00
Sr		220.00	187.50	247.00	199.50	155.50
Ta		0.60	0.50	0.60	1.30	1.60
Tb		0.81	0.77	0.76	1.59	1.79
Th		0.72	0.54	0.62	1.37	1.64
Tm		0.37	0.32	0.34	0.73	0.80
U		0.28	0.25	0.26	0.59	0.69
V		285.00	273.00	258.00	195.00	128.00
W		1.00	1.00	1.00	3.00	13.00
Y		24.20	21.10	23.10	46.10	53.50
Yb		2.34	2.07	2.08	4.55	5.40
Zr		171.00	144.00	162.00	338.00	404.00
As		3.20	1.70	1.00	1.40	2.00
Bi		0.01	0.02	0.02	0.04	0.03
Hg		<0.005	<0.005	<0.005	<0.005	<0.005
In		0.01	0.05	0.06	0.09	0.10

Abbreviations:

D = depth

WL = wavelength

Units:

MD = mafic dyke

MBX = mafic breccia

MT = mafic tuff

MLT = mafic lapilli tuff

Table C.1.1. Whole Rock Geochemistry and Terraspec™ Data for Argyle Samples

Sample ID		150420	150421	150422	150423	150424
Hole ID		AE-16-14	AE-16-14	AE-16-14	AE-16-14	AE-16-14
Depth (m)		6.9	16.36	20.44	26.76	34.62
Lithology		Gabbro	Gabbro	Gabbro	Gabbro	Gabbro
Alteration Assemblage		Ep-Ab	Rut-Chl-Py-Ab	Rut-Chl-Qt	Rut-Chl	Rut-Chl-Ab
Alteration		Intermediate	Intermediate	Proximal	Intermediate	Intermediate
Re		<0.001	<0.001	0.00	<0.001	<0.001
Sb		0.50	0.10	0.10	0.12	0.25
Se		<0.2	0.30	0.20	0.30	<0.2
Te		0.01	0.01	0.02	0.02	<0.01
Tl		<0.02	<0.02	<0.02	<0.02	<0.02
Ag		<0.5	<0.5	<0.5	<0.5	<0.5
Cd		<0.5	<0.5	<0.5	<0.5	<0.5
Co		47	37	32	29	21
Cu		26	11	9	5	3
Li		20	30	20	20	10
Mo		<1	<1	<1	<1	<1
Ni		69	31	26	2	1
Pb		<2	<2	<2	6	2
Sc		31	31	28	20	14
Zn		73	47	50	68	78
Au		0.00	0.00	0.00	0.00	0.09
C	*%*	0.16	2.50	2.44	2.24	2.04
CO_2		0.60	9.20	9.00	8.20	7.50
AlOH WL	*nm*	-	2200.17	2201.40	-	2199.19
AlOH D		-	0.09	0.14	-	0.17
FeOH WL		2253.52	2257.03	2255.75	2257.83	2240.99
FeOH D		0.16	0.11	0.20	0.14	0.08
AlOH D/FeOH D		-	0.80	0.71	-	2.19

Abbreviations:
D = depth
WL = wavelength

Units:
MD = mafic dyke
MBX = mafic breccia
MT = mafic tuff
MLT = mafic lapilli tuff

Table C.1.1. Whole Rock Geochemistry and Terraspec™ Data for Argyle Samples

Sample ID		150425	150426	150427	150428	150429
Hole ID		AE-16-14	AE-16-14	AE-16-14	AE-16-14	AE-16-14
Depth (m)		38.47	43.35	52.76	60.28	69.72
Lithology		Gabbro	Gabbro	Gabbro	Gabbro	MD
Alteration Assemblage		Ank-Ab-Chl-Py	Ab-Py-Rut	Ep-Ab-Chl	Ep	-
Alteration		Proximal	Intermediate	Proximal	Distal	Distal
SiO_2	*%*	43.60	42.10	45.30	44.40	44.20
Al_2O_3		12.10	12.25	16.00	16.05	15.20
Fe_2O_3		12.85	12.60	12.05	11.10	14.00
CaO		7.39	8.12	11.35	10.15	10.90
MgO		3.56	3.58	5.85	6.51	5.06
Na_2O		3.94	4.58	2.30	2.82	2.80
K_2O		0.21	0.09	0.06	0.11	0.29
Cr_2O_3		<0.01	<0.01	0.01	0.03	<0.01
TiO_2		3.72	3.31	2.18	1.98	3.14
MnO		0.25	0.22	0.16	0.15	0.20
P_2O_5		0.45	0.47	0.25	0.20	0.52
SrO		0.02	0.02	0.05	0.04	0.06
BaO		<0.01	<0.01	<0.01	<0.01	0.01
LOI		11.55	12.20	4.24	5.87	2.89
Total		99.64	99.54	99.80	99.41	99.27
C		2.78	3.09	0.28	0.68	0.07
S		0.01	0.01	0.01	0.01	0.14
Ba	*ppm*	38.90	26.60	22.20	28.90	50.00
Ce		47.00	46.30	21.00	21.50	48.40
Cr		<10	<10	70.00	240.00	30.00
Cs		0.06	0.04	0.03	0.04	0.05
Dy		8.48	7.45	4.08	3.98	6.29
Er		4.40	4.11	2.16	2.32	3.59
Eu		2.81	2.69	1.49	1.50	2.60
Ga		21.30	22.30	20.10	19.20	26.10
Gd		8.79	8.83	4.68	4.51	7.38
Ge		<5	<5	<5	<5	<5
Hf		7.00	6.00	2.80	3.20	5.90
Ho		1.70	1.53	0.85	0.87	1.30
La		18.10	18.10	7.80	8.30	20.10
Lu		0.58	0.52	0.26	0.29	0.47
Nb		19.50	17.80	6.90	7.50	18.40
Nd		32.10	31.20	15.30	15.20	30.10
Pr		6.75	6.47	3.14	3.15	6.50
Rb		3.00	1.60	1.00	1.90	2.10
Sm		8.64	7.93	4.24	4.25	7.03
Sn		2.00	4.00	1.00	2.00	2.00
Sr		160.50	146.00	427.00	339.00	503.00
Ta		1.30	1.20	0.50	0.50	1.20
Tb		1.45	1.35	0.70	0.68	1.12
Th		1.27	1.00	0.45	0.57	1.64
Tm		0.68	0.57	0.30	0.33	0.51
U		0.57	0.44	0.21	0.23	0.62
V		271.00	275.00	354.00	292.00	339.00
W		11.00	6.00	1.00	<1	<1
Y		42.50	38.70	20.40	21.10	32.80
Yb		4.17	3.76	1.88	1.89	3.09
Zr		313.00	268.00	122.00	144.00	301.00
As		1.00	1.00	3.00	2.10	19.00
Bi		0.02	0.01	0.01	0.01	0.02
Hg		<0.005	<0.005	<0.005	<0.005	<0.005
In		0.09	0.09	0.02	0.03	0.01

Abbreviations:

D = depth

WL = wavelength

Units:

MD = mafic dyke

MBX = mafic breccia

MT = mafic tuff

MLT = mafic lapilli tuff

Table C.1.1. Whole Rock Geochemistry and Terraspec™ Data for Argyle Samples

Sample ID	150425	150426	150427	150428	150429
Hole ID	AE-16-14	AE-16-14	AE-16-14	AE-16-14	AE-16-14
Depth (m)	38.47	43.35	52.76	60.28	69.72
Lithology	Gabbro	Gabbro	Gabbro	Gabbro	MD
Alteration Assemblage	Ank-Ab-Chl-Py	Ab-Py-Rut	Ep-Ab-Chl	Ep	-
Alteration	Proximal	Intermediate	Proximal	Distal	Distal
Re	<0.001	<0.001	<0.001	<0.001	<0.001
Sb	0.21	0.13	0.64	0.41	0.22
Se	<0.2	0.40	0.20	0.20	0.30
Te	0.01	<0.01	0.01	0.01	0.02
Tl	<0.02	<0.02	<0.02	<0.02	<0.02
Ag	<0.5	<0.5	<0.5	<0.5	<0.5
Cd	<0.5	1	1	1	1
Co	29	31	41	43	41
Cu	5	3	48	31	29
Li	20	20	10	20	10
Mo	<1	<1	<1	<1	1
Ni	<1	1	37	57	42
Pb	<2	3	2	<2	8
Sc	25	23	38	38	27
Zn	86	77	71	62	105
Au	0.00	0.04	0.00	0.00	0.00
C *%*	2.67	2.96	0.18	0.61	0.07
CO_2	9.80	10.80	0.70	2.20	0.30
AlOH WL *nm*	-	2203.30	-	-	2226.79
AlOH D	-	0.05	-	-	0.04
FeOH WL	2259.32	2263.49	2253.56	2252.05	2253.79
FeOH D	0.11	0.16	0.25	0.24	0.14
AlOH D/FeOH D	-	0.31	-	-	0.28

Abbreviations:
D = depth
WL = wavelength

Units:
MD = mafic dyke
MBX = mafic breccia
MT = mafic tuff
MLT = mafic lapilli tuff

Table C.1.1. Whole Rock Geochemistry and Terraspec™ Data for Argyle Samples

Sample ID		150430	150431	150432	150433	150434
Hole ID		AE-16-14	AE-16-15	AE-16-15	AE-16-15	AE-16-15
Depth (m)		74.31	3.48	9.84	14.4	19.09
Lithology		MF	Gabbro	Gabbro	Gabbro	MD
Alteration Assemblage		-	Ep-Ab-Chl	Rut-Py-Chl-Ab	Rut-Ab-Chl	-
Alteration		-	Intermediate	Intermediate	Proximal	Distal
SiO_2	*%*	54.50	45.50	40.60	42.00	43.50
Al_2O_3		15.20	16.40	14.40	12.85	14.95
Fe_2O_3		7.15	11.60	10.55	13.15	14.65
CaO		4.17	9.74	10.40	9.42	7.89
MgO		8.20	5.50	4.58	5.10	5.61
Na_2O		5.49	2.73	3.95	3.36	4.11
K_2O		0.65	0.16	0.41	0.20	0.03
Cr_2O_3		0.05	0.01	0.01	<0.01	0.01
TiO_2		0.90	2.18	2.02	2.54	3.47
MnO		0.11	0.16	0.15	0.18	0.18
P_2O_5		0.17	0.24	0.21	0.32	0.51
SrO		0.02	0.05	0.02	0.05	0.02
BaO		0.01	<0.01	<0.01	0.01	<0.01
LOI		3.62	6.25	12.10	10.15	4.96
Total		100.24	100.52	99.40	99.33	99.89
C		0.09	0.79	2.57	1.98	0.54
S		0.01	0.01	0.01	0.04	0.19
Ba	*ppm*	122.50	34.80	37.30	72.50	18.50
Ce		34.80	23.40	21.30	32.90	43.80
Cr		370.00	90.00	70.00	10.00	80.00
Cs		0.18	0.22	0.12	0.14	0.04
Dy		3.35	4.59	4.10	5.74	6.66
Er		1.85	2.40	2.20	3.04	3.57
Eu		1.18	1.72	1.53	2.14	2.48
Ga		15.70	20.10	18.80	20.30	22.60
Gd		3.73	5.40	4.40	6.45	7.60
Ge		<5	<5	<5	<5	<5
Hf		2.50	3.50	3.10	4.20	5.50
Ho		0.70	0.90	0.81	1.25	1.30
La		16.50	8.90	8.00	12.50	17.80
Lu		0.26	0.30	0.29	0.37	0.47
Nb		9.90	8.90	7.40	11.30	16.60
Nd		17.60	17.30	15.60	23.00	29.20
Pr		4.08	3.46	3.08	4.94	6.15
Rb		8.80	2.70	6.40	3.40	0.30
Sm		3.85	4.78	4.17	5.93	7.31
Sn		2.00	1.00	1.00	1.00	2.00
Sr		163.50	377.00	169.00	376.00	195.50
Ta		0.60	0.60	0.50	0.70	1.10
Tb		0.57	0.81	0.66	1.04	1.14
Th		3.56	0.59	0.55	0.70	1.01
Tm		0.26	0.34	0.30	0.46	0.48
U		2.18	0.26	0.23	0.29	0.43
V		131.00	323.00	304.00	347.00	371.00
W		1.00	<1	1.00	<1	<1
Y		17.60	23.50	20.30	30.10	33.40
Yb		1.82	2.36	2.03	2.77	3.28
Zr		115.00	159.00	138.00	189.00	256.00
As		55.10	2.90	4.10	3.60	8.00
Bi		0.02	0.01	0.01	0.01	0.01
Hg		<0.005	<0.005	<0.005	<0.005	<0.005
In		0.01	0.03	0.05	0.06	0.02

Abbreviations:
D = depth
WL = wavelength

Units:
MD = mafic dyke
MBX = mafic breccia
MT = mafic tuff
MLT = mafic lapilli tuff

Table C.1.1. Whole Rock Geochemistry and Terraspec™ Data for Argyle Samples

Sample ID		150430	150431	150432	150433	150434
Hole ID		AE-16-14	AE-16-15	AE-16-15	AE-16-15	AE-16-15
Depth (m)		74.31	3.48	9.84	14.4	19.09
Lithology		MF	Gabbro	Gabbro	Gabbro	MD
Alteration Assemblage		-	Ep-Ab-Chl	Rut-Py-Chl-Ab	Rut-Ab-Chl	-
Alteration		-	Intermediate	Intermediate	Proximal	Distal
Re		<0.001	<0.001	<0.001	0.00	0.00
Sb		0.38	0.38	0.11	0.13	0.46
Se		<0.2	0.40	0.20	<0.2	0.20
Te		0.01	0.01	0.01	0.01	0.01
Tl		<0.02	<0.02	<0.02	<0.02	<0.02
Ag		<0.5	<0.5	<0.5	<0.5	<0.5
Cd		<0.5	<0.5	<0.5	1	<0.5
Co		35	40	37	43	48
Cu		4	46	40	61	44
Li		10	20	30	10	10
Mo		<1	<1	<1	<1	<1
Ni		217	37	28	23	51
Pb		<2	5	4	2	3
Sc		20	34	32	33	31
Zn		31	74	67	94	114
Au		0.00	0.00	0.00	0.00	0.00
C	*%*	0.08	0.71	2.41	1.82	0.48
CO_2		0.30	2.60	8.80	6.70	1.80
AlOH WL	*nm*	-	-	-	2214.03	2227.07
AlOH D		-	-	-	0.04	0.03
FeOH WL		2251.24	2253.69	2256.49	2254.93	2259.49
FeOH D		0.15	0.16	0.24	0.08	0.11
AlOH D/FeOH D		-	-	-	0.53	0.29

Abbreviations:
D = depth
WL = wavelength

Units:
MD = mafic dyke
MBX = mafic breccia
MT = mafic tuff
MLT = mafic lapilli tuff

Table C.1.1. Whole Rock Geochemistry and Terraspec™ Data for Argyle Samples

Sample ID		150435	150436	150437	150438	150439
Hole ID		AE-16-15	AE-16-15	AE-16-15	AE-16-15	AE-16-15
Depth (m)		21.47	36.35	37.13	42.7	49.9
Lithology		Gabbro	Gabbro	Gabbro	MF	MD
Alteration Assemblage		Rut-Chl-Ab	Ank-Ab-Py-Rut	Chl-Rut	-	Chl
Alteration		Proximal	Proximal	Proximal	-	Distal
SiO_2	*%*	49.40	49.60	44.10	48.60	44.60
Al_2O_3		14.70	13.95	13.65	15.75	16.25
Fe_2O_3		13.40	11.30	15.45	7.22	10.35
CaO		5.53	4.83	5.43	5.27	10.35
MgO		2.94	2.12	3.92	7.76	8.77
Na_2O		5.68	5.48	0.59	3.33	2.05
K_2O		0.17	1.00	1.85	1.21	0.84
Cr_2O_3		<0.01	<0.01	<0.01	0.05	0.03
TiO_2		2.29	1.68	3.39	0.85	1.46
MnO		0.18	0.25	0.20	0.09	0.15
P_2O_5		0.77	0.73	0.51	0.12	0.23
SrO		0.02	0.02	0.01	0.01	0.04
BaO		0.01	0.01	0.01	0.01	0.01
LOI		4.94	9.35	10.30	8.78	4.56
Total		100.03	100.32	99.41	99.05	99.69
C		0.83	2.46	1.98	1.36	0.26
S		0.03	0.03	0.25	0.01	0.02
Ba	*ppm*	58.00	110.00	88.70	90.20	59.80
Ce		63.50	76.80	48.80	23.50	16.30
Cr		<10	10.00	<10	360.00	220.00
Cs		0.16	0.17	0.39	0.23	0.20
Dy		10.00	11.15	8.35	2.97	3.94
Er		5.48	6.23	4.55	1.87	2.10
Eu		3.48	3.58	2.89	1.02	1.44
Ga		24.50	25.30	24.60	16.90	16.90
Gd		11.60	12.45	9.38	3.27	3.93
Ge		<5	<5	<5	<5	<5
Hf		7.20	9.40	6.40	2.20	2.30
Ho		1.96	2.26	1.82	0.67	0.74
La		24.10	29.80	18.50	11.30	6.20
Lu		0.69	0.82	0.58	0.31	0.29
Nb		21.20	25.80	19.10	6.00	4.20
Nd		43.40	49.00	35.00	12.20	12.80
Pr		9.07	10.75	6.89	2.92	2.44
Rb		2.80	13.50	26.10	19.70	15.80
Sm		11.10	12.85	8.97	2.91	3.76
Sn		3.00	3.00	2.00	1.00	1.00
Sr		198.50	194.00	125.50	108.00	331.00
Ta		1.40	1.70	1.20	0.40	0.30
Tb		1.66	1.93	1.47	0.48	0.60
Th		1.48	1.99	1.22	2.84	0.34
Tm		0.74	0.93	0.65	0.31	0.31
U		0.62	0.86	0.49	1.76	0.14
V		116.00	60.00	294.00	121.00	207.00
W		2.00	2.00	8.00	1.00	<1
Y		49.90	58.10	42.50	17.20	19.70
Yb		4.84	5.74	4.16	1.92	1.87
Zr		349.00	475.00	303.00	102.00	98.00
As		3.50	9.70	31.60	1.30	37.10
Bi		0.01	0.01	0.02	0.02	0.01
Hg		<0.005	<0.005	<0.005	<0.005	<0.005
In		0.09	0.08	0.09	0.02	0.01

Abbreviations:
D = depth
WL = wavelength

Units:
MD = mafic dyke
MBX = mafic breccia
MT = mafic tuff
MLT = mafic lapilli tuff

Table C.1.1. Whole Rock Geochemistry and Terraspec™ Data for Argyle Samples

Sample ID	150435	150436	150437	150438	150439
Hole ID	AE-16-15	AE-16-15	AE-16-15	AE-16-15	AE-16-15
Depth (m)	21.47	36.35	37.13	42.7	49.9
Lithology	Gabbro	Gabbro	Gabbro	MF	MD
Alteration Assemblage	Rut-Chl-Ab	Ank-Ab-Py-Rut	Chl-Rut	-	Chl
Alteration	Proximal	Proximal	Proximal	-	Distal
Re	<0.001	<0.001	0.00	<0.001	<0.001
Sb	0.22	0.11	0.21	0.14	0.40
Se	<0.2	0.20	0.60	0.20	<0.2
Te	0.01	0.01	0.03	0.01	0.01
Tl	0	0	0	<0.02	<0.02
Ag	<0.5	<0.5	<0.5	<0.5	<0.5
Cd	<0.5	<0.5	<0.5	<0.5	<0.5
Co	25	18	35	35	47
Cu	10	13	21	6	53
Li	10	<10	<10	30	30
Mo	<1	1	3	<1	<1
Ni	<1	<1	3	176	142
Pb	3	<2	3	2	<2
Sc	15	12	27	22	29
Zn	116	118	112	59	73
Au	<0.001	0.00	0.01	0.00	0.00
C *%*	0.76	2.25	1.90	1.25	0.24
CO_2	2.80	8.30	7.00	4.60	0.90
AlOH WL *nm*	2208.67	2202.00	2197.53	-	-
AlOH D	0.05	0.14	0.24	-	-
FeOH WL	2253.06	2259.67	2253.61	2250.45	2253.93
FeOH D	0.07	0.10	0.19	0.30	0.19
AlOH D/FeOH D	0.66	1.36	1.25	-	-

Abbreviations:
D = depth
WL = wavelength

Units:
MD = mafic dyke
MBX = mafic breccia
MT = mafic tuff
MLT = mafic lapilli tuff

Table C.1.1. Whole Rock Geochemistry and Terraspec™ Data for Argyle Samples

Sample ID		150440	150441	150442	150443	150444
Hole ID		AE-16-15	AE-16-17	AE-16-17	AE-16-17	AE-16-17
Depth (m)		52.83	9.91	19.7	22.85	37.67
Lithology		MLT	Gabbro	MD	Gabbro	Gabbro
Alteration Assemblage		-	Ep-Ab-Chl	-	Ep-Ab-Chl	Ep-Ab-Chl
Alteration		-	Intermediate	Distal	Intermediate	Intermediate
SiO_2	*%*	55.50	46.00	44.60	46.60	46.60
Al_2O_3		17.40	16.95	15.60	17.05	14.95
Fe_2O_3		7.03	10.45	15.20	11.15	12.65
CaO		4.16	9.97	6.62	10.50	8.22
MgO		5.72	6.22	6.43	5.32	6.86
Na_2O		5.70	3.34	4.20	3.77	3.60
K_2O		0.47	0.16	0.15	0.08	0.09
Cr_2O_3		0.03	0.03	0.01	0.01	<0.01
TiO_2		1.10	1.83	3.55	2.11	2.23
MnO		0.05	0.14	0.21	0.16	0.19
P_2O_5		0.21	0.22	0.52	0.28	0.28
SrO		0.03	0.05	0.02	0.05	0.04
BaO		0.01	<0.01	<0.01	<0.01	<0.01
LOI		3.00	5.02	3.89	3.38	3.41
Total		100.41	100.38	101.00	100.46	99.12
C		0.01	0.53	0.16	0.18	0.15
S		0.01	0.13	0.08	0.07	0.04
Ba	*ppm*	64.70	27.50	41.00	31.10	28.70
Ce		34.70	24.70	44.60	28.80	28.30
Cr		190.00	220.00	90.00	80.00	20.00
Cs		0.11	0.15	0.09	0.05	0.11
Dy		4.27	4.27	6.89	5.53	5.27
Er		2.33	2.56	3.89	2.68	3.11
Eu		1.43	1.58	2.48	1.84	1.76
Ga		18.00	21.20	23.40	22.70	20.40
Gd		4.51	5.25	8.12	5.64	6.01
Ge		<5	<5	<5	<5	<5
Hf		2.90	5.30	5.90	4.40	4.30
Ho		0.87	0.94	1.46	1.06	1.02
La		16.20	9.50	17.80	11.00	10.50
Lu		0.38	0.34	0.45	0.37	0.38
Nb		8.70	8.80	17.40	10.60	10.10
Nd		18.40	17.00	29.20	19.60	19.10
Pr		4.31	3.57	6.11	4.05	4.05
Rb		5.30	2.30	1.40	1.20	1.40
Sm		4.73	4.76	7.36	5.43	5.03
Sn		1.00	1.00	2.00	1.00	2.00
Sr		245.00	400.00	164.50	424.00	327.00
Ta		0.60	0.60	1.20	0.70	0.60
Tb		0.65	0.78	1.19	0.88	0.87
Th		3.81	0.77	1.11	0.77	0.80
Tm		0.40	0.38	0.57	0.39	0.40
U		2.12	0.32	0.42	0.30	0.29
V		120.00	262.00	388.00	290.00	304.00
W		1.00	1.00	1.00	<1	<1
Y		23.50	21.80	33.50	25.20	25.40
Yb		2.38	2.25	3.30	2.61	2.48
Zr		138.00	219.00	280.00	192.00	188.00
As		16.80	54.30	85.40	49.00	38.40
Bi		0.01	0.01	0.02	0.01	0.01
Hg		<0.005	<0.005	<0.005	<0.005	<0.005
In		<0.005	0.02	0.02	0.02	0.01

Abbreviations:
D = depth
WL = wavelength

Units:
MD = mafic dyke
MBX = mafic breccia
MT = mafic tuff
MLT = mafic lapilli tuff

Table C.1.1. Whole Rock Geochemistry and Terraspec™ Data for Argyle Samples

Sample ID		150440	150441	150442	150443	150444
Hole ID		AE-16-15	AE-16-17	AE-16-17	AE-16-17	AE-16-17
Depth (m)		52.83	9.91	19.7	22.85	37.67
Lithology		MLT	Gabbro	MD	Gabbro	Gabbro
Alteration Assemblage		-	Ep-Ab-Chl	-	Ep-Ab-Chl	Ep-Ab-Chl
Alteration		-	Intermediate	Distal	Intermediate	Intermediate
Re		<0.001	<0.001	0.00	0.00	<0.001
Sb		0.15	0.38	0.26	0.48	0.38
Se		<0.2	0.30	0.20	0.30	0.20
Te		<0.01	0.02	0.02	<0.01	<0.01
Tl		<0.02	<0.02	<0.02	<0.02	<0.02
Ag		<0.5	<0.5	<0.5	<0.5	<0.5
Cd		<0.5	<0.5	<0.5	1	<0.5
Co		27	40	45	36	51
Cu		5	62	46	48	41
Li		20	10	20	10	10
Mo		<1	<1	<1	<1	<1
Ni		110	57	54	33	39
Pb		2	<2	3	<2	<2
Sc		18	33	32	32	31
Zn		32	67	113	69	88
Au		0.00	0.00	0.00	0.00	<0.001
C	*%*	<0.05	0.45	0.14	0.17	0.14
CO_2		0.20	1.70	0.50	0.60	0.50
AlOH WL	*nm*	-	-	2220.90	-	-
AlOH D		-	-	0.04	-	-
FeOH WL		2252.25	2255.06	2255.62	2255.16	2253.66
FeOH D		0.32	0.21	0.11	0.22	0.15
AlOH D/FeOH D		-	-	0.33	-	-

Abbreviations:	**Units:**	
D = depth	MD = mafic dyke	MT = mafic tuff
WL = wavelength	MBX = mafic breccia	MLT = mafic lapilli tuff

Table C.1.1. Whole Rock Geochemistry and Terraspec™ Data for Argyle Samples

Sample ID		150445	150446	150447	150448	150449
Hole ID		AE-16-17	AE-16-17	AE-16-17	AE-16-17	AE-16-17
Depth (m)		42.1	43.3	55.82	69	81.5
Lithology		Gabbro	Gabbro	MF	MF	MF
Alteration Assemblage		Rut-Chl	Rut-Chl-Ab	-	-	Ep-Ab
Alteration		Proximal	Proximal	-	-	Distal
SiO_2	*%*	42.40	43.80	52.30	52.50	52.60
Al_2O_3		13.60	15.60	15.00	16.15	15.10
Fe_2O_3		11.10	9.68	7.03	7.54	7.06
CaO		8.69	7.77	3.72	4.18	6.45
MgO		5.11	2.17	8.51	8.53	7.13
Na_2O		4.10	4.19	3.32	3.94	4.64
K_2O		0.16	1.72	0.99	1.16	0.65
Cr_2O_3		<0.01	<0.01	0.05	0.05	0.05
TiO_2		1.98	2.65	0.82	0.88	0.84
MnO		0.16	0.20	0.09	0.08	0.13
P_2O_5		0.27	0.79	0.06	0.14	0.18
SrO		0.03	0.02	0.01	0.02	0.03
BaO		<0.01	0.02	0.01	0.01	0.01
LOI		10.50	9.70	8.04	3.75	3.50
Total		98.10	98.31	99.95	98.93	98.37
C		2.18	2.37	1.11	0.01	0.26
S		0.08	0.31	0.01	0.01	0.02
Ba	*ppm*	44.80	134.00	135.00	87.00	60.80
Ce		28.10	87.20	28.60	22.40	33.20
Cr		20.00	10.00	420.00	340.00	340.00
Cs		0.09	0.34	0.23	0.26	0.07
Dy		5.13	12.80	3.35	3.62	3.22
Er		2.96	7.48	2.11	1.95	1.85
Eu		1.86	3.81	0.86	0.97	1.09
Ga		19.60	26.30	16.90	17.20	17.00
Gd		5.64	14.90	3.34	3.34	3.48
Ge		<5	<5	<5	<5	<5
Hf		4.30	13.10	2.80	2.60	2.60
Ho		1.07	2.74	0.69	0.78	0.69
La		10.60	34.60	12.90	10.00	16.20
Lu		0.37	0.96	0.25	0.29	0.27
Nb		10.30	33.50	8.00	5.60	9.40
Nd		19.10	56.00	13.60	11.50	16.60
Pr		4.10	12.25	3.27	2.70	4.20
Rb		2.70	22.40	18.80	24.90	9.30
Sm		5.00	13.50	3.22	3.22	3.80
Sn		2.00	3.00	1.00	1.00	2.00
Sr		247.00	180.00	105.50	186.00	268.00
Ta		0.60	2.10	0.60	0.40	0.60
Tb		0.86	2.21	0.52	0.57	0.51
Th		0.73	2.52	3.91	2.85	3.42
Tm		0.37	1.07	0.29	0.32	0.30
U		0.27	1.06	1.40	1.58	1.84
V		275.00	147.00	92.00	117.00	124.00
W		1.00	19.00	1.00	<1	1.00
Y		24.80	64.80	15.40	18.00	16.80
Yb		2.25	6.52	1.77	2.24	1.57
Zr		189.00	598.00	124.00	107.00	111.00
As		48.40	61.60	0.90	2.20	8.80
Bi		0.02	0.04	0.01	0.03	0.06
Hg		<0.005	<0.005	<0.005	<0.005	<0.005
In		0.07	0.06	0.02	0.01	0.01

Abbreviations:

D = depth

WL = wavelength

Units:

MD = mafic dyke

MBX = mafic breccia

MT = mafic tuff

MLT = mafic lapilli tuff

Table C.1.1. Whole Rock Geochemistry and Terraspec™ Data for Argyle Samples

Sample ID		150445	150446	150447	150448	150449
Hole ID		AE-16-17	AE-16-17	AE-16-17	AE-16-17	AE-16-17
Depth (m)		42.1	43.3	55.82	69	81.5
Lithology		Gabbro	Gabbro	MF	MF	MF
Alteration Assemblage		Rut-Chl	Rut-Chl-Ab	-	-	Ep-Ab
Alteration		Proximal	Proximal	-	-	Distal
Re		<0.001	0.00	<0.001	<0.001	<0.001
Sb		0.15	0.11	0.13	0.18	0.30
Se		0.20	0.20	<0.2	<0.2	0.30
Te		0.01	0.07	0.01	<0.01	<0.01
Tl		<0.02	<0.02	<0.02	<0.02	<0.02
Ag		<0.5	<0.5	<0.5	<0.5	<0.5
Cd		<0.5	<0.5	<0.5	<0.5	1
Co		39	26	35	31	32
Cu		52	54	19	32	36
Li		20	10	30	20	20
Mo		<1	3	<1	<1	<1
Ni		25	<1	234	152	207
Pb		4	<2	<2	<2	9
Sc		29	14	19	22	19
Zn		79	102	65	61	61
Au		0.00	2.07	0.00	0.00	0.00
C	*%*	2.02	2.24	1.03	<0.05	0.23
CO_2		7.40	8.20	3.80	0.20	0.80
AlOH WL	*nm*	-	2201.05	-	-	-
AlOH D		-	0.17	-	-	-
FeOH WL		2257.35	2256.16	2251.16	2249.73	2253.30
FeOH D		0.23	0.12	0.28	0.28	0.30
AlOH D/FeOH D		-	1.43	-	-	-

Abbreviations:
D = depth
WL = wavelength

Units:
MD = mafic dyke
MBX = mafic breccia
MT = mafic tuff
MLT = mafic lapilli tuff

Table C.1.1. Whole Rock Geochemistry and Terraspec™ Data for Argyle Samples

Sample ID		150450	166359	166360	166361	183063
Hole ID		AE-16-17	AE-16-20	AE-16-20	AE-16-20	AE-16-17
Depth (m)		97	61.67	70.74	72.14	101.39
Lithology		MF	MD	MD	MF	Gabbro
Alteration Assemblage		Ab-Ank	Qt-Cal	Qt-Cal	-	Rut-Chl
Alteration		Proximal	Distal	Distal	-	Distal
SiO_2	*%*	43.90	48.80	50.20	51.10	43.20
Al_2O_3		13.75	20.10	17.40	17.05	12.45
Fe_2O_3		5.93	8.93	7.52	8.43	9.48
CaO		8.99	4.65	7.80	6.94	8.20
MgO		4.40	5.87	4.97	7.24	5.70
Na_2O		3.01	5.60	4.96	4.46	2.67
K_2O		2.51	0.28	0.81	0.53	1.27
Cr_2O_3		0.02	0.02	0.01	0.03	0.02
TiO_2		0.87	1.24	1.02	1.16	1.44
MnO		0.11	0.09	0.09	0.13	0.14
P_2O_5		0.15	0.16	0.13	0.16	0.17
SrO		0.02	0.02	0.03	0.05	0.02
BaO		0.01	<0.01	0.02	0.01	0.01
LOI		14.75	3.76	4.08	2.96	14.00
Total		98.42	99.52	99.04	100.25	98.77
C		3.74	0.08	0.52	0.07	3.40
S		0.05	0.01	0.08	0.03	<0.01
Ba	*ppm*	125.00	41.10	143.50	69.90	75.90
Ce		25.60	25.00	19.60	23.40	18.80
Cr		110.00	120.00	90.00	230.00	130.00
Cs		0.41	0.12	0.10	0.08	0.23
Dy		3.33	4.54	3.55	4.06	3.92
Er		1.96	2.39	2.01	2.31	2.21
Eu		1.24	1.37	1.03	1.24	1.32
Ga		15.20	22.10	15.90	17.10	16.90
Gd		3.21	4.30	3.41	4.22	3.88
Ge		<5	<5	<5	<5	<5
Hf		2.50	2.80	2.50	2.80	2.90
Ho		0.70	0.94	0.74	0.85	0.79
La		11.50	11.00	8.70	10.30	7.30
Lu		0.29	0.35	0.28	0.33	0.26
Nb		6.60	6.10	4.70	5.70	6.60
Nd		13.20	14.40	11.00	13.60	13.40
Pr		3.17	3.35	2.50	3.03	2.72
Rb		33.30	4.60	9.40	7.20	17.50
Sm		3.21	3.75	3.13	3.71	3.54
Sn		5.00	2.00	1.00	1.00	1.00
Sr		152.00	193.00	288.00	365.00	159.50
Ta		0.40	0.40	0.30	0.40	0.40
Tb		0.51	0.68	0.51	0.66	0.66
Th		2.74	2.78	2.20	2.04	0.63
Tm		0.28	0.38	0.32	0.36	0.29
U		2.16	1.91	1.48	1.29	0.27
V		157.00	209.00	171.00	166.00	232.00
W		4.00	1.00	1.00	1.00	5.00
Y		17.50	23.30	18.70	22.00	19.80
Yb		1.93	2.26	1.93	2.31	1.97
Zr		111.00	128.00	103.00	124.00	122.00
As		1.10	36.30	93.40	40.80	0.50
Bi		0.04	0.04	0.05	0.05	0.02
Hg		<0.005	<0.005	<0.005	<0.005	<0.005
In		0.04	0.02	0.01	0.01	0.04

Abbreviations:
D = depth
WL = wavelength

Units:
MD = mafic dyke
MBX = mafic breccia

MT = mafic tuff
MLT = mafic lapilli tuff

Table C.1.1. Whole Rock Geochemistry and Terraspec™ Data for Argyle Samples

Sample ID	150450	166359	166360	166361	183063
Hole ID	AE-16-17	AE-16-20	AE-16-20	AE-16-20	AE-16-17
Depth (m)	97	61.67	70.74	72.14	101.39
Lithology	MF	MD	MD	MF	Gabbro
Alteration Assemblage	Ab-Ank	Qt-Cal	Qt-Cal	-	Rut-Chl
Alteration	Proximal	Distal	Distal	-	Distal
Re	0.00	<0.001	<0.001	<0.001	0.00
Sb	0.29	0.27	0.43	0.44	0.10
Se	0.30	0.20	<0.2	0.20	<0.2
Te	0.01	<0.01	0.01	<0.01	0.01
Tl	0	<0.02	<0.02	0	0
Ag	<0.5	<0.5	<0.5	<0.5	<0.5
Cd	<0.5	<0.5	<0.5	<0.5	<0.5
Co	18	31	23	29	34
Cu	153	82	65	44	76
Li	<10	20	10	20	20
Mo	<1	2	1	1	1
Ni	51	40	28	104	69
Pb	4	6	6	7	5
Sc	17	28	27	21	29
Zn	28	70	60	61	66
Au	0.00	0.00	0.00	0.00	0.02
C *%*	3.59	0.06	0.45	0.05	3.24
CO_2	13.20	0.20	1.60	0.20	11.90
AlOH WL *nm*	2199.44	-	-	-	2204.48
AlOH D	0.29	-	-	-	0.11
FeOH WL	2251.71	2253.51	2253.57	2253.19	2257.53
FeOH D	0.13	0.33	0.19	0.31	0.17
AlOH D/FeOH D	2.29	-	-	-	0.64

Abbreviations:

D = depth
WL = wavelength

Units:

MD = mafic dyke
MBX = mafic breccia
MT = mafic tuff
MLT = mafic lapilli tuff

Table C.1.1. Whole Rock Geochemistry and Terraspec™ Data for Argyle Samples

Sample ID		183064	183065	183066	183067	183068
Hole ID		AE-16-17	AE-16-17	AE-16-17	AE-16-17	AE-16-17
Depth (m)		110.35	116	121.8	130.74	140.3
Lithology		Gabbro	MD	Gabbro	Gabbro	Gabbro
Alteration Assemblage		Rut-Chl	Chl-Qt	Ep-Ab-Chl-Hem	Ep-Ab-Chl	Ep-Chl-Qt
Alteration		Distal	Distal	Intermediate	Distal	Distal
SiO_2	*%*	45.20	45.90	51.80	47.30	48.50
Al_2O_3		13.45	15.00	14.45	12.55	14.90
Fe_2O_3		9.63	12.50	10.40	17.00	12.10
CaO		8.59	7.86	8.45	8.14	9.70
MgO		5.97	6.64	6.11	5.13	6.26
Na_2O		3.70	2.79	4.33	3.48	3.31
K_2O		0.13	0.04	0.07	0.17	0.19
Cr_2O_3		0.02	0.01	0.02	<0.01	0.02
TiO_2		1.53	2.65	1.78	3.35	1.84
MnO		0.13	0.18	0.15	0.21	0.17
P_2O_5		0.17	0.36	0.19	0.20	0.20
SrO		0.02	0.05	0.02	0.03	0.03
BaO		<0.01	<0.01	<0.01	0.01	<0.01
LOI		10.25	5.42	2.33	2.44	3.51
Total		98.79	99.40	100.10	100.01	100.73
C		1.93	0.46	0.08	0.15	0.26
S		<0.01	<0.01	<0.01	0.11	0.01
Ba	*ppm*	25.60	31.40	29.00	89.20	40.60
Ce		18.20	38.40	20.10	22.70	20.00
Cr		130.00	90.00	110.00	10.00	110.00
Cs		0.06	0.16	0.06	0.46	0.04
Dy		3.67	5.53	4.59	4.77	4.23
Er		2.21	2.89	2.57	2.61	2.47
Eu		1.23	2.02	1.41	1.55	1.39
Ga		17.50	23.70	18.80	22.50	21.30
Gd		3.76	6.31	4.82	5.40	4.74
Ge		<5	<5	<5	<5	<5
Hf		2.90	5.20	3.70	3.50	3.10
Ho		0.77	1.10	0.93	0.99	0.87
La		7.20	15.80	7.10	8.70	8.30
Lu		0.30	0.38	0.34	0.37	0.33
Nb		6.50	16.60	8.20	8.60	7.20
Nd		12.70	24.20	14.80	16.00	13.90
Pr		2.68	5.28	3.04	3.33	2.91
Rb		2.30	0.70	0.90	3.00	1.80
Sm		3.77	6.25	4.28	4.58	4.14
Sn		1.00	2.00	1.00	1.00	1.00
Sr		199.50	411.00	224.00	226.00	215.00
Ta		0.40	1.10	0.50	0.60	0.50
Tb		0.64	0.97	0.75	0.81	0.69
Th		0.54	1.09	0.77	0.74	0.65
Tm		0.29	0.37	0.37	0.38	0.37
U		0.25	0.39	0.37	0.32	0.20
V		258.00	306.00	283.00	695.00	323.00
W		1.00	<1	1.00	1.00	1.00
Y		19.20	25.80	22.30	24.60	20.80
Yb		1.85	2.61	2.28	2.53	2.18
Zr		115.00	219.00	143.00	148.00	121.00
As		0.70	3.60	16.10	29.90	100.50
Bi		0.03	0.01	0.01	0.01	0.01
Hg		<0.005	<0.005	<0.005	<0.005	<0.005
In		0.05	0.03	0.02	0.02	0.01

Abbreviations: **Units:**
D = depth MD = mafic dyke MT = mafic tuff
WL = wavelength MBX = mafic breccia MLT = mafic lapilli tuff

Table C.1.1. Whole Rock Geochemistry and Terraspec™ Data for Argyle Samples

Sample ID	183064	183065	183066	183067	183068
Hole ID	AE-16-17	AE-16-17	AE-16-17	AE-16-17	AE-16-17
Depth (m)	110.35	116	121.8	130.74	140.3
Lithology	Gabbro	MD	Gabbro	Gabbro	Gabbro
Alteration Assemblage	Rut-Chl	Chl-Qt	Ep-Ab-Chl-Hem	Ep-Ab-Chl	Ep-Chl-Qt
Alteration	Distal	Distal	Intermediate	Distal	Distal
Re	0.00	0.00	<0.001	0.00	0.00
Sb	0.07	0.36	0.58	0.86	0.38
Se	<0.2	0.30	0.20	0.30	0.20
Te	<0.01	0.01	0.01	0.01	0.01
Tl	<0.02	<0.02	<0.02	<0.02	<0.02
Ag	<0.5	<0.5	<0.5	<0.5	<0.5
Cd	<0.5	<0.5	<0.5	1	<0.5
Co	36	47	38	60	44
Cu	67	45	38	171	51
Li	20	20	10	<10	20
Mo	<1	1	<1	1	1
Ni	61	60	53	39	58
Pb	2	4	<2	<2	<2
Sc	32	28	35	42	35
Zn	59	102	68	132	74
Au	0.01	0.00	0.00	0.00	0.00
C *%*	1.78	0.40	0.05	0.12	0.22
CO_2	6.50	1.50	0.20	0.40	0.80
AlOH WL *nm*	-	-	2227.39	-	-
AlOH D	-	-	0.03	-	-
FeOH WL	2255.29	2253.90	2255.22	2254.19	2254.00
FeOH D	0.18	0.13	0.14	0.11	0.15
AlOH D/FeOH D	-	-	0.22	-	-

Abbreviations:
D = depth
WL = wavelength

Units:
MD = mafic dyke
MBX = mafic breccia
MT = mafic tuff
MLT = mafic lapilli tuff

Table C.1.1. Whole Rock Geochemistry and Terraspec™ Data for Argyle Samples

Sample ID		183069	183070	183071	183072	183073
Hole ID		AE-16-17	AE-16-03	AE-16-03	AE-16-03	AE-16-03
Depth (m)		149	4.37	13.16	18.95	21.36
Lithology		Gabbro	Gabbro	Gabbro	Gabbro	Gabbro
Alteration Assemblage		Ep-Chl-Qt	Chl-Ank-Py-Ab	Chl-Ab-Ank-Py	Chl-Ab-Ank-Py-Fuch	Rut-Chl-Ab-Py
Alteration		Distal	Proximal	Proximal	Proximal	Intermediate
SiO_2	*%*	50.80	49.60	40.30	38.90	45.90
Al_2O_3		15.45	14.20	13.00	11.00	17.30
Fe_2O_3		11.00	13.05	14.40	5.63	7.64
CaO		8.73	4.77	5.10	12.45	4.51
MgO		6.62	2.38	3.19	6.29	8.51
Na_2O		4.04	3.82	4.59	1.20	1.14
K_2O		0.32	0.61	0.72	2.76	3.42
Cr_2O_3		0.02	<0.01	<0.01	0.05	0.06
TiO_2		1.62	1.86	3.39	0.57	0.93
MnO		0.17	0.24	0.31	0.18	0.08
P_2O_5		0.18	1.11	0.67	0.14	0.10
SrO		0.04	0.02	0.02	0.03	0.01
BaO		0.01	0.01	0.01	0.02	0.03
LOI		2.46	8.00	13.95	19.90	10.90
Total		101.46	99.67	99.65	99.12	100.53
C		0.03	1.66	3.90	5.21	1.88
S		0.01	0.03	0.30	<0.01	0.01
Ba	*ppm*	74.30	71.10	58.80	180.00	264.00
Ce		19.60	82.40	61.00	14.50	30.30
Cr		120.00	10.00	10.00	330.00	390.00
Cs		0.09	0.15	0.17	0.48	0.55
Dy		3.99	12.35	10.55	2.74	3.30
Er		2.53	6.38	6.15	1.87	1.95
Eu		1.32	4.37	3.63	0.89	1.09
Ga		19.70	27.20	24.30	14.70	17.50
Gd		3.96	14.10	11.85	2.59	3.65
Ge		<5	<5	<5	<5	<5
Hf		3.40	9.50	9.10	1.70	3.00
Ho		0.81	2.57	2.33	0.63	0.67
La		7.60	31.60	22.60	6.60	13.70
Lu		0.31	0.88	0.81	0.22	0.28
Nb		7.00	23.80	27.20	4.00	7.40
Nd		13.60	56.30	42.70	7.90	14.70
Pr		2.85	12.05	8.53	1.82	3.58
Rb		3.90	8.40	9.90	40.50	56.70
Sm		4.18	14.20	11.00	2.17	3.55
Sn		1.00	4.00	3.00	3.00	1.00
Sr		306.00	157.50	193.50	248.00	113.50
Ta		0.40	1.50	1.60	0.30	0.50
Tb		0.66	2.22	1.75	0.46	0.54
Th		0.62	2.02	1.55	2.01	3.60
Tm		0.35	0.97	0.87	0.25	0.28
U		0.27	0.80	0.64	1.14	1.50
V		276.00	71.00	153.00	100.00	97.00
W		1.00	2.00	9.00	3.00	4.00
Y		20.00	61.70	53.40	14.70	15.80
Yb		2.16	5.92	5.20	1.63	1.85
Zr		130.00	459.00	392.00	73.00	123.00
As		61.60	3.70	32.10	1.20	0.90
Bi		0.01	0.01	0.04	0.01	0.01
Hg		<0.005	<0.005	<0.005	<0.005	<0.005
In		0.01	0.11	0.12	0.05	0.01

Abbreviations: **Units:**

D = depth
MD = mafic dyke
MT = mafic tuff
WL = wavelength
MBX = mafic breccia
MLT = mafic lapilli tuff

Table C.1.1. Whole Rock Geochemistry and Terraspec™ Data for Argyle Samples

Sample ID	183069	183070	183071	183072	183073
Hole ID	AE-16-17	AE-16-03	AE-16-03	AE-16-03	AE-16-03
Depth (m)	149	4.37	13.16	18.95	21.36
Lithology	Gabbro	Gabbro	Gabbro	Gabbro	Gabbro
Alteration Assemblage	Ep-Chl-Qt	Chl-Ank-Py-Ab	Chl-Ab-Ank-Py	Chl-Ab-Ank-Py-Fuch	Rut-Chl-Ab-Py
Alteration	Distal	Proximal	Proximal	Proximal	Intermediate
Re	0.00	0.00	0.00	<0.001	<0.001
Sb	0.41	0.10	0.13	0.10	0.11
Se	0.20	<0.2	0.70	0.20	0.20
Te	0.01	0.01	0.04	4.62	0.04
Tl	<0.02	<0.02	<0.02	0	0
Ag	<0.5	<0.5	<0.5	<0.5	<0.5
Cd	1	<0.5	<0.5	<0.5	<0.5
Co	39	25	25	23	31
Cu	89	6	13	1	13
Li	20	20	<10	<10	30
Mo	<1	1	2	<1	<1
Ni	61	<1	2	144	175
Pb	<2	<2	<2	4	2
Sc	31	11	21	16	19
Zn	83	151	112	42	56
Au	0.00	0.01	0.69	0.02	0.00
C *%*	<0.05	1.35	3.68	4.98	1.75
CO_2	0.20	4.90	13.50	18.30	6.40
AlOH WL *nm*	-	2193.28	2192.49	2201.36	2206.06
AlOH D	-	0.17	0.31	0.45	0.33
FeOH WL	2255.66	2258.00	-	-	2241.41
FeOH D	0.17	0.15	-	-	0.25
AlOH D/FeOH D	-	1.10	-	-	1.36

Abbreviations:
D = depth
WL = wavelength

Units:
MD = mafic dyke
MBX = mafic breccia
MT = mafic tuff
MLT = mafic lapilli tuff

Table C.1.1. Whole Rock Geochemistry and Terraspec™ Data for Argyle Samples

Sample ID		183074	183075	183076	183077	183078
Hole ID		AE-16-03	AE-16-03	AE-16-03	AE-16-06	AE-16-06
Depth (m)		25.55	35.16	45.16	4.63	8.7
Lithology		Gabbro	MF	Gabbro	Gabbro	Gabbro
Alteration Assemblage		Rut-Ep-Ab	Chl-Ep	Least altered?	Ank-Chl-Ab-Py-Qt	Chl-Ab-Ank-Py
Alteration		Intermediate	Distal	Distal	Proximal	Proximal
SiO_2	*%*	46.40	50.90	46.90	33.30	56.10
Al_2O_3		14.75	16.65	14.20	11.35	15.75
Fe_2O_3		7.39	7.07	10.95	12.15	8.76
CaO		6.57	5.52	7.46	13.30	3.92
MgO		6.45	6.34	6.13	3.74	1.42
Na_2O		1.72	3.69	3.99	2.30	6.17
K_2O		2.87	1.98	0.24	1.40	1.02
Cr_2O_3		0.03	0.02	0.02	<0.01	<0.01
TiO_2		1.07	0.97	1.69	3.36	1.38
MnO		0.12	0.09	0.16	0.27	0.12
P_2O_5		0.17	0.13	0.20	0.56	0.45
SrO		0.02	0.02	0.03	0.03	0.01
BaO		0.03	0.03	0.01	0.01	0.01
LOI		12.20	7.98	8.23	16.45	6.32
Total		99.79	101.39	100.21	98.22	101.43
C		2.65	1.19	1.37	4.77	1.31
S		<0.01	<0.01	0.05	1.55	0.74
Ba	*ppm*	221.00	224.00	75.60	68.30	54.50
Ce		21.60	18.80	21.00	48.30	89.20
Cr		210.00	110.00	120.00	10.00	10.00
Cs		0.44	0.43	0.19	0.29	0.19
Dy		3.85	3.35	4.45	9.57	12.15
Er		2.04	2.22	2.45	4.94	7.01
Eu		1.27	1.02	1.49	3.15	3.92
Ga		13.60	15.20	16.60	18.70	22.40
Gd		3.72	3.14	4.65	9.99	13.15
Ge		<5	<5	<5	<5	<5
Hf		2.80	2.40	3.20	7.20	14.50
Ho		0.83	0.79	0.91	1.81	2.40
La		9.50	8.40	8.10	18.20	34.90
Lu		0.29	0.30	0.32	0.63	0.98
Nb		5.20	4.50	7.60	20.60	31.10
Nd		13.10	11.00	15.10	35.30	55.40
Pr		2.78	2.41	2.94	6.97	12.35
Rb		42.80	37.30	4.40	17.40	13.60
Sm		3.25	2.76	4.12	9.44	13.65
Sn		1.00	1.00	1.00	3.00	3.00
Sr		212.00	159.00	249.00	256.00	98.50
Ta		0.40	0.30	0.50	1.10	1.90
Tb		0.60	0.55	0.68	1.59	1.97
Th		1.90	2.21	0.80	1.24	2.88
Tm		0.29	0.28	0.35	0.73	0.97
U		1.21	1.43	0.26	0.59	1.14
V		128.00	158.00	251.00	219.00	61.00
W		1.00	1.00	1.00	22.00	9.00
Y		19.70	17.70	21.00	45.20	58.90
Yb		2.13	2.17	2.15	4.47	6.72
Zr		118.00	106.00	131.00	321.00	665.00
As		0.60	1.00	6.60	93.30	107.50
Bi		0.03	0.07	0.02	1.32	0.06
Hg		<0.005	<0.005	<0.005	<0.005	<0.005
In		0.04	0.02	0.06	0.09	0.07

Abbreviations:

D = depth
WL = wavelength

Units:

MD = mafic dyke
MBX = mafic breccia
MT = mafic tuff
MLT = mafic lapilli tuff

Table C.1.1. Whole Rock Geochemistry and Terraspec™ Data for Argyle Samples

Sample ID	183074	183075	183076	183077	183078
Hole ID	AE-16-03	AE-16-03	AE-16-03	AE-16-06	AE-16-06
Depth (m)	25.55	35.16	45.16	4.63	8.7
Lithology	Gabbro	MF	Gabbro	Gabbro	Gabbro
Alteration Assemblage	Rut-Ep-Ab	Chl-Ep	Least altered?	Ank-Chl-Ab-Py-Qt	Chl-Ab-Ank-Py
Alteration	Intermediate	Distal	Distal	Proximal	Proximal
Re	<0.001	0.00	0.00	<0.001	<0.001
Sb	0.10	0.20	0.34	0.22	0.11
Se	0.20	0.20	0.30	2.10	1.20
Te	0.01	<0.01	0.01	0.85	0.08
Tl	0	0	<0.02	<0.02	<0.02
Ag	<0.5	<0.5	<0.5	1	<0.5
Cd	<0.5	<0.5	<0.5	1	<0.5
Co	32	27	40	44	10
Cu	43	55	73	22	144
Li	10	20	10	<10	<10
Mo	<1	<1	<1	1	1
Ni	103	37	59	1	<1
Pb	4	<2	<2	4	<2
Sc	21	25	32	23	11
Zn	78	56	84	91	74
Au	0.02	0.00	0.00	8.59	1.90
C *%*	2.44	1.09	1.23	4.50	1.23
CO_2	9.00	4.00	4.50	16.50	4.50
AlOH WL *nm*	2208.75	2220.99	-	2194.84	2199.60
AlOH D	0.30	0.19	-	0.30	0.07
FeOH WL	2249.64	2250.29	2255.72	2252.16	2260.03
FeOH D	0.22	0.24	0.13	0.05	0.12
AlOH D/FeOH D	1.35	0.80	-	6.12	0.56

Abbreviations:
D = depth
WL = wavelength

Units:
MD = mafic dyke
MBX = mafic breccia
MT = mafic tuff
MLT = mafic lapilli tuff

Table C.1.1. Whole Rock Geochemistry and Terraspec™ Data for Argyle Samples

Sample ID	183079	183080	183081	183082	183083
Hole ID	AE-16-06	AE-16-06	AE-16-06	AE-16-06	AE-16-06
Depth (m)	12.2	20.9	24	33.87	42.64
Lithology	Gabbro	Gabbro	Gabbro	MF	MD
Alteration Assemblage	Chl-Py-Rut-Ab	Chl-Ep-Py-Ab	Ep-Ab-Chl	Cal	Least altered?
Alteration	Intermediate	Intermediate	Proximal	Distal	Distal
SiO_2 *%*	48.50	45.70	48.20	49.60	53.90
Al_2O_3	15.45	13.25	15.80	14.55	17.20
Fe_2O_3	15.10	16.15	9.33	6.91	7.49
CaO	4.15	9.56	10.40	7.01	8.09
MgO	3.03	4.83	5.98	8.31	5.22
Na_2O	4.86	2.49	3.79	4.50	5.04
K_2O	0.33	0.18	0.10	0.60	0.44
Cr_2O_3	<0.01	<0.01	0.01	0.06	0.01
TiO_2	2.27	3.55	1.53	0.71	1.04
MnO	0.19	0.23	0.14	0.11	0.10
P_2O_5	1.19	0.34	0.18	0.09	0.14
SrO	0.02	0.04	0.03	0.01	0.03
BaO	<0.01	0.02	<0.01	0.01	0.01
LOI	6.02	3.45	3.90	7.43	2.20
Total	101.11	99.79	99.39	99.90	100.91
C	0.91	0.15	0.43	1.14	0.05
S	<0.01	0.41	<0.01	<0.01	<0.01
Ba *ppm*	38.90	208.00	27.60	81.60	85.30
Ce	91.60	37.90	20.90	22.40	21.70
Cr	10.00	10.00	70.00	410.00	100.00
Cs	0.13	1.84	0.08	0.16	0.08
Dy	13.55	6.52	4.14	3.11	4.08
Er	7.57	3.69	2.15	1.91	2.43
Eu	4.57	2.24	1.47	0.95	1.18
Ga	29.20	24.00	19.50	15.00	19.30
Gd	15.95	7.03	4.64	2.93	4.02
Ge	<5	<5	<5	<5	<5
Hf	11.10	5.80	3.50	2.40	2.80
Ho	2.63	1.36	0.89	0.66	0.82
La	34.80	14.40	7.80	10.50	9.70
Lu	0.85	0.46	0.28	0.24	0.30
Nb	28.70	12.80	7.10	5.20	5.30
Nd	60.10	25.80	14.90	10.90	12.20
Pr	12.95	5.27	3.04	2.72	2.74
Rb	4.70	4.50	1.60	11.60	4.50
Sm	15.25	7.00	4.13	2.87	3.33
Sn	3.00	2.00	1.00	2.00	1.00
Sr	161.00	352.00	293.00	98.20	241.00
Ta	1.90	0.80	0.40	0.40	0.30
Tb	2.34	1.10	0.66	0.50	0.63
Th	2.23	0.98	0.56	2.99	2.57
Tm	1.00	0.53	0.34	0.31	0.33
U	0.89	0.42	0.23	1.88	1.76
V	77.00	528.00	226.00	107.00	171.00
W	6.00	1.00	<1	1.00	1.00
Y	65.00	32.60	19.70	15.60	20.20
Yb	6.20	3.31	1.92	1.78	2.19
Zr	516.00	250.00	143.00	98.00	120.00
As	28.10	49.90	17.80	35.20	41.70
Bi	0.01	0.01	0.01	0.01	0.02
Hg	<0.005	<0.005	<0.005	<0.005	<0.005
In	0.10	0.02	0.01	0.02	0.01

Abbreviations:
D = depth
WL = wavelength

Units:
MD = mafic dyke
MBX = mafic breccia
MT = mafic tuff
MLT = mafic lapilli tuff

Table C.1.1. Whole Rock Geochemistry and Terraspec™ Data for Argyle Samples

Sample ID		183079	183080	183081	183082	183083
Hole ID		AE-16-06	AE-16-06	AE-16-06	AE-16-06	AE-16-06
Depth (m)		12.2	20.9	24	33.87	42.64
Lithology		Gabbro	Gabbro	Gabbro	MF	MD
Alteration Assemblage		Chl-Py-Rut-Ab	Chl-Ep-Py-Ab	Ep-Ab-Chl	Cal	Least altered?
Alteration		Intermediate	Intermediate	Proximal	Distal	Distal
Re		<0.001	0.00	<0.001	0.00	<0.001
Sb		0.12	0.78	0.50	0.14	0.40
Se		<0.2	0.50	0.20	0.30	<0.2
Te		0.02	0.01	<0.01	0.01	<0.01
Tl		<0.02	<0.02	<0.02	<0.02	<0.02
Ag		<0.5	<0.5	<0.5	<0.5	<0.5
Cd		<0.5	1	<0.5	<0.5	<0.5
Co		25	49	38	40	29
Cu		8	48	65	2	67
Li		20	10	20	20	10
Mo		2	1	<1	1	1
Ni		<1	10	37	248	34
Pb		<2	<2	<2	6	2
Sc		10	37	38	23	27
Zn		134	107	62	55	62
Au		0.02	0.08	0.01	0.00	0.00
C	*%*	0.83	0.11	0.38	1.02	<0.05
CO_2		3.00	0.40	1.40	3.70	0.20
AlOH WL	*nm*	-	-	-	-	-
AlOH D		-	-	-	-	-
FeOH WL		2261.40	2253.58	2253.87	2251.92	2253.89
FeOH D		0.13	0.14	0.26	0.26	0.32
AlOH D/FeOH D		-	-	-	-	-

Abbreviations:
D = depth
WL = wavelength

Units:
MD = mafic dyke
MBX = mafic breccia

MT = mafic tuff
MLT = mafic lapilli tuff

Table C.1.1. Whole Rock Geochemistry and Terraspec™ Data for Argyle Samples

Sample ID		183084	183085	183086	183087	183088
Hole ID		AE-16-04	AE-16-04	AE-16-04	AE-16-04	AE-16-04
Depth (m)		6.11	13.6	20.66	26.15	33
Lithology		Gabbro	Gabbro	Gabbro	Gabbro	Gabbro
Alteration Assemblage		Ep-Chl-Qt-Rut-Py	Ep-Chl-Ab-Rut	Ab-Rut-Qt-Chl	Ep-Ab-Rut-Chl	Ep-Ab-Rut-Chl-Qt
Alteration		Intermediate	Intermediate	Proximal	Intermediate	Intermediate
SiO_2	*%*	40.70	44.00	39.90	40.50	42.20
Al_2O_3		14.35	14.10	13.05	14.65	13.70
Fe_2O_3		9.57	9.21	9.29	8.98	11.05
CaO		9.10	8.31	10.55	8.92	10.05
MgO		6.10	5.30	4.16	4.37	4.88
Na_2O		2.14	2.33	3.63	3.77	3.13
K_2O		1.81	2.34	0.46	1.69	0.18
Cr_2O_3		0.03	0.03	0.01	0.01	<0.01
TiO_2		1.64	1.61	1.95	1.74	2.15
MnO		0.15	0.13	0.15	0.14	0.17
P_2O_5		0.18	0.18	0.19	0.19	0.26
SrO		0.02	0.02	0.03	0.03	0.03
BaO		0.01	0.01	<0.01	0.01	<0.01
LOI		13.40	13.30	15.65	14.30	10.75
Total		99.20	100.87	99.02	99.30	98.55
C		2.92	3.15	3.98	3.58	2.11
S		<0.01	<0.01	<0.01	<0.01	<0.01
Ba	*ppm*	113.50	126.00	28.60	111.00	45.80
Ce		19.40	20.50	11.60	21.30	27.90
Cr		200.00	190.00	90.00	50.00	30.00
Cs		0.41	0.54	0.11	0.55	0.19
Dy		3.66	3.82	3.82	3.86	5.22
Er		2.05	2.19	2.09	1.98	2.67
Eu		1.25	1.29	1.30	1.38	1.81
Ga		17.50	16.50	15.40	18.80	18.50
Gd		4.25	4.05	4.04	4.32	5.54
Ge		<5	<5	<5	<5	<5
Hf		2.80	3.00	3.10	3.10	4.20
Ho		0.76	0.80	0.77	0.80	1.00
La		7.50	7.90	3.70	8.30	10.60
Lu		0.26	0.30	0.26	0.26	0.36
Nb		7.00	7.40	7.90	7.20	9.60
Nd		13.10	14.40	10.30	14.70	19.00
Pr		2.75	3.02	1.93	2.99	3.99
Rb		26.10	36.00	6.00	25.80	2.60
Sm		3.33	3.95	3.45	3.60	4.77
Sn		1.00	2.00	1.00	1.00	1.00
Sr		166.00	163.50	236.00	217.00	267.00
Ta		0.50	0.50	0.50	0.40	0.60
Tb		0.60	0.64	0.62	0.63	0.87
Th		0.50	0.56	0.48	0.57	0.73
Tm		0.31	0.28	0.29	0.28	0.39
U		0.20	0.17	0.19	0.21	0.31
V		228.00	233.00	227.00	286.00	296.00
W		1.00	1.00	8.00	10.00	1.00
Y		17.90	18.50	19.10	19.00	25.50
Yb		1.67	1.84	1.98	2.02	2.34
Zr		123.00	135.00	129.00	138.00	179.00
As		1.00	1.50	1.60	1.50	1.90
Bi		0.01	0.01	<0.01	0.01	0.01
Hg		<0.005	<0.005	<0.005	<0.005	<0.005
In		0.03	0.03	0.05	0.04	0.06

Abbreviations:
D = depth
WL = wavelength

Units:
MD = mafic dyke
MBX = mafic breccia

MT = mafic tuff
MLT = mafic lapilli tuff

Table C.1.1. Whole Rock Geochemistry and Terraspec™ Data for Argyle Samples

Sample ID	183084	183085	183086	183087	183088
Hole ID	AE-16-04	AE-16-04	AE-16-04	AE-16-04	AE-16-04
Depth (m)	6.11	13.6	20.66	26.15	33
Lithology	Gabbro	Gabbro	Gabbro	Gabbro	Gabbro
Alteration Assemblage	Ep-Chl-Qt-Rut-Py	Ep-Chl-Ab-Rut	Ab-Rut-Qt-Chl	Ep-Ab-Rut-Chl	Ep-Ab-Rut-Chl-Qt
Alteration	Intermediate	Intermediate	Proximal	Intermediate	Intermediate
Re	0.00	<0.001	0.00	<0.001	<0.001
Sb	0.09	0.14	0.11	0.14	0.18
Se	<0.2	<0.2	0.20	<0.2	<0.2
Te	0.01	0.01	0.01	0.01	<0.01
Tl	0	0	<0.02	0	<0.02
Ag	<0.5	<0.5	<0.5	<0.5	<0.5
Cd	<0.5	<0.5	<0.5	<0.5	1
Co	40	35	31	30	36
Cu	20	9	6	35	55
Li	30	10	10	10	30
Mo	<1	<1	<1	<1	<1
Ni	62	48	26	22	28
Pb	<2	<2	<2	<2	<2
Sc	29	27	26	28	32
Zn	59	47	55	48	81
Au	0.00	0.00	0.18	0.03	0.00
C *%*	2.70	2.84	3.70	3.40	1.94
CO_2	9.90	10.40	13.50	12.40	7.10
AlOH WL *nm*	2205.55	2205.51	2191.09	2200.71	2227.23
AlOH D	0.19	0.12	0.32	0.23	0.05
FeOH WL	2254.44	2247.15	2255.41	2251.83	2257.07
FeOH D	0.25	0.08	0.08	0.11	0.16
AlOH D/FeOH D	0.74	1.63	4.14	2.04	0.33

Abbreviations:
D = depth
WL = wavelength

Units:
MD = mafic dyke
MBX = mafic breccia
MT = mafic tuff
MLT = mafic lapilli tuff

Table C.1.1. Whole Rock Geochemistry and Terraspec™ Data for Argyle Samples

Sample ID		183089	183090	183091	183092	183093
Hole ID		AE-16-04	AE-16-04	AE-16-04	AE-16-04	AE-16-20
Depth (m)		39.9	47.49	55.73	61.13	5.7
Lithology		Gabbro	Gabbro	Gabbro	MLT	Gabbro
Alteration Assemblage		Ab-Ank-Py	Chl-Ab-Rut	Ep-Ab-Chl	Ep-Chl	Ab-Chl-Rut
Alteration		Proximal	Proximal	Proximal	Distal	Intermediate
SiO_2	*%*	48.30	42.90	42.60	52.10	44.90
Al_2O_3		17.25	12.75	13.85	13.30	17.95
Fe_2O_3		11.20	12.50	10.55	5.70	11.85
CaO		3.22	8.47	10.50	7.70	5.27
MgO		1.34	4.84	5.90	6.60	5.50
Na_2O		6.82	3.37	2.77	3.98	4.85
K_2O		1.16	0.23	0.47	0.27	0.36
Cr_2O_3		<0.01	<0.01	0.03	0.02	<0.01
TiO_2		1.18	2.44	1.91	0.86	2.45
MnO		0.15	0.16	0.16	0.12	0.13
P_2O_5		0.37	0.25	0.21	0.16	0.29
SrO		0.02	0.02	0.03	0.03	0.03
BaO		0.01	<0.01	0.01	<0.01	0.01
LOI		8.50	11.55	11.70	9.15	6.65
Total		99.52	99.48	100.69	99.99	100.24
C		1.76	2.52	2.28	1.68	0.86
S		2.73	<0.01	<0.01	<0.01	<0.01
Ba	*ppm*	82.80	44.50	46.10	37.30	95.90
Ce		101.50	31.10	25.60	20.00	30.70
Cr		10.00	20.00	180.00	150.00	20.00
Cs		0.16	0.08	0.23	0.06	0.13
Dy		15.15	5.31	4.70	2.83	5.44
Er		8.69	2.95	2.41	1.56	2.79
Eu		4.16	1.73	1.59	1.18	1.68
Ga		25.10	18.90	16.50	12.70	22.00
Gd		15.40	6.40	5.27	3.09	5.78
Ge		<5	<5	<5	<5	<5
Hf		16.40	4.40	4.00	2.20	4.30
Ho		3.08	1.07	0.94	0.57	1.03
La		38.70	12.00	9.60	8.80	11.90
Lu		1.32	0.39	0.32	0.25	0.38
Nb		38.30	10.40	9.10	4.60	10.80
Nd		62.10	21.60	17.40	10.80	21.50
Pr		13.75	4.30	3.59	2.43	4.35
Rb		15.50	3.50	7.40	4.70	5.90
Sm		15.70	5.48	4.69	2.56	5.29
Sn		2.00	1.00	1.00	2.00	1.00
Sr		144.50	160.50	240.00	222.00	202.00
Ta		2.40	0.70	0.60	0.30	0.70
Tb		2.40	0.95	0.79	0.43	0.85
Th		3.36	0.80	0.61	1.80	0.80
Tm		1.23	0.44	0.36	0.23	0.37
U		1.37	0.33	0.31	1.16	0.33
V		86.00	356.00	267.00	120.00	304.00
W		11.00	1.00	1.00	1.00	1.00
Y		80.20	26.70	22.70	15.20	26.40
Yb		8.75	2.68	2.34	1.53	2.68
Zr		769.00	199.00	163.00	95.00	184.00
As		162.00	2.00	1.50	0.60	12.50
Bi		0.07	0.01	0.01	0.01	0.01
Hg		<0.005	<0.005	<0.005	<0.005	<0.005
In		0.10	0.07	0.05	0.07	0.06

Abbreviations:

D = depth

WL = wavelength

Units:

MD = mafic dyke

MBX = mafic breccia

MT = mafic tuff

MLT = mafic lapilli tuff

Table C.1.1. Whole Rock Geochemistry and Terraspec™ Data for Argyle Samples

Sample ID		183089	183090	183091	183092	183093
Hole ID		AE-16-04	AE-16-04	AE-16-04	AE-16-04	AE-16-20
Depth (m)		39.9	47.49	55.73	61.13	5.7
Lithology		Gabbro	Gabbro	Gabbro	MLT	Gabbro
Alteration Assemblage		Ab-Ank-Py	Chl-Ab-Rut	Ep-Ab-Chl	Ep-Chl	Ab-Chl-Rut
Alteration		Proximal	Proximal	Proximal	Distal	Intermediate
Re		<0.001	0.00	<0.001	0.00	<0.001
Sb		0.11	0.15	0.11	0.14	0.13
Se		5.70	0.30	<0.2	0.30	0.20
Te		0.41	0.01	<0.01	<0.01	<0.01
Tl		<0.02	<0.02	<0.02	<0.02	<0.02
Ag		1	<0.5	<0.5	<0.5	<0.5
Cd		<0.5	<0.5	<0.5	<0.5	<0.5
Co		11	40	37	21	38
Cu		41	54	83	5	29
Li		<10	30	40	20	20
Mo		2	1	<1	<1	<1
Ni		1	25	48	58	25
Pb		<2	<2	<2	<2	<2
Sc		7	36	32	19	30
Zn		71	76	65	36	85
Au		8.60	0.02	0.01	0.00	0.00
C	*%*	1.59	2.39	2.16	1.59	0.77
CO_2		5.80	8.70	7.90	5.80	2.80
AlOH WL	*nm*	2195.95	-	-	-	-
AlOH D		0.27	-	-	-	-
FeOH WL		-	2256.19	2255.59	2251.68	2255.43
FeOH D		-	0.20	0.23	0.30	0.25
AlOH D/FeOH D		-	-	-	-	-

Abbreviations:
D = depth
WL = wavelength

Units:
MD = mafic dyke
MBX = mafic breccia
MT = mafic tuff
MLT = mafic lapilli tuff

Table C.1.1. Whole Rock Geochemistry and Terraspec™ Data for Argyle Samples

Sample ID		183094	183095	183096	183097	183098
Hole ID		AE-16-20	AE-16-20	AE-16-20	AE-16-20	AE-16-20
Depth (m)		11.4	16.76	21.42	33.5	39.2
Lithology		Gabbro	Gabbro	Gabbro	Gabbro	Gabbro
Alteration Assemblage		Ep-Ab-Chl	Ab-Chl-Rut-Ank spots	Ab-Rut-Qt-Chl-Ank-Py	Ab-Rut-Chl-Ank	Rut-Py-Qt
Alteration		Proximal	Proximal	Proximal	Proximal	Proximal
SiO_2	*%*	47.30	38.60	50.80	42.40	40.50
Al_2O_3		15.50	15.40	14.50	13.10	14.35
Fe_2O_3		13.40	17.80	10.60	13.75	13.50
CaO		7.31	5.62	5.86	6.86	6.56
MgO		5.95	3.82	1.93	3.70	5.01
Na_2O		3.46	2.28	3.22	4.22	3.55
K_2O		0.10	0.90	1.22	0.29	0.72
Cr_2O_3		<0.01	<0.01	<0.01	<0.01	<0.01
TiO_2		2.29	4.89	2.42	3.41	3.10
MnO		0.20	0.27	0.20	0.22	0.18
P_2O_5		0.32	0.51	1.00	0.43	0.48
SrO		0.05	0.02	0.02	0.03	0.02
BaO		<0.01	0.01	0.01	0.01	0.01
LOI		3.35	9.95	7.14	10.90	10.25
Total		99.23	100.07	98.92	99.32	98.23
C		0.12	1.96	1.52	2.70	2.32
S		<0.01	0.12	0.35	0.01	0.17
Ba	*ppm*	38.40	82.00	130.00	54.70	64.20
Ce		36.70	58.20	80.90	52.50	50.10
Cr		10.00	10.00	10.00	10.00	30.00
Cs		0.03	0.23	0.18	0.07	0.14
Dy		6.15	9.67	12.25	8.38	6.24
Er		3.35	5.18	6.51	4.44	3.08
Eu		2.12	3.30	4.15	2.61	2.40
Ga		22.30	29.20	27.20	22.30	22.50
Gd		6.60	10.85	14.20	8.98	7.61
Ge		<5	<5	<5	<5	<5
Hf		5.40	8.70	9.60	7.10	6.30
Ho		1.22	1.97	2.44	1.64	1.24
La		14.10	21.80	31.30	20.20	20.20
Lu		0.46	0.71	0.82	0.56	0.48
Nb		12.60	23.10	26.70	18.10	18.20
Nd		25.10	39.50	55.00	35.40	30.60
Pr		5.15	8.16	11.50	7.34	6.66
Rb		1.40	12.80	15.40	4.50	10.70
Sm		6.58	10.25	14.15	8.86	7.37
Sn		2.00	3.00	3.00	2.00	2.00
Sr		373.00	140.00	144.50	211.00	137.00
Ta		0.80	1.50	1.70	1.30	1.20
Tb		1.08	1.64	2.08	1.40	1.16
Th		1.05	1.56	1.88	1.22	1.68
Tm		0.50	0.75	0.88	0.64	0.47
U		0.40	0.70	0.84	0.48	0.68
V		274.00	348.00	106.00	282.00	312.00
W		1.00	10.00	2.00	4.00	3.00
Y		31.40	50.00	61.60	41.30	31.40
Yb		3.05	4.90	5.84	4.12	3.28
Zr		232.00	389.00	441.00	305.00	302.00
As		16.70	23.60	57.60	3.20	4.00
Bi		<0.01	0.01	0.01	0.01	0.01
Hg		<0.005	<0.005	<0.005	<0.005	<0.005
In		0.02	0.11	0.09	0.09	0.07

Abbreviations:

D = depth

WL = wavelength

Units:

MD = mafic dyke

MBX = mafic breccia

MT = mafic tuff

MLT = mafic lapilli tuff

Table C.1.1. Whole Rock Geochemistry and Terraspec™ Data for Argyle Samples

Sample ID		183094	183095	183096	183097	183098
Hole ID		AE-16-20	AE-16-20	AE-16-20	AE-16-20	AE-16-20
Depth (m)		11.4	16.76	21.42	33.5	39.2
Lithology		Gabbro	Gabbro	Gabbro	Gabbro	Gabbro
Alteration Assemblage		Ep-Ab-Chl	Ab-Chl-Rut-Ank spots	Ab-Rut-Qt-Chl-Ank-Py	Ab-Rut-Chl-Ank	Rut-Py-Qt
Alteration		Proximal	Proximal	Proximal	Proximal	Proximal
Re		<0.001	0.00	0.00	0.00	0.00
Sb		0.61	0.38	0.18	0.16	0.12
Se		0.40	0.20	0.40	0.40	0.30
Te		<0.01	<0.01	<0.01	<0.01	<0.01
Tl		<0.02	<0.02	<0.02	<0.02	<0.02
Ag		<0.5	<0.5	<0.5	<0.5	<0.5
Cd		<0.5	1	1	<0.5	<0.5
Co		46	46	23	32	37
Cu		49	12	23	11	31
Li		10	20	10	20	30
Mo		1	2	2	1	2
Ni		25	2	<1	<1	43
Pb		3	<2	<2	<2	5
Sc		29	31	16	23	24
Zn		113	221	132	112	115
Au		0.00	0.01	0.04	0.03	0.00
C	*%*	0.10	1.76	1.41	2.44	2.11
CO_2		0.40	6.40	5.20	9.00	7.70
AlOH WL	*nm*	-	2197.11	2194.88	2203.42	2207.16
AlOH D		-	0.11	0.15	0.06	0.07
FeOH WL		2252.01	2257.52	2257.61	2261.70	2256.03
FeOH D		0.16	0.10	0.18	0.17	0.17
AlOH D/FeOH D		-	1.09	0.85	0.35	0.40

Abbreviations:	**Units:**	
D = depth	MD = mafic dyke	MT = mafic tuff
WL = wavelength	MBX = mafic breccia	MLT = mafic lapilli tuff

Table C.1.1. Whole Rock Geochemistry and Terraspec™ Data for Argyle Samples

Sample ID		183099	183100	195902	195904	195905
Hole ID		AE-16-20	AE-16-20	BN-14-187	BN-14-187	BN-14-187
Depth (m)		43.85	52	7	15.64	24.24
Lithology		MF	MD	Gabbro	Gabbro	Gabbro
Alteration Assemblage		Qt-Cal	Ep-Ab-Chl	Ab-Rut	Ab-Rut	Ab-Hem-Qt-Py
Alteration		Distal	Distal	Moderate	Moderate	Strong
SiO_2	*%*	47.60	50.80	45.10	39.60	54.50
Al_2O_3		14.30	18.55	14.40	13.70	16.25
Fe_2O_3		5.96	7.66	9.11	10.15	10.70
CaO		9.12	7.10	7.98	8.68	3.89
MgO		6.11	5.34	5.84	7.37	1.84
Na_2O		4.70	5.49	4.13	2.68	5.95
K_2O		0.14	0.29	0.24	1.08	0.89
Cr_2O_3		0.04	0.02	0.03	0.03	<0.01
TiO_2		0.75	1.03	1.24	1.53	1.61
MnO		0.18	0.11	0.17	0.17	0.18
P_2O_5		0.15	0.16	0.14	0.19	0.56
SrO		0.02	0.03	0.02	0.02	0.02
BaO		<0.01	0.01	<0.01	0.01	0.01
LOI		9.85	3.65	12.85	14.70	5.32
Total		98.92	100.24	101.25	99.91	101.72
C		1.91	0.33	2.97	3.39	1.14
S		<0.01	0.01	<0.01	<0.01	0.24
Ba	*ppm*	30.10	52.50	22.60	108.00	114.00
Ce		21.70	21.20	15.50	20.10	89.50
Cr		280.00	130.00	190.00	200.00	10.00
Cs		0.02	0.08	0.11	0.15	0.20
Dy		2.59	3.50	4.22	3.70	13.70
Er		1.60	2.12	2.37	1.93	7.80
Eu		0.89	1.10	1.16	1.27	4.10
Ga		15.90	18.20	16.00	15.40	27.50
Gd		2.64	3.57	3.93	3.62	14.20
Ge		<5	<5	<5	<5	<5
Hf		2.20	2.50	2.50	3.00	12.90
Ho		0.58	0.78	0.93	0.78	2.95
La		10.00	9.40	5.90	7.90	35.00
Lu		0.26	0.29	0.38	0.23	1.06
Nb		5.20	7.30	3.30	6.90	32.10
Nd		11.10	12.40	11.60	14.00	58.10
Pr		2.57	2.65	2.23	2.94	12.75
Rb		2.20	4.40	3.50	16.20	12.90
Sm		2.66	3.35	3.78	3.89	14.50
Sn		1.00	1.00	1.00	1.00	5.00
Sr		185.50	246.00	186.50	175.00	184.00
Ta		0.30	0.30	0.20	0.40	1.90
Tb		0.42	0.59	0.70	0.65	2.31
Th		2.62	2.29	0.81	0.48	2.44
Tm		0.26	0.28	0.35	0.30	1.16
U		1.89	1.48	0.44	0.22	1.02
V		121.00	171.00	231.00	212.00	40.00
W		1.00	1.00	3.00	4.00	35.00
Y		14.50	19.20	23.20	18.60	72.50
Yb		1.76	2.09	2.29	1.89	7.03
Zr		93.00	107.00	88.00	116.00	544.00
As		1.80	51.60	0.80	0.30	0.80
Bi		0.14	0.02	0.02	0.02	0.05
Hg		<0.005	<0.005	<0.005	<0.005	<0.005
In		0.03	0.01	0.05	0.03	0.07

Abbreviations:
D = depth
WL = wavelength

Units:
MD = mafic dyke
MBX = mafic breccia
MT = mafic tuff
MLT = mafic lapilli tuff

Table C.1.1. Whole Rock Geochemistry and Terraspec™ Data for Argyle Samples

Sample ID	183099	183100	195902	195904	195905
Hole ID	AE-16-20	AE-16-20	BN-14-187	BN-14-187	BN-14-187
Depth (m)	43.85	52	7	15.64	24.24
Lithology	MF	MD	Gabbro	Gabbro	Gabbro
Alteration Assemblage	Qt-Cal	Ep-Ab-Chl	Ab-Rut	Ab-Rut	Ab-Hem-Qt-Py
Alteration	Distal	Distal	Moderate	Moderate	Strong
Re	<0.001	<0.001	<0.001	0.00	0.00
Sb	0.18	0.34	<0.05	<0.05	<0.05
Se	0.40	0.20	<0.2	<0.2	0.20
Te	<0.01	0.01	<0.01	<0.01	0.01
Tl	<0.02	<0.02	<0.02	<0.02	<0.02
Ag	<0.5	<0.5	<0.5	<0.5	<0.5
Cd	1	<0.5	<0.5	<0.5	<0.5
Co	23	24	30	41	11
Cu	58	72	13	68	4
Li	10	10	30	30	10
Mo	<1	1	<1	2	3
Ni	135	39	44	111	2
Pb	13	4	<2	<2	<2
Sc	19	25	36	26	14
Zn	89	60	152	64	110
Au	0.00	0.00	0.00	0.00	0.13
C *%*	1.75	0.28	2.99	3.34	1.16
CO_2	6.40	1.00	11.00	12.20	4.30
AlOH WL *nm*	-	2227.24	-	-	-
AlOH D	-	0.12	-	-	-
FeOH WL	2253.72	2255.33	-	-	-
FeOH D	0.31	0.27	-	-	-
AlOH D/FeOH D	-	0.45	-	-	-

Abbreviations:
D = depth
WL = wavelength

Units:
MD = mafic dyke
MBX = mafic breccia
MT = mafic tuff
MLT = mafic lapilli tuff

Table C.1.1. Whole Rock Geochemistry and Terraspec™ Data for Argyle Samples

Sample ID		195906	195907	195908	195909	195910
Hole ID		BN-14-187	BN-14-187	BN-14-187	BN-14-187	BN-14-187
Depth (m)		30.84	35.02	39.81	45.35	47.85
Lithology		Gabbro	Gabbro	Gabbro	Gabbro	Gabbro
Alteration Assemblage		Ab-Hem-Chl-Py	Chl-Py-Ab-Hem	Ab-Py-Qt	Ab-Chl	Chl-Ab
Alteration		Strong	Strong	Strong	Strong	Strong
SiO_2	*%*	45.10	49.50	45.30	45.90	47.60
Al_2O_3		12.65	13.65	13.60	17.00	14.50
Fe_2O_3		13.50	12.25	10.25	12.75	12.60
CaO		7.18	6.35	7.81	4.37	5.89
MgO		3.47	2.89	2.50	2.75	2.95
Na_2O		4.18	5.02	7.75	5.63	4.58
K_2O		0.60	0.52	0.13	0.95	0.71
Cr_2O_3		<0.01	<0.01	<0.01	<0.01	<0.01
TiO_2		2.94	2.51	0.44	3.13	2.20
MnO		0.25	0.24	0.21	0.18	0.21
P_2O_5		0.50	0.48	0.39	0.70	0.95
SrO		0.02	0.03	0.03	0.03	0.02
BaO		0.01	0.01	<0.01	0.01	0.01
LOI		10.20	8.53	9.76	6.69	7.45
Total		100.60	101.98	98.17	100.09	99.67
C		2.55	2.09	2.88	1.37	1.64
S		0.10	0.07	4.31	0.04	0.10
Ba	*ppm*	91.10	102.00	26.10	101.50	113.00
Ce		53.40	56.90	48.30	67.30	75.40
Cr		<10	<10	<10	<10	<10
Cs		0.10	0.17	0.02	0.26	0.13
Dy		9.95	9.30	6.92	9.44	11.40
Er		5.10	5.19	4.20	5.29	6.14
Eu		2.74	2.95	2.39	3.03	4.17
Ga		23.40	23.40	10.10	25.90	25.10
Gd		9.77	9.54	7.94	10.50	13.10
Ge		<5	<5	<5	<5	<5
Hf		8.30	9.00	8.60	9.40	9.40
Ho		2.02	1.93	1.51	1.97	2.43
La		20.00	22.10	19.20	25.90	28.90
Lu		0.68	0.73	0.53	0.71	0.79
Nb		20.80	23.80	13.50	25.30	22.90
Nd		36.90	39.80	30.50	44.80	53.60
Pr		7.52	8.00	6.50	9.59	11.05
Rb		10.30	8.50	1.80	13.30	11.40
Sm		9.87	9.91	7.93	11.30	12.85
Sn		3.00	3.00	1.00	3.00	3.00
Sr		190.50	234.00	282.00	212.00	196.50
Ta		1.30	1.30	1.00	1.70	1.40
Tb		1.54	1.52	1.27	1.59	2.06
Th		1.38	1.58	1.69	1.87	1.93
Tm		0.80	0.83	0.68	0.77	0.88
U		0.68	0.67	0.89	0.79	0.83
V		199.00	135.00	19.00	153.00	115.00
W		8.00	4.00	7.00	38.00	4.00
Y		47.40	48.10	37.20	48.20	58.40
Yb		4.96	5.11	4.16	4.86	5.53
Zr		346.00	376.00	368.00	416.00	398.00
As		3.50	1.10	10.40	0.90	3.20
Bi		0.03	0.02	3.10	0.04	0.02
Hg		<0.005	<0.005	0.01	<0.005	<0.005
In		0.08	0.08	0.04	0.07	0.06

Abbreviations: **Units:**

D = depth
MD = mafic dyke
MT = mafic tuff
WL = wavelength
MBX = mafic breccia
MLT = mafic lapilli tuff

Table C.1.1. Whole Rock Geochemistry and Terraspec™ Data for Argyle Samples

Sample ID		195906	195907	195908	195909	195910
Hole ID		BN-14-187	BN-14-187	BN-14-187	BN-14-187	BN-14-187
Depth (m)		30.84	35.02	39.81	45.35	47.85
Lithology		Gabbro	Gabbro	Gabbro	Gabbro	Gabbro
Alteration Assemblage		Ab-Hem-Chl-Py	Chl-Py-Ab-Hem	Ab-Py-Qt	Ab-Chl	Chl-Ab
Alteration		Strong	Strong	Strong	Strong	Strong
Re		0.00	0.00	0.00	0.00	0.00
Sb		<0.05	<0.05	<0.05	<0.05	<0.05
Se		0.20	<0.2	3.90	<0.2	0.50
Te		<0.01	<0.01	1.97	0.02	0.01
Tl		<0.02	<0.02	<0.02	<0.02	<0.02
Ag		<0.5	<0.5	<0.5	<0.5	<0.5
Cd		<0.5	<0.5	<0.5	<0.5	<0.5
Co		26	19	65	23	21
Cu		7	8	10	42	17
Li		10	10	<10	10	10
Mo		2	3	10	4	3
Ni		<1	1	12	1	2
Pb		<2	<2	4	2	<2
Sc		25	18	6	15	16
Zn		130	122	30	115	123
Au		0.00	0.00	7.84	0.05	0.01
C	*%*	2.56	2.04	2.78	1.41	2.05
CO_2		9.40	7.50	10.20	5.20	7.50
AlOH WL	*nm*	-	-	-	-	-
AlOH D		-	-	-	-	-
FeOH WL		-	-	-	-	-
FeOH D		-	-	-	-	-
AlOH D/FeOH D		-	-	-	-	-

Abbreviations:
D = depth
WL = wavelength

Units:
MD = mafic dyke
MBX = mafic breccia
MT = mafic tuff
MLT = mafic lapilli tuff

Table C.1.1. Whole Rock Geochemistry and Terraspec™ Data for Argyle Samples

Sample ID		195913	195915	195917	195918	195922
Hole ID		BN-14-189	BN-14-189	BN-14-189	BN-14-189	BN-14-188
Depth (m)		10.46	13.82	18	21.68	5.52
Lithology		Gabbro	Gabbro	Gabbro	Gabbro	Gabbro
Alteration Assemblage		Qt-Ank-Ab	Ab-Chl	Ab-Chl-Ank	Ab-Rut	Cal
Alteration		Strong	Strong	Strong	Moderate	Weak
SiO_2	*%*	38.90	38.00	52.80	51.10	43.40
Al_2O_3		9.85	9.48	14.50	15.05	15.50
Fe_2O_3		16.05	16.35	9.58	10.40	10.75
CaO		8.68	8.87	4.86	6.25	7.97
MgO		4.59	5.43	2.42	2.71	7.32
Na_2O		2.58	2.39	5.72	4.23	3.36
K_2O		0.45	0.23	0.61	1.43	0.11
Cr_2O_3		<0.01	<0.01	<0.01	<0.01	0.03
TiO_2		4.82	4.08	2.07	2.20	1.71
MnO		0.26	0.25	0.14	0.16	0.13
P_2O_5		0.32	0.21	0.26	0.48	0.22
SrO		0.02	0.02	0.02	0.02	0.02
BaO		<0.01	<0.01	0.01	0.04	<0.01
LOI		13.05	13.55	7.48	6.70	10.35
Total		99.57	98.86	100.47	100.77	100.87
C		3.41	3.43	1.72	1.26	1.70
S		0.20	0.21	0.32	0.01	<0.01
Ba	*ppm*	43.30	17.90	79.10	364.00	14.10
Ce		33.00	24.90	67.40	63.30	23.00
Cr		<10	<10	<10	<10	240.00
Cs		0.08	0.06	0.10	0.48	0.20
Dy		6.30	5.37	10.40	9.55	4.27
Er		3.62	2.95	6.59	5.62	2.22
Eu		2.07	1.84	2.61	2.88	1.33
Ga		17.90	18.00	21.80	24.80	17.80
Gd		6.64	5.65	10.55	10.00	4.24
Ge		<5	<5	<5	<5	<5
Hf		5.80	4.30	14.60	10.00	3.40
Ho		1.38	1.21	2.33	2.03	0.91
La		12.30	9.10	25.80	24.10	8.90
Lu		0.43	0.36	0.89	0.73	0.29
Nb		16.60	10.70	23.80	23.60	7.80
Nd		24.00	18.80	42.20	41.60	16.20
Pr		4.76	3.77	9.25	8.48	3.41
Rb		7.00	4.20	10.30	27.20	2.00
Sm		6.72	5.14	10.50	9.97	4.49
Sn		2.00	2.00	2.00	3.00	1.00
Sr		177.50	199.00	187.50	160.00	189.50
Ta		1.00	0.70	1.70	1.80	0.50
Tb		1.09	0.91	1.78	1.70	0.72
Th		0.91	0.65	2.75	2.12	0.63
Tm		0.54	0.44	1.06	0.80	0.34
U		0.37	0.30	1.15	0.87	0.20
V		467.00	603.00	166.00	162.00	228.00
W		2.00	1.00	21.00	4.00	2.00
Y		32.30	26.90	57.80	49.20	21.00
Yb		3.01	2.60	6.25	4.93	2.10
Zr		229.00	173.00	626.00	400.00	144.00
As		1.90	1.00	2.60	1.40	1.00
Bi		0.02	0.02	0.03	0.02	0.01
Hg		0.01	<0.005	<0.005	<0.005	<0.005
In		0.08	0.08	0.06	0.05	0.06

Abbreviations:	**Units:**	
D = depth	MD = mafic dyke	MT = mafic tuff
WL = wavelength	MBX = mafic breccia	MLT = mafic lapilli tuff

Table C.1.1. Whole Rock Geochemistry and Terraspec™ Data for Argyle Samples

Sample ID	195913	195915	195917	195918	195922
Hole ID	BN-14-189	BN-14-189	BN-14-189	BN-14-189	BN-14-188
Depth (m)	10.46	13.82	18	21.68	5.52
Lithology	Gabbro	Gabbro	Gabbro	Gabbro	Gabbro
Alteration Assemblage	Qt-Ank-Ab	Ab-Chl	Ab-Chl-Ank	Ab-Rut	Cal
Alteration	Strong	Strong	Strong	Moderate	Weak
Re	0.00	0.00	0.00	0.00	<0.001
Sb	0.07	0.07	<0.05	0.06	<0.05
Se	<0.2	0.20	0.40	<0.2	<0.2
Te	<0.01	<0.01	0.01	<0.01	<0.01
Tl	<0.02	<0.02	<0.02	0	<0.02
Ag	<0.5	<0.5	<0.5	<0.5	<0.5
Cd	1	<0.5	<0.5	<0.5	<0.5
Co	39	50	21	19	41
Cu	18	13	45	35	15
Li	10	20	10	10	40
Mo	2	1	2	2	<1
Ni	4	2	3	4	87
Pb	2	2	<2	<2	<2
Sc	34	44	18	16	27
Zn	119	139	69	83	69
Au	0.00	0.00	1.78	0.01	0.00
C *%*	3.41	3.34	1.70	1.24	1.65
CO_2	12.50	12.20	6.20	4.50	6.00
AlOH WL *nm*	-	-	-	-	-
AlOH D	-	-	-	-	-
FeOH WL	-	-	-	-	-
FeOH D	-	-	-	-	-
AlOH D/FeOH D	-	-	-	-	-

Abbreviations:
D = depth
WL = wavelength

Units:
MD = mafic dyke
MBX = mafic breccia
MT = mafic tuff
MLT = mafic lapilli tuff

Table C.1.1. Whole Rock Geochemistry and Terraspec™ Data for Argyle Samples

Sample ID		195923	195924	195925	195926	195928
Hole ID		BN-14-188	BN-14-188	BN-14-188	BN-14-188	BN-14-188
Depth (m)		11.72	15.46	20.5	26.56	34.61
Lithology		Gabbro	Gabbro	Gabbro	Gabbro	Gabbro
Alteration Assemblage		Ab	Ab-Chl-Ank-Rut	Ab-Chl-Ank	Chl-Ank-Ab	Ab-Chl-Ank
Alteration		Moderate	Strong	Strong	Strong	Strong
SiO_2	*%*	40.60	41.20	38.40	44.10	48.40
Al_2O_3		14.85	12.20	10.55	11.65	14.70
Fe_2O_3		8.48	16.90	17.30	14.40	13.60
CaO		10.35	7.26	8.13	9.42	5.58
MgO		5.90	3.80	5.08	4.16	3.17
Na_2O		2.62	3.60	1.63	2.89	4.89
K_2O		0.84	0.34	0.55	0.10	0.43
Cr_2O_3		0.03	<0.01	<0.01	<0.01	<0.01
TiO_2		1.39	3.32	4.42	3.63	2.10
MnO		0.14	0.28	0.27	0.28	0.19
P_2O_5		0.16	1.29	0.36	0.59	0.88
SrO		0.03	0.02	0.02	0.02	0.02
BaO		0.01	<0.01	0.01	<0.01	0.01
LOI		15.70	9.23	13.00	9.53	7.25
Total		101.10	99.44	99.72	100.77	101.22
C		3.70	2.21	3.08	1.96	1.61
S		<0.01	0.21	0.07	0.10	0.31
Ba	*ppm*	50.60	35.30	57.70	28.80	53.30
Ce		16.10	68.30	37.00	58.90	74.30
Cr		250.00	10.00	<10	<10	<10
Cs		0.31	0.09	0.08	0.06	0.06
Dy		3.13	11.45	7.05	9.27	11.10
Er		1.64	5.87	4.02	5.06	6.10
Eu		1.21	3.82	2.46	3.67	3.67
Ga		15.70	23.20	23.00	21.10	22.90
Gd		3.47	13.30	8.00	10.95	12.35
Ge		<5	<5	<5	<5	<5
Hf		2.40	7.40	5.40	8.50	9.70
Ho		0.65	2.31	1.50	1.95	2.41
La		5.80	25.10	14.20	22.40	28.40
Lu		0.22	0.68	0.45	0.66	0.77
Nb		5.20	25.50	13.30	18.00	16.40
Nd		11.70	52.00	26.90	40.80	51.40
Pr		2.37	10.10	5.34	8.32	10.80
Rb		12.40	5.40	9.10	1.90	6.40
Sm		3.31	13.30	7.04	10.50	12.85
Sn		1.00	3.00	2.00	2.00	2.00
Sr		283.00	192.50	152.00	165.00	174.00
Ta		0.30	1.50	0.80	1.20	1.10
Tb		0.55	2.00	1.25	1.61	1.90
Th		0.44	1.21	0.79	1.61	1.90
Tm		0.25	0.82	0.52	0.76	0.91
U		0.19	0.55	0.37	0.62	1.02
V		209.00	138.00	509.00	263.00	128.00
W		7.00	7.00	10.00	2.00	23.00
Y		16.00	55.50	35.60	46.40	56.50
Yb		1.46	5.04	3.40	4.39	5.27
Zr		92.00	313.00	202.00	337.00	409.00
As		0.60	1.40	2.30	2.80	3.00
Bi		0.05	0.03	0.01	0.01	0.05
Hg		<0.005	<0.005	<0.005	<0.005	<0.005
In		0.03	0.09	0.08	0.14	0.09

Abbreviations:
D = depth
WL = wavelength

Units:
MD = mafic dyke
MBX = mafic breccia
MT = mafic tuff
MLT = mafic lapilli tuff

Table C.1.1. Whole Rock Geochemistry and Terraspec™ Data for Argyle Samples

Sample ID		195923	195924	195925	195926	195928
Hole ID		BN-14-188	BN-14-188	BN-14-188	BN-14-188	BN-14-188
Depth (m)		11.72	15.46	20.5	26.56	34.61
Lithology		Gabbro	Gabbro	Gabbro	Gabbro	Gabbro
Alteration Assemblage		Ab	Ab-Chl-Ank-Rut	Ab-Chl-Ank	Chl-Ank-Ab	Ab-Chl-Ank
Alteration		Moderate	Strong	Strong	Strong	Strong
Re		<0.001	0.00	0.00	0.00	0.00
Sb		0.08	<0.05	<0.05	<0.05	<0.05
Se		0.20	<0.2	<0.2	0.20	0.40
Te		<0.01	0.01	<0.01	<0.01	0.03
Tl		<0.02	<0.02	<0.02	<0.02	<0.02
Ag		<0.5	<0.5	<0.5	<0.5	<0.5
Cd		<0.5	<0.5	<0.5	<0.5	<0.5
Co		34	31	43	34	24
Cu		104	29	6	10	280
Li		30	10	10	20	10
Mo		<1	3	1	1	3
Ni		60	1	1	<1	3
Pb		<2	<2	<2	<2	4
Sc		36	19	41	26	15
Zn		57	167	150	128	106
Au		0.04	0.04	0.00	<0.001	0.16
C	*%*	3.58	2.09	3.02	1.92	1.58
CO_2		13.10	7.70	11.10	7.00	5.80
AlOH WL	*nm*	-	-	-	-	-
AlOH D		-	-	-	-	-
FeOH WL		-	-	-	-	-
FeOH D		-	-	-	-	-
AlOH D/FeOH D		-	-	-	-	-

Abbreviations:
D = depth
WL = wavelength

Units:
MD = mafic dyke
MBX = mafic breccia

MT = mafic tuff
MLT = mafic lapilli tuff

Table C.1.1. Whole Rock Geochemistry and Terraspec™ Data for Argyle Samples

Sample ID		195931	195932	195934	195935	195936
Hole ID		AP-05-01	AP-05-01	AP-05-01	AP-05-01	AP-05-01
Depth (m)		6.14	16.9	28.86	44.04	65.3
Lithology		Gabbro	Gabbro	Gabbro	Gabbro	Gabbro
Alteration Assemblage		-	Ep-Ab	Ep-Ab	Ep-Ab-Rut	Ep-Ab-Chl
Alteration		Distal	Distal	Distal	Intermediate	Intermediate
SiO_2	*%*	45.00	47.40	56.00	45.80	52.50
Al_2O_3		13.90	13.95	15.65	17.00	14.80
Fe_2O_3		11.80	13.80	10.25	10.45	13.30
CaO		8.32	7.96	4.63	9.35	4.63
MgO		3.41	4.97	2.05	4.16	2.90
Na_2O		4.65	4.03	6.66	4.45	5.99
K_2O		0.28	0.13	0.38	0.26	0.41
Cr_2O_3		<0.01	<0.01	<0.01	<0.01	<0.01
TiO_2		2.42	2.77	1.29	2.03	1.81
MnO		0.22	0.19	0.18	0.16	0.26
P_2O_5		0.45	0.35	0.54	0.25	0.74
SrO		0.03	0.02	0.03	0.04	0.03
BaO		0.01	<0.01	0.01	0.01	0.01
LOI		8.12	4.08	3.96	6.47	3.06
Total		98.61	99.65	101.63	100.43	100.44
C		1.67	0.47	0.71	0.99	0.35
S		0.08	0.01	0.02	0.05	0.01
Ba	*ppm*	61.00	33.80	82.90	45.90	90.50
Ce		43.40	35.60	68.60	31.80	66.40
Cr		20.00	10.00	10.00	10.00	10.00
Cs		0.23	0.24	0.36	0.12	0.70
Dy		7.30	6.96	11.05	5.41	10.95
Er		3.78	3.58	6.06	2.65	5.46
Eu		2.23	2.10	3.62	1.87	3.85
Ga		20.80	19.80	25.20	20.30	25.60
Gd		8.35	7.05	11.50	5.42	11.85
Ge		<5	<5	<5	<5	<5
Hf		5.90	5.20	10.90	5.10	8.90
Ho		1.43	1.39	2.18	1.06	2.04
La		17.00	14.10	27.20	12.40	26.20
Lu		0.47	0.41	0.83	0.35	0.69
Nb		12.50	10.80	23.50	10.60	20.40
Nd		29.20	25.20	45.50	20.50	45.00
Pr		6.43	5.30	9.87	4.72	10.20
Rb		4.70	1.90	6.60	4.40	3.90
Sm		7.53	6.65	10.50	5.23	10.85
Sn		2.00	1.00	2.00	1.00	3.00
Sr		260.00	196.00	254.00	322.00	268.00
Ta		0.80	0.60	1.50	0.80	1.40
Tb		1.19	1.06	1.77	0.91	1.73
Th		1.18	0.93	2.15	0.94	1.76
Tm		0.57	0.44	0.91	0.44	0.84
U		0.45	0.33	0.87	0.36	0.69
V		218.00	370.00	45.00	257.00	73.00
W		1.00	1.00	<1	1.00	2.00
Y		37.20	33.10	57.20	28.00	55.00
Yb		3.27	3.07	5.83	2.64	4.95
Zr		241.00	204.00	462.00	204.00	372.00
As		10.30	3.40	1.90	22.20	3.60
Bi		0.01	0.01	0.01	0.01	0.01
Hg		<0.005	<0.005	<0.005	<0.005	<0.005
In		0.07	0.03	0.05	0.02	0.07

Abbreviations:

D = depth

WL = wavelength

Units:

MD = mafic dyke

MBX = mafic breccia

MT = mafic tuff

MLT = mafic lapilli tuff

Table C.1.1. Whole Rock Geochemistry and Terraspec™ Data for Argyle Samples

Sample ID	195931	195932	195934	195935	195936
Hole ID	AP-05-01	AP-05-01	AP-05-01	AP-05-01	AP-05-01
Depth (m)	6.14	16.9	28.86	44.04	65.3
Lithology	Gabbro	Gabbro	Gabbro	Gabbro	Gabbro
Alteration Assemblage	-	Ep-Ab	Ep-Ab	Ep-Ab-Rut	Ep-Ab-Chl
Alteration	Distal	Distal	Distal	Intermediate	Intermediate
Re	0.00	0.00	0.00	0.00	<0.001
Sb	0.06	0.49	0.13	0.35	0.38
Se	<0.2	<0.2	<0.2	<0.2	<0.2
Te	<0.01	<0.01	<0.01	<0.01	<0.01
Tl	0	<0.02	0	<0.02	<0.02
Ag	<0.5	<0.5	<0.5	<0.5	<0.5
Cd	<0.5	<0.5	<0.5	<0.5	<0.5
Co	29	46	13	31	21
Cu	17	77	27	64	16
Li	10	10	10	20	<10
Mo	2	1	2	1	2
Ni	16	18	2	14	2
Pb	<2	<2	<2	<2	<2
Sc	22	38	12	27	14
Zn	103	98	85	77	135
Au	<0.001	0.00	<0.001	<0.001	<0.001
C *%*	1.67	0.46	0.70	0.97	0.36
CO_2	6.10	1.70	2.60	3.60	1.30
AlOH WL *nm*	-	-	-	-	-
AlOH D	-	-	-	-	-
FeOH WL	-	-	-	-	-
FeOH D	-	-	-	-	-
AlOH D/FeOH D	-	-	-	-	-

Abbreviations:
D = depth
WL = wavelength

Units:
MD = mafic dyke
MBX = mafic breccia
MT = mafic tuff
MLT = mafic lapilli tuff

Table C.1.1. Whole Rock Geochemistry and Terraspec™ Data for Argyle Samples

Sample ID	195937	195939	195941	195941	195943
Hole ID	AP-05-01	AP-05-02	-	AP-05-02	AP-05-03
Depth (m)	66.05	15.32	-	63.24	4.46
Lithology	Gabbro	Gabbro	Gabbro	Gabbro	Gabbro
Alteration Assemblage	Ep	Chl-Ab	Ep-Ab-Chl	Ep-Ab-Chl	Ep
Alteration	Distal	Distal	Least Altered Gabbro	Weak	Intermediate
SiO$_2$ *%*	54.90	49.40	49.10	49.10	48.60
Al$_2$O$_3$	14.25	14.85	15.50	15.50	17.80
Fe$_2$O$_3$	11.50	14.05	12.95	12.95	10.50
CaO	9.80	4.96	7.19	7.19	10.05
MgO	2.05	3.19	3.87	3.87	4.20
Na$_2$O	4.00	5.79	4.50	4.50	3.28
K$_2$O	0.41	0.06	0.62	0.62	0.20
Cr$_2$O$_3$	<0.01	<0.01	<0.01	<0.01	<0.01
TiO$_2$	2.13	1.91	2.68	2.68	2.05
MnO	0.23	0.18	0.22	0.22	0.15
P$_2$O$_5$	0.66	0.88	0.40	0.40	0.25
SrO	0.05	0.02	0.06	0.06	0.06
BaO	0.01	<0.01	0.02	0.02	0.01
LOI	1.35	4.50	3.46	3.46	3.38
Total	101.34	99.79	100.57	100.57	100.53
C	0.11	0.65	0.39	0.39	0.19
S	0.01	0.01	0.04	0.04	0.01
Ba *ppm*	67.50	28.10	169.50	169.50	62.70
Ce	70.90	77.70	47.40	47.40	29.60
Cr	10.00	<10	<10	<10	20.00
Cs	0.70	0.06	0.61	0.61	0.34
Dy	11.75	12.75	8.43	8.43	4.84
Er	6.32	6.57	4.31	4.31	2.52
Eu	3.86	3.94	2.67	2.67	1.75
Ga	31.60	27.70	25.80	25.80	21.20
Gd	12.55	13.35	9.08	9.08	5.35
Ge	<5	<5	<5	<5	<5
Hf	10.80	10.70	7.10	7.10	4.10
Ho	2.33	2.43	1.57	1.57	1.02
La	28.20	30.60	18.80	18.80	11.80
Lu	0.77	0.79	0.56	0.56	0.30
Nb	24.50	25.00	14.70	14.70	10.10
Nd	46.30	54.30	32.30	32.30	20.30
Pr	10.55	11.75	7.00	7.00	4.47
Rb	3.50	0.90	9.10	9.10	3.80
Sm	11.80	13.45	8.37	8.37	5.08
Sn	3.00	3.00	2.00	2.00	1.00
Sr	454.00	162.00	568.00	568.00	573.00
Ta	1.60	1.80	1.00	1.00	0.70
Tb	1.90	2.04	1.36	1.36	0.79
Th	1.99	1.99	1.37	1.37	0.87
Tm	0.94	0.93	0.60	0.60	0.35
U	0.90	0.90	0.55	0.55	0.36
V	131.00	62.00	319.00	319.00	276.00
W	1.00	2.00	1.00	1.00	<1
Y	60.60	62.80	42.10	42.10	25.30
Yb	5.94	6.10	3.78	3.78	2.53
Zr	452.00	459.00	292.00	292.00	178.00
As	3.50	3.60	3.70	3.70	4.20
Bi	0.01	<0.01	0.01	0.01	0.01
Hg	<0.005	<0.005	<0.005	<0.005	<0.005
In	0.04	0.11	0.04	0.04	0.02

Abbreviations:
D = depth
WL = wavelength

Units:
MD = mafic dyke
MBX = mafic breccia

MT = mafic tuff
MLT = mafic lapilli tuff

Table C.1.1. Whole Rock Geochemistry and Terraspec™ Data for Argyle Samples

Sample ID		195937	195939	195941	195941	195943
Hole ID		AP-05-01	AP-05-02	-	AP-05-02	AP-05-03
Depth (m)		66.05	15.32	-	63.24	4.46
Lithology		Gabbro	Gabbro	Gabbro	Gabbro	Gabbro
Alteration Assemblage		Ep	Chl-Ab	Ep-Ab-Chl	Ep-Ab-Chl	Ep
Alteration		Distal	Distal	Least Altered Gabbro	Weak	Intermediate
Re		<0.001	<0.001	0.00	0.00	<0.001
Sb		1.07	0.22	0.60	0.60	0.61
Se		<0.2	<0.2	<0.2	<0.2	<0.2
Te		<0.01	<0.01	<0.01	<0.01	<0.01
Tl		<0.02	<0.02	<0.02	<0.02	<0.02
Ag		<0.5	<0.5	<0.5	<0.5	<0.5
Cd		<0.5	<0.5	<0.5	<0.5	<0.5
Co		16	23	33	33	33
Cu		8	9	26	26	27
Li		<10	10	<10	<10	<10
Mo		3	2	2	2	<1
Ni		1	2	3	3	25
Pb		<2	<2	<2	<2	21
Sc		19	15	30	30	27
Zn		107	157	98	98	72
Au		<0.001	<0.001	<0.001	<0.001	<0.001
C	*%*	0.12	0.66	0.40	0.40	0.21
CO_2		0.40	2.40	1.50	1.50	0.80
AlOH WL	*nm*	-	-		-	-
AlOH D		-	-		-	-
FeOH WL		-	-		-	-
FeOH D		-	-		-	-
AlOH D/FeOH D		-	-		-	-

Abbreviations:
D = depth
WL = wavelength

Units:
MD = mafic dyke
MBX = mafic breccia

MT = mafic tuff
MLT = mafic lapilli tuff

Table C.1.1. Whole Rock Geochemistry and Terraspec™ Data for Argyle Samples

Sample ID		195944	195945	195946	195947	195948
Hole ID		AP-05-03	AP-05-03	AP-05-03	AE-16-12	AE-16-12
Depth (m)		21.52	39.42	60.25	6.25	19.2
Lithology		Gabbro	Gabbro	Gabbro	Gabbro	Gabbro
Alteration Assemblage		Chl-Rut	Ep-Ab-Chl	Chl-Rut	Rut-Cal	Ep-Ab
Alteration		Intermediate	Proximal	Intermediate	Distal	Proximal
SiO_2	*%*	43.90	61.20	44.30	42.50	44.20
Al_2O_3		14.25	15.75	16.45	14.75	14.90
Fe_2O_3		12.20	6.68	10.40	9.95	10.05
CaO		8.20	3.59	8.24	9.77	11.30
MgO		2.85	0.74	3.86	6.28	5.26
Na_2O		4.72	7.51	3.26	3.47	3.15
K_2O		0.22	0.33	1.37	0.38	0.09
Cr_2O_3		<0.01	<0.01	<0.01	0.03	0.01
TiO_2		3.67	0.95	2.10	1.73	1.89
MnO		0.19	0.10	0.14	0.14	0.16
P_2O_5		0.39	0.21	0.28	0.19	0.24
SrO		0.03	0.02	0.02	0.03	0.04
BaO		<0.01	0.01	0.01	0.01	<0.01
LOI		8.76	3.40	9.75	10.20	8.19
Total		99.38	100.49	100.18	99.43	99.48
C		1.82	0.68	1.77	1.83	1.43
S		0.08	0.01	0.05	0.01	0.02
Ba	*ppm*	29.30	129.50	106.50	62.50	33.80
Ce		38.60	86.60	31.30	19.40	21.60
Cr		10.00	10.00	10.00	230.00	100.00
Cs		0.21	0.14	0.33	0.13	0.12
Dy		6.75	13.75	5.23	4.02	4.30
Er		3.31	8.11	2.87	2.07	2.27
Eu		2.21	3.99	1.67	1.46	1.52
Ga		21.60	28.90	19.10	17.80	17.30
Gd		7.20	13.45	5.89	3.98	4.23
Ge		<5	<5	<5	<5	<5
Hf		5.30	16.90	4.50	2.70	3.10
Ho		1.29	2.72	1.13	0.76	0.84
La		14.90	35.50	12.50	7.30	8.10
Lu		0.40	1.08	0.32	0.23	0.29
Nb		13.70	36.70	10.70	6.90	7.60
Nd		26.10	52.70	21.70	13.90	15.90
Pr		5.75	12.15	4.61	2.87	3.13
Rb		3.20	5.40	21.70	6.60	1.60
Sm		6.51	12.85	5.30	3.60	4.00
Sn		1.00	7.00	1.00	1.00	1.00
Sr		279.00	210.00	196.50	227.00	309.00
Ta		1.00	2.40	0.70	0.40	0.50
Tb		1.09	2.17	0.90	0.64	0.69
Th		0.99	3.55	0.75	0.48	0.50
Tm		0.47	1.22	0.40	0.29	0.30
U		0.42	1.45	0.33	0.19	0.21
V		270.00	12.00	235.00	246.00	268.00
W		2.00	2.00	2.00	1.00	1.00
Y		32.70	75.40	27.70	18.40	21.10
Yb		2.99	8.17	2.75	1.75	2.14
Zr		220.00	809.00	187.00	121.00	135.00
As		11.80	1.20	24.90	2.00	4.40
Bi		0.01	0.01	0.01	0.01	0.01
Hg		<0.005	<0.005	<0.005	<0.005	<0.005
In		0.08	0.11	0.05	0.04	0.02

Abbreviations:

D = depth

WL = wavelength

Units:

MD = mafic dyke

MBX = mafic breccia

MT = mafic tuff

MLT = mafic lapilli tuff

Table C.1.1. Whole Rock Geochemistry and Terraspec™ Data for Argyle Samples

Sample ID		195944	195945	195946	195947	195948
Hole ID		AP-05-03	AP-05-03	AP-05-03	AE-16-12	AE-16-12
Depth (m)		21.52	39.42	60.25	6.25	19.2
Lithology		Gabbro	Gabbro	Gabbro	Gabbro	Gabbro
Alteration Assemblage		Chl-Rut	Ep-Ab-Chl	Chl-Rut	Rut-Cal	Ep-Ab
Alteration		Intermediate	Proximal	Intermediate	Distal	Proximal
Re		0.00	<0.001	0.00	<0.001	<0.001
Sb		0.09	0.09	0.08	0.20	0.33
Se		<0.2	<0.2	<0.2	<0.2	<0.2
Te		<0.01	<0.01	<0.01	0.01	0.01
Tl		0	<0.02	0	<0.02	<0.02
Ag		<0.5	<0.5	<0.5	<0.5	<0.5
Cd		<0.5	<0.5	<0.5	<0.5	<0.5
Co		39	5	30	42	36
Cu		48	8	36	9	27
Li		10	<10	20	10	20
Mo		1	1	1	<1	<1
Ni		5	2	15	64	33
Pb		<2	2	<2	<2	4
Sc		22	7	26	34	32
Zn		86	98	84	62	62
Au		0.00	<0.001	0.00	0.00	0.01
C	*%*	1.76	0.69	1.69	1.70	1.34
CO_2		6.50	2.50	6.20	6.20	4.90
AlOH WL	*nm*	-	-	-	-	-
AlOH D		-	-	-	-	-
FeOH WL		-	-	-	2253.83	2256.97
FeOH D		-	-	-	0.22	0.16
AlOH D/FeOH D		-	-	-	-	-

Abbreviations:
D = depth
WL = wavelength

Units:
MD = mafic dyke
MBX = mafic breccia

MT = mafic tuff
MLT = mafic lapilli tuff

Table C.1.1. Whole Rock Geochemistry and Terraspec™ Data for Argyle Samples

Sample ID		195949	195950	294827	294828	294829
Hole ID		AE-16-12	AE-16-12	AE-17-50	AE-17-50	AE-17-50
Depth (m)		23	27.1	30.7	76.6	83.1
Lithology		Gabbro	Gabbro	MF	MF	Gabbro
Alteration Assemblage		Ank-Chl	Ank-Chl-Ab-Rut-Qt	Calc-Qt-Chl	Ser-Chl-Qt	Ab-Ser-Qt-Fuch-Rut-Chl
Alteration		Proximal	Proximal	Distal	Intermediate	Proximal
SiO_2	*%*	36.40	43.70	44.90	38.20	38.40
Al_2O_3		14.80	15.10	16.45	14.05	15.15
Fe_2O_3		9.99	9.75	11.50	10.30	9.30
CaO		10.45	6.72	10.65	10.15	9.16
MgO		4.81	2.20	6.45	4.01	4.94
Na_2O		3.41	5.66	2.74	2.23	2.47
K_2O		1.67	0.88	0.32	0.63	0.79
Cr_2O_3		0.01	<0.01	0.02	0.01	0.02
TiO_2		1.96	2.24	1.55	1.45	1.72
MnO		0.17	0.24	0.16	0.18	0.13
P_2O_5		0.22	0.64	0.17	0.18	0.22
SrO		0.02	0.02	0.04	0.02	0.03
BaO		0.02	0.01	0.01	<0.01	0.01
LOI		15.45	10.95	4.89	17.85	17.95
Total		99.38	98.11	99.85	99.26	100.29
C		3.80	2.92	0.51	4.43	4.46
S		0.05	0.15	0.03	<0.01	0.01
Ba	*ppm*	146.00	78.20	54.40	44.80	70.90
Ce		24.90	82.70	17.20	15.50	25.10
Cr		90.00	10.00	120.00	100.00	170.00
Cs		0.34	0.21	0.07	0.12	0.17
Dy		4.44	11.90	5.66	5.21	4.73
Er		2.44	6.94	3.23	3.37	2.51
Eu		1.61	3.80	1.51	1.24	1.27
Ga		19.30	22.70	21.80	16.70	17.90
Gd		4.68	12.60	5.04	4.48	4.55
Ge		<5	<5	<5	<5	<5
Hf		3.50	11.00	2.70	2.80	4.00
Ho		0.86	2.55	1.18	1.18	0.90
La		9.80	33.00	6.60	5.80	9.60
Lu		0.33	0.91	0.56	0.47	0.29
Nb		8.70	26.20	5.70	5.20	8.60
Nd		17.30	51.00	13.00	11.30	15.80
Pr		3.51	11.40	2.61	2.37	3.62
Rb		23.90	13.00	5.30	9.10	12.30
Sm		4.36	12.55	4.33	3.73	4.13
Sn		1.00	3.00	1.00	3.00	1.00
Sr		210.00	193.50	341.00	202.00	304.00
Ta		0.60	1.80	0.40	0.30	0.60
Tb		0.73	1.92	0.88	0.79	0.69
Th		0.59	2.35	0.53	0.49	0.69
Tm		0.36	1.01	0.51	0.46	0.35
U		0.25	0.97	0.25	0.26	0.27
V		280.00	131.00	242.00	218.00	233.00
W		3.00	10.00	1.00	10.00	12.00
Y		20.90	62.70	30.90	28.50	22.40
Yb		1.99	6.27	3.15	3.26	1.98
Zr		160.00	535.00	116.00	108.00	164.00
As		2.80	3.00	10.10	0.80	1.60
Bi		0.02	0.03	0.01	0.01	0.01
Hg		<0.005	<0.005	<0.005	<0.005	<0.005
In		0.04	0.09	0.01	0.07	0.05

Abbreviations:
D = depth
WL = wavelength

Units:
MD = mafic dyke
MBX = mafic breccia
MT = mafic tuff
MLT = mafic lapilli tuff

Table C.1.1. Whole Rock Geochemistry and Terraspec™ Data for Argyle Samples

Sample ID	195949	195950	294827	294828	294829
Hole ID	AE-16-12	AE-16-12	AE-17-50	AE-17-50	AE-17-50
Depth (m)	23	27.1	30.7	76.6	83.1
Lithology	Gabbro	Gabbro	MF	MF	Gabbro
Alteration Assemblage	Ank-Chl	Ank-Chl-Ab-Rut-Qt	Calc-Qt-Chl	Ser-Chl-Qt	Ab-Ser-Qt-Fuch-Rut-Chl
Alteration	Proximal	Proximal	Distal	Intermediate	Proximal
Re	0.00	0.00	0.00	<0.001	<0.001
Sb	0.19	0.13	0.14	0.08	0.11
Se	<0.2	<0.2	<0.2	<0.2	<0.2
Te	0.01	0.03	<0.01	<0.01	<0.01
Tl	<0.02	0	0	<0.02	<0.02
Ag	<0.5	<0.5	<0.5	<0.5	<0.5
Cd	<0.5	<0.5	<0.5	<0.5	<0.5
Co	35	18	43	33	35
Cu	50	14	56	1	8
Li	10	<10	20	10	20
Mo	<1	1	<1	<1	1
Ni	34	<1	73	50	48
Pb	<2	2	<2	<2	2
Sc	31	13	29	29	27
Zn	61	66	87	58	53
Au	0.01	0.01	<0.001	0.00	0.01
C *%*	3.80	2.77	0.48	3.69	3.55
CO_2	13.90	10.10	1.80	13.50	13.00
AlOH WL *nm*	2196.17	2195.18	-	2188.89	2188.79
AlOH D	0.23	0.30	-	0.44	0.43
FeOH WL	2256.71	2253.66	2255.25	2255.95	2240.80
FeOH D	0.17	0.09	0.38	0.05	0.06
AlOH D/FeOH D	1.39	3.54	-	-	6.69

Abbreviations:
D = depth
WL = wavelength

Units:
MD = mafic dyke
MBX = mafic breccia
MT = mafic tuff
MLT = mafic lapilli tuff

Table C.1.1. Whole Rock Geochemistry and Terraspec™ Data for Argyle Samples

Sample ID		294830	294831	294832	294833	294834
Hole ID		AE-17-50	AE-17-50	AE-17-50	AE-17-50	AE-17-50
Depth (m)		93	101.6	105.7	107	113.1
Lithology		Gabbro	Gabbro	Gabbro	MD	MD
Alteration Assemblage		Chl-Ab-Qt-Ank-Rut-Py	Ep-Chl-Ab-Rut	Ab-Ank-Rut-Ser-Chl-Qt	Ser-Chl-Qt-Rut	Chl-Ab
Alteration		Intermediate	Distal	Proximal	Intermediate	Distal
SiO_2	*%*	42.00	45.90	33.60	37.50	45.40
Al_2O_3		15.10	12.40	12.30	14.25	14.90
Fe_2O_3		11.00	13.20	15.40	8.75	14.40
CaO		9.64	8.77	7.79	8.70	6.20
MgO		4.93	5.77	4.50	6.89	5.90
Na_2O		4.28	2.22	4.05	2.54	3.70
K_2O		0.09	0.40	0.81	0.79	0.04
Cr_2O_3		0.01	0.00	0.00	0.03	0.01
TiO_2		2.14	2.76	3.54	1.32	3.53
MnO		0.15	0.18	0.21	0.14	0.20
P_2O_5		0.26	0.25	0.33	0.20	0.50
SrO		0.03	0.02	0.02	0.02	0.03
BaO		<0.01	0.01	0.01	0.01	<0.01
LOI		10.75	9.93	17.45	18.85	4.86
Total		100.38	101.81	100.01	99.99	99.67
C		2.03	1.87	4.71	4.74	0.36
S		0.02	<0.01	<0.01	<0.01	<0.01
Ba	*ppm*	21.10	48.10	93.30	90.20	26.30
Ce		27.80	31.10	36.00	14.30	47.50
Cr		60.00	20.00	20.00	200.00	80.00
Cs		0.01	0.47	0.13	0.23	0.01
Dy		5.13	5.54	6.49	3.58	7.01
Er		2.67	3.03	3.13	1.96	3.67
Eu		1.54	2.03	1.97	1.06	2.44
Ga		19.40	20.70	22.70	14.40	23.20
Gd		5.32	5.78	6.59	3.37	7.55
Ge		<5	<5	<5	<5	<5
Hf		4.30	4.50	5.40	2.00	6.10
Ho		1.01	1.14	1.24	0.69	1.41
La		10.50	12.00	13.10	5.30	18.70
Lu		0.35	0.33	0.45	0.25	0.46
Nb		9.90	10.00	12.80	3.90	17.40
Nd		18.50	21.50	24.50	10.20	29.00
Pr		4.05	4.45	5.10	2.11	6.62
Rb		1.40	8.50	13.70	12.60	0.80
Sm		5.17	5.45	6.24	3.27	7.35
Sn		1.00	3.00	2.00	1.00	2.00
Sr		204.00	221.00	163.00	154.00	216.00
Ta		0.60	0.50	0.70	0.10	1.00
Tb		0.85	0.90	0.97	0.58	1.18
Th		0.62	1.22	1.02	0.27	1.08
Tm		0.39	0.38	0.42	0.28	0.51
U		0.30	0.29	0.41	0.09	0.44
V		299.00	458.00	520.00	193.00	390.00
W		2.00	1.00	22.00	3.00	1.00
Y		25.10	27.40	32.20	17.20	35.00
Yb		2.48	2.57	2.95	1.70	3.23
Zr		177.00	176.00	217.00	83.00	257.00
As		1.00	2.20	0.80	2.80	4.60
Bi		0.01	0.01	0.01	0.01	0.01
Hg		<0.005	<0.005	<0.005	<0.005	<0.005
In		0.06	0.05	0.08	0.04	0.04

Abbreviations:	**Units:**	
D = depth	MD = mafic dyke	MT = mafic tuff
WL = wavelength	MBX = mafic breccia	MLT = mafic lapilli tuff

Table C.1.1. Whole Rock Geochemistry and Terraspec™ Data for Argyle Samples

Sample ID	294830	294831	294832	294833	294834
Hole ID	AE-17-50	AE-17-50	AE-17-50	AE-17-50	AE-17-50
Depth (m)	93	101.6	105.7	107	113.1
Lithology	Gabbro	Gabbro	Gabbro	MD	MD
Alteration Assemblage	Chl-Ab-Qt-Ank-Rut-Py	Ep-Chl-Ab-Rut	Ab-Ank-Rut-Ser-Chl-Qt	Ser-Chl-Qt-Rut	Chl-Ab
Alteration	Intermediate	Distal	Proximal	Intermediate	Distal
Re	0.00	<0.001	0.00	0.00	0.00
Sb	0.07	0.26	0.14	0.13	0.36
Se	<0.2	<0.2	<0.2	<0.2	<0.2
Te	<0.01	<0.01	<0.01	<0.01	<0.01
Tl	<0.02	<0.02	<0.02	<0.02	<0.02
Ag	<0.5	<0.5	<0.5	<0.5	<0.5
Cd	<0.5	<0.5	1	<0.5	<0.5
Co	38	43	46	39	45
Cu	72	7	25	40	39
Li	40	30	10	10	20
Mo	4	<1	1	1	2
Ni	27	35	23	101	52
Pb	<2	<2	<2	2	<2
Sc	32	36	36	24	30
Zn	64	72	81	59	114
Au	<0.001	<0.001	<0.001	<0.001	<0.001
C *%*	1.76	1.60	3.60	3.70	0.34
CO_2	6.40	5.90	13.20	13.60	1.30
AlOH WL *nm*	2227.24	2197.54	2191.70	2189.19	2222.25
AlOH D	0.09	0.11	0.24	0.48	0.15
FeOH WL	2254.12	2253.09	2261.72	-	2259.92
FeOH D	0.27	0.15	0.06	-	0.19
AlOH D/FeOH D	0.32	0.72	3.81	-	0.77

Abbreviations:
D = depth
WL = wavelength

Units:
MD = mafic dyke
MBX = mafic breccia
MT = mafic tuff
MLT = mafic lapilli tuff

Table C.1.1. Whole Rock Geochemistry and Terraspec™ Data for Argyle Samples

Sample ID		294835	294836	294837	294838	294839
Hole ID		AE-17-50	AE-17-50	AE-17-50	AE-16-44	AE-16-44
Depth (m)		114.55	131	144.65	5.6	63.25
Lithology		Gabbro	MCT	MLT	MF	Gabbro
Alteration Assemblage		Chl-Ep-mt-Calc	Chl-Ab-carb	carb-Chl	Chl	Chl-Rut
Alteration		Intermediate	Distal	Distal	Distal	Distal
SiO_2	*%*	45.20	50.10	51.70	43.60	42.60
Al_2O_3		12.90	13.65	14.80	17.05	15.75
Fe_2O_3		15.15	6.26	8.54	12.45	10.10
CaO		9.44	6.05	4.41	8.77	9.52
MgO		6.23	6.59	5.34	8.26	6.52
Na_2O		2.52	3.76	1.15	2.53	3.28
K_2O		0.05	0.85	2.52	0.65	0.81
Cr_2O_3		<0.002	0.04	0.02	0.02	0.03
TiO_2		3.19	0.82	0.96	1.81	1.74
MnO		0.20	0.09	0.06	0.18	0.14
P_2O_5		0.19	0.17	0.11	0.21	0.29
SrO		0.04	0.01	0.02	0.03	0.03
BaO		<0.01	0.01	0.02	0.01	0.01
LOI		4.18	9.71	9.36	4.65	9.41
Total		99.29	98.11	99.01	100.22	100.23
C		0.41	1.90	1.64	0.24	1.57
S		0.01	<0.01	<0.01	0.01	0.01
Ba	*ppm*	42.60	141.50	181.50	79.60	114.50
Ce		24.50	25.00	27.50	18.40	37.00
Cr		20.00	340.00	160.00	120.00	230.00
Cs		0.04	0.18	0.55	0.16	0.30
Dy		5.20	3.28	3.65	6.24	4.52
Er		2.73	1.97	2.03	3.65	2.20
Eu		1.65	0.92	0.96	1.47	1.74
Ga		22.30	14.60	17.40	20.40	18.80
Gd		5.11	3.12	3.92	5.98	5.36
Ge		<5	<5	<5	<5	<5
Hf		4.10	2.80	3.00	3.10	4.00
Ho		1.08	0.69	0.73	1.32	0.81
La		8.90	11.10	12.40	7.00	15.20
Lu		0.34	0.23	0.28	0.54	0.34
Nb		9.00	6.00	7.00	6.50	9.40
Nd		17.30	12.40	14.10	14.40	21.80
Pr		3.55	2.98	3.20	2.68	4.85
Rb		0.90	14.40	40.20	9.90	13.70
Sm		4.37	3.31	3.25	4.47	4.76
Sn		2.00	1.00	1.00	1.00	1.00
Sr		298.00	108.50	123.00	254.00	258.00
Ta		0.50	0.30	0.30	0.20	0.50
Tb		0.86	0.52	0.64	0.99	0.74
Th		0.57	3.08	2.91	0.68	1.88
Tm		0.36	0.28	0.28	0.51	0.32
U		0.21	2.13	1.96	0.28	0.50
V		575.00	118.00	170.00	271.00	251.00
W		1.00	1.00	4.00	<1	1.00
Y		24.70	16.90	18.00	34.40	21.30
Yb		2.16	1.73	2.00	3.37	1.97
Zr		151.00	105.00	121.00	125.00	162.00
As		3.70	1.10	1.80	50.40	3.40
Bi		<0.01	0.01	0.01	0.01	0.01
Hg		<0.005	<0.005	<0.005	<0.005	<0.005
In		0.02	0.03	0.02	0.01	0.04

Abbreviations:
D = depth
WL = wavelength

Units:
MD = mafic dyke
MBX = mafic breccia
MT = mafic tuff
MLT = mafic lapilli tuff

Table C.1.1. Whole Rock Geochemistry and Terraspec™ Data for Argyle Samples

Sample ID		294835	294836	294837	294838	294839
Hole ID		AE-17-50	AE-17-50	AE-17-50	AE-16-44	AE-16-44
Depth (m)		114.55	131	144.65	5.6	63.25
Lithology		Gabbro	MCT	MLT	MF	Gabbro
Alteration Assemblage		Chl-Ep-mt-Calc	Chl-Ab-carb	carb-Chl	Chl	Chl-Rut
Alteration		Intermediate	Distal	Distal	Distal	Distal
Re		<0.001	<0.001	<0.001	0.00	0.00
Sb		0.67	0.33	0.09	0.13	0.34
Se		0.20	<0.2	<0.2	<0.2	0.30
Te		<0.01	<0.01	<0.01	<0.01	<0.01
Tl		<0.02	<0.02	<0.02	<0.02	<0.02
Ag		<0.5	<0.5	<0.5	<0.5	<0.5
Cd		<0.5	<0.5	<0.5	<0.5	<0.5
Co		54	28	30	45	36
Cu		64	3	3	45	47
Li		10	20	10	30	20
Mo		<1	<1	<1	<1	<1
Ni		35	167	96	67	92
Pb		<2	2	<2	<2	<2
Sc		47	17	20	29	27
Zn		102	38	34	96	62
Au		<0.001	<0.001	<0.001	<0.001	0.00
C	*%*	0.34	1.53	1.38	0.18	1.41
CO_2		1.20	5.60	5.00	0.70	5.20
AlOH WL	*nm*	-	2217.60	2198.13	2225.22	-
AlOH D		-	0.18	0.34	0.24	-
FeOH WL		2251.05	2252.84	2250.68	2253.22	2256.67
FeOH D		0.23	0.26	0.22	0.39	0.24
AlOH D/FeOH D		-	0.70	1.53	0.62	-

Abbreviations:
D = depth
WL = wavelength

Units:
MD = mafic dyke
MBX = mafic breccia
MT = mafic tuff
MLT = mafic lapilli tuff

Table C.1.1. Whole Rock Geochemistry and Terraspec™ Data for Argyle Samples

Sample ID		294840	294841	294842	294843	294844
Hole ID		AE-16-44	AE-16-44	AE-16-44	AE-16-44	AE-16-44
Depth (m)		67.2	82	99.7	103	107.2
Lithology		MD	Gabbro	Gabbro	Gabbro	Gabbro
Alteration Assemblage		Chl-Ab-Hem	Chl-Ep-Ab-Carb-Mt	Ab-Ank-Qt-Chl-Rut-Py	Ank-Chl-Ab-Rut	Chl-Ep-carb
Alteration		Distal	Intermediate	Proximal	Proximal	Distal
SiO_2	*%*	44.90	49.30	49.50	41.40	49.50
Al_2O_3		14.50	12.90	14.10	12.10	14.50
Fe_2O_3		13.90	14.45	11.05	14.90	10.40
CaO		7.44	7.82	5.22	7.18	10.70
MgO		5.54	4.73	2.19	4.26	6.00
Na_2O		3.26	3.20	6.07	3.34	2.30
K_2O		0.04	0.04	0.46	0.42	0.04
Cr_2O_3		0.00	<0.002	<0.002	<0.002	0.03
TiO_2		3.39	3.60	1.52	3.49	1.80
MnO		0.20	0.23	0.19	0.17	0.15
P_2O_5		0.52	0.48	0.78	0.30	0.22
SrO		0.04	0.02	0.02	0.02	0.05
BaO		<0.01	<0.01	<0.01	0.01	<0.01
LOI		4.37	4.60	10.85	11.80	5.62
Total		98.10	101.37	101.95	99.39	101.31
C		0.32	0.58	3.03	2.91	0.70
S		0.09	<0.01	0.02	<0.01	<0.01
Ba	*ppm*	45.40	28.70	35.50	88.50	30.50
Ce		56.20	51.40	83.60	32.20	25.40
Cr		30.00	10.00	<10	<10	190.00
Cs		0.02	0.10	0.10	0.17	0.13
Dy		7.69	8.41	11.85	5.60	4.59
Er		3.75	4.44	6.58	2.89	2.38
Eu		2.80	2.79	3.69	1.75	1.41
Ga		24.30	23.60	23.80	21.70	21.60
Gd		8.70	9.54	13.00	5.83	4.83
Ge		<5	<5	<5	<5	<5
Hf		7.30	6.80	11.00	5.10	3.70
Ho		1.54	1.71	2.26	1.15	0.89
La		22.80	19.70	32.00	12.40	9.80
Lu		0.58	0.60	0.82	0.39	0.40
Nb		20.90	18.10	26.40	11.80	8.60
Nd		35.40	36.40	53.50	23.20	17.60
Pr		7.68	7.32	11.85	4.70	3.63
Rb		0.70	1.00	6.70	7.00	0.80
Sm		7.97	8.24	12.00	5.86	4.38
Sn		3.00	2.00	3.00	2.00	3.00
Sr		358.00	201.00	175.00	172.50	399.00
Ta		1.30	1.10	1.60	0.70	0.50
Tb		1.23	1.49	2.09	0.98	0.78
Th		1.65	1.17	2.26	0.81	0.61
Tm		0.54	0.60	0.88	0.41	0.34
U		0.73	0.52	0.97	0.34	0.28
V		366.00	352.00	88.00	551.00	277.00
W		<1	1.00	12.00	1.00	1.00
Y		36.70	43.70	61.10	28.80	22.90
Yb		3.65	3.96	5.56	2.44	2.02
Zr		341.00	293.00	473.00	197.00	152.00
As		4.80	4.60	0.70	1.30	5.10
Bi		0.01	<0.01	0.03	<0.01	<0.01
Hg		0.01	0.01	0.01	<0.005	<0.005
In		0.02	0.03	0.08	0.07	0.02

Abbreviations:
D = depth
WL = wavelength

Units:
MD = mafic dyke
MBX = mafic breccia
MT = mafic tuff
MLT = mafic lapilli tuff

Table C.1.1. Whole Rock Geochemistry and Terraspec™ Data for Argyle Samples

Sample ID	294840	294841	294842	294843	294844
Hole ID	AE-16-44	AE-16-44	AE-16-44	AE-16-44	AE-16-44
Depth (m)	67.2	82	99.7	103	107.2
Lithology	MD	Gabbro	Gabbro	Gabbro	Gabbro
Alteration Assemblage	Chl-Ab-Hem	Chl-Ep-Ab-Carb-Mt	Ab-Ank-Qt-Chl-Rut-Py	Ank-Chl-Ab-Rut	Chl-Ep-carb
Alteration	Distal	Intermediate	Proximal	Proximal	Distal
Re	0.00	0.00	0.02	<0.001	0.00
Sb	0.35	0.44	0.08	0.39	0.63
Se	0.40	<0.2	<0.2	<0.2	<0.2
Te	<0.01	<0.01	0.02	<0.01	<0.01
Tl	<0.02	<0.02	<0.02	<0.02	<0.02
Ag	<0.5	<0.5	<0.5	<0.5	<0.5
Cd	<0.5	<0.5	<0.5	<0.5	<0.5
Co	44	35	18	47	38
Cu	36	17	20	20	24
Li	10	10	10	30	10
Mo	2	1	23	1	<1
Ni	41	8	<1	7	49
Pb	<2	<2	<2	6	<2
Sc	28	33	10	30	31
Zn	113	79	82	107	61
Au	<0.001	<0.001	0.01	<0.001	<0.001
C *%*	0.27	0.52	2.29	2.74	0.64
CO_2	1.00	1.90	8.40	10.00	2.40
AlOH WL *nm*	2216.78	-	2190.12	2193.43	-
AlOH D	0.15	-	0.19	0.21	-
FeOH WL	2255.84	2250.90	2262.48	2252.28	2256.57
FeOH D	0.20	0.14	0.02	0.19	0.20
AlOH D/FeOH D	0.76	-	8.34	1.11	-

Abbreviations:
D = depth
WL = wavelength

Units:
MD = mafic dyke
MBX = mafic breccia
MT = mafic tuff
MLT = mafic lapilli tuff

Table C.1.1. Whole Rock Geochemistry and Terraspec™ Data for Argyle Samples

Sample ID		294845	294846	294847	294848	294849
Hole ID		AE-16-44	AE-16-43	AE-16-43	AE-16-43	AE-16-43
Depth (m)		141.9	27.85	81.65	91.8	105.25
Lithology		MBX	MLT	Gabbro	Gabbro	Gabbro
Alteration Assemblage		Chl-carb-Ep-Qt-Hem	Qt	Chl-Calc-Rut-Ab	Chl-Ab-Rut-Ank	Ab-Qt-Ank-Chl-Py-Rut
Alteration		Distal	Distal	Distal	Intermediate	Proximal
SiO_2	%	57.20	39.00	43.10	48.50	54.80
Al_2O_3		18.55	14.10	17.55	13.60	16.35
Fe_2O_3		5.75	8.69	11.50	14.80	9.23
CaO		3.86	14.60	5.63	5.42	3.80
MgO		4.00	4.71	6.72	3.92	1.64
Na_2O		6.68	1.15	5.25	2.77	6.32
K_2O		1.05	2.79	0.30	0.23	0.91
Cr_2O_3		0.00	0.01	0.03	<0.002	<0.002
TiO_2		1.29	1.43	2.15	3.51	1.42
MnO		0.03	0.13	0.13	0.19	0.10
P_2O_5		0.16	0.16	0.27	0.60	0.50
SrO		0.02	0.01	0.02	0.01	0.02
BaO		0.01	0.02	0.01	<0.01	<0.01
LOI		2.60	13.85	7.45	7.31	5.87
Total		101.20	100.65	100.11	100.86	100.96
C		0.08	2.88	0.98	1.03	1.29
S		0.01	0.03	0.01	0.06	1.48
Ba	*ppm*	145.50	171.50	49.80	32.20	48.50
Ce		37.20	15.00	29.40	63.40	103.50
Cr		30.00	100.00	230.00	<10	<10
Cs		0.11	0.46	0.04	0.03	0.21
Dy		4.92	4.99	5.37	10.45	13.70
Er		2.66	2.95	2.80	5.49	7.69
Eu		1.44	1.19	1.69	3.35	3.63
Ga		20.50	16.00	23.30	28.40	26.10
Gd		4.82	4.53	5.51	11.10	14.10
Ge		<5	<5	<5	<5	<5
Hf		4.50	2.80	4.00	9.20	15.60
Ho		0.94	1.11	1.05	2.05	2.97
La		16.60	6.10	11.30	24.70	41.40
Lu		0.43	0.41	0.32	0.80	1.12
Nb		9.00	5.50	10.10	23.40	34.00
Nd		19.30	12.10	19.70	42.90	60.60
Pr		4.56	2.38	4.19	9.10	13.80
Rb		10.70	62.10	4.70	4.00	13.50
Sm		4.31	3.94	5.25	10.75	14.30
Sn		2.00	1.00	1.00	2.00	2.00
Sr		175.00	111.50	145.00	132.50	125.50
Ta		0.50	0.20	0.50	1.40	2.20
Tb		0.86	0.79	0.83	1.78	2.37
Th		5.15	0.47	0.68	1.67	3.21
Tm		0.40	0.43	0.38	0.79	1.22
U		2.91	0.85	0.30	0.70	1.36
V		163.00	221.00	288.00	285.00	70.00
W		1.00	3.00	5.00	4.00	17.00
Y		25.10	27.20	25.90	52.60	75.40
Yb		2.62	3.10	2.35	4.71	8.22
Zr		181.00	102.00	174.00	378.00	688.00
As		9.60	14.40	1.30	3.10	89.00
Bi		0.01	<0.01	<0.01	0.01	0.05
Hg		<0.005	<0.005	<0.005	<0.005	<0.005
In		<0.005	0.02	0.06	0.11	0.06

Abbreviations:
D = depth
WL = wavelength

Units:
MD = mafic dyke
MBX = mafic breccia

MT = mafic tuff
MLT = mafic lapilli tuff

Table C.1.1. Whole Rock Geochemistry and Terraspec™ Data for Argyle Samples

Sample ID	294845	294846	294847	294848	294849
Hole ID	AE-16-44	AE-16-43	AE-16-43	AE-16-43	AE-16-43
Depth (m)	141.9	27.85	81.65	91.8	105.25
Lithology	MBX	MLT	Gabbro	Gabbro	Gabbro
Alteration Assemblage	Chl-carb-Ep-Qt-Hem	Qt	Chl-Calc-Rut-Ab	Chl-Ab-Rut-Ank	Ab-Qt-Ank-Chl-Py-Rut
Alteration	Distal	Distal	Distal	Intermediate	Proximal
Re	<0.001	0.00	0.00	0.00	0.00
Sb	0.36	0.08	0.15	0.13	0.12
Se	<0.2	<0.2	0.20	0.40	2.80
Te	<0.01	<0.01	<0.01	<0.01	0.44
Tl	<0.02	0	<0.02	<0.02	<0.02
Ag	<0.5	<0.5	<0.5	<0.5	<0.5
Cd	<0.5	<0.5	<0.5	<0.5	<0.5
Co	17	33	41	32	18
Cu	2	40	28	30	67
Li	10	20	20	30	<10
Mo	<1	1	1	2	1
Ni	16	56	60	1	1
Pb	3	<2	<2	<2	<2
Sc	17	27	28	24	9
Zn	24	69	63	88	48
Au	<0.001	<0.001	<0.001	0.02	3.95
C *%*	0.07	2.73	0.92	0.94	1.16
CO_2	0.30	10.00	3.40	3.50	4.20
AlOH WL *nm*	-	2222.70	-	-	2197.63
AlOH D	-	0.27	-	-	0.15
FeOH WL	2251.03	2247.20	2256.26	2259.83	2258.16
FeOH D	0.32	0.26	0.32	0.24	0.22
AlOH D/FeOH D	-	1.04	-	-	0.67

Abbreviations:
D = depth
WL = wavelength

Units:
MD = mafic dyke
MBX = mafic breccia
MT = mafic tuff
MLT = mafic lapilli tuff

Table C.1.1. Whole Rock Geochemistry and Terraspec™ Data for Argyle Samples

Sample ID		294850	294851	294852	294853	294854
Hole ID		AE-16-43	AE-16-43	AE-16-43	AE-16-27	AE-16-27
Depth (m)		111.05	119.6	125.95	21.75	33.35
Lithology		Gabbro	Gabbro	MLT	MBX	Gabbro
Alteration Assemblage		Chl-Ab-carb-Rut	Ep-carb-Chl-Qt-Hem	Chl-Calc	Chl-Calc-Hem	Chl-Calc-Ep
Alteration		Proximal	Intermediate	Distal	Distal	Distal
SiO_2	*%*	41.60	48.00	54.20	50.70	45.40
Al_2O_3		12.75	16.00	15.50	17.85	14.90
Fe_2O_3		15.90	10.30	7.57	11.45	11.50
CaO		8.12	11.55	4.81	4.33	8.69
MgO		4.95	6.63	6.08	5.43	7.24
Na_2O		3.50	2.21	5.51	5.21	3.07
K_2O		0.28	0.16	0.17	0.78	0.18
Cr_2O_3		<0.002	0.03	0.03	0.02	0.03
TiO_2		3.38	1.82	0.87	1.90	2.03
MnO		0.18	0.13	0.09	0.07	0.17
P_2O_5		0.36	0.19	0.12	0.09	0.24
SrO		0.02	0.05	0.01	0.02	0.02
BaO		0.01	0.01	<0.01	0.01	<0.01
LOI		9.78	4.37	6.23	3.98	7.40
Total		100.83	101.45	101.19	101.84	100.87
C		2.03	0.36	0.84	0.19	0.95
S		0.01	0.01	<0.01	0.02	0.02
Ba	*ppm*	50.60	60.80	22.20	72.30	40.70
Ce		41.30	23.60	26.80	16.90	30.10
Cr		10.00	250.00	190.00	130.00	210.00
Cs		0.06	0.14	0.04	0.02	0.11
Dy		7.28	4.34	3.35	4.76	4.89
Er		3.83	2.46	1.88	2.56	2.59
Eu		2.13	1.39	0.91	1.07	1.72
Ga		22.80	18.90	18.20	21.00	17.50
Gd		7.18	4.73	3.04	4.09	5.85
Ge		<5	<5	<5	<5	<5
Hf		6.10	3.20	3.00	3.30	3.70
Ho		1.43	0.88	0.70	0.99	1.04
La		15.90	9.10	11.60	6.00	12.10
Lu		0.53	0.26	0.32	0.40	0.37
Nb		14.70	8.50	7.00	6.70	9.20
Nd		27.50	17.10	13.20	11.80	20.80
Pr		5.70	3.43	3.24	2.40	4.25
Rb		4.80	2.80	2.10	7.90	2.60
Sm		6.88	4.22	3.12	3.24	5.29
Sn		2.00	2.00	1.00	1.00	2.00
Sr		155.00	435.00	122.00	136.00	180.00
Ta		0.80	0.40	0.40	0.30	0.50
Tb		1.15	0.77	0.55	0.69	0.90
Th		1.04	0.61	4.19	0.67	0.63
Tm		0.53	0.34	0.31	0.44	0.29
U		0.42	0.21	2.87	0.44	0.28
V		512.00	278.00	126.00	167.00	281.00
W		2.00	1.00	1.00	1.00	1.00
Y		35.60	21.70	17.50	22.10	26.80
Yb		3.14	2.24	1.62	2.58	2.07
Zr		249.00	139.00	118.00	132.00	156.00
As		1.20	5.00	1.00	56.50	2.70
Bi		<0.01	<0.01	0.01	<0.01	<0.01
Hg		<0.005	<0.005	<0.005	<0.005	<0.005
In		0.08	0.02	0.02	<0.005	0.04

Abbreviations:
D = depth
WL = wavelength

Units:
MD = mafic dyke
MBX = mafic breccia

MT = mafic tuff
MLT = mafic lapilli tuff

Table C.1.1. Whole Rock Geochemistry and Terraspec™ Data for Argyle Samples

Sample ID		294850	294851	294852	294853	294854
Hole ID		AE-16-43	AE-16-43	AE-16-43	AE-16-27	AE-16-27
Depth (m)		111.05	119.6	125.95	21.75	33.35
Lithology		Gabbro	Gabbro	MLT	MBX	Gabbro
Alteration Assemblage		Chl-Ab-carb-Rut	Ep-carb-Chl-Qt-Hem	Chl-Calc	Chl-Calc-Hem	Chl-Calc-Ep
Alteration		Proximal	Intermediate	Distal	Distal	Distal
Re		0.00	0.00	0.00	<0.001	0.00
Sb		0.16	0.88	0.16	0.27	0.47
Se		<0.2	<0.2	<0.2	0.20	<0.2
Te		<0.01	<0.01	<0.01	<0.01	<0.01
Tl		<0.02	<0.02	<0.02	<0.02	<0.02
Ag		<0.5	<0.5	<0.5	<0.5	<0.5
Cd		<0.5	1	<0.5	<0.5	1
Co		48	39	26	47	43
Cu		47	51	2	1	7
Li		30	10	20	20	20
Mo		1	1	1	<1	<1
Ni		20	55	103	71	75
Pb		<2	<2	10	<2	<2
Sc		32	33	17	30	32
Zn		83	47	47	49	50
Au		0.09	0.01	<0.001	<0.001	<0.001
C	*%*	1.84	0.33	0.82	0.18	0.87
CO_2		6.80	1.20	3.00	0.70	3.20
AlOH WL	*nm*	-	-	-	-	-
AlOH D		-	-	-	-	-
FeOH WL		2251.99	2253.21	2258.03	2256.70	2254.60
FeOH D		0.16	0.25	0.32	0.26	0.20
AlOH D/FeOH D		-	-	-	-	-

Abbreviations:	**Units:**	
D = depth	MD = mafic dyke	MT = mafic tuff
WL = wavelength	MBX = mafic breccia	MLT = mafic lapilli tuff

Table C.1.1. Whole Rock Geochemistry and Terraspec™ Data for Argyle Samples

Sample ID		294855	294856	294857	294858	294859
Hole ID		AE-16-27	AE-16-27	AE-16-27	AE-16-27	AE-16-27
Depth (m)		55.5	64.9	68	83.45	90.95
Lithology		Gabbro	Gabbro	Gabbro	Gabbro	Gabbro
Alteration Assemblage		Chl-carb-Ep	Ab-Ank-Chl-Qt-Rut	Chl-Ab-Calc-Mt	Chl-Calc-Ep-Qt-Hem	Chl-carb-Rut
Alteration		Intermediate	Proximal	Proximal	Intermediate	Distal
SiO_2	*%*	45.70	38.40	42.40	41.00	45.10
Al_2O_3		16.80	14.00	12.75	14.60	14.95
Fe_2O_3		11.05	9.46	17.25	11.90	10.70
CaO		10.40	11.75	9.02	12.50	9.22
MgO		6.11	3.29	6.34	5.76	6.22
Na_2O		2.64	3.33	2.01	2.57	3.21
K_2O		0.16	1.63	0.09	0.07	0.62
Cr_2O_3		0.03	0.00	<0.002	0.01	0.03
TiO_2		2.05	2.25	3.75	2.57	1.98
MnO		0.15	0.15	0.22	0.17	0.14
P_2O_5		0.26	0.22	0.23	0.23	0.21
SrO		0.05	0.02	0.03	0.03	0.02
BaO		0.01	0.01	<0.01	<0.01	0.01
LOI		4.41	14.30	7.17	7.39	8.97
Total		99.82	98.81	101.26	98.80	101.38
C		0.32	3.47	1.00	1.15	1.47
S		0.01	0.06	<0.01	0.01	0.02
Ba	*ppm*	54.50	114.00	20.90	20.70	135.50
Ce		27.80	29.20	27.10	23.80	25.20
Cr		190.00	30.00	10.00	60.00	210.00
Cs		0.06	0.31	0.21	0.02	0.30
Dy		5.05	5.47	5.65	4.58	4.52
Er		2.65	2.63	2.97	2.17	2.31
Eu		1.59	1.78	1.65	1.54	1.36
Ga		21.50	19.80	22.50	21.10	18.60
Gd		5.40	5.28	5.75	4.65	5.11
Ge		<5	<5	<5	<5	<5
Hf		4.50	4.00	4.30	3.40	3.50
Ho		0.96	1.05	1.02	0.96	0.90
La		10.80	11.40	10.20	9.10	9.90
Lu		0.38	0.34	0.36	0.32	0.32
Nb		9.90	10.00	9.80	8.50	8.30
Nd		20.00	19.90	20.30	17.30	17.40
Pr		4.09	4.26	4.04	3.59	3.67
Rb		2.10	23.30	1.80	1.20	11.40
Sm		5.12	5.25	5.17	4.36	4.22
Sn		2.00	1.00	2.00	2.00	2.00
Sr		460.00	203.00	285.00	303.00	212.00
Ta		0.60	0.60	0.50	0.50	0.50
Tb		0.86	0.82	0.93	0.72	0.72
Th		0.81	0.72	0.75	0.49	0.57
Tm		0.35	0.33	0.37	0.35	0.33
U		0.33	0.26	0.31	0.21	0.28
V		279.00	287.00	591.00	413.00	272.00
W		1.00	6.00	2.00	38.00	1.00
Y		25.30	25.60	26.20	22.30	22.70
Yb		2.42	1.98	2.48	1.88	2.04
Zr		179.00	170.00	168.00	136.00	147.00
As		4.70	11.80	2.80	3.10	2.00
Bi		<0.01	0.01	<0.01	<0.01	<0.01
Hg		<0.005	<0.005	<0.005	0.01	<0.005
In		0.02	0.04	0.06	0.03	0.04

Abbreviations:

D = depth

WL = wavelength

Units:

MD = mafic dyke

MBX = mafic breccia

MT = mafic tuff

MLT = mafic lapilli tuff

Table C.1.1. Whole Rock Geochemistry and Terraspec™ Data for Argyle Samples

Sample ID	294855	294856	294857	294858	294859
Hole ID	AE-16-27	AE-16-27	AE-16-27	AE-16-27	AE-16-27
Depth (m)	55.5	64.9	68	83.45	90.95
Lithology	Gabbro	Gabbro	Gabbro	Gabbro	Gabbro
Alteration Assemblage	Chl-carb-Ep	Ab-Ank-Chl-Qt-Rut	Chl-Ab-Calc-Mt	Chl-Calc-Ep-Qt-Hem	Chl-carb-Rut
Alteration	Intermediate	Proximal	Proximal	Intermediate	Distal
Re	<0.001	0.00	<0.001	<0.001	<0.001
Sb	0.65	0.11	0.61	0.35	0.29
Se	0.20	0.20	0.30	<0.2	<0.2
Te	<0.01	<0.01	<0.01	<0.01	<0.01
Tl	<0.02	<0.02	<0.02	<0.02	<0.02
Ag	<0.5	<0.5	<0.5	<0.5	<0.5
Cd	<0.5	<0.5	1	<0.5	<0.5
Co	40	33	53	41	38
Cu	46	37	48	33	60
Li	10	20	20	10	10
Mo	<1	1	<1	<1	<1
Ni	49	19	25	32	46
Pb	<2	<2	<2	<2	<2
Sc	28	28	39	36	33
Zn	64	50	100	65	67
Au	<0.001	0.01	<0.001	0.51	0.00
C *%*	0.31	3.29	0.93	1.08	1.39
CO_2	1.10	12.10	3.40	4.00	5.10
AlOH WL *nm*	-	2201.64	2222.35	-	2225.01
AlOH D	-	0.19	0.10	-	0.12
FeOH WL	2255.08	2257.08	2250.94	2253.97	2253.91
FeOH D	0.27	0.14	0.16	0.22	0.25
AlOH D/FeOH D	-	1.35	0.62	-	0.48

Abbreviations:
D = depth
WL = wavelength

Units:
MD = mafic dyke
MBX = mafic breccia
MT = mafic tuff
MLT = mafic lapilli tuff

Table C.1.1. Whole Rock Geochemistry and Terraspec™ Data for Argyle Samples

Sample ID		294860	294861	294862	294863	294864
Hole ID		AE-16-27	AE-16-26	AE-16-26	AE-16-26	AE-16-26
Depth (m)		92.35	21.5	33	43.6	73.55
Lithology		MCT	Gabbro	Gabbro	Gabbro	Gabbro
Alteration Assemblage		Calc-Si-Chl	Chl-carb-Hem	Ab-carb-Chl-Qt-Rut	Chl-Ab-Ep-Calc-Mt	Chl-Calc-Ep-Hem
Alteration		Distal	Distal	Proximal	Proximal	Intermediate
SiO_2	*%*	54.10	47.00	40.00	46.30	47.10
Al_2O_3		14.45	15.70	13.95	13.00	13.50
Fe_2O_3		5.82	10.30	10.20	15.40	15.50
CaO		8.99	7.40	9.21	7.44	8.53
MgO		5.08	6.28	4.95	5.71	5.85
Na_2O		6.14	4.13	1.74	2.89	3.54
K_2O		0.21	0.25	0.90	0.10	0.12
Cr_2O_3		0.02	0.03	0.01	<0.002	<0.002
TiO_2		1.59	1.88	2.02	3.38	2.73
MnO		0.12	0.13	0.13	0.20	0.19
P_2O_5		0.25	0.24	0.19	0.27	0.20
SrO		0.02	0.02	0.03	0.02	0.02
BaO		<0.01	0.01	0.01	<0.01	0.01
LOI		2.37	7.47	15.90	6.00	2.64
Total		99.16	100.84	99.24	100.71	99.93
C		0.24	1.05	3.78	0.78	0.09
S		<0.01	<0.01	0.01	0.01	0.01
Ba	*ppm*	36.80	52.70	52.10	40.30	49.50
Ce		17.90	26.00	20.00	29.30	23.10
Cr		110.00	210.00	60.00	20.00	20.00
Cs		0.06	0.05	0.27	0.05	0.12
Dy		5.88	4.73	3.96	5.85	5.02
Er		3.30	2.12	1.99	2.62	2.88
Eu		1.39	1.66	1.42	1.82	1.41
Ga		14.30	19.90	17.60	20.20	20.10
Gd		5.32	4.57	4.20	5.81	4.66
Ge		<5	<5	<5	<5	<5
Hf		2.70	4.00	2.90	4.30	3.40
Ho		1.24	0.97	0.75	1.14	0.88
La		7.10	9.90	7.70	11.60	9.00
Lu		0.47	0.32	0.22	0.35	0.36
Nb		5.80	8.90	7.30	10.50	7.70
Nd		14.00	16.90	13.80	19.70	15.20
Pr		2.67	3.65	2.93	4.13	3.18
Rb		3.00	4.40	14.30	1.60	1.90
Sm		3.81	4.37	3.66	5.49	4.06
Sn		8.00	2.00	1.00	2.00	2.00
Sr		169.00	169.50	250.00	184.50	221.00
Ta		0.30	0.60	0.30	0.60	0.70
Tb		0.87	0.74	0.70	0.93	0.73
Th		0.54	0.69	0.42	0.71	0.70
Tm		0.47	0.37	0.29	0.41	0.37
U		0.58	0.32	0.22	0.33	0.27
V		236.00	260.00	307.00	510.00	715.00
W		1.00	1.00	5.00	2.00	<1
Y		31.00	22.10	18.70	26.80	25.20
Yb		2.82	2.06	1.88	2.24	2.39
Zr		110.00	151.00	118.00	178.00	137.00
As		10.40	2.30	0.80	3.40	3.70
Bi		<0.01	<0.01	<0.01	<0.01	0.01
Hg		<0.005	<0.005	<0.005	<0.005	<0.005
In		0.02	0.04	0.05	0.05	0.02

Abbreviations:
D = depth
WL = wavelength

Units:
MD = mafic dyke
MBX = mafic breccia

MT = mafic tuff
MLT = mafic lapilli tuff

Table C.1.1. Whole Rock Geochemistry and Terraspec™ Data for Argyle Samples

Sample ID		294860	294861	294862	294863	294864
Hole ID		AE-16-27	AE-16-26	AE-16-26	AE-16-26	AE-16-26
Depth (m)		92.35	21.5	33	43.6	73.55
Lithology		MCT	Gabbro	Gabbro	Gabbro	Gabbro
Alteration Assemblage		Calc-Si-Chl	Chl-carb-Hem	Ab-carb-Chl-Qt-Rut	Chl-Ab-Ep-Calc-Mt	Chl-Calc-Ep-Hem
Alteration		Distal	Distal	Proximal	Proximal	Intermediate
Re		0.00	0.00	<0.001	0.00	0.00
Sb		0.39	0.26	0.10	0.82	0.49
Se		<0.2	<0.2	<0.2	0.50	<0.2
Te		<0.01	<0.01	<0.01	<0.01	<0.01
Tl		<0.02	<0.02	<0.02	<0.02	<0.02
Ag		<0.5	<0.5	<0.5	<0.5	<0.5
Cd		<0.5	<0.5	<0.5	1	1
Co		22	38	36	55	51
Cu		3	6	74	78	88
Li		10	30	20	20	10
Mo		1	<1	<1	2	1
Ni		51	53	30	21	57
Pb		<2	<2	<2	<2	<2
Sc		29	30	33	38	41
Zn		37	48	58	100	89
Au		<0.001	<0.001	0.01	<0.001	<0.001
C	*%*	0.22	0.99	3.45	0.74	0.08
CO_2		0.80	3.60	12.70	2.70	0.30
AlOH WL	*nm*	2222.98	-	2193.02	-	-
AlOH D		0.11	-	0.32	-	-
FeOH WL		2257.71	2255.39	2259.85	2258.55	2260.08
FeOH D		0.13	0.27	0.16	0.14	0.15
AlOH D/FeOH D		0.82	-	2.01	-	-

Abbreviations:
D = depth
WL = wavelength

Units:
MD = mafic dyke
MBX = mafic breccia
MT = mafic tuff
MLT = mafic lapilli tuff

Table C.1.1. Whole Rock Geochemistry and Terraspec™ Data for Argyle Samples

Sample ID		294865	294866	294867	294868	294951
Hole ID		AE-16-26	AE-16-26	AE-16-26	AE-16-26	BN-14-186
Depth (m)		84.45	85.15	89.85	94	2.6
Lithology		MD	Gabbro	Gabbro	MLT	Gabbro
Alteration Assemblage		Calc-Ser-Chl-Ab	Chl-Ab-carb	Chl-Ank-Ab-Rut	Chl-Ab-Calc	Chl-Ab-Rut
Alteration		Distal	Distal	Intermediate	Distal	Distal
SiO_2	*%*	40.20	41.30	44.50	55.90	49.20
Al_2O_3		13.75	11.85	13.45	15.75	16.55
Fe_2O_3		14.05	16.75	10.50	5.52	7.76
CaO		8.50	8.90	8.17	5.84	6.50
MgO		5.35	4.27	5.01	5.04	6.01
Na_2O		3.46	3.56	3.68	7.16	4.94
K_2O		0.02	0.04	0.97	0.04	0.32
Cr_2O_3		0.01	<0.002	0.01	0.02	0.03
TiO_2		3.40	3.25	1.72	1.08	1.06
MnO		0.18	0.19	0.16	0.07	0.12
P_2O_5		0.54	0.23	0.20	0.18	0.16
SrO		0.01	0.02	0.02	0.01	0.02
BaO		<0.01	<0.01	0.01	<0.01	0.01
LOI		9.33	9.79	12.25	4.66	7.89
Total		98.80	100.15	100.65	101.27	100.57
C		1.71	2.10	2.89	0.75	1.31
S		0.18	0.02	0.05	0.01	0.01
Ba	*ppm*	16.90	33.00	89.60	16.20	77.00
Ce		47.40	24.30	22.80	29.90	25.60
Cr		70.00	<10	90.00	150.00	220.00
Cs		0.02	0.09	0.23	0.02	0.09
Dy		6.52	4.79	4.32	4.12	3.52
Er		3.93	2.67	2.45	2.60	2.17
Eu		2.49	1.50	1.42	1.18	1.11
Ga		22.20	21.40	16.60	13.90	18.30
Gd		7.52	5.01	4.15	4.03	3.89
Ge		<5	<5	<5	<5	<5
Hf		6.10	3.70	3.60	3.60	3.30
Ho		1.32	0.94	0.83	0.85	0.77
La		19.00	9.40	8.80	13.20	11.50
Lu		0.47	0.35	0.32	0.33	0.27
Nb		17.40	8.20	7.80	8.70	6.20
Nd		29.60	16.30	14.70	16.20	14.00
Pr		6.59	3.43	3.25	3.59	3.25
Rb		0.50	0.80	16.70	0.40	5.80
Sm		7.73	4.57	4.15	3.68	3.57
Sn		2.00	1.00	1.00	4.00	1.00
Sr		126.50	156.50	179.00	90.90	152.00
Ta		1.30	0.60	0.70	0.70	0.60
Tb		1.11	0.81	0.73	0.69	0.61
Th		0.98	0.71	0.80	3.22	2.51
Tm		0.53	0.40	0.35	0.36	0.30
U		0.42	0.28	0.26	2.54	1.64
V		380.00	805.00	277.00	153.00	174.00
W		1.00	2.00	4.00	<1	3.00
Y		35.70	26.30	23.20	23.70	21.20
Yb		3.05	2.53	2.09	2.43	2.17
Zr		271.00	142.00	140.00	144.00	129.00
As		3.60	2.50	1.80	1.00	0.80
Bi		0.01	<0.01	0.01	<0.01	0.03
Hg		<0.005	<0.005	<0.005	<0.005	<0.005
In		0.08	0.07	0.04	0.03	0.03

Abbreviations:

D = depth

WL = wavelength

Units:

MD = mafic dyke

MBX = mafic breccia

MT = mafic tuff

MLT = mafic lapilli tuff

Table C.1.1. Whole Rock Geochemistry and Terraspec™ Data for Argyle Samples

Sample ID		294865	294866	294867	294868	294951
Hole ID		AE-16-26	AE-16-26	AE-16-26	AE-16-26	BN-14-186
Depth (m)		84.45	85.15	89.85	94	2.6
Lithology		MD	Gabbro	Gabbro	MLT	Gabbro
Alteration Assemblage		Calc-Ser-Chl-Ab	Chl-Ab-carb	Chl-Ank-Ab-Rut	Chl-Ab-Calc	Chl-Ab-Rut
Alteration		Distal	Distal	Intermediate	Distal	Distal
Re		0.00	0.00	0.00	0.00	0.00
Sb		0.09	0.24	0.08	0.17	0.14
Se		<0.2	<0.2	<0.2	0.20	<0.2
Te		<0.01	<0.01	<0.01	<0.01	<0.01
Tl		<0.02	<0.02	<0.02	<0.02	<0.02
Ag		<0.5	<0.5	<0.5	<0.5	<0.5
Cd		<0.5	1	<0.5	<0.5	<0.5
Co		41	56	34	17	33
Cu		40	86	34	8	21
Li		30	20	20	10	30
Mo		2	1	<1	<1	<1
Ni		43	31	47	57	99
Pb		2	<2	<2	<2	<2
Sc		28	34	29	20	22
Zn		113	77	52	41	51
Au		<0.001	<0.001	0.00	<0.001	0.00
C	*%*	1.58	1.96	2.66	0.70	1.16
CO_2		5.80	7.20	9.80	2.60	4.30
AlOH WL	*nm*	-	-	2201.61	2225.02	-
AlOH D		-	-	0.13	0.08	-
FeOH WL		2256.92	2255.23	2258.89	2252.68	2257.72
FeOH D		0.19	0.15	0.16	0.24	0.33
AlOH D/FeOH D		-	-	0.81	0.34	-

Abbreviations:
D = depth
WL = wavelength

Units:
MD = mafic dyke
MBX = mafic breccia
MT = mafic tuff
MLT = mafic lapilli tuff

Table C.1.1. Whole Rock Geochemistry and Terraspec™ Data for Argyle Samples

Sample ID		294951	294952	294952	294953	294953
Hole ID		BN-14-190	BN-14-186	BN-14-190	BN-14-186	BN-14-190
Depth (m)		2.6	17.8	17.8	24.55	24.55
Lithology		Gabbro	Gabbro	Gabbro	Gabbro	Gabbro
Alteration Assemblage		Chl-Ab-Rut	Ab-Ank-Chl-Qt	Ab-ank-Chl-Qt	Ab-Chl-Qt-Ank-Py	Ab-Chl-Qt-Ank-Py
Alteration		Distal	Intermediate	Intermediate	Proximal	Proximal
SiO_2	%	49.20	42.30	42.30	45.60	45.60
Al_2O_3		16.55	14.85	14.85	12.95	12.95
Fe_2O_3		7.76	8.24	8.24	12.55	12.55
CaO		6.50	9.01	9.01	7.21	7.21
MgO		6.01	4.36	4.36	2.75	2.75
Na_2O		4.94	2.36	2.36	4.32	4.32
K_2O		0.32	2.77	2.77	0.79	0.79
Cr_2O_3		0.03	0.01	0.01	<0.002	<0.002
TiO_2		1.06	1.48	1.48	2.31	2.31
MnO		0.12	0.12	0.12	0.21	0.21
P_2O_5		0.16	0.18	0.18	1.07	1.07
SrO		0.02	0.02	0.02	0.03	0.03
BaO		0.01	0.02	0.02	0.01	0.01
LOI		7.89	14.15	14.15	8.24	8.24
Total		100.57	99.87	99.87	98.04	98.04
C		1.31	3.58	3.58	2.34	2.34
S		0.01	0.13	0.13	1.37	1.37
Ba	*ppm*	77.00	157.00	157.00	102.00	102.00
Ce		25.60	20.90	20.90	73.30	73.30
Cr		220.00	90.00	90.00	10.00	10.00
Cs		0.09	0.52	0.52	0.14	0.14
Dy		3.52	3.37	3.37	11.55	11.55
Er		2.17	1.98	1.98	6.44	6.44
Eu		1.11	1.17	1.17	3.76	3.76
Ga		18.30	17.10	17.10	22.50	22.50
Gd		3.89	3.44	3.44	12.80	12.80
Ge		<5	<5	<5	<5	<5
Hf		3.30	2.90	2.90	8.30	8.30
Ho		0.77	0.68	0.68	2.27	2.27
La		11.50	8.00	8.00	27.80	27.80
Lu		0.27	0.25	0.25	0.76	0.76
Nb		6.20	6.90	6.90	21.70	21.70
Nd		14.00	14.00	14.00	48.40	48.40
Pr		3.25	2.93	2.93	10.70	10.70
Rb		5.80	38.10	38.10	11.90	11.90
Sm		3.57	3.61	3.61	12.65	12.65
Sn		1.00	1.00	1.00	3.00	3.00
Sr		152.00	228.00	228.00	262.00	262.00
Ta		0.60	0.60	0.60	1.60	1.60
Tb		0.61	0.59	0.59	1.96	1.96
Th		2.51	0.65	0.65	1.62	1.62
Tm		0.30	0.27	0.27	0.92	0.92
U		1.64	0.25	0.25	0.74	0.74
V		174.00	218.00	218.00	122.00	122.00
W		3.00	12.00	12.00	30.00	30.00
Y		21.20	18.90	18.90	61.80	61.80
Yb		2.17	2.04	2.04	5.29	5.29
Zr		129.00	125.00	125.00	387.00	387.00
As		0.80	2.20	2.20	7.60	7.60
Bi		0.03	0.05	0.05	0.20	0.20
Hg		<0.005	<0.005	<0.005	<0.005	<0.005
In		0.03	0.02	0.02	0.07	0.07

Abbreviations:
D = depth
WL = wavelength

Units:
MD = mafic dyke
MBX = mafic breccia

MT = mafic tuff
MLT = mafic lapilli tuff

Table C.1.1. Whole Rock Geochemistry and Terraspec™ Data for Argyle Samples

Sample ID		294951	294952	294952	294953	294953
Hole ID		BN-14-190	BN-14-186	BN-14-190	BN-14-186	BN-14-190
Depth (m)		2.6	17.8	17.8	24.55	24.55
Lithology		Gabbro	Gabbro	Gabbro	Gabbro	Gabbro
Alteration Assemblage		Chl-Ab-Rut	Ab-Ank-Chl-Qt	Ab-ank-Chl-Qt	Ab-Chl-Qt-Ank-Py	Ab-Chl-Qt-Ank-Py
Alteration		Distal	Intermediate	Intermediate	Proximal	Proximal
Re		0.00	0.00	0.00	0.00	0.00
Sb		0.14	<0.05	<0.05	0.05	0.05
Se		<0.2	0.30	0.30	1.00	1.00
Te		<0.01	0.03	0.03	0.20	0.20
Tl		<0.02	<0.02	<0.02	<0.02	<0.02
Ag		<0.5	<0.5	<0.5	<0.5	<0.5
Cd		<0.5	1	1	<0.5	<0.5
Co		33	31	31	30	30
Cu		21	23	23	36	36
Li		30	10	10	10	10
Mo		<1	1	1	3	3
Ni		99	36	36	2	2
Pb		<2	<2	<2	3	3
Sc		22	28	28	17	17
Zn		51	53	53	73	73
Au		0.00	0.03	0.03	3.64	3.64
C	*%*	1.16	3.31	3.31	2.16	2.16
CO_2		4.30	12.10	12.10	7.90	7.90
AlOH WL	*nm*	-	2197.81	-	2201.75	-
AlOH D		-	0.27	-	0.20	-
FeOH WL		-	2240.84	-	-	-
FeOH D		-	0.13	-	-	-
AlOH D/FeOH D		-	2.19	-	-	-

Abbreviations:
D = depth
WL = wavelength

Units:
MD = mafic dyke
MBX = mafic breccia
MT = mafic tuff
MLT = mafic lapilli tuff

Table C.1.1. Whole Rock Geochemistry and Terraspec™ Data for Argyle Samples

Sample ID		294954	294954	294955	294955	294956
Hole ID		BN-14-186	BN-14-190	BN-14-186	BN-14-190	BN-14-190
Depth (m)		32.95	32.95	40.55	40.55	41.9
Lithology		Gabbro	Gabbro	Gabbro	Gabbro	MF
Alteration Assemblage		Ab-Hem-Chl-Ank-Qt	Ab-Hem-Chl-Ank-Qt	Chl-Ank-Ab-Qt-Rut	Chl-Ank-Ab-Qt-Rut	Chl-Qt
Alteration		Proximal	Proximal	Intermediate	Intermediate	Distal
SiO_2	*%*	42.20	42.20	41.70	41.70	51.90
Al_2O_3		14.95	14.95	13.40	13.40	14.40
Fe_2O_3		10.80	10.80	10.10	10.10	6.52
CaO		8.40	8.40	8.94	8.94	7.33
MgO		3.13	3.13	5.25	5.25	7.43
Na_2O		4.74	4.74	3.11	3.11	4.27
K_2O		1.34	1.34	1.56	1.56	0.11
Cr_2O_3		<0.002	<0.002	0.02	0.02	0.04
TiO_2		2.09	2.09	1.90	1.90	0.71
MnO		0.23	0.23	0.15	0.15	0.12
P_2O_5		0.92	0.92	0.25	0.25	0.15
SrO		0.03	0.03	0.02	0.02	0.02
BaO		0.01	0.01	0.01	0.01	0.01
LOI		10.50	10.50	14.15	14.15	8.97
Total		99.34	99.34	100.56	100.56	101.98
C		2.76	2.76	3.51	3.51	1.54
S		0.47	0.47	0.06	0.06	0.01
Ba	*ppm*	110.50	110.50	89.30	89.30	51.10
Ce		72.10	72.10	30.00	30.00	25.80
Cr		<10	<10	180.00	180.00	320.00
Cs		0.29	0.29	0.26	0.26	0.05
Dy		11.45	11.45	4.68	4.68	2.47
Er		6.37	6.37	2.61	2.61	1.38
Eu		3.84	3.84	1.59	1.59	0.87
Ga		21.80	21.80	16.90	16.90	14.20
Gd		12.80	12.80	5.45	5.45	2.91
Ge		<5	<5	<5	<5	<5
Hf		9.30	9.30	4.50	4.50	2.30
Ho		2.30	2.30	0.94	0.94	0.50
La		27.90	27.90	11.60	11.60	12.30
Lu		0.81	0.81	0.36	0.36	0.16
Nb		26.60	26.60	9.90	9.90	4.40
Nd		46.80	46.80	19.40	19.40	12.60
Pr		10.25	10.25	4.22	4.22	3.13
Rb		20.60	20.60	26.10	26.10	2.40
Sm		11.65	11.65	5.18	5.18	2.74
Sn		3.00	3.00	2.00	2.00	1.00
Sr		257.00	257.00	216.00	216.00	209.00
Ta		1.60	1.60	0.80	0.80	0.40
Tb		2.07	2.07	0.88	0.88	0.43
Th		1.82	1.82	0.79	0.79	2.56
Tm		0.86	0.86	0.36	0.36	0.21
U		0.96	0.96	0.32	0.32	1.42
V		131.00	131.00	266.00	266.00	131.00
W		46.00	46.00	3.00	3.00	1.00
Y		61.60	61.60	26.50	26.50	14.00
Yb		5.82	5.82	2.54	2.54	1.48
Zr		422.00	422.00	189.00	189.00	89.00
As		1.80	1.80	0.60	0.60	0.70
Bi		0.14	0.14	0.02	0.02	0.06
Hg		<0.005	<0.005	<0.005	<0.005	<0.005
In		0.06	0.06	0.03	0.03	0.03

Abbreviations:	**Units:**	
D = depth	MD = mafic dyke	MT = mafic tuff
WL = wavelength	MBX = mafic breccia	MLT = mafic lapilli tuff

Table C.1.1. Whole Rock Geochemistry and Terraspec™ Data for Argyle Samples

Sample ID		294954	294954	294955	294955	294956
Hole ID		BN-14-186	BN-14-190	BN-14-186	BN-14-190	BN-14-190
Depth (m)		32.95	32.95	40.55	40.55	41.9
Lithology		Gabbro	Gabbro	Gabbro	Gabbro	MF
Alteration Assemblage		Ab-Hem-Chl-Ank-Qt	Ab-Hem-Chl-Ank-Qt	Chl-Ank-Ab-Qt-Rut	Chl-Ank-Ab-Qt-Rut	Chl-Qt
Alteration		Proximal	Proximal	Intermediate	Intermediate	Distal
Re		0.00	0.00	<0.001	<0.001	<0.001
Sb		<0.05	<0.05	0.05	0.05	<0.05
Se		0.30	0.30	<0.2	<0.2	<0.2
Te		0.06	0.06	<0.01	<0.01	<0.01
Tl		<0.02	<0.02	<0.02	<0.02	<0.02
Ag		<0.5	<0.5	<0.5	<0.5	<0.5
Cd		<0.5	<0.5	<0.5	<0.5	<0.5
Co		17	17	33	33	30
Cu		30	30	70	70	43
Li		10	10	10	10	20
Mo		10	10	1	1	<1
Ni		5	5	48	48	179
Pb		5	5	4	4	<2
Sc		15	15	31	31	19
Zn		79	79	75	75	55
Au		1.20	1.20	0.01	0.01	0.00
C	*%*	2.54	2.54	3.23	3.23	1.38
CO_2		9.30	9.30	11.80	11.80	5.10
AlOH WL	*nm*	2201.70	-	2203.35	-	-
AlOH D		0.06	-	0.17	-	-
FeOH WL		2266.94	-	2259.84	-	2250.67
FeOH D		0.10	-	0.10	-	0.17
AlOH D/FeOH D		0.64	-	1.63	-	-

Abbreviations:
D = depth
WL = wavelength

Units:
MD = mafic dyke
MBX = mafic breccia
MT = mafic tuff
MLT = mafic lapilli tuff

Table C.1.1. Whole Rock Geochemistry and Terraspec™ Data for Argyle Samples

Sample ID		294957	294958	294958	294959	294959
Hole ID		BN-14-190	BN-14-186	BN-14-190	BN-14-186	BN-14-190
Depth (m)		45.6	51.7	51.7	58.1	58.1
Lithology		DiAbase	Gabbro	Gabbro	Gabbro	Gabbro
Alteration Assemblage		Chl-Qt	Chl-ank-Ab-Qt	Chl-ank-Ab-Qt	Ab-Ank-Hem-Qt-Ser-Chl	Ab-Ank-Hem-Qt-Ser-Chl
Alteration		Distal	Intermediate	Intermediate	Proximal	Proximal
SiO_2	*%*	46.40	47.20	47.20	39.30	39.30
Al_2O_3		14.25	14.35	14.35	12.85	12.85
Fe_2O_3		10.30	7.13	7.13	5.56	5.56
CaO		8.91	7.47	7.47	16.00	16.00
MgO		5.87	6.83	6.83	3.62	3.62
Na_2O		3.98	2.85	2.85	2.48	2.48
K_2O		0.10	1.87	1.87	2.18	2.18
Cr_2O_3		0.02	0.05	0.05	0.05	0.05
TiO_2		1.66	0.80	0.80	0.67	0.67
MnO		0.15	0.09	0.09	0.14	0.14
P_2O_5		0.19	0.16	0.16	0.33	0.33
SrO		0.02	0.02	0.02	0.03	0.03
BaO		<0.01	0.03	0.03	0.01	0.01
LOI		8.99	12.45	12.45	17.55	17.55
Total		100.84	101.30	101.30	100.77	100.77
C		1.68	2.74	2.74	4.51	4.51
S		0.06	0.01	0.01	0.01	0.01
Ba	*ppm*	41.30	281.00	281.00	105.50	105.50
Ce		21.80	33.10	33.10	21.70	21.70
Cr		140.00	390.00	390.00	360.00	360.00
Cs		0.08	0.35	0.35	0.64	0.64
Dy		4.06	2.97	2.97	2.89	2.89
Er		2.27	1.65	1.65	1.59	1.59
Eu		1.43	1.09	1.09	0.96	0.96
Ga		17.40	13.70	13.70	13.20	13.20
Gd		4.37	3.27	3.27	2.90	2.90
Ge		<5	<5	<5	<5	<5
Hf		3.40	2.20	2.20	1.90	1.90
Ho		0.85	0.54	0.54	0.59	0.59
La		8.50	15.70	15.70	10.30	10.30
Lu		0.29	0.21	0.21	0.20	0.20
Nb		7.50	8.00	8.00	4.50	4.50
Nd		14.70	15.80	15.80	11.30	11.30
Pr		3.06	3.94	3.94	2.70	2.70
Rb		2.20	35.00	35.00	38.90	38.90
Sm		3.93	3.31	3.31	2.89	2.89
Sn		1.00	1.00	1.00	1.00	1.00
Sr		175.00	206.00	206.00	312.00	312.00
Ta		0.60	0.60	0.60	0.60	0.60
Tb		0.71	0.52	0.52	0.55	0.55
Th		0.66	3.02	3.02	2.42	2.42
Tm		0.33	0.21	0.21	0.22	0.22
U		0.27	2.05	2.05	1.73	1.73
V		280.00	136.00	136.00	145.00	145.00
W		1.00	14.00	14.00	16.00	16.00
Y		23.10	15.50	15.50	15.90	15.90
Yb		2.00	1.62	1.62	1.43	1.43
Zr		132.00	97.00	97.00	82.00	82.00
As		2.90	0.50	0.50	0.40	0.40
Bi		0.01	0.02	0.02	0.06	0.06
Hg		<0.005	<0.005	<0.005	<0.005	<0.005
In		0.04	0.01	0.01	0.02	0.02

Abbreviations:
D = depth
WL = wavelength

Units:
MD = mafic dyke
MBX = mafic breccia

MT = mafic tuff
MLT = mafic lapilli tuff

Table C.1.1. Whole Rock Geochemistry and Terraspec™ Data for Argyle Samples

Sample ID	294957	294958	294958	294959	294959
Hole ID	BN-14-190	BN-14-186	BN-14-190	BN-14-186	BN-14-190
Depth (m)	45.6	51.7	51.7	58.1	58.1
Lithology	DiAbase	Gabbro	Gabbro	Gabbro	Gabbro
Alteration Assemblage	Chl-Qt	Chl-ank-Ab-Qt	Chl-ank-Ab-Qt	Ab-Ank-Hem-Qt-Ser-Chl	Ab-Ank-Hem-Qt-Ser-Chl
Alteration	Distal	Intermediate	Intermediate	Proximal	Proximal
Re	0.00	<0.001	<0.001	<0.001	<0.001
Sb	0.12	<0.05	<0.05	<0.05	<0.05
Se	0.20	<0.2	<0.2	<0.2	<0.2
Te	<0.01	<0.01	<0.01	13.20	13.20
Tl	<0.02	<0.02	<0.02	<0.02	<0.02
Ag	<0.5	<0.5	<0.5	<0.5	<0.5
Cd	<0.5	<0.5	<0.5	<0.5	<0.5
Co	36	33	33	25	25
Cu	63	42	42	22	22
Li	20	10	10	10	10
Mo	1	1	1	1	1
Ni	61	215	215	136	136
Pb	<2	4	4	23	23
Sc	33	19	19	19	19
Zn	94	67	67	34	34
Au	<0.001	<0.001	<0.001	0.07	0.07
C *%*	1.47	2.58	2.58	4.15	4.15
CO_2	5.40	9.50	9.50	15.20	15.20
AlOH WL *nm*	-	2208.71	-	2197.83	-
AlOH D	-	0.22	-	0.30	-
FeOH WL	2256.04	2249.94	-	2243.17	-
FeOH D	0.22	0.27	-	0.14	-
AlOH D/FeOH D	-	0.83	-	2.06	-

Abbreviations:
D = depth
WL = wavelength

Units:
MD = mafic dyke
MBX = mafic breccia
MT = mafic tuff
MLT = mafic lapilli tuff

Table C.1.1. Whole Rock Geochemistry and Terraspec™ Data for Argyle Samples

Sample ID		294960	294960	294961	294961	294962
Hole ID		BN-14-186	BN-14-190	BN-14-186	BN-14-190	BN-14-186
Depth (m)		68.3	68.3	81.45	81.45	8
Lithology		Gabbro	Gabbro	Gabbro	Gabbro	Gabbro
Alteration Assemblage		Ab-Hem-Qt-Fuch-Chl-Ser	Ab-Hem-Qt-Fuch-Chl-Ser	Chl-Ank-Ab	Chl-Ank-Ab	Chl-Ab-Qt
Alteration		Proximal	Proximal	Intermediate	Intermediate	Distal
SiO_2	*%*	49.90	49.90	47.20	47.20	41.30
Al_2O_3		17.30	17.30	14.70	14.70	12.55
Fe_2O_3		5.70	5.70	7.73	7.73	10.25
CaO		6.71	6.71	7.06	7.06	10.35
MgO		2.52	2.52	5.09	5.09	9.09
Na_2O		4.01	4.01	4.96	4.96	1.80
K_2O		3.12	3.12	1.04	1.04	0.07
Cr_2O_3		0.01	0.01	0.02	0.02	0.03
TiO_2		0.86	0.86	1.07	1.07	1.51
MnO		0.08	0.08	0.16	0.16	0.15
P_2O_5		0.23	0.23	0.12	0.12	0.18
SrO		0.02	0.02	0.02	0.02	0.03
BaO		0.02	0.02	0.01	0.01	<0.01
LOI		9.94	9.94	11.70	11.70	13.25
Total		100.42	100.42	100.88	100.88	100.56
C		2.54	2.54	2.87	2.87	2.57
S		0.36	0.36	0.01	0.01	0.01
Ba	*ppm*	150.00	150.00	82.70	82.70	8.00
Ce		15.80	15.80	19.70	19.70	19.80
Cr		110.00	110.00	170.00	170.00	250.00
Cs		0.65	0.65	0.16	0.16	0.08
Dy		3.32	3.32	3.33	3.33	3.55
Er		1.88	1.88	2.05	2.05	1.99
Eu		0.84	0.84	1.02	1.02	1.25
Ga		19.20	19.20	14.10	14.10	14.40
Gd		3.17	3.17	3.51	3.51	3.88
Ge		<5	<5	<5	<5	<5
Hf		2.20	2.20	2.60	2.60	3.00
Ho		0.58	0.58	0.72	0.72	0.70
La		7.10	7.10	8.50	8.50	7.60
Lu		0.25	0.25	0.29	0.29	0.28
Nb		3.90	3.90	3.90	3.90	6.90
Nd		9.20	9.20	11.60	11.60	13.20
Pr		2.14	2.14	2.51	2.51	2.94
Rb		53.30	53.30	16.00	16.00	1.40
Sm		2.61	2.61	3.02	3.02	3.29
Sn		1.00	1.00	1.00	1.00	1.00
Sr		207.00	207.00	171.50	171.50	255.00
Ta		0.50	0.50	0.40	0.40	0.60
Tb		0.51	0.51	0.52	0.52	0.60
Th		1.55	1.55	1.62	1.62	0.47
Tm		0.26	0.26	0.27	0.27	0.27
U		0.68	0.68	1.11	1.11	0.19
V		190.00	190.00	168.00	168.00	222.00
W		17.00	17.00	13.00	13.00	2.00
Y		17.90	17.90	19.30	19.30	18.50
Yb		1.67	1.67	1.88	1.88	1.85
Zr		96.00	96.00	109.00	109.00	125.00
As		0.80	0.80	0.20	0.20	1.00
Bi		0.07	0.07	0.01	0.01	<0.01
Hg		<0.005	<0.005	<0.005	<0.005	<0.005
In		0.02	0.02	0.02	0.02	0.05

Abbreviations:
D = depth
WL = wavelength

Units:
MD = mafic dyke
MBX = mafic breccia
MT = mafic tuff
MLT = mafic lapilli tuff

Table C.1.1. Whole Rock Geochemistry and Terraspec™ Data for Argyle Samples

Sample ID		294960	294960	294961	294961	294962
Hole ID		BN-14-186	BN-14-190	BN-14-186	BN-14-190	BN-14-186
Depth (m)		68.3	68.3	81.45	81.45	8
Lithology		Gabbro	Gabbro	Gabbro	Gabbro	Gabbro
Alteration Assemblage		Ab-Hem-Qt-Fuch-Chl-Ser	Ab-Hem-Qt-Fuch-Chl-Ser	Chl-Ank-Ab	Chl-Ank-Ab	Chl-Ab-Qt
Alteration		Proximal	Proximal	Intermediate	Intermediate	Distal
Re		<0.001	<0.001	<0.001	<0.001	<0.001
Sb		<0.05	<0.05	<0.05	<0.05	<0.05
Se		<0.2	<0.2	<0.2	<0.2	<0.2
Te		0.10	0.10	0.02	0.02	<0.01
Tl		0	0	<0.02	<0.02	<0.02
Ag		<0.5	<0.5	<0.5	<0.5	<0.5
Cd		<0.5	<0.5	<0.5	<0.5	<0.5
Co		18	18	28	28	50
Cu		75	75	19	19	4
Li		<10	<10	20	20	30
Mo		<1	<1	<1	<1	<1
Ni		24	24	67	67	164
Pb		3	3	3	3	<2
Sc		16	16	24	24	26
Zn		26	26	47	47	47
Au		0.20	0.20	0.00	0.00	<0.001
C	*%*	2.32	2.32	2.68	2.68	2.22
CO_2		8.50	8.50	9.80	9.80	8.10
AlOH WL	*nm*	2203.66	-	2201.78	-	2227.39
AlOH D		0.41	-	0.19	-	0.11
FeOH WL		-	-	2254.88	-	2255.05
FeOH D		-	-	0.26	-	0.26
AlOH D/FeOH D		-	-	0.75	-	0.42

Abbreviations:
D = depth
WL = wavelength

Units:
MD = mafic dyke
MBX = mafic breccia
MT = mafic tuff
MLT = mafic lapilli tuff

Table C.1.1. Whole Rock Geochemistry and Terraspec™ Data for Argyle Samples

Sample ID		294963	294964	294965	294966	294967
Hole ID		BN-14-186	BN-14-186	BN-14-186	BN-14-186	BN-14-186
Depth (m)		20.9	29.2	34.5	42.75	48.5
Lithology		Gabbro	Gabbro	Gabbro	Gabbro	Gabbro
Alteration Assemblage		Ank-Ab-Chl-Qt-Rut	Ab-Hem-Qt-Chl-Ank-Rut	Chl-Ab-Qt-Ank	Chl-Ab	Chl-Ab-Ank-Qt
Alteration		Intermediate	Proximal	Proximal	Distal	Intermediate
SiO_2	*%*	37.80	40.20	46.30	52.00	47.80
Al_2O_3		17.45	15.50	13.35	15.80	14.95
Fe_2O_3		9.19	13.40	15.15	6.49	6.43
CaO		9.21	7.46	6.29	5.14	6.81
MgO		4.07	3.60	3.18	5.92	5.83
Na_2O		3.65	2.82	3.49	5.77	4.36
K_2O		2.36	1.91	0.70	0.11	1.31
Cr_2O_3		<0.002	<0.002	<0.002	0.02	0.03
TiO_2		1.84	2.50	2.80	0.93	0.90
MnO		0.14	0.17	0.27	0.09	0.09
P_2O_5		0.22	1.07	1.09	0.14	0.22
SrO		0.03	0.02	0.02	0.02	0.03
BaO		0.02	0.02	0.01	<0.01	0.01
LOI		14.35	9.42	8.07	7.63	11.80
Total		100.33	98.09	100.72	100.06	100.57
C		3.58	2.32	1.89	1.42	2.79
S		0.04	1.65	0.15	0.01	0.02
Ba	*ppm*	153.00	157.00	93.50	25.40	92.20
Ce		28.20	79.70	80.70	28.40	30.20
Cr		10.00	10.00	<10	180.00	230.00
Cs		0.49	0.36	0.18	0.06	0.22
Dy		4.34	11.80	11.75	3.74	3.53
Er		2.32	6.55	6.72	1.98	1.92
Eu		1.31	4.44	4.21	1.02	1.24
Ga		18.90	26.90	24.60	15.40	14.50
Gd		4.70	14.05	13.95	2.99	3.59
Ge		<5	<5	<5	<5	<5
Hf		4.00	8.60	8.80	2.90	2.80
Ho		0.83	2.32	2.35	0.66	0.66
La		11.10	30.00	31.10	13.50	13.90
Lu		0.29	0.82	0.78	0.28	0.25
Nb		9.20	26.70	27.50	6.60	7.50
Nd		18.10	53.50	54.30	13.50	15.20
Pr		4.07	11.65	11.75	3.35	3.73
Rb		36.90	30.40	11.30	1.60	20.20
Sm		4.18	13.80	13.35	3.48	3.54
Sn		1.00	4.00	4.00	1.00	1.00
Sr		287.00	237.00	197.50	155.00	245.00
Ta		0.70	1.70	2.00	0.70	0.80
Tb		0.73	2.13	2.07	0.51	0.58
Th		0.71	1.66	1.69	3.20	3.47
Tm		0.37	0.91	0.86	0.25	0.24
U		0.27	1.17	0.73	2.85	2.29
V		230.00	213.00	107.00	137.00	117.00
W		19.00	49.00	9.00	8.00	19.00
Y		22.20	63.50	64.40	18.90	19.50
Yb		2.18	5.51	5.39	1.88	2.06
Zr		166.00	397.00	402.00	119.00	121.00
As		1.70	5.00	3.00	0.50	0.30
Bi		0.01	0.35	0.02	<0.01	0.04
Hg		<0.005	<0.005	<0.005	<0.005	<0.005
In		0.02	0.05	0.07	0.03	0.02

Abbreviations:
D = depth
WL = wavelength

Units:
MD = mafic dyke
MBX = mafic breccia
MT = mafic tuff
MLT = mafic lapilli tuff

Table C.1.1. Whole Rock Geochemistry and Terraspec™ Data for Argyle Samples

Sample ID	294963	294964	294965	294966	294967
Hole ID	BN-14-186	BN-14-186	BN-14-186	BN-14-186	BN-14-186
Depth (m)	20.9	29.2	34.5	42.75	48.5
Lithology	Gabbro	Gabbro	Gabbro	Gabbro	Gabbro
Alteration Assemblage	Ank-Ab-Chl-Qt-Rut	Ab-Hem-Qt-Chl-Ank-Rut	Chl-Ab-Qt-Ank	Chl-Ab	Chl-Ab-Ank-Qt
Alteration	Intermediate	Proximal	Proximal	Distal	Intermediate
Re	0.00	0.01	<0.001	<0.001	<0.001
Sb	<0.05	<0.05	0.06	<0.05	<0.05
Se	<0.2	1.20	<0.2	<0.2	<0.2
Te	<0.01	0.26	<0.01	<0.01	0.02
Tl	<0.02	0	<0.02	<0.02	<0.02
Ag	<0.5	<0.5	<0.5	<0.5	<0.5
Cd	<0.5	1	<0.5	<0.5	<0.5
Co	29	29	29	25	24
Cu	11	10	25	4	31
Li	10	10	20	20	20
Mo	<1	15	2	<1	<1
Ni	20	16	<1	87	118
Pb	3	5	3	2	2
Sc	24	18	16	20	17
Zn	56	106	157	33	54
Au	0.00	2.10	0.01	0.01	0.01
C *%*	3.21	2.12	1.66	1.22	2.57
CO_2	11.80	7.80	6.10	4.50	9.40
AlOH WL *nm*	2193.92	2204.33	-	-	2199.99
AlOH D	0.25	0.14	-	-	0.18
FeOH WL	2254.76	2253.96	-	-	2252.17
FeOH D	0.19	0.11	-	-	0.17
AlOH D/FeOH D	1.35	1.19	-	-	1.07

Abbreviations:
D = depth
WL = wavelength

Units:
MD = mafic dyke
MBX = mafic breccia
MT = mafic tuff
MLT = mafic lapilli tuff

Table C.1.1. Whole Rock Geochemistry and Terraspec™ Data for Argyle Samples

Sample ID		294968	294969	294970	I951351	I951352
Hole ID		BN-14-186	BN-14-186	BN-14-186	AE-17-46	AE-17-46
Depth (m)		55.6	63.7	67	11.30	37.60
Lithology		Gabbro	Gabbro	Gabbro	MBX	Gabbro
Alteration Assemblage		Ab-Ank-Qt-Chl	Ab-Hem-Ank-Qt-Chl	Ab-Chl-Ank	Ep-Chl	Chl-Ab-Ep-Rut
Alteration		Proximal	Proximal	Intermediate	Distal	Intermediate
SiO_2	*%*	38.40	47.20	51.10	42.20	44.20
Al_2O_3		13.00	16.55	17.30	14.45	13.05
Fe_2O_3		5.79	5.98	6.35	10.25	10.50
CaO		14.50	7.14	5.37	9.02	8.37
MgO		3.83	2.96	3.29	5.48	5.32
Na_2O		3.81	3.65	1.97	4.00	3.82
K_2O		1.68	2.83	3.81	0.04	0.17
Cr_2O_3		0.04	0.01	0.01	0.01	<0.01
TiO_2		0.78	1.21	1.18	1.55	1.97
MnO		0.13	0.10	0.06	0.15	0.16
P_2O_5		0.18	0.22	0.22	0.19	0.28
SrO		0.04	0.02	0.02	0.01	0.03
BaO		0.01	0.01	0.01	<0.01	0.01
LOI		17.50	10.85	9.80	11.80	9.48
Total		99.69	98.73	100.49	99.15	97.36
C		4.61	2.72	2.11	1.82	1.79
S		0.01	0.18	0.03	0.02	0.10
Ba	*ppm*	77.30	142.00	122.50	13.30	44.40
Ce		25.00	30.50	35.90	18.10	28.40
Cr		320.00	100.00	40.00	120.00	20.00
Cs		0.43	0.55	1.02	0.06	0.03
Dy		2.71	3.67	3.74	6.59	5.01
Er		1.73	2.34	2.52	3.86	3.17
Eu		1.00	1.23	1.30	1.16	1.63
Ga		12.80	18.30	19.20	14.10	16.20
Gd		2.98	4.01	3.98	4.91	5.59
Ge		<5	<5	<5	<5	<5
Hf		2.40	3.40	4.10	2.70	4.30
Ho		0.53	0.72	0.82	1.30	1.09
La		11.50	13.80	15.80	6.80	11.00
Lu		0.21	0.32	0.34	0.53	0.38
Nb		6.00	6.60	8.10	6.10	10.00
Nd		12.40	15.90	17.10	14.10	18.80
Pr		2.89	3.79	4.08	2.52	3.84
Rb		29.00	46.90	80.90	0.40	2.10
Sm		2.76	4.05	3.47	4.47	5.08
Sn		1.00	2.00	2.00	4.00	2.00
Sr		311.00	191.00	165.00	126.50	221.00
Ta		0.60	0.60	0.70	0.30	0.60
Tb		0.50	0.54	0.59	0.99	0.84
Th		2.81	3.34	4.46	0.54	0.94
Tm		0.25	0.31	0.33	0.60	0.38
U		1.82	2.11	2.91	0.22	0.34
V		135.00	234.00	143.00	261.00	204.00
W		15.00	23.00	10.00	3.00	2.00
Y		15.90	21.50	22.90	29.90	23.60
Yb		1.49	2.32	2.65	3.76	2.31
Zr		96.00	146.00	171.00	129.00	202.00
As		0.10	0.80	0.30	45.80	3.60
Bi		0.01	0.03	0.01	0.03	0.01
Hg		<0.005	<0.005	<0.005	<0.005	<0.005
In		0.02	0.03	0.01	0.06	0.06

Abbreviations:
D = depth
WL = wavelength

Units:
MD = mafic dyke
MBX = mafic breccia
MT = mafic tuff
MLT = mafic lapilli tuff

Table C.1.1. Whole Rock Geochemistry and Terraspec™ Data for Argyle Samples

Sample ID		294968	294969	294970	I951351	I951352
Hole ID		BN-14-186	BN-14-186	BN-14-186	AE-17-46	AE-17-46
Depth (m)		55.6	63.7	67	11.30	37.60
Lithology		Gabbro	Gabbro	Gabbro	MBX	Gabbro
Alteration Assemblage		Ab-Ank-Qt-Chl	Ab-Hem-Ank-Qt-Chl	Ab-Chl-Ank	Ep-Chl	Chl-Ab-Ep-Rut
Alteration		Proximal	Proximal	Intermediate	Distal	Intermediate
Re		<0.001	<0.001	<0.001	<0.001	0.00
Sb		<0.05	<0.05	<0.05	0.11	0.09
Se		<0.2	<0.2	<0.2	<0.2	<0.2
Te		3.65	0.16	0.01	<0.01	<0.01
Tl		<0.02	<0.02	0	<0.02	<0.02
Ag		<0.5	<0.5	<0.5	<0.5	<0.5
Cd		<0.5	<0.5	<0.5	1	<0.5
Co		24	22	19	39	38
Cu		30	84	103	1	49
Li		<10	<10	10	30	10
Mo		<1	1	<1	<1	<1
Ni		143	49	27	59	30
Pb		5	6	4	4	<2
Sc		18	19	17	31	32
Zn		35	32	51	82	83
Au		0.01	0.35	0.05	<0.001	<0.001
C	*%*	4.26	2.47	1.92	1.73	1.69
CO_2		15.60	9.10	7.00	6.30	6.20
AlOH WL	*nm*	2198.50	2199.67	2201.88	-	-
AlOH D		0.28	0.33	0.43	-	-
FeOH WL		2251.35	-	2251.04	2256.51	2255.53
FeOH D		0.14	-	0.25	0.34	0.19
AlOH D/FeOH D		2.00	-	1.75	-	-

Abbreviations:
D = depth
WL = wavelength

Units:
MD = mafic dyke
MBX = mafic breccia
MT = mafic tuff
MLT = mafic lapilli tuff

Table C.1.1. Whole Rock Geochemistry and Terraspec™ Data for Argyle Samples

Sample ID		I951353	I951354	I951355	I951356	I951357
Hole ID		AE-17-46	AE-17-46	AE-17-46	AE-17-46	AE-17-46
Depth (m)		50.35	67.60	69.60	71.75	73.85
Lithology		Gabbro	Gabbro	Gabbro	MD	MD
Alteration Assemblage		Ank-Ab-Chl-Rut	Qt-Ank-AB-Ms-Chl-Py	Ab-Qt-Chl-Ank-Py	Ank-Ab-Ep	Chl-Ep-Rut
Alteration		Intermediate	Proximal	Proximal	Proximal	Distal
SiO_2	*%*	44.30	52.20	54.70	40.40	40.30
Al_2O_3		13.05	16.35	15.85	13.85	13.40
Fe_2O_3		14.95	10.05	9.06	8.55	13.55
CaO		5.67	2.78	3.15	10.60	6.40
MgO		4.29	1.08	1.21	3.80	5.17
Na_2O		4.28	6.92	6.74	2.12	4.41
K_2O		0.23	0.54	0.88	2.63	0.08
Cr_2O_3		<0.01	<0.01	<0.01	<0.01	<0.01
TiO_2		3.42	1.14	1.10	3.02	3.15
MnO		0.22	0.10	0.20	0.24	0.19
P_2O_5		0.52	0.40	0.39	0.43	0.53
SrO		0.03	0.01	0.02	0.02	0.01
BaO		0.01	<0.01	0.01	0.02	<0.01
LOI		8.25	4.30	7.11	15.60	9.70
Total		99.22	95.87	100.42	101.28	96.89
C		1.83	0.90	2.01	4.05	2.10
S		0.25	2.65	0.23	0.15	0.19
Ba	*ppm*	62.60	45.20	76.00	214.00	19.80
Ce		58.80	97.70	87.20	41.30	55.70
Cr		<10	<10	<10	30.00	30.00
Cs		0.05	0.08	0.18	0.35	0.05
Dy		10.30	14.95	13.75	6.22	7.89
Er		5.82	8.56	8.09	3.17	4.19
Eu		3.22	4.11	3.89	2.11	2.85
Ga		25.90	25.20	28.10	21.00	25.70
Gd		11.40	15.05	13.55	6.92	8.64
Ge		<5	<5	<5	<5	<5
Hf		7.30	13.90	12.50	4.70	6.30
Ho		2.04	3.07	2.86	1.15	1.57
La		22.90	38.60	34.40	17.10	22.80
Lu		0.74	1.16	1.08	0.43	0.51
Nb		20.60	34.70	34.00	15.40	21.10
Nd		40.60	59.50	54.50	25.60	34.10
Pr		7.86	12.45	11.15	5.35	6.97
Rb		3.30	8.00	11.70	34.90	1.10
Sm		10.35	14.95	13.35	6.10	8.65
Sn		3.00	2.00	4.00	2.00	3.00
Sr		262.00	120.00	187.50	197.50	166.50
Ta		1.30	2.20	2.10	1.00	1.30
Tb		1.76	2.40	2.30	1.03	1.41
Th		1.46	3.33	2.83	1.17	1.55
Tm		0.84	1.33	1.22	0.49	0.59
U		0.56	1.29	1.18	0.47	0.58
V		342.00	38.00	21.00	321.00	377.00
W		4.00	13.00	6.00	8.00	1.00
Y		45.10	67.40	62.50	26.60	34.50
Yb		4.72	7.93	7.28	2.77	3.73
Zr		364.00	745.00	679.00	259.00	360.00
As		3.00	244.00	4.50	18.20	19.90
Bi		0.05	0.33	0.02	0.02	0.02
Hg		0.01	0.01	<0.005	<0.005	0.01
In		0.12	0.09	0.09	0.05	0.09

Abbreviations:
D = depth
WL = wavelength

Units:
MD = mafic dyke
MBX = mafic breccia
MT = mafic tuff
MLT = mafic lapilli tuff

Table C.1.1. Whole Rock Geochemistry and Terraspec™ Data for Argyle Samples

Sample ID	I951353	I951354	I951355	I951356	I951357
Hole ID	AE-17-46	AE-17-46	AE-17-46	AE-17-46	AE-17-46
Depth (m)	50.35	67.60	69.60	71.75	73.85
Lithology	Gabbro	Gabbro	Gabbro	MD	MD
Alteration Assemblage	Ank-Ab-Chl-Rut	Qt-Ank-AB-Ms-Chl-Py	Ab-Qt-Chl-Ank-Py	Ank-Ab-Ep	Chl-Ep-Rut
Alteration	Intermediate	Proximal	Proximal	Proximal	Distal
Re	0.00	0.00	<0.001	0.00	0.00
Sb	0.14	0.14	0.06	0.16	0.09
Se	0.20	3.40	<0.2	<0.2	<0.2
Te	<0.01	0.47	0.05	0.02	<0.01
Tl	0	0	<0.02	0	<0.02
Ag	<0.5	<0.5	<0.5	<0.5	<0.5
Cd	<0.5	<0.5	<0.5	1	<0.5
Co	42	12	8	32	42
Cu	28	60	5	36	34
Li	10	<10	<10	<10	30
Mo	1	1	1	1	2
Ni	2	2	1	29	40
Pb	<2	5	<2	3	4
Sc	30	8	8	23	26
Zn	129	75	95	75	116
Au	<0.001	10.65	0.29	1.18	<0.001
C *%*	1.69	0.83	1.82	3.84	2.01
CO_2	6.20	3.00	6.70	14.10	7.40
AlOH WL *nm*	2220.30	2196.91	2195.34	2197.84	-
AlOH D	0.04	0.15	0.35	0.39	-
FeOH WL	2259.11	2259.46	-	-	2258.77
FeOH D	0.08	0.05	-	-	0.15
AlOH D/FeOH D	0.48	3.13	-	-	-

Abbreviations:
D = depth
WL = wavelength

Units:
MD = mafic dyke
MBX = mafic breccia
MT = mafic tuff
MLT = mafic lapilli tuff

Table C.1.1. Whole Rock Geochemistry and Terraspec™ Data for Argyle Samples

Sample ID		I951363	I951364	I951365	I951366	I951367
Hole ID		AE-16-40	AE-16-40	AE-16-40	AE-16-40	AE-16-40
Depth (m)		44.20	54.85	66.50	69.90	85.50
Lithology		Gabbro	Gabbro	MD	Gabbro	MLT
Alteration Assemblage		Ab-Chl-Ank-Rut	Ab-Chl-Ep-Ank-Rut	Chl-Ep	Chl-Ank-Ep	Ep-Chl
Alteration		Proximal	Intermediate	Distal	Intermediate	Distal
SiO_2	*%*	50.70	51.30	42.30	47.80	54.90
Al_2O_3		13.55	15.00	14.10	16.50	17.45
Fe_2O_3		8.69	13.05	14.70	10.95	6.73
CaO		4.21	5.78	7.41	10.55	4.69
MgO		1.03	3.37	5.69	6.64	6.03
Na_2O		3.04	5.14	3.46	3.00	5.88
K_2O		1.81	0.25	0.39	0.69	0.72
Cr_2O_3		<0.01	<0.01	<0.01	0.03	0.03
TiO_2		1.04	2.56	3.45	1.87	1.15
MnO		0.18	0.19	0.21	0.16	0.07
P_2O_5		0.33	0.70	0.56	0.23	0.22
SrO		0.01	0.03	0.04	0.05	0.03
BaO		0.02	0.01	0.01	0.01	0.01
LOI		6.91	3.42	4.46	2.88	2.67
Total		91.52	100.80	96.78	101.36	100.58
C		1.49	0.46	0.40	0.13	0.02
S		0.08	0.27	0.20	0.03	0.01
Ba	*ppm*	140.50	98.00	100.50	112.50	91.40
Ce		74.50	55.90	49.30	24.00	37.80
Cr		<10	<10	20.00	210.00	230.00
Cs		0.38	0.23	0.08	0.10	0.09
Dy		11.80	9.09	7.21	4.49	4.94
Er		7.38	5.00	4.18	2.55	2.56
Eu		3.08	2.69	2.54	1.57	1.45
Ga		35.70	19.60	23.80	18.20	19.70
Gd		11.35	9.10	8.50	4.59	4.95
Ge		<5	<5	<5	<5	<5
Hf		11.40	6.60	5.60	3.70	3.30
Ho		2.44	1.80	1.48	0.86	0.97
La		29.30	22.20	20.50	9.30	17.30
Lu		0.97	0.59	0.48	0.33	0.37
Nb		30.90	19.40	19.40	8.40	10.00
Nd		44.00	36.20	31.70	15.60	19.10
Pr		9.66	7.20	6.45	3.20	4.26
Rb		27.40	2.80	4.00	8.70	7.60
Sm		11.75	9.52	7.43	4.63	4.91
Sn		5.00	3.00	2.00	2.00	2.00
Sr		111.00	215.00	341.00	380.00	255.00
Ta		1.80	1.20	1.10	0.50	0.60
Tb		1.93	1.48	1.23	0.74	0.78
Th		2.58	1.43	0.97	0.70	4.33
Tm		1.10	0.74	0.54	0.38	0.40
U		1.02	0.58	0.37	0.24	2.31
V		19.00	120.00	368.00	254.00	148.00
W		1.00	1.00	1.00	<1	1.00
Y		55.80	38.50	32.10	19.60	22.10
Yb		6.25	4.14	3.29	2.15	2.57
Zr		629.00	340.00	294.00	175.00	156.00
As		1.80	4.70	5.20	25.40	17.50
Bi		0.01	<0.01	0.01	<0.01	0.02
Hg		<0.005	0.01	0.01	<0.005	<0.005
In		0.09	0.05	0.02	0.01	<0.005

Abbreviations:
D = depth
WL = wavelength

Units:
MD = mafic dyke
MBX = mafic breccia
MT = mafic tuff
MLT = mafic lapilli tuff

Table C.1.1. Whole Rock Geochemistry and Terraspec™ Data for Argyle Samples

Sample ID		I951363	I951364	I951365	I951366	I951367
Hole ID		AE-16-40	AE-16-40	AE-16-40	AE-16-40	AE-16-40
Depth (m)		44.20	54.85	66.50	69.90	85.50
Lithology		Gabbro	Gabbro	MD	Gabbro	MLT
Alteration Assemblage		Ab-Chl-Ank-Rut	Ab-Chl-Ep-Ank-Rut	Chl-Ep	Chl-Ank-Ep	Ep-Chl
Alteration		Proximal	Intermediate	Distal	Intermediate	Distal
Re		<0.001	0.00	0.00	0.00	<0.001
Sb		0.11	0.25	0.31	0.40	0.12
Se		<0.2	0.30	<0.2	<0.2	<0.2
Te		<0.01	0.01	<0.01	<0.01	<0.01
Tl		0	0	<0.02	<0.02	<0.02
Ag		<0.5	<0.5	<0.5	<0.5	<0.5
Cd		<0.5	<0.5	1	<0.5	<0.5
Co		9	30	49	42	28
Cu		5	16	38	88	4
Li		<10	10	20	10	10
Mo		2	2	1	1	1
Ni		<1	2	46	59	109
Pb		2	4	6	2	3
Sc		9	20	30	34	18
Zn		122	119	123	66	42
Au		0.01	0.00	<0.001	<0.001	0.08
C	*%*	1.39	0.42	0.36	0.14	<0.05
CO_2		5.10	1.50	1.30	0.50	<0.2
AlOH WL	*nm*	2196.77	2221.16	-	2227.31	-
AlOH D		0.24	0.12	-	0.11	-
FeOH WL		2251.05	2252.04	2255.81	2255.04	2251.89
FeOH D		0.06	0.18	0.11	0.25	0.33
AlOH D/FeOH D		4.12	0.70	-	0.43	-

Abbreviations:
D = depth
WL = wavelength

Units:
MD = mafic dyke
MBX = mafic breccia
MT = mafic tuff
MLT = mafic lapilli tuff

Table C.1.1. Whole Rock Geochemistry and Terraspec™ Data for Argyle Samples

Sample ID		I951368	I951369	I951370	I951371	I951372
Hole ID		AE-16-34	AE-16-34	AE-16-34	AE-16-34	AE-16-34
Depth (m)		4.90	11.20	20.85	32.00	33.50
Lithology		MBX	Gabbro	Gabbro	Gabbro	Gabbro
Alteration Assemblage		Calc-Chl-Ep	Ep-Chl	Ank-Chl-Ep-Rut	Qt-Chl-Ank-Ab-Py	Qt-Chl-Ank-Ab-Py
Alteration		Distal	Distal	Intermediate	Proximal	Proximal
SiO_2	*%*	51.50	43.40	46.30	58.50	73.10
Al_2O_3		16.15	15.50	16.95	6.82	3.44
Fe_2O_3		8.05	10.25	11.00	7.34	6.91
CaO		5.68	9.22	10.65	8.69	6.02
MgO		3.81	6.66	6.63	3.35	1.48
Na_2O		6.14	2.57	2.38	0.86	1.21
K_2O		0.26	0.39	0.19	0.85	0.19
Cr_2O_3		0.02	0.03	0.03	<0.01	<0.01
TiO_2		1.65	1.80	1.93	0.88	0.62
MnO		0.08	0.11	0.15	0.20	0.17
P_2O_5		0.28	0.22	0.24	0.21	0.16
SrO		0.01	0.03	0.06	0.02	0.01
BaO		<0.01	<0.01	<0.01	0.01	<0.01
LOI		6.61	7.45	4.56	12.20	6.16
Total		100.24	97.63	101.07	99.93	99.47
C		1.17	1.04	0.35	3.14	2.01
S		0.01	0.01	0.02	0.02	1.69
Ba	*ppm*	46.00	44.10	33.90	70.40	18.60
Ce		18.10	22.60	28.00	17.50	11.60
Cr		120.00	220.00	240.00	20.00	30.00
Cs		0.06	0.30	0.07	0.19	0.04
Dy		6.43	4.43	5.02	4.38	2.58
Er		4.28	2.17	2.87	2.12	1.45
Eu		1.90	1.48	1.71	1.48	0.96
Ga		16.90	20.10	22.90	13.10	4.00
Gd		6.56	4.53	5.48	4.39	2.61
Ge		<5	<5	<5	<5	<5
Hf		2.60	2.90	3.60	2.10	1.70
Ho		1.50	0.87	1.10	0.78	0.55
La		8.20	8.60	11.20	6.80	4.30
Lu		0.59	0.23	0.36	0.24	0.19
Nb		5.80	7.80	9.90	8.50	6.40
Nd		15.70	15.80	18.70	12.60	8.10
Pr		2.78	3.07	3.78	2.41	1.73
Rb		3.10	6.10	3.00	12.30	2.40
Sm		4.65	4.49	4.87	3.61	2.27
Sn		4.00	2.00	2.00	5.00	2.00
Sr		113.00	285.00	609.00	197.50	96.60
Ta		0.30	0.50	0.60	0.40	0.30
Tb		1.05	0.68	0.87	0.64	0.42
Th		0.53	0.50	0.71	0.39	0.30
Tm		0.68	0.36	0.42	0.32	0.20
U		0.37	0.15	0.30	0.19	0.15
V		177.00	276.00	315.00	154.00	36.00
W		2.00	1.00	1.00	12.00	9.00
Y		34.50	18.90	22.40	18.00	12.90
Yb		3.78	1.97	2.41	2.00	1.26
Zr		122.00	136.00	180.00	102.00	73.00
As		1.50	4.20	6.30	1.40	-250.00
Bi		<0.01	<0.01	<0.01	<0.01	0.32
Hg		<0.005	<0.005	<0.005	0.01	<0.005
In		0.03	0.03	0.02	0.06	0.05

Abbreviations:
D = depth
WL = wavelength

Units:
MD = mafic dyke
MBX = mafic breccia
MT = mafic tuff
MLT = mafic lapilli tuff

Table C.1.1. Whole Rock Geochemistry and Terraspec™ Data for Argyle Samples

Sample ID		I951368	I951369	I951370	I951371	I951372
Hole ID		AE-16-34	AE-16-34	AE-16-34	AE-16-34	AE-16-34
Depth (m)		4.90	11.20	20.85	32.00	33.50
Lithology		MBX	Gabbro	Gabbro	Gabbro	Gabbro
Alteration Assemblage		Calc-Chl-Ep	Ep-Chl	Ank-Chl-Ep-Rut	Qt-Chl-Ank-Ab-Py	Qt-Chl-Ank-Ab-Py
Alteration		Distal	Distal	Intermediate	Proximal	Proximal
Re		<0.001	<0.001	<0.001	0.00	0.00
Sb		0.07	0.41	0.67	0.05	0.07
Se		0.30	<0.2	0.20	<0.2	1.90
Te		<0.01	0.01	0.01	<0.01	0.44
Tl		<0.02	<0.02	<0.02	<0.02	<0.02
Ag		<0.5	<0.5	<0.5	<0.5	<0.5
Cd		<0.5	<0.5	<0.5	<0.5	<0.5
Co		31	44	44	17	9
Cu		9	6	31	1	3
Li		20	20	20	10	<10
Mo		<1	<1	<1	1	2
Ni		54	71	59	16	1
Pb		4	<2	<2	2	<2
Sc		31	32	33	18	7
Zn		28	45	62	67	23
Au		<0.001	<0.001	<0.001	0.01	4.95
C	*%*	1.06	0.95	0.33	2.93	1.87
CO_2		3.90	3.50	1.20	<0.2	10.70
AlOH WL	*nm*	-	-	-	2196.72	2196.76
AlOH D		-	-	-	0.26	0.03
FeOH WL		2256.27	2252.26	2253.74	2257.55	2252.35
FeOH D		0.27	0.22	0.27	0.04	0.01
AlOH D/FeOH D		-	-	-	6.82	1.94

Abbreviations:
D = depth
WL = wavelength

Units:
MD = mafic dyke
MBX = mafic breccia
MT = mafic tuff
MLT = mafic lapilli tuff

Table C.1.1. Whole Rock Geochemistry and Terraspec™ Data for Argyle Samples

Sample ID		I951373	I951374	I951375	I951376	I951377
Hole ID		AE-16-34	AE-16-34	AE-16-34	AE-16-34	AE-16-09
Depth (m)		35.10	48.05	60.20	68.10	14.90
Lithology		Gabbro	Gabbro	MD	MD	Gabbro
Alteration Assemblage		Chl-Ab-Ank-Rut-Qt	Chl-Ab-Ank-Ep-Rut	Ep-Chl	Chl-Ep	Chl-Ep
Alteration		Proximal	Intermediate	Intermediate	Distal	Distal
SiO_2	*%*	49.80	44.80	37.00	44.90	45.00
Al_2O_3		14.00	13.15	16.10	15.10	13.05
Fe_2O_3		14.30	12.25	12.20	14.85	17.10
CaO		4.57	7.29	6.63	7.60	5.60
MgO		2.88	3.41	7.11	6.07	4.99
Na_2O		4.69	4.68	1.86	2.68	3.63
K_2O		0.17	0.22	2.29	0.45	0.12
Cr_2O_3		<0.01	<0.01	0.03	<0.01	<0.01
TiO_2		2.17	2.48	2.15	3.45	3.64
MnO		0.24	0.20	0.12	0.20	0.19
P_2O_5		1.10	0.62	0.27	0.57	0.36
SrO		0.02	0.02	0.02	0.06	0.01
BaO		0.01	0.01	0.01	0.01	<0.01
LOI		6.13	10.10	12.85	4.03	6.18
Total		100.08	99.23	98.64	99.97	99.87
C		1.20	2.42	2.63	0.13	1.00
S		0.04	0.05	0.06	0.10	0.02
Ba	*ppm*	83.70	73.30	133.50	81.80	38.60
Ce		83.00	57.70	29.80	60.40	39.50
Cr		<10	<10	250.00	30.00	10.00
Cs		0.05	0.07	0.40	0.10	0.16
Dy		12.50	9.44	5.17	7.61	7.27
Er		6.72	4.97	2.77	4.17	3.78
Eu		4.02	2.98	1.73	2.55	2.33
Ga		27.20	22.70	21.40	25.20	23.50
Gd		14.25	10.05	5.43	8.28	7.58
Ge		<5	<5	<5	<5	<5
Hf		9.70	6.90	4.40	7.90	5.90
Ho		2.58	1.91	1.04	1.59	1.45
La		31.40	21.80	11.20	24.40	14.90
Lu		0.87	0.64	0.34	0.58	0.49
Nb		25.90	17.80	10.20	21.90	13.90
Nd		54.60	38.00	19.70	36.10	27.00
Pr		11.90	8.24	4.30	8.17	5.74
Rb		2.50	3.40	31.40	3.40	1.80
Sm		13.80	9.39	5.23	8.22	7.00
Sn		4.00	3.00	2.00	3.00	4.00
Sr		172.00	229.00	183.00	510.00	110.00
Ta		1.70	1.20	0.70	1.40	0.90
Tb		2.10	1.52	0.85	1.30	1.20
Th		1.84	1.30	0.76	1.94	0.95
Tm		0.96	0.68	0.37	0.60	0.56
U		0.84	0.55	0.35	0.75	0.43
V		95.00	174.00	309.00	369.00	557.00
W		2.00	2.00	6.00	1.00	1.00
Y		63.50	45.30	25.10	37.20	35.20
Yb		5.63	4.27	2.43	3.71	3.34
Zr		437.00	295.00	188.00	379.00	252.00
As		1.90	2.10	3.30	2.40	2.30
Bi		<0.01	0.02	0.01	0.01	<0.01
Hg		<0.005	<0.005	<0.005	0.01	<0.005
In		0.10	0.09	0.04	0.04	0.08

Abbreviations:
D = depth
WL = wavelength

Units:
MD = mafic dyke
MBX = mafic breccia
MT = mafic tuff
MLT = mafic lapilli tuff

Table C.1.1. Whole Rock Geochemistry and Terraspec™ Data for Argyle Samples

Sample ID	I951373	I951374	I951375	I951376	I951377
Hole ID	AE-16-34	AE-16-34	AE-16-34	AE-16-34	AE-16-09
Depth (m)	35.10	48.05	60.20	68.10	14.90
Lithology	Gabbro	Gabbro	MD	MD	Gabbro
Alteration Assemblage	Chl-Ab-Ank-Rut-Qt	Chl-Ab-Ank-Ep-Rut	Ep-Chl	Chl-Ep	Chl-Ep
Alteration	Proximal	Intermediate	Intermediate	Distal	Distal
Re	<0.001	0.00	<0.001	0.00	0.00
Sb	0.13	0.12	0.23	0.22	0.21
Se	<0.2	<0.2	<0.2	0.30	<0.2
Te	<0.01	<0.01	0.03	<0.01	0.01
Tl	<0.02	<0.02	0	<0.02	<0.02
Ag	<0.5	<0.5	<0.5	<0.5	<0.5
Cd	<0.5	<0.5	1	1	<0.5
Co	24	26	49	47	50
Cu	10	28	75	34	41
Li	30	20	40	10	20
Mo	1	1	<1	1	<1
Ni	<1	2	75	46	17
Pb	5	3	2	6	<2
Sc	14	23	31	29	36
Zn	149	89	78	121	111
Au	0.01	0.01	0.01	0.01	<0.001
C *%*	1.09	2.27	2.47	0.15	0.93
CO_2	6.90	4.00	8.30	9.00	0.50
AlOH WL *nm*	-	-	2203.34	2227.42	-
AlOH D	-	-	0.31	0.03	-
FeOH WL	2260.87	2259.28	2253.80	2255.36	2257.35
FeOH D	0.13	0.18	0.22	0.11	0.11
AlOH D/FeOH D	-	-	1.39	0.24	-

Abbreviations:
D = depth
WL = wavelength

Units:
MD = mafic dyke
MBX = mafic breccia
MT = mafic tuff
MLT = mafic lapilli tuff

Table C.1.1. Whole Rock Geochemistry and Terraspec™ Data for Argyle Samples

Sample ID		I951378	I951379	I951380	I951381	I951382
Hole ID		AE-16-09	AE-16-09	AE-16-09	AE-16-09	AE-16-09
Depth (m)		22.20	26.35	33.20	42.50	55.15
Lithology		Gabbro	Gabbro	Gabbro	MD	MD
Alteration Assemblage		Chl-Ank-Ab-Ep-Rut	Ab-Ms-Ank-Chl-Py	Chl-Ank-Ab-Ep-Rut	Chl	Chl
Alteration		Proximal	Proximal	Proximal	Distal	Distal
SiO_2	*%*	43.90	51.20	40.60	43.30	44.70
Al_2O_3		12.30	16.20	13.85	16.95	15.00
Fe_2O_3		14.05	9.64	9.06	12.50	14.75
CaO		7.19	4.10	9.44	10.45	8.51
MgO		3.25	1.52	5.77	9.01	5.84
Na_2O		3.74	6.76	3.27	1.76	2.75
K_2O		0.38	0.72	1.21	0.96	1.25
Cr_2O_3		<0.01	<0.01	0.05	0.03	<0.01
TiO_2		2.87	1.35	1.52	2.03	3.30
MnO		0.23	0.11	0.15	0.18	0.21
P_2O_5		0.63	0.36	0.18	0.32	0.54
SrO		0.02	0.01	0.02	0.04	0.05
BaO		0.01	0.01	0.01	0.01	0.02
LOI		10.70	6.84	14.75	4.37	2.98
Total		99.27	98.82	99.88	101.91	99.90
C		2.50	1.40	3.53	0.17	0.09
S		0.01	2.28	0.01	0.10	0.17
Ba	*ppm*	66.90	47.40	93.00	81.00	176.00
Ce		59.60	113.50	17.20	24.10	55.30
Cr		<10	<10	320.00	230.00	30.00
Cs		0.12	0.21	0.29	0.21	0.10
Dy		9.92	15.60	3.21	5.66	6.98
Er		5.34	9.17	1.77	3.05	3.78
Eu		3.14	4.46	1.07	1.78	2.62
Ga		23.00	21.60	14.10	18.30	23.70
Gd		9.99	15.05	3.30	5.37	7.75
Ge		<5	<5	<5	<5	<5
Hf		8.00	17.60	2.70	3.50	7.30
Ho		2.00	3.28	0.66	1.12	1.41
La		22.60	44.60	6.30	8.90	22.60
Lu		0.69	1.27	0.21	0.41	0.51
Nb		21.80	38.20	5.90	6.40	19.90
Nd		39.00	66.90	11.60	17.50	32.30
Pr		8.47	15.45	2.48	3.54	7.44
Rb		5.70	10.20	17.60	15.90	14.60
Sm		9.81	15.55	3.16	4.83	7.48
Sn		3.00	3.00	1.00	1.00	2.00
Sr		184.00	134.50	209.00	351.00	407.00
Ta		1.40	2.60	0.40	0.40	1.30
Tb		1.56	2.52	0.52	0.85	1.19
Th		1.52	3.63	0.44	0.42	1.78
Tm		0.75	1.36	0.26	0.45	0.54
U		0.65	1.54	0.16	0.19	0.70
V		202.00	68.00	231.00	290.00	350.00
W		3.00	12.00	3.00	1.00	1.00
Y		47.50	81.60	16.30	27.60	35.00
Yb		4.49	8.67	1.57	2.79	3.35
Zr		354.00	811.00	107.00	142.00	349.00
As		1.10	74.10	0.50	106.00	25.90
Bi		<0.01	0.07	0.01	0.01	0.01
Hg		<0.005	0.01	0.01	<0.005	0.01
In		0.10	0.09	0.04	0.01	0.01

Abbreviations:

D = depth
WL = wavelength

Units:

MD = mafic dyke
MBX = mafic breccia
MT = mafic tuff
MLT = mafic lapilli tuff

Table C.1.1. Whole Rock Geochemistry and Terraspec™ Data for Argyle Samples

Sample ID		I951378	I951379	I951380	I951381	I951382
Hole ID		AE-16-09	AE-16-09	AE-16-09	AE-16-09	AE-16-09
Depth (m)		22.20	26.35	33.20	42.50	55.15
Lithology		Gabbro	Gabbro	Gabbro	MD	MD
Alteration Assemblage		Chl-Ank-Ab-Ep-Rut	Ab-Ms-Ank-Chl-Py	Chl-Ank-Ab-Ep-Rut	Chl	Chl
Alteration		Proximal	Proximal	Proximal	Distal	Distal
Re		0.00	0.00	<0.001	0.00	0.00
Sb		0.17	0.14	0.07	0.38	0.20
Se		<0.2	3.40	<0.2	<0.2	0.30
Te		<0.01	0.40	0.01	<0.01	<0.01
Tl		<0.02	<0.02	<0.02	<0.02	<0.02
Ag		<0.5	<0.5	<0.5	<0.5	<0.5
Cd		<0.5	<0.5	<0.5	<0.5	1
Co		28	14	37	52	47
Cu		10	46	34	53	40
Li		10	<10	20	30	10
Mo		<1	2	1	<1	2
Ni		1	1	57	112	47
Pb		3	2	2	2	8
Sc		20	9	36	34	27
Zn		104	47	60	88	119
Au		0.00	5.05	0.04	0.01	0.00
C	*%*	2.34	1.32	3.36	0.17	0.09
CO_2		3.40	8.60	4.80	12.30	0.60
AlOH WL	*nm*	2196.99	2196.18	2195.04	2224.20	-
AlOH D		0.05	0.20	0.24	0.12	-
FeOH WL		2258.26	2257.16	2256.17	2253.70	2255.66
FeOH D		0.10	0.10	0.19	0.18	0.17
AlOH D/FeOH D		0.53	1.90	1.28	0.67	-

Abbreviations:

D = depth

WL = wavelength

Units:

MD = mafic dyke

MBX = mafic breccia

MT = mafic tuff

MLT = mafic lapilli tuff

Table C.1.1. Whole Rock Geochemistry and Terraspec™ Data for Argyle Samples

Sample ID		I951383	I951384	I951385	I951386	I951387
Hole ID		AE-16-09	AE-16-32	AE-16-32	AE-16-32	AE-16-32
Depth (m)		62.40	8.90	20.05	23.35	32.30
Lithology		MLT	MLT	Gabbro	MD	Gabbro
Alteration Assemblage		Chl	Chl-Hem-Ep	Chl-Ep-Rut	Ep-Chl	Ep-Calc-Chl-Ab
Alteration		Distal	Distal	Distal	Distal	Intermediate
SiO_2	*%*	53.40	52.20	43.90	40.70	46.20
Al_2O_3		16.50	16.60	16.55	14.25	15.65
Fe_2O_3		7.34	10.70	11.10	14.05	11.60
CaO		3.46	4.35	5.60	7.47	10.40
MgO		7.88	5.70	7.06	5.96	6.69
Na_2O		4.13	5.08	3.13	2.09	3.19
K_2O		1.15	1.88	1.26	0.74	0.11
Cr_2O_3		0.03	0.02	0.03	0.01	0.02
TiO_2		0.99	1.72	1.90	3.32	2.10
MnO		0.10	0.15	0.11	0.17	0.17
P_2O_5		0.14	0.21	0.24	0.48	0.25
SrO		0.02	0.02	0.02	0.02	0.03
BaO		0.02	0.03	0.01	0.01	<0.01
LOI		4.44	2.56	8.33	9.31	3.09
Total		99.60	101.22	99.24	98.58	99.50
C		0.23	0.02	1.18	1.54	0.17
S		0.01	0.01	0.01	0.28	0.01
Ba	*ppm*	192.50	274.00	80.80	67.00	34.80
Ce		27.70	19.10	27.60	45.10	26.40
Cr		240.00	120.00	220.00	80.00	140.00
Cs		0.20	0.32	0.39	0.09	0.07
Dy		3.50	6.13	4.83	6.54	5.02
Er		2.07	3.74	2.62	3.52	2.65
Eu		1.12	1.46	1.46	2.21	1.55
Ga		16.70	18.30	19.10	22.10	18.70
Gd		3.39	5.64	5.06	7.20	5.06
Ge		<5	<5	<5	<5	<5
Hf		2.80	3.20	3.90	5.80	3.80
Ho		0.76	1.30	0.95	1.32	0.97
La		12.30	6.90	10.30	18.00	9.80
Lu		0.31	0.53	0.33	0.46	0.35
Nb		7.20	6.20	9.20	16.60	8.70
Nd		14.30	14.00	18.10	28.30	17.70
Pr		3.41	2.85	3.86	6.27	3.79
Rb		19.50	35.70	21.30	10.70	1.30
Sm		3.28	4.48	4.58	6.75	4.74
Sn		2.00	1.00	2.00	2.00	1.00
Sr		144.00	165.50	156.00	149.50	295.00
Ta		0.50	0.40	0.60	1.10	0.60
Tb		0.52	0.94	0.76	1.10	0.82
Th		2.94	0.57	0.70	1.02	0.63
Tm		0.31	0.56	0.37	0.51	0.36
U		1.86	0.44	0.31	0.42	0.28
V		164.00	242.00	275.00	366.00	315.00
W		<1	1.00	2.00	11.00	1.00
Y		18.40	32.30	23.40	32.70	23.70
Yb		1.92	3.48	2.24	3.08	2.35
Zr		123.00	124.00	168.00	256.00	158.00
As		1.60	2.70	1.30	22.40	6.60
Bi		0.04	0.01	0.01	0.03	<0.01
Hg		0.01	0.01	0.01	0.01	0.01
In		0.01	0.01	0.03	0.07	0.01

Abbreviations:
D = depth
WL = wavelength

Units:
MD = mafic dyke
MBX = mafic breccia

MT = mafic tuff
MLT = mafic lapilli tuff

Table C.1.1. Whole Rock Geochemistry and Terraspec™ Data for Argyle Samples

Sample ID	I951383	I951384	I951385	I951386	I951387
Hole ID	AE-16-09	AE-16-32	AE-16-32	AE-16-32	AE-16-32
Depth (m)	62.40	8.90	20.05	23.35	32.30
Lithology	MLT	MLT	Gabbro	MD	Gabbro
Alteration Assemblage	Chl	Chl-Hem-Ep	Chl-Ep-Rut	Ep-Chl	Ep-Calc-Chl-Ab
Alteration	Distal	Distal	Distal	Distal	Intermediate
Re	<0.001	<0.001	<0.001	0.00	<0.001
Sb	0.13	0.26	0.09	0.09	0.51
Se	<0.2	<0.2	<0.2	0.50	<0.2
Te	0.01	0.01	<0.01	0.05	<0.01
Tl	<0.02	0	<0.02	<0.02	<0.02
Ag	<0.5	<0.5	<0.5	<0.5	<0.5
Cd	<0.5	<0.5	<0.5	1	1
Co	28	41	44	42	39
Cu	43	43	61	41	45
Li	20	10	30	40	20
Mo	<1	<1	1	2	<1
Ni	106	69	67	50	48
Pb	3	2	2	3	2
Sc	19	31	31	29	40
Zn	62	90	80	109	66
Au	<0.001	<0.001	<0.001	0.01	0.00
C *%*	0.22	<0.05	1.09	1.43	0.15
CO_2	0.30	0.80	<0.2	4.00	5.20
AlOH WL *nm*	2226.72	-	2220.22	-	-
AlOH D	0.29	-	0.14	-	-
FeOH WL	2249.97	2243.27	2252.21	2256.42	2255.14
FeOH D	0.35	0.16	0.22	0.24	0.27
AlOH D/FeOH D	0.83	-	0.62	-	-

Abbreviations:

D = depth

WL = wavelength

Units:

MD = mafic dyke

MBX = mafic breccia

MT = mafic tuff

MLT = mafic lapilli tuff

Table C.1.1. Whole Rock Geochemistry and Terraspec™ Data for Argyle Samples

Sample ID		I951388	I951389	I951390	I951391	I951392
Hole ID		AE-16-32	AE-16-32	AE-16-32	AE-16-32	AE-16-32
Depth (m)		50.35	55.00	66.25	69.80	79.85
Lithology		Gabbro	Gabbro	MD	Gabbro	MLT
Alteration Assemblage		Ab-Ms-Ank-Chl-Qt-Py	Ab-Ep-Chl	Chl-Ep	Ep-Ank-Chl	Ep-Chl
Alteration		Proximal	Proximal	Distal	Distal	Distal
SiO_2	*%*	46.20	45.40	44.40	44.70	54.40
Al_2O_3		15.00	12.25	14.75	16.25	16.40
Fe_2O_3		15.40	14.50	14.95	10.60	6.21
CaO		5.48	7.48	6.94	8.28	4.04
MgO		3.26	3.77	5.81	6.52	4.16
Na_2O		2.99	3.43	3.38	3.96	6.59
K_2O		1.09	0.11	0.15	0.23	0.46
Cr_2O_3		<0.01	<0.01	<0.01	0.04	0.01
TiO_2		2.49	3.65	3.47	1.90	1.21
MnO		0.19	0.20	0.21	0.14	0.08
P_2O_5		1.17	0.47	0.58	0.23	0.21
SrO		0.01	0.02	0.03	0.03	0.02
BaO		0.01	<0.01	<0.01	0.01	0.01
LOI		6.14	8.35	5.28	5.68	2.03
Total		99.43	99.63	99.95	98.57	95.83
C		0.92	1.67	0.53	0.69	0.07
S		0.22	0.01	0.18	0.01	0.02
Ba	*ppm*	107.50	40.60	38.80	46.90	55.10
Ce		93.00	51.50	56.20	26.80	38.60
Cr		<10	<10	30.00	260.00	80.00
Cs		0.19	0.10	0.08	0.06	0.05
Dy		15.60	8.90	7.35	4.60	4.18
Er		8.24	4.73	4.09	2.62	2.51
Eu		4.32	2.79	2.68	1.58	1.18
Ga		26.40	21.10	23.40	19.00	17.70
Gd		16.50	9.37	8.05	4.88	4.04
Ge		<5	<5	<5	<5	<5
Hf		11.20	8.00	7.40	4.10	3.80
Ho		3.18	1.79	1.53	0.94	0.88
La		35.00	19.90	22.90	10.10	18.00
Lu		1.06	0.62	0.53	0.37	0.36
Nb		28.60	20.60	20.60	9.40	9.40
Nd		59.70	34.20	34.00	18.00	18.00
Pr		13.35	7.40	7.74	3.79	4.54
Rb		16.40	1.40	1.50	3.50	4.30
Sm		14.80	8.44	7.73	4.60	4.10
Sn		2.00	2.00	2.00	2.00	2.00
Sr		114.50	211.00	280.00	270.00	208.00
Ta		1.80	1.40	1.30	0.60	0.70
Tb		2.57	1.47	1.26	0.76	0.68
Th		2.39	1.34	1.44	0.71	5.20
Tm		1.12	0.70	0.56	0.37	0.35
U		1.29	0.67	0.66	0.32	3.69
V		138.00	248.00	352.00	272.00	139.00
W		10.00	3.00	1.00	1.00	1.00
Y		77.20	44.20	36.30	23.30	22.10
Yb		7.00	4.14	3.54	2.20	2.35
Zr		510.00	349.00	348.00	175.00	164.00
As		39.00	2.70	15.60	3.10	14.30
Bi		0.05	<0.01	0.01	<0.01	0.01
Hg		<0.005	<0.005	<0.005	<0.005	0.01
In		0.08	0.12	0.03	0.02	0.01

Abbreviations:
D = depth
WL = wavelength

Units:
MD = mafic dyke
MBX = mafic breccia

MT = mafic tuff
MLT = mafic lapilli tuff

Table C.1.1. Whole Rock Geochemistry and Terraspec™ Data for Argyle Samples

Sample ID		I951388	I951389	I951390	I951391	I951392
Hole ID		AE-16-32	AE-16-32	AE-16-32	AE-16-32	AE-16-32
Depth (m)		50.35	55.00	66.25	69.80	79.85
Lithology		Gabbro	Gabbro	MD	Gabbro	MLT
Alteration Assemblage		Ab-Ms-Ank-Chl-Qt-Py	Ab-Ep-Chl	Chl-Ep	Ep-Ank-Chl	Ep-Chl
Alteration		Proximal	Proximal	Distal	Distal	Distal
Re		0.00	0.00	0.00	<0.001	0.00
Sb		0.12	0.09	0.31	0.34	0.15
Se		0.30	<0.2	<0.2	<0.2	<0.2
Te		0.09	0.01	<0.01	<0.01	0.01
Tl		<0.02	<0.02	<0.02	<0.02	<0.02
Ag		<0.5	<0.5	<0.5	<0.5	<0.5
Cd		<0.5	1	<0.5	<0.5	<0.5
Co		28	33	45	39	17
Cu		31	8	34	19	9
Li		20	10	20	20	10
Mo		3	1	1	<1	1
Ni		1	1	42	55	44
Pb		3	2	6	<2	5
Sc		18	24	28	35	16
Zn		138	115	118	67	45
Au		0.78	0.04	0.00	<0.001	<0.001
C	*%*	0.84	1.43	0.48	0.63	0.07
CO_2		0.60	3.10	5.30	1.80	<0.2
AlOH WL	*nm*	2205.84	-	-	-	-
AlOH D		0.06	-	-	-	-
FeOH WL		2259.32	2257.88	2261.12	2256.72	2254.18
FeOH D		0.10	0.06	0.12	0.18	0.28
AlOH D/FeOH D		0.54	-	-	-	-

Abbreviations:	**Units:**	
D = depth	MD = mafic dyke	MT = mafic tuff
WL = wavelength	MBX = mafic breccia	MLT = mafic lapilli tuff

Table C.1.1. Whole Rock Geochemistry and Terraspec™ Data for Argyle Samples

Sample ID		I951393	I951394	I951395	I951396	I951397
Hole ID		AE-17-46	AE-16-21	AE-16-21	AE-16-21	AE-16-21
Depth (m)		91.95	8.80	23.65	29.35	34.50
Lithology		MLT	Gabbro	MD	Gabbro	Gabbro
Alteration Assemblage		Ep-Chl	Chl-Ep	Ep-Chl	Ab-Ank-Chl-Rut	Ab-Ank-Ser-Qt-Chl-Rut-Py
Alteration		Distal	Intermediate	Distal	Proximal	Proximal
SiO_2	*%*	44.40	34.30	42.80	39.00	41.90
Al_2O_3		15.70	19.25	14.85	13.95	14.70
Fe_2O_3		8.17	12.40	14.90	11.65	11.45
CaO		5.00	10.15	6.29	8.61	7.37
MgO		9.36	6.37	6.23	5.05	2.47
Na_2O		1.74	0.80	3.75	2.31	3.97
K_2O		2.41	3.64	0.18	2.03	2.10
Cr_2O_3		0.05	0.03	0.01	<0.01	<0.01
TiO_2		0.90	2.41	3.57	2.10	2.33
MnO		0.09	0.14	0.20	0.18	0.23
P_2O_5		0.14	0.25	0.54	0.26	0.95
SrO		0.02	0.02	0.01	0.02	0.02
BaO		0.02	0.02	<0.01	0.02	0.01
LOI		11.20	12.20	5.97	13.20	11.10
Total		99.20	101.98	99.30	98.38	98.60
C		2.05	2.12	0.66	3.06	3.01
S		0.01	0.13	0.26	0.04	0.54
Ba	*ppm*	159.00	182.00	28.30	159.00	126.00
Ce		24.70	31.00	48.70	30.10	78.90
Cr		390.00	210.00	80.00	10.00	<10
Cs		0.33	0.54	0.05	0.45	0.38
Dy		3.39	5.50	6.95	5.24	12.15
Er		2.02	2.95	3.88	3.03	6.55
Eu		1.01	1.71	2.48	1.71	3.68
Ga		15.90	25.00	22.00	20.70	24.00
Gd		3.22	5.70	7.62	5.48	12.80
Ge		<5	<5	<5	<5	<5
Hf		2.50	4.20	6.20	4.60	9.80
Ho		0.73	1.13	1.41	1.05	2.41
La		11.40	12.20	19.30	11.50	29.90
Lu		0.29	0.37	0.49	0.37	0.86
Nb		5.80	10.20	18.00	10.10	26.40
Nd		12.70	20.40	30.80	19.80	51.40
Pr		3.05	4.41	6.85	4.34	11.35
Rb		38.00	46.50	2.80	36.50	29.50
Sm		3.09	5.23	7.56	5.21	12.60
Sn		1.00	2.00	2.00	2.00	3.00
Sr		158.00	164.50	100.00	197.00	194.00
Ta		0.40	0.70	1.20	0.60	1.70
Tb		0.55	0.89	1.16	0.89	1.99
Th		2.81	1.21	1.30	0.86	1.92
Tm		0.27	0.40	0.53	0.41	0.91
U		1.71	0.35	0.45	0.34	0.81
V		124.00	352.00	390.00	304.00	129.00
W		2.00	24.00	1.00	4.00	29.00
Y		17.80	27.10	34.80	26.50	59.70
Yb		1.87	2.46	3.29	2.59	5.66
Zr		107.00	171.00	271.00	196.00	451.00
As		0.40	20.50	44.00	40.60	34.60
Bi		<0.01	0.01	0.01	0.01	0.02
Hg		<0.005	<0.005	<0.005	<0.005	<0.005
In		0.01	0.03	0.07	0.05	0.07

Abbreviations:
D = depth
WL = wavelength

Units:
MD = mafic dyke
MBX = mafic breccia

MT = mafic tuff
MLT = mafic lapilli tuff

Table C.1.1. Whole Rock Geochemistry and Terraspec™ Data for Argyle Samples

Sample ID	I951393	I951394	I951395	I951396	I951397
Hole ID	AE-17-46	AE-16-21	AE-16-21	AE-16-21	AE-16-21
Depth (m)	91.95	8.80	23.65	29.35	34.50
Lithology	MLT	Gabbro	MD	Gabbro	Gabbro
Alteration Assemblage	Ep-Chl	Chl-Ep	Ep-Chl	Ab-Ank-Chl-Rut	Ab-Ank-Ser-Qt-Chl-Rut-Py
Alteration	Distal	Intermediate	Distal	Proximal	Proximal
Re	<0.001	0.00	0.00	0.00	0.00
Sb	0.05	0.14	0.25	0.12	0.10
Se	<0.2	<0.2	0.20	<0.2	0.50
Te	<0.01	0.01	<0.01	0.01	0.03
Tl	0	<0.02	<0.02	0	0
Ag	<0.5	<0.5	<0.5	<0.5	<0.5
Cd	<0.5	1	1	1	<0.5
Co	39	51	45	40	18
Cu	1	26	42	52	38
Li	40	30	20	10	<10
Mo	<1	1	2	1	2
Ni	185	62	50	25	<1
Pb	<2	<2	3	<2	<2
Sc	21	32	31	30	13
Zn	57	82	110	85	89
Au	<0.001	0.00	<0.001	<0.001	0.37
C *%*	1.94	2.01	0.59	2.84	2.84
CO_2	2.30	0.20	7.10	7.40	2.20
AlOH WL *nm*	2211.75	2205.69	-	2203.13	2198.32
AlOH D	0.23	0.33	-	0.21	0.23
FeOH WL	2249.94	2250.23	2259.28	2253.50	-
FeOH D	0.22	0.25	0.16	0.09	-
AlOH D/FeOH D	1.05	1.31	-	2.29	-

Abbreviations:
D = depth
WL = wavelength

Units:
MD = mafic dyke
MBX = mafic breccia
MT = mafic tuff
MLT = mafic lapilli tuff

Table C.1.1. Whole Rock Geochemistry and Terraspec™ Data for Argyle Samples

Sample ID		I951398	I951399	I951400	I951451	I951452
Hole ID		AE-16-21	AE-16-21	AE-16-21	AE-16-21	AE-16-21
Depth (m)		41.15	61.75	65.75	84.70	105.90
Lithology		Gabbro	MD	MF	MD	Gabbro
Alteration Assemblage		Ab-Ank-Ms-Chl-Ep	Chl-Ep	Ep-Chl	Ep-Chl	Chl-Ep
Alteration		Proximal	Distal	Distal	Distal	Distal
SiO_2	*%*	47.20	46.30	53.40	40.80	45.90
Al_2O_3		13.65	15.55	16.85	13.75	14.60
Fe_2O_3		15.55	11.15	8.06	10.70	10.60
CaO		5.54	10.55	4.93	10.00	8.03
MgO		3.11	6.69	6.03	7.18	6.44
Na_2O		3.99	3.44	5.66	1.12	4.27
K_2O		0.33	0.17	0.77	1.95	0.10
Cr_2O_3		<0.01	0.03	0.01	0.02	0.02
TiO_2		2.36	1.97	1.23	1.83	1.50
MnO		0.29	0.15	0.10	0.18	0.15
P_2O_5		1.08	0.26	0.14	0.33	0.19
SrO		0.02	0.03	0.02	0.01	0.02
BaO		0.01	<0.01	0.01	0.02	<0.01
LOI		7.72	3.18	2.44	11.55	7.67
Total		100.85	99.47	99.65	99.44	99.49
C		1.71	0.18	0.01	2.09	1.28
S		0.15	0.03	0.02	0.23	0.02
Ba	*ppm*	65.20	32.50	72.10	193.50	31.00
Ce		77.30	27.90	27.50	26.00	20.20
Cr		<10	210.00	100.00	140.00	140.00
Cs		0.05	0.06	0.08	0.32	0.06
Dy		12.95	4.81	4.31	4.42	4.23
Er		6.78	2.64	2.63	2.38	2.24
Eu		3.78	1.54	1.24	1.33	1.19
Ga		25.30	18.60	17.80	16.20	16.90
Gd		13.45	5.17	4.08	4.76	4.14
Ge		<5	<5	<5	<5	<5
Hf		9.90	4.00	3.20	3.30	2.90
Ho		2.56	0.99	0.90	0.90	0.83
La		28.80	10.70	12.40	10.10	7.80
Lu		0.86	0.33	0.39	0.35	0.29
Nb		26.20	9.40	6.10	6.80	6.90
Nd		51.20	18.20	14.50	16.60	13.30
Pr		11.25	4.05	3.38	3.64	2.94
Rb		4.60	1.40	7.90	35.20	1.30
Sm		12.75	4.81	3.66	4.39	3.70
Sn		3.00	2.00	2.00	1.00	1.00
Sr		176.50	246.00	181.50	118.50	183.00
Ta		1.70	0.70	0.50	0.40	0.40
Tb		2.04	0.77	0.67	0.74	0.66
Th		1.90	0.67	3.16	0.63	0.63
Tm		0.99	0.37	0.38	0.34	0.33
U		0.95	0.33	2.04	0.33	0.28
V		84.00	279.00	182.00	236.00	246.00
W		2.00	1.00	1.00	2.00	1.00
Y		62.60	23.60	22.90	23.00	20.00
Yb		5.85	2.27	2.59	2.23	2.05
Zr		445.00	167.00	132.00	138.00	119.00
As		13.50	30.80	3.10	12.30	4.20
Bi		<0.01	<0.01	0.01	0.08	0.02
Hg		<0.005	<0.005	0.01	<0.005	<0.005
In		0.11	0.01	0.01	0.03	0.04

Abbreviations:
D = depth
WL = wavelength

Units:
MD = mafic dyke
MBX = mafic breccia
MT = mafic tuff
MLT = mafic lapilli tuff

Table C.1.1. Whole Rock Geochemistry and Terraspec™ Data for Argyle Samples

Sample ID	I951398	I951399	I951400	I951451	I951452
Hole ID	AE-16-21	AE-16-21	AE-16-21	AE-16-21	AE-16-21
Depth (m)	41.15	61.75	65.75	84.70	105.90
Lithology	Gabbro	MD	MF	MD	Gabbro
Alteration Assemblage	Ab-Ank-Ms-Chl-Ep	Chl-Ep	Ep-Chl	Ep-Chl	Chl-Ep
Alteration	Proximal	Distal	Distal	Distal	Distal
Re	<0.001	<0.001	<0.001	0.00	<0.001
Sb	0.07	0.36	0.15	0.09	0.43
Se	<0.2	<0.2	<0.2	0.20	0.20
Te	0.01	<0.01	<0.01	<0.01	0.01
Tl	<0.02	<0.02	<0.02	0	<0.02
Ag	<0.5	<0.5	<0.5	<0.5	<0.5
Cd	<0.5	1	<0.5	<0.5	<0.5
Co	27	41	26	42	41
Cu	16	84	4	40	108
Li	30	20	10	20	20
Mo	2	<1	<1	<1	<1
Ni	<1	58	44	80	70
Pb	<2	<2	<2	3	<2
Sc	14	35	22	25	33
Zn	163	60	34	82	86
Au	0.01	<0.001	<0.001	<0.001	<0.001
C *%*	1.59	0.15	<0.05	1.91	1.17
CO_2	10.40	10.40	5.80	0.60	<0.2
AlOH WL *nm*	-	-	-	2226.77	-
AlOH D	-	-	-	0.15	-
FeOH WL	2260.06	2255.12	2253.98	2253.97	2255.56
FeOH D	0.14	0.26	0.33	0.26	0.14
AlOH D/FeOH D	-	-	-	0.58	-

Abbreviations:
D = depth
WL = wavelength

Units:
MD = mafic dyke
MBX = mafic breccia
MT = mafic tuff
MLT = mafic lapilli tuff

Table C.1.1. Whole Rock Geochemistry and Terraspec™ Data for Argyle Samples

Sample ID		I951453	I951454	I951455	I951456	I951457
Hole ID		AE-16-39	AE-16-39	AE-16-39	AE-16-39	AE-16-39
Depth (m)		34.35	62.15	84.60	85.40	91.70
Lithology		MLT	Gabbro	MD	Gabbro	Gabbro
Alteration Assemblage		Ep-Chl	Ep-Ank-Chl-Ab-Rut	Ep-Calc-Chl	Ank-Ab-Chl-Ep-Rut	Ab-Ank-Chl-Ep-Rut-Py
Alteration		Distal	Intermediate	Intermediate	Proximal	Proximal
SiO_2	*%*	36.20	39.10	39.50	40.10	42.00
Al_2O_3		13.65	15.10	13.45	14.30	13.20
Fe_2O_3		7.79	10.65	14.95	13.65	14.10
CaO		16.90	9.52	7.18	7.57	7.21
MgO		4.49	4.94	4.88	3.79	3.48
Na_2O		3.72	2.35	0.99	2.20	1.08
K_2O		1.01	1.05	1.24	1.58	2.42
Cr_2O_3		0.01	0.02	<0.01	<0.01	<0.01
TiO_2		1.42	2.01	3.22	2.89	3.08
MnO		0.13	0.15	0.17	0.22	0.25
P_2O_5		0.13	0.26	0.53	0.34	0.51
SrO		0.02	0.03	0.02	0.02	0.02
BaO		0.01	0.01	0.01	0.01	0.02
LOI		13.35	15.40	12.85	12.70	11.15
Total		98.83	100.59	98.99	99.37	98.52
C		2.97	3.67	2.73	2.99	2.66
S		0.02	0.02	0.09	0.17	0.58
Ba	*ppm*	85.50	70.10	102.50	105.50	156.50
Ce		14.60	28.10	51.40	40.50	56.30
Cr		90.00	60.00	30.00	10.00	<10
Cs		0.26	0.18	0.24	0.34	0.27
Dy		5.10	4.73	6.98	6.62	9.06
Er		2.99	2.34	3.78	3.52	5.05
Eu		1.13	1.51	2.49	2.25	3.17
Ga		14.90	18.00	20.70	21.20	21.80
Gd		4.32	4.96	7.44	6.78	9.60
Ge		<5	<5	<5	<5	<5
Hf		2.50	3.70	6.10	5.40	7.50
Ho		1.05	0.93	1.32	1.33	1.78
La		5.60	10.90	20.30	15.50	21.10
Lu		0.44	0.33	0.50	0.46	0.63
Nb		5.10	8.80	18.60	15.00	20.70
Nd		11.40	18.30	30.90	25.80	36.20
Pr		2.27	3.98	6.98	5.77	8.07
Rb		18.90	14.20	16.60	24.00	35.80
Sm		3.75	4.65	7.24	6.51	8.99
Sn		1.00	1.00	2.00	2.00	3.00
Sr		222.00	241.00	199.00	225.00	195.50
Ta		0.30	0.60	1.20	0.90	1.40
Tb		0.75	0.77	1.14	1.10	1.47
Th		0.45	0.64	1.33	1.10	1.38
Tm		0.46	0.36	0.52	0.52	0.70
U		1.62	0.29	0.55	0.57	0.77
V		295.00	273.00	330.00	410.00	273.00
W		<1	5.00	9.00	9.00	8.00
Y		26.80	22.80	33.50	33.60	45.40
Yb		2.85	2.22	3.18	3.05	4.32
Zr		101.00	157.00	297.00	254.00	347.00
As		3.00	7.00	7.70	14.60	31.90
Bi		<0.01	0.01	0.02	0.01	0.07
Hg		0.01	<0.005	<0.005	<0.005	<0.005
In		0.01	0.05	0.07	0.08	0.10

Abbreviations:

D = depth

WL = wavelength

Units:

MD = mafic dyke

MBX = mafic breccia

MT = mafic tuff

MLT = mafic lapilli tuff

Table C.1.1. Whole Rock Geochemistry and Terraspec™ Data for Argyle Samples

Sample ID	I951453	I951454	I951455	I951456	I951457
Hole ID	AE-16-39	AE-16-39	AE-16-39	AE-16-39	AE-16-39
Depth (m)	34.35	62.15	84.60	85.40	91.70
Lithology	MLT	Gabbro	MD	Gabbro	Gabbro
Alteration Assemblage	Ep-Chl	Ep-Ank-Chl-Ab-Rut	Ep-Calc-Chl	Ank-Ab-Chl-Ep-Rut	Ab-Ank-Chl-Ep-Rut-Py
Alteration	Distal	Intermediate	Intermediate	Proximal	Proximal
Re	<0.001	0.00	0.00	0.00	0.00
Sb	0.24	0.73	0.16	0.24	0.15
Se	<0.2	<0.2	0.20	0.20	1.00
Te	0.01	<0.01	0.01	0.01	0.07
Tl	<0.02	<0.02	<0.02	<0.02	0
Ag	<0.5	<0.5	<0.5	<0.5	<0.5
Cd	<0.5	1	1	1	<0.5
Co	41	36	43	42	30
Cu	30	43	33	45	9
Li	20	10	10	10	<10
Mo	<1	1	1	1	2
Ni	61	30	37	23	2
Pb	<2	<2	2	<2	<2
Sc	28	30	25	22	20
Zn	79	66	107	88	95
Au	<0.001	<0.001	0.03	<0.001	0.85
C *%*	2.78	3.49	2.61	2.84	2.56
CO_2	7.00	4.30	10.20	12.80	9.60
AlOH WL *nm*	-	2191.61	2194.56	2195.58	2199.34
AlOH D	-	0.41	0.23	0.21	0.24
FeOH WL	2252.88	2249.95	2254.10	2253.30	2254.98
FeOH D	0.22	0.10	0.12	0.08	0.16
AlOH D/FeOH D	-	4.01	1.93	2.74	1.48

Abbreviations:
D = depth
WL = wavelength

Units:
MD = mafic dyke
MBX = mafic breccia
MT = mafic tuff
MLT = mafic lapilli tuff

Table C.1.1. Whole Rock Geochemistry and Terraspec™ Data for Argyle Samples

Sample ID		I951458	I951459	I951460	I951461	I951462
Hole ID		AE-16-39	AE-16-39	AE-16-38	AE-16-38	AE-16-38
Depth (m)		98.00	108.15	7.10	44.35	69.35
Lithology		Gabbro	MLT	MF	Gabbro	Gabbro
Alteration Assemblage		Ab-Chl-Ank-Ep	Ep-Chl	Ep-Chl	Chl-Ep-Rut	Ab-Ank-Chl-Ep-Rut-Qt
Alteration		Proximal	Distal	Intermediate	Distal	Proximal
SiO_2	*%*	41.90	52.20	45.60	43.90	42.10
Al_2O_3		9.69	16.00	15.65	18.50	12.50
Fe_2O_3		17.25	8.03	10.65	11.90	14.90
CaO		7.30	4.97	9.79	4.62	8.71
MgO		4.78	7.23	6.35	7.48	4.08
Na_2O		0.80	5.40	3.80	4.12	1.59
K_2O		0.71	0.06	0.70	1.26	1.18
Cr_2O_3		<0.01	0.04	0.01	0.03	<0.01
TiO_2		3.77	1.03	1.54	2.14	3.41
MnO		0.33	0.09	0.15	0.14	0.25
P_2O_5		0.71	0.19	0.16	0.26	0.52
SrO		0.02	0.02	0.03	0.01	0.02
BaO		0.01	<0.01	0.01	0.01	0.01
LOI		11.60	3.83	5.83	6.30	10.90
Total		98.87	99.09	100.27	100.67	100.17
C		2.69	0.24	0.84	0.67	2.21
S		0.27	0.02	0.04	0.09	0.10
Ba	*ppm*	82.30	20.50	56.80	107.00	91.60
Ce		68.70	25.00	16.40	28.90	57.10
Cr		<10	300.00	110.00	230.00	<10
Cs		0.11	0.06	0.07	0.12	0.18
Dy		10.80	4.34	5.63	5.09	9.29
Er		5.94	2.62	3.35	2.78	5.22
Eu		3.38	1.28	1.45	1.69	3.00
Ga		18.20	13.80	16.30	19.80	22.50
Gd		11.95	4.24	5.10	5.66	9.97
Ge		<5	<5	<5	<5	<5
Hf		8.50	2.50	2.80	4.20	7.80
Ho		2.13	0.93	1.17	1.02	1.84
La		26.00	11.20	6.10	10.90	21.90
Lu		0.76	0.37	0.50	0.34	0.67
Nb		25.10	5.80	5.60	10.00	21.90
Nd		43.30	13.60	12.40	19.10	36.80
Pr		9.68	3.20	2.51	4.11	8.05
Rb		11.10	0.70	9.60	18.60	17.00
Sm		10.80	3.53	3.70	4.98	8.92
Sn		3.00	1.00	1.00	2.00	3.00
Sr		200.00	200.00	253.00	132.00	215.00
Ta		1.60	0.40	0.30	0.70	1.50
Tb		1.80	0.69	0.89	0.89	1.54
Th		1.59	2.43	0.50	0.66	1.41
Tm		0.78	0.38	0.51	0.40	0.74
U		0.72	1.50	0.24	0.29	0.61
V		204.00	152.00	262.00	310.00	243.00
W		11.00	1.00	1.00	1.00	3.00
Y		54.20	23.80	30.60	25.80	47.20
Yb		5.15	2.57	3.24	2.39	4.46
Zr		388.00	112.00	114.00	182.00	357.00
As		39.40	1.60	1.80	53.10	22.50
Bi		0.05	0.04	0.01	0.02	0.01
Hg		<0.005	<0.005	<0.005	<0.005	<0.005
In		0.10	0.01	0.01	0.04	0.10

Abbreviations:
D = depth
WL = wavelength

Units:
MD = mafic dyke
MBX = mafic breccia

MT = mafic tuff
MLT = mafic lapilli tuff

Table C.1.1. Whole Rock Geochemistry and Terraspec™ Data for Argyle Samples

Sample ID	I951458	I951459	I951460	I951461	I951462
Hole ID	AE-16-39	AE-16-39	AE-16-38	AE-16-38	AE-16-38
Depth (m)	98.00	108.15	7.10	44.35	69.35
Lithology	Gabbro	MLT	MF	Gabbro	Gabbro
Alteration Assemblage	Ab-Chl-Ank-Ep	Ep-Chl	Ep-Chl	Chl-Ep-Rut	Ab-Ank-Chl-Ep-Rut-Qt
Alteration	Proximal	Distal	Intermediate	Distal	Proximal
Re	0.00	<0.001	<0.001	0.00	<0.001
Sb	0.16	0.16	0.18	0.10	0.11
Se	0.70	0.40	0.40	0.60	0.60
Te	0.04	0.01	<0.01	0.01	0.01
Tl	0	<0.02	<0.02	<0.02	0
Ag	<0.5	<0.5	<0.5	<0.5	<0.5
Cd	1	<0.5	1	<0.5	1
Co	40	30	43	47	33
Cu	26	5	47	27	24
Li	20	20	20	30	10
Mo	3	1	1	1	3
Ni	<1	122	74	68	2
Pb	<2	<2	<2	<2	<2
Sc	25	20	30	28	25
Zn	153	42	85	91	129
Au	0.04	<0.001	<0.001	<0.001	0.00
C *%*	2.58	0.22	0.77	0.60	2.10
CO_2	10.40	9.40	9.50	0.80	2.80
AlOH WL *nm*	2205.37	-	-	2227.32	2205.43
AlOH D	0.08	-	-	0.18	0.11
FeOH WL	2258.94	2253.36	2253.71	2252.07	2259.40
FeOH D	0.16	0.29	0.28	0.23	0.11
AlOH D/FeOH D	0.50	-	-	0.78	0.96

Abbreviations:
D = depth
WL = wavelength

Units:
MD = mafic dyke
MBX = mafic breccia
MT = mafic tuff
MLT = mafic lapilli tuff

Table C.1.1. Whole Rock Geochemistry and Terraspec™ Data for Argyle Samples

Sample ID		I951463	I951464	I951465	I951466	I951467
Hole ID		AE-16-38	AE-16-38	AE-16-38	AE-16-38	AE-16-38
Depth (m)		72.50	77.00	79.40	110.45	99.50
Lithology		Gabbro	Gabbro	MD	MF	Gabbro
Alteration Assemblage		Ab-Ank-Chl-Ep-Rut	Ab-Ank-Chl-Ep-Qt-Rut	Chl-Ab	Chl	Chl-Calc-Ab-Rut
Alteration		Proximal	Proximal	Distal	Distal	Intermediate
SiO_2	*%*	44.50	47.00	43.40	55.10	48.80
Al_2O_3		12.75	14.60	14.20	16.65	15.45
Fe_2O_3		14.20	11.90	14.40	7.29	10.70
CaO		6.38	5.81	6.45	4.81	8.21
MgO		3.81	2.64	5.74	5.88	7.04
Na_2O		2.39	4.76	3.34	5.83	3.97
K_2O		1.29	0.84	0.06	0.72	0.18
Cr_2O_3		<0.01	<0.01	<0.01	0.01	0.03
TiO_2		3.27	1.91	3.51	1.24	2.03
MnO		0.24	0.24	0.20	0.10	0.17
P_2O_5		0.52	0.97	0.55	0.17	0.26
SrO		0.01	0.03	0.02	0.03	0.03
BaO		0.01	0.01	<0.01	0.01	<0.01
LOI		10.35	8.58	8.17	2.34	3.09
Total		99.72	99.29	100.04	100.18	99.96
C		2.37	1.92	1.28	0.04	0.13
S		0.21	0.03	0.05	0.01	0.03
Ba	*ppm*	78.00	104.00	25.00	91.70	41.40
Ce		61.90	87.20	54.60	27.80	33.20
Cr		<10	<10	30.00	90.00	220.00
Cs		0.15	0.16	0.08	0.12	0.05
Dy		10.40	13.60	7.62	4.19	5.27
Er		5.89	7.31	4.27	2.63	2.86
Eu		3.08	4.23	2.78	1.29	1.79
Ga		21.40	23.90	21.80	15.50	15.10
Gd		10.95	14.45	8.18	4.08	5.67
Ge		<5	<5	<5	<5	<5
Hf		9.30	11.10	6.80	3.20	4.30
Ho		2.08	2.68	1.51	0.90	1.06
La		23.50	33.10	22.10	12.30	12.50
Lu		0.75	0.97	0.54	0.37	0.37
Nb		24.80	26.60	21.00	6.90	12.00
Nd		39.60	56.20	32.40	14.30	21.50
Pr		8.85	12.50	7.53	3.43	4.70
Rb		18.40	12.20	1.10	9.80	2.20
Sm		9.82	13.65	7.82	3.71	5.55
Sn		3.00	4.00	2.00	2.00	2.00
Sr		138.50	243.00	198.00	281.00	259.00
Ta		1.60	1.80	1.40	0.50	0.70
Tb		1.74	2.27	1.30	0.67	0.92
Th		1.71	2.19	1.35	3.37	0.94
Tm		0.83	1.07	0.58	0.37	0.40
U		0.76	0.95	0.70	2.23	0.34
V		213.00	83.00	376.00	181.00	303.00
W		8.00	6.00	1.00	1.00	1.00
Y		53.40	67.40	38.10	23.50	27.30
Yb		5.10	6.55	3.56	2.51	2.55
Zr		428.00	534.00	338.00	143.00	184.00
As		10.20	2.00	2.70	8.80	16.80
Bi		0.02	0.01	0.02	0.01	0.01
Hg		<0.005	<0.005	0.01	<0.005	<0.005
In		0.09	0.11	0.09	0.01	0.01

Abbreviations:

D = depth
WL = wavelength

Units:

MD = mafic dyke
MBX = mafic breccia
MT = mafic tuff
MLT = mafic lapilli tuff

Table C.1.1. Whole Rock Geochemistry and Terraspec™ Data for Argyle Samples

Sample ID		I951463	I951464	I951465	I951466	I951467
Hole ID		AE-16-38	AE-16-38	AE-16-38	AE-16-38	AE-16-38
Depth (m)		72.50	77.00	79.40	110.45	99.50
Lithology		Gabbro	Gabbro	MD	MF	Gabbro
Alteration Assemblage		Ab-Ank-Chl-Ep-Rut	Ab-Ank-Chl-Ep-Qt-Rut	Chl-Ab	Chl	Chl-Calc-Ab-Rut
Alteration		Proximal	Proximal	Distal	Distal	Intermediate
Re		0.00	0.00	0.00	<0.001	0.00
Sb		0.11	0.08	0.10	0.16	0.25
Se		0.60	0.20	0.40	0.40	0.40
Te		0.07	0.02	0.02	<0.01	<0.01
Tl		<0.02	<0.02	<0.02	<0.02	<0.02
Ag		<0.5	<0.5	<0.5	<0.5	<0.5
Cd		<0.5	<0.5	1	<0.5	1
Co		30	19	49	26	41
Cu		25	12	34	6	80
Li		10	<10	40	10	20
Mo		3	2	2	1	1
Ni		<1	<1	44	44	47
Pb		2	<2	2	6	<2
Sc		23	13	29	23	36
Zn		123	98	137	49	82
Au		0.13	0.01	0.00	<0.001	<0.001
C	*%*	2.29	1.84	1.23	0.07	0.14
CO_2		<0.2	2.20	7.70	8.40	6.70
AlOH WL	*nm*	2200.98	2201.72	-	-	-
AlOH D		0.17	0.02	-	-	-
FeOH WL		2257.54	2261.59	2258.95	2253.48	2254.22
FeOH D		0.15	0.05	0.13	0.32	0.27
AlOH D/FeOH D		1.16	0.45	-	-	-

Abbreviations:
D = depth
WL = wavelength

Units:
MD = mafic dyke
MBX = mafic breccia
MT = mafic tuff
MLT = mafic lapilli tuff

Table C.1.1. Whole Rock Geochemistry and Terraspec™ Data for Argyle Samples

Sample ID	I951468	I951469	I951470	I951471	I951472
Hole ID	AE-16-36	AE-16-36	AE-16-36	AE-16-36	AE-16-36
Depth (m)	6.40	13.00	16.30	26.00	44.05
Lithology	Gabbro	Gabbro	MD	Gabbro	Gabbro
Alteration Assemblage	Ep-Chl-Ank-Rut	Chl-Ab-Calc-Ep-Rut-Py	Chl-Ep-Ab-Py	Ep-Ank-Chl	Ep-Ab-Ank-Chl
Alteration	Intermediate	Intermediate	Distal	Intermediate	Intermediate
SiO_2 *%*	45.10	41.30	42.40	48.40	47.50
Al_2O_3	16.40	16.25	13.80	15.40	15.10
Fe_2O_3	10.90	11.00	13.45	11.60	14.15
CaO	9.94	8.60	8.55	10.35	8.77
MgO	7.11	6.99	5.78	6.88	4.94
Na_2O	3.08	3.19	3.32	3.57	3.60
K_2O	0.29	1.36	0.21	0.15	0.20
Cr_2O_3	0.03	0.03	0.01	0.01	<0.01
TiO_2	1.98	2.02	3.32	2.09	2.83
MnO	0.16	0.15	0.19	0.18	0.21
P_2O_5	0.23	0.26	0.47	0.27	0.34
SrO	0.05	0.02	0.02	0.04	0.06
BaO	<0.01	0.01	<0.01	<0.01	0.02
LOI	4.34	9.66	8.56	2.58	2.58
Total	99.61	100.84	100.08	101.52	100.30
C	0.36	1.62	1.55	0.04	0.06
S	0.06	0.07	0.18	0.01	0.15
Ba *ppm*	33.20	130.00	33.30	44.30	157.00
Ce	27.00	27.20	44.50	32.00	42.80
Cr	250.00	240.00	70.00	50.00	10.00
Cs	0.07	0.19	0.01	0.04	1.01
Dy	4.74	4.73	6.22	5.32	6.56
Er	2.62	2.70	3.36	2.87	3.76
Eu	1.63	1.95	2.47	1.86	2.23
Ga	17.20	19.80	18.60	17.00	20.70
Gd	4.98	5.25	6.53	5.58	7.03
Ge	<5	<5	<5	<5	<5
Hf	3.70	3.70	5.20	4.40	5.50
Ho	0.92	0.96	1.24	1.00	1.30
La	10.20	10.10	17.40	11.90	16.30
Lu	0.34	0.33	0.44	0.39	0.50
Nb	9.40	9.00	16.00	10.60	14.50
Nd	18.20	18.40	28.00	20.90	27.50
Pr	3.94	4.05	6.18	4.64	6.20
Rb	4.60	20.80	3.10	1.60	3.90
Sm	4.74	4.78	6.71	5.49	7.06
Sn	2.00	1.00	2.00	2.00	2.00
Sr	435.00	154.50	184.50	364.00	507.00
Ta	0.60	0.60	1.00	0.70	1.00
Tb	0.76	0.79	1.06	0.90	1.12
Th	0.68	0.61	0.98	0.81	0.98
Tm	0.38	0.36	0.47	0.42	0.51
U	0.27	0.28	0.43	0.35	0.41
V	298.00	306.00	375.00	297.00	413.00
W	2.00	2.00	2.00	1.00	<1
Y	23.70	24.90	32.20	27.90	34.30
Yb	2.17	2.17	2.94	2.44	3.10
Zr	159.00	158.00	247.00	195.00	242.00
As	55.40	36.90	60.10	35.80	25.10
Bi	0.01	0.01	0.02	0.01	0.01
Hg	<0.005	<0.005	<0.005	<0.005	<0.005
In	0.01	0.04	0.08	0.01	0.01

Abbreviations:
D = depth
WL = wavelength

Units:
MD = mafic dyke
MBX = mafic breccia
MT = mafic tuff
MLT = mafic lapilli tuff

Table C.1.1. Whole Rock Geochemistry and Terraspec™ Data for Argyle Samples

Sample ID		I951468	I951469	I951470	I951471	I951472
Hole ID		AE-16-36	AE-16-36	AE-16-36	AE-16-36	AE-16-36
Depth (m)		6.40	13.00	16.30	26.00	44.05
Lithology		Gabbro	Gabbro	MD	Gabbro	Gabbro
Alteration Assemblage		Ep-Chl-Ank-Rut	Chl-Ab-Calc-Ep-Rut-Py	Chl-Ep-Ab-Py	Ep-Ank-Chl	Ep-Ab-Ank-Chl
Alteration		Intermediate	Intermediate	Distal	Intermediate	Intermediate
Re		0.00	<0.001	0.00	0.00	<0.001
Sb		0.31	0.07	0.08	0.29	0.37
Se		0.40	0.30	0.50	0.20	0.70
Te		0.02	0.02	0.02	0.01	0.01
Tl		<0.02	<0.02	<0.02	<0.02	<0.02
Ag		<0.5	<0.5	<0.5	<0.5	<0.5
Cd		<0.5	1	<0.5	<0.5	1
Co		44	45	45	44	45
Cu		74	7	42	23	53
Li		20	30	20	20	10
Mo		1	1	1	1	1
Ni		65	64	51	41	20
Pb		<2	<2	<2	<2	<2
Sc		29	32	29	37	27
Zn		76	70	109	81	109
Au		0.01	0.00	0.00	<0.001	<0.001
C	*%*	0.35	1.50	1.41	0.05	0.06
CO_2		4.50	0.20	0.50	1.30	5.50
AlOH WL	*nm*	-	2221.29	-	-	-
AlOH D		-	0.18	-	-	-
FeOH WL		2254.26	2251.93	2255.71	2255.11	2254.50
FeOH D		0.25	0.25	0.24	0.25	0.23
AlOH D/FeOH D		-	0.75	-	-	-

Abbreviations:	**Units:**	
D = depth	MD = mafic dyke	MT = mafic tuff
WL = wavelength	MBX = mafic breccia	MLT = mafic lapilli tuff

Table C.1.1. Whole Rock Geochemistry and Terraspec™ Data for Argyle Samples

Sample ID		I951473	I951474	I951475	I951476	I951477
Hole ID		AE-16-36	AE-16-36	AE-16-35	AE-16-35	AE-16-35
Depth (m)		51.15	60.50	18.35	24.40	28.25
Lithology		Gabbro	MF	Gabbro	Gabbro	Gabbro
Alteration Assemblage		Ab-Chl-Ank-Ep-Rut	Chl	Ab-Ank-Chl-Ep-Rut	Ab-Ank-Ms-Chl-Qt-Rut-Py	Ab-Chl-Ep-Rut
Alteration		Intermediate	Distal	Proximal	Proximal	Intermediate
SiO_2	*%*	51.50	53.30	48.10	54.90	48.10
Al_2O_3		14.50	16.55	14.60	14.85	12.55
Fe_2O_3		11.45	7.46	12.95	10.15	13.10
CaO		5.47	4.45	5.34	3.74	7.47
MgO		2.79	7.14	3.13	1.90	4.17
Na_2O		5.06	5.72	4.86	5.73	4.08
K_2O		0.24	0.34	0.29	0.57	0.11
Cr_2O_3		<0.01	0.03	<0.01	<0.01	<0.01
TiO_2		2.19	1.13	2.33	1.88	3.37
MnO		0.16	0.11	0.23	0.14	0.23
P_2O_5		0.65	0.14	0.78	0.70	0.43
SrO		0.02	0.02	0.03	0.02	0.02
BaO		0.01	<0.01	0.01	0.01	<0.01
LOI		5.68	2.78	6.12	5.26	6.41
Total		99.72	99.17	98.77	99.85	100.04
C		1.03	0.01	1.22	0.64	1.23
S		0.12	0.01	0.32	1.08	0.13
Ba	*ppm*	58.00	41.20	77.70	130.50	38.80
Ce		79.60	26.60	79.60	108.00	54.20
Cr		<10	180.00	<10	<10	<10
Cs		0.08	0.07	0.07	0.12	0.04
Dy		11.55	3.87	11.15	14.75	8.10
Er		6.49	2.35	6.11	8.39	4.95
Eu		3.44	1.24	3.68	4.31	2.81
Ga		22.40	13.70	23.20	18.50	18.50
Gd		12.15	3.65	12.15	15.55	8.68
Ge		<5	<5	<5	<5	<5
Hf		10.00	2.90	9.10	14.30	7.20
Ho		2.28	0.81	2.23	2.92	1.65
La		30.80	11.40	30.50	41.80	20.80
Lu		0.83	0.33	0.80	1.06	0.64
Nb		25.80	6.10	23.40	33.60	18.90
Nd		50.50	14.70	50.50	63.20	35.00
Pr		11.25	3.40	11.30	14.95	7.74
Rb		3.50	3.50	4.10	9.80	1.70
Sm		12.10	3.35	12.25	15.10	8.64
Sn		4.00	1.00	3.00	4.00	2.00
Sr		189.00	174.00	279.00	193.50	202.00
Ta		1.70	0.40	1.60	2.30	1.30
Tb		1.90	0.60	1.89	2.49	1.36
Th		2.13	2.58	1.80	3.15	1.40
Tm		0.89	0.35	0.82	1.25	0.66
U		0.91	1.49	0.77	1.40	0.59
V		99.00	157.00	129.00	81.00	315.00
W		3.00	<1	2.00	3.00	3.00
Y		60.00	20.90	58.30	75.70	41.90
Yb		5.39	2.17	5.49	7.43	3.94
Zr		463.00	129.00	416.00	671.00	329.00
As		20.60	4.40	16.80	93.60	5.20
Bi		0.01	0.02	0.02	0.03	0.01
Hg		0.01	<0.005	0.01	<0.005	<0.005
In		0.10	0.01	0.11	0.06	0.09

Abbreviations:
D = depth
WL = wavelength

Units:
MD = mafic dyke
MBX = mafic breccia
MT = mafic tuff
MLT = mafic lapilli tuff

Table C.1.1. Whole Rock Geochemistry and Terraspec™ Data for Argyle Samples

Sample ID	I951473	I951474	I951475	I951476	I951477
Hole ID	AE-16-36	AE-16-36	AE-16-35	AE-16-35	AE-16-35
Depth (m)	51.15	60.50	18.35	24.40	28.25
Lithology	Gabbro	MF	Gabbro	Gabbro	Gabbro
Alteration Assemblage	Ab-Chl-Ank-Ep-Rut	Chl	Ab-Ank-Chl-Ep-Rut	Ab-Ank-Ms-Chl-Qt-Rut-Py	Ab-Chl-Ep-Rut
Alteration	Intermediate	Distal	Proximal	Proximal	Intermediate
Re	0.00	0.00	0.00	<0.001	0.00
Sb	0.08	0.20	0.07	0.06	0.31
Se	<0.2	0.50	0.50	1.40	<0.2
Te	<0.01	0.01	0.03	0.04	0.01
Tl	<0.02	<0.02	<0.02	<0.02	<0.02
Ag	<0.5	<0.5	<0.5	<0.5	<0.5
Cd	<0.5	<0.5	<0.5	1	1
Co	20	29	26	18	31
Cu	14	9	15	72	23
Li	10	20	20	10	10
Mo	2	<1	2	3	2
Ni	<1	82	<1	<1	1
Pb	<2	<2	<2	<2	<2
Sc	14	22	17	12	27
Zn	124	58	115	95	101
Au	0.02	<0.001	0.33	0.59	0.01
C *%*	0.95	<0.05	1.12	0.57	1.11
CO_2	5.20	0.20	0.20	3.50	<0.2
AlOH WL *nm*	2223.99	-	-	2218.38	-
AlOH D	0.07	-	-	0.06	-
FeOH WL	2255.83	2252.07	2261.13	2256.75	2256.71
FeOH D	0.15	0.37	0.09	0.11	0.14
AlOH D/FeOH D	0.51	-	-	0.56	-

Abbreviations:
D = depth
WL = wavelength

Units:
MD = mafic dyke
MBX = mafic breccia

MT = mafic tuff
MLT = mafic lapilli tuff

Table C.1.1. Whole Rock Geochemistry and Terraspec™ Data for Argyle Samples

Sample ID		I951478	I951479	I951480	I951481	I951482
Hole ID		AE-16-35	AE-16-35	AE-16-35	AE-16-35	AE-16-35
Depth (m)		36.60	46.55	49.60	63.40	69.70
Lithology		MD	MD	MLT	Gabbro	MD
Alteration Assemblage		Chl-Ank-Ep-Ab	Chl-Ep-Ab	Ep-Chl	Rut-Ep	Chl-Calc-Ep-Rut-Qt-Ab
Alteration		Intermediate	Distal	Distal	Distal	Proximal
SiO_2	*%*	42.50	43.60	56.70	47.50	38.70
Al_2O_3		12.10	14.80	16.65	14.05	13.55
Fe_2O_3		8.20	15.10	6.78	10.00	7.28
CaO		10.85	7.74	5.64	8.21	11.30
MgO		7.85	6.21	5.45	6.05	4.86
Na_2O		2.37	3.64	5.54	3.48	3.38
K_2O		0.58	0.30	0.56	0.13	2.11
Cr_2O_3		0.05	<0.01	0.02	0.02	0.02
TiO_2		1.19	3.69	1.14	1.57	1.58
MnO		0.15	0.21	0.09	0.14	0.17
P_2O_5		0.51	0.59	0.34	0.20	0.20
SrO		0.05	0.03	0.03	0.02	0.03
BaO		0.01	0.01	0.01	<0.01	0.02
LOI		11.60	4.91	2.56	7.82	16.45
Total		98.01	100.83	101.51	99.19	99.65
C		2.22	0.54	0.11	1.26	4.29
S		<0.01	0.25	<0.01	<0.01	0.02
Ba	*ppm*	62.60	56.80	66.30	43.40	153.00
Ce		100.00	55.90	38.00	23.60	19.80
Cr		340.00	30.00	120.00	120.00	140.00
Cs		0.17	0.05	0.10	0.10	0.36
Dy		3.90	7.29	4.31	4.32	4.17
Er		2.01	3.97	2.76	2.36	2.25
Eu		1.88	2.77	1.38	1.38	1.44
Ga		12.70	21.40	15.20	14.10	13.60
Gd		5.74	8.12	4.40	4.31	4.12
Ge		<5	<5	<5	<5	<5
Hf		5.50	6.50	3.60	3.20	2.90
Ho		0.74	1.49	0.91	0.85	0.83
La		44.60	22.10	17.20	9.30	7.30
Lu		0.25	0.53	0.38	0.33	0.30
Nb		13.50	20.40	9.50	7.40	7.00
Nd		46.40	33.70	18.60	14.90	14.00
Pr		12.35	7.70	4.60	3.34	2.94
Rb		9.00	3.70	7.90	2.50	30.70
Sm		8.28	8.00	4.36	4.06	4.04
Sn		1.00	2.00	2.00	1.00	1.00
Sr		428.00	305.00	319.00	184.50	251.00
Ta		0.70	1.30	0.60	0.50	0.40
Tb		0.71	1.24	0.70	0.69	0.66
Th		7.63	1.22	4.22	0.75	0.64
Tm		0.30	0.54	0.41	0.34	0.32
U		1.60	0.52	3.34	0.32	0.28
V		178.00	389.00	134.00	267.00	241.00
W		1.00	<1	1.00	1.00	2.00
Y		19.40	37.80	24.20	21.80	21.30
Yb		1.63	3.48	2.54	2.04	2.10
Zr		230.00	314.00	153.00	134.00	122.00
As		2.90	18.90	5.40	1.70	2.20
Bi		0.01	0.03	0.07	0.02	0.01
Hg		<0.005	<0.005	<0.005	<0.005	<0.005
In		0.05	0.02	0.01	0.04	0.04

Abbreviations:
D = depth
WL = wavelength

Units:
MD = mafic dyke
MBX = mafic breccia

MT = mafic tuff
MLT = mafic lapilli tuff

Table C.1.1. Whole Rock Geochemistry and Terraspec™ Data for Argyle Samples

Sample ID	I951478	I951479	I951480	I951481	I951482
Hole ID	AE-16-35	AE-16-35	AE-16-35	AE-16-35	AE-16-35
Depth (m)	36.60	46.55	49.60	63.40	69.70
Lithology	MD	MD	MLT	Gabbro	MD
Alteration Assemblage	Chl-Ank-Ep-Ab	Chl-Ep-Ab	Ep-Chl	Rut-Ep	Chl-Calc-Ep-Rut-Qt-Ab
Alteration	Intermediate	Distal	Distal	Distal	Proximal
Re	0.00	0.00	<0.001	0.00	<0.001
Sb	0.11	0.12	0.19	0.15	0.06
Se	0.40	0.40	0.30	0.20	0.20
Te	0.01	0.01	<0.01	0.01	0.01
Tl	<0.02	<0.02	<0.02	<0.02	0
Ag	<0.5	<0.5	<0.5	<0.5	<0.5
Cd	<0.5	1	<0.5	1	<0.5
Co	33	46	21	36	23
Cu	15	38	102	68	174
Li	20	20	20	10	10
Mo	<1	2	1	1	1
Ni	237	46	70	58	45
Pb	<2	<2	11	<2	<2
Sc	18	29	15	30	30
Zn	85	118	59	65	39
Au	<0.001	<0.001	0.00	<0.001	0.00
C *%*	2.03	0.50	0.10	1.15	4.14
CO_2	4.10	2.10	4.10	7.40	1.90
AlOH WL *nm*	-	-	-	-	2199.68
AlOH D	-	-	-	-	0.42
FeOH WL	2253.21	2257.69	2252.70	2255.29	2249.40
FeOH D	0.28	0.16	0.35	0.28	0.12
AlOH D/FeOH D	-	-	-	-	3.50

Abbreviations:
D = depth
WL = wavelength

Units:
MD = mafic dyke
MBX = mafic breccia
MT = mafic tuff
MLT = mafic lapilli tuff

Table C.1.2. Whole Rock Geochemistry of SLV_MC Reference Material

Sample ID Reference	199504060 SLV_MC	199504061 SLV_MC	199504062 SLV_MC	199504063 SLV_MC	199504066 SLV_MC	199504069 SLV_MC	199504070 SLV_MC	199504075 SLV_MC
SiO_2 (%)	49.50	50.20	51.40	50.80	51.60	49.00	50.30	50.50
Al_2O_3	15.40	15.60	15.60	15.50	15.60	15.70	15.95	16.10
Fe_2O_3	12.85	13.35	12.85	12.80	12.95	13.00	13.25	13.35
CaO	8.60	8.73	8.72	8.71	8.71	8.74	8.84	8.85
MgO	7.57	7.74	7.72	7.68	7.51	7.54	7.53	7.61
Na_2O	3.53	3.52	3.57	3.54	3.52	3.59	3.58	3.60
K_2O	0.57	0.54	0.53	0.53	0.52	0.56	0.53	0.52
Cr_2O_3	0.03	0.03	0.03	0.03	0.03	0.03	0.03	0.03
TiO_2	1.52	1.52	1.53	1.52	1.52	1.54	1.54	1.55
MnO	0.17	0.17	0.17	0.17	0.16	0.17	0.16	0.16
P_2O_5	0.24	0.26	0.25	0.24	0.24	0.26	0.24	0.25
SrO	0.05	0.05	0.05	0.05	0.05	0.06	0.06	0.06
BaO	0.02	0.02	0.02	0.02	0.02	0.02	0.02	0.02
LOI	0.00	0.00	0.00	0.00	0.00	0.00	0.00	0.00
Total	99.27	100.88	101.58	100.71	101.65	99.50	101.28	101.97
C	0.01	0.01	0.02	0.01	0.01	0.01	BDL	BDL
S	0.01	0.01	0.01	BDL	BDL	0.01	0.01	0.01
Ba (ppm)	175.50	158.50	160.00	165.00	167.00	168.50	162.00	172.50
Ce	23.10	21.80	22.30	22.90	22.60	22.30	22.00	24.30
Cr	250.00	230.00	240.00	230.00	240.00	230.00	240.00	240.00
Cs	0.07	0.07	0.06	0.07	0.06	0.06	0.07	0.08
Dy	4.09	3.52	3.77	3.65	3.65	3.94	3.53	3.52
Er	2.24	1.79	1.91	1.89	1.81	1.83	1.88	1.95
Eu	1.45	1.26	1.42	1.37	1.32	1.35	1.40	1.44
Ga	23.50	20.70	19.30	17.80	21.80	21.30	21.20	21.50
Gd	4.69	4.04	4.25	4.07	4.34	3.88	4.14	4.43
Ge	2.50	2.50	2.50	2.50	2.50	2.50	2.50	2.50
Hf	2.60	2.70	2.70	2.50	2.70	2.80	2.60	2.80
Ho	0.83	0.70	0.71	0.67	0.74	0.76	0.62	0.65
La	10.10	9.40	9.50	9.70	9.60	10.00	9.80	10.80
Lu	0.25	0.23	0.22	0.21	0.21	0.23	0.23	0.24
Nb	9.20	8.40	8.80	8.60	9.00	8.80	8.60	8.60
Nd	15.80	14.00	14.20	14.40	14.80	14.30	14.10	15.10
Pr	2.96	3.05	3.19	3.21	3.02	3.06	3.12	3.46
Rb	6.10	5.40	5.70	5.60	5.60	5.70	5.90	6.10
Sm	4.65	3.84	3.63	3.83	4.05	4.06	4.72	3.83
Sn	2.00	2.00	2.00	2.00	2.00	2.00	2.00	2.00
Sr	482.00	452.00	482.00	485.00	474.00	479.00	496.00	508.00
Ta	0.50	0.50	0.50	0.50	0.40	0.50	0.60	0.70
Tb	0.67	0.59	0.63	0.64	0.59	0.71	0.60	0.59
Th	0.93	0.81	0.85	0.89	0.89	0.92	0.80	0.80
Tm	0.28	0.24	0.25	0.27	0.27	0.24	0.25	0.29
U	0.32	0.31	0.29	0.30	0.55	0.30	0.29	0.34
V	215.00	198.00	217.00	208.00	201.00	195.00	197.00	203.00
W	1.00	1.00	1.00	1.00	BDL	BDL	1.00	1.00
Y	17.20	17.00	18.00	17.80	17.70	17.80	18.60	18.70
Yb	1.76	1.52	1.51	1.52	1.29	1.29	1.55	1.57
Zr	115.00	101.00	106.00	104.00	101.00	101.00	104.00	108.00
As	0.80	0.70	0.70	1.00	0.80	0.90	0.90	0.90
Bi	0.01	BDL	0.01	0.01	BDL	BDL	0.01	BDL
Hg	BDL	0.01	BDL	BDL	0.01	BDL	BDL	BDL
In	0.02	0.02	0.02	0.02	0.02	0.02	0.02	0.02

Abbreviations: BDL = Below detection limit

Table C.1.2. Whole Rock Geochemistry of SLV_MC Reference Material

Sample ID Reference	199504060 SLV_MC	199504061 SLV_MC	199504062 SLV_MC	199504063 SLV_MC	199504066 SLV_MC	199504069 SLV_MC	199504070 SLV_MC	199504075 SLV_MC
Re	0.00	BDL	BDL	0.00	0.00	0.00	BDL	BDL
Sb	0.15	0.16	0.16	0.16	0.13	0.15	0.14	0.14
Se	0.20	BDL	0.20	0.20	BDL	BDL	BDL	BDL
Te	BDL	BDL	0.01	BDL	BDL	BDL	BDL	BDL
Tl	BDL	BDL	BDL	BDL	BDL	BDL	BDL	BDL
Ag	BDL	BDL	BDL	BDL	BDL	BDL	BDL	BDL
Cd	BDL	0.50	0.60	0.50	BDL	BDL	BDL	BDL
Co	49.00	48.00	49.00	48.00	48.00	49.00	46.00	45.00
Cu	58.00	57.00	57.00	56.00	58.00	58.00	59.00	58.00
Li	10.00	10.00	10.00	10.00	10.00	10.00	10.00	10.00
Mo	3.00	3.00	4.00	4.00	4.00	4.00	5.00	3.00
Ni	159.00	156.00	155.00	154.00	154.00	155.00	159.00	155.00
Pb	8.00	11.00	5.00	2.00	BDL	3.00	2.00	6.00
Sc	20.00	19.00	19.00	18.00	18.00	19.00	20.00	19.00
Zn	117.00	116.00	115.00	114.00	116.00	116.00	118.00	115.00
Au	BDL	BDL	0.02	0.02	BDL	BDL	BDL	0.00
C (%)	BDL	BDL	BDL	BDL	BDL	BDL	BDL	BDL
CO_2	BDL	BDL	BDL	BDL	BDL	BDL	BDL	BDL

Abbreviations: BDL = Below detection limit

Table C.1.2. Whole Rock Geochemistry of SLV_MC Reference Material

Sample ID	Average	STDEV	%RSD	2s	%RD	Avg. other*
Reference	SLV_MC	SLV_MC	SLV_MC	SLV_MC	SLV_MC	SLV_MC
SiO_2 (%)	50.41	0.88	1.75	0.62	-0.01	50.42
Al_2O_3	15.68	0.23	1.49	0.16	0.74	15.57
Fe_2O_3	13.05	0.23	1.77	0.16	0.64	12.97
CaO	8.74	0.08	0.91	0.06	0.41	8.70
MgO	7.61	0.09	1.18	0.06	-0.19	7.63
Na_2O	3.56	0.03	0.91	0.02	0.32	3.55
K_2O	0.54	0.02	3.41	0.01	-0.77	0.54
Cr_2O_3	0.03	0.00	2.88	0.00	0.82	0.03
TiO_2	1.53	0.01	0.78	0.01	0.33	1.53
MnO	0.17	0.01	3.11	0.00	-1.24	0.17
P_2O_5	0.25	0.01	3.58	0.01	-0.34	0.25
SrO	0.05	0.01	9.63	0.00	4.03	0.05
BaO	0.02	0.00	0.00	0.00	0.00	0.02
LOI	0.00	0.00	0.00	0.06	-3.70	-0.81
Total	100.86	1.00	0.99	0.70	0.26	100.60
C	0.01	0.00	34.99	0.00	0.00	0.01
S	0.01	0.00	0.00	0.00	0.00	0.01
Ba (ppm)	166.13	5.96	3.59	4.22	0.23	165.75
Ce	22.66	0.79	3.49	0.56	0.72	22.50
Cr	237.50	7.07	2.98	5.00	0.35	236.67
Cs	0.07	0.01	10.48	0.01	3.85	0.07
Dy	3.71	0.21	5.70	0.15	-1.62	3.77
Er	1.91	0.14	7.46	0.10	0.04	1.91
Eu	1.38	0.06	4.71	0.05	1.07	1.36
Ga	20.89	1.71	8.17	1.21	0.74	20.73
Gd	4.23	0.26	6.04	0.18	0.44	4.21
Ge	2.50	0.00	0.00	0.00	0.00	2.50
Hf	2.68	0.10	3.87	0.07	0.31	2.67
Ho	0.71	0.07	9.40	0.05	-3.40	0.74
La	9.86	0.45	4.53	0.32	1.50	9.72
Lu	0.23	0.01	6.10	0.01	1.11	0.23
Nb	8.75	0.26	2.93	0.18	-0.57	8.80
Nd	14.59	0.61	4.20	0.43	0.03	14.58
Pr	3.13	0.16	4.99	0.11	1.69	3.08
Rb	5.76	0.25	4.34	0.18	1.39	5.68
Sm	4.08	0.40	9.82	0.28	1.65	4.01
Sn	2.00	0.00	0.00	0.00	0.00	2.00
Sr	482.25	16.27	3.37	11.51	1.38	475.67
Ta	0.53	0.09	16.88	0.06	8.62	0.48
Tb	0.63	0.04	7.06	0.03	-1.70	0.64
Th	0.86	0.05	6.22	0.04	-2.32	0.88
Tm	0.26	0.02	7.22	0.01	1.13	0.26
U	0.34	0.09	25.92	0.06	-2.17	0.35
V	204.25	8.29	4.06	5.86	-0.69	205.67
W	1.00	0.00	0.00	0.00	0.00	1.00
Y	17.85	0.60	3.33	0.42	1.52	17.58
Yb	1.50	0.15	10.20	0.11	1.32	1.48
Zr	105.00	4.78	4.55	3.38	0.32	104.67
As	0.84	0.11	12.66	0.07	2.55	0.82
Bi	0.01	0.00	0.00	0.00	0.00	0.01
Hg	0.01	0.00	7.44	0.00	0.00	0.01
In	0.02	0.00	6.67	0.00	1.25	0.02

Abbreviations: BDL = Below detection limit
Avg. other* = Average of other internal ALS-tested SLV_MC standards

Table C.1.2. Whole Rock Geochemistry of SLV_MC Reference Material

Sample ID Reference	Average SLV_MC	STDEV SLV_MC	%RSD SLV_MC	2s SLV_MC	%RD SLV_MC	Avg. other* SLV_MC
Re	0.00	0.00	0.00	0.00	0.00	0.00
Sb	0.15	0.01	7.57	0.01	-1.92	0.15
Se	0.20	0.00	0.00	0.00	0.00	0.20
Te	BDL	-	-	-	-	-
Tl	BDL	-	-	-	-	-
Ag	BDL	-	-	-	-	-
Cd	0.53	0.06	10.83	0.07	0.00	0.53
Co	47.75	1.49	3.12	1.05	-1.55	48.50
Cu	57.63	0.92	1.59	0.65	0.51	57.33
Li	10.00	0.00	0.00	0.00	0.00	10.00
Mo	3.75	0.71	18.86	0.50	2.27	3.67
Ni	155.88	2.03	1.30	1.44	0.24	155.50
Pb	5.29	3.35	63.42	2.53	-8.87	5.80
Sc	19.00	0.76	3.98	0.53	0.88	18.83
Zn	115.88	1.25	1.08	0.88	0.18	115.67
Au	0.01	0.01	83.21	0.01	30.00	0.01
C (%)	BDL	-	-	-	-	-
CO_2	BDL	-	-	-	-	-

Abbreviations:
BDL = Below detection limit
Avg. other* = Average of other internal ALS-tested SLV_MC standards

Appendix D: Electron Microprobe Analysis Data

Table D.1.1. Summary of electron microprobe conditions for white mica and chlorite analysis

Element	X-ray	Crystal	Spectro-meter	Accelerating voltage (kV)	Intensity (nA)	Spot size (μm)	Peak Position	Back-ground lower (mm)	Back-ground upper (mm)
F	Kα	LDE1	1	15	20	1	85.2	6.0	5.0
Cu	Kα	LIFL	2	15	20	1	107.0	3.0	3.0
Ni	Kα	LIFL	2	15	20	1	115.1	2.0	2.0
Fe	Kα	LIFL	2	15	20	1	134.4	3.5	3.6
Mn	Kα	LIFL	2	15	20	1	146.0	6.0	3.3
Cl	Kα	PETL	3	15	20	1	151.3	2.0	2.0
K	Kα	PETL	3	15	20	1	119.6	3.0	7.0
Ca	Kα	PETL	3	15	20	1	107.4	3.0	2.0
Na	Kα	TAP	4	15	20	1	129.4	4.7	6.2
Al	Kα	TAP	4	15	20	1	90.6	5.5	3.3
Si	Kα	TAP	4	15	20	1	77.4	3.3	4.1
Mg	Kα	TAP	4	15	20	1	107.5	6.0	5.0
Cr	Kα	LIFH	5	15	20	1	159.3	2.5	3.0
V	Kα	LIFH	5	15	20	1	174.2	2.0	3.0
Ti	Kα	LIFH	5	15	20	1	191.2	3.0	5.0
Ba	Lα	LIFH	5	15	20	1	193.0	4.0	2.5

Table D.1.2. Summary of electron microprobe conditions for carbonate analysis

Element	X-ray	Crystal	Spectrometer	Accelerating voltage (kV)	Intensity (nA)	Spot size (μm)	Peak Position	Background lower (mm)	Background upper (mm)
Fe	Kα	LIFL	2	15	20	1	134.5	3.5	3.6
Mn	Kα	LIFL	2	15	20	1	146.0	6.0	3.3
Ca	Kα	PETL	3	15	20	1	107.4	3.0	2.0
Sr	Kα	PETL	3	15	20	1	219.7	2.3	2.0
Mg	Kα	TAP	4	15	20	1	107.5	7.2	5.5
Ba	Kα	LIFH	5	15	20	1	193.0	3.0	2.0

Table D.1.3. Electron microprobe analyses: chlorite values

Probe Analysis	183067-1-chl-1	183067-1-chl-2	183067-1-chl-3	183067-1-chl-4	183067-1-chl-5
Sample	183067	183067	183067	183067	183067
Deposit	Argyle	Argyle	Argyle	Argyle	Argyle
Alteration Zone	Distal	Distal	Distal	Distal	Distal
SiO_2 *wt.%*	28.96	26.99	27.04	29.02	28.50
Al_2O_3	16.28	18.01	17.91	15.90	16.60
FeO	23.28	25.00	25.07	22.57	22.84
MgO	16.74	16.13	15.94	16.65	17.79
CaO	0.80	0.03	0.06	0.62	0.15
Na_2O	0.04	0.02	0.05	0.04	0.06
K_2O	0.01	0.01	0.01	0.02	0.02
MnO	0.24	0.27	0.28	0.26	0.26
Cr_2O_3	0.01	BDL	BDL	0.02	BDL
BaO	BDL	BDL	BDL	BDL	BDL
TiO_2	0.02	BDL	BDL	0.32	0.05
NiO	BDL	BDL	0.03	0.03	0.04
F	BDL	BDL	0.26	BDL	BDL
Cl	0.01	BDL	0.01	0.02	0.03
Total	85.93	86.02	86.64	84.96	85.91
Si *apfu*	6.11	5.76	5.74	6.16	6.01
Al^{iv}	1.89	2.24	2.26	1.84	1.99
Fe^{2+}	3.95	4.44	4.35	3.78	3.94
Mg	5.26	5.13	5.04	5.27	5.59
Ca	0.18	0.01	0.01	0.14	0.03
Na	0.03	0.01	0.04	0.03	0.05
K	0.01	0.01	0.01	0.01	0.01
Mn	0.04	0.05	0.05	0.05	0.05
Cr	0.00	0.00	0.00	0.00	0.00
Ba	0.00	0.00	0.00	0.00	0.00
Ti	0.00	0.00	0.00	0.05	0.01
Ni	0.00	0.00	0.00	0.01	0.01
F	0.00	0.00	0.35	0.00	0.00
Cl	0.01	0.00	0.01	0.02	0.02
Thermometers (°C)					
Kranidiotis and MacLean (1987)	227.7	265.3	268.0	222.4	238.2
Cathelineau (1988)	242.3	298.3	302.3	234.6	258.8
Zang and Fyfe (1995)	260.1	317.5	321.6	251.9	275.3
Xie et al. (1997)	218.1	253.2	255.6	213.4	230.5
Jowett (1991)	256.3	313.4	317.5	248.2	272.3

Abbreviations: BDL = Below detection limit

Table D.1.3. Electron microprobe analyses: chlorite values

Probe Analysis	183067-2-chl-1	183067-5-chl-1	183067-5-chl-2	183067-3-chl-1	183067-4-chl-1
Sample	183067	183067	183067	183067	183067
Deposit	Argyle	Argyle	Argyle	Argyle	Argyle
Alteration Zone	Distal	Distal	Distal	Distal	Distal
SiO_2 *wt.%*	28.57	26.52	26.25	27.11	28.65
Al_2O_3	16.67	18.92	18.88	17.82	16.49
FeO	23.05	25.15	25.67	25.21	23.38
MgO	17.40	15.21	14.95	15.57	16.98
CaO	0.21	0.15	0.07	0.16	0.35
Na_2O	0.10	0.03	0.01	0.01	0.02
K_2O	0.07	0.04	0.01	0.01	0.01
MnO	0.22	0.27	0.30	0.25	0.24
Cr_2O_3	BDL	BDL	BDL	BDL	BDL
BaO	BDL	BDL	BDL	BDL	BDL
TiO_2	BDL	BDL	BDL	BDL	BDL
NiO	0.01	BDL	BDL	0.02	BDL
F	BDL	BDL	BDL	BDL	0.22
Cl	0.03	0.03	0.03	0.01	0.04
Total	85.93	85.99	85.80	85.85	86.32
Si *apfu*	6.02	5.67	5.65	5.81	6.02
Al^{iv}	1.98	2.33	2.35	2.19	1.98
Fe^{2+}	3.97	4.43	4.57	4.45	3.92
Mg	5.47	4.85	4.79	4.98	5.32
Ca	0.05	0.03	0.02	0.04	0.08
Na	0.08	0.02	0.01	0.01	0.01
K	0.04	0.02	0.01	0.01	0.01
Mn	0.04	0.05	0.05	0.05	0.04
Cr	0.00	0.00	0.00	0.00	0.00
Ba	0.00	0.00	0.00	0.00	0.00
Ti	0.00	0.00	0.00	0.00	0.00
Ni	0.00	0.00	0.00	0.00	0.00
F	0.00	0.00	0.00	0.00	0.29
Cl	0.02	0.02	0.02	0.01	0.03
Thermometers (°C)					
Kranidiotis and MacLean (1987)	236.7	275.2	278.1	260.5	236.8
Cathelineau (1988)	256.2	312.8	316.9	290.6	256.3
Zang and Fyfe (1995)	273.2	332.8	337.6	310.5	273.7
Xie et al. (1997)	228.2	261.6	263.7	247.4	227.5
Jowett (1991)	269.9	328.4	332.9	306.0	270.1

Abbreviations: BDL = Below detection limit

Table D.1.3. Electron microprobe analyses: chlorite values

Probe Analysis	183067-5-chl-3	183067-5-chl-4	183067-5-chl-5	I951364-1-chl-1	I951364-1-chl-2
Sample	183067	183067	183067	I951364	I951364
Deposit	Argyle	Argyle	Argyle	Argyle	Argyle
Alteration Zone	Distal	Distal	Distal	Intermediate	Intermediate
SiO_2 *wt.%*	26.03	27.04	25.65	25.47	25.51
Al_2O_3	19.38	17.46	19.43	19.74	19.51
FeO	25.91	23.44	25.89	25.57	26.29
MgO	14.64	16.81	14.42	14.81	14.55
CaO	0.05	0.04	0.15	0.01	0.03
Na_2O	0.03	BDL	0.07	BDL	0.02
K_2O	0.01	0.01	0.04	0.01	0.01
MnO	0.30	0.26	0.29	0.43	0.37
Cr_2O_3	BDL	BDL	BDL	BDL	BDL
BaO	BDL	BDL	BDL	BDL	BDL
TiO_2	BDL	BDL	0.16	BDL	0.03
NiO	BDL	BDL	0.03	0.01	BDL
F	BDL	BDL	BDL	BDL	BDL
Cl	0.03	0.02	0.05	BDL	0.01
Total	85.90	84.71	85.79	85.60	85.90
Si *apfu*	5.59	5.82	5.53	5.50	5.51
Al^{iv}	2.41	2.18	2.47	2.50	2.49
Fe^{2+}	4.60	4.17	4.64	4.61	4.75
Mg	4.69	5.40	4.64	4.77	4.68
Ca	0.01	0.01	0.03	0.00	0.01
Na	0.03	0.00	0.06	0.00	0.02
K	0.00	0.01	0.02	0.00	0.00
Mn	0.05	0.05	0.05	0.08	0.07
Cr	0.00	0.00	0.00	0.00	0.00
Ba	0.00	0.00	0.00	0.00	0.00
Ti	0.00	0.00	0.03	0.00	0.01
Ni	0.00	0.00	0.01	0.00	0.00
F	0.00	0.00	0.00	0.00	0.00
Cl	0.02	0.01	0.04	0.00	0.01
Thermometers (°C)					
Kranidiotis and MacLean (1987)	284.2	258.3	290.5	294.0	293.1
Cathelineau (1988)	325.8	288.6	335.4	341.0	339.1
Zang and Fyfe (1995)	346.9	306.2	356.6	361.5	360.5
Xie et al. (1997)	269.0	248.7	275.1	279.5	277.5
Jowett (1991)	342.0	302.8	351.7	357.0	355.6

Abbreviations: BDL = Below detection limit

Table D.1.3. Electron microprobe analyses: chlorite values

Probe Analysis	I951364-1-chl-3	I951364-1-chl-4	I951364-1-chl-5	I951364-1-chl-6	I951364-1-chl-7
Sample	I951364	I951364	I951364	I951364	I951364
Deposit	Argyle	Argyle	Argyle	Argyle	Argyle
Alteration Zone	Intermediate	Intermediate	Intermediate	Intermediate	Intermediate
SiO_2 *wt.%*	26.19	26.23	25.92	26.32	27.05
Al_2O_3	19.17	18.75	19.42	18.90	17.76
FeO	24.48	24.57	25.67	24.90	24.03
MgO	15.52	15.77	14.94	15.57	16.49
CaO	0.03	0.03	0.01	0.02	0.04
Na_2O	BDL	0.02	BDL	BDL	BDL
K_2O	BDL	0.01	BDL	BDL	0.01
MnO	0.42	0.39	0.37	0.41	0.42
Cr_2O_3	0.03	0.02	BDL	BDL	0.01
BaO	BDL	BDL	BDL	BDL	BDL
TiO_2	BDL	0.03	0.02	0.02	0.03
NiO	BDL	BDL	BDL	BDL	BDL
F	BDL	BDL	BDL	BDL	BDL
Cl	BDL	0.01	BDL	0.01	0.01
Total	85.46	85.46	85.89	85.62	85.40
Si *apfu*	5.62	5.64	5.57	5.64	5.79
Al^{iv}	2.38	2.36	2.43	2.36	2.21
Fe^{2+}	4.34	4.39	4.58	4.42	4.26
Mg	4.97	5.06	4.78	4.98	5.26
Ca	0.01	0.01	0.00	0.00	0.01
Na	0.00	0.02	0.00	0.00	0.00
K	0.00	0.01	0.00	0.00	0.00
Mn	0.08	0.07	0.07	0.07	0.08
Cr	0.00	0.00	0.00	0.00	0.00
Ba	0.00	0.00	0.00	0.00	0.00
Ti	0.00	0.00	0.00	0.00	0.01
Ni	0.00	0.00	0.00	0.00	0.00
F	0.00	0.00	0.00	0.00	0.00
Cl	0.00	0.00	0.00	0.00	0.00
Thermometers (°C)					
Kranidiotis and MacLean (1987)	280.2	278.3	286.5	278.1	261.8
Cathelineau (1988)	320.8	318.0	329.6	317.5	293.5
Zang and Fyfe (1995)	340.0	337.1	350.2	337.0	311.8
Xie et al. (1997)	267.8	266.2	272.1	265.3	251.2
Jowett (1991)	336.0	333.1	345.6	332.8	308.1

Abbreviations: BDL = Below detection limit

Table D.1.3. Electron microprobe analyses: chlorite values

Probe Analysis	I951364-2-chl-1	I951364-2-chl-2	I951364-2-chl-3	I951364-2-chl-4	I951364-3-chl-1
Sample	I951364	I951364	I951364	I951364	I951364
Deposit	Argyle	Argyle	Argyle	Argyle	Argyle
Alteration Zone	Intermediate	Intermediate	Intermediate	Intermediate	Intermediate
SiO_2 *wt.%*	26.09	26.49	25.41	25.56	25.46
Al_2O_3	19.71	18.61	19.71	19.49	19.27
FeO	25.33	24.58	26.06	25.95	27.17
MgO	15.29	15.98	14.28	14.41	13.76
CaO	0.03	0.02	0.02	0.03	0.02
Na_2O	BDL	0.01	BDL	0.02	BDL
K_2O	0.02	0.01	0.01	BDL	0.01
MnO	0.43	0.40	0.40	0.40	0.44
Cr_2O_3	BDL	BDL	BDL	BDL	BDL
BaO	0.03	BDL	BDL	BDL	BDL
TiO_2	BDL	BDL	BDL	BDL	BDL
NiO	BDL	BDL	BDL	0.01	BDL
F	BDL	BDL	BDL	BDL	BDL
Cl	BDL	0.00	BDL	BDL	BDL
Total	86.49	85.65	85.48	85.46	85.65
Si *apfu*	5.56	5.67	5.51	5.54	5.54
Al^{iv}	2.44	2.33	2.49	2.46	2.46
Fe^{2+}	4.48	4.38	4.69	4.67	4.93
Mg	4.85	5.10	4.61	4.65	4.46
Ca	0.01	0.01	0.00	0.01	0.00
Na	0.00	0.01	0.00	0.01	0.00
K	0.01	0.00	0.00	0.00	0.00
Mn	0.08	0.07	0.07	0.07	0.08
Cr	0.00	0.00	0.00	0.00	0.00
Ba	0.01	0.00	0.00	0.00	0.00
Ti	0.00	0.00	0.00	0.00	0.00
Ni	0.00	0.00	0.00	0.00	0.00
F	0.00	0.00	0.00	0.00	0.00
Cl	0.00	0.00	0.00	0.00	0.00
Thermometers (°C)					
Kranidiotis and MacLean (1987)	287.7	274.8	293.2	289.9	290.1
Cathelineau (1988)	331.7	312.7	339.3	334.4	333.9
Zang and Fyfe (1995)	351.7	331.7	360.7	355.7	356.7
Xie et al. (1997)	274.1	262.9	277.4	274.4	272.4
Jowett (1991)	347.4	327.8	355.8	350.8	351.1

Abbreviations: BDL = Below detection limit

Table D.1.3. Electron microprobe analyses: chlorite values

Probe Analysis	I951364-3-chl-2	I951364-3-chl-3	I951364-3-chl-4	I951364-3-chl-5	I951364-3-chl-6
Sample	I951364	I951364	I951364	I951364	I951364
Deposit	Argyle	Argyle	Argyle	Argyle	Argyle
Alteration Zone	Intermediate	Intermediate	Intermediate	Intermediate	Intermediate
SiO_2 *wt.%*	26.64	26.20	26.09	26.91	26.37
Al_2O_3	19.05	18.45	18.97	17.84	18.78
FeO	26.53	26.61	26.48	24.72	26.12
MgO	14.80	14.40	14.36	15.61	14.86
CaO	0.02	0.05	0.03	0.06	0.02
Na_2O	BDL	0.03	0.02	BDL	BDL
K_2O	0.01	0.02	0.01	BDL	BDL
MnO	0.43	0.45	0.42	0.34	0.45
Cr_2O_3	BDL	BDL	0.02	BDL	BDL
BaO	BDL	BDL	0.03	0.03	BDL
TiO_2	BDL	BDL	BDL	BDL	BDL
NiO	BDL	BDL	BDL	BDL	BDL
F	BDL	BDL	BDL	BDL	BDL
Cl	0.00	BDL	0.01	BDL	BDL
Total	87.03	85.80	86.03	84.99	86.17
Si *apfu*	5.66	5.67	5.63	5.80	5.66
Al^{iv}	2.34	2.33	2.37	2.20	2.34
Fe^{2+}	4.66	4.79	4.73	4.38	4.65
Mg	4.69	4.65	4.62	5.02	4.76
Ca	0.00	0.01	0.01	0.01	0.01
Na	0.00	0.03	0.02	0.00	0.00
K	0.00	0.01	0.01	0.00	0.00
Mn	0.08	0.08	0.08	0.06	0.08
Cr	0.00	0.00	0.00	0.00	0.00
Ba	0.00	0.00	0.00	0.01	0.00
Ti	0.00	0.00	0.00	0.00	0.00
Ni	0.00	0.00	0.00	0.00	0.00
F	0.00	0.00	0.00	0.00	0.00
Cl	0.00	0.00	0.00	0.00	0.00
Thermometers (°C)					
Kranidiotis and MacLean (1987)	276.8	275.8	280.7	261.1	276.8
Cathelineau (1988)	314.5	312.7	320.3	291.8	314.8
Zang and Fyfe (1995)	335.8	334.6	342.0	311.4	335.8
Xie et al. (1997)	261.3	259.6	264.6	248.6	261.9
Jowett (1991)	330.8	329.3	336.8	307.1	330.9

Abbreviations: BDL = Below detection limit

Table D.1.3. Electron microprobe analyses: chlorite values

Probe Analysis	I951364-4-chl-1	I951364-4-chl-2	I951457-2-chl-2	I951457-2-chl-3	I951457-2-chl-4
Sample	I951364	I951364	I951457	I951457	I951457
Deposit	Argyle	Argyle	Argyle	Argyle	Argyle
Alteration Zone	Intermediate	Intermediate	Proximal	Proximal	Proximal
SiO_2 *wt.%*	26.62	25.75	25.37	25.72	26.08
Al_2O_3	18.84	19.53	18.57	18.40	18.24
FeO	25.08	25.97	36.18	36.54	36.70
MgO	15.38	14.55	5.91	6.28	6.46
CaO	0.02	0.02	0.09	0.05	0.04
Na_2O	0.01	BDL	0.06	0.03	0.02
K_2O	BDL	BDL	0.08	0.02	0.03
MnO	0.36	0.38	0.07	0.04	0.06
Cr_2O_3	BDL	BDL	BDL	BDL	BDL
BaO	BDL	BDL	BDL	BDL	BDL
TiO_2	0.02	0.03	BDL	BDL	0.02
NiO	BDL	BDL	BDL	BDL	0.01
F	BDL	BDL	BDL	0.48	BDL
Cl	BDL	BDL	0.02	0.01	BDL
Total	85.92	85.85	86.05	87.34	87.37
Si *apfu*	5.69	5.55	5.75	5.69	5.82
Al^{iv}	2.31	2.45	2.25	2.31	2.18
Fe^{2+}	4.41	4.64	6.60	6.40	6.60
Mg	4.90	4.68	2.00	2.07	2.15
Ca	0.01	0.01	0.02	0.01	0.01
Na	0.01	0.00	0.05	0.02	0.02
K	0.00	0.00	0.05	0.01	0.02
Mn	0.07	0.07	0.01	0.01	0.01
Cr	0.00	0.00	0.00	0.00	0.00
Ba	0.00	0.00	0.00	0.00	0.00
Ti	0.00	0.00	0.00	0.00	0.00
Ni	0.00	0.00	0.00	0.00	0.00
F	0.00	0.00	0.00	0.68	0.00
Cl	0.00	0.00	0.02	0.01	0.00
Thermometers (°C)					
Kranidiotis and MacLean (1987)	273.3	288.7	273.6	278.9	265.9
Cathelineau (1988)	310.1	332.7	300.8	309.2	289.4
Zang and Fyfe (1995)	329.9	353.8	339.5	347.2	327.4
Xie et al. (1997)	260.1	273.4	232.5	238.6	225.9
Jowett (1991)	325.6	349.0	326.1	334.1	314.3

Abbreviations: BDL = Below detection limit

Table D.1.3. Electron microprobe analyses: chlorite values

Probe Analysis	I951457-3-chl-1	I951457-4-chl-1	I951457-4-chl-2	I951457-4-chl-3	I951457-6-chl-1
Sample	I951457	I951457	I951457	I951457	I951457
Deposit	Argyle	Argyle	Argyle	Argyle	Argyle
Alteration Zone	Proximal	Proximal	Proximal	Proximal	Proximal
SiO_2 *wt.%*	24.58	25.28	24.48	25.57	26.41
Al_2O_3	20.09	19.66	19.02	18.72	20.45
FeO	36.29	36.59	36.12	36.05	30.26
MgO	5.53	6.09	5.57	6.04	8.08
CaO	0.06	0.05	0.07	0.06	0.04
Na_2O	0.03	0.04	0.07	0.04	0.08
K_2O	0.06	0.06	0.11	0.15	0.84
MnO	0.02	0.05	0.02	0.05	BDL
Cr_2O_3	BDL	BDL	BDL	BDL	BDL
BaO	BDL	BDL	BDL	BDL	BDL
TiO_2	BDL	0.03	0.10	0.04	0.04
NiO	BDL	0.04	BDL	BDL	BDL
F	BDL	BDL	BDL	BDL	BDL
Cl	0.02	0.01	0.01	0.01	0.05
Total	86.31	87.61	85.27	86.41	85.96
Si *apfu*	5.55	5.62	5.61	5.75	5.75
Al^{iv}	2.45	2.38	2.39	2.25	2.25
Fe^{2+}	6.60	6.58	6.72	6.53	5.16
Mg	1.86	2.02	1.90	2.03	2.62
Ca	0.01	0.01	0.02	0.01	0.01
Na	0.03	0.04	0.06	0.04	0.07
K	0.03	0.04	0.06	0.09	0.47
Mn	0.00	0.01	0.00	0.01	0.00
Cr	0.00	0.00	0.00	0.00	0.00
Ba	0.00	0.00	0.00	0.00	0.00
Ti	0.00	0.00	0.02	0.01	0.01
Ni	0.00	0.01	0.00	0.00	0.00
F	0.00	0.00	0.00	0.00	0.00
Cl	0.02	0.00	0.01	0.01	0.04
Thermometers (°C)					
Kranidiotis and MacLean (1987)	295.1	286.6	288.0	272.9	270.8
Cathelineau (1988)	333.0	320.5	322.3	299.8	299.9
Zang and Fyfe (1995)	372.2	358.9	361.5	338.3	332.2
Xie et al. (1997)	252.9	245.7	245.9	232.1	238.7
Jowett (1991)	358.7	345.7	348.0	325.0	321.7

Abbreviations: BDL = Below detection limit

Table D.1.3. Electron microprobe analyses: chlorite values

Probe Analysis	I951457-6-chl-2	I951457-6-chl-3	I951457-6-chl-4	I951457-6-chl-5
Sample	I951457	I951457	I951457	I951457
Deposit	Argyle	Argyle	Argyle	Argyle
Alteration Zone	Proximal	Proximal	Proximal	Proximal
SiO_2 *wt.%*	25.21	24.54	25.19	24.49
Al_2O_3	19.50	19.55	19.69	19.99
FeO	36.13	34.66	35.64	36.35
MgO	6.01	5.78	5.93	5.56
CaO	0.05	0.07	0.06	0.04
Na_2O	0.01	0.06	0.08	0.05
K_2O	0.04	0.10	0.13	0.07
MnO	0.03	0.05	0.03	0.05
Cr_2O_3	BDL	BDL	BDL	BDL
BaO	BDL	BDL	BDL	BDL
TiO_2	0.04	0.03	0.03	0.06
NiO	BDL	0.02	BDL	0.02
F	BDL	BDL	BDL	BDL
Cl	0.02	0.05	0.04	0.01
Total	86.66	84.56	86.44	86.28
Si *apfu*	5.65	5.61	5.64	5.53
Al^{iv}	2.35	2.39	2.36	2.47
Fe^{2+}	6.50	6.34	6.41	6.64
Mg	2.01	1.97	1.98	1.87
Ca	0.01	0.02	0.02	0.01
Na	0.01	0.05	0.07	0.04
K	0.02	0.06	0.08	0.04
Mn	0.00	0.01	0.01	0.01
Cr	0.00	0.00	0.00	0.00
Ba	0.00	0.00	0.00	0.00
Ti	0.01	0.00	0.00	0.01
Ni	0.00	0.00	0.00	0.00
F	0.00	0.00	0.00	0.00
Cl	0.01	0.04	0.03	0.01
Thermometers (°C)				
Kranidiotis and MacLean (1987)	283.7	287.5	284.5	296.4
Cathelineau (1988)	316.2	322.1	317.5	335.0
Zang and Fyfe (1995)	354.6	360.3	355.8	374.2
Xie et al. (1997)	242.8	246.7	243.7	254.2
Jowett (1991)	341.4	347.2	342.7	360.7

Abbreviations: BDL = Below detection limit

Table D.1.4. Electron microprobe analysis: white mica values

Probe Analysis	I951457-1-wm-1	I951457-1-wm-2	I951457-1-wm-3	I951457-1-wm-4	I951457-1-wm-5
Sample	I951457	I951457	I951457	I951457	I951457
Deposit	Argyle	Argyle	Argyle	Argyle	Argyle
Alteration Zone	Proximal	Proximal	Proximal	Proximal	Proximal
SiO_2 *wt.%*	47.54	47.41	47.70	46.74	47.52
Al_2O_3	36.15	37.50	36.82	36.72	36.76
FeO	1.06	0.67	1.00	0.71	0.87
MgO	0.73	0.51	0.64	0.51	0.73
CaO	0.01	0.01	0.03	BDL	0.01
Na_2O	0.56	0.63	0.50	0.52	0.46
K_2O	10.31	10.29	10.33	10.59	10.39
MnO	BDL	BDL	0.01	BDL	BDL
Cr_2O_3	BDL	BDL	BDL	BDL	BDL
BaO	BDL	0.03	0.06	0.05	0.05
TiO_2	0.11	0.10	0.08	0.08	0.06
NiO	BDL	BDL	BDL	BDL	BDL
F	BDL	BDL	BDL	BDL	BDL
Cl	0.01	BDL	BDL	0.00	BDL
Total	96.59	97.22	97.20	96.04	96.95
Si *apfu*	3.09	3.07	3.09	3.07	3.09
Al	2.77	2.86	2.81	2.84	2.82
Fe	0.06	0.04	0.05	0.04	0.05
Mg	0.07	0.05	0.06	0.05	0.07
Ca	0.00	0.00	0.00	0.00	0.00
Na	0.07	0.08	0.06	0.07	0.06
K	0.43	0.42	0.43	0.44	0.43
Mn	0.00	0.00	0.00	0.00	0.00
Cr	0.00	0.00	0.00	0.00	0.00
Ba	0.00	0.00	0.00	0.00	0.00
Ti	0.01	0.00	0.00	0.00	0.00
Ni	0.00	0.00	0.00	0.00	0.00
F	0.00	0.00	0.00	0.00	0.00
Cl	0.00	0.00	0.00	0.00	0.00

Abbreviations: BDL = Below detection limit

Table D.1.4. Electron microprobe analysis: white mica values

Probe Analysis	I951457-2-wm-1	I951457-2-wm-2	I951457-2-wm-3	I951457-2-wm-4	I951457-3-wm-1
Sample	I951457	I951457	I951457	I951457	I951457
Deposit	Argyle	Argyle	Argyle	Argyle	Argyle
Alteration Zone	Proximal	Proximal	Proximal	Proximal	Proximal
SiO_2 *wt.%*	47.39	47.15	46.95	47.01	47.70
Al_2O_3	36.62	36.87	36.07	37.44	34.97
FeO	0.92	0.83	1.78	0.79	1.48
MgO	0.61	0.55	0.62	0.47	1.03
CaO	0.01	BDL	0.01	BDL	BDL
Na_2O	0.48	0.56	0.48	0.53	0.30
K_2O	10.49	10.26	10.52	10.20	10.70
MnO	BDL	BDL	BDL	0.03	0.01
Cr_2O_3	BDL	BDL	0.01	0.01	BDL
BaO	BDL	BDL	0.07	0.06	0.08
TiO_2	0.10	0.09	0.09	0.07	0.10
NiO	BDL	0.02	BDL	BDL	BDL
F	BDL	BDL	BDL	BDL	BDL
Cl	0.01	BDL	0.00	0.00	0.01
Total	96.70	96.61	96.71	96.76	96.49
Si *apfu*	3.08	3.08	3.08	3.06	3.12
Al	2.81	2.84	2.79	2.87	2.70
Fe	0.05	0.05	0.10	0.04	0.08
Mg	0.06	0.05	0.06	0.05	0.10
Ca	0.00	0.00	0.00	0.00	0.00
Na	0.06	0.07	0.06	0.07	0.04
K	0.43	0.43	0.44	0.42	0.45
Mn	0.00	0.00	0.00	0.00	0.00
Cr	0.00	0.00	0.00	0.00	0.00
Ba	0.00	0.00	0.00	0.00	0.00
Ti	0.00	0.00	0.00	0.00	0.00
Ni	0.00	0.00	0.00	0.00	0.00
F	0.00	0.00	0.00	0.00	0.00
Cl	0.00	0.00	0.00	0.00	0.00

Abbreviations: BDL = Below detection limit

Table D.1.4. Electron microprobe analysis: white mica values

Probe Analysis	I951457-4-wm-1	I951457-4-wm-2	I951457-4-wm-3	I951457-5-wm-1	I951457-5-wm-2
Sample	I951457	I951457	I951457	I951457	I951457
Deposit	Argyle	Argyle	Argyle	Argyle	Argyle
Alteration Zone	Proximal	Proximal	Proximal	Proximal	Proximal
SiO_2 *wt.%*	48.28	47.15	47.63	47.27	48.50
Al_2O_3	36.81	37.41	37.10	35.81	37.56
FeO	0.70	1.13	1.58	0.96	0.68
MgO	0.64	0.53	0.72	0.64	0.41
CaO	0.01	BDL	0.01	0.01	0.02
Na_2O	0.46	0.45	0.48	0.44	0.64
K_2O	9.74	10.62	10.41	10.53	9.77
MnO	BDL	BDL	BDL	BDL	BDL
Cr_2O_3	BDL	BDL	BDL	BDL	BDL
BaO	0.03	0.04	BDL	BDL	BDL
TiO_2	0.06	0.18	0.09	0.06	0.09
NiO	BDL	BDL	BDL	BDL	BDL
F	BDL	BDL	BDL	BDL	BDL
Cl	0.01	BDL	0.01	0.01	BDL
Total	96.88	97.56	98.06	95.78	97.81
Si *apfu*	3.12	3.05	3.07	3.11	3.11
Al	2.80	2.86	2.82	2.78	2.84
Fe	0.04	0.06	0.09	0.05	0.04
Mg	0.06	0.05	0.07	0.06	0.04
Ca	0.00	0.00	0.00	0.00	0.00
Na	0.06	0.06	0.06	0.06	0.08
K	0.40	0.44	0.43	0.44	0.40
Mn	0.00	0.00	0.00	0.00	0.00
Cr	0.00	0.00	0.00	0.00	0.00
Ba	0.00	0.00	0.00	0.00	0.00
Ti	0.00	0.01	0.00	0.00	0.00
Ni	0.00	0.00	0.00	0.00	0.00
F	0.00	0.00	0.00	0.00	0.00
Cl	0.00	0.00	0.00	0.00	0.00

Abbreviations: BDL = Below detection limit

Table D.1.4. Electron microprobe analysis: white mica values

Probe Analysis	I951457-5-wm-3	I951457-6-wm-1	I951457-6-wm-2	I951457-6-wm-3	I951457-6-wm-4
Sample	I951457	I951457	I951457	I951457	I951457
Deposit	Argyle	Argyle	Argyle	Argyle	Argyle
Alteration Zone	Proximal	Proximal	Proximal	Proximal	Proximal
SiO_2 *wt.%*	47.13	46.55	46.81	46.34	47.19
Al_2O_3	34.78	37.21	37.45	36.92	37.41
FeO	2.22	1.95	0.80	2.39	1.29
MgO	0.87	0.33	0.36	0.66	0.39
CaO	0.17	BDL	0.01	0.02	0.03
Na_2O	0.26	0.59	0.77	0.56	0.60
K_2O	10.77	10.54	10.27	9.78	10.31
MnO	BDL	BDL	BDL	BDL	BDL
Cr_2O_3	0.01	BDL	BDL	BDL	BDL
BaO	0.07	0.06	0.03	0.05	BDL
TiO_2	0.13	0.24	0.12	0.17	0.58
NiO	0.01	BDL	BDL	0.01	BDL
F	BDL	BDL	BDL	BDL	BDL
Cl	BDL	0.01	BDL	0.01	0.01
Total	96.48	97.56	96.68	97.00	97.89
Si *apfu*	3.11	3.02	3.05	3.02	3.04
Al	2.71	2.85	2.88	2.84	2.84
Fe	0.12	0.11	0.04	0.13	0.07
Mg	0.09	0.03	0.03	0.06	0.04
Ca	0.01	0.00	0.00	0.00	0.00
Na	0.03	0.07	0.10	0.07	0.08
K	0.45	0.44	0.43	0.41	0.42
Mn	0.00	0.00	0.00	0.00	0.00
Cr	0.00	0.00	0.00	0.00	0.00
Ba	0.00	0.00	0.00	0.00	0.00
Ti	0.01	0.01	0.01	0.01	0.03
Ni	0.00	0.00	0.00	0.00	0.00
F	0.00	0.00	0.00	0.00	0.00
Cl	0.00	0.00	0.00	0.00	0.00

Abbreviations: BDL = Below detection limit

Table D.1.4. Electron microprobe analysis: white mica values

Probe Analysis	I951457-6-wm-5	I951457-6-wm-6	I951457-6-wm-7	I951457-6-wm-8
Sample	I951457	I951457	I951457	I951457
Deposit	Argyle	Argyle	Argyle	Argyle
Alteration Zone	Proximal	Proximal	Proximal	Proximal
SiO_2 *wt.%*	48.38	47.34	46.61	47.48
Al_2O_3	37.72	36.82	37.51	37.26
FeO	0.66	0.74	0.89	1.08
MgO	0.48	0.50	0.41	0.54
CaO	0.01	0.01	BDL	0.01
Na_2O	0.61	0.53	0.62	0.61
K_2O	9.66	9.91	9.95	10.22
MnO	BDL	BDL	BDL	BDL
Cr_2O_3	BDL	BDL	BDL	BDL
BaO	0.03	BDL	BDL	0.05
TiO_2	0.10	0.07	0.12	0.15
NiO	BDL	BDL	BDL	0.02
F	BDL	BDL	BDL	BDL
Cl	0.02	0.01	0.01	0.01
Total	97.81	96.04	96.22	97.55
Si *apfu*	3.07	3.08	3.04	3.06
Al	2.83	2.83	2.89	2.83
Fe	0.03	0.04	0.05	0.06
Mg	0.05	0.05	0.04	0.05
Ca	0.00	0.00	0.00	0.00
Na	0.08	0.07	0.08	0.08
K	0.39	0.41	0.41	0.42
Mn	0.00	0.00	0.00	0.00
Cr	0.00	0.00	0.00	0.00
Ba	0.00	0.00	0.00	0.00
Ti	0.00	0.00	0.01	0.01
Ni	0.00	0.00	0.00	0.00
F	0.00	0.00	0.00	0.00
Cl	0.00	0.00	0.00	0.00

Abbreviations: BDL = Below detection limit

Table D.1.5. Electron microprobe analysis: secondary standard compilation

Probe Analysis	Astimex chlorite	Astimex chlorite	Astimex chlorite	Astimex chlorite	Astimex chlorite
Sample					
Deposit	Standard	Standard	Standard	Standard	Standard
Alteration Zone					
SiO_2 *wt.%*	30.19	30.20	29.95	30.14	30.23
Al_2O_3	18.64	18.40	18.57	18.46	18.70
FeO	3.10	3.02	2.97	3.07	3.09
MgO	31.13	30.98	30.78	30.98	30.95
CaO	0.01	BDL	0.01	0.00	0.00
Na_2O	BDL	BDL	BDL	BDL	0.01
K_2O	BDL	BDL	BDL	BDL	BDL
MnO	BDL	0.01	0.02	0.02	BDL
Cr_2O_3	1.84	1.84	1.84	1.80	1.75
BaO	BDL	0.03	BDL	BDL	BDL
TiO_2	0.05	BDL	0.03	0.03	0.02
NiO	0.21	0.23	0.20	0.22	0.23
F	BDL	BDL	BDL	BDL	BDL
Cl	BDL	BDL	BDL	BDL	BDL
Total	84.50	84.02	83.76	84.02	84.27

Abbreviations: BDL = Below detection limit

Table D.1.5. Electron microprobe analysis: secondary standard compilation

Probe Analysis	Astimex chlorite	Astimex chlorite	Astimex chlorite	Astimex chlorite	Astimex chlorite
Sample					
Deposit	Standard	Standard	Standard	Standard	Standard
Alteration Zone					
SiO_2 *wt.%*	30.10	30.13	30.02	30.29	30.47
Al_2O_3	18.69	18.81	18.51	18.89	18.68
FeO	3.10	3.06	3.06	3.11	3.10
MgO	31.01	31.14	31.38	31.61	31.17
CaO	BDL	BDL	0.01	0.01	BDL
Na_2O	BDL	BDL	BDL	0.01	BDL
K_2O	BDL	BDL	BDL	BDL	BDL
MnO	0.03	0.01	BDL	0.04	0.02
Cr_2O_3	1.78	1.83	1.85	1.81	1.86
BaO	BDL	BDL	BDL	BDL	BDL
TiO_2	BDL	0.03	0.02	0.02	BDL
NiO	0.20	0.22	0.23	0.22	0.23
F	BDL	BDL	BDL	BDL	BDL
Cl	BDL	BDL	BDL	BDL	BDL
Total	84.19	84.56	84.44	85.31	84.89

Abbreviations: BDL = Below detection limit

Table D.1.5. Electron microprobe analysis: secondary standard compilation

Probe Analysis	Astimex chlorite	Astimex chlorite	Astimex chlorite	Astimex chlorite	Astimex biotite
Sample					
Deposit	Standard	Standard	Standard	Standard	Standard
Alteration Zone					
SiO_2 *wt.%*	30.17	30.27	30.31	30.02	38.49
Al_2O_3	18.75	18.63	18.69	18.55	16.07
FeO	3.05	3.22	3.00	2.99	9.50
MgO	31.06	31.31	31.42	31.23	19.74
CaO	BDL	BDL	0.01	BDL	0.16
Na_2O	BDL	BDL	BDL	BDL	0.09
K_2O	BDL	BDL	BDL	0.01	9.57
MnO	0.01	0.02	0.04	0.02	0.10
Cr_2O_3	1.86	1.79	1.80	1.81	0.10
BaO	BDL	BDL	BDL	BDL	0.11
TiO_2	0.02	BDL	BDL	BDL	1.31
NiO	0.21	0.24	0.23	0.23	0.07
F	BDL	BDL	BDL	BDL	BDL
Cl	0.01	BDL	0.01	0.00	0.02
Total	84.43	85.46	84.85	84.19	95.29

Abbreviations: BDL = Below detection limit

Table D.1.5. Electron microprobe analysis: secondary standard compilation

Probe Analysis	Astimex biotite	Astimex biotite	Astimex biotite	Astimex biotite	Astimex biotite
Sample					
Deposit	Standard	Standard	Standard	Standard	Standard
Alteration Zone					
SiO_2 *wt.%*	38.68	37.55	37.73	37.30	38.12
Al_2O_3	16.18	15.34	16.33	16.09	15.77
FeO	9.44	9.38	13.09	12.98	9.56
MgO	19.80	18.96	16.26	16.35	19.59
CaO	0.15	0.17	0.18	0.14	0.21
Na_2O	0.11	0.09	0.06	0.07	0.12
K_2O	9.60	9.65	8.71	9.62	9.18
MnO	0.09	0.11	0.24	0.22	0.12
Cr_2O_3	0.09	0.09	0.07	0.06	0.10
BaO	0.06	0.09	0.08	0.10	BDL
TiO_2	1.29	1.44	1.71	1.69	1.38
NiO	0.04	0.06	0.07	0.06	0.05
F	BDL	BDL	BDL	BDL	BDL
Cl	0.01	0.02	0.03	0.02	0.01
Total	95.41	93.06	94.48	94.72	94.06

Abbreviations: BDL = Below detection limit

Table D.1.5. Electron microprobe analysis: secondary standard compilation

Probe Analysis	Astimex biotite	Astimex biotite	Astimex biotite	Astimex biotite	Astimex biotite
Sample					
Deposit	Standard	Standard	Standard	Standard	Standard
Alteration Zone					
SiO_2 *wt.%*	38.84	36.65	36.88	37.43	38.17
Al_2O_3	15.93	15.75	15.51	16.01	16.39
FeO	9.48	13.03	9.41	12.96	13.04
MgO	19.68	15.88	18.48	16.21	16.62
CaO	0.15	0.13	0.14	0.16	0.15
Na_2O	0.10	0.04	0.10	0.09	0.06
K_2O	9.46	9.66	9.84	9.77	9.10
MnO	0.08	0.21	0.12	0.24	0.23
Cr_2O_3	0.09	0.06	0.10	0.08	0.06
BaO	0.07	0.05	0.10	0.10	0.10
TiO_2	1.52	1.95	1.53	1.83	1.67
NiO	0.03	0.05	0.05	0.03	0.04
F	BDL	0.14	0.11	BDL	BDL
Cl	0.02	0.03	0.02	0.01	0.02
Total	95.30	93.58	92.39	94.78	95.51

Abbreviations: BDL = Below detection limit

Table D.1.5. Electron microprobe analysis: secondary standard compilation

Probe Analysis Sample	Astimex biotite
Deposit Alteration Zone	Standard
SiO_2 *wt.%*	39.39
Al_2O_3	16.41
FeO	9.39
MgO	20.05
CaO	0.21
Na_2O	0.15
K_2O	9.71
MnO	0.11
Cr_2O_3	0.07
BaO	0.11
TiO_2	1.33
NiO	0.03
F	BDL
Cl	0.01
Total	96.88

Abbreviations: BDL = Below detection limit

Table D.1.6. Electron microprobe analysis: carbonates compilation

Probe Analysis	I951364-2-carb-1	I951364-2-carb-2	I951364-3-carb-1	I951364-3-carb-2	I951364-3-carb-3
Sample	I951364	I951364	I951364	I951364	I951364
Deposit	Argyle	Argyle	Argyle	Argyle	Argyle
Alteration Zone	Intermediate	Intermediate	Intermediate	Intermediate	Intermediate
FeO *wt.%*	0.33	0.27	0.42	0.27	0.19
MnO	0.39	0.34	0.32	0.17	0.35
CaO	54.87	54.94	53.58	55.57	54.56
SrO	BDL	0.11	0.09	BDL	0.07
MgO	0.07	0.07	0.07	0.03	0.10
BaO	0.01	BDL	0.03	BDL	0.03
CO_2	44.19	44.19	44.19	44.19	44.19
Total	100.00	100.00	100.00	100.00	100.00
Fe *apfu*	0.98	0.98	0.96	0.99	0.97
Mn	0.00	0.00	0.00	0.00	0.00
Ca	0.01	0.00	0.00	0.00	0.00
Sr	0.00	0.00	0.01	0.00	0.00
Mg	0.00	0.00	0.00	0.00	0.00
Ba	0.00	0.00	0.00	0.00	0.00
C	0.99	0.99	0.97	1.00	0.98
O	2.97	2.97	2.91	2.99	2.95
Total	0.99	0.99	0.97	1.00	0.98

***CO_2 calculated by difference from 100% Total Oxide**

Table D.1.6. Electron microprobe analysis: carbonates compilation

Probe Analysis	I951364-3-carb-4	I951364-4-carb-1	I951364-4-carb-2	I951364-4-carb-3	I951364-4-carb-4
Sample	I951364	I951364	I951364	I951364	I951364
Deposit	Argyle	Argyle	Argyle	Argyle	Argyle
Alteration Zone	Intermediate	Intermediate	Intermediate	Intermediate	Intermediate
FeO *wt.%*	0.25	0.25	1.10	0.33	0.25
MnO	0.43	0.34	0.26	0.28	0.35
CaO	54.17	54.73	52.17	55.35	55.55
SrO	0.13	0.14	0.01	0.09	0.07
MgO	0.11	0.05	0.41	0.08	0.04
BaO	0.01	0.01	0.02	0.01	BDL
CO_2	44.19	44.19	44.19	44.19	44.19
Total	100.00	100.00	100.00	100.00	100.00
Fe *apfu*	0.97	0.98	0.93	0.99	0.99
Mn	0.00	0.00	0.01	0.00	0.00
Ca	0.01	0.00	0.00	0.00	0.00
Sr	0.00	0.00	0.02	0.00	0.00
Mg	0.00	0.00	0.00	0.00	0.00
Ba	0.00	0.00	0.00	0.00	0.00
C	0.98	0.99	0.96	1.00	1.00
O	2.94	2.96	2.88	3.00	3.00
Total	0.98	0.99	0.96	1.00	1.00

***CO_2 calculated by difference from 100% Total Oxide**

Table D.1.6. Electron microprobe analysis: carbonates compilation

Probe Analysis	I951457-4-carb-1	I951457-5-carb-1	I951457-5-carb-2	I951457-5-carb-3	I951457-5-carb-4
Sample	I951457	I951457	I951457	I951457	I951457
Deposit	Argyle	Argyle	Argyle	Argyle	Argyle
Alteration Zone	Proximal	Proximal	Proximal	Proximal	Proximal
FeO *wt.%*	0.45	0.27	0.35	18.56	15.05
MnO	1.45	1.33	1.82	0.45	2.44
CaO	53.72	52.21	48.99	28.10	28.28
SrO	0.10	BDL	0.01	0.10	0.04
MgO	0.13	0.04	0.07	8.21	9.27
BaO	0.05	BDL	0.04	BDL	0.02
CO_2	44.19	44.19	44.19	44.19	44.19
Total	100.00	100.00	100.00	100.00	100.00
Fe *apfu*	0.96	0.93	0.87	0.50	0.50
Mn	0.00	0.00	0.00	0.20	0.23
Ca	0.02	0.02	0.03	0.01	0.03
Sr	0.01	0.00	0.00	0.26	0.21
Mg	0.00	0.00	0.00	0.00	0.00
Ba	0.00	0.00	0.00	0.00	0.00
C	0.99	0.95	0.91	0.97	0.98
O	2.97	2.86	2.72	2.91	2.94
Total	0.99	0.95	0.91	0.97	0.98

***CO_2 calculated by difference from 100% Total Oxide**

Table D.1.6. Electron microprobe analysis: carbonates compilation

Probe Analysis	I951457-5-carb-5	I951457-5-carb-6	I951457-6-carb-1	I951457-6-carb-2	I951457-6-carb-3
Sample	I951457	I951457	I951457	I951457	I951457
Deposit	Argyle	Argyle	Argyle	Argyle	Argyle
Alteration Zone	Proximal	Proximal	Proximal	Proximal	Proximal
FeO *wt.%*	17.70	17.83	18.61	0.45	0.58
MnO	0.71	1.68	0.44	0.94	1.15
CaO	28.66	28.25	28.00	53.71	54.62
SrO	0.09	0.13	BDL	BDL	BDL
MgO	8.39	7.79	8.58	0.07	0.02
BaO	BDL	BDL	BDL	0.07	0.00
CO_2	44.19	44.19	44.19	44.19	44.19
Total	100.00	100.00	100.00	100.00	100.00
Fe *apfu*	0.51	0.50	0.50	0.96	0.97
Mn	0.21	0.19	0.21	0.00	0.00
Ca	0.01	0.02	0.01	0.01	0.02
Sr	0.25	0.25	0.26	0.01	0.01
Mg	0.00	0.00	0.00	0.00	0.00
Ba	0.00	0.00	0.00	0.00	0.00
C	0.98	0.97	0.98	0.98	1.00
O	2.93	2.91	2.93	2.94	3.00
Total	0.98	0.97	0.98	0.98	1.00

***CO_2 calculated by difference from 100% Total Oxide**

Table D.1.6. Electron microprobe analysis: carbonates compilation

Probe Analysis	I951457-6-carb-4	I951457-6-carb-5	I951457-6-carb-6
Sample	I951457	I951457	I951457
Deposit	Argyle	Argyle	Argyle
Alteration Zone	Proximal	Proximal	Proximal
FeO *wt.%*	0.31	19.16	0.31
MnO	1.59	0.44	2.27
CaO	54.50	28.23	53.69
SrO	0.05	0.08	0.04
MgO	0.05	8.40	0.09
BaO	BDL	0.00	0.01
CO_2	44.19	44.19	44.19
Total	100.00	100.00	100.00
Fe *apfu*	0.97	0.50	0.96
Mn	0.00	0.21	0.00
Ca	0.02	0.01	0.03
Sr	0.00	0.27	0.00
Mg	0.00	0.00	0.00
Ba	0.00	0.00	0.00
C	1.00	0.99	1.00
O	3.00	2.96	2.99
Total	1.00	0.99	1.00

***CO_2 calculated by difference from 100% Total Oxide**

Table D.1.7. Electron microprobe analysis: secondary standards compilation

Probe Analysis	Astimex dolomite	Astimex dolomite	Astimex dolomite	Astimex dolomite	Astimex dolomite
Sample	Standard	Standard	Standard	Standard	Standard
Deposit					
Alteration Zone					
FeO *wt.%*	0.11	0.15	0.14	0.14	0.12
MnO	0.00	0.03	0.03	0.02	0.03
CaO	30.70	30.80	30.70	30.35	30.85
SrO	0.00	0.12	0.04	0.03	0.03
MgO	20.96	20.82	20.75	20.80	20.93
BaO	0.08	0.01	0.03	0.05	-0.01
CO_2	48.16	48.08	48.32	48.62	48.05
Total	100.00	100.00	100.00	100.00	100.00

***CO_2 calculated by difference from 100% Total Oxide**

Table D.1.7. Electron microprobe analysis: secondary standards compilation

Probe Analysis	Astimex dolomite	Astimex dolomite	Astimex dolomite	Astimex dolomite	Astimex dolomite
Sample	Standard	Standard	Standard	Standard	Standard
Deposit					
Alteration Zone					
FeO *wt.%*	0.13	0.13	0.14	0.12	0.12
MnO	0.02	0.03	0.01	0.05	0.03
CaO	30.68	30.65	30.50	30.71	30.39
SrO	-0.02	0.00	0.02	-0.01	-0.01
MgO	20.91	20.96	21.00	20.74	20.92
BaO	0.08	-0.05	0.07	0.03	0.00
CO_2	48.19	48.29	48.25	48.37	48.55
Total	100.00	100.00	100.00	100.00	100.00

***CO_2 calculated by difference from 100% Total Oxide**

Table D.1.7. Electron microprobe analysis: secondary standards compilation

Probe Analysis	Astimex dolomite	Astimex dolomite	Astimex dolomite
Sample	Standard	Standard	Standard
Deposit			
Alteration Zone			
FeO *wt.%*	0.10	0.15	0.11
MnO	0.01	0.04	0.00
CaO	30.61	30.50	30.59
SrO	-0.01	0.03	-0.04
MgO	21.08	20.85	21.10
BaO	-0.01	0.02	0.05
CO_2	48.23	48.41	48.19
Total	100.00	100.00	100.00

***CO_2 calculated by difference from 100% Total Oxide**

Appendix E: Principal Component Analysis

Table E.1.1. Total variance

Principal component	Eigenvalues	% of Variance	Cumulative %
PC1	**8.29**	**31.88**	**31.88**
PC2	**5.06**	**19.46**	**51.34**
PC3	**3.79**	**14.57**	**65.91**
PC4	**2.06**	**7.92**	**73.83**
PC5	**1.33**	**5.12**	**78.95**
PC6	1.06	4.06	83.01
PC7	0.83	3.19	86.2
PC8	0.69	2.66	88.86
PC9	0.56	2.14	90.99
PC10	0.45	1.75	92.74
PC11	0.39	1.49	94.23
PC12	0.26	1.01	95.24
PC13	0.22	0.85	96.09
PC14	0.19	0.73	96.82
PC15	0.16	0.61	97.43
PC16	0.15	0.58	98.02
PC17	0.13	0.48	98.5
PC18	0.11	0.41	98.91
PC19	0.08	0.32	99.23
PC20	0.06	0.24	99.47
PC21	0.04	0.16	99.64
PC22	0.03	0.13	99.77
PC23	0.02	0.09	99.86
PC24	0.02	0.09	99.95
PC25	0.01	0.03	99.98
PC26	0.00	0.02	100

PC1-PC5 = Significant Principal Components

Table E.1.2. Scaled co-ordinates

	PC1	PC2	PC3	PC4	PC5
SiO_2	0.342	0.454	-0.642	-0.021	-0.352
Al_2O_3	-0.020	0.014	-0.521	-0.481	0.410
Fe_2O_3	-0.025	0.667	0.658	-0.135	0.092
CaO	-0.805	-0.219	0.212	0.121	-0.067
MgO	-0.913	-0.113	0.090	-0.090	-0.058
Na_2O	0.314	0.390	-0.493	0.188	0.380
K_2O	0.503	-0.743	0.221	-0.302	-0.011
TiO_2	-0.112	0.540	0.748	-0.023	0.183
MnO	0.311	0.434	0.668	0.187	-0.276
P_2O_5	0.753	0.443	0.287	0.049	0.004
LOI	0.174	-0.706	0.450	0.378	0.203
Ba	0.376	-0.558	0.248	-0.436	-0.244
Cs	0.199	-0.611	0.221	-0.437	-0.229
Lu	0.871	0.410	0.089	-0.071	0.075
Rb	0.483	-0.761	0.239	-0.297	-0.013
Sr	-0.591	0.165	-0.161	-0.022	-0.220
V	-0.825	0.104	0.444	-0.073	0.149
W	0.547	-0.236	0.354	0.025	0.262
Y	0.866	0.425	0.138	-0.037	0.077
As	0.296	0.294	0.001	-0.663	0.092
Sb	-0.608	0.410	-0.048	-0.286	-0.115
Co	-0.855	0.079	0.386	-0.157	0.097
Cu	-0.321	0.181	-0.089	-0.506	0.485
Sc	-0.927	0.027	0.261	-0.049	0.032
Zn	0.419	0.565	0.476	-0.175	-0.195
CO_2	0.232	-0.387	0.198	0.405	0.399

PC1-PC5 = Significant Principal Components

Appendix F: Mass Change Calculations

Table F.1.1 Pearson's correlation coefficients of Argyle lithogeochemical samples

	SiO_2	Al_2O_3	Fe_2O_3	CaO	MgO	Na_2O	K_2O	Cr_2O_3	TiO_2	MnO	P_2O_5	SrO	BaO	LOI	C	S	Ba	Ce	Cr	Cs	Dy	Er	Eu	Ga	Gd	Ge	Hf	Ho	La	Lu	Nb	Nd	Pr	Rb
SiO_2	1																																	
Al_2O_3	-0.12	1																																
Fe_2O_3	-0.23	-0.19	1																															
CaO	-0.48	-0.03	-0.16	1																														
MgO	-0.34	0.29	-0.07	0.61	1																													
Na_2O	0.35	0.29	-0.10	-0.56	-0.49	1																												
K_2O	-0.32	0.08	-0.26	-0.08	-0.10	-0.34	1																											
Cr_2O_3	-0.13	0.40	-0.50	0.34	0.66	-0.30	0.24	1																										
TiO_2	-0.37	-0.26	0.88	-0.04	-0.08	-0.16	-0.19	-0.48	1																									
MnO	-0.08	-0.46	0.63	-0.20	-0.43	-0.03	-0.05	-0.54	0.64	1																								
P_2O_5	0.18	-0.07	0.36	-0.56	-0.66	0.35	0.02	-0.47	0.25	0.60	1																							
SrO	-0.05	0.31	-0.07	0.58	0.46	-0.16	-0.38	0.25	-0.08	-0.16	-0.31	1																						
BaO	-0.18	0.01	-0.10	-0.10	-0.02	-0.25	0.66	0.14	-0.07	0.00	0.00	-0.19	1																					
LOI	-0.63	-0.35	-0.17	0.16	-0.14	-0.27	0.55	0.01	0.02	0.09	-0.05	-0.37	0.29	1																				
C	-0.52	-0.43	-0.17	0.07	-0.30	-0.17	0.53	-0.10	0.02	0.20	0.06	-0.41	0.26	0.97	1																			
S	0.31	-0.03	-0.10	-0.38	-0.50	0.33	0.13	-0.22	-0.15	-0.04	0.15	-0.26	0.01	-0.07	0.03	1																		
Ba	-0.21	0.06	-0.13	-0.11	-0.05	-0.23	0.75	0.18	-0.11	0.02	0.07	-0.20	0.85	0.32	0.30	0.03	1																	
Ce	0.32	0.07	0.19	-0.74	-0.81	0.57	0.11	-0.48	0.11	0.40	0.81	-0.40	0.08	-0.11	0.01	0.51	0.11	1																
Cr	-0.14	0.42	-0.49	0.41	0.72	-0.32	0.18	0.98	-0.47	-0.59	-0.53	0.31	0.10	-0.01	-0.14	-0.25	0.12	-0.55	1															
Cs	-0.18	0.01	0.01	0.09	0.03	-0.28	0.44	0.09	0.02	0.00	-0.09	0.02	0.55	0.16	0.14	0.05	0.64	-0.05	0.06	1														
Dy	0.29	0.02	0.26	-0.72	-0.82	0.54	0.07	-0.53	0.18	0.47	0.83	-0.41	0.05	-0.10	0.02	0.50	0.07	0.99	-0.60	-0.07	1													
Er	0.32	0.03	0.22	-0.73	-0.82	0.56	0.09	-0.51	0.14	0.45	0.79	-0.40	0.06	-0.11	0.02	0.52	0.09	0.98	-0.58	-0.05	0.99	1												
Eu	0.28	0.00	0.29	-0.71	-0.81	0.53	0.05	-0.55	0.22	0.53	0.87	-0.38	0.02	-0.10	0.03	0.44	0.06	0.97	-0.61	-0.07	0.98	0.97	1											
Ga	-0.01	0.26	0.46	-0.49	-0.50	0.34	0.04	-0.43	0.36	0.40	0.60	-0.18	0.10	-0.17	-0.12	0.09	0.08	0.67	-0.45	0.04	0.70	0.69	0.70	1										
Gd	0.28	0.02	0.28	-0.71	-0.81	0.53	0.06	-0.53	0.20	0.50	0.87	-0.39	0.03	-0.10	0.02	0.45	0.07	0.98	-0.60	-0.07	0.99	0.98	0.99	0.71	1									
Ge	-0.10	-0.05	0.13	0.16	0.15	-0.07	-0.17	-0.04	0.13	-0.15	-0.18	-0.02	0.04	0.06	0.01	-0.12	-0.17	-0.16	0.06	-0.11	-0.16	-0.19	-0.20	0.01	-0.18	1								
Hf	0.33	0.09	0.16	-0.73	-0.81	0.60	0.08	-0.49	0.10	0.34	0.70	-0.39	0.06	-0.12	0.00	0.57	0.06	0.98	-0.55	-0.05	0.97	0.97	0.94	0.66	0.95	-0.14	1							
Ho	0.30	0.02	0.24	-0.73	-0.82	0.55	0.08	-0.52	0.17	0.46	0.81	-0.41	0.05	-0.11	0.02	0.51	0.08	0.98	-0.59	-0.06	1.00	0.99	0.98	0.70	0.99	-0.18	0.97	1						
La	0.32	0.07	0.17	-0.74	-0.81	0.57	0.12	-0.47	0.09	0.38	0.79	-0.41	0.09	-0.10	0.02	0.51	0.12	1.00	-0.54	-0.04	0.98	0.98	0.96	0.67	0.98	-0.15	0.98	0.98	1					
Lu	0.32	0.05	0.21	-0.73	-0.82	0.57	0.10	-0.50	0.12	0.42	0.75	-0.40	0.07	-0.12	0.01	0.56	0.08	0.98	-0.57	-0.05	0.99	0.99	0.96	0.69	0.97	-0.17	0.98	0.99	0.98	1				
Nb	0.31	0.02	0.20	-0.74	-0.84	0.55	0.10	-0.51	0.16	0.45	0.76	-0.41	0.06	-0.09	0.05	0.53	0.07	0.98	-0.58	-0.06	0.98	0.98	0.96	0.69	0.97	-0.18	0.98	0.98	0.98	0.98	1			
Nd	0.30	0.04	0.24	-0.73	-0.82	0.56	0.08	-0.51	0.16	0.45	0.84	-0.39	0.05	-0.11	0.02	0.48	0.08	0.99	-0.58	-0.06	0.99	0.99	0.99	0.70	0.99	-0.16	0.97	0.99	0.99	0.98	0.98	1		
Pr	0.31	0.06	0.21	-0.73	-0.81	0.56	0.09	-0.49	0.13	0.42	0.83	-0.40	0.06	-0.11	0.01	0.48	0.09	1.00	-0.56	-0.06	0.99	0.98	0.98	0.67	0.99	-0.15	0.97	0.98	0.99	0.98	0.97	1.00	1	
Rb	-0.32	0.07	-0.27	-0.09	-0.07	-0.35	0.99	0.26	-0.20	-0.07	-0.01	-0.38	0.68	0.55	0.53	0.11	0.77	0.08	0.20	0.46	0.04	0.06	0.02	0.02	0.03	-0.14	0.06	0.05	0.09	0.06	0.07	0.05	0.06	1
Sm	0.30	0.04	0.25	-0.73	-0.82	0.55	0.06	-0.52	0.17	0.47	0.85	-0.39	0.03	-0.12	0.01	0.48	0.07	0.99	-0.59	-0.06	0.99	0.99	0.99	0.71	0.99	-0.18	0.96	0.99	0.98	0.98	0.98	1.00	0.99	0.03
Sn	0.31	-0.25	0.18	-0.49	-0.60	0.19	0.09	-0.36	0.16	0.52	0.60	-0.31	0.11	-0.04	0.07	0.18	0.11	0.66	-0.42	0.00	0.68	0.68	0.68	0.50	0.68	-0.13	0.62	0.67	0.66	0.65	0.68	0.67	0.66	0.07
Sr	-0.05	0.29	-0.08	0.59	0.47	-0.21	-0.36	0.28	-0.09	-0.15	-0.31	0.95	-0.14	-0.37	-0.41	-0.25	-0.16	-0.39	0.33	0.05	-0.39	-0.38	-0.37	-0.18	-0.38	-0.01	-0.38	-0.39	-0.39	-0.39	-0.40	-0.38	-0.39	-0.35
Ta	0.31	0.04	0.21	-0.74	-0.83	0.56	0.10	-0.50	0.16	0.44	0.76	-0.41	0.06	-0.09	0.03	0.52	0.08	0.98	-0.57	-0.06	0.98	0.98	0.96	0.67	0.97	-0.21	0.98	0.98	0.98	0.98	0.99	0.98	0.98	0.07
Tb	0.30	0.02	0.27	-0.72	-0.82	0.54	0.07	-0.54	0.19	0.48	0.84	-0.39	0.04	-0.11	0.02	0.47	0.07	0.99	-0.60	-0.07	1.00	0.99	0.99	0.71	0.99	-0.17	0.96	0.99	0.98	0.98	0.98	0.99	0.99	0.03
Th	0.32	0.13	-0.03	-0.72	-0.67	0.48	0.32	-0.25	-0.10	0.18	0.59	-0.43	0.30	-0.04	0.06	0.55	0.30	0.89	-0.33	0.07	0.84	0.86	0.80	0.54	0.82	-0.15	0.88	0.85	0.90	0.88	0.86	0.85	0.86	0.31
Tm	0.33	0.04	0.20	-0.73	-0.82	0.56	0.09	-0.50	0.12	0.42	0.77	-0.40	0.06	-0.12	0.01	0.54	0.08	0.98	-0.57	-0.05	0.99	0.99	0.96	0.69	0.97	-0.20	0.98	0.99	0.98	0.99	0.98	0.98	0.97	0.06
U	0.31	0.09	-0.03	-0.70	-0.65	0.42	0.34	-0.23	-0.08	0.21	0.60	-0.44	0.34	-0.01	0.09	0.52	0.32	0.86	-0.32	0.06	0.83	0.84	0.79	0.49	0.81	-0.18	0.86	0.83	0.87	0.86	0.84	0.83	0.85	0.34
V	-0.43	-0.12	0.54	0.46	0.51	-0.38	-0.24	-0.07	0.53	0.01	-0.46	0.23	-0.06	-0.05	-0.13	-0.33	-0.13	-0.56	0.01	0.12	-0.52	-0.54	-0.52	-0.12	-0.52	0.38	-0.53	-0.53	-0.56	-0.53	-0.55	-0.54	-0.55	-0.23
W	-0.22	-0.10	0.04	-0.04	-0.36	-0.04	0.40	-0.22	0.12	0.22	0.24	-0.29	0.12	0.37	0.43	0.37	0.13	0.32	-0.24	0.08	0.33	0.31	0.30	0.20	0.32	0.07	0.32	0.33	0.32	0.33	0.34	0.32	0.32	0.36
Y	0.30	0.02	0.26	-0.73	-0.82	0.55	0.07	-0.53	0.18	0.47	0.82	-0.41	0.05	-0.10	0.02	0.50	0.07	0.99	-0.60	-0.07	0.99	0.99	0.98	0.69	0.99	-0.15	0.97	0.99	0.98	0.98	0.98	0.99	0.99	0.04
Yb	0.33	0.05	0.19	-0.74	-0.83	0.58	0.09	-0.50	0.11	0.40	0.75	-0.39	0.06	-0.11	0.01	0.56	0.08	0.98	-0.57	-0.05	0.99	0.99	0.96	0.68	0.97	-0.19	0.99	0.99	0.98	0.99	0.98	0.98	0.98	0.06
Zr	0.33	0.09	0.12	-0.73	-0.82	0.59	0.11	-0.47	0.05	0.33	0.69	-0.39	0.06	-0.11	0.01	0.58	0.08	0.97	-0.54	-0.03	0.97	0.98	0.93	0.67	0.95	-0.18	0.99	0.97	0.97	0.98	0.98	0.96	0.96	0.08
As	0.23	0.22	-0.03	-0.29	-0.33	0.31	0.13	-0.15	-0.13	-0.04	0.17	-0.14	-0.04	-0.21	-0.13	0.81	0.06	0.44	-0.18	0.06	0.44	0.46	0.40	0.21	0.42	-0.19	0.50	0.44	0.45	0.49	0.45	0.42	0.42	0.10
Bi	-0.04	-0.21	-0.04	0.09	-0.18	-0.02	0.09	-0.10	0.04	0.14	0.08	-0.07	-0.02	0.14	0.21	0.48	-0.03	0.10	-0.12	0.01	0.14	0.13	0.14	-0.09	0.13	-0.08	0.12	0.13	0.10	0.13	0.14	0.11	0.10	0.06
Hg	0.12	0.01	0.09	-0.11	0.00	0.10	-0.16	-0.09	0.11	0.01	-0.06	0.07	-0.03	-0.14	-0.14	0.04	-0.07	0.01	-0.06	-0.08	0.03	0.02	0.01	0.05	0.00	0.23	0.05	0.03	0.01	0.03	0.04	0.03	0.01	-0.15
In	0.01	-0.34	0.35	-0.61	-0.75	0.31	0.08	-0.55	0.38	0.60	0.68	-0.57	0.02	0.32	0.41	0.26	0.01	0.71	-0.62	-0.16	0.75	0.73	0.77	0.53	0.75	-0.13	0.68	0.74	0.70	0.72	0.75	0.73	0.72	0.06
Re	0.04	-0.05	0.05	-0.12	-0.15	0.15	0.00	-0.14	0.00	0.05	0.14	-0.10	0.04	0.07	0.12	-0.01	-0.04	0.15	-0.12	-0.01	0.13	0.12	0.13	0.08	0.13	0.26	0.14	0.11	0.15	0.12	0.12	0.15	0.15	-0.01
Sb	0.04	0.21	0.20	0.43	0.48	-0.25	-0.39	0.18	0.13	-0.10	-0.34	0.59	-0.19	-0.52	-0.55	-0.19	-0.26	-0.38	0.23	0.08	-0.37	-0.37	-0.37	-0.05	-0.36	0.21	-0.36	-0.37	-0.38	-0.36	-0.38	-0.37	-0.38	-0.39
Se	0.26	0.04	-0.08	-0.35	-0.41	0.33	0.10	-0.19	-0.15	-0.08	0.08	-0.20	-0.01	-0.07	0.00	0.95	-0.01	0.45	-0.20	0.01	0.44	0.45	0.38	0.08	0.40	-0.05	0.53	0.44	0.46	0.51	0.48	0.42	0.43	0.08
Te	-0.06	-0.17	-0.26	0.13	-0.02	-0.10	0.27	0.21	-0.22	-0.01	-0.06	-0.02	0.19	0.26	0.28	0.19	0.19	-0.01	0.18	0.12	-0.02	0.00	-0.04	-0.14	-0.04	-0.05	0.00	-0.01	0.00	0.01	-0.01	-0.03	-0.02	0.27
Tl	-0.12	-0.11	0.10	-0.02	-0.03	-0.16	0.26	-0.05	0.10	0.03	0.00	-0.14	0.30	0.17	0.16	0.00	0.22	0.01	-0.05	0.10	0.00	0.00	-0.04	0.05	-0.02	0.42	-0.03	-0.01	0.02	-0.01	-0.01	-0.01	-0.01	0.28
Ag	-0.13	-0.03	0.11	0.14	0.06	-0.01	-0.11	-0.07	0.11	-0.12	-0.15	-0.03	0.05	0.10	0.07	0.13	-0.16	-0.07	0.01	-0.09	-0.06	-0.09	-0.11	0.03	-0.09	0.89	-0.02	-0.08	-0.07	-0.05	-0.07	-0.07	-0.07	-0.10
Cd	-0.21	-0.10	0.34	0.27	0.14	-0.27	-0.06	-0.07	0.39	0.12	-0.13	0.10	0.06	0.00	-0.03	-0.07	0.01	-0.13	-0.04	0.13	-0.13	-0.16	-0.13	0.02	-0.13	0.46	-0.14	-0.15	-0.14	-0.15	-0.14	-0.14	-0.13	-0.06
Co	-0.51	0.10	0.42	0.58	0.78	-0.49	-0.20	0.23	0.40	-0.11	-0.49	0.39	-0.08	-0.10	-0.23	-0.44	-0.11	-0.69	0.30	0.09	-0.66	-0.68	-0.64	-0.24	-0.64	0.24	-0.68	-0.67	-0.69	-0.68	-0.70	-0.67	-0.68	-0.19
Cu	0.03	0.16	0.02	0.18	0.24	0.04	-0.16	0.05	-0.09	-0.29	-0.32	0.22	-0.04	-0.28	-0.30	0.08	-0.07	-0.20	0.08	0.03	-0.22	-0.20	-0.26	-0.18	-0.23	0.08	-0.14	-0.22	-0.19	-0.17	-0.22	-0.22	-0.21	-0.16
Li	-0.27	0.15	0.09	0.17	0.44	-0.15	-0.15	0.22	0.09	-0.23	-0.15	-0.01	-0.11	0.08	-0.06	-0.41	-0.12	-0.34	0.27	-0.12	-0.36	-0.39	-0.33	-0.14	-0.33	0.18	-0.38	-0.37	-0.34	-0.39	-0.38	-0.34	-0.33	-0.13
Mo	0.13	-0.07	0.08	-0.25	-0.29	0.17	0.03	-0.20	0.02	0.16	0.32	-0.17	0.06	0.04	0.10	0.08	-0.02	0.33	-0.20	-0.05	0.32	0.31	0.31	0.17	0.32	0.17	0.32	0.30	0.33	0.30	0.31	0.33	0.34	0.02
Ni	-0.20	0.32	-0.43	0.44	0.82	-0.39	0.21	0.84	-0.45	-0.60	-0.64	0.27	0.20	0.02	-0.12	-0.32	0.19	-0.66	0.87	0.12	-0.72	-0.70	-0.74	-0.52	-0.72	0.09	-0.67	-0.71	-0.65	-0.68	-0.71	-0.70	-0.68	0.24
Pb	-0.13	-0.14	0.04	0.02	-0.11	-0.03	0.06	-0.09	0.07	0.05	0.07	-0.11	0.03	0.18	0.21	0.08	0.01	0.04	-0.08	-0.05	0.05	0.04	0.04	0.07	0.06	0.10	0.01	0.05	0.05	0.03	0.05	0.05	0.03	0.05
Sc	-0.43	0.07	0.23	0.68	0.80	-0.46	-0.30	0.26	0.27	-0.23	-0.65	0.42	-0.17	-0.11	-0.24	-0.49	-0.21	-0.79	0.34	0.01	-0.76	-0.77	-0.75	-0.37	-0.75	0.24	-0.76	-0.76	-0.80	-0.77	-0.78	-0.77	-0.78	-0.28
Zn	0.02	-0.13	0.70	-0.47	-0.37	0.07	-0.04	-0.47	0.59	0.69	0.65	-0.19	0.08	-0.16	-0.11	-0.04	0.12	0.50	-0.53	0.00	0.56	0.53	0.59	0.60	0.58	-0.24	0.45	0.54	0.49	0.50	0.52	0.54	0.52	-0.06
Au	0.20	-0.03	-0.15	-0.23	-0.41	0.28	0.11	-0.16	-0.18	-0.08	0.08	-0.21	-0.03	-0.01	0.08	0.92	-0.04	0.38	-0.18	-0.01	0.38	0.40	0.33	0.04	0.35	-0.07	0.45	0.39	0.39	0.44	0.41	0.36	0.36	0.08
CO_2	-0.40	-0.39	-0.16	0.07	-0.28	-0.09	0.38	-0.12	0.01	0.18	0.02	-0.29	0.22	0.78	0.83	0.10	0.22	0.02	-0.13	0.12	0.01	0.01	0.02	-0.14	0.02	0.03	0.02	0.02	0.02	0.02	0.05	0.02	0.01	0.38

Table F.1.1 Pearson's correlation coefficients of Argyle lithogeochemical samples

	Sm	Sn	Sr	Ta	Tb	Th	Tm	U	V	W	Y	Yb	Zr	As	Bi	Hg	In	Re	Sb	Se	Te	Tl	Ag	Cd	Co	Cu	Li	Mo	Ni	Pb	Sc	Zn	Au	CO_2
SiO_2																																		
Al_2O_3																																		
Fe_2O_3																																		
CaO																																		
MgO																																		
Na_2O																																		
K_2O																																		
Cr_2O_3																																		
TiO_2																																		
MnO																																		
P_2O_5																																		
SrO																																		
BaO																																		
LOI																																		
C																																		
S																																		
Ba																																		
Ce																																		
Cr																																		
Cs																																		
Dy																																		
Er																																		
Eu																																		
Ga																																		
Gd																																		
Ge																																		
Hf																																		
Ho																																		
La																																		
Lu																																		
Nb																																		
Nd																																		
Pr																																		
Rb																																		
Sm	1																																	
Sn	0.68	1																																
Sr	-0.38	-0.26	1																															
Ta	0.97	0.66	-0.40	1																														
Tb	0.99	0.68	-0.38	0.97	1																													
Th	0.84	0.55	-0.41	0.86	0.84	1																												
Tm	0.98	0.67	-0.38	0.98	0.98	0.87	1																											
U	0.82	0.54	-0.42	0.84	0.82	0.98	0.85	1																										
V	-0.53	-0.38	0.22	-0.54	-0.52	-0.59	-0.54	-0.60	1																									
W	0.31	0.22	-0.27	0.31	0.32	0.29	0.32	0.28	-0.12	1																								
Y	0.99	0.66	-0.39	0.98	0.99	0.84	0.98	0.84	-0.51	0.32	1																							
Yb	0.98	0.65	-0.39	0.98	0.98	0.88	0.99	0.86	-0.54	0.32	0.99	1																						
Zr	0.96	0.64	-0.38	0.98	0.96	0.89	0.98	0.86	-0.56	0.32	0.96	0.98	1																					
As	0.43	0.10	-0.13	0.44	0.42	0.47	0.48	0.42	-0.25	0.27	0.42	0.48	0.52	1																				
Bi	0.13	0.10	-0.06	0.11	0.13	0.10	0.14	0.11	-0.13	0.30	0.12	0.14	0.13	0.36	1																			
Hg	0.02	0.03	0.09	0.01	0.04	-0.01	0.04	-0.03	0.07	-0.03	0.03	0.03	0.01	-0.04	0.00	1																		
In	0.74	0.61	-0.55	0.74	0.74	0.55	0.72	0.57	-0.35	0.26	0.74	0.71	0.68	0.09	0.13	0.02	1																	
Re	0.12	0.06	-0.10	0.10	0.14	0.12	0.11	0.11	-0.02	0.16	0.14	0.11	0.11	-0.03	-0.02	0.09	0.09	1																
Sb	-0.36	-0.27	0.61	-0.39	-0.36	-0.38	-0.36	-0.39	0.48	-0.26	-0.37	-0.36	-0.36	-0.08	-0.07	0.06	-0.56	-0.08	1															
Se	0.42	0.11	-0.20	0.46	0.41	0.50	0.47	0.47	-0.27	0.30	0.45	0.51	0.53	0.75	0.39	0.01	0.21	0.00	-0.14	1														
Te	-0.03	0.11	-0.03	-0.01	-0.02	0.19	0.01	0.25	-0.17	0.08	-0.01	0.02	0.01	0.11	0.20	-0.04	0.03	-0.03	-0.10	0.19	1													
Tl	-0.01	0.08	-0.14	-0.03	-0.01	0.04	-0.01	0.05	0.10	0.16	-0.02	-0.02	-0.02	-0.09	-0.04	0.10	0.04	0.15	-0.03	-0.01	0.06	1												
Ag	-0.09	-0.10	-0.03	-0.11	-0.07	-0.05	-0.10	-0.08	0.31	0.16	-0.04	-0.07	-0.07	0.00	0.20	0.19	-0.06	0.22	0.17	0.25	0.02	0.36	1											
Cd	-0.14	-0.11	0.10	-0.15	-0.13	-0.18	-0.17	-0.18	0.48	0.12	-0.11	-0.16	-0.17	-0.05	0.07	-0.01	-0.10	0.16	0.36	-0.03	-0.06	0.17	0.44	1										
Co	-0.66	-0.50	0.37	-0.69	-0.65	-0.70	-0.68	-0.70	0.86	-0.22	-0.66	-0.70	-0.71	-0.27	-0.07	0.00	-0.53	-0.09	0.54	-0.37	-0.17	0.03	0.18	0.40	1									
Cu	-0.22	-0.39	0.20	-0.22	-0.22	-0.15	-0.19	-0.17	0.36	-0.12	-0.22	-0.18	-0.15	0.25	-0.04	-0.03	-0.39	-0.02	0.34	0.10	-0.10	-0.09	0.07	0.24	0.33	1								
Li	-0.34	-0.33	-0.04	-0.37	-0.35	-0.35	-0.39	-0.35	0.26	-0.30	-0.35	-0.40	-0.41	-0.34	-0.23	0.06	-0.18	-0.06	-0.07	-0.34	-0.22	-0.11	0.08	0.03	0.41	-0.02	1							
Mo	0.30	0.22	-0.16	0.30	0.33	0.27	0.29	0.28	-0.19	0.17	0.33	0.29	0.29	0.04	0.02	0.11	0.23	0.93	-0.16	0.07	-0.02	0.12	0.17	0.09	-0.24	-0.08	-0.09	1						
Ni	-0.72	-0.52	0.28	-0.70	-0.72	-0.34	-0.69	-0.32	0.19	-0.28	-0.71	-0.68	-0.66	-0.22	-0.15	-0.06	-0.70	-0.12	0.26	-0.26	0.26	0.00	0.03	-0.02	0.43	0.20	0.30	-0.25	1					
Pb	0.05	0.11	-0.11	0.04	0.05	0.08	0.04	0.11	-0.01	0.10	0.04	0.04	0.04	0.01	0.17	-0.04	0.14	-0.01	-0.09	0.06	0.18	0.22	0.11	-0.03	-0.05	-0.08	0.06	0.00	-0.04	1				
Sc	-0.77	-0.59	0.42	-0.78	-0.76	-0.80	-0.77	-0.80	0.80	-0.30	-0.76	-0.78	-0.78	-0.35	-0.17	0.04	-0.61	-0.13	0.54	-0.42	-0.20	-0.02	0.14	0.31	0.88	0.35	0.37	-0.29	0.45	-0.11	1			
Zn	0.56	0.49	-0.21	0.52	0.57	0.33	0.51	0.35	-0.02	0.03	0.54	0.49	0.44	0.07	-0.02	0.05	0.55	0.01	-0.08	-0.08	-0.15	-0.01	-0.23	0.10	-0.04	-0.10	-0.06	0.16	-0.52	0.02	-0.22	1		
Au	0.36	0.09	-0.20	0.39	0.36	0.43	0.42	0.40	-0.29	0.38	0.37	0.44	0.46	0.77	0.67	0.00	0.19	-0.02	-0.14	0.88	0.22	-0.03	0.22	-0.06	-0.35	0.06	-0.35	0.04	-0.24	0.14	-0.41	-0.11	1	
CO_2	0.01	0.01	-0.30	0.04	0.02	0.08	0.02	0.11	-0.12	0.29	0.02	0.02	0.03	-0.08	0.25	-0.12	0.32	0.08	-0.48	0.08	0.31	0.17	0.09	-0.01	-0.21	-0.22	-0.06	0.05	-0.09	0.23	-0.23	-0.12	0.14	1

Table F.1.2. Calculated mass changes for gabbro samples

Sample ID	16SJP006	16SJP007	16SJP008	183076	I951385	195947	150428
Hole ID	-	-	-	AE-16-03	AE-16-09	AE-16-12	AE-16-14
Depth	-	-	-	45.16	33.2	6.25	60.28
Alteration	Distal	Distal	Distal	Distal	Distal	Distal	Distal
SiO_2	-5.92	-2.00	6.98	2.09	-7.99	-4.44	-6.22
Al_2O_3	0.00	0.00	0.00	0.00	0.00	0.00	0.00
Fe_2O_3	-2.20	-0.60	2.26	-1.00	-2.55	-2.49	-2.23
CaO	0.59	1.80	0.00	0.95	-1.95	3.08	2.61
MgO	1.93	2.07	0.96	2.82	2.74	2.73	2.42
Na_2O	-0.80	-0.82	0.46	-0.14	-1.57	-0.85	-1.78
K_2O	-0.59	-0.57	-0.47	-0.36	0.56	-0.22	-0.51
Cr_2O_3	0.00	0.01	0.00	0.02	0.02	0.03	0.02
TiO_2	-0.76	-0.54	1.04	-0.84	-0.90	-0.86	-0.77
MnO	-0.06	-0.07	0.01	-0.05	-0.12	-0.07	-0.08
P_2O_5	-0.14	-0.17	0.18	-0.18	-0.18	-0.20	-0.21
SrO	-0.01	-0.02	-0.03	-0.03	-0.04	-0.03	-0.02
BaO	-0.02	-0.02	-0.01	-0.01	-0.01	-0.01	-0.02
LOI	-0.23	0.81	4.19	5.52	4.34	7.26	2.21
C	-0.25	0.03	0.98	1.11	0.72	1.53	0.27
S	-0.04	-0.04	0.16	0.01	-0.03	-0.03	-0.03
Ba	-146.71	-144.50	-108.31	-86.98	-93.83	-103.82	-141.59
Ce	-18.61	-20.30	19.71	-24.48	-21.55	-27.01	-26.64
Cr	22.68	85.00	0.81	125.99	201.04	236.69	226.78
Cs	-0.55	-0.59	-0.46	-0.40	-0.24	-0.47	-0.57
Dy	-3.35	-3.35	2.83	-3.57	-3.91	-4.21	-4.59
Er	-1.63	-1.45	1.89	-1.64	-1.86	-2.13	-2.07
Eu	-0.96	-0.92	0.74	-1.04	-1.30	-1.14	-1.22
Ga	-7.72	-6.40	-1.88	-7.68	-7.91	-7.09	-7.26
Gd	-3.75	-3.95	2.70	-4.00	-4.34	-4.90	-4.72
Ge	-0.19	0.00	0.40	0.23	-0.16	0.13	-0.09
Hf	-2.67	-2.80	3.23	-3.61	-3.45	-4.26	-4.01
Ho	-0.55	-0.48	0.75	-0.58	-0.68	-0.77	-0.73
La	-7.73	-8.50	6.63	-9.96	-9.15	-11.13	-10.78
Lu	-0.19	-0.20	0.19	-0.21	-0.25	-0.32	-0.28
Nb	-4.83	-5.60	6.55	-6.40	-6.08	-7.45	-7.46
Nd	-12.09	-13.80	13.21	-15.82	-15.35	-17.69	-17.62
Pr	-2.97	-3.18	2.35	-3.79	-3.38	-3.98	-3.96
Rb	-8.64	-8.30	-6.55	-4.30	10.85	-2.16	-7.27
Sm	-3.13	-2.97	3.59	-3.87	-4.08	-4.59	-4.27
Sn	-1.08	-1.00	0.32	-0.91	-0.13	-0.95	-0.07
Sr	-186.96	-238.00	-321.86	-296.20	-421.90	-329.46	-240.62
Ta	-0.35	-0.50	0.51	-0.45	-0.44	-0.58	-0.52
Tb	-0.47	-0.46	0.63	-0.62	-0.65	-0.69	-0.70
Th	-0.65	-0.65	0.48	-0.50	-0.71	-0.87	-0.82
Tm	-0.18	-0.19	0.20	-0.22	-0.25	-0.30	-0.28
U	-0.27	-0.29	0.20	-0.27	-0.26	-0.35	-0.33
V	-82.81	13.00	-55.44	-45.02	-61.45	-60.49	-37.01
W	-0.08	0.00	0.16	0.09	0.87	0.05	-0.52
Y	-17.00	-17.00	13.75	-19.18	-20.18	-22.76	-21.72
Yb	-1.28	-1.06	2.13	-1.43	-1.68	-1.94	-1.95
Zr	-118.55	-124.00	129.46	-149.01	-134.66	-164.85	-152.93
As	0.18	24.50	18.13	3.50	-2.48	-1.60	-1.67
Bi	0.02	0.01	0.01	0.01	0.00	0.00	0.00
Hg	0.01	0.01	0.00	0.00	0.00	0.00	0.00
In	-0.03	-0.03	0.04	0.02	-0.01	0.00	-0.02
Re	0.00	0.00	0.00	0.00	0.00	0.00	0.00
Sb	-0.15	-0.24	-0.51	-0.23	-0.52	-0.39	-0.20
Se	0.08	0.00	0.25	0.23	-0.01	0.01	0.09
Te	0.00	0.00	0.00	0.01	0.00	0.01	0.00
Tl	0.00	0.00	0.00	0.00	0.00	0.00	0.00
Ag	-0.02	0.00	0.04	0.02	-0.02	0.01	-0.01
Cd	-0.02	0.00	0.04	0.02	-0.02	0.01	0.23
Co	2.98	8.00	0.67	10.66	8.21	11.14	8.53
Cu	18.29	-12.00	-1.62	53.68	31.13	-16.54	3.94
Li	13.45	5.00	6.61	5.92	23.10	5.51	14.31
Mo	-1.08	-1.00	0.32	-1.45	-1.06	-1.47	-1.52
Ni	31.14	33.00	-2.42	61.40	59.75	64.25	52.05
Pb	-0.08	0.00	0.16	0.09	0.87	0.05	-0.03
Sc	-6.01	7.00	3.67	4.93	-0.97	5.73	6.70
Zn	-24.19	-15.00	6.49	-6.31	-23.08	-32.85	-38.12
Au	0.00	0.00	0.00	0.00	0.00	0.00	0.00
C	-0.26	0.01	0.97	0.94	0.62	1.39	0.19
CO_2	-0.95	0.00	3.49	3.41	-1.41	5.02	0.62

Table F.1.2. Calculated mass changes for gabbro samples

Sample ID	183063	183064	183067	183068	183069	I951452	294861
Hole ID	AE-16-17	AE-16-17	AE-16-17	AE-16-17	AE-16-17	AE-16-21	AE-16-26
Depth	101.39	110.35	130.74	140.3	149	41.15	21.5
Alteration	Distal	Distal	Distal	Distal	Distal	Distal	Distal
SiO_2	4.68	2.99	9.32	1.35	1.86	-0.37	-2.70
Al_2O_3	0.00	0.00	0.00	0.00	0.00	0.00	0.00
Fe_2O_3	-1.15	-1.85	8.05	-0.36	-1.91	-1.70	-2.78
CaO	3.02	2.71	2.86	2.90	1.57	1.34	0.12
MgO	3.23	3.01	2.47	2.64	2.77	2.97	2.33
Na_2O	-1.18	-0.24	-0.20	-1.06	-0.45	0.03	-0.42
K_2O	0.96	-0.47	-0.41	-0.42	-0.30	-0.51	-0.37
Cr_2O_3	0.02	0.02	0.00	0.02	0.02	0.02	0.02
TiO_2	-0.89	-0.92	1.46	-0.77	-1.05	-1.09	-0.82
MnO	-0.05	-0.07	0.04	-0.04	-0.05	-0.06	-0.09
P_2O_5	-0.19	-0.20	-0.15	-0.19	-0.22	-0.20	-0.16
SrO	-0.04	-0.04	-0.02	-0.03	-0.02	-0.04	-0.04
BaO	-0.01	-0.01	-0.01	-0.01	-0.01	-0.01	-0.01
LOI	13.97	8.35	-0.45	0.19	-0.99	4.68	3.91
C	3.84	1.83	-0.20	-0.12	-0.36	0.97	0.65
S	-0.03	-0.03	0.10	-0.03	-0.03	-0.02	-0.03
Ba	-75.01	-140.00	-59.33	-127.27	-94.96	-136.59	-117.47
Ce	-23.99	-26.43	-19.36	-26.59	-27.74	-25.95	-21.73
Cr	156.85	144.81	7.35	109.43	115.39	143.63	202.32
Cs	-0.32	-0.54	-0.04	-0.57	-0.52	-0.55	-0.56
Dy	-3.55	-4.20	-2.54	-4.03	-4.43	-3.94	-3.76
Er	-1.56	-1.76	-1.09	-1.74	-1.77	-1.93	-2.22
Eu	-1.03	-1.25	-0.76	-1.22	-1.35	-1.41	-1.03
Ga	-4.76	-5.63	1.99	-3.64	-6.04	-7.86	-6.15
Gd	-4.25	-4.75	-2.41	-4.15	-5.11	-4.68	-4.57
Ge	0.61	0.38	0.59	0.10	0.01	0.15	2.44
Hf	-3.49	-3.76	-2.78	-3.88	-3.69	-4.02	-3.15
Ho	-0.59	-0.68	-0.35	-0.66	-0.76	-0.69	-0.61
La	-9.71	-10.50	-8.05	-10.17	-11.18	-10.52	-9.03
Lu	-0.24	-0.21	-0.10	-0.22	-0.25	-0.25	-0.24
Nb	-6.48	-7.21	-4.08	-7.21	-7.68	-7.37	-5.91
Nd	-15.62	-17.66	-12.54	-17.84	-18.66	-18.18	-15.62
Pr	-3.61	-3.91	-2.89	-3.97	-4.14	-3.88	-3.40
Rb	12.69	-6.45	-5.39	-7.23	-5.19	-7.72	-4.76
Sm	-3.96	-4.03	-2.71	-4.06	-4.18	-4.44	-4.06
Sn	-0.76	-0.85	-0.76	-0.96	-1.00	-0.94	-0.03
Sr	-369.43	-338.09	-288.88	-344.34	-261.01	-373.72	-400.66
Ta	-0.50	-0.54	-0.26	-0.48	-0.60	-0.58	-0.41
Tb	-0.54	-0.62	-0.36	-0.64	-0.70	-0.66	-0.63
Th	-0.59	-0.75	-0.46	-0.69	-0.75	-0.70	-0.69
Tm	-0.24	-0.27	-0.13	-0.22	-0.25	-0.25	-0.23
U	-0.21	-0.26	-0.15	-0.34	-0.28	-0.25	-0.23
V	-30.16	-21.68	539.37	17.01	-42.11	-57.84	-62.31
W	5.22	0.15	0.24	0.04	0.00	0.06	-0.01
Y	-17.45	-19.97	-11.72	-20.46	-22.04	-20.87	-20.28
Yb	-1.33	-1.65	-0.66	-1.51	-1.61	-1.60	-1.75
Zr	-140.11	-159.47	-109.21	-166.13	-161.58	-165.66	-142.92
As	-3.08	-2.89	33.23	100.85	58.10	0.76	-1.43
Bi	0.01	0.02	0.00	0.00	0.00	0.01	0.00
Hg	0.00	0.00	0.00	0.00	0.00	0.00	0.00
In	0.01	0.02	-0.02	-0.03	-0.03	0.00	0.00
Re	0.00	0.00	0.00	0.00	0.00	0.00	0.00
Sb	-0.48	-0.52	0.46	-0.20	-0.19	-0.14	-0.34
Se	0.02	0.02	0.27	0.11	0.10	0.11	0.10
Te	0.01	0.00	0.01	0.01	0.01	0.01	0.00
Tl	0.01	0.00	0.00	0.00	0.00	0.00	0.01
Ag	0.06	0.04	0.06	0.01	0.00	0.02	0.24
Cd	0.06	0.04	0.86	0.01	0.25	0.02	0.24
Co	9.33	8.49	41.10	12.77	6.13	10.53	4.52
Cu	68.62	51.21	185.20	27.05	63.29	88.66	-20.08
Li	19.90	18.05	1.18	15.81	15.06	16.23	24.62
Mo	-0.76	-1.42	-0.76	-0.96	-1.50	-1.47	-1.01
Ni	82.90	67.30	45.17	57.34	58.20	71.32	49.32
Pb	5.22	1.30	0.24	0.04	0.00	0.06	0.97
Sc	6.10	6.88	21.87	6.41	1.10	5.03	-0.38
Zn	-15.83	-30.01	65.03	-21.02	-14.73	-6.70	-50.61
Au	0.02	0.01	0.00	0.00	0.00	0.00	0.00
C	3.63	1.65	-0.25	-0.17	-0.37	0.84	0.58
CO_2	13.32	5.99	-1.01	-0.67	-1.30	-1.39	2.05

Table F.1.2. Calculated mass changes for gabbro samples

Sample ID	294866	294854	294859	I951391	I951369	I951377	I951481
Hole ID	AE-16-26	AE-16-27	AE-16-27	AE-16-32	AE-16-34	AE-16-34	AE-16-35
Depth	85.15	33.35	90.95	55	11.2	48.05	63.4
Alteration	Distal	Distal	Distal	Distal	Distal	Distal	Distal
SiO_2	4.92	-1.87	-2.34	-6.46	-5.70	4.35	3.30
Al_2O_3	0.00	0.00	0.00	0.00	0.00	0.00	0.00
Fe_2O_3	8.96	-0.99	-1.86	-2.84	-2.70	7.36	-1.92
CaO	4.45	1.85	2.37	0.71	2.03	-0.54	1.87
MgO	1.72	3.66	2.58	2.35	2.79	2.06	2.80
Na_2O	0.16	-1.31	-1.17	-0.72	-1.93	-0.19	-0.66
K_2O	-0.57	-0.43	0.02	-0.40	-0.23	-0.48	-0.48
Cr_2O_3	0.00	0.02	0.02	0.03	0.03	0.00	0.02
TiO_2	1.57	-0.57	-0.63	-0.87	-0.88	1.64	-0.95
MnO	0.03	-0.04	-0.07	-0.09	-0.11	0.01	-0.07
P_2O_5	-0.10	-0.15	-0.18	-0.18	-0.18	0.03	-0.18
SrO	-0.03	-0.04	-0.04	-0.03	-0.03	-0.05	-0.04
BaO	-0.01	-0.01	-0.01	-0.01	-0.02	-0.01	-0.01
LOI	9.35	4.24	5.84	1.96	3.99	3.88	5.17
C	2.36	0.60	1.13	0.27	0.65	0.80	1.00
S	-0.01	-0.02	-0.02	-0.03	-0.03	-0.02	-0.03
Ba	-126.34	-127.16	-29.02	-124.76	-125.40	-123.65	-121.62
Ce	-15.62	-16.09	-21.27	-21.84	-24.80	-0.48	-21.36
Cr	8.08	213.46	212.73	243.00	215.00	6.88	127.38
Cs	-0.49	-0.50	-0.30	-0.55	-0.31	-0.42	-0.50
Dy	-2.16	-3.34	-3.74	-4.04	-4.00	0.20	-3.66
Er	-0.82	-1.62	-1.92	-1.81	-2.14	0.18	-1.71
Eu	-0.71	-0.88	-1.26	-1.16	-1.19	0.10	-1.15
Ga	2.19	-7.60	-6.52	-7.68	-5.70	2.11	-10.24
Gd	-2.53	-2.99	-3.78	-4.43	-4.55	-0.08	-4.33
Ge	4.04	2.70	2.68	-0.12	0.00	0.47	0.26
Hf	-2.26	-3.25	-3.47	-3.19	-4.20	-0.09	-3.57
Ho	-0.34	-0.49	-0.64	-0.67	-0.70	0.15	-0.63
La	-6.50	-6.21	-8.54	-9.17	-10.20	-1.10	-8.54
Lu	-0.10	-0.18	-0.23	-0.21	-0.33	0.02	-0.20
Nb	-3.97	-5.13	-6.09	-5.73	-6.90	1.81	-6.54
Nd	-10.98	-10.66	-14.26	-15.13	-16.50	-0.23	-15.86
Pr	-2.51	-2.58	-3.19	-3.38	-3.93	-0.18	-3.32
Rb	-8.05	-6.40	2.72	-5.76	-3.00	-6.96	-6.34
Sm	-2.39	-2.87	-3.99	-3.98	-3.88	-0.06	-3.89
Sn	-0.69	0.08	0.07	-0.09	0.00	2.75	-0.90
Sr	-363.30	-380.75	-348.20	-310.46	-283.00	-437.35	-364.46
Ta	-0.22	-0.48	-0.48	-0.43	-0.50	0.07	-0.45
Tb	-0.30	-0.42	-0.61	-0.64	-0.68	0.07	-0.60
Th	-0.44	-0.71	-0.78	-0.69	-0.87	-0.24	-0.54
Tm	-0.08	-0.30	-0.26	-0.25	-0.24	0.07	-0.22
U	-0.18	-0.26	-0.26	-0.24	-0.40	-0.04	-0.20
V	733.95	-26.68	-36.99	-59.55	-43.00	342.57	-24.44
W	1.62	0.04	0.04	-0.05	0.00	0.19	0.10
Y	-7.70	-14.22	-18.56	-19.88	-23.20	-0.29	-18.05
Yb	-0.47	-1.63	-1.66	-1.68	-1.81	0.19	-1.53
Zr	-106.26	-129.72	-139.59	-125.08	-156.00	7.31	-144.17
As	-0.43	-0.89	-1.63	-0.74	0.50	-0.97	-1.82
Bi	0.00	0.00	0.00	-0.01	-0.01	0.00	0.01
Hg	0.00	0.00	0.00	0.00	0.00	0.00	0.00
In	0.05	0.00	0.00	-0.02	-0.01	0.05	0.01
Re	0.00	0.00	0.00	0.00	0.00	0.00	0.00
Sb	-0.29	-0.11	-0.30	-0.28	-0.19	-0.35	-0.43
Se	0.16	0.11	0.11	0.00	0.00	0.02	0.12
Te	0.01	0.01	0.01	0.00	0.01	0.01	0.01
Tl	0.02	0.01	0.01	0.00	0.00	0.00	0.00
Ag	0.40	0.27	0.27	-0.01	0.00	0.05	0.03
Cd	0.40	0.27	0.27	-0.01	0.00	0.05	0.30
Co	40.25	11.73	6.40	4.20	11.00	26.39	6.72
Cu	86.49	-18.72	36.21	-7.88	-20.00	22.70	49.02
Li	21.16	15.81	5.37	14.08	15.00	18.75	6.03
Mo	-0.69	-0.96	-0.96	-1.52	-1.50	-1.41	-0.90
Ni	37.55	75.02	44.69	49.46	68.00	17.19	60.99
Pb	1.62	1.08	1.07	-0.05	0.00	0.19	0.10
Sc	14.47	3.29	4.21	3.38	2.00	12.76	3.10
Zn	2.72	-45.99	-28.54	-34.09	-53.00	33.84	-26.29
Au	0.00	0.00	0.00	0.00	0.00	0.00	0.00
C	2.16	0.51	1.04	0.20	0.55	0.70	0.87
CO_2	7.92	1.83	3.79	0.22	2.00	-0.91	6.66

Table F.1.2. Calculated mass changes for gabbro samples

Sample ID	I951461	294847	294839	294844	294831	183073	183074
Hole ID	AE-16-39	AE-16-43	AE-16-44	AE-16-44	AE-17-50	AE-16-03	AE-16-03
Depth	98	81.65	63.25	107.2	101.6	21.36	25.55
Alteration	Distal	Distal	Distal	Distal	Distal	Intermediate	Intermediate
SiO_2	-12.32	-11.03	-7.18	3.81	8.28	-7.98	-0.34
Al_2O_3	0.00	0.00	0.00	0.00	0.00	0.00	0.00
Fe_2O_3	-2.98	-2.79	-3.01	-1.83	3.55	-6.10	-5.18
CaO	-3.32	-2.22	2.18	4.25	3.77	-3.15	-0.29
MgO	2.40	2.07	2.55	2.54	3.34	3.75	2.91
Na_2O	-1.05	0.14	-1.27	-2.04	-1.73	-3.48	-2.69
K_2O	0.44	-0.36	0.18	-0.58	-0.12	2.44	2.40
Cr_2O_3	0.02	0.02	0.03	0.02	0.00	0.05	0.03
TiO_2	-0.89	-0.78	-0.97	-0.76	0.77	-1.85	-1.56
MnO	-0.10	-0.11	-0.08	-0.06	0.00	-0.15	-0.09
P_2O_5	-0.18	-0.16	-0.11	-0.16	-0.09	-0.31	-0.22
SrO	-0.05	-0.04	-0.03	-0.01	-0.04	-0.05	-0.04
BaO	-0.01	-0.01	-0.01	-0.01	-0.01	0.01	0.01
LOI	1.82	3.12	5.80	2.55	8.95	6.31	9.36
C	0.17	0.48	1.16	0.36	1.95	1.29	2.39
S	0.04	-0.03	-0.03	-0.03	-0.03	-0.03	-0.03
Ba	-79.85	-125.52	-56.82	-136.90	-109.38	67.03	62.74
Ce	-23.19	-21.43	-10.99	-20.25	-8.53	-20.25	-24.70
Cr	187.70	198.13	221.35	198.10	20.00	344.42	215.68
Cs	-0.51	-0.57	-0.31	-0.47	-0.02	-0.12	-0.15
Dy	-4.17	-3.69	-3.98	-3.52	-1.51	-5.47	-4.38
Er	-1.98	-1.84	-2.14	-1.77	-0.52	-2.56	-2.17
Eu	-1.25	-1.18	-0.96	-1.16	-0.13	-1.69	-1.34
Ga	-9.21	-5.22	-7.30	-2.71	0.07	-10.12	-11.51
Gd	-4.34	-4.21	-3.81	-3.92	-1.86	-5.81	-5.17
Ge	-0.41	1.92	2.42	2.84	3.75	-0.26	0.13
Hf	-3.58	-3.57	-3.16	-3.14	-1.48	-4.41	-4.16
Ho	-0.72	-0.64	-0.77	-0.62	-0.15	-0.97	-0.70
La	-9.67	-8.82	-3.84	-8.32	-3.80	-6.53	-8.82
Lu	-0.28	-0.28	-0.23	-0.13	-0.15	-0.31	-0.26
Nb	-6.32	-5.78	-5.45	-5.51	-2.20	-8.07	-9.24
Nd	-16.30	-14.90	-10.85	-13.49	-5.43	-19.13	-18.53
Pr	-3.56	-3.30	-2.23	-3.12	-1.44	-3.79	-4.08
Rb	6.48	-4.95	4.38	-8.24	1.53	41.70	35.88
Sm	-4.20	-3.73	-3.69	-3.69	-1.56	-5.19	-4.95
Sn	-0.32	-1.12	-1.02	1.21	1.75	-1.10	-0.95
Sr	-457.41	-439.94	-314.10	-141.48	-291.75	-466.31	-345.22
Ta	-0.41	-0.56	-0.51	-0.47	-0.38	-0.55	-0.58
Tb	-0.61	-0.63	-0.63	-0.53	-0.24	-0.88	-0.73
Th	-0.82	-0.77	0.48	-0.72	0.16	1.86	0.63
Tm	-0.26	-0.26	-0.29	-0.24	-0.13	-0.35	-0.30
U	-0.31	-0.29	-0.06	-0.25	-0.19	0.79	0.72
V	-59.27	-64.64	-71.98	-22.90	253.50	-232.09	-184.49
W	-0.16	3.42	-0.02	0.07	0.25	2.58	0.05
Y	-20.48	-19.23	-21.14	-17.62	-7.85	-27.94	-21.40
Yb	-1.78	-1.70	-1.84	-1.62	-0.57	-2.12	-1.54
Zr	-139.51	-138.32	-132.57	-129.52	-72.00	-181.80	-168.00
As	40.79	-2.55	-0.35	1.75	-0.95	-2.89	-3.07
Bi	0.01	0.00	0.00	0.00	0.00	0.00	0.02
Hg	0.00	0.00	0.00	0.00	0.00	0.00	0.00
In	-0.01	0.01	-0.01	-0.02	0.03	-0.04	-0.01
Re	0.00	0.00	0.00	0.00	0.00	0.00	0.00
Sb	-0.52	-0.47	-0.27	0.07	-0.28	-0.50	-0.49
Se	0.40	0.08	0.20	0.11	0.15	0.08	0.11
Te	0.00	0.00	0.00	0.01	0.01	0.03	0.01
Tl	0.00	0.01	0.01	0.01	0.02	0.01	0.01
Ag	-0.04	0.19	0.24	0.28	0.38	-0.03	0.01
Cd	-0.04	0.19	0.24	0.28	0.38	-0.03	0.01
Co	6.38	3.21	2.43	7.62	20.75	-5.23	0.63
Cu	-3.38	-1.27	20.25	-0.34	-17.25	-14.35	19.19
Li	20.14	12.66	14.68	5.69	32.50	21.88	5.51
Mo	-1.16	-1.12	-1.02	-0.93	-0.75	-1.55	-1.47
Ni	53.97	49.99	87.54	49.38	40.75	153.79	105.24
Pb	-0.16	0.77	0.97	1.14	1.50	0.79	3.20
Sc	-6.54	-5.27	-3.43	3.14	15.00	-12.98	-7.93
Zn	-21.76	-42.36	-36.98	-32.79	-8.00	-47.83	-16.03
Au	0.00	0.00	0.00	0.00	0.00	0.00	0.02
C	0.10	0.41	0.99	0.28	1.60	1.17	2.16
CO_2	-0.83	1.50	3.62	1.07	5.88	4.23	7.96

Table F.1.2. Calculated mass changes for gabbro samples

Sample ID	183084	183085	183087	183088	183079	183080	150416
Hole ID	AE-16-04	AE-16-04	AE-16-04	AE-16-04	AE-16-06	AE-16-06	AE-16-12
Depth	6.11	13.6	26.15	33	12.2	20.9	39.9
Alteration	Intermediate	Intermediate	Intermediate	Intermediate	Intermediate	Intermediate	Intermediate
SiO_2	-5.14	-0.73	-6.25	-1.36	-0.44	4.36	2.72
Al_2O_3	0.00	0.00	0.00	0.00	0.00	0.00	0.00
Fe_2O_3	-2.61	-2.83	-3.45	-0.45	2.20	5.94	2.38
CaO	2.64	1.95	2.25	4.18	-3.03	3.99	-0.13
MgO	2.72	1.96	0.75	1.65	-0.83	1.78	-0.42
Na_2O	-2.19	-1.94	-0.51	-0.96	0.38	-1.59	0.89
K_2O	1.34	1.95	1.17	-0.42	-0.29	-0.41	-0.33
Cr_2O_3	0.03	0.03	0.01	0.00	0.00	0.00	0.00
TiO_2	-0.91	-0.91	-0.84	-0.25	-0.40	1.47	1.15
MnO	-0.06	-0.08	-0.07	-0.03	-0.03	0.05	0.07
P_2O_5	-0.21	-0.20	-0.20	-0.11	0.79	0.00	0.19
SrO	-0.04	-0.04	-0.03	-0.03	-0.04	-0.01	-0.04
BaO	-0.01	-0.01	-0.01	-0.01	-0.01	0.00	-0.01
LOI	11.01	11.16	11.67	8.70	2.58	0.58	6.72
C	2.76	3.07	3.40	2.00	0.52	-0.21	2.08
S	-0.03	-0.03	-0.03	-0.03	-0.03	0.44	0.06
Ba	-46.90	-30.99	-52.06	-117.68	-130.47	73.82	-103.84
Ce	-26.45	-24.86	-24.86	-15.83	44.50	-3.06	8.88
Cr	211.03	203.87	47.90	28.94	5.03	6.70	6.44
Cs	-0.17	-0.02	-0.03	-0.40	-0.48	1.54	-0.54
Dy	-4.48	-4.23	-4.35	-2.52	5.16	-0.80	1.06
Er	-2.10	-1.90	-2.22	-1.29	3.28	0.01	1.11
Eu	-1.32	-1.25	-1.21	-0.62	1.91	-0.05	0.56
Ga	-6.90	-7.66	-5.91	-4.87	3.49	2.28	0.85
Gd	-4.49	-4.63	-4.51	-2.81	6.92	-0.86	1.16
Ge	0.20	0.25	0.15	0.33	0.01	0.42	0.36
Hf	-4.08	-3.80	-3.82	-2.35	4.04	-0.32	0.56
Ho	-0.75	-0.69	-0.72	-0.44	1.07	0.02	0.39
La	-10.70	-10.12	-10.02	-6.81	16.11	-1.95	2.82
Lu	-0.28	-0.23	-0.28	-0.15	0.29	-0.02	0.13
Nb	-7.14	-6.57	-7.08	-3.84	14.09	0.27	8.41
Nd	-18.15	-16.47	-16.75	-10.80	27.99	-2.12	6.36
Pr	-4.03	-3.68	-3.84	-2.49	5.99	-0.84	1.17
Rb	19.09	30.47	18.20	-6.16	-4.38	-3.84	-4.75
Sm	-4.77	-4.03	-4.56	-2.97	6.93	-0.18	1.30
Sn	-0.92	0.20	-0.94	-0.87	1.01	0.34	0.29
Sr	-388.70	-388.27	-338.41	-265.92	-406.48	-156.23	-358.66
Ta	-0.46	-0.45	-0.58	-0.32	0.91	-0.06	0.49
Tb	-0.71	-0.66	-0.69	-0.38	0.99	-0.07	0.23
Th	-0.83	-0.75	-0.77	-0.54	0.87	-0.22	0.00
Tm	-0.27	-0.29	-0.30	-0.16	0.40	0.02	0.15
U	-0.33	-0.36	-0.33	-0.20	0.34	-0.06	0.06
V	-72.73	-62.87	-16.41	15.89	-241.75	298.66	-78.78
W	0.08	0.10	9.58	0.13	5.02	0.17	0.14
Y	-22.77	-21.76	-22.00	-13.25	23.11	-3.96	5.83
Yb	-1.98	-1.76	-1.64	-1.13	2.44	0.09	0.73
Zr	-159.14	-143.60	-145.99	-89.48	225.67	0.45	60.32
As	-2.62	-2.05	-2.11	-1.55	24.49	54.67	0.42
Bi	0.00	0.00	0.00	0.00	0.00	0.00	0.01
Hg	0.00	0.00	0.00	0.00	0.00	0.00	0.00
In	-0.01	-0.01	0.00	0.02	0.06	-0.02	0.07
Re	0.00	0.00	0.00	0.00	0.00	0.00	0.00
Sb	-0.50	-0.45	-0.45	-0.40	-0.48	0.31	-0.45
Se	0.01	0.01	0.01	0.01	0.00	0.48	0.36
Te	0.01	0.01	0.01	0.00	0.02	0.01	0.01
Tl	0.01	0.01	0.01	0.00	0.00	0.00	0.00
Ag	0.02	0.02	0.01	0.03	0.00	0.04	0.04
Cd	0.02	0.02	0.01	0.32	0.00	0.45	0.04
Co	10.21	5.48	-1.26	7.73	-7.92	24.32	1.32
Cu	-4.40	-16.11	11.03	36.23	-17.97	30.15	1.45
Li	27.40	5.99	5.58	28.94	15.06	6.70	17.88
Mo	-1.46	-1.45	-1.47	-1.43	0.01	-0.83	0.29
Ni	63.97	49.77	20.28	28.68	-2.50	8.70	-0.71
Pb	0.08	0.10	0.06	0.13	0.00	0.17	5.86
Sc	1.32	-0.32	-0.38	6.20	-19.97	13.28	-8.27
Zn	-34.27	-46.33	-47.22	-6.36	36.43	27.17	18.68
Au	0.00	0.00	0.03	0.00	0.02	0.09	0.00
C	2.52	2.72	3.20	1.79	0.43	-0.27	1.95
CO_2	9.19	9.93	11.62	6.53	1.51	-1.03	7.08

Table F.1.2. Calculated mass changes for gabbro samples

Sample ID	150420	150421	150423	150424	150426	150431	150432
Hole ID	AE-16-14	AE-16-14	AE-16-14	AE-16-14	AE-16-14	AE-16-15	AE-16-15
Depth	6.9	16.36	26.76	34.62	43.35	3.48	9.84
Alteration	Intermediate	Intermediate	Intermediate	Intermediate	Intermediate	Intermediate	Intermediate
SiO_2	-7.08	-5.74	5.83	5.77	4.17	-6.10	-5.40
Al_2O_3	0.00	0.00	0.00	0.00	0.00	0.00	0.00
Fe_2O_3	-2.65	-2.06	0.43	0.51	2.99	-1.99	-1.59
CaO	-0.09	1.91	1.11	0.51	3.08	2.02	4.00
MgO	2.58	1.19	0.08	-0.83	0.66	1.33	1.06
Na_2O	-1.47	-0.83	1.30	0.81	1.30	-1.92	-0.25
K_2O	-0.57	0.39	-0.41	-0.13	-0.51	-0.47	-0.18
Cr_2O_3	0.02	0.01	0.00	0.00	0.00	0.00	0.01
TiO_2	-0.75	-0.55	0.56	-0.19	1.51	-0.62	-0.51
MnO	-0.09	-0.07	0.04	0.07	0.06	-0.07	-0.06
P_2O_5	-0.18	-0.15	0.38	0.44	0.19	-0.17	-0.17
SrO	-0.03	-0.04	-0.04	-0.04	-0.03	-0.01	-0.04
BaO	-0.02	-0.01	-0.01	-0.01	-0.01	-0.02	-0.01
LOI	0.43	9.11	8.50	7.23	11.98	2.45	9.56
C	-0.23	2.36	2.44	2.13	3.52	0.36	2.38
S	-0.03	-0.03	-0.03	-0.03	-0.03	-0.03	-0.03
Ba	-143.34	-96.82	-123.53	-120.85	-135.84	-136.61	-129.35
Ce	-23.03	-23.31	16.72	29.31	11.18	-25.28	-24.47
Cr	201.07	78.78	6.79	6.31	1.33	80.06	70.35
Cs	-0.54	-0.32	-0.53	-0.42	-0.56	-0.40	-0.48
Dy	-3.96	-4.04	2.39	3.00	1.00	-4.09	-4.02
Er	-1.86	-1.94	1.71	2.09	0.89	-2.04	-1.94
Eu	-1.08	-0.98	0.95	1.47	0.73	-1.04	-1.02
Ga	-8.69	-6.63	-0.34	5.31	2.42	-6.80	-5.56
Gd	-4.44	-4.06	3.71	4.67	2.09	-3.98	-4.34
Ge	-0.26	0.12	0.45	0.33	0.66	-0.14	0.19
Hf	-3.78	-3.75	1.50	2.52	0.49	-3.79	-3.76
Ho	-0.66	-0.63	0.69	0.89	0.37	-0.72	-0.70
La	-9.48	-9.58	5.95	11.18	4.10	-10.39	-10.19
Lu	-0.27	-0.26	0.14	0.24	0.10	-0.28	-0.25
Nb	-6.01	-5.69	9.23	12.79	7.82	-6.29	-6.73
Nd	-15.81	-15.33	12.02	19.29	7.18	-15.95	-15.51
Pr	-3.39	-3.52	2.12	4.06	1.19	-3.73	-3.68
Rb	-8.20	6.71	-5.92	-1.29	-7.08	-6.55	-2.21
Sm	-3.75	-4.09	3.31	5.15	1.66	-3.85	-3.88
Sn	-0.21	-0.95	2.71	0.26	3.06	-1.05	-0.92
Sr	-370.89	-371.63	-332.85	-392.07	-383.27	-211.69	-386.09
Ta	-0.46	-0.48	0.53	0.81	0.52	-0.43	-0.46
Tb	-0.63	-0.55	0.51	0.67	0.35	-0.59	-0.65
Th	-0.72	-0.80	0.24	0.49	-0.10	-0.81	-0.78
Tm	-0.27	-0.26	0.26	0.31	0.12	-0.28	-0.28
U	-0.30	-0.29	0.15	0.23	0.01	-0.30	-0.30
V	-63.65	-33.09	-89.15	-174.18	28.96	-13.73	8.22
W	-0.10	0.05	2.54	13.71	6.59	-0.53	0.08
Y	-20.42	-20.00	12.24	18.43	6.87	-19.89	-20.25
Yb	-1.68	-1.61	1.58	2.33	0.98	-1.55	-1.59
Zr	-138.79	-141.19	106.40	165.08	47.10	-141.73	-143.46
As	-0.83	-1.92	-2.05	-1.44	-2.43	-0.96	0.71
Bi	0.00	0.01	0.04	0.02	0.00	0.00	0.00
Hg	0.00	0.00	0.00	0.00	0.00	0.00	0.00
In	-0.03	0.01	0.07	0.07	0.08	-0.02	0.01
Re	0.00	0.00	0.00	0.00	0.00	0.00	0.00
Sb	-0.15	-0.50	-0.46	-0.32	-0.44	-0.24	-0.48
Se	-0.01	0.21	0.25	0.01	0.41	0.28	0.12
Te	0.00	0.01	0.02	0.00	0.00	0.00	0.01
Tl	0.00	0.00	0.00	0.00	0.00	0.00	0.00
Ag	-0.03	0.01	0.04	0.03	0.07	-0.01	0.02
Cd	-0.03	0.01	0.04	0.03	0.64	-0.01	0.02
Co	9.11	5.75	1.18	-9.24	6.22	4.80	6.83
Cu	-2.71	-14.48	-20.11	-22.61	-22.20	17.48	17.06
Li	12.92	26.42	18.57	6.31	20.31	13.90	27.29
Mo	-1.55	-1.48	-1.41	-1.43	-1.37	-1.53	-1.46
Ni	58.82	29.47	-0.64	-1.87	-1.73	31.97	27.14
Pb	-0.10	0.05	6.07	1.26	2.80	3.73	3.31
Sc	-2.23	2.47	-6.43	-14.16	-0.90	2.13	4.44
Zn	-32.60	-48.78	-17.85	-9.75	-0.57	-28.06	-25.88
Au	0.00	0.00	0.00	0.10	0.05	0.00	0.00
C	-0.26	2.22	2.24	1.91	3.35	0.27	2.19
CO_2	-0.96	8.14	8.17	6.99	12.17	0.96	7.97

Table F.1.2. Calculated mass changes for gabbro samples

Sample ID	150441	150443	150444	183066	183093	I951454	294864
Hole ID	AE-16-17	AE-16-17	AE-16-17	AE-16-17	AE-16-20	AE-16-21	AE-16-26
Depth	9.91	22.85	37.67	121.8	5.7	105.9	73.55
Alteration	Intermediate	Intermediate	Intermediate	Intermediate	Intermediate	Intermediate	Intermediate
SiO_2	-7.04	-6.74	-0.79	6.46	-10.33	-8.96	4.98
Al_2O_3	0.00	0.00	0.00	0.00	0.00	0.00	0.00
Fe_2O_3	-3.39	-2.81	0.17	-1.79	-2.72	-2.02	4.85
CaO	1.93	2.36	1.33	1.87	-2.64	2.58	2.60
MgO	1.82	0.97	3.24	2.68	0.88	1.20	2.85
Na_2O	-1.45	-1.07	-0.77	0.14	-0.31	-2.09	-0.44
K_2O	-0.47	-0.55	-0.53	-0.54	-0.31	0.46	-0.48
Cr_2O_3	0.02	0.00	0.00	0.02	0.00	0.02	0.00
TiO_2	-1.01	-0.76	-0.37	-0.77	-0.56	-0.62	0.45
MnO	-0.09	-0.07	-0.02	-0.06	-0.11	-0.07	0.00
P_2O_5	-0.20	-0.15	-0.11	-0.20	-0.15	-0.13	-0.17
SrO	-0.01	-0.01	-0.02	-0.04	-0.03	-0.03	-0.04
BaO	-0.02	-0.02	-0.01	-0.01	-0.01	-0.01	-0.01
LOI	1.13	-0.39	0.08	-0.96	2.28	12.35	-0.43
C	0.09	-0.23	-0.23	-0.30	0.35	3.38	-0.29
S	0.08	0.02	0.00	-0.03	-0.04	-0.02	-0.03
Ba	-144.35	-141.23	-139.74	-138.39	-86.69	-97.54	-112.67
Ce	-24.81	-21.22	-18.06	-25.84	-20.89	-18.56	-20.88
Cr	196.18	67.73	15.74	112.99	12.27	56.59	17.96
Cs	-0.47	-0.56	-0.50	-0.55	-0.50	-0.43	-0.47
Dy	-4.53	-3.40	-2.97	-3.51	-3.73	-3.57	-2.67
Er	-1.97	-1.87	-1.09	-1.55	-1.90	-1.91	-1.00
Eu	-1.23	-1.00	-0.85	-1.16	-1.22	-1.12	-1.05
Ga	-6.41	-5.16	-4.65	-5.63	-6.80	-7.32	-2.72
Gd	-4.28	-3.95	-2.85	-3.91	-4.09	-3.99	-3.73
Ge	-0.21	-0.23	0.09	0.18	-0.34	0.07	3.24
Hf	-2.25	-3.10	-2.64	-3.13	-3.39	-3.30	-3.20
Ho	-0.71	-0.61	-0.51	-0.57	-0.68	-0.62	-0.56
La	-10.11	-8.80	-7.91	-11.18	-8.52	-7.61	-8.47
Lu	-0.25	-0.22	-0.17	-0.20	-0.23	-0.22	-0.15
Nb	-6.65	-5.06	-4.23	-5.90	-5.37	-5.67	-5.86
Nd	-16.75	-14.48	-12.50	-16.42	-13.73	-13.52	-14.85
Pr	-3.74	-3.32	-2.80	-3.74	-3.24	-2.91	-3.35
Rb	-7.00	-8.01	-7.65	-8.13	-4.01	5.48	-6.92
Sm	-4.02	-3.43	-3.15	-3.78	-3.80	-3.60	-3.71
Sn	-1.09	-1.09	0.07	-0.93	-1.14	-0.97	0.30
Sr	-202.22	-182.55	-228.97	-327.72	-393.57	-320.62	-314.26
Ta	-0.45	-0.36	-0.38	-0.46	-0.40	-0.38	-0.20
Tb	-0.65	-0.56	-0.46	-0.56	-0.63	-0.57	-0.52
Th	-0.67	-0.67	-0.54	-0.54	-0.68	-0.71	-0.57
Tm	-0.25	-0.25	-0.19	-0.20	-0.28	-0.23	-0.18
U	-0.26	-0.28	-0.25	-0.15	-0.27	-0.25	-0.24
V	-79.41	-55.36	-3.82	-15.44	-56.49	-38.77	501.93
W	-0.09	-0.55	-0.48	0.07	-0.14	4.13	0.15
Y	-22.16	-19.19	-15.77	-18.18	-19.30	-18.70	-13.17
Yb	-1.72	-1.41	-1.21	-1.33	-1.47	-1.50	-1.04
Zr	-91.73	-117.45	-97.08	-138.61	-133.11	-130.84	-134.70
As	45.95	40.85	36.11	13.57	7.09	3.49	0.55
Bi	0.00	0.00	0.00	0.00	0.00	0.00	0.00
Hg	0.00	0.00	0.00	0.00	0.00	0.00	0.00
In	-0.02	-0.02	-0.03	-0.02	0.01	0.01	-0.02
Re	0.00	0.00	0.00	0.00	0.00	0.00	0.00
Sb	-0.25	-0.16	-0.21	0.02	-0.49	0.15	-0.04
Se	0.17	0.17	0.11	0.11	0.07	0.00	0.13
Te	0.01	0.00	0.00	0.01	0.00	0.00	0.01
Tl	0.00	0.00	0.00	0.00	0.00	0.00	0.01
Ag	-0.02	-0.02	0.01	0.02	-0.03	0.01	0.32
Cd	-0.02	0.20	0.01	0.02	-0.03	0.26	0.32
Co	3.58	-0.27	19.88	7.76	-0.19	3.95	25.56
Cu	30.70	17.64	16.51	14.76	-0.96	18.14	75.04
Li	4.14	4.09	5.37	5.73	12.27	5.26	6.48
Mo	-1.54	-1.55	-1.48	-1.46	-1.57	-0.97	-0.85
Ni	49.12	27.00	37.43	53.85	18.59	27.79	62.44
Pb	-0.09	-0.09	0.04	0.07	-0.14	0.03	1.30
Sc	0.18	-0.91	2.14	7.54	-4.09	0.79	17.07
Zn	-36.73	-35.27	-6.76	-25.06	-24.60	-30.25	4.19
Au	0.00	0.00	0.00	0.00	0.00	0.00	0.00
C	0.01	-0.25	-0.25	-0.35	0.26	3.18	-0.31
CO_2	0.05	-0.95	-0.98	-1.29	0.92	2.91	-1.16

Table F.1.2. Calculated mass changes for gabbro samples

Sample ID	294867	294855	294858	I951387	I951394	I951370	I951374
Hole ID	AE-16-26	AE-16-27	AE-16-27	AE-16-32	AE-16-32	AE-16-34	AE-16-34
Depth	89.85	55.5	83.45	20.05	69.8	20.85	35.1
Alteration	Intermediate	Intermediate	Intermediate	Intermediate	Intermediate	Intermediate	Intermediate
SiO_2	2.18	-6.94	-5.57	-3.34	-21.48	-6.76	3.71
Al_2O_3	0.00	0.00	0.00	0.00	0.00	0.00	0.00
Fe_2O_3	-0.85	-2.76	-0.32	-1.46	-2.97	-2.89	1.49
CaO	2.23	2.41	6.08	3.11	0.98	2.55	1.40
MgO	1.90	1.77	2.25	2.76	1.26	2.19	0.15
Na_2O	-0.26	-2.06	-1.77	-1.34	-3.86	-2.32	1.02
K_2O	0.50	-0.47	-0.55	-0.51	2.31	-0.45	-0.36
Cr_2O_3	0.01	0.02	0.00	0.01	0.02	0.02	0.00
TiO_2	-0.70	-0.79	0.05	-0.60	-0.74	-0.92	0.24
MnO	-0.04	-0.08	-0.04	-0.05	-0.11	-0.08	0.02
P_2O_5	-0.17	-0.16	-0.16	-0.15	-0.20	-0.18	0.33
SrO	-0.04	-0.01	-0.03	-0.03	-0.04	-0.01	-0.04
BaO	-0.01	-0.01	-0.01	-0.02	0.00	-0.02	-0.01
LOI	10.66	0.61	4.39	-0.40	6.36	0.71	8.44
C	2.94	-0.09	0.83	-0.22	1.32	-0.07	2.46
S	0.02	-0.03	-0.03	-0.03	0.06	-0.02	0.02
Ba	-66.24	-119.22	-147.52	-135.03	-22.95	-138.50	-83.10
Ce	-21.12	-21.75	-22.13	-21.25	-22.44	-21.80	20.61
Cr	98.72	170.30	58.70	133.66	164.09	214.47	0.89
Cs	-0.34	-0.55	-0.59	-0.54	-0.18	-0.55	-0.53
Dy	-3.45	-3.77	-3.57	-3.46	-4.00	-3.84	2.70
Er	-1.49	-1.87	-2.01	-1.69	-1.93	-1.69	1.55
Eu	-1.03	-1.20	-1.04	-1.13	-1.29	-1.11	0.84
Ga	-6.67	-5.96	-3.40	-7.28	-5.67	-4.86	0.96
Gd	-4.30	-4.10	-4.14	-4.07	-4.49	-4.07	2.77
Ge	3.26	2.11	2.81	-0.02	-0.49	-0.21	0.45
Hf	-2.95	-2.95	-3.49	-3.34	-3.72	-3.81	1.03
Ho	-0.61	-0.68	-0.55	-0.61	-0.66	-0.56	0.68
La	-8.66	-8.84	-9.14	-9.09	-8.98	-8.56	6.90
Lu	-0.19	-0.21	-0.22	-0.21	-0.26	-0.23	0.19
Nb	-5.71	-5.57	-5.68	-6.08	-6.49	-5.65	6.28
Nd	-15.36	-13.85	-13.93	-14.77	-15.87	-15.20	12.49
Pr	-3.25	-3.23	-3.19	-3.25	-3.45	-3.54	2.71
Rb	10.15	-7.16	-7.83	-7.81	28.34	-6.36	-5.09
Sm	-3.59	-3.65	-3.74	-3.68	-4.16	-3.92	2.70
Sn	-0.85	-0.15	0.12	-1.01	-0.39	-0.17	1.54
Sr	-361.72	-143.60	-246.32	-275.83	-435.55	-11.10	-298.08
Ta	-0.19	-0.45	-0.47	-0.41	-0.44	-0.45	0.41
Tb	-0.52	-0.57	-0.60	-0.55	-0.64	-0.56	0.43
Th	-0.45	-0.62	-0.85	-0.75	-0.40	-0.72	0.16
Tm	-0.20	-0.28	-0.23	-0.24	-0.28	-0.22	0.20
U	-0.25	-0.25	-0.33	-0.27	-0.27	-0.28	0.10
V	0.22	-61.59	119.46	-7.02	-35.57	-30.95	-113.90
W	3.61	-0.08	39.34	-0.01	18.32	-0.09	1.36
Y	-15.36	-18.76	-18.43	-18.63	-20.28	-21.62	11.30
Yb	-1.37	-1.55	-1.78	-1.45	-1.80	-1.58	1.25
Zr	-130.66	-126.85	-147.62	-135.51	-154.31	-127.40	55.72
As	-1.63	0.64	-0.41	2.84	12.81	2.06	-1.22
Bi	0.00	0.00	0.00	-0.01	0.00	-0.01	0.01
Hg	0.00	0.00	0.00	0.00	0.00	0.00	0.00
In	0.01	-0.02	-0.01	-0.03	-0.02	-0.02	0.07
Re	0.00	0.00	0.00	0.00	0.00	0.00	0.00
Sb	-0.51	0.00	-0.23	-0.09	-0.49	0.01	-0.46
Se	0.13	0.08	0.11	0.00	-0.02	0.08	0.02
Te	0.01	0.00	0.01	0.00	0.00	0.00	0.00
Tl	0.01	0.01	0.01	0.00	0.00	0.00	0.00
Ag	0.33	0.21	0.28	0.00	-0.05	-0.02	0.04
Cd	0.33	0.21	0.28	0.25	0.23	-0.02	0.04
Co	6.18	3.90	10.53	5.63	8.06	7.24	-2.35
Cu	13.18	16.44	9.03	18.57	-5.06	2.35	7.00
Li	18.05	4.23	5.62	14.81	19.16	13.29	18.57
Mo	-0.85	-1.08	-0.94	-1.50	-1.19	-1.54	-0.82
Ni	51.16	42.21	30.97	44.54	46.92	50.95	-0.64
Pb	1.30	0.85	1.12	0.98	-0.19	-0.09	2.54
Sc	3.42	-4.17	8.22	9.62	-4.23	0.18	-2.89
Zn	-38.07	-38.95	-28.99	-32.63	-31.97	-41.30	6.90
Au	0.00	0.00	0.54	0.00	0.00	0.00	0.01
C	2.67	-0.11	0.75	-0.25	1.22	-0.10	2.28
CO_2	9.79	-0.49	2.75	3.65	-1.34	-0.40	3.21

Table F.1.2. Calculated mass changes for gabbro samples

Sample ID	I951477	I951468	I951469	I951471	I951472	I951473	I951467
Hole ID	AE-16-35	AE-16-36	AE-16-36	AE-16-36	AE-16-36	AE-16-36	AE-16-38
Depth	28.25	6.4	13	26	44.05	51.15	77
Alteration	Intermediate	Intermediate	Intermediate	Intermediate	Intermediate	Intermediate	Intermediate
SiO_2	10.31	-6.47	-9.71	-0.39	-0.34	5.95	-0.14
Al_2O_3	0.00	0.00	0.00	0.00	0.00	0.00	0.00
Fe_2O_3	3.23	-2.65	-2.46	-1.27	1.57	-0.71	-2.22
CaO	2.04	2.20	1.01	3.23	1.81	-1.34	1.05
MgO	1.28	2.85	2.80	3.05	1.20	-0.89	3.19
Na_2O	0.54	-1.59	-1.46	-0.91	-0.80	0.91	-0.52
K_2O	-0.48	-0.35	0.68	-0.47	-0.41	-0.36	-0.44
Cr_2O_3	0.00	0.02	0.02	0.01	0.00	0.00	0.03
TiO_2	1.48	-0.81	-0.75	-0.58	0.22	-0.34	-0.64
MnO	0.06	-0.07	-0.08	-0.04	0.00	-0.05	-0.05
P_2O_5	0.13	-0.18	-0.15	-0.13	-0.05	0.29	-0.14
SrO	-0.04	-0.01	-0.04	-0.02	0.00	-0.04	-0.03
BaO	-0.01	-0.02	-0.01	-0.01	0.00	-0.01	-0.01
LOI	4.46	0.64	5.75	-0.86	-0.81	2.61	-0.36
C	1.13	-0.05	1.16	-0.35	-0.33	0.71	-0.26
S	0.12	0.02	0.03	-0.03	0.11	0.09	-0.01
Ba	-121.58	-138.12	-45.50	-124.91	-8.34	-107.50	-127.97
Ce	19.54	-21.88	-21.46	-15.19	-3.47	37.69	-14.09
Cr	1.18	231.28	223.92	45.32	5.26	0.34	215.71
Cs	-0.56	-0.54	-0.43	-0.57	0.43	-0.52	-0.56
Dy	1.57	-3.95	-3.92	-3.08	-1.70	3.92	-3.14
Er	1.80	-1.83	-1.73	-1.42	-0.45	2.63	-1.44
Eu	0.80	-1.13	-0.81	-0.80	-0.38	1.01	-0.87
Ga	-2.95	-9.54	-6.91	-8.69	-4.55	-1.86	-10.65
Gd	1.64	-4.37	-4.07	-3.46	-1.86	3.91	-3.39
Ge	0.59	-0.14	-0.12	0.02	0.07	0.17	0.01
Hf	1.79	-3.60	-3.57	-2.67	-1.45	3.59	-2.79
Ho	0.47	-0.70	-0.65	-0.56	-0.24	0.87	-0.51
La	6.89	-9.16	-9.17	-6.82	-2.07	14.12	-6.26
Lu	0.23	-0.24	-0.25	-0.17	-0.05	0.33	-0.19
Nb	8.64	-5.82	-6.12	-4.03	0.18	12.88	-2.66
Nd	10.93	-15.10	-14.75	-11.26	-4.07	21.68	-10.73
Pr	2.56	-3.28	-3.14	-2.33	-0.64	5.03	-2.28
Rb	-7.00	-4.75	10.74	-7.49	-5.10	-5.36	-6.89
Sm	2.30	-3.89	-3.81	-2.84	-1.12	4.56	-2.80
Sn	0.47	-0.11	-1.05	0.01	0.05	2.28	0.01
Sr	-318.52	-156.87	-420.63	-201.64	-47.57	-365.97	-308.16
Ta	0.61	-0.43	-0.43	-0.30	0.03	0.82	-0.30
Tb	0.32	-0.64	-0.61	-0.45	-0.21	0.67	-0.44
Th	0.36	-0.73	-0.79	-0.55	-0.36	0.91	-0.43
Tm	0.22	-0.24	-0.26	-0.18	-0.08	0.35	-0.20
U	0.18	-0.29	-0.28	-0.20	-0.13	0.42	-0.21
V	70.04	-37.35	-27.12	-20.07	104.94	-213.17	-15.02
W	2.71	0.89	0.91	0.01	-0.49	2.21	0.00
Y	9.65	-19.70	-18.35	-14.02	-6.89	22.04	-14.71
Yb	1.09	-1.73	-1.71	-1.32	-0.60	1.98	-1.22
Zr	114.33	-141.73	-141.29	-95.73	-43.59	202.93	-107.40
As	2.72	48.66	31.50	32.33	22.06	18.32	13.15
Bi	0.00	0.00	0.00	0.00	0.00	0.00	0.00
Hg	0.00	0.00	0.00	0.00	0.00	0.00	0.00
In	0.07	-0.03	-0.01	-0.03	-0.03	0.06	-0.03
Re	0.00	0.00	0.00	0.00	0.00	0.00	0.00
Sb	-0.22	-0.31	-0.53	-0.31	-0.22	-0.51	-0.35
Se	0.02	0.28	0.19	0.10	0.62	0.01	0.30
Te	0.01	0.01	0.01	0.01	0.01	0.00	0.00
Tl	0.00	0.00	0.00	0.00	0.00	0.00	0.00
Ag	0.06	-0.01	-0.01	0.00	0.01	0.02	0.00
Cd	0.61	-0.01	0.23	0.00	0.37	0.02	0.25
Co	5.29	8.59	9.92	11.29	13.19	-11.62	8.13
Cu	2.41	43.94	-19.32	-2.85	28.40	-11.03	54.26
Li	7.35	13.90	23.62	15.13	5.26	5.69	15.06
Mo	0.47	-1.05	-1.05	-0.99	-0.97	0.14	-1.00
Ni	-1.76	58.43	58.05	38.27	17.53	-2.47	44.15
Pb	0.24	-0.05	-0.05	0.01	0.03	0.07	0.00
Sc	3.35	-2.59	0.52	7.24	-2.28	-15.03	6.12
Zn	26.74	-26.17	-31.23	-16.47	13.89	34.55	-15.73
Au	0.01	0.01	0.00	0.00	0.00	0.02	0.00
C	0.97	-0.07	1.03	-0.35	-0.34	0.62	-0.26
CO_2	-1.38	2.75	-1.31	-0.19	4.15	4.06	5.22

Table F.1.2. Calculated mass changes for gabbro samples

Sample ID	I951360	I951364	I951366	294848	294851	294841	I951352
Hole ID	AE-16-40	AE-16-40	AE-16-40	AE-16-43	AE-16-43	AE-16-44	AE-17-46
Depth	16.85	54.85	69.9	91.8	119.6	82	37.6
Alteration	Intermediate	Intermediate	Intermediate	Intermediate	Intermediate	Intermediate	Intermediate
SiO_2	-7.33	3.91	-4.20	6.18	-2.60	10.14	3.40
Al_2O_3	0.00	0.00	0.00	0.00	0.00	0.00	0.00
Fe_2O_3	-2.27	0.54	-2.66	3.92	-2.97	4.41	-0.48
CaO	1.79	-1.22	2.72	-1.01	4.00	2.21	2.75
MgO	2.81	-0.39	2.37	0.60	2.55	1.81	2.45
Na_2O	-2.30	0.81	-1.68	-1.34	-2.36	-0.66	0.04
K_2O	-0.39	-0.36	0.03	-0.36	-0.47	-0.57	-0.42
Cr_2O_3	0.02	0.00	0.02	0.00	0.03	0.00	0.00
TiO_2	-0.82	-0.03	-0.92	1.32	-0.92	1.65	-0.34
MnO	-0.09	-0.02	-0.07	0.00	-0.09	0.06	-0.03
P_2O_5	-0.18	0.32	-0.18	0.28	-0.22	0.18	-0.07
SrO	-0.01	-0.03	-0.01	-0.05	-0.01	-0.04	-0.02
BaO	-0.02	-0.01	-0.01	-0.01	-0.01	-0.01	-0.01
LOI	2.22	0.07	-0.75	4.87	0.77	2.07	7.80
C	0.12	0.09	-0.27	0.78	-0.04	0.31	1.74
S	0.00	0.24	-0.01	0.03	-0.03	-0.03	0.08
Ba	-132.88	-68.23	-63.82	-132.80	-110.60	-135.02	-116.76
Ce	-22.58	10.36	-24.85	24.86	-24.54	14.36	-13.67
Cr	219.77	0.17	192.27	6.40	237.19	7.02	18.75
Cs	-0.08	-0.37	-0.52	-0.58	-0.47	-0.49	-0.57
Dy	-3.44	0.96	-4.21	3.48	-4.23	1.68	-2.48
Er	-1.70	0.86	-1.91	1.95	-1.93	1.02	-0.54
Eu	-1.16	0.11	-1.20	1.15	-1.32	0.68	-0.73
Ga	-5.85	-5.55	-8.70	6.57	-7.49	2.56	-6.56
Gd	-4.09	0.32	-4.77	3.57	-4.50	2.38	-2.44
Ge	-0.16	0.08	-0.15	3.20	2.34	3.51	0.47
Hf	-3.26	-0.28	-3.62	3.39	-4.00	1.07	-1.99
Ho	-0.65	0.29	-0.76	0.77	-0.72	0.48	-0.28
La	-9.25	4.14	-10.06	9.35	-9.98	4.87	-5.73
Lu	-0.21	0.05	-0.25	0.35	-0.31	0.16	-0.11
Nb	-5.15	5.35	-6.81	11.97	-6.47	7.05	-2.82
Nd	-15.63	5.11	-17.65	16.59	-15.73	11.44	-9.97
Pr	-3.68	0.44	-3.99	3.37	-3.68	1.80	-2.44
Rb	-5.92	-6.21	-0.93	-4.54	-6.39	-7.90	-6.61
Sm	-3.65	1.47	-4.02	3.88	-4.28	1.53	-2.34
Sn	-0.13	1.10	-0.12	0.28	-0.06	0.40	0.38
Sr	-126.88	-345.83	-211.03	-416.99	-146.59	-326.49	-305.51
Ta	-0.44	0.24	-0.53	0.60	-0.61	0.32	-0.29
Tb	-0.59	0.17	-0.66	0.67	-0.61	0.43	-0.36
Th	-0.60	0.11	-0.71	0.53	-0.78	0.04	-0.25
Tm	-0.20	0.16	-0.24	0.30	-0.27	0.12	-0.15
U	-0.25	0.05	-0.32	0.25	-0.35	0.07	-0.15
V	-34.29	-195.00	-80.39	5.82	-49.69	103.95	-76.70
W	-0.06	0.03	-0.53	3.56	-0.03	0.20	1.38
Y	-20.93	-2.32	-23.69	17.85	-21.08	10.41	-14.07
Yb	-1.43	0.50	-1.76	1.59	-1.61	0.98	-1.04
Zr	-105.63	59.33	-127.61	138.81	-157.34	60.05	-52.08
As	4.07	1.16	20.16	-0.17	1.14	1.83	0.58
Bi	0.00	0.00	-0.01	0.00	0.00	0.00	0.00
Hg	0.00	0.00	0.00	0.00	0.00	0.00	0.00
In	-0.01	0.00	-0.03	0.09	-0.03	0.00	0.02
Re	0.00	0.00	0.00	0.00	0.00	0.00	0.00
Sb	0.06	-0.34	-0.22	-0.45	0.25	-0.07	-0.49
Se	-0.01	0.21	-0.01	0.36	0.09	0.14	0.02
Te	0.00	0.01	0.00	0.01	0.00	0.01	0.00
Tl	0.00	0.05	0.00	0.01	0.01	0.01	0.00
Ag	-0.02	0.01	-0.02	0.32	0.23	0.35	0.05
Cd	-0.02	0.01	-0.02	0.32	0.33	0.35	0.05
Co	6.34	-2.00	6.45	3.47	4.78	9.05	12.13
Cu	9.59	-9.47	56.67	8.19	23.41	-5.57	32.20
Li	13.73	5.33	4.39	29.19	4.69	7.02	6.88
Mo	-1.53	0.07	-1.06	0.28	-1.03	-0.80	-1.41
Ni	63.50	-0.93	52.42	-1.86	50.28	6.61	32.63
Pb	-0.06	3.13	0.88	1.28	0.94	1.40	0.19
Sc	-0.97	-9.33	1.94	-2.65	1.97	9.65	8.01
Zn	-40.87	24.97	-36.00	2.29	-52.47	-3.08	0.58
Au	0.00	0.00	0.00	0.03	0.00	0.00	0.00
C	0.07	0.03	-0.27	0.67	-0.08	0.22	1.61
CO_2	0.19	0.05	-1.03	2.49	-0.34	0.78	5.86

Table F.1.2. Calculated mass changes for gabbro samples

Sample ID	I951353	I951358	294830	294835	16SJP003	16SJP005	183070
Hole ID	AE-17-46	AE-17-46	AE-17-50	AE-17-50	-	-	AE-16-03
Depth	50.35	76.75	93	114.55	-	-	4.37
Alteration	Intermediate	Intermediate	Intermediate	Intermediate	Proximal	Proximal	Proximal
SiO_2	3.52	1.99	-5.99	5.21	11.66	5.55	5.04
Al_2O_3	0.00	0.00	0.00	0.00	0.00	0.00	0.00
Fe_2O_3	4.81	1.68	-1.66	5.25	6.83	-2.28	1.29
CaO	-0.46	5.33	2.71	4.15	-1.57	-3.24	-1.98
MgO	1.23	3.88	1.19	3.62	1.35	-2.07	-1.27
Na_2O	0.58	-0.98	-0.11	-1.47	-0.11	1.65	-0.33
K_2O	-0.35	-0.46	-0.53	-0.56	-0.41	-0.17	0.05
Cr_2O_3	0.00	0.00	0.00	0.00	0.00	0.00	0.00
TiO_2	1.38	-0.16	-0.48	1.15	2.49	-0.53	-0.65
MnO	0.04	-0.02	-0.07	0.02	0.09	0.00	0.04
P_2O_5	0.22	-0.14	-0.13	-0.17	0.08	0.17	0.81
SrO	-0.02	-0.02	-0.03	-0.01	-0.04	-0.03	-0.04
BaO	-0.01	0.00	-0.01	-0.01	-0.01	-0.01	-0.01
LOI	6.34	9.99	7.57	1.56	2.50	2.47	5.27
C	1.78	2.16	1.69	0.10	0.50	0.81	1.42
S	0.26	0.11	-0.02	-0.03	0.75	-0.01	-0.01
Ba	-95.15	72.92	-147.84	-118.31	-93.36	-53.75	-91.89
Ce	22.44	-12.80	-18.86	-17.96	12.00	21.95	42.54
Cr	0.94	32.20	56.59	19.03	7.40	5.06	5.92
Cs	-0.55	-0.34	-0.60	-0.56	-0.40	-0.51	-0.45
Dy	3.80	-1.44	-3.16	-2.18	2.94	2.29	5.05
Er	2.60	-0.61	-1.57	-1.03	1.75	2.08	2.65
Eu	1.15	-0.50	-1.09	-0.69	0.95	0.90	2.10
Ga	4.96	0.24	-5.89	0.99	1.73	-0.54	3.89
Gd	4.46	-1.95	-3.62	-2.94	2.41	2.34	6.31
Ge	0.47	0.60	2.63	3.51	0.60	0.02	0.23
Hf	1.57	-2.39	-2.69	-2.17	2.82	3.17	3.27
Ho	0.85	-0.23	-0.53	-0.27	0.85	0.70	1.24
La	8.40	-5.66	-8.02	-8.11	4.14	7.67	15.69
Lu	0.32	-0.10	-0.20	-0.15	0.26	0.23	0.40
Nb	9.77	-3.66	-4.54	-3.89	11.84	12.78	11.28
Nd	15.92	-8.24	-13.31	-11.51	11.47	15.61	29.15
Pr	2.34	-2.44	-2.84	-2.73	1.67	2.73	6.15
Rb	-5.18	-6.00	-7.66	-8.02	-5.26	-2.16	0.07
Sm	3.92	-1.93	-3.06	-3.12	3.03	3.31	7.13
Sn	1.56	0.48	-0.97	0.40	1.72	1.02	2.37
Sr	-256.81	-120.36	-358.60	-209.94	-339.84	-314.36	-396.08
Ta	0.54	-0.38	-0.38	-0.40	0.74	0.61	0.64
Tb	0.73	-0.28	-0.49	-0.33	0.51	0.59	1.06
Th	0.36	-0.51	-0.73	-0.69	0.22	0.53	0.83
Tm	0.40	-0.05	-0.20	-0.17	0.33	0.28	0.46
U	0.12	-0.29	-0.24	-0.30	0.21	0.25	0.32
V	87.21	203.04	-12.08	371.89	40.60	-243.51	-241.50
W	3.75	0.24	1.05	0.20	0.24	1.01	1.18
Y	11.47	-13.08	-16.34	-12.42	14.07	14.46	25.25
Yb	1.83	-0.51	-1.23	-1.18	1.95	1.70	2.68
Zr	140.34	-67.56	-110.31	-110.57	112.24	140.79	209.02
As	-0.14	-0.85	-2.67	0.75	43.17	-2.39	0.34
Bi	0.05	0.00	0.00	0.00	0.08	0.02	0.00
Hg	0.00	0.01	0.00	0.00	0.03	0.02	0.00
In	0.10	0.02	0.02	-0.02	0.08	0.04	0.07
Re	0.00	0.00	0.00	0.00	0.00	0.00	0.00
Sb	-0.43	-0.41	-0.53	0.21	-0.34	-0.53	-0.49
Se	0.14	0.02	0.11	0.14	0.64	0.20	0.01
Te	0.00	0.01	0.01	0.01	0.02	0.00	0.01
Tl	0.03	0.00	0.01	0.01	0.00	0.00	0.00
Ag	0.05	0.06	0.26	0.35	0.06	0.00	0.02
Cd	0.05	0.06	0.26	0.35	0.06	0.00	0.02
Co	16.89	20.32	6.01	31.88	7.92	-17.90	-5.71
Cu	7.26	60.80	47.91	50.90	12.44	-16.94	-19.45
Li	6.88	19.80	36.06	7.02	7.40	15.13	16.83
Mo	-0.81	-0.76	2.11	-0.80	0.48	0.01	-0.91
Ni	-0.62	39.16	24.72	39.05	-2.38	-0.99	-2.45
Pb	0.19	1.48	1.05	1.40	0.24	0.01	0.09
Sc	5.63	17.12	2.85	26.47	8.44	-16.92	-17.99
Zn	55.22	-3.76	-32.30	24.56	68.16	20.77	66.82
Au	0.00	0.01	0.00	0.00	0.03	0.00	0.01
C	1.61	2.03	1.41	0.01	0.47	0.76	1.07
CO_2	5.86	7.43	5.07	-0.06	1.72	2.73	3.85

Table F.1.2. Calculated mass changes for gabbro samples

Sample ID	183071	183072	183086	183089	183090	183091	183077
Hole ID	AE-16-03	AE-16-03	AE-16-04	AE-16-04	AE-16-04	AE-16-04	AE-16-06
Depth	13.16	18.95	20.66	39.9	47.49	55.73	4.63
Alteration	Proximal	Proximal	Proximal	Proximal	Proximal	Proximal	Proximal
SiO_2	-1.05	5.71	-1.71	-5.70	3.05	-1.42	-3.62
Al_2O_3	0.00	0.00	0.00	0.00	0.00	0.00	0.00
Fe_2O_3	4.22	-5.02	-1.92	-2.89	2.25	-1.14	3.64
CaO	-1.11	10.35	5.34	-4.30	3.11	4.56	10.97
MgO	-0.07	4.99	1.07	-2.67	2.01	2.73	1.24
Na_2O	0.97	-2.81	-0.19	1.63	-0.40	-1.40	-1.36
K_2O	0.24	3.27	-0.07	0.42	-0.34	-0.09	1.29
Cr_2O_3	0.00	0.07	0.01	0.00	0.00	0.03	0.00
TiO_2	1.36	-1.88	-0.36	-1.62	0.29	-0.54	1.91
MnO	0.15	0.03	-0.04	-0.09	-0.03	-0.04	0.15
P_2O_5	0.40	-0.20	-0.17	-0.07	-0.10	-0.16	0.36
SrO	-0.04	-0.02	-0.02	-0.04	-0.04	-0.03	-0.02
BaO	-0.01	0.01	-0.01	-0.01	-0.01	-0.01	-0.01
LOI	13.17	24.58	15.13	4.18	10.58	9.63	19.00
C	4.26	6.95	4.34	1.19	2.67	2.16	6.12
S	0.32	-0.03	-0.03	2.41	-0.03	-0.03	2.08
Ba	-99.39	84.14	-135.53	-95.10	-115.40	-117.91	-76.23
Ce	25.33	-26.97	-33.62	43.80	-9.59	-18.75	18.56
Cr	6.92	460.00	101.90	3.99	19.31	196.44	8.66
Cs	-0.41	0.07	-0.48	-0.47	-0.51	-0.35	-0.21
Dy	4.15	-4.57	-3.89	5.18	-1.97	-3.17	4.64
Er	3.02	-1.68	-1.83	3.50	-0.72	-1.61	2.44
Eu	1.66	-1.42	-1.13	1.07	-0.57	-0.89	1.63
Ga	3.17	-5.09	-7.51	-3.25	-2.82	-7.33	-0.26
Gd	5.05	-5.43	-4.28	4.76	-1.30	-3.18	4.56
Ge	0.48	1.02	0.47	-0.25	0.54	0.30	0.91
Hf	3.75	-4.70	-3.42	7.64	-1.75	-2.62	2.73
Ho	1.21	-0.68	-0.66	1.20	-0.27	-0.52	0.90
La	8.15	-9.50	-14.41	15.97	-4.21	-8.06	6.05
Lu	0.41	-0.25	-0.25	0.63	-0.09	-0.20	0.30
Nb	17.73	-9.06	-5.32	19.71	-2.06	-4.52	13.43
Nd	18.61	-21.17	-20.07	23.50	-6.04	-12.83	15.91
Pr	3.17	-4.44	-4.71	5.36	-1.77	-2.98	2.52
Rb	2.70	47.97	-1.97	4.83	-4.85	-0.82	14.66
Sm	4.75	-5.31	-4.27	5.74	-1.71	-3.12	4.52
Sn	1.58	2.23	-0.81	-0.20	-0.78	-0.88	2.10
Sr	-337.29	-218.55	-287.69	-438.16	-372.88	-299.41	-218.40
Ta	0.91	-0.58	-0.41	1.16	-0.15	-0.33	0.50
Tb	0.73	-0.71	-0.62	0.80	-0.21	-0.48	0.81
Th	0.48	1.46	-0.80	1.65	-0.40	-0.69	0.32
Tm	0.44	-0.25	-0.26	0.51	-0.07	-0.20	0.40
U	0.21	1.06	-0.32	0.68	-0.15	-0.20	0.26
V	-136.58	-178.09	-49.38	-241.72	113.78	-20.19	-19.93
W	9.73	3.23	8.50	8.88	0.22	0.12	29.04
Y	21.57	-21.39	-19.41	29.96	-9.64	-16.70	19.63
Yb	2.42	-1.48	-1.43	4.08	-0.52	-1.16	2.32
Zr	175.38	-189.14	-138.78	398.99	-50.08	-109.58	146.37
As	34.57	-2.01	-1.80	141.87	-1.27	-2.02	123.71
Bi	0.04	0.00	0.00	0.05	0.00	0.00	1.79
Hg	0.00	0.00	0.00	0.00	0.00	0.00	0.00
In	0.10	0.03	0.02	0.05	0.04	0.02	0.07
Re	0.00	0.00	0.00	0.00	0.00	0.00	0.00
Sb	-0.45	-0.46	-0.47	-0.50	-0.42	-0.48	-0.30
Se	0.73	0.18	0.14	5.02	0.26	0.01	2.77
Te	0.04	6.51	0.01	0.36	0.01	0.00	1.16
Tl	0.00	0.02	0.00	0.00	0.00	0.00	0.00
Ag	0.05	0.10	0.05	0.38	0.05	0.03	0.57
Cd	0.05	0.10	0.05	-0.03	0.05	0.03	0.57
Co	-3.19	-0.59	3.82	-23.12	15.63	8.41	27.09
Cu	-10.50	-24.59	-18.87	10.84	39.65	66.89	4.04
Li	0.96	2.05	6.88	-0.51	31.47	39.77	1.83
Mo	0.38	-1.30	-1.41	-0.20	-0.78	-1.44	-0.63
Ni	-0.62	199.91	27.88	-2.10	27.39	50.72	-1.63
Pb	0.19	4.64	0.19	-0.10	0.22	0.12	4.46
Sc	-4.96	-7.45	0.88	-23.71	13.76	5.81	1.41
Zn	35.54	-38.82	-32.67	-34.20	-5.61	-25.26	26.27
Au	0.82	0.02	0.21	7.73	0.02	0.01	11.73
C	3.99	6.62	3.99	1.03	2.51	2.02	5.75
CO_2	14.60	24.29	14.53	3.71	9.08	7.34	21.03

Table F.1.2. Calculated mass changes for gabbro samples

Sample ID	183078	183081	I951378	I951379	I951380	195948	195949
Hole ID	AE-16-06	AE-16-06	AE-16-09	AE-16-09	AE-16-09	AE-16-12	AE-16-12
Depth	8.7	24	14.9	22.2	26.35	19.2	23
Alteration	Proximal	Proximal	Proximal	Proximal	Proximal	Proximal	Proximal
SiO_2	6.11	-1.82	6.22	-0.11	-3.66	-3.12	-10.98
Al_2O_3	0.00	0.00	0.00	0.00	0.00	0.00	0.00
Fe_2O_3	-4.33	-3.80	4.76	-3.73	-2.81	-2.50	-2.49
CaO	-3.33	3.01	1.87	-3.27	3.37	4.57	3.75
MgO	-2.47	2.00	0.23	-2.42	2.59	1.60	1.17
Na_2O	1.57	-0.78	0.21	1.97	-0.84	-1.22	-0.93
K_2O	0.38	-0.52	-0.14	0.07	0.73	-0.53	1.13
Cr_2O_3	0.00	0.00	0.00	0.00	0.05	0.01	0.01
TiO_2	-1.32	-1.18	0.94	-1.39	-0.98	-0.71	-0.63
MnO	-0.10	-0.08	0.07	-0.11	-0.05	-0.05	-0.04
P_2O_5	0.04	-0.22	0.39	-0.06	-0.20	-0.15	-0.17
SrO	-0.05	-0.03	-0.03	-0.05	-0.04	-0.02	-0.04
BaO	-0.01	-0.02	-0.01	-0.01	-0.01	-0.01	0.00
LOI	2.76	0.37	10.02	3.08	13.05	5.06	12.72
C	0.90	0.03	2.76	0.95	3.56	1.10	3.59
S	0.69	-0.04	-0.03	2.14	-0.03	-0.02	0.01
Ba	-115.87	-142.42	-85.20	-124.15	-65.42	-134.34	-16.59
Ce	40.38	-26.90	27.71	61.20	-28.15	-24.93	-21.32
Cr	4.84	63.67	1.30	-0.22	353.12	99.03	89.26
Cs	-0.42	-0.53	-0.46	-0.41	-0.29	-0.49	-0.25
Dy	3.53	-4.37	4.07	6.50	-4.84	-3.96	-3.78
Er	2.59	-2.20	2.42	4.46	-2.33	-1.95	-1.75
Eu	1.19	-1.23	1.29	1.60	-1.47	-1.09	-0.98
Ga	-3.76	-6.67	3.18	-5.13	-10.02	-7.80	-5.59
Gd	3.86	-4.53	3.51	5.32	-5.39	-4.68	-4.18
Ge	-0.04	-0.05	0.65	-0.11	0.30	0.10	0.12
Hf	7.17	-3.67	2.98	9.74	-4.08	-3.88	-3.43
Ho	0.79	-0.70	0.95	1.57	-0.83	-0.70	-0.67
La	15.55	-11.15	9.68	23.87	-11.75	-10.37	-8.54
Lu	0.40	-0.29	0.31	0.66	-0.32	-0.26	-0.21
Nb	15.91	-7.73	12.77	21.85	-8.10	-6.79	-5.59
Nd	22.22	-17.68	16.85	31.71	-19.32	-15.76	-14.18
Pr	5.15	-4.02	3.67	7.78	-4.22	-3.74	-3.32
Rb	4.28	-7.53	-1.92	0.66	10.60	-7.44	15.93
Sm	5.06	-4.32	3.99	6.51	-4.83	-4.21	-3.80
Sn	0.95	-1.02	1.78	0.87	-0.88	-0.96	-0.95
Sr	-471.06	-280.56	-336.13	-439.31	-334.10	-246.56	-348.07
Ta	0.87	-0.61	0.76	1.49	-0.55	-0.48	-0.37
Tb	0.58	-0.71	0.61	1.05	-0.78	-0.64	-0.60
Th	1.46	-0.82	0.55	2.10	-0.88	-0.85	-0.75
Tm	0.35	-0.27	0.35	0.70	-0.31	-0.29	-0.22
U	0.57	-0.32	0.27	0.92	-0.37	-0.33	-0.29
V	-258.97	-97.29	-64.45	-253.94	-60.48	-40.21	-25.76
W	7.86	-0.51	2.78	10.48	2.36	0.04	2.14
Y	15.87	-22.77	17.76	35.97	-23.86	-20.15	-20.21
Yb	2.83	-1.90	1.88	4.52	-2.02	-1.55	-1.70
Zr	362.44	-151.72	154.10	483.96	-172.25	-151.56	-124.43
As	102.09	13.76	-2.31	67.20	-3.14	0.88	-0.77
Bi	0.05	0.00	0.00	0.06	0.00	0.00	0.01
Hg	0.00	0.00	0.00	0.00	0.00	0.00	0.00
In	0.03	-0.03	0.08	0.04	0.00	-0.02	0.00
Re	0.00	0.00	0.00	0.00	0.00	0.00	0.00
Sb	-0.49	-0.11	-0.39	-0.47	-0.52	-0.26	-0.40
Se	1.08	0.10	0.03	3.15	0.01	0.00	0.00
Te	0.07	0.00	0.00	0.38	0.01	0.01	0.01
Tl	0.00	0.00	0.00	0.00	0.00	0.00	0.00
Ag	0.00	0.00	0.07	-0.01	0.03	0.01	0.01
Cd	0.00	0.00	0.07	-0.01	0.03	0.01	0.01
Co	-23.16	4.28	2.28	-19.60	8.41	4.45	3.66
Cu	115.71	37.77	-13.40	18.01	12.05	2.09	26.36
Li	-0.08	14.62	7.60	-0.22	17.38	15.81	5.47
Mo	-1.02	-1.51	-1.37	-0.09	-0.88	-1.48	-1.48
Ni	-2.51	33.30	-1.74	-2.04	60.79	31.33	32.61
Pb	-0.02	-0.02	2.78	0.91	1.24	3.16	0.05
Sc	-19.17	7.28	-4.80	-21.39	10.29	3.29	2.47
Zn	-25.17	-37.18	33.06	-53.03	-30.85	-33.50	-34.11
Au	1.86	0.01	0.01	4.83	0.04	0.01	0.01
C	0.81	-0.03	2.55	0.86	3.36	0.99	3.58
CO_2	2.93	-0.13	2.78	6.73	3.87	3.60	13.06

Table F.1.2. Calculated mass changes for gabbro samples

Sample ID	183081	I951378	I951379	I951380	195948	195949	195950
Hole ID	AE-16-06	AE-16-09	AE-16-09	AE-16-09	AE-16-12	AE-16-12	AE-16-12
Depth	24	14.9	22.2	26.35	19.2	23	27.1
Alteration	Proximal	Proximal	Proximal	Proximal	Proximal	Proximal	Proximal
SiO_2	-1.82	6.22	-0.11	-3.66	-3.12	-10.98	-4.24
Al_2O_3	0.00	0.00	0.00	0.00	0.00	0.00	0.00
Fe_2O_3	-3.80	4.76	-3.73	-2.81	-2.50	-2.49	-2.94
CaO	3.01	1.87	-3.27	3.37	4.57	3.75	-0.29
MgO	2.00	0.23	-2.42	2.59	1.60	1.17	-1.61
Na_2O	-0.78	0.21	1.97	-0.84	-1.22	-0.93	1.31
K_2O	-0.52	-0.14	0.07	0.73	-0.53	1.13	0.28
Cr_2O_3	0.00	0.00	0.00	0.05	0.01	0.01	0.00
TiO_2	-1.18	0.94	-1.39	-0.98	-0.71	-0.63	-0.38
MnO	-0.08	0.07	-0.11	-0.05	-0.05	-0.04	0.03
P_2O_5	-0.22	0.39	-0.06	-0.20	-0.15	-0.17	0.26
SrO	-0.03	-0.03	-0.05	-0.04	-0.02	-0.04	-0.04
BaO	-0.02	-0.01	-0.01	-0.01	-0.01	0.00	-0.01
LOI	0.37	10.02	3.08	13.05	5.06	12.72	7.78
C	0.03	2.76	0.95	3.56	1.10	3.59	2.61
S	-0.04	-0.03	2.14	-0.03	-0.02	0.01	0.11
Ba	-142.42	-85.20	-124.15	-65.42	-134.34	-16.59	-89.23
Ce	-26.90	27.71	61.20	-28.15	-24.93	-21.32	37.49
Cr	63.67	1.30	-0.22	353.12	99.03	89.26	5.26
Cs	-0.53	-0.46	-0.41	-0.29	-0.49	-0.25	-0.39
Dy	-4.37	4.07	6.50	-4.84	-3.96	-3.78	3.79
Er	-2.20	2.42	4.46	-2.33	-1.95	-1.75	2.81
Eu	-1.23	1.29	1.60	-1.47	-1.09	-0.98	1.23
Ga	-6.67	3.18	-5.13	-10.02	-7.80	-5.59	-2.50
Gd	-4.53	3.51	5.32	-5.39	-4.68	-4.18	3.85
Ge	-0.05	0.65	-0.11	0.30	0.10	0.12	0.07
Hf	-3.67	2.98	9.74	-4.08	-3.88	-3.43	4.19
Ho	-0.70	0.95	1.57	-0.83	-0.70	-0.67	1.05
La	-11.15	9.68	23.87	-11.75	-10.37	-8.54	15.07
Lu	-0.29	0.31	0.66	-0.32	-0.26	-0.21	0.37
Nb	-7.73	12.77	21.85	-8.10	-6.79	-5.59	12.19
Nd	-17.68	16.85	31.71	-19.32	-15.76	-14.18	20.05
Pr	-4.02	3.67	7.78	-4.22	-3.74	-3.32	4.70
Rb	-7.53	-1.92	0.66	10.60	-7.44	15.93	4.24
Sm	-4.32	3.99	6.51	-4.83	-4.21	-3.80	4.51
Sn	-1.02	1.78	0.87	-0.88	-0.96	-0.95	1.08
Sr	-280.56	-336.13	-439.31	-334.10	-246.56	-348.07	-369.37
Ta	-0.61	0.76	1.49	-0.55	-0.48	-0.37	0.85
Tb	-0.71	0.61	1.05	-0.78	-0.64	-0.60	0.61
Th	-0.82	0.55	2.10	-0.88	-0.85	-0.75	1.04
Tm	-0.27	0.35	0.70	-0.31	-0.29	-0.22	0.44
U	-0.32	0.27	0.92	-0.37	-0.33	-0.29	0.45
V	-97.29	-64.45	-253.94	-60.48	-40.21	-25.76	-184.53
W	-0.51	2.78	10.48	2.36	0.04	2.14	9.26
Y	-22.77	17.76	35.97	-23.86	-20.15	-20.21	22.26
Yb	-1.90	1.88	4.52	-2.02	-1.55	-1.70	2.66
Zr	-151.72	154.10	483.96	-172.25	-151.56	-124.43	257.17
As	13.76	-2.31	67.20	-3.14	0.88	-0.77	-0.62
Bi	0.00	0.00	0.06	0.00	0.00	0.01	0.02
Hg	0.00	0.00	0.00	0.00	0.00	0.00	0.00
In	-0.03	0.08	0.04	0.00	-0.02	0.00	0.05
Re	0.00	0.00	0.00	0.00	0.00	0.00	0.00
Sb	-0.11	-0.39	-0.47	-0.52	-0.26	-0.40	-0.47
Se	0.10	0.03	3.15	0.01	0.00	0.00	0.00
Te	0.00	0.00	0.38	0.01	0.01	0.01	0.03
Tl	0.00	0.00	0.00	0.00	0.00	0.00	0.01
Ag	0.00	0.07	-0.01	0.03	0.01	0.01	0.01
Cd	0.00	0.07	-0.01	0.03	0.01	0.01	0.01
Co	4.28	2.28	-19.60	8.41	4.45	3.66	-14.52
Cu	37.77	-13.40	18.01	12.05	2.09	26.36	-11.63
Li	14.62	7.60	-0.22	17.38	15.81	5.47	0.13
Mo	-1.51	-1.37	-0.09	-0.88	-1.48	-1.48	-0.97
Ni	33.30	-1.74	-2.04	60.79	31.33	32.61	-2.49
Pb	-0.02	2.78	0.91	1.24	3.16	0.05	1.05
Sc	7.28	-4.80	-21.39	10.29	3.29	2.47	-16.66
Zn	-37.18	33.06	-53.03	-30.85	-33.50	-34.11	-30.25
Au	0.01	0.01	4.83	0.04	0.01	0.01	0.01
C	-0.03	2.55	0.86	3.36	0.99	3.58	2.44
CO_2	-0.13	2.78	6.73	3.87	3.60	13.06	8.87

Table F.1.2. Calculated mass changes for gabbro samples

Sample ID	150415	150417	150422	150425	150427	150433	150435
Hole ID	AE-16-12	AE-16-12	AE-16-14	AE-16-14	AE-16-14	AE-16-15	AE-16-15
Depth	32.7	53.2	20.44	38.47	52.76	14.4	21.47
Alteration	Proximal	Proximal	Proximal	Proximal	Proximal	Proximal	Proximal
SiO_2	2.10	-6.98	-3.56	6.75	-5.22	1.56	2.99
Al_2O_3	0.00	0.00	0.00	0.00	0.00	0.00	0.00
Fe_2O_3	-2.30	-3.73	-2.48	3.51	-1.28	2.91	1.18
CaO	-2.57	2.80	1.69	2.28	3.81	4.17	-1.36
MgO	-2.05	1.83	0.90	0.69	1.80	2.28	-0.77
Na_2O	0.35	-1.86	0.52	0.55	-2.27	-0.45	1.49
K_2O	0.14	-0.35	-0.01	-0.35	-0.56	-0.38	-0.44
Cr_2O_3	0.00	0.04	0.01	0.00	0.00	0.00	0.00
TiO_2	-0.78	-1.13	-0.58	2.09	-0.57	0.38	-0.27
MnO	-0.01	-0.09	-0.06	0.10	-0.07	0.00	-0.03
P_2O_5	0.03	-0.23	-0.14	0.18	-0.16	-0.01	0.41
SrO	-0.04	-0.01	-0.03	-0.03	-0.01	0.00	-0.04
BaO	-0.01	-0.01	-0.01	-0.01	-0.02	-0.01	-0.01
LOI	3.52	-0.72	9.69	11.34	0.65	8.78	1.75
C	1.11	-0.27	2.71	3.17	-0.12	2.00	0.49
S	0.06	-0.02	-0.03	-0.03	-0.03	0.01	-0.01
Ba	-98.49	-118.71	-84.09	-119.67	-147.99	-82.05	-108.34
Ce	45.40	-28.69	-20.14	12.81	-27.06	-7.72	19.56
Cr	4.90	293.25	37.76	1.40	62.81	7.06	0.27
Cs	-0.44	-0.50	-0.45	-0.53	-0.58	-0.44	-0.44
Dy	5.58	-4.90	-3.62	2.43	-4.48	-1.51	2.11
Er	3.51	-2.43	-1.58	1.33	-2.22	-0.64	1.47
Eu	1.48	-1.31	-0.79	0.93	-1.23	-0.09	1.00
Ga	1.63	-8.45	-6.45	1.49	-6.33	-1.31	0.03
Gd	5.28	-4.99	-3.63	2.18	-4.55	-1.30	3.15
Ge	-0.02	-0.24	0.17	0.70	-0.08	0.52	0.14
Hf	6.96	-4.39	-3.36	1.87	-4.39	-2.03	0.49
Ho	1.28	-0.82	-0.58	0.61	-0.75	-0.06	0.50
La	16.66	-11.66	-8.54	4.39	-11.24	-3.72	6.61
Lu	0.51	-0.33	-0.21	0.18	-0.31	-0.11	0.17
Nb	24.12	-8.10	-4.65	10.28	-8.02	-1.07	7.65
Nd	26.04	-18.74	-13.59	8.82	-17.48	-4.56	13.46
Pr	5.78	-4.32	-3.09	1.65	-3.96	-1.04	2.56
Rb	1.89	-4.67	0.52	-5.26	-8.13	-5.00	-6.15
Sm	6.39	-5.01	-3.67	2.70	-4.26	-1.22	3.33
Sn	2.95	-1.10	-0.93	0.56	-1.03	-0.79	1.16
Sr	-404.58	-63.69	-303.97	-362.40	-154.34	-114.46	-358.70
Ta	1.48	-0.55	-0.36	0.67	-0.52	-0.16	0.48
Tb	0.98	-0.76	-0.55	0.50	-0.68	-0.11	0.39
Th	1.47	-0.89	-0.71	0.26	-0.93	-0.53	0.19
Tm	0.58	-0.35	-0.24	0.27	-0.31	-0.05	0.18
U	0.68	-0.36	-0.27	0.18	-0.35	-0.20	0.10
V	-283.35	-88.53	-43.21	28.15	23.94	99.56	-196.69
W	1.97	-0.55	0.07	13.09	-0.03	-0.40	1.11
Y	28.81	-24.20	-17.41	12.34	-22.34	-5.79	10.52
Yb	3.96	-2.07	-1.56	1.56	-1.96	-0.44	1.32
Zr	419.12	-172.70	-118.83	108.95	-173.81	-64.02	75.99
As	-0.73	-0.63	-2.63	-2.42	-0.79	0.64	-0.01
Bi	0.02	0.00	0.01	0.02	0.00	0.00	0.00
Hg	0.00	0.00	0.00	0.00	0.00	0.00	0.00
In	0.09	-0.03	0.02	0.08	-0.03	0.03	0.05
Re	0.00	0.00	0.00	0.00	0.00	0.00	0.00
Sb	-0.48	-0.12	-0.49	-0.33	0.02	-0.44	-0.37
Se	0.00	0.08	0.11	0.03	0.09	0.02	0.01
Te	0.05	0.01	0.02	0.01	0.00	0.01	0.01
Tl	0.00	0.00	0.00	0.00	0.00	0.00	0.01
Ag	0.00	-0.02	0.02	0.07	-0.01	0.05	0.01
Cd	0.00	0.29	0.02	0.07	0.23	0.35	0.01
Co	-23.10	2.25	1.21	4.15	6.72	18.87	-6.64
Cu	-19.07	46.30	-16.38	-19.60	20.50	47.58	-15.46
Li	-0.05	4.04	16.38	20.62	4.69	7.06	5.54
Mo	-0.02	-1.55	-1.47	-1.36	-1.52	-1.40	-1.47
Ni	-2.01	48.52	24.79	-2.36	32.84	24.74	-2.47
Pb	1.97	1.71	0.07	0.28	0.94	1.41	2.16
Sc	-16.13	-2.89	-0.07	2.02	6.81	9.81	-14.18
Zn	-2.92	-40.16	-44.55	12.17	-29.22	15.39	24.31
Au	0.00	0.00	0.00	0.00	0.00	0.00	0.00
C	1.05	-0.29	2.21	3.02	-0.23	1.80	0.40
CO_2	3.85	-1.14	8.12	11.05	-0.82	6.58	1.45

Table F.1.2. Calculated mass changes for gabbro samples

Sample ID	150436	150437	150445	150446	183094	183095	183096
Hole ID	AE-16-15	AE-16-15	AE-16-17	AE-16-17	AE-16-20	AE-16-20	AE-16-20
Depth	36.35	37.13	42.1	43.3	11.4	16.76	21.42
Alteration	Proximal	Proximal	Proximal	Proximal	Proximal	Proximal	Proximal
SiO_2	6.01	0.98	-0.78	-5.58	-1.80	-10.25	5.20
Al_2O_3	0.00	0.00	0.00	0.00	0.00	0.00	0.00
Fe_2O_3	-0.39	4.59	-0.30	-3.33	0.45	4.97	-1.62
CaO	-1.82	-1.02	2.71	0.53	0.12	-1.53	-0.93
MgO	-1.51	0.58	1.95	-1.71	2.08	-0.03	-1.81
Na_2O	1.59	-3.83	0.17	-0.34	-1.04	-2.21	-1.06
K_2O	0.49	1.48	-0.44	1.09	-0.52	0.29	0.68
Cr_2O_3	0.00	0.00	0.00	0.00	0.00	0.00	0.00
TiO_2	-0.81	1.17	-0.42	-0.05	-0.39	2.24	-0.09
MnO	0.06	0.01	-0.04	-0.02	-0.02	0.05	-0.01
P_2O_5	0.41	0.18	-0.09	0.38	-0.08	0.11	0.67
SrO	-0.04	-0.05	-0.03	-0.04	-0.01	-0.04	-0.04
BaO	-0.01	-0.01	-0.01	0.00	-0.02	-0.01	-0.01
LOI	6.93	8.24	8.51	6.18	-0.11	6.55	4.17
C	2.34	1.86	2.09	1.96	-0.27	1.58	1.23
S	-0.01	0.24	0.05	0.27	-0.04	0.08	0.33
Ba	-47.28	-68.78	-118.44	-36.36	-131.10	-86.97	-30.53
Ce	37.93	8.01	-15.37	39.24	-10.70	11.18	39.08
Cr	6.11	0.68	17.79	4.94	5.00	5.06	5.69
Cs	-0.42	-0.17	-0.51	-0.27	-0.58	-0.38	-0.42
Dy	3.96	1.05	-2.58	4.29	-2.28	1.30	4.66
Er	2.61	0.86	-0.94	3.12	-0.96	0.90	2.65
Eu	1.31	0.61	-0.55	1.12	-0.55	0.65	1.77
Ga	2.31	2.13	-3.46	0.33	-3.50	3.59	3.28
Gd	4.75	1.57	-2.65	5.72	-2.48	1.84	6.10
Ge	0.28	0.34	0.35	-0.02	0.00	0.02	0.17
Hf	3.34	0.17	-2.20	5.92	-1.70	1.66	3.16
Ho	0.94	0.50	-0.35	1.15	-0.35	0.41	1.04
La	14.31	2.21	-6.72	15.58	-4.70	3.14	14.66
Lu	0.35	0.10	-0.14	0.39	-0.10	0.15	0.32
Nb	13.97	6.99	-2.96	18.59	-2.10	8.55	13.84
Nd	22.14	7.44	-10.53	23.34	-7.20	7.46	26.49
Pr	4.94	0.82	-2.33	5.17	-1.85	1.21	5.29
Rb	5.90	20.54	-6.02	13.16	-7.70	3.78	7.36
Sm	5.91	1.82	-2.67	5.04	-1.79	1.95	6.76
Sn	1.33	0.27	0.28	0.98	0.00	1.02	1.21
Sr	-352.44	-425.49	-286.49	-389.15	-195.00	-427.09	-413.53
Ta	0.89	0.36	-0.32	1.09	-0.20	0.51	0.82
Tb	0.78	0.31	-0.38	0.84	-0.28	0.29	0.86
Th	0.84	0.02	-0.54	1.13	-0.32	0.20	0.64
Tm	0.43	0.14	-0.18	0.46	-0.10	0.15	0.34
U	0.41	0.01	-0.24	0.50	-0.15	0.15	0.35
V	-252.33	14.85	-5.58	-172.94	-45.00	31.26	-205.69
W	1.22	8.08	0.14	17.88	0.00	9.06	1.14
Y	22.46	6.16	-13.84	22.28	-10.70	8.22	23.75
Yb	2.60	0.94	-1.22	2.70	-0.73	1.15	2.46
Zr	235.78	52.07	-76.60	302.17	-60.00	99.53	179.41
As	7.08	32.18	51.46	57.51	13.00	20.05	57.87
Bi	0.00	0.01	0.01	0.03	-0.01	0.00	0.00
Hg	0.00	0.00	0.00	0.00	0.00	0.00	0.00
In	0.05	0.06	0.03	0.02	-0.02	0.07	0.05
Re	0.00	0.00	0.00	0.00	0.00	0.00	0.00
Sb	-0.48	-0.36	-0.43	-0.49	0.01	-0.22	-0.41
Se	0.12	0.58	0.13	0.10	0.30	0.10	0.33
Te	0.01	0.03	0.01	0.06	0.00	0.00	0.00
Tl	0.01	0.01	0.00	0.00	0.00	0.00	0.00
Ag	0.03	0.03	0.03	0.00	0.00	0.00	0.02
Cd	0.03	0.03	0.03	0.00	0.00	0.45	0.39
Co	-13.00	6.74	11.45	-7.17	13.00	13.30	-8.41
Cu	-11.56	-2.15	33.26	27.65	23.00	-13.92	-1.41
Li	0.56	0.68	17.79	4.94	5.00	15.13	5.69
Mo	-0.89	1.41	-1.43	0.98	-1.00	0.01	0.14
Ni	-2.44	0.41	25.49	-2.50	22.00	-0.99	-2.47
Pb	0.11	2.41	3.56	-0.01	2.00	0.01	0.07
Sc	-16.67	0.66	3.05	-16.09	-1.00	1.20	-12.90
Zn	33.11	29.18	-7.96	3.35	15.00	124.44	43.10
Au	0.00	0.01	0.00	2.06	0.00	0.01	0.04
C	2.10	1.76	1.90	1.83	-0.30	1.37	1.11
CO_2	7.72	6.45	6.93	6.65	-1.10	4.94	4.06

Table F.1.2. Calculated mass changes for gabbro samples

Sample ID	183097	183098	I951396	I951397	I951398	294862	294863
Hole ID	AE-16-20	AE-16-20	AE-16-21	AE-16-21	AE-16-21	AE-16-26	AE-16-26
Depth	33.5	39.2	8.8	29.35	34.5	33	43.6
Alteration	Proximal	Proximal	Proximal	Proximal	Proximal	Proximal	Proximal
SiO_2	1.07	-5.35	-5.77	-4.92	4.50	-4.66	6.10
Al_2O_3	0.00	0.00	0.00	0.00	0.00	0.00	0.00
Fe_2O_3	3.32	1.63	-0.01	-0.88	4.71	-1.62	5.41
CaO	0.93	-0.10	2.38	0.58	-0.90	3.04	1.68
MgO	0.51	1.54	1.74	-1.27	-0.34	1.63	2.94
Na_2O	0.49	-0.67	-1.93	-0.31	0.03	-2.57	-1.05
K_2O	-0.28	0.16	1.64	1.59	-0.25	0.38	-0.50
Cr_2O_3	0.00	0.00	0.00	0.00	0.00	0.00	0.00
TiO_2	1.35	0.67	-0.35	-0.22	0.00	-0.44	1.35
MnO	0.04	-0.03	-0.02	0.02	0.11	-0.08	0.02
P_2O_5	0.11	0.12	-0.11	0.60	0.83	-0.19	-0.08
SrO	-0.02	-0.04	-0.04	-0.04	-0.04	-0.03	-0.04
BaO	-0.01	-0.01	0.00	-0.01	-0.01	-0.01	-0.01
LOI	9.44	7.61	11.21	8.24	5.31	14.21	3.69
C	2.80	2.12	3.01	2.78	1.55	3.81	0.54
S	-0.03	0.14	0.00	0.53	0.13	-0.03	-0.03
Ba	-104.78	-100.16	7.17	-36.64	-95.46	-111.61	-121.45
Ce	14.72	6.71	-13.96	35.79	40.38	-25.18	-12.47
Cr	6.83	27.40	6.11	0.27	0.68	61.67	18.85
Cs	-0.53	-0.46	-0.11	-0.21	-0.55	-0.31	-0.55
Dy	1.49	-1.69	-2.61	4.38	6.28	-4.03	-1.46
Er	0.94	-0.98	-0.94	2.60	3.39	-2.10	-1.19
Eu	0.42	-0.08	-0.77	1.21	1.62	-1.09	-0.50
Ga	0.59	-1.50	-2.80	-0.49	2.93	-6.24	-1.72
Gd	1.55	-0.86	-2.99	4.42	6.19	-4.41	-2.15
Ge	0.46	0.20	0.28	0.14	0.34	3.06	3.46
Hf	1.30	-0.30	-1.99	3.23	4.14	-3.88	-1.97
Ho	0.37	-0.23	-0.40	0.97	1.34	-0.74	-0.21
La	5.10	3.02	-6.02	12.73	13.90	-10.24	-4.97
Lu	0.10	-0.04	-0.15	0.35	0.42	-0.32	-0.14
Nb	6.72	4.96	-3.48	13.14	15.05	-6.59	-2.18
Nd	9.59	0.75	-10.30	21.90	25.84	-16.97	-8.81
Pr	1.68	0.19	-2.18	4.97	5.77	-3.74	-2.08
Rb	-3.78	2.46	31.46	22.01	-3.88	6.79	-7.19
Sm	2.11	-0.41	-2.58	4.92	6.11	-4.30	-1.82
Sn	0.37	0.16	0.22	1.16	1.41	-0.89	0.38
Sr	-318.34	-420.02	-349.11	-363.44	-367.58	-290.22	-348.02
Ta	0.54	0.30	-0.33	0.79	0.93	-0.67	-0.28
Tb	0.30	-0.11	-0.37	0.74	0.96	-0.58	-0.25
Th	0.07	0.44	-0.41	0.65	0.79	-0.90	-0.52
Tm	0.16	-0.09	-0.14	0.36	0.52	-0.28	-0.11
U	0.02	0.18	-0.17	0.30	0.53	-0.31	-0.16
V	14.66	18.00	18.78	-182.98	-223.62	22.11	289.08
W	3.73	2.24	3.44	29.58	1.27	4.56	1.38
Y	6.77	-8.18	-12.66	20.85	28.98	-21.32	-10.15
Yb	1.09	-0.24	-0.90	2.19	2.86	-1.69	-1.11
Zr	68.88	34.20	-74.22	183.54	213.31	-160.89	-79.77
As	0.09	0.62	41.41	32.78	11.63	-2.81	0.35
Bi	0.00	0.00	0.00	0.01	0.00	0.00	0.00
Hg	0.00	0.00	0.00	0.00	0.00	0.00	0.00
In	0.06	0.03	0.01	0.03	0.09	0.01	0.01
Re	0.00	0.00	0.00	0.00	0.00	0.00	0.00
Sb	-0.41	-0.47	-0.47	-0.49	-0.52	-0.49	0.38
Se	0.37	0.22	0.01	0.43	0.01	0.12	0.50
Te	0.00	0.00	0.01	0.03	0.01	0.01	0.01
Tl	0.00	0.00	0.02	0.01	0.00	0.01	0.01
Ag	0.05	0.02	0.03	0.01	0.03	0.31	0.35
Cd	0.05	0.02	0.42	0.01	0.03	0.31	0.70
Co	4.86	6.97	11.44	-14.02	-2.34	7.00	32.58
Cu	-12.98	7.48	31.78	14.07	-7.83	56.22	67.00
Li	18.66	27.40	6.11	0.27	29.07	17.22	18.85
Mo	-0.82	0.16	-0.89	0.11	0.27	-0.89	0.38
Ni	-2.41	43.45	24.78	-2.47	-2.43	30.33	22.04
Pb	0.18	4.40	0.11	0.05	0.14	1.22	1.38
Sc	-2.79	-4.08	3.33	-16.29	-14.10	6.67	15.31
Zn	34.52	26.22	-3.56	-4.16	87.09	-33.56	21.23
Au	0.04	0.00	0.00	0.39	0.01	0.01	0.00
C	2.49	1.88	2.76	2.59	1.41	3.43	0.48
CO_2	9.15	6.82	6.72	0.82	10.31	12.61	1.72

Table F.1.2. Calculated mass changes for gabbro samples

Sample ID	294856	294857	I951388	I951389	I951371	I951373	I951475
Hole ID	AE-16-27	AE-16-27	AE-16-32	AE-16-32	AE-16-34	AE-16-34	AE-16-35
Depth	64.9	68	32.3	50.35	32	33.5	18.35
Alteration	Proximal	Proximal	Proximal	Proximal	Proximal	Proximal	Proximal
SiO_2	-6.59	2.45	-1.36	8.34	83.85	6.04	1.97
Al_2O_3	0.00	0.00	0.00	0.00	0.00	0.00	0.00
Fe_2O_3	-2.48	8.02	2.96	5.40	3.73	2.88	0.80
CaO	5.82	3.78	-1.53	2.27	12.56	-2.13	-1.52
MgO	-0.23	3.84	-0.50	0.90	3.74	-0.68	-0.55
Na_2O	-0.81	-2.06	-1.41	-0.16	-2.55	0.69	0.66
K_2O	1.18	-0.51	0.51	-0.48	1.31	-0.43	-0.31
Cr_2O_3	0.00	0.00	0.00	0.00	0.01	0.00	0.00
TiO_2	-0.19	1.88	-0.11	1.94	-0.68	-0.28	-0.21
MnO	-0.05	0.05	-0.02	0.03	0.23	0.05	0.02
P_2O_5	-0.16	-0.12	0.81	0.19	0.08	0.82	0.43
SrO	-0.04	-0.02	-0.05	-0.03	-0.01	-0.04	-0.03
BaO	-0.01	-0.01	-0.01	-0.01	0.00	-0.01	-0.01
LOI	12.37	5.26	2.88	7.11	24.27	3.33	3.04
C	3.45	0.83	0.56	1.72	6.75	0.94	0.91
S	0.03	-0.03	0.19	-0.03	0.01	0.00	0.30
Ba	-43.29	-144.09	-58.42	-118.13	-9.50	-76.83	-87.01
Ce	-15.07	-14.45	48.70	17.76	-7.63	44.49	37.11
Cr	28.21	7.16	0.17	1.33	40.45	0.54	0.31
Cs	-0.27	-0.35	-0.41	-0.48	-0.18	-0.55	-0.54
Dy	-2.37	-1.56	7.69	2.83	1.52	5.41	3.41
Er	-1.40	-0.70	4.20	1.67	0.51	3.13	2.18
Eu	-0.70	-0.66	1.79	0.86	0.69	1.78	1.24
Ga	-3.88	1.55	1.48	0.90	3.97	4.31	-1.17
Gd	-3.23	-2.09	7.97	2.78	0.90	6.70	3.82
Ge	3.04	3.58	0.08	0.66	3.18	0.27	0.15
Hf	-2.67	-1.87	4.47	3.02	-2.33	3.64	2.56
Ho	-0.41	-0.33	1.72	0.69	0.20	1.29	0.80
La	-6.18	-6.40	17.37	6.38	-3.35	15.96	13.58
Lu	-0.18	-0.12	0.54	0.22	-0.01	0.40	0.29
Nb	-3.63	-2.79	14.85	11.37	4.62	13.98	10.14
Nd	-10.27	-7.62	29.39	10.97	-3.66	28.15	21.31
Pr	-2.28	-2.09	6.80	2.36	-1.52	6.18	5.00
Rb	16.70	-6.91	7.85	-7.33	18.85	-6.33	-4.75
Sm	-2.56	-2.08	6.92	2.31	-0.17	6.91	4.64
Sn	-0.89	0.43	0.07	0.53	9.36	2.43	1.18
Sr	-343.25	-221.53	-449.68	-301.02	-119.14	-377.57	-271.80
Ta	-0.34	-0.39	0.86	0.77	-0.09	0.88	0.70
Tb	-0.45	-0.23	1.30	0.50	0.09	0.97	0.65
Th	-0.57	-0.46	1.10	0.33	-0.48	0.67	0.54
Tm	-0.23	-0.15	0.56	0.29	0.13	0.46	0.27
U	-0.26	-0.17	0.78	0.30	-0.12	0.38	0.27
V	-1.25	399.47	-176.40	-5.20	31.00	-213.82	-182.05
W	5.64	1.43	9.33	2.80	26.27	1.21	1.12
Y	-13.76	-10.25	37.67	13.83	-1.19	28.20	19.79
Yb	-1.59	-0.77	3.45	1.46	0.77	2.45	2.05
Zr	-103.79	-87.76	235.00	149.59	-60.18	191.82	149.64
As	9.36	-0.30	36.60	-0.28	-0.52	-1.60	14.14
Bi	0.00	0.00	0.04	0.00	0.00	0.00	0.01
Hg	0.00	0.00	0.00	0.00	0.01	0.00	0.00
In	0.01	0.02	0.04	0.11	0.08	0.07	0.07
Re	0.00	0.00	0.00	0.00	0.00	0.00	0.00
Sb	-0.48	0.14	-0.48	-0.49	-0.49	-0.46	-0.53
Se	0.12	0.26	0.21	0.03	0.13	0.01	0.43
Te	0.01	0.01	0.09	0.01	0.01	0.00	0.03
Tl	0.01	0.01	0.00	0.00	0.01	0.00	0.00
Ag	0.30	0.36	0.01	0.07	0.32	0.03	0.02
Cd	0.30	0.36	0.01	0.51	0.32	0.03	0.02
Co	3.54	31.43	-4.07	8.76	5.64	-6.43	-5.40
Cu	14.96	32.35	6.03	-15.88	-23.73	-14.93	-10.08
Li	17.14	19.31	15.67	7.65	17.73	28.21	16.23
Mo	-0.89	-0.78	1.10	-0.73	0.27	-0.89	0.12
Ni	18.04	27.39	-1.97	-1.73	33.36	-2.45	-2.47
Pb	1.21	1.43	2.10	1.53	3.55	4.54	0.06
Sc	1.00	17.41	-11.40	0.37	10.91	-14.50	-11.95
Zn	-42.64	23.57	44.60	47.51	54.27	66.96	24.09
Au	0.01	0.00	0.80	0.05	0.02	0.01	0.35
C	3.24	0.73	0.47	1.41	6.26	0.81	0.79
CO_2	11.90	2.63	-0.88	2.42	-1.27	6.14	-1.29

Table F.1.2. Calculated mass changes for gabbro samples

Sample ID	I951476	I951462	I951463	I951464	I951456	I951457	I951458
Hole ID	AE-16-35	AE-16-38	AE-16-38	AE-16-38	AE-16-39	AE-16-39	AE-16-39
Depth	24.4	44.35	69.35	72.5	62.15	85.4	91.7
Alteration	Proximal	Proximal	Proximal	Proximal	Proximal	Proximal	Proximal
SiO_2	8.20	3.10	5.00	0.80	-5.63	0.22	17.92
Al_2O_3	0.00	0.00	0.00	0.00	0.00	0.00	0.00
Fe_2O_3	-2.36	5.53	4.31	-0.32	1.85	3.61	14.64
CaO	-3.29	3.61	0.57	-1.02	1.02	1.28	4.49
MgO	-1.89	1.19	0.76	-1.07	0.24	0.22	3.78
Na_2O	1.48	-2.53	-1.59	0.55	-2.12	-3.23	-3.22
K_2O	-0.03	0.84	0.95	0.27	1.09	2.22	0.52
Cr_2O_3	0.00	0.00	0.00	0.00	0.00	0.00	0.00
TiO_2	-0.72	1.55	1.30	-0.65	0.45	0.94	3.35
MnO	-0.07	0.09	0.07	0.03	0.02	0.07	0.31
P_2O_5	0.33	0.24	0.23	0.63	-0.03	0.20	0.74
SrO	-0.04	-0.04	-0.05	-0.03	-0.04	-0.04	-0.03
BaO	-0.01	-0.01	-0.01	-0.01	-0.01	0.00	0.00
LOI	2.03	10.06	9.12	5.65	10.31	9.63	15.10
C	0.28	2.35	2.49	1.65	2.85	2.73	3.91
S	1.09	0.08	0.22	-0.01	0.14	0.64	0.39
Ba	-33.29	-55.92	-74.68	-59.09	-55.15	14.27	-37.85
Ce	65.33	23.40	27.85	45.18	-3.50	18.71	62.49
Cr	0.22	1.20	1.08	0.31	5.84	0.87	3.00
Cs	-0.48	-0.39	-0.43	-0.44	-0.24	-0.29	-0.43
Dy	6.97	3.09	4.21	6.01	-1.25	2.21	8.85
Er	4.45	2.16	2.85	3.45	-0.49	1.62	5.19
Eu	1.83	1.05	1.07	1.82	-0.23	1.05	2.74
Ga	-6.49	2.10	0.22	-0.43	-2.82	-0.20	3.31
Gd	7.15	3.28	4.23	6.26	-1.73	2.19	10.04
Ge	0.11	0.60	0.54	0.15	0.21	0.44	1.50
Hf	7.83	2.57	4.21	4.68	-1.25	1.71	6.50
Ho	1.48	0.71	0.96	1.28	-0.13	0.52	1.84
La	24.83	8.36	9.77	16.34	-2.00	5.98	22.79
Lu	0.55	0.27	0.35	0.47	-0.06	0.18	0.66
Nb	20.37	12.46	15.45	13.54	1.56	9.61	25.45
Nd	33.67	13.33	15.84	27.36	-4.33	10.21	36.96
Pr	8.60	2.98	3.76	6.27	-0.75	2.48	8.48
Rb	1.13	11.98	13.27	3.85	16.91	32.94	8.66
Sm	7.39	2.69	3.57	6.12	-1.31	2.19	8.91
Sn	2.18	1.72	1.65	2.25	0.17	1.52	2.80
Sr	-366.03	-301.40	-399.63	-310.02	-324.12	-338.44	-248.08
Ta	1.40	0.86	0.95	0.91	-0.02	0.64	1.56
Tb	1.24	0.55	0.76	1.05	-0.17	0.37	1.52
Th	1.92	0.38	0.71	0.96	-0.18	0.25	1.17
Tm	0.70	0.32	0.41	0.54	-0.04	0.22	0.65
U	0.91	0.21	0.37	0.46	0.07	0.35	0.60
V	-234.45	-17.68	-60.06	-230.88	125.41	1.57	7.32
W	2.13	2.72	8.73	5.37	8.76	8.39	16.60
Y	36.91	16.43	22.82	29.45	-5.68	11.21	44.60
Yb	3.98	1.75	2.42	3.17	-0.47	1.29	4.46
Zr	408.37	150.68	228.31	274.92	-16.69	115.46	328.64
As	94.00	24.20	8.70	-1.58	12.13	33.76	59.32
Bi	0.02	0.00	0.01	0.00	0.00	0.07	0.07
Hg	0.00	0.00	0.00	0.00	0.00	0.00	0.00
In	0.02	0.08	0.07	0.07	0.04	0.07	0.12
Re	0.00	0.00	0.00	0.00	0.00	0.00	0.00
Sb	-0.54	-0.46	-0.47	-0.52	-0.34	-0.42	-0.34
Se	1.36	0.64	0.63	0.11	0.12	1.07	1.02
Te	0.04	0.01	0.08	0.02	0.01	0.08	0.06
Tl	0.00	0.01	0.00	0.00	0.00	0.04	0.02
Ag	0.01	0.06	0.05	0.02	0.02	0.04	0.15
Cd	0.27	0.37	0.05	0.02	0.51	0.04	0.87
Co	-14.21	7.92	3.47	-12.83	12.52	2.23	30.98
Cu	49.15	3.76	4.39	-13.26	22.78	-15.43	15.59
Li	5.44	7.40	7.16	0.31	5.84	0.87	26.99
Mo	1.13	1.72	1.65	0.12	-0.92	0.35	2.80
Ni	-2.48	-0.52	-2.39	-2.47	21.93	-0.65	-2.20
Pb	0.04	0.24	1.43	0.06	0.08	0.17	0.60
Sc	-17.47	1.00	-2.04	-16.20	-6.15	-6.52	9.99
Zn	1.16	61.96	51.53	6.04	-2.62	13.55	146.74
Au	0.62	0.00	0.16	0.01	0.00	1.00	0.06
C	0.19	2.20	2.38	1.55	2.68	2.61	3.73
CO_2	2.15	1.97	-1.38	0.84	12.37	9.77	15.14

Table F.1.2. Calculated mass changes for gabbro samples

Sample ID	I951361	I951362	I951363	294849	294850	294842	294843
Hole ID	AE-16-40	AE-16-40	AE-16-40	AE-16-43	AE-16-43	AE-16-44	AE-16-44
Depth	28.35	36.4	44.2	105.25	111.05	99.7	103
Alteration	Proximal	Proximal	Proximal	Proximal	Proximal	Proximal	Proximal
SiO_2	-6.55	-2.39	8.90	2.85	1.47	5.31	3.93
Al_2O_3	0.00	0.00	0.00	0.00	0.00	0.00	0.00
Fe_2O_3	6.94	0.14	-3.01	-4.20	6.38	-0.80	6.14
CaO	5.74	-1.51	-2.37	-3.59	2.68	-1.45	2.01
MgO	1.82	-1.64	-2.69	-2.32	2.15	-1.46	1.59
Na_2O	-3.99	-0.16	-1.02	1.49	-0.25	2.17	-0.22
K_2O	2.17	1.08	1.45	0.24	-0.28	-0.11	-0.08
Cr_2O_3	0.00	0.00	0.00	0.00	0.00	0.00	0.00
TiO_2	1.88	-0.65	-1.49	-1.33	1.43	-1.01	1.79
MnO	0.09	0.04	-0.01	-0.13	0.00	-0.01	0.00
P_2O_5	0.03	0.37	-0.02	0.07	0.04	0.46	-0.02
SrO	-0.03	-0.05	-0.05	-0.04	-0.04	-0.04	-0.03
BaO	-0.01	-0.01	0.00	-0.01	-0.01	-0.01	-0.01
LOI	16.50	4.92	4.44	2.10	8.43	8.47	11.66
C	4.45	2.09	1.31	0.83	2.08	2.94	3.34
S	0.34	1.12	0.05	1.36	-0.03	-0.02	-0.03
Ba	-24.54	-62.75	-8.78	-123.52	-107.99	-130.48	-56.13
Ce	7.57	40.57	37.82	50.72	2.81	44.50	-6.15
Cr	7.55	5.26	0.72	4.48	7.16	5.99	7.81
Cs	-0.16	-0.29	-0.18	-0.41	-0.54	-0.50	-0.39
Dy	1.05	5.02	5.07	4.56	0.42	4.60	-1.26
Er	0.60	3.56	4.13	2.98	0.35	2.92	-0.61
Eu	-0.07	1.47	0.85	0.77	-0.08	1.39	-0.43
Ga	5.45	-0.45	15.04	-1.06	1.92	0.36	2.00
Gd	1.27	5.19	3.90	4.29	-0.35	5.21	-1.61
Ge	0.64	0.07	0.36	2.24	3.58	3.00	3.90
Hf	-0.57	4.29	5.94	7.69	0.32	4.99	-0.57
Ho	0.24	1.25	1.22	1.25	0.17	0.91	-0.10
La	2.29	15.90	14.72	20.45	0.53	16.38	-2.92
Lu	0.12	0.47	0.55	0.50	0.08	0.34	-0.06
Nb	4.13	16.30	20.65	17.53	3.17	14.32	0.42
Nd	4.72	24.67	18.03	25.15	1.13	26.51	-2.58
Pr	0.28	4.45	4.05	6.08	-0.07	6.03	-0.98
Rb	28.05	13.79	22.24	3.70	-3.26	-1.73	-0.13
Sm	1.43	6.10	5.07	5.19	-0.01	4.82	-0.86
Sn	1.77	1.08	3.72	-0.10	0.43	1.30	0.56
Sr	-344.60	-416.59	-441.03	-449.02	-379.57	-375.62	-347.03
Ta	0.13	0.85	1.06	1.09	-0.03	0.76	-0.10
Tb	0.31	0.96	0.85	0.89	0.04	0.94	-0.10
Th	-0.14	1.28	1.58	1.67	-0.11	1.11	-0.33
Tm	0.12	0.57	0.66	0.56	0.04	0.37	-0.07
U	-0.04	0.41	0.62	0.74	-0.04	0.52	-0.11
V	307.28	-208.14	-297.27	-252.64	303.43	-222.26	386.83
W	34.14	12.34	0.14	15.12	1.43	12.19	0.28
Y	0.07	19.49	21.73	29.38	1.18	25.07	-5.21
Yb	0.27	2.66	3.37	4.01	0.04	2.33	-0.65
Zr	39.34	338.26	427.52	360.23	10.71	227.96	-39.64
As	17.89	181.07	-1.64	80.67	-2.24	-2.93	-2.03
Bi	0.02	0.04	0.00	0.04	0.00	0.02	0.00
Hg	0.00	0.00	0.00	0.00	0.00	0.00	0.00
In	0.05	0.04	0.07	0.01	0.05	0.05	0.05
Re	0.00	0.00	0.00	0.00	0.00	0.02	0.00
Sb	-0.46	-0.49	-0.47	-0.49	-0.41	-0.51	-0.10
Se	0.28	1.34	0.01	2.55	0.14	0.12	0.16
Te	0.01	0.11	0.00	0.41	0.01	0.02	0.01
Tl	0.03	0.00	0.01	0.01	0.01	0.01	0.02
Ag	0.06	0.01	0.04	0.22	0.36	0.30	0.39
Cd	0.50	0.01	0.04	0.22	0.36	0.30	0.39
Co	27.24	-9.39	-22.70	-15.94	25.35	-13.21	27.21
Cu	7.89	28.40	-20.28	37.52	31.14	-4.01	-0.38
Li	7.55	0.13	0.72	4.48	31.47	5.99	33.43
Mo	-0.74	0.05	0.29	-1.05	-0.78	23.28	-0.72
Ni	14.57	-0.95	-2.43	-2.05	21.31	-1.90	5.97
Pb	6.53	2.08	1.29	0.90	1.43	1.20	6.69
Sc	10.16	-16.66	-19.70	-21.47	8.90	-19.01	8.43
Zn	37.55	7.73	41.56	-52.50	2.90	-7.86	39.07
Au	0.04	2.56	0.01	3.74	0.11	0.01	0.00
C	4.33	1.80	1.19	0.70	1.84	2.12	3.11
CO_2	15.82	6.51	4.33	2.48	6.77	7.73	11.31

Table F.1.2. Calculated mass changes for gabbro samples

Sample ID	I951354	I951355	294829	294832
Hole ID	AE-17-46	AE-17-46	AE-17-50	AE-17-50
Depth	67.6	69.6	83.1	105.7
Alteration	Proximal	Proximal	Proximal	Proximal
SiO_2	0.39	4.39	-9.81	-6.76
Al_2O_3	0.00	0.00	0.00	0.00
Fe_2O_3	-3.42	-4.09	-3.44	6.46
CaO	-4.55	-4.11	2.18	2.63
MgO	-2.85	-2.69	1.18	1.80
Na_2O	2.06	2.09	-1.97	0.60
K_2O	-0.11	0.24	0.19	0.40
Cr_2O_3	0.00	0.00	0.02	0.00
TiO_2	-1.60	-1.60	-0.92	1.78
MnO	-0.13	-0.02	-0.09	0.04
P_2O_5	-0.02	-0.02	-0.17	0.02
SrO	-0.05	-0.04	-0.03	-0.03
BaO	-0.02	-0.01	-0.01	-0.01
LOI	0.62	3.49	14.90	18.53
C	0.46	1.58	4.17	5.55
S	2.47	0.18	-0.03	-0.03
Ba	-126.65	-95.18	-96.96	-51.93
Ce	45.22	37.87	-21.72	-2.03
Cr	-0.26	-0.11	168.93	20.20
Cs	-0.53	-0.43	-0.44	-0.45
Dy	5.74	5.02	-3.59	-0.25
Er	3.80	3.60	-1.74	-0.37
Eu	1.23	1.13	-1.37	-0.19
Ga	-1.91	1.68	-7.49	2.81
Gd	5.19	4.17	-4.42	-0.78
Ge	-0.13	-0.06	2.62	3.80
Hf	6.08	5.12	-3.01	-0.30
Ho	1.34	1.23	-0.65	-0.01
La	17.79	14.84	-8.98	-2.29
Lu	0.54	0.50	-0.26	0.01
Nb	18.20	18.55	-5.90	1.43
Nd	24.11	21.00	-16.13	-1.43
Pr	4.80	3.90	-3.30	-0.57
Rb	-1.52	2.34	3.48	8.16
Sm	5.80	4.69	-4.14	-0.51
Sn	-0.10	1.91	-0.98	0.52
Sr	-454.24	-384.64	-256.98	-362.59
Ta	1.09	1.05	-0.39	-0.12
Tb	0.92	0.89	-0.65	-0.14
Th	1.79	1.40	-0.66	-0.08
Tm	0.66	0.59	-0.24	-0.07
U	0.67	0.60	-0.27	-0.03
V	-282.98	-298.46	-80.62	336.28
W	11.32	4.87	11.28	26.72
Y	21.80	19.02	-19.18	-1.52
Yb	3.74	3.34	-1.75	-0.06
Zr	414.27	372.01	-124.21	-18.54
As	227.61	0.70	-2.06	-2.69
Bi	0.30	0.01	0.00	0.00
Hg	0.00	0.00	0.00	0.00
In	0.04	0.04	0.01	0.06
Re	0.00	0.00	0.00	0.00
Sb	-0.47	-0.54	-0.49	-0.42
Se	3.12	0.00	0.10	0.15
Te	0.44	0.04	0.01	0.01
Tl	0.01	0.00	0.01	0.02
Ag	-0.01	-0.01	0.26	0.38
Cd	-0.01	-0.01	0.26	0.38
Co	-21.62	-25.18	2.81	24.97
Cu	30.88	-21.11	-17.82	5.50
Li	-0.26	-0.11	15.46	7.60
Mo	-1.05	-1.02	-0.98	-0.74
Ni	-1.10	-2.02	46.11	25.98
Pb	3.74	-0.02	1.05	1.52
Sc	-22.42	-22.18	-2.38	15.37
Zn	-26.90	-5.10	-43.78	4.07
Au	10.10	0.28	0.01	0.00
C	0.39	1.38	3.23	4.14
CO_2	1.34	5.05	11.80	15.13

Appendix F.2. Mass changes by element and alteration zone

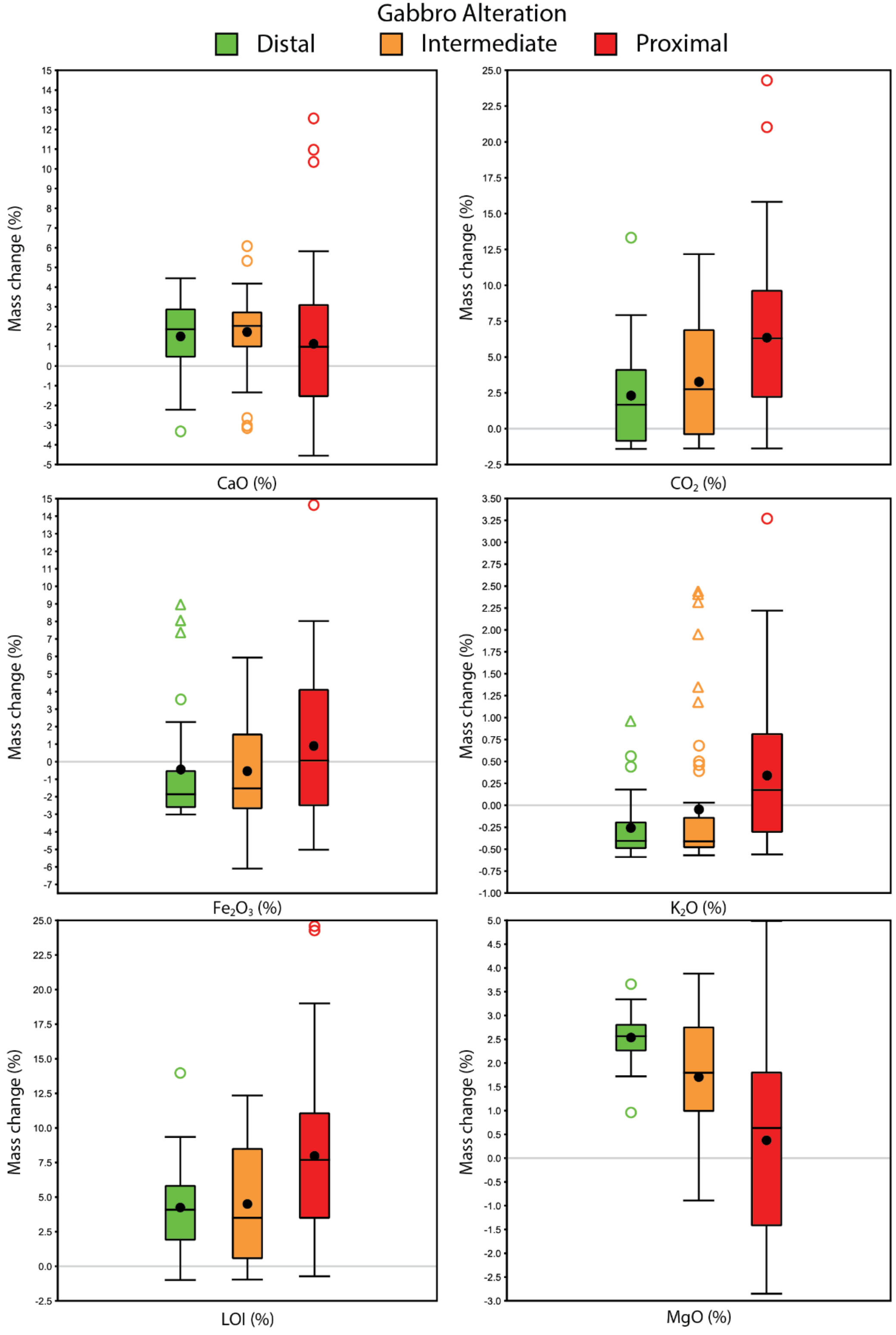

Appendix F.2.1. Mass changes for CaO, CO_2, Fe_2O_3, K_2O, LOI and MgO.

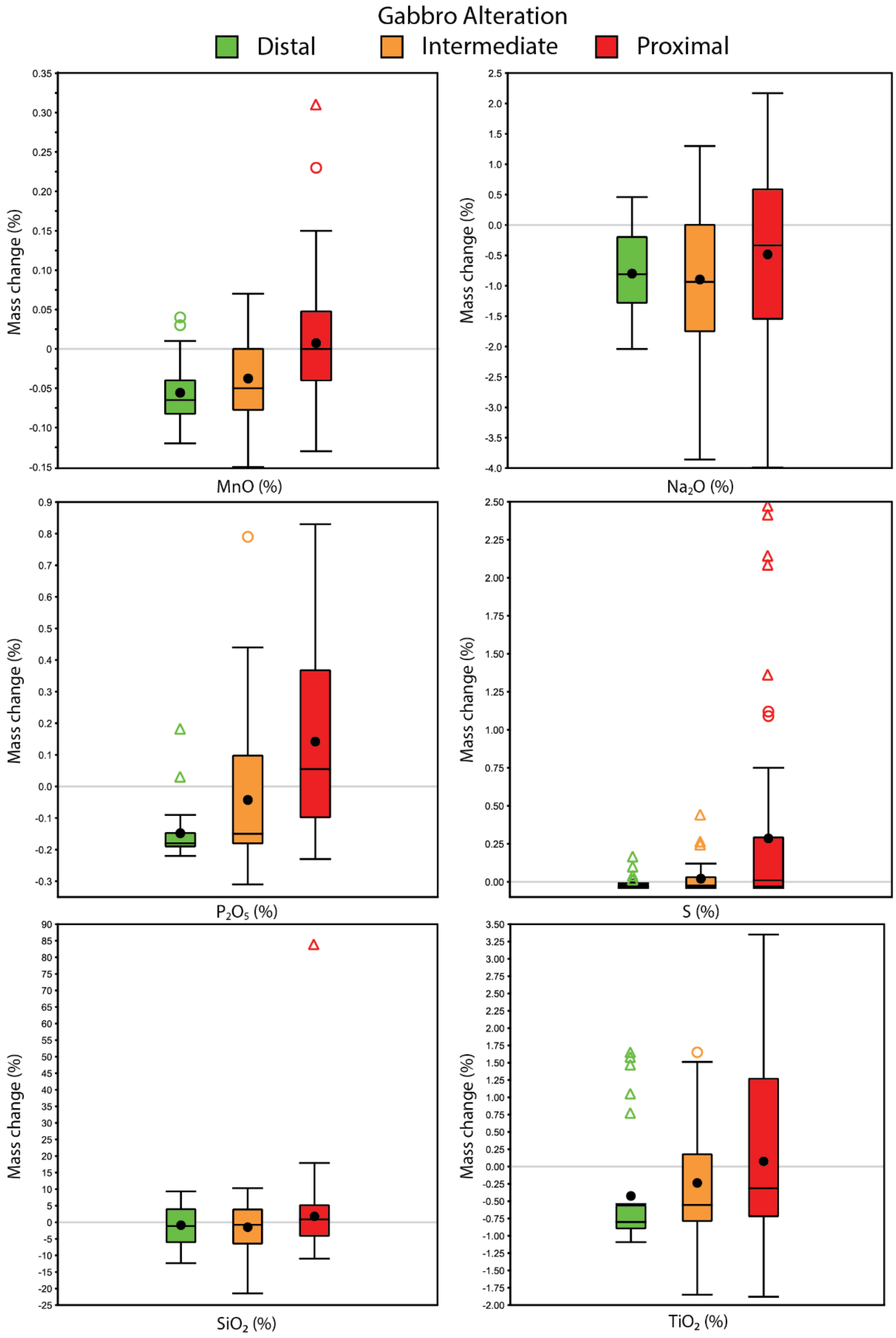

Appendix F.2.2. Mass changes for MnO, Na$_2$O, P$_2$O$_5$, S, SiO$_2$, TiO$_2$.

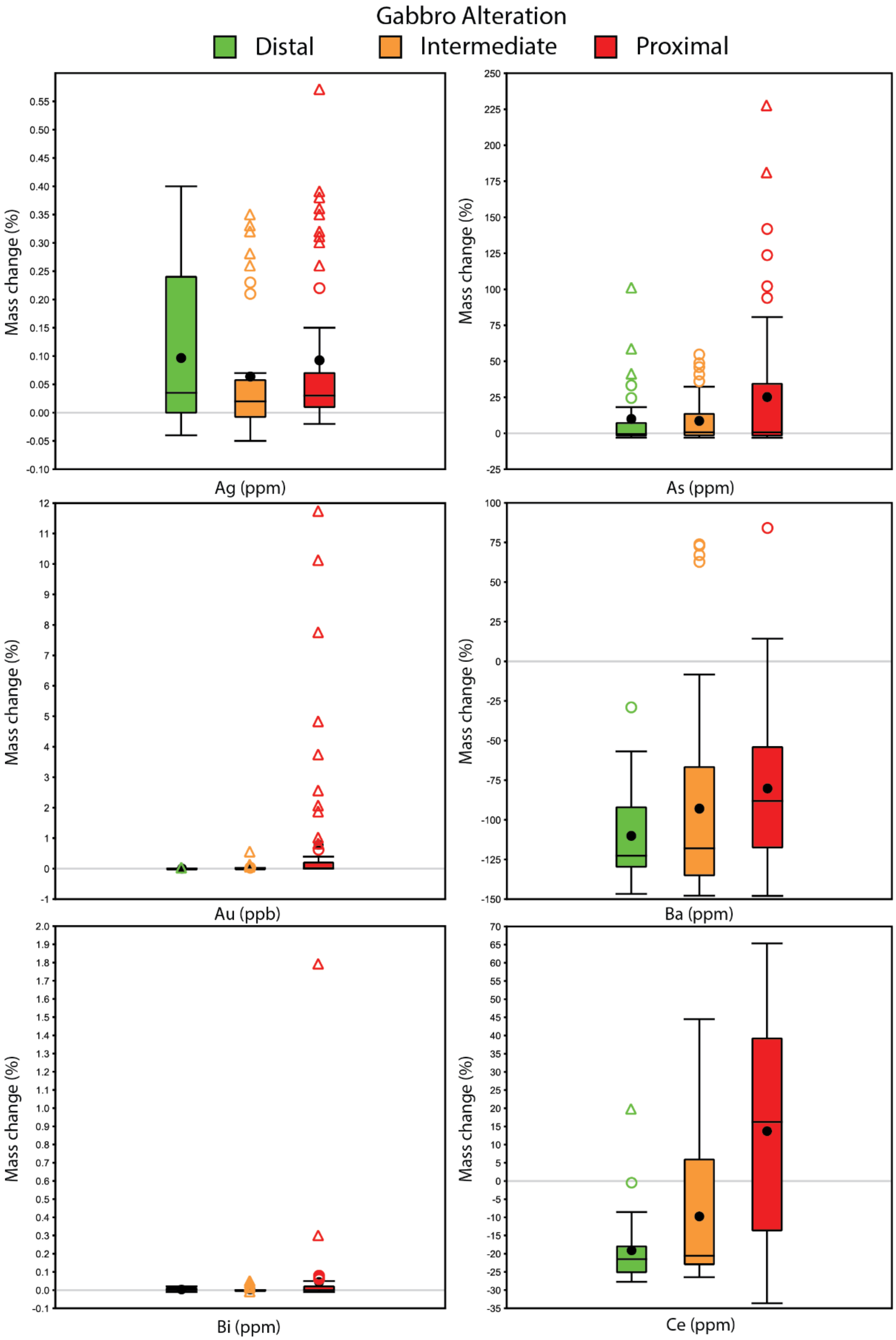

Appendix F.2.3. Mass changes for Ag, As, Au, Ba, Bi, Ce.

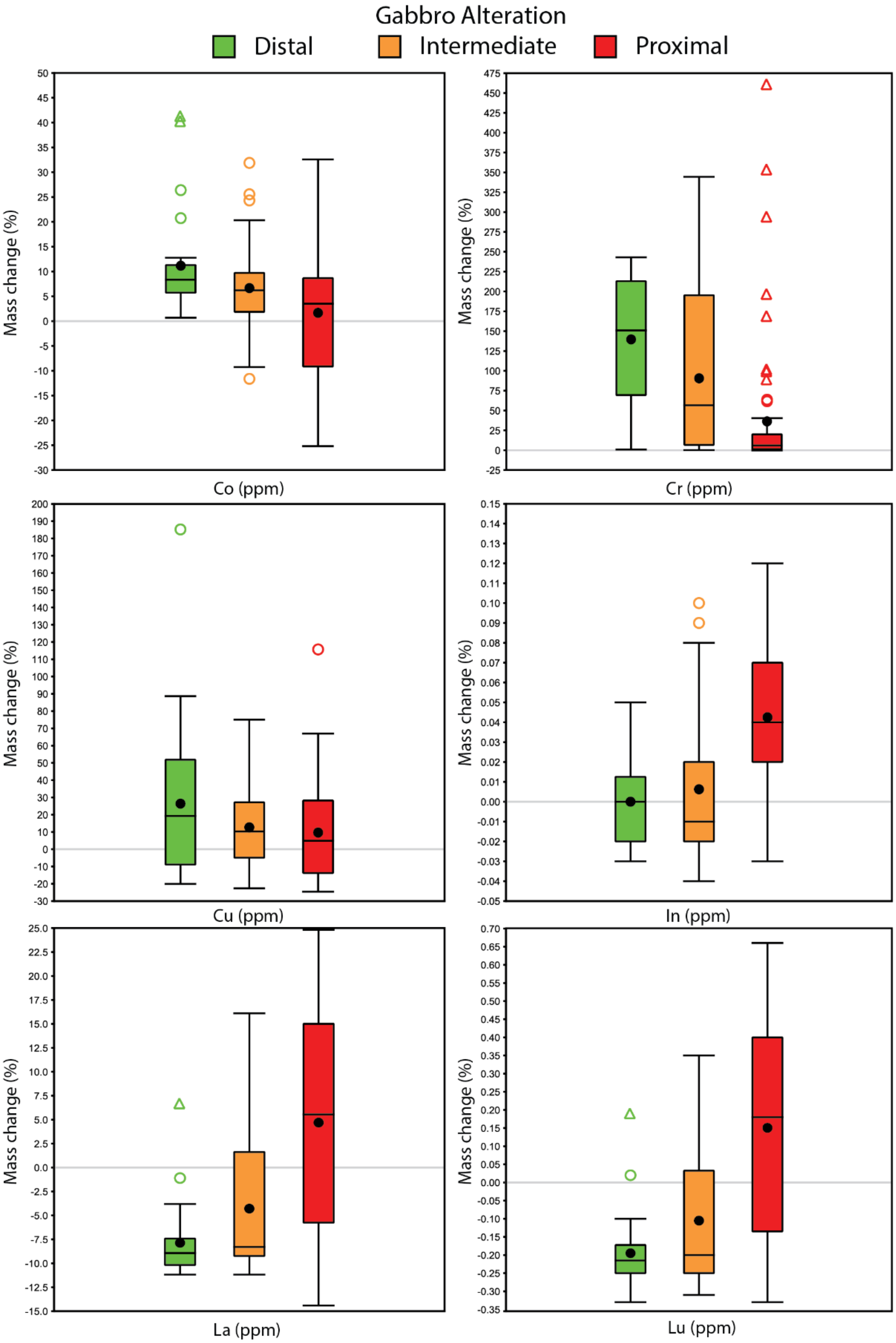

Appendix F.2.4. Mass changes for Co, Cr, Cu, In, La, Lu.

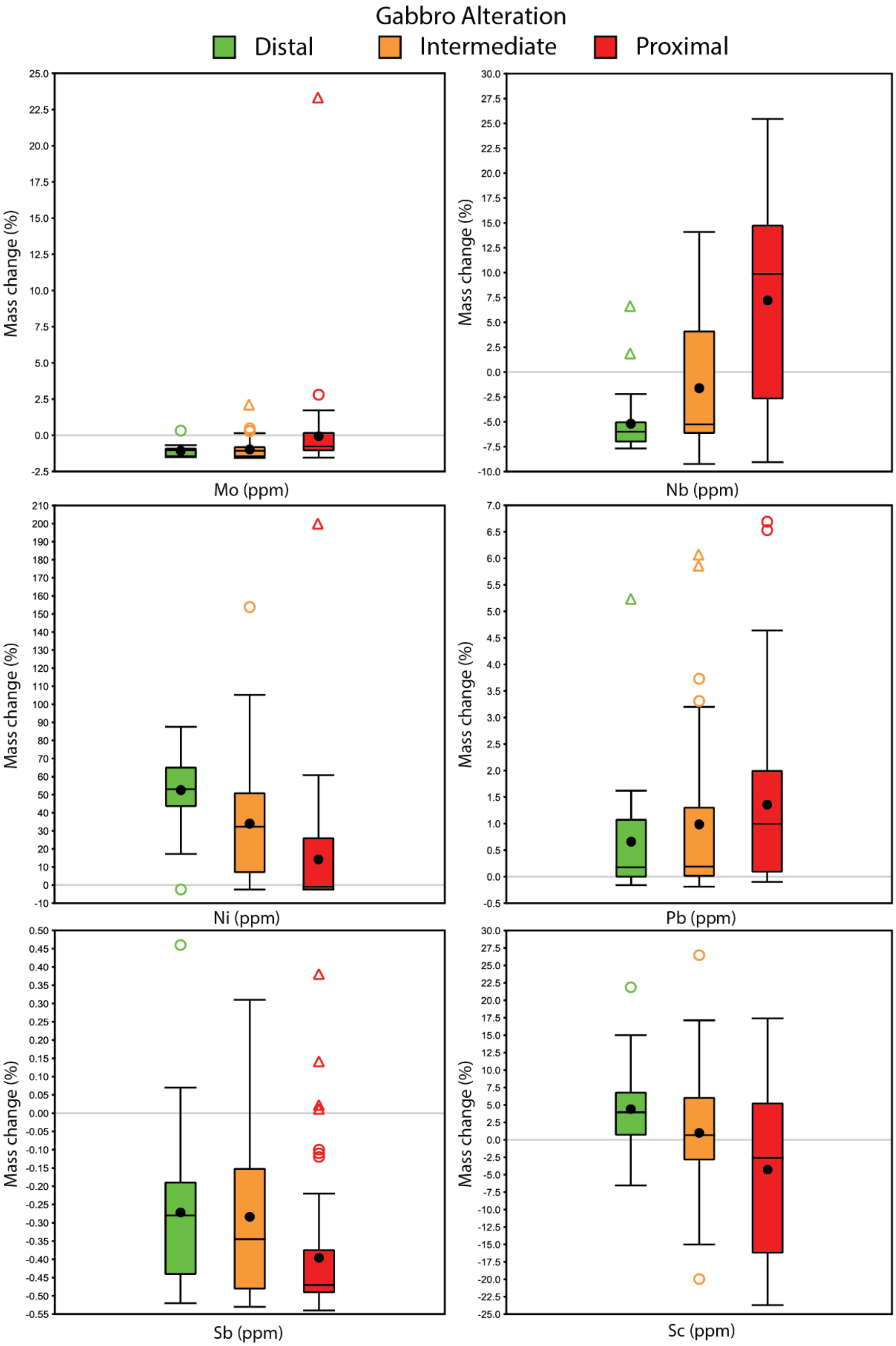

Appendix F.2.5. Mass changes for Mo, Nb, Ni, Pb, Sb, Sc.

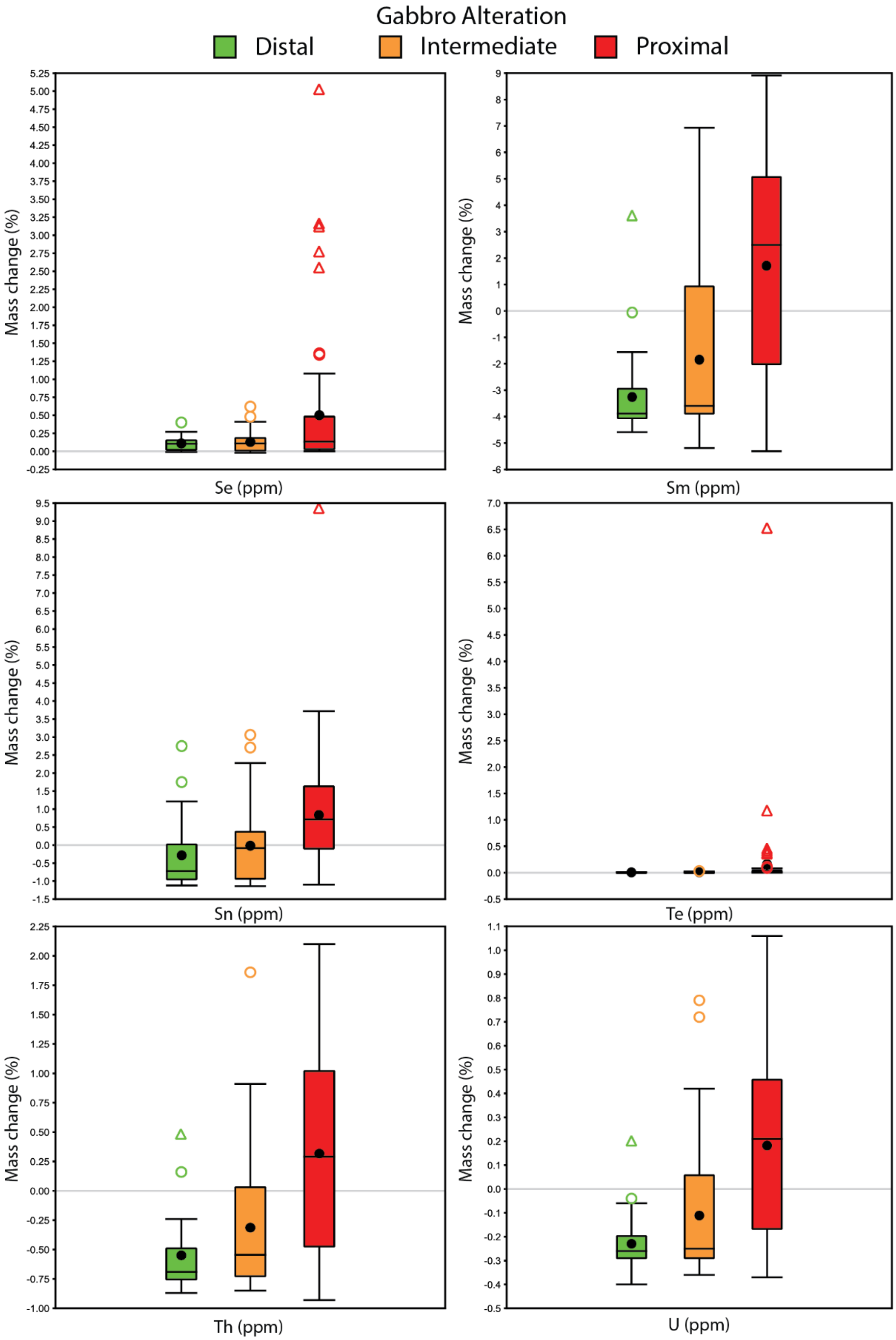

Appendix F.2.6. Mass changes for Se, Sm, Sn, Te, Th, U.

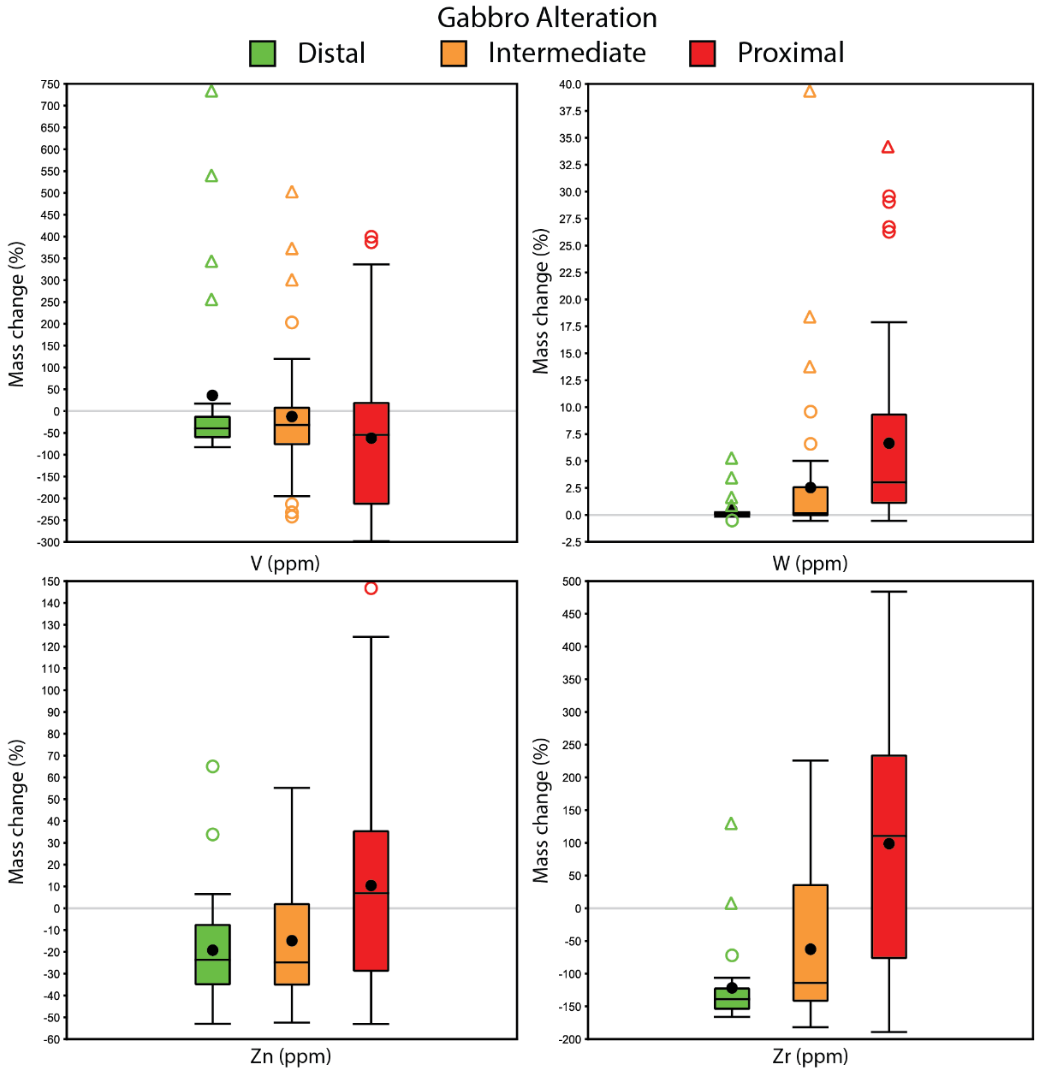

Appendix F.2.7. Mass changes for V, W, Zn, Zr.

Appendix G: Scanning Electron Microscope Analysis

Appendix G.1. Supplementary Scanning Electron Microscope Methods

Scanning electron microscope (SEM) analyses have been used to investigate and document the nano-scale mineralogy, mineral chemistry, and textural relationships between minerals in the gabbro, in addition to evaluating semi-quantitative variations in mineral chemistry as a function of paragenesis and proximity to mineralization. Analyses took place at the Memorial University's Department of Earth Sciences scanning electron microscope laboratory using a JEOL JSM 7100F scanning electron microscope. Analyses were undertaken on polished thin sections (25x45 mm) at 25 kV. Backscatter electron imaging was used to identify mineral phases and textures, whereas semi-quantitative energy dispersive spectrometer (EDS) point analysis was used to determine the mineral chemistry. The backscatter images below represent typical mineral phases observed in gabbro samples from distal, intermediate and proximal alteration zones at Argyle, Animal Pond and Stog'er Tight deposits.

Characterization of representative samples of the alteration assemblages has been achieved through optical microscopy and scanning electron microscopy (SEM) for imaging, and electron microprobe analysis (EMPA) for quantitative mineral chemical variations of micas, chlorites and carbonates. Selected drill core samples were sent to Vancouver Petrographics for polished thin section preparation for petrographic analysis of mineralogy, textural relationships, mineral volume estimation and the determination of mineral chemical variations in alteration facies.

Appendix G.2. Scanning Electron Microscope Images Compilation

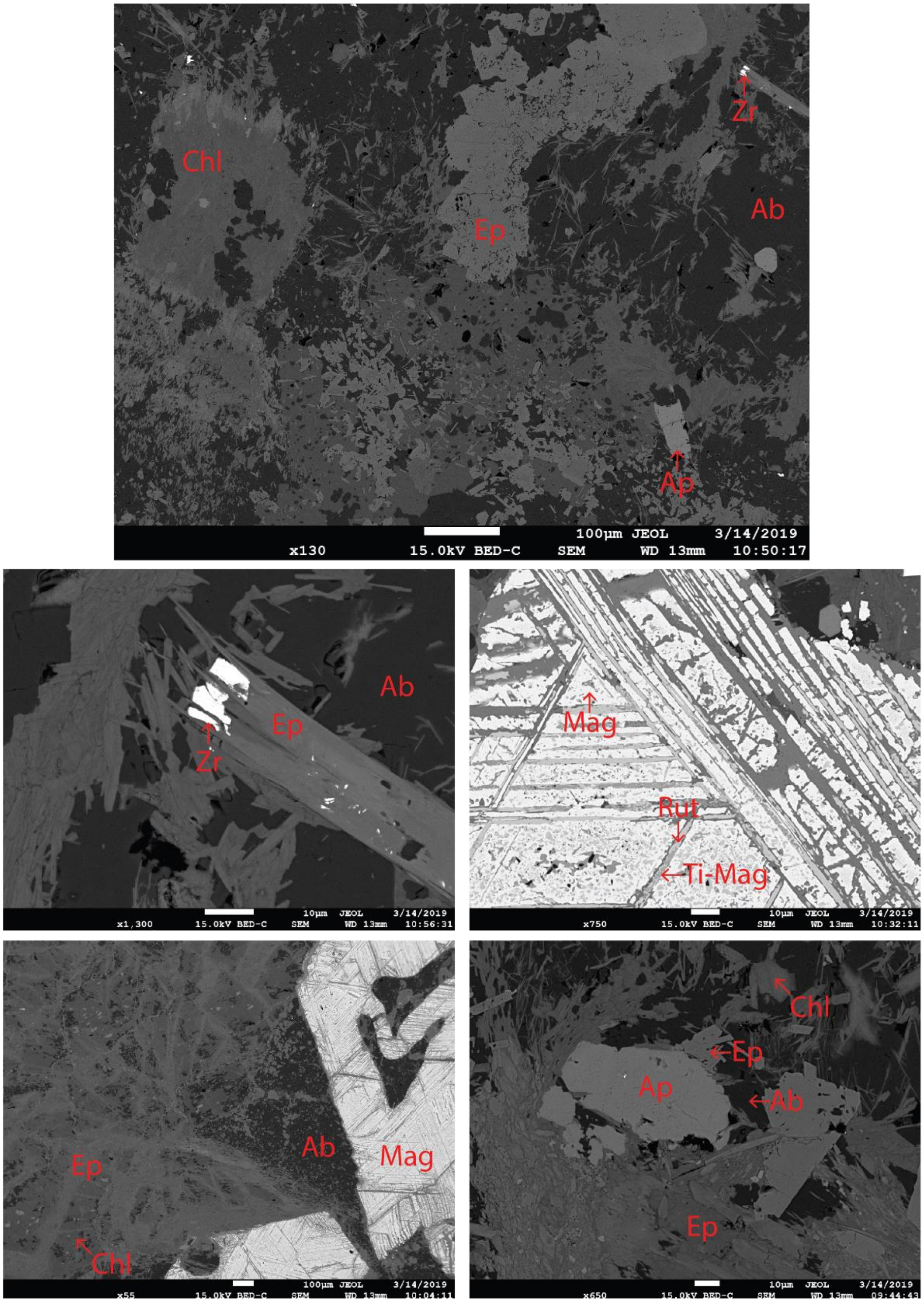

Appendix G.2.1. Scanning Electron Microscope image: sample 183067

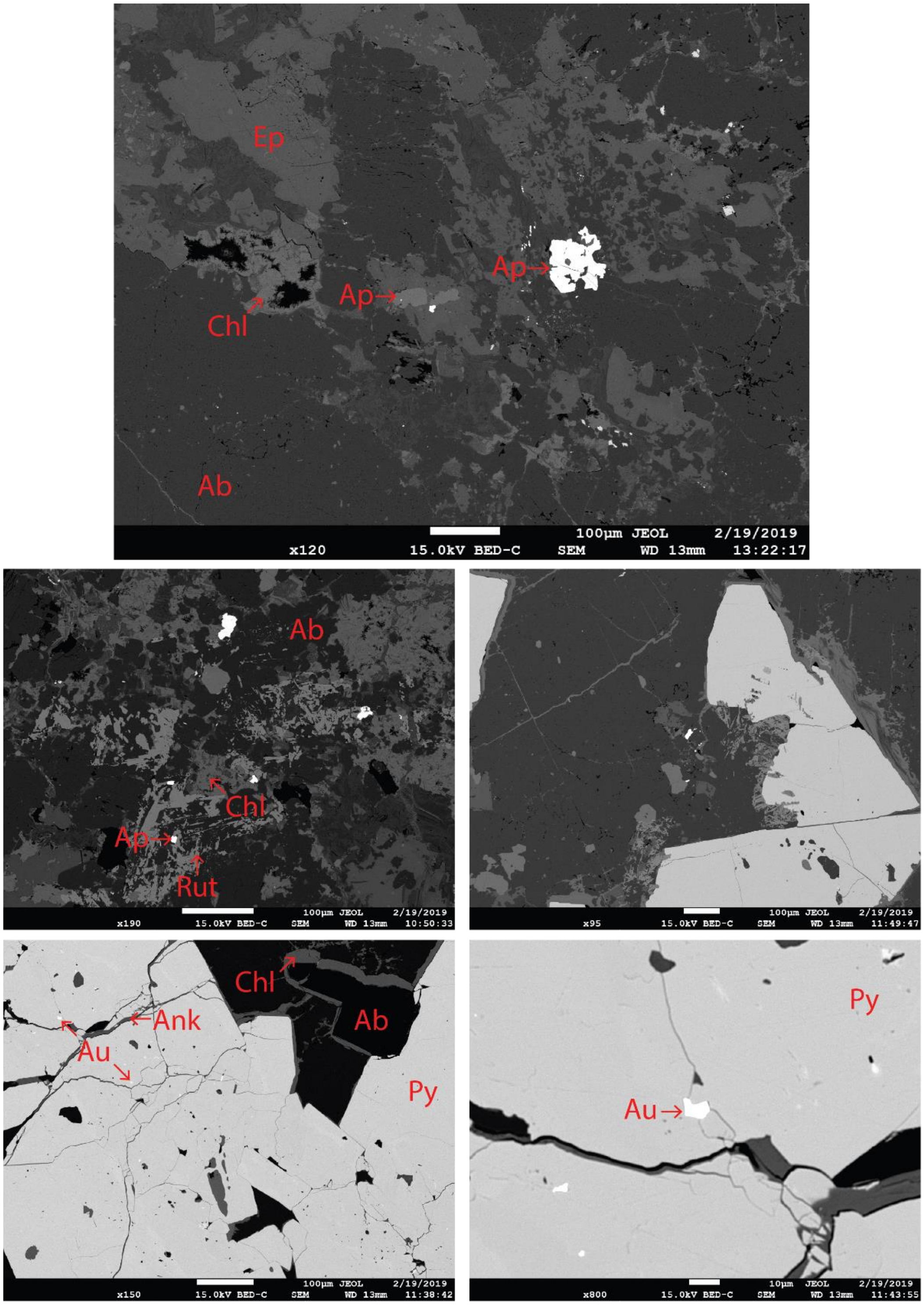

Appendix G.2.2. Scanning Electron Microscope image: sample 294849

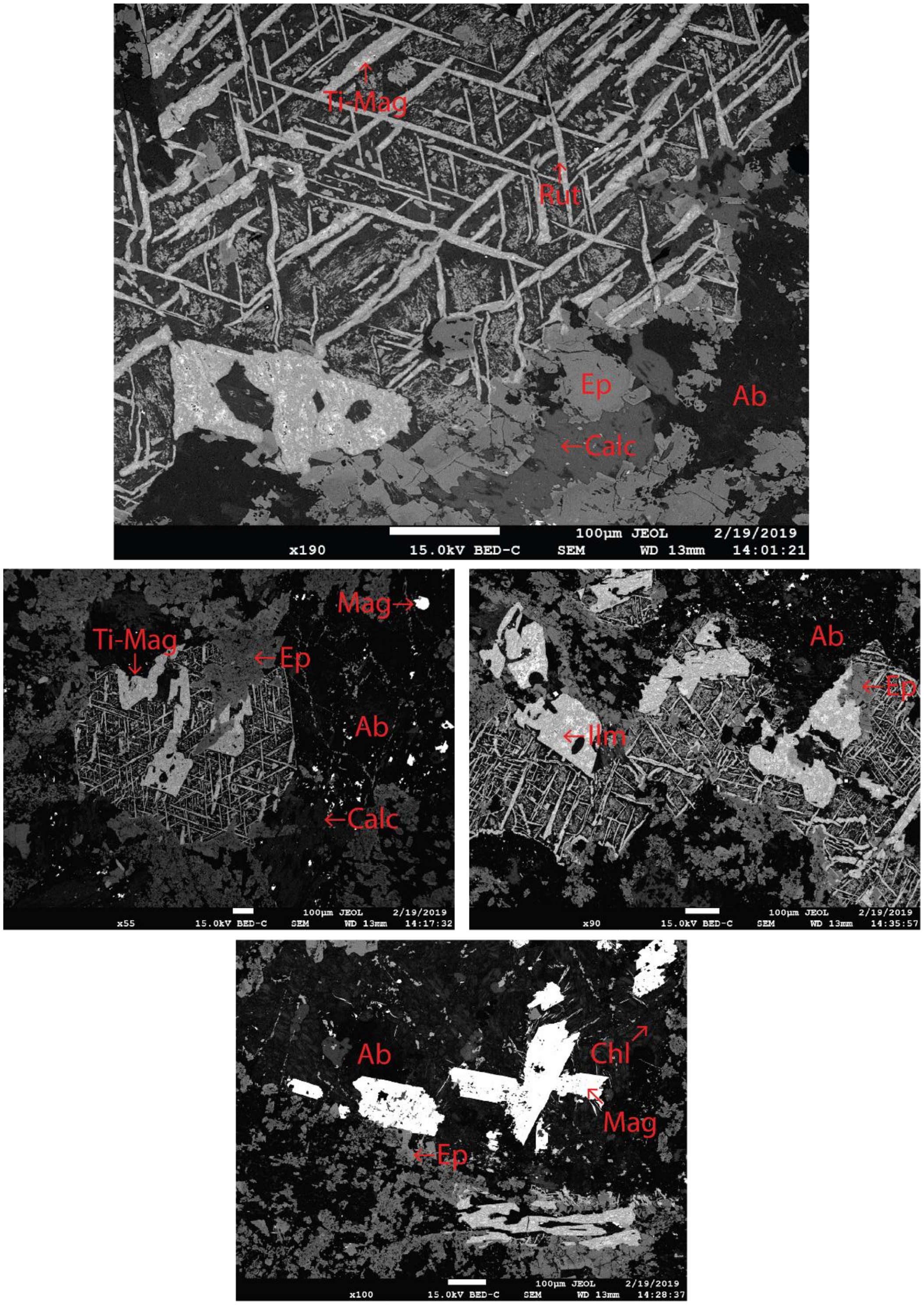

Appendix G.2.3. Scanning Electron Microscope image: sample 294851

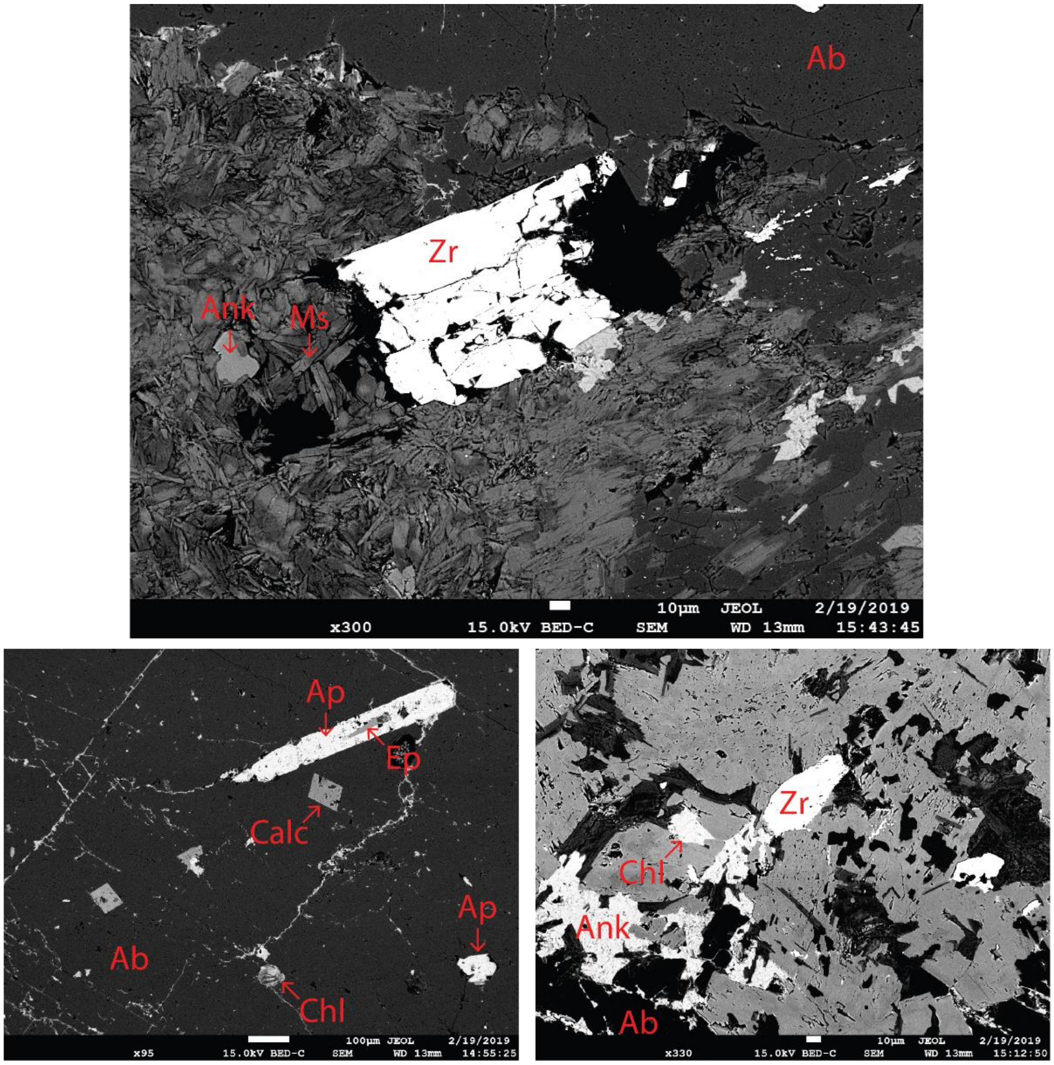

Appendix G.2.4. Scanning Electron Microscope image: sample I951354

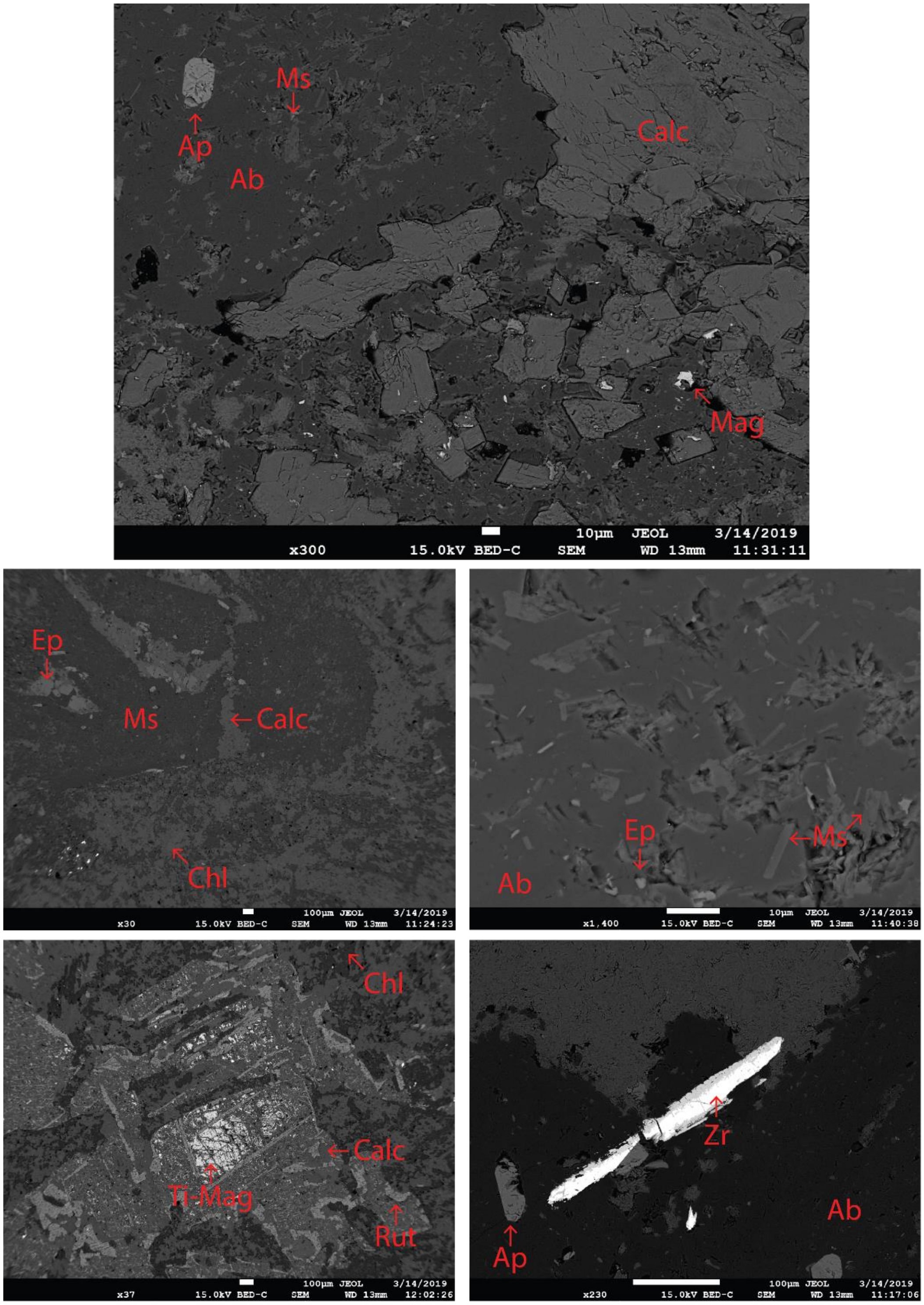

Appendix G.2.5. Scanning Electron Microscope image: sample I951358

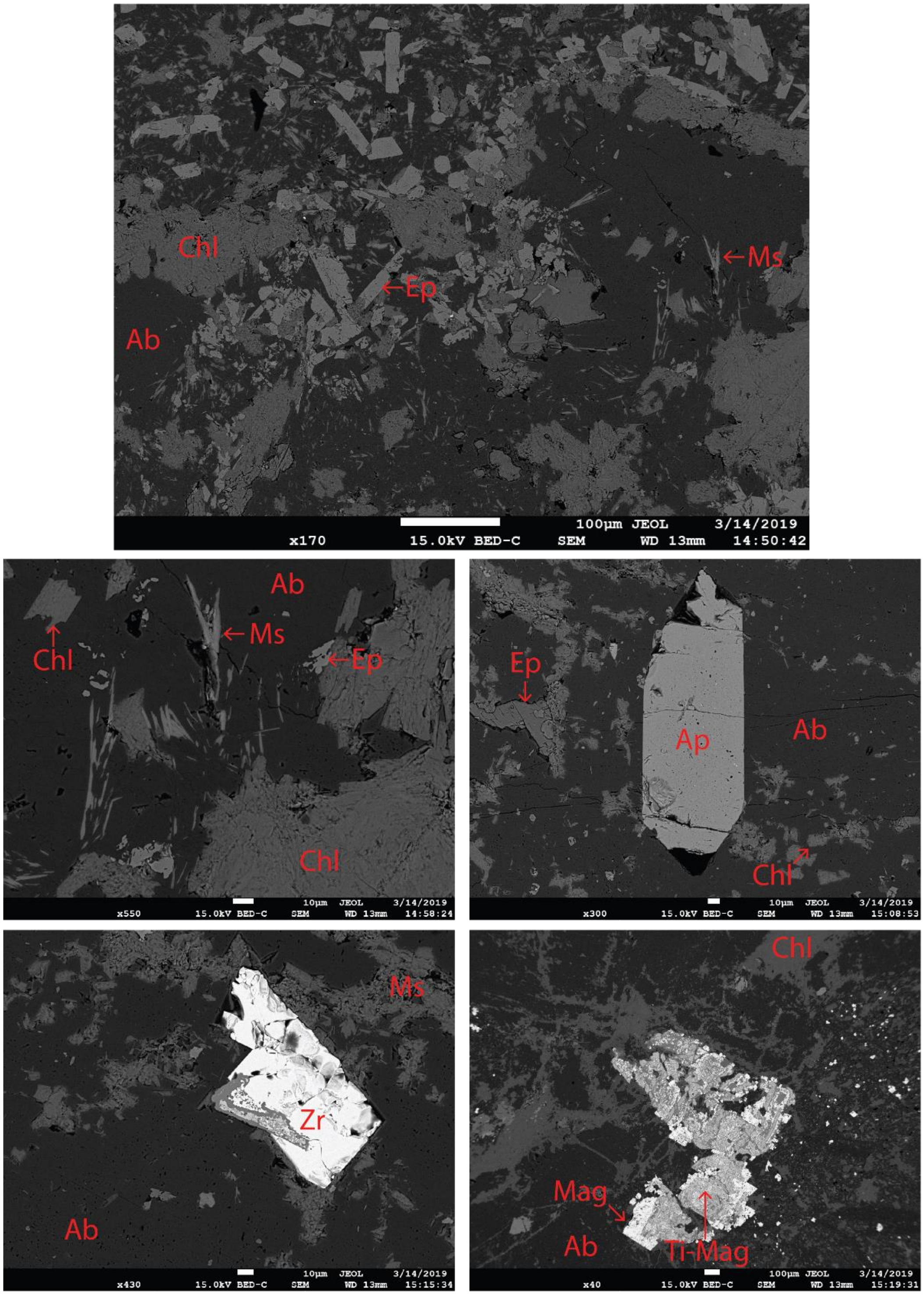

Appendix G.2.6. Scanning Electron Microscope image: sample I951364

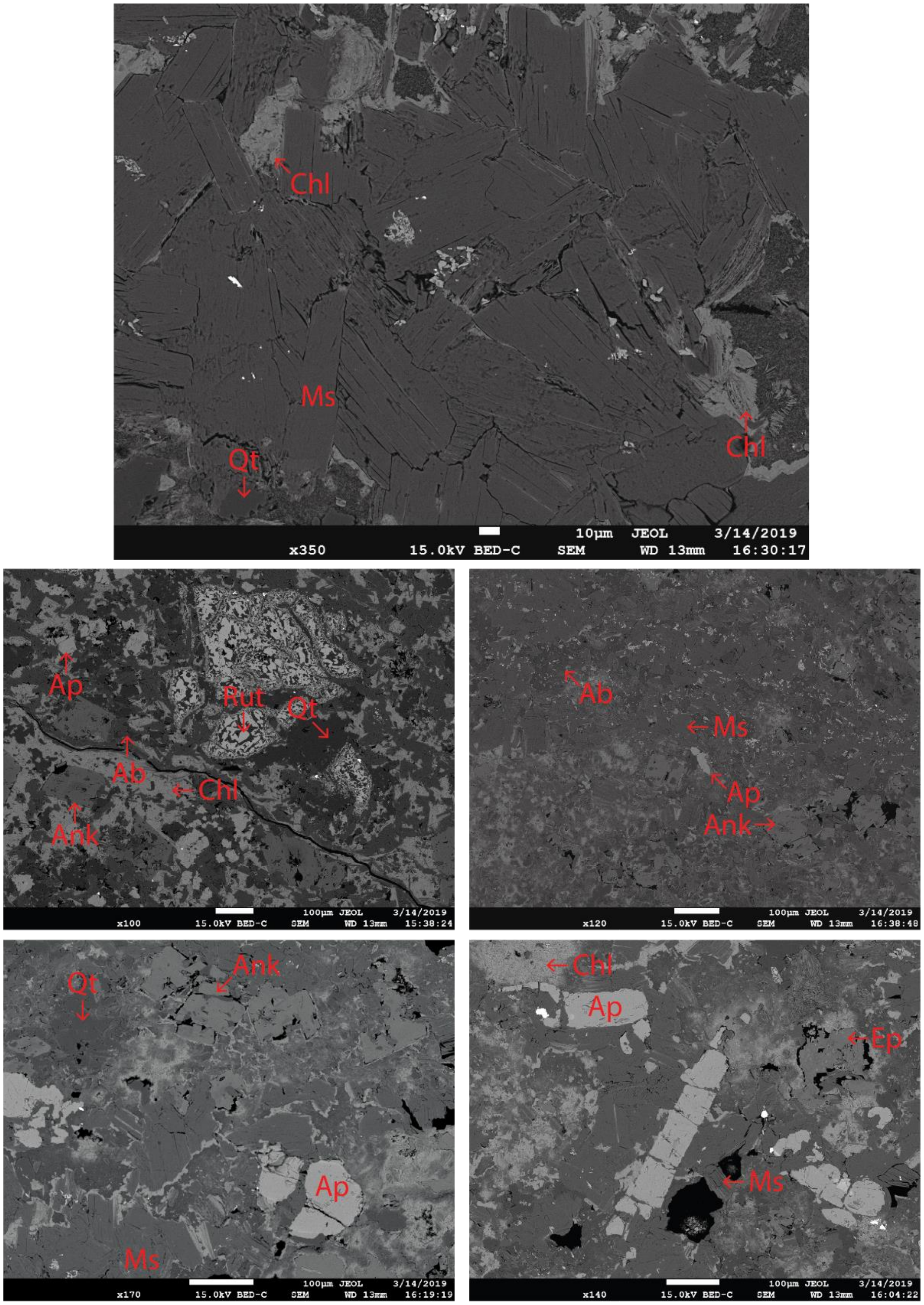

Appendix G.2.7. Scanning Electron Microscope image: sample I951457

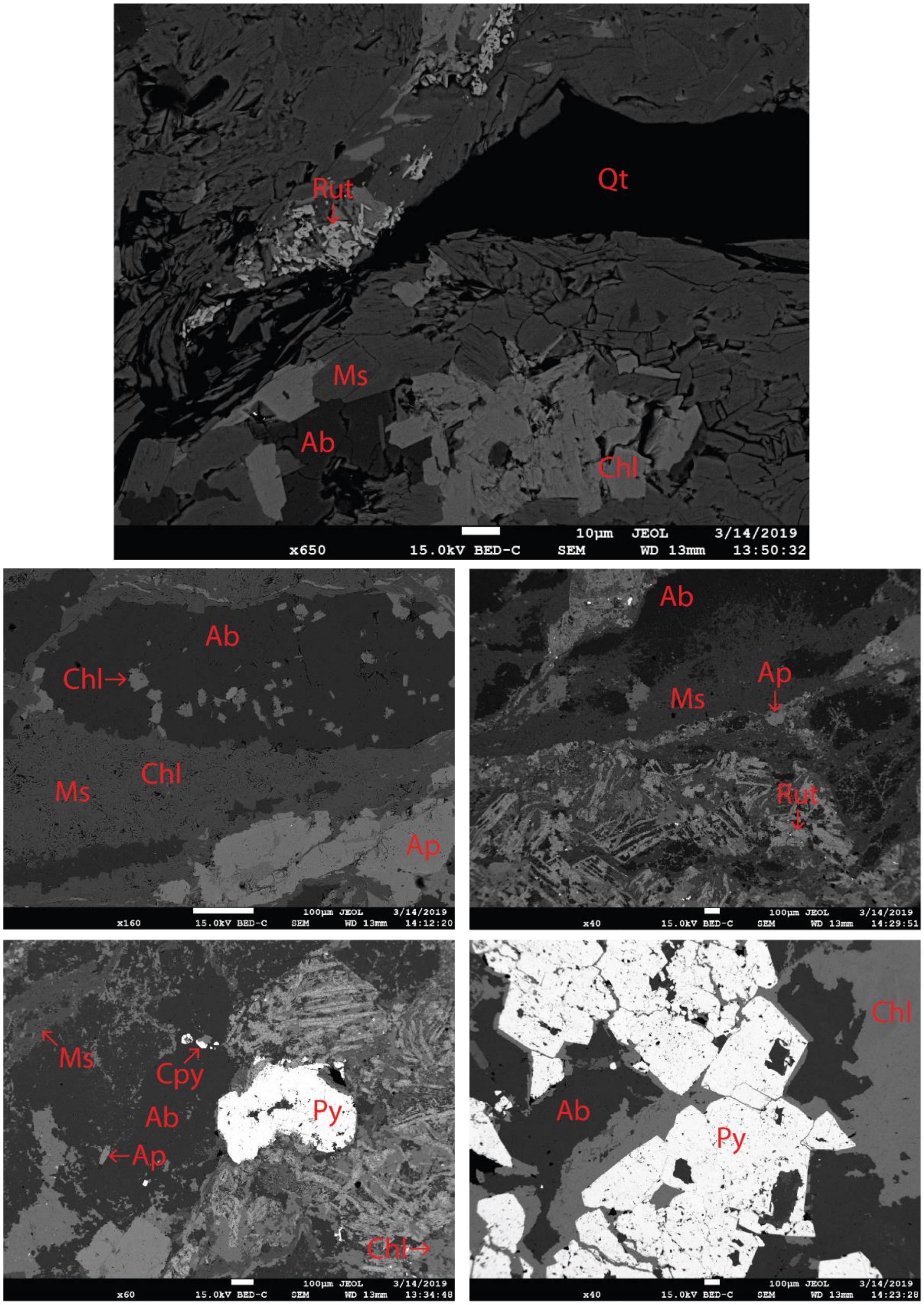

Appendix G.2.8. Scanning Electron Microscope image: sample I951476

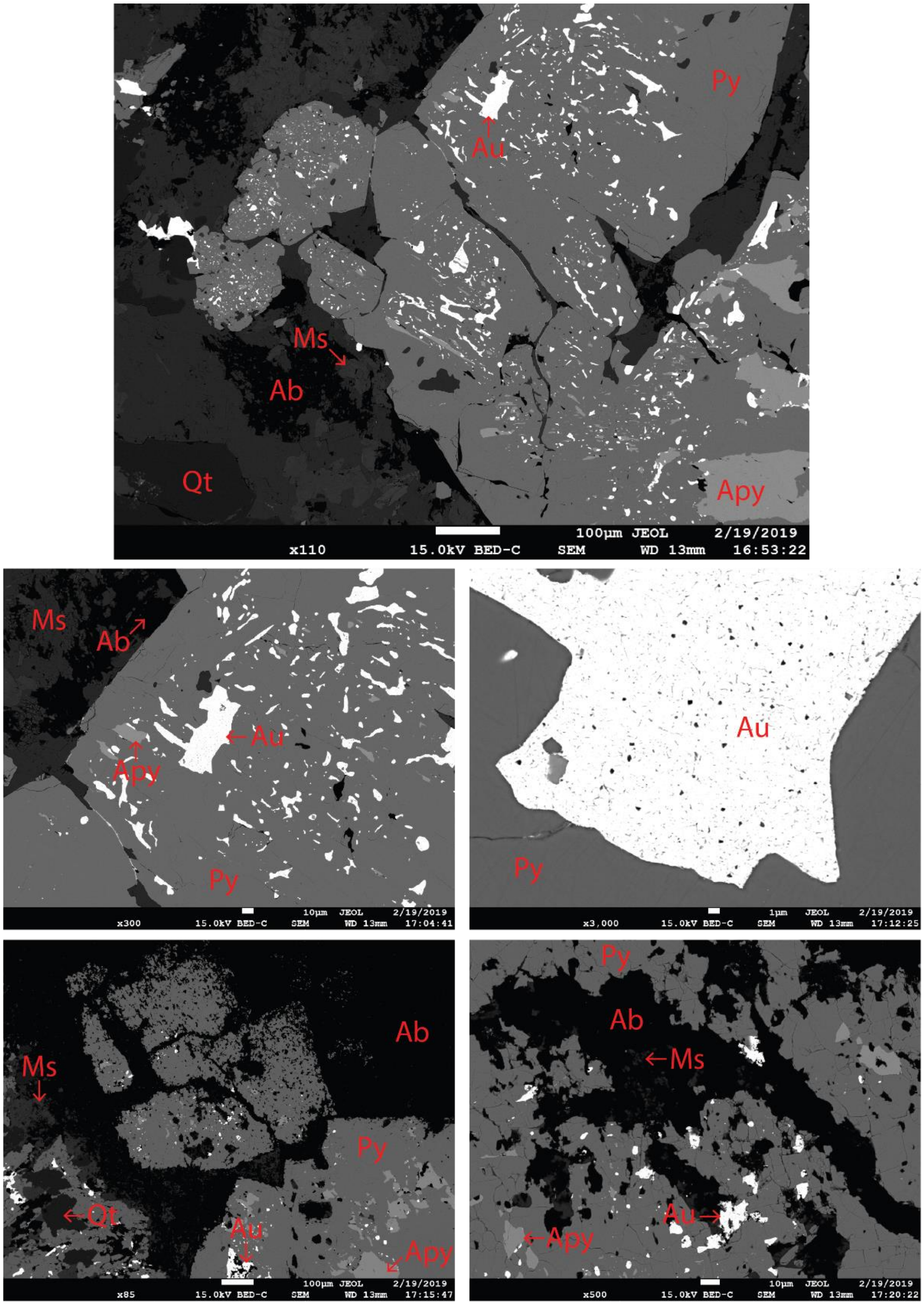

Appendix G.2.9. Scanning Electron Microscope Image sample MP18001-2